BIOKINETIC PROCESSES OF EXTRACELLULAR POLYSACCHARIDE (EPS) STABILIZATION OF SURFACE SOILS AGAINST DUST GENERATION

by

Humphrey O. Zebulun

A dissertation submitted to the faculty of
The University of North Carolina at Charlotte
in partial fulfillment of the requirements
for the degree of Doctor of Philosophy in
Infrastructure and Environmental Systems

Charlotte

2009

Approved by:

_____
Dr. Hilary Inyang

_____
Dr. Jy Wu

_____
Dr. James Oliver

_____
Dr. Helene Hilger

_____
Dr. Ronald Smelser

_____
Dr. John Daniels

_____
Dr. Sunyoung Bae

ABSTRACT

HUMPHREY ZEBULUN. Biokinetic Processes of Extracellular Polysaccharides (EPS) stabilization of surface soils against Dust Generation (Under the direction of Prof. HILARY INYANG).

Extracellular polysaccharide produced by a copiotrophic and nonpathogenic bacteria, *Arthrobacter viscosus*, promises to be an effective alternative to the use of chemical substances in dust control on exposed soil surfaces. The feasibility of this biokinetic stabilization approach to dust control depends in part on the capacity of injected microbes to produce EPS that can increase the resistance of soil to drying (desiccation) stresses. Initial laboratory based biokinetic investigations were performed to determine the rate of EPS production by *Arthrobacter viscosus* in both Haggstrom media (EPS production media) and sterilized samples of silty clay, sandy clay, and sandy silty clay soils and the effects of EPS on dusting resistance indices such as cohesion and retention of intergranular pore liquid. To achieve this objective, both Haggstrom media and the soil samples were inoculated with nutrient broth (20 to 100 ml/mL of Haggstrom media) containing *Arthrobacter viscosus* and changes in dusting resistance indices (soil cohesion, frictional resistance, and desiccation rate) in response to EPS growth were monitored. It was initially determined through tests that an optimum EPS quantity of 12.5 g/mL of Haggstrom media is produced by microbial broth concentration of 60 ml/mL of Haggstrom media. EPS-CM production rate in soil after initial injection of microbial broth concentrations (5 to 25 mL/g of soil) was tracked using thermogravimetric analysis (TGA), which has been shown to be an effective tool in determining the thermal decomposition of polymeric materials mixed with other composites. TGA results indicate that optimum EPS production in silty clay soil samples occurs at between 48 and 72 hr

after soil injection with the highest EPS quantity determined to be 3.8 mg/mg of soil observed when a microbial broth concentration of 20 mL/g of soil is used. In sandy clay and sandy silty clay soils, EPS quantity of 2.5 mg/mg of soil and 3.3 mg/mg of soil occurred in both soils respectively. To further investigate the effectiveness of EPS-CM in surface soil stabilization against dust generation, a direct application of different concentrations (5 to 25 mL/g of soil) of extracted EPS from the Haggstrom media and an indirect application of extracellular polysaccharide-Culture Media (EPS-CM) to the soil through injection of microbial broth with cells of different concentrations (5 to 25 ml/g of soil) for in situ EPS production with time were compared using deionized water as control. Three soil mixes were used, which include silty clay soil (original sample), sandy clay soil, and sandy silty clay soil were prepared from the sieve analyses of the soil samples collected. As part of the characterization of these soil samples, their specific surface areas were determined to be 8.397 m^2/g for silty clay soil; 8.121 m^2/g for sandy clay soil; and 8.193 m^2/g for sandy silty clay soil.

As an indirect measurement of the potential resistance of the stabilized soil to in situ stresses that can be caused by drying, direct shear and unconfined compression tests were performed on replicates of the treated soil samples. The equations developed in chapter 2 to compare the effects of EPS-CM treatment of soil friability indices, deformation resistance indices, coefficient of soil failure, and effective porosity were evaluated in chapter 8. The results of unconfined compression tests show that in EPS-CM amended silty clay soil samples, a strain of 0.34 to 0.20 from day 1 to day 3 occurred at EPS-CM concentration of 5 mL/g of soil but at higher EPS-CM concentrations, soil strain is observed to fluctuate with time. The least strain (0.25) occurs in silty clay soils treated

with EPS-CM concentration of 25 mL/g of soil compared to sandy clay and sandy silty clay soils. Thus soils with higher specific surface and clay minerals can develop cohesion more effectively than coarser-grained soils following EPS-CM amendment.

Desiccation tests performed on treated and control soil samples at 34 % relative humidity and temperature of 37 ^{o}C show that soil liquid content decreases with time. At relatively high EPS-CM concentrations of 15 to 25 mL/g of soil, EPS-CM-amended silty clay soils retain 5 % more liquid with time than sandy clay and silty clay soils. Fluorescence microscopic imaging of the treated soil samples clearly show the presence of EPS-CM as intergranular pore material and as smears on soil particles in EPS-CM-amended and microbial broth-amended soil samples whereas they are absent in the control samples.

The effects of EPS-CM amendment of the following selected indices of soil resistance to dust generation from exposed ground surfaces were investigated (soil cohesion, frictional resistance, effective porosity, desiccation rate). Data show that effective porosity in EPS-CM amended silty clay soil decreases with time due to continued EPS production by *A. viscosus* while changes in effective porosity with time in sandy clay and sandy silty clay fluctuated with time and EPS-CM production. After a 21-day monitoring with sampling at three 7-day intervals, unconfined compression and direct shear tests indicate that increase in cohesion from 37 to 45 kN/m^2 occurs in EPS-CM-amended silty clay soil at EPS-CM concentrations ranging 5 to 25 mL/g of soil. In sandy clay and sandy silty clay soils, maximum cohesion levels of 27 kN/m^2 and 24 kN/m^2 were observed, respectively, for the same EPS-CM concentrations within this sampling time while control samples show cohesion increments of only 0 to 15 kN/m^2.

Generally, it is observed that despite cyclical fluctuations in EPS-CM content in response to microbial dynamics in soil, frictional resistance decreases with increase in concentration of EPS-CM. Thus EPS-CM increase in intergranular pore space reduces intergranular friction but enhances cohesion within an overall increase in shear strength especially in fine grained soils that are prone to dusting. Liquid retention capacity, which is known to affect dust generation, improves favorably in EPS-CM-amended soils. With respect to practical use of duct control in the field, this research indicates that mixing of EPS-CM with microbial broth and scarified soil surfaces before compaction can be effective.

ACKNOWLEDGEMENTS

I would like to first thank God for His grace throughout this time of study. My deepest gratitude goes to my doctoral degree supervisor, Prof. Hilary Inyang, for his instruction, direction, and encouragement. I also wish to express my great thanks to the members of my dissertation committee, Prof. Jy Wu, Prof. James Oliver, Dr. Helene Hilger, Dr. John Daniels, Dr. Sunyoung Bae, and Dr. Ronald Smelser for their selfless encouragements and advice.

I would especially like to thank Prof. David Young for his great assistance and advice and Dr. Brian Anderson for his benevolence in helping me with the geotechnical experiments. My gratitude also goes to Prof. Mark Clemens for his help with the fluorescence microscope. I would like to acknowledge the help of the following faculty members, staff, and students of our university's Global Institute of Energy and Environmental Systems (GIEES) and the Department of Civil and Environmental Engineering; Dr. Vincent Ogunro for his help; Ms. Patricia Espinoza and Ms. Elizabeth Scott for their immense help and logistical support; I thank Mr. Ted Brown for construction of the sandboxes; and Allen Cottingham, Scott Ward for their help on the use of geotechnical equipment. Also I am grateful to Dr. Candace Davison at Penn State University for helping with soil sterilization using gamma irradiation.

I would like to thank the families of my uncle Mike and Stella Essien, Dr. Ekene and my parents, Mr. & Mrs. Zebulon Onyendi for their support throughout this period of study. Finally, I am greatly indebted to my wife, Amaka, and my daughter, Adaora for their love, support, and understanding during my doctoral work.

TABLE OF CONTENTS

LIST OF FIGURES

LIST OF TABLES

LIST OF ABBREVIATIONS

EPS	Extracellular polysaccharides
EPS-CM	Extracellular polysaccharides-Culture Media
TGA	Thermogravimetric analysis
SCSoil	Silty clay soil
SDCSoil	Sandy clay soil
SSCSoil	Sandy silty clay soil
D_N	Deformation index
ASTM	American Society for Testing and Materials
PL	Plasticity limit
PI	Plasticity index
LL	Liquid limit
YMA	Yeast mold agar
PBS	Phosphate buffered solution
EtBr	Ethidium bromide

CHAPTER 1: INTRODUCTION

1.1 Background and Problem Statement

Fugitive or airborne dust has been identified as a significant contributor to health hazards in the United States. The amendment of the Clean Air Act in 1990 required the establishment of a National Ambient Air Quality Standards (NAAQS) by the United States Environmental Protection Agency to regulate the air quality in both rural and urban areas (USEPA, 2004). Under this amendment, airborne particulate matter, especially those in the size fraction ranging from clay to silt with diameters from 0 to 10 µm, (PM_{10}), is used as a regulatory standard for determining air quality (Zobeck and Pelt, 2006; Stefanov et al. 2003; Pulugurtha and James, 2006; Singer et al. 2003). The small particle size range of this airborne particulate matter makes it easy for the material to be inhaled into the respiratory system, thereby increasing the risk of respiratory disorders in humans and animals. Also, farm crops can be contaminated by dusts with indirect health effects in humans through the food chain (Inyang and Bae, 2005; Rice et al. 1996; Miller and Woodbury, 2003). Control of fugitive dust has become the target of many agencies at various jurisdictional levels. Figure 3 shows the mechanisms of dust generation by moving vehicles on unpaved roads, resulting in human dust inhalation that can lead to respiratory problems.

Two main sources of fugitive dust that have been identified as a) anthropogenic sources such as vehicular traffic, industrial emissions, combustion of fossil fuels,

pesticide and herbicide applications; and b) natural sources such as windblown soil and unpaved road dust (Chow et al., 1992; Pewe et al., 1981; Iskander et al., 1997; Stefanov et al., 2003). A report by the Federal Highway Administration (1996) indicates that nearly 39 % of the road network in the United States is unpaved and the concentration of daily vehicular traffic on these roads coupled with wind action, has increased the concentration of dust generated from these roads (Amy and Ehsan 2002).

According to another report by the United States Environmental Protection Agency (2002), increase in population growth rate in arid regions of the U.S. has increased the need for the use of dust suppressants to reduce airborne particulate matter. This is also the case in many parts of the world where vulnerable ground surface is exposed. This need has resulted in a wide application of chemical agents as dust suppressants in these regions. Chemical dust suppressants can alter the physical characteristics of soil for control of dust emission from unpaved roads, mining and construction sites, military sites, forest pathways, agricultural lands, and livestock facilities, vacant lands, landfills, and steel mills (USEPA, 2002). The most commonly used chemical dust suppressants include salts and brines, petroleum-based organics, non-petroleum-based organic, synthetic polymers, electrochemical products, and clay additives (Bollander 1999a).

In particular, physico-chemical interactions between a variety of polymers and various soils have been theoretically modeled and experimentally investigated by Bae et al. (2006). Despite the efficiency of these chemicals in abating dust emission from surface soils, their potential environmental impacts remain a problem. Such impacts include surface and groundwater contamination, soil and soil water contamination, air

pollution, toxicity to soil and aquatic organisms through bioaccumulation, and hazards to humans through inhalation and dermal contact. Since dust emission still remains a global problem that especially results in an increase of respiratory diseases, it has become necessary to develop alternative methods for their control without any negative environmental impact. The development of such methods requires the utilization of natural materials such as slimes from snails and synthesized soil-binding products such as the natural polymer, extracellular polysaccharides (EPS) from microorganisms.

Most research studies involving the environmental application of microorganisms in both natural and laboratory scale investigations have been largely focused on bioremediation of anthropogenic environmental contaminants in soil and water. The production of natural polymers by soil microorganisms has been studied, but most of these studies have been largely focused on the application of these polymers in soil stabilization against water erosion (Tolhurst et al. 1999; deBrouwer et al. 2005; Barry et al. 1991; Gonsalves et al. 1991; Sojka et al. 2005).

Different species of *Arthrobacter* have been studied for their ability to produce natural polymers and among those identified, *Arthrobacter viscosus* has been isolated from soil samples in various parts of the United States, including, Illinois, Indiana, New York, and Arizona; Ontario, Canada; and Central and South America (Gasdorf et al., 1965). An understanding of the interactions between soil particles and this bacterium in soil is essential to the prediction of the cohesion of soil particles as a result of the presence of EPS that is produced in soil. Generally, soil microorganisms ride on solid particles and the spatial arrangement of these particles results in the formation of a complex pattern of pore spaces. Water and/or air that are trapped in these soil pore spaces

are of different shapes and sizes, thus making them attractive habitats for microorganisms (Chenu and Stotzky, 2002). According to Mills and Powelson (1996), the soil environment is made up of both microbes living in an organic-and inorganic-containing broth and microbes living in a surface-rich environment with the surfaces coated with a thin film of water.

An important phenomenon that is essential for the survival of microbes in soil is microbial adhesion to soil particles. Microbial adhesion has been described as the energy involved in the formation of the adhesive joint which can be measured in terms of the work required to remove a microbial cell from a substratum to which it adheres (Rutter et al., 1984). Mechanisms of adhesion of microbial cells to soil particles have been discussed as well, and it has also been noted that these mechanisms involve various interactions between the microbial cell surface and the soil particles (Mills and Powelson, 1996). According to Chenu and Stotzky (2002), the interactions between soil particles and microorganisms can be classified as both biotic and abiotic. The biotic interactions involve cell growth and multiplication, as well the secretion of enzymes and biopolymers while the abiotic interactions involve physical interactions such as cohesion of soil matrix facilitated by the biopolymers produced *in situ* (Robb, 1984; Chenu and Stotzky, 2002).

Such interactions include electrostatic and electrodynamic interactions, hydrophobic interactions, and the adhesion of polymers (Mills and Powelson, 1996). They also involve adhesion processes (Chenu and Stotzky, 2002). Studies of microbial adhesion to soil particles (Deflaun et al., 1999; Mills and Powelson, 1996) have indicated that cell surface charge affects the electrostatic interactions between microbial cells and substratum, hydrophobicity of microbial cells, and the secretion of EPS by these

microorganisms (Deflaun et al., 1999). While the existence and the activities of microorganisms in subsurface and deep soil have been demonstrated by Balkwill and Boone (1997), Stevens and Holbert (1995), Kinkel et al. (1992), Mayer et al. (1999), and Tunlid and White (1992), other studies (Lopez et al. 2003; Park et al., 2000; Jeanes et al., 1965; Bejar et al., 1998; and Ben-Hur, 2006; Blume et al., 2002) have also focused on the secretion of different exopolymers by microorganisms. However, these studies have failed to discuss the effects of microbial biopolymers on the stabilization of surface soils with consideration of their particle sizes and textures.

Based on the polymer-producing capacity of *Arthrobacter viscosus*, this research project focuses on exploring the potential application of using EPS from this bacterium to produce EPS that can stabilize surface soils. To ensure maximum production of the EPS, an appropriate growth nutrient such as glucose is typically used to grow the microorganism. Through the extraction and quantification of the EPS produced, the concentration of the EPS produced will be correlated with the concentrations of the biomass *x* and substrate *s* using differential equations 1 and 2 (Bader, 1982).

$$\frac{dx}{dt} = R_p + x_f \tag{1}$$

$$\frac{ds}{dt} = R_p + s_f \tag{2}$$

where R_p is the rate of production of biomass per unit volume of culture ($m^3\ g^{-1}\ hr^{-1}$), and x_f and s_f are the concentrations of the biomass and substrate respectively (g/m^3).

Bacterial adhesion to solid particles is an important step in soil stabilization. The Derjaguin-Landau-Verwey-Overbeek (DLVO) theory, developed for macromolecules and particles, is commonly used to describe the interactions between charged colloidal

particles and solid surfaces. Bacterial adhesion can be enhanced by exopolymers (Azeredo et al., 1999; Behrens, 1998). According to this theory, two principal forces of attraction involved in these interactions are *Van der Waals* forces and electrostatic double-layer forces while other interactions such as ion bridging, steric interactions in the presence of polymers, and hydrophobic interactions in polar media also contribute to bacterial adhesion to solid particles (Oliveira, 1997; Hayashi et al., 2001; Sharma and Rao, 2003). To apply the DLVO theory to bacterial adhesion studies, it is assumed that the interacting surfaces are smooth with homogenous chemical properties. However, studies involving solid particles such as soil particles have shown that the DLVO interaction energy, E_{DLVO} can also be applied to rough surfaces, and equations that express this phenomenon as well the aggregation of charged particles, have been developed (Bhattacharjee et al., 1998; Behrens et al., 1998). Furthermore, EPS has been reported to significantly influence the adhesion of bacteria to solid surfaces (Tsuneda et al. 2003). By altering the physicochemical characteristics such as charge, hydrophobicity, and polymeric property, EPS covering cell surfaces enable bacterial adhesion onto solid surfaces of solid surfaces, which is correlated with the zeta potential of both the bacterial cell surface and solid surface. Previous studies by Tsuneda et al. (2003) and Kaya and Yukselen (2005) concluded that based on the amount and chemical composition (75-89 % protein and polysaccharides) of EPS, cell adhesion onto solid surfaces can be inhibited by electrostatic interaction or enhanced by polymeric interaction.

These equations also explain the adhesion mechanisms of bacterial surfaces to solids (Mills and Powelson, 1996) which can be described as follows.

$$E_{DLVO}(h) = E_{VDW}(h) + E_{EDL}(h) \ . \tag{3}$$

$$E_{DLVO}(h) = -\frac{A_H}{12\pi h^2} + \frac{\varepsilon\varepsilon_0\kappa}{2}\left[(\psi_s^2 + \psi_r^2)(1-\coth\kappa h) + 2\psi_s\psi_r \cos ech\,\kappa h\right] \quad (4)$$

$$A_H = g_a.12\pi h^2 \quad (5)$$

where E_{VDW} is the van der Waals interaction energy (kPa) per unit area between two infinite flat plates, E_{EDL} is the electrostatic double-layer interaction energy (kPa) per unit area between two infinite flat plates, ε is the dielectric constant of solvent, ε_0 is the dielectric permittivity of vacuum, κ is the inverse Debye screening length (nm), Ψ_s (mV) is the surface potential of the smooth surface, and Ψ_r (mV) is the surface potential of the rough surface. In equation 5, A_H is the Hamaker constant, g_a and h (m) represent the Gibbs energy of attraction per unit cross-sectional area and the local distance between a rough surface and a smooth planar surface respectively (m^2). The differential area of the aggregate surface dS can also be determined using the expression,

$$dS = r^2 \sin\theta\, d\theta\, d\phi \quad (6)$$

where Θ and ø represent the angular coordinates in a spherical coordinate system. The net nonretarded r interaction energy of a pair of colloid particles $V(r)$ (kPa), which comprises of the van der Waals forces of attraction $V_{vdw}(r)$(N) and a repulsive double layer $V_{dl}(r)$ (N) can be applied to calculate the interaction energy between the soil particles and the EPS expressed as

$$V(r) = V_{vdw}(r) + V_{dl}(r) \quad (7)$$

The energy of bacterial adhesion, E_{ba} can also be calculated using a modified version of the van't Hoff equation (Mills and Powelson, 1996) expressed as,

$$E_{ba} = \ln\left(\frac{K}{M}\frac{d}{}\right) = \frac{\Delta H^0}{RT} + C \quad (8)$$

where k_d is modified to represent the coefficient of bacterial distribution in solution and soil, $_M$ is the number of adhesion sites per gram, ΔH^0 is the standard enthalpy, R is the gas constant, T is the absolute temperature, and C is a constant. Replacing k_d in equation 8, the energy of the bacterial adhesion E_{ba} (kPa) can now be calculated as follows,

$$E_{ba} = \ln\left(\frac{\frac{c_s^{soln}}{c_s^{soil}}}{M}\right) = \frac{\Delta H^0}{RT} + C \tag{9}$$

where C^{soln} and C^{soil} are the concentrations of the bacterial EPS in soil solution and soil solid respectively, which will be determined from a sorption test. By modifying the Arrhenius equation, the adhesion energy can also be estimated as follows,

$$k = A\exp^{-E_{ba}/RT} \tag{10}$$

where k is a rate constant, A is a pre-exponential factor, E_{ba} is the energy of bacterial adhesion, R is the universal gas constant, and T is the absolute temperature. Mechanisms of cohesion of soil particles as a result of bacterial adhesion have been described (Munkholm and Kay, 2002; Konrad and Ayad, 1997; Snyder and Miller, 1985; Marder and Fineberg, 1996; Briones and Uehara, 1977). The relevant equations for the determination of these soil properties include but not limited to the following,

$$\frac{dU}{dA} = \frac{d}{dc}\left[\pi\sigma^2 c^2 / 2E\right] = \pi\sigma^2 c / E \tag{11}$$

Equation 11 can be applied to measure the rupture of soil solid where U is the strain-energy, A is the area of rupture (m^2), E is the Young's modulus (N/m^2), c is the semi-major axis of a pre-existing crack, and σ is the limiting stress (N/m^2) (Briones and Uehara, 1977). In a uniformly packed soil with no cracks and an unpacked soil with

potential cracking spaces, the tensile failure *x* can be determined by equation 12 as described by Snyder and Miller (1985).

$$x = -\frac{(\sigma - u_a)_m}{(u_a - u_w)} \tag{12}$$

Where σ the uniform normal stress (N/m^2), μ_a is the air pressure (N/m^2), and μ_w is the water pressure (N/m^2), while the expression $(\sigma - u_a)_m$ represents the maximum stress applied (N/m^2) and $(\sigma - u_a)$ is the relative tensile stress. Aggregate tensile strength *Y* and aggregate friability *k*, can also be determined by the application of equation 13 and 14 (Munkholm and Kay, 2002)

$$Y = a\frac{F}{d^2} \tag{13}$$

$$\log Y = -k \log V + A \tag{14}$$

where *a* is a constant, *F* is the polar force needed to fracture the aggregate (N), and *d* is the average aggregate diameter (m), *A* is the predicted log strength of 1 m^3 of soil (kPa), and V is the volume of the aggregate (m^3).

Previous studies have shown the existence of a relationship between the concentration of the EPS produced and the cell growth of *Arthrobacter viscosus* (Novak et al. 1992; Perkins et al. 2004; Bader 2000; Pickett, 2000; Yallop et al. 2000). It has also been shown that the rate, concentration, and quality of EPS produced by this bacterium depend on the composition of the growth medium in terms of nutrients and environmental conditions (Lopez et al. 2003; Jeanes et al. 1965; Taylor et al. 1999). Characterization of EPS has revealed the mechanisms of their formation, chemical composition, and rheological properties (Bejar et al. 1998). Different bacteria species synthesize extracellular polysaccharides (EPS) as a construction material for the formation of biofilms and sludge, which enables them to exist as a consortium in both

soil and water environments (Flemming and Wingender, 2001; Miyazaki and Seki, 2006; Xavier et al. 2004). In soil, bacteria interact with the surfaces of the soil particles through a mechanism termed, adhesion. This adhesion mechanism involves electrostatic and electrodynamic interactions, which is facilitated by the production of EPS (Chenu and Stotzky, 2002). Through these interactions, these bacteria are able to attach firmly to the soil particles thereby acting as a bridge between the soil particles and the surfaces of the bacteria cells (Mills and Powelson, 1996; Chenu and Stotzky, 2002; Bos et al. 1999). This is the phenomenon applied in soil stabilization using EPS. Bacteria cells also synthesize EPS in response to unfavorable conditions such as desiccation and nutrient starvation, which enables them to retain water and nutrients for long term survival. In order words, the production of EPS, which are major contents of biofilms, is induced by desiccation and this does not destroy the inherent water-binding properties of biofilms polymers. This makes it possible for the dried biofilms to act as a sponge, rapidly absorbing any moisture that becomes available (McArthur, 2006). In liquid media, the production of EPS also enables bacteria to attach to sediments or any solid surface and to form a cluster, which is able to withstand the effect of shear stress in such environments **(**Dunsmore et al. 2002; Brouwer and Stal, 2001).

Compositional analysis of EPS produced by *Arthrobacter viscosus* has shown the carbon sources of the polysaccharides as well their carbon-chain structures (Novak et al. 1992). EPS is composed of different monomers such as xylose, glucose, galactose, mannose, and 2-*O*-methylglucose and some percentages of proteins (Hu et al. 2003; Novak et al. 1992; Taylor et al. 1999). Sorption of EPS to soil particles affects adhesive mechanisms that bind soil particles together (de Brouwer et al. 2002). Other studies have

also indicated the presence of interrelationships among rates of microbial production, EPS production, microbial biomass, and soil stability while the cohesive strength of soils have been determined based on their shear stress (Yallop et al. 2000; Tolhurst et al. 1999). Essentially, the adhesion of EPS to the surfaces of soils that are most vulnerable to dust generation (silty clay soils) is expected to improve their cohesion and liquid retention capacity. Finally, it is expected that all these interactions will result in the reduction of potential of dust emission from soil samples.

CHAPTER 2: QUANTIFICATION OF SIGNIFICANT PARAMETERS

2.1 Hypotheses and Research Objectives

2.1.1 Conceptual model

The theoretical basis for this research is that the introduction of EPS into soil with supporting nutrients, for the growth of resident bacteria will result in the production and growth of EPS to partially or completely fill the existing pore space over a given time interval. The required time interval for such an occurrence should depend on soil porosity, biomass content, nutrient quantities and characteristics; and physico-chemical conditions of the system. Consistent with the growth of biomass to fill intergranular pore spaces in soil should be the generation of cohesion among soil grains in ways that constrain the evaporation of moisture from the exposed soil while enhancing the resistance of the soil to desiccation stresses that produce dust.

In order to analyze soil textural characteristics and their possible alteration by the production of EPS, it is necessary to quantitatively scale the important textural parameters. By definition, the porosity of any given soil can be estimated by equation 15.

$$n = \frac{V_v}{V_b} \tag{15}$$

where n is porosity, V_v is the volume of voids in the soil (L^3), V_b is the bulk volume of soil (L^3). Upon the introduction of EPS of a known volume (V_{EPS}) (L^3) and density ρ_{EPS} (m/L^3) into a given soil of known volume V_s (L^3) and density ρ_s (m/L^3), only a fraction α

of the initial volume of void is occupied. The relevant relationship is shown in equation 16 and hypothetically illustrated in Figure 1.

$$V_{vt} = V_a + V_{eps} + [V_{int} + V_{epsin}] \quad (16)$$

where V_{vt} is the volume of voids (L^3) at time t, V_a is the volume of air in soil (L^3), V_{int} is the volume of intragranular pores (L^3), and V_{EPSin} (L^3) is the volume of EPS in the intergranular pores (L^3). A hypothetical representation of the relationships among these parameters is shown in Figure 1.

Specifically, the hypotheses of this research are;

1. The adhesion of the bacteria in soil will be enhanced through the production of the extracellular polysaccharide (EPS)
2. The production of the EPS in soil will increase the forces of cohesion between soil particles.
3. Increased soil cohesion will increase soil surface resistance to desiccation and hence, dust generation potential.

The objectives of this research include;

1. Generally, to investigate the effectiveness of EPS, produced by *Arthrobacter viscosus,* in the stabilization of different soils against dust generation.
2. To quantify and estimate the amount of EPS produced by *Arthrobacter viscosus* in both Haggstrom and soil media.
3. To establish a relationship between the amount of EPS produced in these media and amount of broth (with cells) added.
4. To determine the effectiveness of both direct application of extracted EPS and microbial broth concentrations in the stabilization of three different soils (silty

clay, sandy clay, and sandy silty clay) against dust generation.

5. To monitor changes in soil property such as effective porosity based on EPS produced *in situ*.
6. To quantify and compare the indices of soil resistance against dust generation achieved through EPS-CM application in these soils.
7. To empirically determine the effects of EPS-CM application on soil friability, deformation resistance index, coefficient of soil failure, and adhesion Gibbs energy.
8. To statistically determine the effect of different levels of EPS produced in Haggstrom media
9. To make recommendations on the implementation of soil stabilization projects involving the potential use of EPS.

2.2 Strength indices of soils

For any of the soils tested in this research, it is expected that the potential of dust formation in each soil will depend on the magnitude of soil strength indices such as cohesion and frictional resistance. For any of soil types that have been selected for this research, the relative magnitudes of increases or decreases in cohesion and frictional resistance following EPS amendment are indices of the resistance levels of the soils to stresses that cause dust generation from exposed ground surfaces. As shown in Figure 2, the summation of these strength indices over time will show the total strength in each soil as well.

2.3 Approach

The purpose of this research is to investigate the feasibility of using EPS,

produced by *Arthrobacter viscosus*, to stabilize soil against dust generation. The proposed method of achieving this objective is growing the microorganism with appropriate nutrients that will ensure maximum production of the EPS. By extracting and applying this EPS to different soil types and by growing the microorganism in the soil (to induce real-time EPS production), it is expected that the EPS will increase the moisture retention capacity of the soil, as well as the indices of soil resistance against stresses that generate dusts. Figure 4 illustrates this soil stabilization approach.

The application of EPS to different soil types will be carried out and based on this application, the stability of the soil will be tested through shear strength testing and dust generation potential. The objective of the experimental work in this research is to determine how much EPS is necessary to stabilize soil particles against dust generation, what microbial concentration yields the highest concentration of EPS, and what structural components of the EPS facilitate the soil stability. In the second phase of this research, *Arthrobacter viscosus* will be directly applied to the soil and supplied with the essential nutrients necessary for EPS production. The objective of this aspect of the research is to compare the soil stability against dust generation achieved through the application of the extracted EPS and that achieved by the direct production of EPS in soil by the inoculum.

2.4 Significant parameters

In order to develop a model that will be applied to future research projects involving the application of EPS in the stabilization of surface soils, the following will be evaluated,

a) Relationship between changes in soil porosity and volume of EPS.

b) Determining of the effect of EPS production on soil stability against

desiccation by scaling of liquid retention in EPS-amended soil under desiccation.

c) Determination of soil failure under stress based on Mohr's theory.

d) Determination of the effects of EPS-CM application on soil friability.

e) Determination of the effects of EPS-CM application deformation resistance index.

f) Determination of the effects of EPS-CM application coefficient of soil failure.

g) Relationship between amounts of EPS produced in Haggstrom media and empirically derived amounts of EPS.

h) Relationship between all soil strength parameters tested.

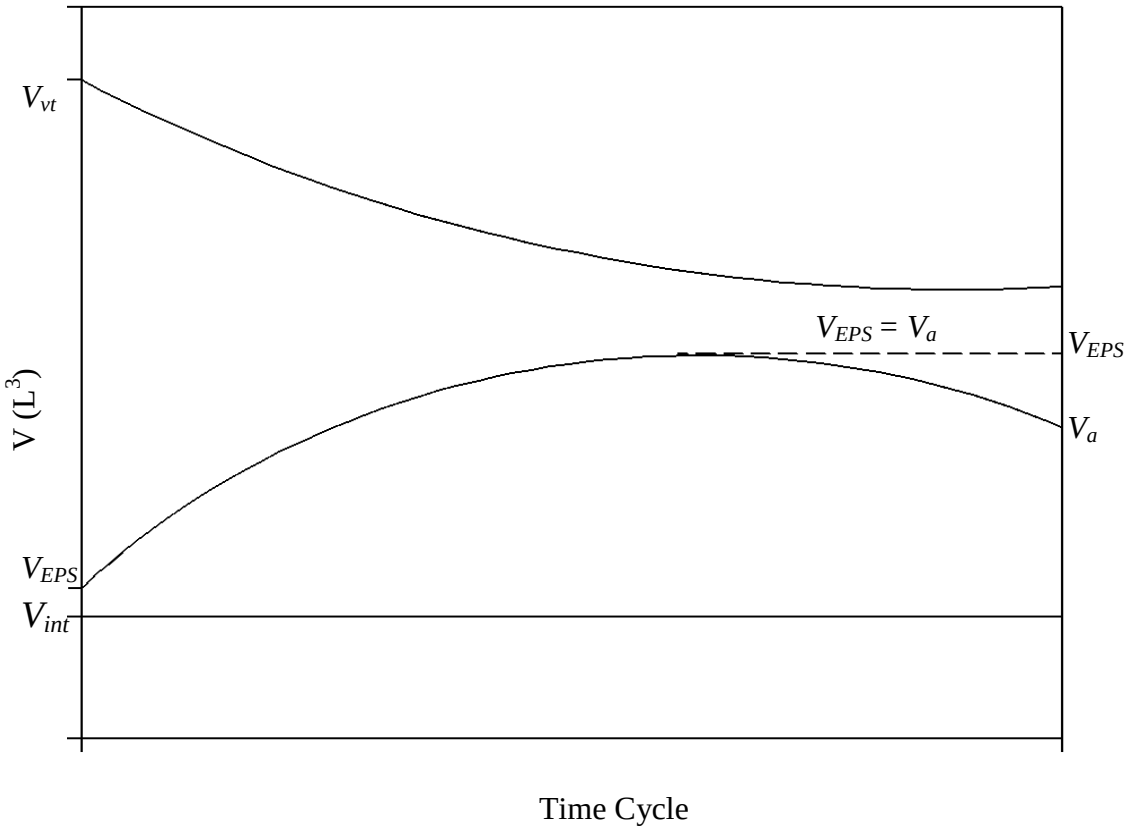

Figure 1: Hypothetical representation of changes in soil textural parameters in response to one cycle of bacterial growth and associated EPS content with time

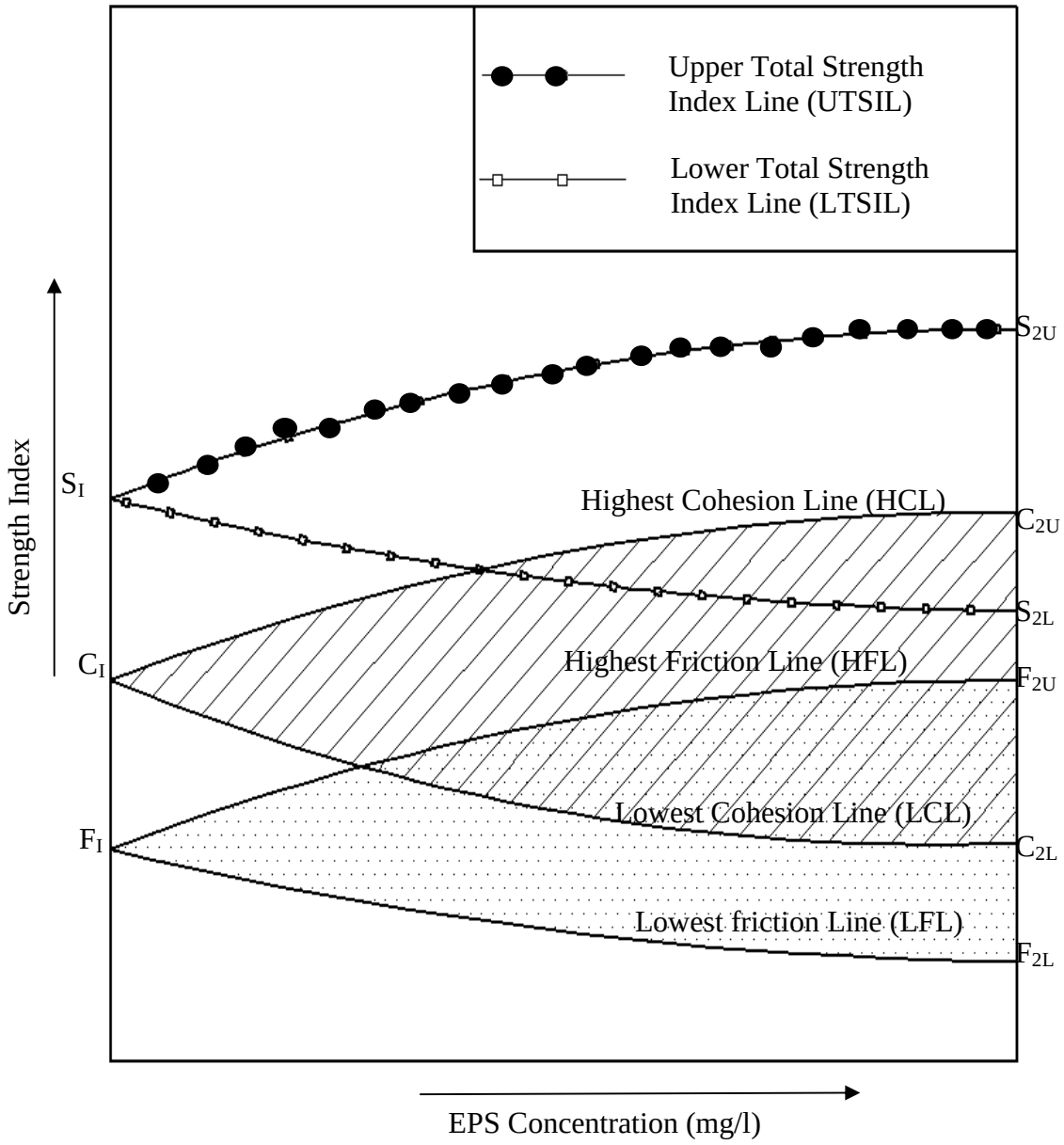

Figure 2: Hypothetical representation of relationship among significant soil strength parameters with time; S_I is the initial shear strength, C_I is the initial cohesion, F_I is the initial frictional resistance of the tested samples, S_{2U} is the final upper shear strength, C_{2U} is the final upper cohesion, S_{2L} is the final lower shear strength, F_{2U} is the final upper frictional resistance, C_{2L} is the final lower cohesion, and F_{2L} is final lower frictional resistance.

Figure 3: Illustration of the human health hazard of road dust generation on exposed soils (Inyang et al., 2006)

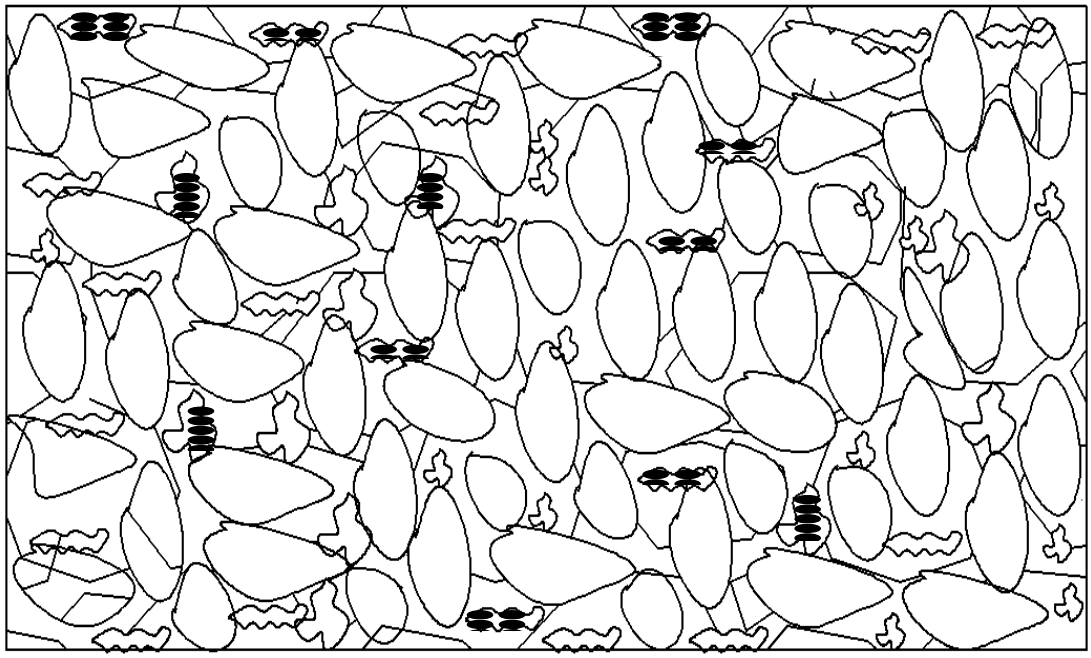

Figure 4: Schematic representation of cohesion development due to EPS impregnation of friable soils (EPS polymer molecules are exaggerated in size)

2.5 Relationship between changes in soil porosity and volume of EPS

Knowing that changes in EPS production will directly affect the porosity of soil, a relationship between soil parameters such as soil density, soil specific surface area, volume of voids, mass of soil, and the area of the soil can be derived starting from equation 17,

$$n_t = \frac{[V_a + V_{eps}]_t + V_{int} + V_{epsin}}{V_b} \tag{17}$$

where n_t is porosity at time t.

Knowing that for each material, the following relationships apply,

$$V_{eps} = \frac{M_{eps}}{\rho_{eps_b}} \tag{18}$$

$$V_{int} = \frac{M_s}{\rho_s} \tag{19}$$

Assuming that V_{int} and V_{epsin} are negligible, from equation 17,

$$n_t = \frac{V_{at} + \frac{M_{eps_t}}{\rho_{eps_b}}}{V_b} \tag{20}$$

where V_{at} is volume of air (L^3) in soil at time t (hr), M_{eps_t} is the mass of EPS (m) at time t, and ρ_{eps_b} is the bulk density of EPS (m/L^3). With the introduction of EPS in the soil, the initial porosity of the soil is expected to decrease with time therefore; an estimation of the effective porosity of the soil can then be estimated from equations 21 and 22,

$$n_{et} = n_i - \frac{\frac{M_{eps_t}}{\rho_{eps_b}}}{V_b} \tag{21}$$

Knowing $n_i = 1 - \frac{\rho_{bs_t}}{\rho_p}$ (22)

$$n_{et} = \left[1 - \left(\frac{\rho_{bs}}{\rho_p}\right)\right] - \left[\frac{\frac{M_{eps_t}}{\rho_{eps_b}}}{V_b}\right] \tag{23}$$

where n_{et} is effective porosity, ρ_{bs_t} is bulk density of soil at time t (m/L^3), and ρ_p is soil particle density (m/L^3). With ρ_{bs} calculated for different mass and volumes of samples used and ρ_p calculated from equation 24,

$$\rho_p = [x_1 * \rho_{\rho s}] + [x_2 * \rho_{eps}] \quad (24)$$

where x_1 is the mass of soil in sample (m), x_2 is mass of EPS in sample (m), and $\rho_{\rho s}$ is the effective soil particle density (m/L^3).

2.6 Determining of the effect of EPS production on soil stability against desiccation

One of the main factors behind soil cracking that will eventually lead to dust formation is a low liquid content. As earlier discussed in the introductory part of this research, soil cracking can also be induced by repeated intermittent stresses on the surface by vehicular activities, wind action, and other anthropogenic activities. Consistent with the direct or indirect introduction of EPS in the soil is the development of cohesion between the soil particles as a result of the caused by the sorption of the slimy EPS soil particles and the filling up of the intergranular spaces between the soil particles by EPS as well.

In order to analyze the strength characteristics of the soil in response to the introduction of EPS, it is necessary to quantitatively determine the shear strength and unconfined compressive strength. A relationship between these strength parameters and different types of soils is illustrated in Figure 5.

As a definition, the shear strength of soil is the maximum strength at which the soil deforms due to applied shear stress and soils generally deform by shear. The normal shear stress acting on the soil sample can be simply calculated from equation 25,

$$\tau_s = \frac{F_s}{A_s} \quad (25)$$

where τ_s is the nominal shear stress is applied to the soil (w/L^2), F_s is the shear force applied to the soil (w), and $A_s$is the initial area of the soil (L^2). For each soil type, represented by S_1, S_2, and S_3, the cohesion, frictional resistance, and shear strength can be determined. A diagrammatically representation of relationship expected between EPS concentration and effect on soil strength is shown in Figure 5.

From the determined deformation force *F*, a deformation index D_N can be estimated with the following equations based on EPS concentration and cohesion obtained in each soil,

$$D_N = \int_{C_0}^{C_f} [a \ ln \ M_{eps_t}] dC \tag{26}$$

or based on microbial broth concentrations and cohesion obtained in soil thus,

$$D_N = \int_{C_0}^{C_f} [a \ ln \ M_{b_t}] \ dC \tag{27}$$

By integrating equation 26 and 27,

$$D_N = a\left[C_f lnM_{eps_t} - C_f - C_o lnM_{eps_t} + C_o\right] \tag{28}$$

or

$$D_N = a\left[C_f lnM_{b_t} - C_f - C_o lnM_{b_t} + C_o\right] \tag{29}$$

where C_o and C_f are the least and final cohesion *C* (kN/m^2) respectively of soil sample before deformation occurs, M_{eps_t} is the initial concentration (mL/g of soil) of EPS at time *t* before final soil deformation, M_{b_t} is initial concentration of microbial broth at time *t* before final soil deformation, and *a* is the EPS production constant obtained from the equation of the line of EPS production based on time and microbial concentration.

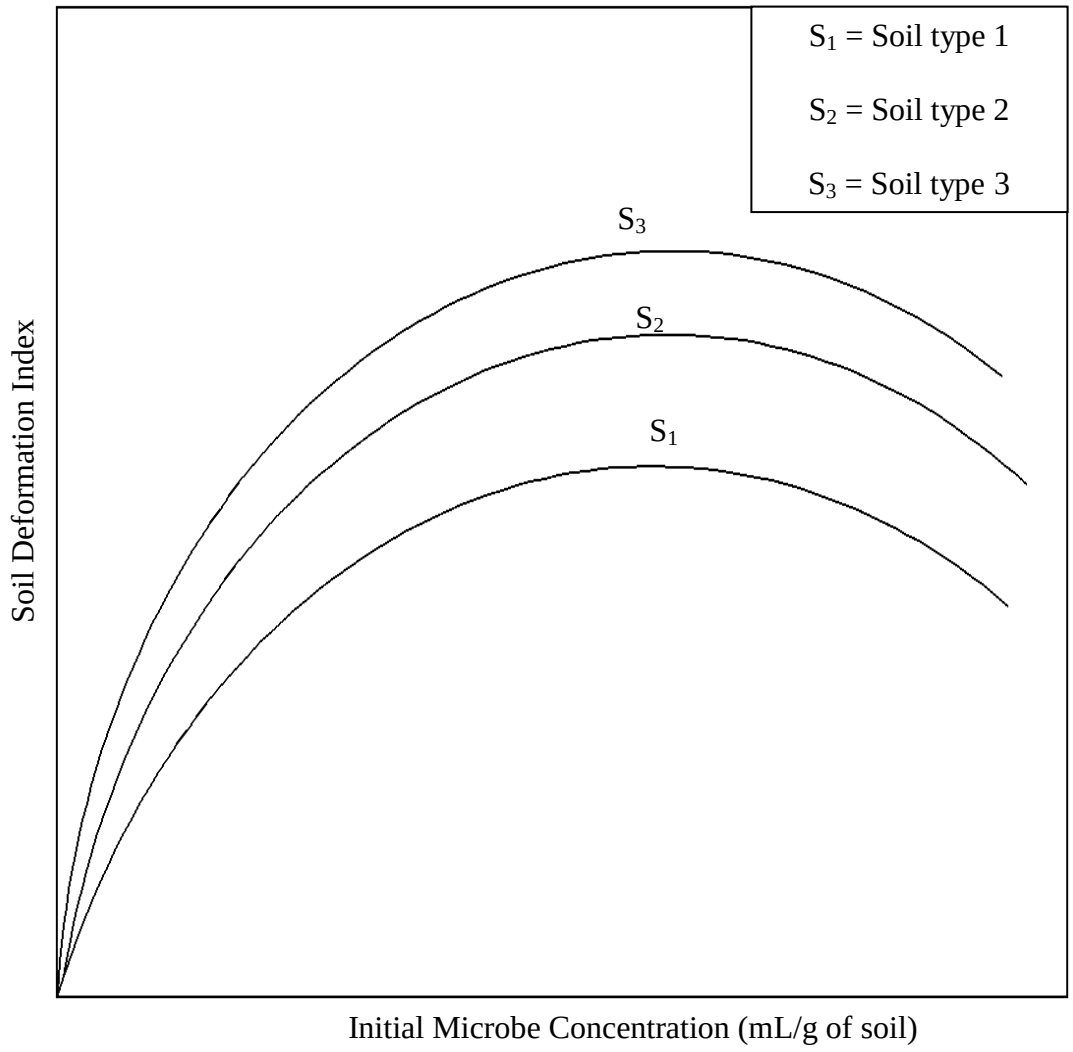

Figure 5: Hypothetical relationships between soil strength and EPS concentration

2.7 Mohr's theory of soil failure under stress

Following the Mohr's theory of soil failure under stress, the following equations can also be used to determine the effect of EPS adhesion on soil stability through cohesion;

$$\tau = Ce^{-\mu\theta M_{eps}} + \sigma tan\phi \quad (30)$$

Solving for μ (positive for clayey soils),

$$\frac{\tau - \sigma tan\phi}{C} = e^{-\mu\theta M_{eps}} \quad (31)$$

Taking log of both sides

$$ln\left[\frac{\tau - \sigma tan\phi}{C}\right] = lne^{-\mu\theta M_{eps}} \quad (32)$$

$$\mu = -\left[\frac{ln\left[\frac{\tau - \sigma tan\phi}{C}\right]}{\theta M_{eps}}\right] \quad (33)$$

where τ is the shear strength (kN/m^2), σ is the net normal stress (N), θ is the volumetric water content (m^{-3}), ϕ' is the effective angle of shearing resistance, C is a hypothetical maximum value of cohesion (when θ=0) (kN/m^2), and μ is a coefficient of failure in soil strength (μ>0 for clayey soils) (dimensionless). The determination of the failure pattern in these soils is based on the EPS amendments.

2.8 Determination of soil friability based on soil deformation values

Soil friability essentially indicates the potential of each soil type to disintegrate into various fragments and particles under stress therefore leading to dusting. This relationship is illustrated in Figure 6. According to Utomo and Dexter (1981), the

equation 34 can be used for the determination of aggregate size and aggregate strength as an index of friability,

$$\log Y = -k \log V + A \tag{34}$$

where A (kPa) is the estimated log strength of 1 m^3 soil and V (m^3) is the volume of the aggregate and k is the friability of the soil. For the purpose of this research and in terms of shear strength and cohesion of the soil, equation 34 can be modified thus,

$$logS_s = -\lambda logV + C \tag{35}$$

Solving for λ,

$$\lambda = -\left[\frac{logS_s + C}{\log V}\right] \tag{36}$$

since the shear strength of the soils are dependent on the initial microbial broth concentration (inducing EPS) in the soil, equation 37 can be applied to determine the friability index λ of each soil based on EPS-amendment, cohesion, and shear strength,

$$\lambda = -\left[\frac{logS_s + C}{\log V_b}\right] bM_{b_{eps}} \tag{37}$$

where S_s is the shear strength (kN/m^2) of the soil, C (kN/m^2) is the estimated cohesion of the soil, V_s (m^3) is the bulk volume of the soil, b is the EPS production constant in each soil at different microbial broth concentrations, and $M_{b_{eps}}$ is the initial microbial broth concentration (mL/g of soil). It is assumed that soil type 1 S_1 is more likely to generate dust due to its high friability index as is the case with silty clay soils; soil type 2 is less likely to generate dust compared to S_1 while soil type 3 S_3 is least likely to generate dust compared to S_1 and S_2. The expected relationship between the concentrations of EPS, M_{eps} added to a soil and the friability index is shown in Figure 6 and it is expected that EPS-amendment of these soils will reduce these friability indices. The models developed in this chapter are tested in chapter 8, and their results are discussed as well.

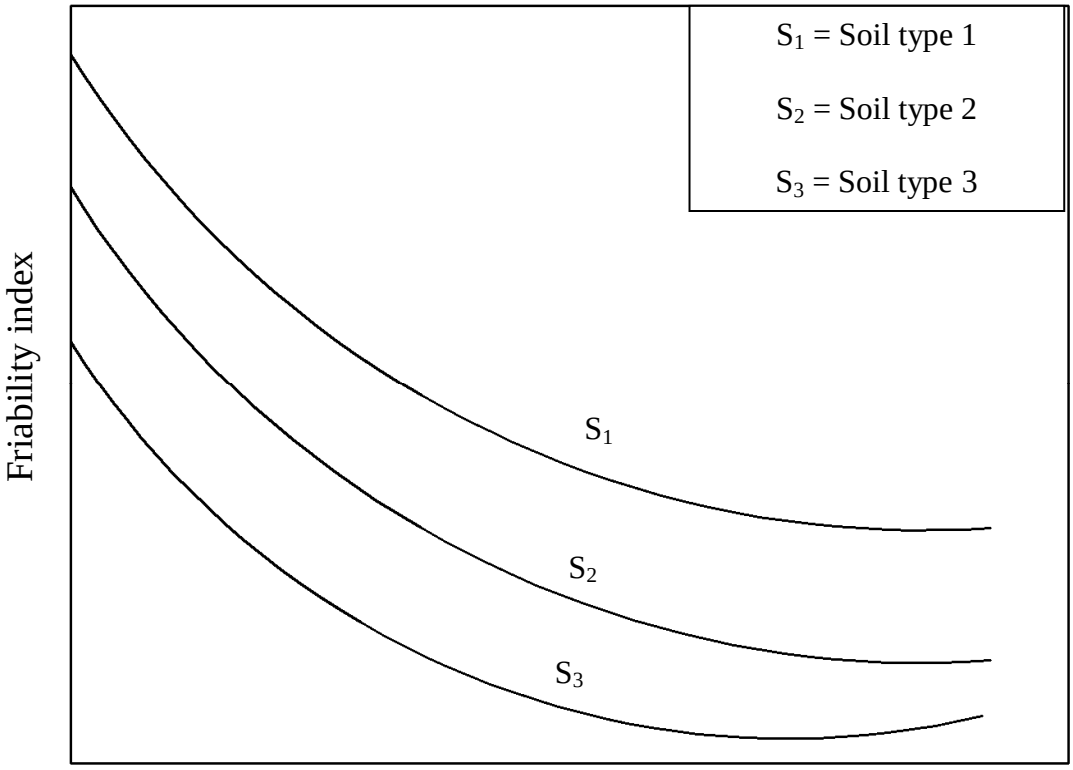

Figure 6: Hypothetical relationship between soil treatment with EPS and friability

CHAPTER 3: MICROBIAL GROWTH AND INTERACTIONS WITH SOIL

3.1 Introduction

3.1.1 Microbes in soil: quantification in soil and growth dynamics

Understanding the interactions between soil particles and microorganisms in soil is essential to prediction of the cohesion of soil particles. This cohesion results from microbial-mediated production of extracellular polysaccharides and can promote soil stability. Soil is made up many kinds of microorganisms but the predominant ones are bacteria, fungi, and actinomycetes. There are approximately 10^7 to 10^8 bacteria in 1g of soil and about 10 to 1000 bacteria per 1 cm^2 of soil particle surface (Miyazaki, 2006). Soil microorganisms occupy areas that are characterized by solid soil particles and the spatial arrangement of these soil particles result in the formation of a complex pattern of pore spaces. Water and/or air are trapped in these pore spaces in soil. Pore spaces are of different shapes and sizes, and are attractive habitats for microorganisms (Chenu and Stotzky, 2002). According to Mills and Powelson (1996), the soil environment is made up of both microbes living in an organic-and inorganic-containing broth and microbes living in a surface-rich environment with the surfaces coated with thin films of water.

3.1.2 Adhesion dynamics and effects on soil cohesion

An important phenomenon that is essential for the survival of microbes in soil is microbial adhesion to soil particles. Microbial adhesion has been described as the energy involved in the formation of the adhesive joint and can be measured in terms of the work

required to remove a microbial cell from a substratum to which it adheres (Rutter et al., 1984). The mechanisms of adhesion of microbial cells to soil particles have been discussed as well (Robb, 1984; Chenu and Stotzky, 2002; Mills and Powelson, 1996). It has also been noted that these mechanisms involve various interactions between the microbial cell surface and the soil particles. According to Chenu and Stotzky (2002), the interactions between soil particles and microorganism can be classified as both biotic and abiotic. The biotic interactions involve cell growth and multiplication, as well the secretion enzymes and biopolymers while the abiotic interactions involve physical interactions such as cohesion of soil matrix by microbial secreted polymers (Robb, 1984; Chenu and Stotzky, 2002). Such interactions include electrostatic and electrodynamic interactions, hydrophobic interactions, and the adhesion of polymers (Mills and Powelson, 1996). These direct surface interactions between the microorganisms and soil particles involve adhesion processes (Chenu and Stotzky, 2002).

Studies of microbial adhesion to soil particles have indicated that a number of factors affect the adhesiveness of microbes to soil surfaces (Deflaun et al., 1999; Mills and Powelson, 1996). These factors include cell surface charge, which affects the electrostatic interactions between microbial cells and substratum, hydrophobicity of microbial cells, and the secretion of extracellular polysaccharides by these microorganisms (Deflaun et al., 1999). While the existence and activity of microorganisms in subsurface and deep soils have been demonstrated by Balkwill and Boone (1997), Stevens and Holbert (1995), Kinkel et al. (1992), Mayer et al. (1999), Tunlid and White (1992), other studies have focused on various factors that influence the secretion of different exopolymers by microorganisms (Lopez et al. 2003; Park et al.,

2000; Jeanes et al., 1965; Bejar et al., 1998; and Ben-Hur, 2006; Blume et al., 2002). However, these studies have failed to discuss the effects of microbial biopolymer on the stabilization of different types of soil. To elucidate the interactions that determine microbial growth and effects in soil, bacterial adhesion, soil cohesion, and the relationship between bacterial adhesion and soil cohesion in different types of soil, it is therefore necessary to discuss the following topics, a) the influence of soil type and climatic factors on soil microbes, b) the population dynamics of microbes in soil, c) the influence of water and nutrient availability in soil on microbial survival, d) the effect of the production of extracellular polysaccharides by soil microbes. These are discussed in detail in the following sections.

3.2 Climatic and Soil Type Controls on Species of Microbes

Soil has a complex structure, and the range of living organisms including microorganisms, inhabiting soil varies extensively. For the purposes of this analysis, soil profile can be divided into three layers namely, upper layer where most weathering actions occur, middle layer which contains mainly fine soil particles and soluble substances washed in from above while the third (most inner layer) is an area with no weathering actions (Varnam and Evans, 2000; Paul and Clark, 1989; Paul and Clark, 1996; Miyazaki 2006). It has also been noted that humus-rich soil maintains a large population of microorganisms which enhances soil stability (Varnam and Evans, 2000).

In many regions, soil is subjected to periodic environmental changes such as dehydration due to drought and waterlogging from floods. According to Varnam and Evans (2000), the climatic factors that affect microorganisms in the environment include temperature, atmosphere, water availability, and light radiation. Most environments are

dominated by low temperatures and microorganisms that inhabit such areas are grouped as psychrotrophs (grow at low temperatures but at a maximum of 20^{o}C) and psychrophiles (grow at optimum temperature of 15^{o}C or lower).

Based on their ability to utilize atmospheric oxygen, microorganisms can be classified as aerobe or anaerobe. Aerobes utilize oxygen for their metabolic activities while anaerobes metabolize without oxygen. A few examples of aerobic organisms include *Pseudomonas* spp, *Neisseria* spp, and *Arthrobacter* spp (Levett, 1990; Loveland et al., 1994; Mosso et al., 1994). Other microbial groups such as micro-aerophiles exist which include those microorganism that are aerobic but can only survive under reduced concentrations of oxygen and facultative anaerobes are anaerobes that survive by the fermentation of carbohydrates, nitrate respiration, and dihydrolase pathway (Varnam and Evans, 2000). The production of EPS in soil requires oxygen availability therefore, it is important that the microorganism for this purpose be aerobic. This forms the basis of the selected microbe for this study. Other climatic factors such as the availability of water help microorganisms to balance their internal osmotic pressure in response to that of the surrounding environments while light radiation determines the concentration of ultraviolet and visible radiation that is available for the photosynthetic activity of both terrestrial and aquatic microorganisms. In contrast, the absence of atmospheric O_2 in the soil creates an anaerobic condition that permits the growth of anaerobes. Anaerobic microorganisms do not need oxygen to grow and such organisms have also been grouped as obligate anaerobes (Levett, 1990; Kourtev et al., 2006) and examples of such organisms include *Enterobacter* species and *Pantoea*. In between the aerobic and anaerobic microorganisms, two other groups of microorganisms exist. They have been

identified as facultative anaerobes and micro-aerophiles. Facultative anaerobes are organisms that can survive under both anaerobic and aerobic conditions and possess the ability to grow anaerobically by carbohydrate fermentation, while micro-aerophiles are aerobic microorganisms that can only grow in environments with lower oxygen concentrations (Varnam and Evans, 2000; Levett, 1990). A distinguishing factor between aerobic and anaerobic conditions in soil is the nature of the end-product of the microbial metabolic processes under each condition. Under an aerobic condition, carbon dioxide (CO_2) is produced as an end-product while methane (CH_4) is produced anaerobically (Hanson and Hanson, 1996; Dedysh, et al., 2000; Coles and Yavitt, 2004; Warren et al., 2005).

Various studies have been performed to determine the effects of climate and soil type on microbial population in soil. Working with two soil samples collected from Purdue University's Piney and O'Neil Agricultural Research Centers, Blume et al. (2002) studied the effect of soil depth and seasonal changes on the microbial biomass, metabolic activity, and community structure of microorganisms. The results of that study show that no changes occurred in microbial biomass as a result of soil depth and seasonal changes contrary to the expected result of the study. In contrast, a study by Grayston et al. (2001) to account for the variability of soil microbial communities of a temperate grassland ecosystem indicate that soil microbial biomass is influenced by the vegetation type (improved and unimproved grassland). It was also shown that depending on the sampling time, a change in phospholipids fatty acid analysis (PFLA) is indicative of the formation of more microbial biomass during winter. On another hand, the study by Blume et al. (2002) showed a strong relationship between temperature and microbial activity in soil

samples as microbial activity increased significantly during the summer period compared to winter at all soil depths. In their study, Sohlenuis and Bostrom (1999) also showed that a climatic change can influence soil factors such as soil temperature, soil water concentration, and nutrient availability. This in turn affects the microbial metabolic process as well the microbial biomass

Working at depths of 10 – 15 cm in different surface soils in New South Wales (NSW), Australia, Banu et al. (2004) studied the influence of various physicochemical properties and climatic zones on microbial biomass and microbial diversity of soil in NSW. According to these authors, microbial diversity and microbial community structure in soil samples is a function of the carbon and nitrogen concentrations and factors such as soil moisture concentration, total organic carbon, total nitrogen, and electrical conductivity can have a significant influence on both microbial diversity and microbial community structure. From their study, the authors also concluded that a relationship exists between gravimetric soil moisture, microbial diversity and microbial community structure.

By investigating the effect of soil properties on microbial activity across a 500 m elevation in a semi-arid environment, Smith et al. (2002) found that climatic changes can affect soil carbon (C) and nitrogen cycles. It was noted that changes in these cycles result in changes in annual precipitation, soil processes and microbial community structure of the area as well. Working at a the Arid Land Ecology (ALE) Reserve contained in the United States Department of Energy's Hanford Site in southeastern Washington State, the authors sampled different locations to determine the microbial biomass and the different biochemical processes in soil. They observed that changes in soil temperature and

precipitation affect the nutrient cycle of the areas as well as the microbial activity. They suggest that climatic change in the area affected the nitrogen cycle which in turn affected the shrub-steppe ecosystem as well as microbial population and activity (Smith et al., 2002). A similar study carried out by Acea et al. (2003) also reported that temperature differences in soils affect soil microorganisms as a result of changes in the C and N cycles. Other studies have also shown that bacterial diversity, population, distribution, and metabolic activity in soils are significantly affected by seasonal changes, large scale variation in soil temperature and moisture as well as soil depth (Papatheodorou et al., 2004; Waldrop and Firestone, 2006; Monokrousos et al., 2004; Fierer et al., 2003).

The result and conclusions that arise from all these studies show that climatic factors as well soil type, play important roles in the activities of microbial populations in different regions. To incorporate this fact into this present study, the temperature, moisture, and humidity of the different types of soil samples to be used for experiment will be controlled in order to improve the validity of expected results.

3.3 Population Dynamics of Microbes in Soils

Different molecular biology techniques have been applied to identify and quantify microbial population in different soils. The efficiencies of these techniques have been recently reviewed by Dubey et al (2006). Examples of these techniques are polymerase chain reaction (La Rosa et al., 2006; Nemergut et al., 2005), fluorescent in situ hybridization (Hill et al., 2000; Jjemba et al., 2000), and fluorescence-activated cell sorting (Park et al., 2005; Hansen et al., 2001),

The population dynamics of microbes in soil varies with differences in soil type, soil depth, elevation, and regional climate. According to Brockman and Murray (1997),

microbial populations exhibit different patterns of distribution in the soil such as randomness, clumping, uniformity, and various forms of regular spatial distributions. Microorganisms have been identified in terrestrial subsurface environments where they exist in pores or pore networks with different mineral or organic matter (Brockman and Murray, 1997). According to Varnam and Evans (2000), the growth and development of a diverse microbial population in soil is facilitated by the presence of a physicochemical gradient in the soil. A diverse microbial population promotes interactions between microorganisms and often leads to the formation of biofilms. This is essential for the long-term stability of the microbial population especially in the event of an environmental change. This can be attributed to the fact that a diverse microbial population is less affected by environmental change and can recover faster than ecosystems with a lower microbial diversity (Varnam and Evans, 2000). Barbhuiya et al. (2004) also noted that air temperature, soil temperature and light intensity are significant in studies involving undisturbed and disturbed forest soils.

The spatial distribution of microbial population in soil can be statistically determined by the use of variogram analysis. A variogram can be developed through the calculation of the average squared difference between all pairs of points separated by a given vector and the formula below is adapted from Brockman and Murray (1997) and is as follows:

$$\gamma(h) = \frac{1}{2} N(h) \Sigma \left[z(x_i) - z(x_i + h) \right]^2 \tag{38}$$

where $\gamma(h)$ is the estmated variogram value for the vector separation of h; z is the variable of interest (e.g., number of culturable aerobes at a sample point), x_i and $x_i + h$ are a pair of locations in the field approximately separated by the vector h, and N(h) is the number of

pairs approximately separated by that vector distance. In summarizing the population dynamics of microbes in soil, Varnam and Evans (2000) noted that the growth and distribution of microbial population in soil is organized either horizontally or vertically, depending on the direction of the physicochemical gradients. Thus, the oxygen gradient across small soil particles facilitates the growth of such microbes as aerobes, micro-aerophils, and anaerobes within close proximity to each other.

Different types of models have been developed for the study of microbial population dynamics. Bader (1982) has classified the models into segregated, distributed, structured, unstructured, deterministic, and stochastic models. The author also noted that the development of these models can be based on the following;

A. Quasichemical reactions that involve the reaction between the microbial biomass (x) and the growth substrate (*S*) expressed as

$$x + \alpha S \rightarrow 2x \tag{39}$$

This equation was also proposed by Williams (1985).

B. Differential equations that describe the quasichemical reaction expressed as

$$\frac{dx}{dt} = R_p + (x_f - \frac{x}{\theta}) \tag{40}$$

$$\frac{dS}{dt} = \alpha R_p + (S_f - \frac{S}{\theta}) \tag{41}$$

$$\text{and } \theta = \frac{V}{Q} \tag{42}$$

where V is the volume of the system, Q is the flow rate through system and Θ = V/Q describes the holding time of the system, R_p is the rate of production of biomass per unit volume of culture, and x_f and S_f are the concentrations of the biomass and substrate respectively.

C. Linearized Stability Analysis (LSA) which can be applied to determine the stability and dynamic behavior of a specific steady state in an analysis of the set of differential equations expressed as;

$$\frac{dV_i}{dt} = f_i(V_1, V_2 .....V_n) \tag{43}$$

where i = 1, 2, 3…..n.

Growth models for microbial populations in particular environments have also been developed by different authors. These growth models are also based on chemical reaction kinetics that involves the relationship between an increase of substrate concentrations and the rate of microbial growth (Bader 2000; Pickett, 2000). These chemical reaction kinetics include,

A. Blackman Kinetics (BK), which focuses on the specific growth rate of microorganisms in a given environment controlled by the substrate concentration. According to this model, growth is considered to be directly proportional to substrate concentration expressed as follows;

$$\frac{dx}{dt} = (\frac{\mu}{2}\frac{S_1}{K_1})x \quad \text{for } S_1 < 2K_1 \tag{44}$$

$$\frac{dx}{dt} = \mu x \quad \text{for } S_1 \geq 2K_1 \tag{45}$$

where μ is the maximum specific growth rate (hr^{-1}), S_1 is substrate concentration, and K_1 is the constant.

B. Monod Kinetics (MK) which focuses on the relationship between microbial growth rate, substrate concentration, and enzymatic kinetics expressed as,

$$\frac{dx}{dt} = (\frac{\mu S_1}{K_1 + S_1})x \tag{46}$$

C. Exponential Kinetics (EK) which combines the Blackman and Monod models and is expressed as,

$$\frac{dx}{dt} = (1 - \exp\left\{-0.6931\frac{S_1}{K_1}\right\})x \tag{47}$$

or

$$\frac{\mu^1}{\mu} = (1 - \exp\left\{-0.6931\frac{S_1}{K_1}\right\})x \tag{48}$$

where μ is the maximum specific growth rate (hr^{-1}), μ^1 is the actual specific growth rate at a particular concentration of substrate S_1, and K_1 is a constant.

The development of a growth model is a significant step in this current research because it is important for the quantification of the extracellular polysaccharide that is produced by the bacteria, *Arthrobabcter viscocus*. From the quantification, it is possible to show from the experiment, how the concentration of EPS produced affects the soil stabilization.

3.4 Nutrients, aerobic and anaerobic conditions

Based on their nutrient needs, microorganisms in the environment can be classified as oligotrophs and copiotrophs. Maloney et al. (1997) have studied the effect of soil nutrients on these two groups of microorganisms. Oligotrophs are characterized by a low growth rate, efficient substrate utilization, and accumulation of nutrients over a long period to enable multiplication while copiotrophs are characterized by their low substrate affinity at high nutrient levels and have high growth rate. Oligotrophs also possess adaptive measures, which can sustain them in the presence of low nutrients (Varnam and Evans, 2000; Koch, 2001; Maloney et al., 1997). As a general description of these two groups of microorganisms, Koch (2001) described oligotrophs as those microorganisms

that can survive chronic starvation conditions and are not able to persist in nutrient-rich environments. Examples include *Caulobacter crescentus* and *Arthrobacter* spp (the organism of interest in this research), *Cycloclasticus oligotrophus* RB1, *Rhodomicrobium vanneilii*. On the other hand, copiotrophs are those organisms that can only survive in nutrient-rich environments where they rapidly utilize available nutrients. Examples include with *Bacillus* spp, *Bacillus subtilis*, and *Escherichia coli*, and *Pseudomonas* spp (Giongo et. al., 2007; Peix et al., 2005). Most environments are made up of low levels of nutrients leading to the starvation of microorganisms which favors the persistence of oligotrophs. This assessment has been supported by the work of Williams (1985) and extensively discussed by Varnam and Evans (2000). The persistence of heterotrophs, microorganisms that require organic nutrients to survive in the environment, is controlled by the availability of carbon and low levels of inorganic phosphates may limit the development of microbial population as well (Peretyazhko and Sposito, 2005; Gyaneshwar et al., 2002).

The presence or absence of oxygen in a soil environment creates two different conditions that determine the group of microorganisms that can inhabit such soil. The presence of O_2 in the soil creates an aerobic condition which permits the existence of aerobes in such soil.

From the standpoint of this research, the first few centimeters of the ground surface that needs to be stabilized is porous to air from the atmosphere. It thus represents a largely aerobic condition. As earlier pointed out, a successful production EPS by soil microbe requires adequate oxygen availability. It is therefore important for the microorganism of interest in this research, *Arthrobacter viscosus*, to be supplied with

adequate concentration of O_2 under both laboratory and field experiments since it is an aerobe. This will ensure the growth of the microorganism that will facilitate optimum production of the EPS needed for the soil stability against dust generation.

Since the availability of nutrients in soil plays a significant role in soil microbial processes, several studies have been carried out to determine the effects of different nutrients and atmospheric CO_2, N_2, and O_2, and P on the microbial communities in soil. In their research performed to investigate the effects of carbon and nitrogen availability on the growth of soil microbial community in boreal forests, Ekblad and Nordgren (2002) applied sucrose from sugar cane, C_4-sucrose, and NH_4Cl to the organic layer of the soil. The authors monitored microbial activity in the soil for nine days and sampled the soil for evolved CO_2 from soil respiration. From the results of their study, it was shown that the growth of the microbial biomass in the soil was primarily limited by carbon rather than nitrogen. It was also reported that the C/N ratio in the organic matter of the microbial nutrient determined the growth limitation of the microbes either by carbon or nitrogen. The study concluded that despite the possibility of nitrogen limitation in the growth of soil microorganisms, the latter is largely dependent on the concentration of available carbon in the soil (Ekblad and Norgren, 2002).

Blagodatsky and Richter (1998) also carried out a similar study to investigate the relationship between microbial growth in soil and nitrogen turnover. They hypothesized that the efficiency of microbial biosynthesis and respiration is controlled by the ratio of nitrogen to carbon. By modifying the Monod's model for microbial growth, they were able to develop different models for microbial growth based on the ratio of carbon and nitrogen turnover. A summary of these models is presented in Table 1.

Table 1: Summary of models of microbial growth in soil as a function of carbon and nitrogen concentrations

Variable	Equation
Watersoluble substrate C_s, mg C (g soil)$^{-1}$	$C_s = C_b r.(-\frac{\mu(C_s)}{Y_s} + q(C_h).Y_r)$
Microbial biomass C_b, mg C (g soil)$^{-1}$	$C_b = C_b.r.(\mu(C_s) - a(C_s) - a_{max}.(1 - Y_r))$
CO_2 C_{CO2}, mg C (g soil)$^{-1}$	$C_{CO2} = C_b.r.(\mu(C_s).\frac{1-Y_s}{Y_s} + a_{max}(1 - Y_r) + q(C_h).(1 - Y_r)$
Insoluble organic C, mg C (g soil)$^{-1}$	$C_h = C_b.r.(a(C_s) - q(C_h)$
Insoluble N_i. mg C (g soil)$^{-1}$	$N_i = -\mu(N_i).C_b.r(nc_{max} - \frac{N_b}{C_b}) + q(C_h).N_h.C_b.r/C_r$
Microbial biomass N_b, mg C (g soil)$^{-1}$	$N_b = \mu(N_i).C_b.r\left(nc_{max} - \frac{N_b}{C_b}\right) - a(C_s).N_b.r$
Insoluble organic N_h , mg C (g soil)$^{-1}$	$N_h = a(C_s).N_b.r - q(C_h).N_h.C_b.r/C_h$

Source: Blagodatsky and Richter (1998)

where a is the specific death rate of the microorganism (d^{-1}), a_{max} is the maximal specific death rate of microbe (d^{-1}), C_h is the specific rate of organic matter decomposition (d^{-1}), Y_s is the efficiency of substrate uptake (dimensionless), Y_r is the efficiency of organic matter mineralization (dimensionless), r is the index of physiological state, q is the specific rate of decomposition (d^{-1}), μ is the specific rate of microbial, growth (d^{-1}), , and nc_{max} is the maximal N:C ratio in microbial biomass (dimensionless).

From the models developed from their study, Blagodatsky and Richter (1998) suggested that rates of microbial activities in soil, including microbial death and reutilization, depend on nitrogen to carbon (N-to-C), ratio as well as soil organic matter decomposition. The biological effects of mineral nitrogen fertilization on soil microorganisms have also been reviewed by Barabasz et al. (2002). According to these authors, soil microorganism are involved in biochemical transformations of mineral fertilizers in soil especially NPK fertilizers. They noted that soil microorganisms are

involved in the synthesis of biological elements such as amino acids, vitamins, antibiotics, and toxins as well as nitrogen fixation. Through their metabolic and enzymatic activities, these microorganisms are able to regulate and circulate different soil nutrients thereby making them available for uptake by plants (DeBoer et al. 1996; Nannipieri et al. 2003). According to Barabasz et al. (2002), some microorganisms, especially those belonging to the genera *Arthrobacter* and *Eubacter*, through a co-metabolic process, can breakdown nitrosamines to simple compounds and use them as nutrients. It was also noted that a high rate of mineral nitrogen fertilizers in soil will result in 50% growth retardation in microorganisms of the genera *Arthrobacter* and *Streptomyces* as well as completely eliminating *Azobacter, Rhizobium,* and *Bradyrhzobium* from the soil. This makes it necessary for the mineral nitrogen concentration of the experimental soil samples to be determined to ensure that it is will not negatively affect the growth of the microorganisms for this present research study.

A similar study by Galicia and Garcia-Oliva (2004) examined the effects of carbon, nitrogen, and phosphorus additions on soil microbial activity in a tropical seasonal pasture. Working in Chemela, located in the western part of Mexico, the authors sampled soils in the area during both dry season and rainy season (two dominant weather conditions in the area). The sampling for the dry season was carried out in April while that of the rainy season was done in September. Using ANOVA as a statistical tool, the results of the study showed that addition of C, N, and P had an effect on the microbial activity in the pasture comprised of plant species such as *Panicum maximum* and *Cordia elaeagnoides* in the dry season. Results of the soil sampling showed various concentrations of N, P, and C when different plants were used. These results show that

there is relationship between the soil microorganisms and the surrounding vegetation in terms of nutrient utilization and storage. In this present research study, it is anticipated that the application of nutrients to the soil to enhance the growth of the target microorganism will result in the growth of some plant species as well therefore; measures will be put in place to check such a situation. While this can be controlled in the laboratory work by sterilizing the soil, it will be difficult to control plant growth when the EPS is applied to the field therefore, we can only expect that the target microorganism persists in the soil despite such situations.

Other research studies that have shown the effects of nutrients on soil microorganisms include those involving the assimilation of CO_2 and nutrient transformation into soil organic matter (Miltner et al., 2004; Powlson, et al., 2001); the consumption of oxygen by soil microorganism as affected by the levels of CO_2 and O_2 in the soil (Sierra and Renault, 1995); and the response of soil microorganisms to the addition of C, N, and P in a forest zone (Joergensen and Scheu, 1999). It has also been reported that phosphate solubilizing bacteria from subtropical soil such as those belonging to the genus *Bacillus, Rhodococcus,* and *Arthrobacter* can convert insoluble forms of phosphorus to an available form that can be utilized for their growth and development as well plant growth (Chen et al., 2006).

3.5 Water Availability and Microbial Distribution in Soil

The availability of water is important for microbial growth since it controls the osmolarity of the environment surrounding the microorganism and fluctuations in the osmolarity of the environment will result in stress which affects the growth and survival of microorganisms (Varnam and Evans, 2000; Booth et al., 1990). Therefore, a positive

pressure difference between internal osmotic pressure and that of the environment is necessary for good microbial growth in soil as well. In addition to maintaining osmotic pressure, soil water affects the moisture available to microorganisms, the concentration and type of soluble minerals in soil, and the pH of the soil solution. It has also been reported that water influences the soil microorganisms through the effects of diffusion, mass flow, and concentration of nutrients. Therefore, under a condition of limited soil moisture, diffusion and mass flow of nutrients such as phosphorus is impaired (Paul and Clark, 1996). Osmolytes such as potassium are involved in maintaining turgor pressure as well. As osmolarity of the environment increases, potassium is taken up by the cell to maintain turgor by raising the intracellular osmotic pressure and vice versa. The importance of turgor pressure regulation is highlighted by the fact that it mediates synthesis or accumulation of compatible solutes, and it is also responsible for differential gene expression.

Many regional soils experience periodic dehydration for prolonged periods. Many microorganisms need to be drought-resistant to survive in such regions. Survival of soil microbes is generally impaired at the higher temperatures associated with dehydration. To survive in such environments, microorganisms such as bacteria produce endospores. Bacterial endospores are highly efficient in resisting both dehydration and high temperatures and based on this ability, endospore-forming bacteria are the most common microorganism found in such soils. Another important characteristic that enables microorganisms to survive in harsh environments is the production of biofilms. Biofilms are very important in protecting vegetative bacteria from dehydration and they can be formed on any surface exposed to microbes, which has sufficient water and nutrients to

promote growth (McArthur, 2006). The production of extracellular polymeric substances, which are major concentrations of biofilms, is induced by desiccation and this does not destroy the inherent water-binding properties of biofilms polymers. This makes it possible for the dried biofilms to act as a sponge, rapidly absorbing any moisture that becomes available (McArthur, 2006).

CHAPTER 4: SOIL CHARACTERISTICS AND THEORETICAL MODELS OF ADHESION DYNAMICS OF MICROBES AND EXTRACELLULAR POLYSACCHARIDES IN SOIL

4.1 Soil texture

The relative proportion of grain sizes and minerals in a soil constitute the soil texture. Different pore sizes in soil is as a result of different soil textures and when only one soil particle size is involved, pore size S_p (in diameter) is directly proportional to particle size P_s thus,

$$S_p = P_s \tag{49}$$

Based on their particle sizes, soils can be grouped into four classes namely, sand, loam, silt, and clay soils. Sandy soils do not form aggregates because they are single-grained and are mainly coars*e* textured, loamy soils are medium textured and contains are even mixture of sand, silt, and clay soils, silt soils are also medium textured and similar to loamy soil in terms of particle sizes and soil properties, while clay soils are fine textured and usually hardens when dry and very sticky when wet (Brown, 2003). These soil particles are arranged spatially in a way that gives them a complex and discontinuous pattern of pore spaces of various sizes and shapes that are filled with water or air, which forms the habitats of soil microorganisms.

According to Chenu and Stotzky (2002), the ratio of the surface area of the solid particles in soil to the volume of the liquid phase is high. Therefore, the surfaces of soil particles act as sinks for microbial metabolites (Chenu and Stotzky). Based on the

percentage composition of a mixture of these soil particles, other groups of soils can also be identified such as loamy sand, sandy loam, clay loam, silt loam, silty clay loam, silty clay, and sandy clay soils and each soil type has a unique property in terms of mineral composition, engineering and microbiological applications. As shown in Table 2, these different soil types comprise of different particles sizes.

Table 2: Particle sizes of the different classes of soil

Class of Soil	Particle size (diameter in mm)
Sand	0.10 – 2.00
Silt	0.05 – 0.002
Clay	< 0.002

Source: Brown (2003)

The dynamics of microbial adhesions and EPS production are different for each type of soil. This is due to available pores spaces between the soil particles in which microorganisms can grow and adhere to soil particles through the production EPS (main constituents of biofilms). The proportion of the pore spaces that is filled with water also determines the maximum concentration of microorganisms that can inhabit the spaces among the soil particles. According to Mills and Powelson (1996), in medium texture soils such as silt and loam with porosities between 0.25 and 0.60, the total space available for microbial habitation is approximately 25 - 60 mL/g. In these pore spaces, an interaction occurs between the bacterial cells and the soil particles, which enables them to remain attached to the particles. This direct surface interaction between the bacterial cells

and the soil particles has been termed, adhesion. The next section discusses the relevant aspect of this phenomenon in this present research study with a review of previous studies.

4.2 Adhesion dynamics and theory

Bacterial adhesion to solid particles is an important step in the soil stabilization. Studies have also shown a positive correlation between increased bacterial productions of biofilms to sediment stability (Yallop et al. 1993; Yallop et al. 2000; Paterson et al. 1991). The Derjaguin Landau Verwey Overbeek (DLVO) theory, developed for macromolecules and particles, is commonly used to describe the interactions between charged colloidal particles, solid surfaces and bacterial adhesion enhanced by exopolymers (Azeredo et al., 1999; Behrens, 1998). According to this theory, the two principal forces of attraction involved in these interactions are *Van der Waals* forces and electrostatic double-layer forces while other interactions such as ion bridging, steric interactions in the presence of polymer, and hydrophobic interactions in polar media also contribute to bacterial adhesion to solid particles (Oliveira, 1997; Hayashi et al., 2001; Sharma and Rao, 2003). To apply of the DLVO theory to bacterial adhesion studies, it is assumed that the interacting surfaces are smooth and have homogenous chemical properties. However, studies involving solid particles such as soil have shown that the DLVO interaction energy E_{DLVO} also applies to rough surfaces. As earlier noted, equations expressing this phenomenon, as well the aggregation of charged particles, have been developed (Bhattacharjee et al., 1998; Behrens et al., 1998).

The DLVO interaction energy between soil particle surfaces can also be calculated from the equation developed by Hayashi et al. (2001) and Bos et al. (1999), which can be modified to include other soil parameters thus,

$$V_{T(h)} = \varepsilon_0 \varepsilon_r a_b \left[\left(\psi_1 + \psi_2\right)^2 \log\left(1 + e^{-\kappa h}\right) + \left(\psi_1 + \psi_2\right)^2 \log\left(1 - e^{-\kappa h}\right) \right] - \frac{A}{6}\left[\frac{a_b}{h} + \frac{a_b}{h + 2a_b} + \log\left(\frac{h}{h + 2a_b} \right) \right] \quad (50)$$

where $V_{T(h)}$ is the total interaction energy, a_b is the cell radius, ψ_1 and ψ_2 are surface potentials of cell and solid respectively, *A* is the Hamaka constant as already given in equation 5, ε_0 is the permittivity of vacuum, and ε_r is the relative permittivity of the medium. It has been documented that the initial microbial adhesion to soil particles is reversible process, which can further develop over time to an irreversible interaction. The strength of these interactions is also based on the ability of the microorganism breakdown energy barriers involved in the interfacial energy of adhesion (Bos et al. 1999). Suffice it to say that the entire process of surface interactions between the soil particles and the microorganisms is based on the outer electrostatic charges of the EPS produced and the soil surface charge. This creates the need to discuss the excretion of polymeric substances by soil microorganisms as part of the processes involved in the adhesion dynamics of microbes to soil particles. As part of the objectives of this research study, more emphasis is placed on previous investigations involving the production of EPS by *Arthrobacter viscosus* with a brief discussion of other polymeric substances produced by different microorganisms.

4.3 Excretion of polymeric substances

The production of natural polymers by microorganisms has been studied as far back as the late 1960s and early 1970s, which focused mainly on their medical

significance as well as their application in the textile, cosmetic, pharmaceutical, and food industries (Lopez et al. 2003; van der Aa and Dufrene, 2002). Different areas involving the production of extracellular polymers by microorganisms that have received much attention in recent years are the aquatic environment, wastewater treatment facilities, and municipal landfill sites (de Brouwer and Stal, 2001; Hilger et al. 2000; Gorner et al. 2003; McSwain et al. 2005; Radic et al. 2005; Daniels and Cherukuri, 2005). Different parameters responsible for improving bonding mechanisms that enhance soil strength (cohesion) have been outlined to include cementation, electrostatic and electromagnetic attractions, and primary valence bonding and adhesion (Mitchell, 1976). In addition to acting as a physical bridge between soil particles, the production of EPS by soil bacteria can be correlated to the improvement of the electrostatic and electromagnetic attractions between soil particles therefore increasing soil cohesion as well.

Different microorganisms have been studied for their ability to produce exopolymers (Momeni, 2001; Gasdorf et al. 1965). The extraction and characterization of these exopolymers have also revealed that they are made of different carbon-based structures, which makes each of them unique in their physical and chemical properties. In a study focused on determining the EPS production ability of different strains of the species of *Halomonas eurihalina* isolated from saline soils and to characterize the EPS produced, Bejar et al. (1998) used different culture mediums to grow the microorganisms. Using thin layer and ion exchange chromatography, the authors determined the composition of the EPS, which showed that the EPS produced by the organism was composed of carbohydrates, proteins, uronic acids, amines, acetyls, and a significant concentration of sulfates. It was also observed that the EPS produced by the different

strains of the microorganisms differed in the concentration of each of those components, which gave them other unique properties such as gel forming at certain pH and high viscosity. It was concluded that such properties made the EPS attractive for industrial applications. A similar study was also carried out by Zinkevich et al. (1996), which involved the characterization of the EPS produced by sulfate-reducing bacteria isolated from marine environments in Alaska and off the coast of Indonesia. The results of this study also showed the effect of changes in environmental conditions on the ability of the microorganisms to produce EPS under unfavorable conditions. Such studies suggest that the production of EPS as the main component of biofilms produced by microorganisms is in response to harsh environmental conditions, which makes them withstand dehydration. Other microorganisms that have also been studied for their exopolymer production under unfavorable environmental conditions include *Pseudoalteromonas antarctica* (Maza et al. 199; Cocera et al. 2000), *Pseudomonas* spp. (Bueno and Garcia-Cruz, 2006; Priester et al. 2006), *Anabaena cylindrical* (Lama et al. 1996), Bacillus spp. (Gandhi et al. 1997), *Microcoleus vaginatus, Scytonema javanicum, Phormidium tenue,* and *Nostoc* sp. (Hu et al. 2003), *Rhodopseudomonas acidophila* (Sheng et al. 2005), and *Clostridium acetobutylicum* (Haggstrom and Forberg, 1986; Dennis and Turner, 1998; Daniels et al. 2005).

Focusing on the microorganism selected for this present research study, different species of *Arthrobacter* have been studied for their ability to produce natural polymers. Working with 34 soil samples collected from different parts of the United States including, Illinois, Indiana, New York, and Arizona; Ontario, Canada; and Central and South America, Gasdorf et al. (1965) were able to identify these *Arthrobacter* species.

The species identified include *Arthrobacter globiformis, Arthrobacter pascens, Arthrobacter aurescens, Arthrobacter citreus, Arthrobacter tumescens, Arthrobacter atrocyaneus, Arthrobacter simplex,* and *Arthrobacter ramosus*. In further studies to distinguish between two polymer-producing microorganisms isolated from soil samples in Guatemala and designated as NRRL B-1973 and NRRL B-1797, Gasdorf et al. (1965) cultured both organisms to produce extracellular polysaccharide. From the results of their study, the authors showed that both cultures produced large concentrations of the EPS and based on the similarities in their morphology and physiology, these organisms were grouped as a different species called, *Arthrobacter viscosus*. Lopez et al. (2003) also noted that the rate, quantity, and quality of the EPS produced by *A. viscosus* depend on the composition of the medium used and environmental parameters such as pH and temperature. The EPS produced by these bacteria is commonly polysaccharide in nature and occurs in two basic forms in soil, a) as capsule associated with cells surface and covalently bound, b) as slime loosely associated with the cells surface (Vandevivere and Baveye, 1992). Using EPS, these microorganisms form biofilms that enable them to establish a stable arrangement and function multicellularly as synergistic microconsortia (Flemming and Wingender, 2001) and these EPS contain high concentrations of negatively charged functional groups like -COOH, PO_4^-, SO_4^- (Wuertz et al. 2001). In order to utilize the EPS produced by these microorganisms in industrial and engineering applications, it is important to study their rheological behavior, which involves the determination of their shear rate and viscosity as well as the effects of temperature and salt concentration (Bodie et al. 1985; Lopez et al. 2003; Barbaro et al. 2001; Knutson et al. 1979; Pfiffner et al. 1986).

The production of these exopolymers in soil could affect hydraulic conductivity in saturated soil by increasing the viscosity of the percolating solution. This could also enhance cell adhesion and retention and increase the frictional resistance at the solid- liquid interfaces, which also decreases porosity in soil (Vandevivere and Baveye, 1992). Banu et al. (2006) also noted that these polymers are able to adhere to soil structure by their adhesion to soil minerals, and they do not penetrate soil aggregates but adhere mainly to their external surfaces. The exopolymer produced by these microorganisms can either be nonionic (not dependent on a surface-active anion for effect) or cationic (characterized by an active and especially surface-active cation). The interaction of nonionic polymers with the particles of a clay soil for example, is mainly through hydrogen bonds between the hydroxyl group (-OH) of the polymer and the silicate O_2 at the clay surface. This may also involve various dipole-dipole or charge-dipole interactions. Conversely, cationic polymers are adhered to the surface of the soil particles through interactions between the cationic groups of the polymer and the positively charged clay surface and these adhesions on soil surfaces is also associated with the molecular sizes and conformation of the soil particles (Banu et al. 2006).

Generally, the effectiveness of soil strength improvement by a polymer is related to its ability to enhance flocculation (or coagulation) of dispersed soil particles which can occur in 2 ways, a) electrostatic adhesion of polymer molecules on the soil particles which helps to neutralize the soil surface charge and b) bridging soil particles together when one polymer molecule adheres some soil particles together. The adhesion of these polymers to soil particles is also enhanced by the roughness of the soil surfaces (Banu et al. 2006; Chenu and Stotzky, 2002; Van der Aa and Dufrene, 2002).

Studies have also shown that the concentration of EPS produced by these microorganisms is dependent on both time and pH. From the graphical results obtained from a study by Torino et al. (2005) on the EPS production by *Lactobacillus helveticus* ATCC 15807, the relationship between the production of EPS, using glucose, galactose, and lactose as different energy sources, and time can be obtained through the use of the following equation,

$$Q_{eps} = \ln(kx) \tag{51}$$

or $$Q_{eps} = k\ln(k_1 x + k_2) \tag{52}$$

where Q_{eps} is the quantity of EPS produced (mg/l), x is the time (hrs), and k, k_1, k_2 are growth constants already determined from previous studies. It has also been shown that under laboratory investigations, approximately 85 ml/g of the EPS produced by these microorganisms occurs during the growth phase and involves the use of repeated pH-controlled batch cultures in order to increase biomass concentration thus, high EPS productivity (Bergmaier et al. 2003). In relating the concentration of biomass to the quantity of EPS produced as time dependent variables, the following equation can be developed based on the results obtained graphically,

$$Q_{eps} = ke^{at+\psi_1} + e^{at+\psi_2} \tag{53}$$

where Q_{eps} is the quantity of EPS produced (mg/l), k is a growth constant, a is the biomass concentration (g/l), t is the time (hrs), and ψ_1 and ψ_2 are surface charges of the soil and polymer respectively. In the application of EPS to improve soil strength by inoculating soils with the microorganism, equation 53 can also be expanded to include other soil parameters such as porosity *p*, temperature *T*, humidity *H*, bulk density ρ, and

particle sizes ε, pH, and the contact angle of the *Arthrobacter viscosus*, which has been determined to be 60^o (Loosdrecht et al. 1988). So the equation becomes

$$Q_{eps} = ke^{ax+\psi_1} + e^{ax+\psi_2} 60(p + \mathrm{T} + \mathrm{H} + \rho + \varepsilon + pH) \tag{54}$$

Similar studies by Velasco et al. (2006) reported that high EPS concentrations (4.1g l^{-1}) were obtained under high biomass concentrations as well and at controlled pH of 5.2. This led to the conclusion that EPS production continues in microbial culture media from the growth phase into the stationary phase.

In concluding this section, another important factor in the adherence of these bacterial cells to soil surfaces, which is facilitated by the EPS production, is the energy involved in the adhesion process. This energy is referred to as adhesion Gibbs energy of bacteria ($\Delta_{adh}G^{\sigma}$) can be calculated from the equation modified from Loosdrecht et al. (1988) and Volmer (1925) as follows,

$$e^{(\Delta_{adh}G^{\sigma}/RT)} = \frac{[\frac{A}{(1-A)}]exp[\frac{A}{(1-A)}]}{[\frac{X}{(1-X)}]} \tag{55}$$

Taking natural log of both sides of the equation and solving for $\Delta_{adh}G^{\sigma}$,

$$\Delta_{adh}G^{\sigma} = RT\left[ln\frac{[\frac{A}{(1-A)}]exp[\frac{A}{(1-A)}]}{[\frac{X}{(1-X)}]}\right] \tag{56}$$

where A is the area of the surface covered (m^2), X is the concentration of EPS added (mg/l), R is the gas constant, and T is the absolute temperature (K). This adhesion energy is critical in the improvement of soil strength against dust generation. This adherence also increases the forces of cohesion between the soil particles making it possible for the soil to withstand the effect of wind erosion.

4.4 The role of excreted polymer in soil cohesion against dusting

4.4.1 Defining soil cohesion

The cohesion of a soil has been defined as the existence of tensile or shear strength in the soil when it is tested in the absence of lateral load or effective stress being applied to it (Mitchell, 1976; Lambe, 1951). Studies have shown that soil cohesion changes with the moisture content of a soil therefore, the cohesive component in the shear strength of a soil can be determined in an unsaturated soil as a function of the moisture content (Matsushi and Matsukura, 2006; Lambe, 1951). To determine this relationship, a model has been proposed, which takes into account the angle of shearing resistance in the soil and the stress applied to a soil sample. According to Matsushi and Matsukur (2006) and Milligan and Houlsby (1984), such model can be presented as the following equation,

$$\tau = \sigma' \tan\phi' + Ce^{-\mu\theta} \tag{57}$$

$$\tau = C' + \sigma' \tan\phi' \tag{58}$$

where τ is the shear strength (kN/m^2), σ' is the net normal stress (N), θ is the volumetric water concentration (mL), ϕ' is the effective angle of shearing resistance, C is a hypothetical maximum value of cohesion (when θ =0) (kN/m^2),, and μ is a coefficient related to susceptibility of soil strength reduction (μ >0) (dimensionless).

It is also known that the production of EPS in soils increases the moisture retention capacity of a soil under desiccation and on rehydration (Chenu, 1993). With this in mind, it is also possible to determine the soil cohesion as a function of the quantity of EPS Q_{EPS} thus equations 57 and 58 can be empirically modified to reflect the following,

$$\tau = Ce^{-\mu Q_{eps}} + \sigma' \tan\phi' \tag{59}$$

For clay soils, μQ_{eps} become positive, thus equation 59 becomes

$$\tau = Ce^{\mu Q_{eps}} + \sigma' \tan \phi' \quad (60)$$

It has also been suggested that these parameters can be obtained by simple shear test and a subsequent regression analysis and provides an acceptable alternative for engineering applications.

As already noted the cohesion induced in soil through EPS production or application is achieved by electrostatic and electromagnetic. These electromagnetic attractions are due to van der Waals forces and can be a source of tensile strength and cohesion between closely packed soil particles of very small sizes (<1 μm) (Mitchell, 1976). It is important to note that cohesive forces exist between the matrices of microbial polymers (biofilms), which maintains their viscosity. This makes the polymers attractive for engineering applications as well (Chen and Stewart, 2002) and can be a factor in measuring the tensile strength of cohesive soils. The tensile strength of a soil indicates the concentration of tensile stress (axially directed pulling forces) that can be applied to it before it fails and this tensile stress can be in the form of a wind blowing over a soil surface (Mazeover et al. 2005). The two tests that have been developed to determine the tensile strength of a cohesive soil include shear tests and unconfined compression test. In a shear test, a shear failure is induced by a shear force applied along a predetermined horizontal surface while the unconfined compression test measures the compressive strength of a cohesive soil in a cylinder in the absence of a lateral support (Liu and Evett, 2000; Lambe, 1951; Horvath, 1973). To determine the shear strength of an unsaturated cohesive soil under stress and air and water pressure, two equation are commonly used, which are

$$\psi_f = c' + (\sigma_f - \mu_a)\tan\varphi' + (\mu_a - \mu_w)\tan\varphi^b \quad (61)$$

$$\psi_f = c' + (\sigma_f - \mu_a) + \chi(\mu_a - \mu_w)\tan\varphi' \quad (62)$$

Where c' is the cohesion intercept, σ_f is the normal stress at failure, μ_a is the air pressure, μ_w is the water pressure, φ' and φ^b are friction angles, and χ is the degree of soil saturation (Fredlund and Rahardjo, 1993; Bishop and Blight, 1963). Replacing soil saturation with the concentration of EPS and eliminating the effect of water pressure, equation 63 can be modified to determine the shear strength of surface soil against dust generation based on EPS concentration, Q_{eps} and air pressure (force of wind). This equation becomes,

$$\psi_f = c' + (\sigma_f - \mu_a) + Q_{eps}(\mu_a)\tan\varphi' \quad (64)$$

Another important aspect of determining the strength as well as the dust generating potential of surface soils is the testing of soil friability. Soil friability has been defined as the ability of reducing a mass of soil into smaller pieces or crumbles under an applied stress (Watts and Dexter, 1998; Utomo and Dexter, 1981). The testing of soil friability has been widely applied in determining soil tillage potential in agriculture and as a method of determining the organic carbon concentration of soil (Munkholm and Kay, 2002; Imhoff et al. 2002; Dexter, 2004; Utomo and Dexter, 1981; Watts and Dexter, 1998), and some of these research studies have also established a relationship between soil tensile strength and soil friability (Munkholm and Kay, 2002; Imhoff et al. 2002; Dexter, 2004; Utomo and Dexter, 1981). In this current research study, the testing of soil friability can be applied to determine the potential of an EPS amended and unamended cohesive soil to break down to smaller particles under a tensile stress applied by the force of a wind, which can lead to dust generation from surface soils.

According to Utomo and Dexter (1981), the index of friability, D of a soil aggregate can be obtained from,

$$\log Y_v = -\mathrm{D}\log V + S \tag{65}$$

where S (kPa) is the estimated log strength of 1 m^3 soil and V (m^3) is the volume of the aggregate and the aggregate strength value Y_v can be obtained from

$$Y_v = c\frac{P_f}{D^2} \tag{66}$$

where c is a constant with a value of 0.576 based on the assumption of spherical shape and elastic behavior of aggregates (Dexter, 1975), P_f is the polar force (N) needed to fracture the aggregate and D (m) is the mean aggregate diameter, which is obtained from

$$D = d\left(\frac{X}{\bar{X}}\right)^{\frac{1}{3}} \tag{67}$$

where d (mm) is the mean diameter constant of all aggregates in a batch (determined from the experiment), X is the mass (g) of an individual aggregate, and $\bar{X}$ is the mean mass (g) of the aggregates in the population (Dexter and Kroebergen, 1985).

In order to obtain a representative value of Y_v, which identifies the characteristics of each soil type to be used, equation 67 can be expanded to also include soil parameters such as porosity p, temperature T, humidity H, bulk density ρ, and particle sizes ε, pH, and the contact angle of the *Arthrobacter viscosus*, which has been determined to be 60^o (Loosdrecht et al. 1988). So the equation becomes,

$$Y_v = c\frac{P_f}{D^2}60(p + \mathrm{T} + \mathrm{H} + \rho + \varepsilon + pH) \tag{68}$$

Applying this equation to derive the soil friability index involves solving for Dthus,

$$e^{\log Y_v} = -\mathrm{D}e^{\log V} + S$$

$$\mathrm{D} = -\frac{c\frac{P_f}{D^2}60(p + \mathrm{T} + \mathrm{H} + \rho + \varepsilon + pH) - S}{V} \tag{69}$$

The determination of different soil friability values, *F* for different soil types can be used to establish a relationship between the concentrations of EPS, Q_{eps} added to a soil and the friability, F_X measured, which will involve an analysis using the following equation,

$$Q_{eps} = \ln(F_X) + C \tag{70}$$

where *C* is a constant.

4.5 Mohr circle representation of cohesion of soils

The shear strengths of geologic materials such as rocks and cohesive soils is mostly represented by the Mohr-Coulomb theory (Milligan and Houlsby, 1984; Kezdi and Horvath, 1973; Vesga and Vallejo, 2006; Favaretti, 1995; Ramamurthy, 2001; Palchik, 2006; Francois and Royer-Carfagni, 2005). The theory elucidates the response of materials such as soils to the effect of shear stress and normal stress and the resultant equation takes into account that soil deformation under any stress is controlled by friction between the soil particles and this occurs when the shear stress, τ in a cohesive soil exceeds a percentage of the effective normal stress, σ. The frictional resistance between soil particles has also been noted as the basic factor responsible for the strength of different soils (Mitchell, 1976). This relationship is represented in equation 71 and further expanded for cohesive soil by Milligan and Houlsby (1984).

$$\tau = \mu\sigma = \sigma tan\varphi \tag{71}$$

where μ is a constant for proportionality and φ is the angle of internal friction of the soil. The Mohr-Coulomb theory has been represented diagrammatically to define the shear strength of soils at different effective stresses as shown in Figure 7.

4.6 Test methods for soil cohesion

Different test methods for soil cohesion have been documented and one of these methods involves the use of a Cohesion Strength Meter (CSM), which measures the stability of soils and sediments through shear stress (Tolhurst et al. 1999; Yallop et al. 2000; Paterson, 1988; Paterson, 1989). In a majority of the literature sources consulted, it was observed that the major tests that can be applied to determine the magnitude of the

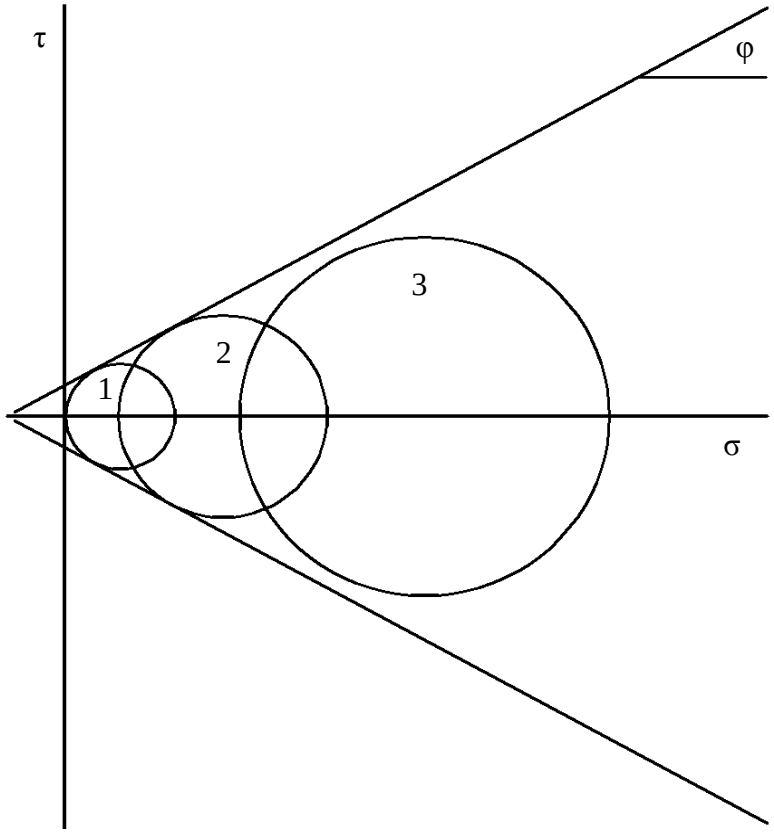

Figure 7: Mohr's circle of states of stress occurring at different points in a soil mass. τ = shear stress, φ = angle of internal friction of soil, σ = effective normal stress. Initial soil failure occurs when a circle first touches the line such as in circle1, circle 2 indicates a state of stress without an occurrence of failure, while circle 3 indicates a state of stress that will not occur due to prior failures.

cohesion in soils include, unconfined compressive strength test, triaxial compression test, and a direct shear test (Lambe, 1951; Liu and Evett, 2000; Milligan and Houlsby, 1984; Bonala and Reddi, 1999; Palchik, 2006; Ramamurthy, 2001; Kedzi and Horvath, 1973; Aly and Letey, 1989).

Other investigations have also shown that soil cohesion can be determined as a function of soil water concentration. Based on this criterion, soil cohesion have been determined through desiccation tests (Konrad and Ayad, 1996; Abu-Hejleh and Znidarcic, 1995; Bae et al. 2006), a combination of testing soil moisture concentration and shear test (Matsushi and Matsukura, 2006), a correlation of change in soil water volume and shear strength in unsaturated soil (Kim and Hwang, 2003), a determination of shrinkage stress in soil as a result of changes in pore water and vapor pressure (Karalis et al. 2003; Munkholm et al. 2002; Chertkov, 2005), and measuring the hydraulic conductivity of the soil (Dexter, 2004; Ben-Hur et al. 1990; Al-Shayea, 2001; Sivapullaiah et al. 2003).

Direct shear tests and unconfined compression tests are determinants of soil resistance against deformations and this can be correlated with dust formation from surface soils. In direct shear tests, soils are tested under consolidated drained conditions to determine the deformation of a soil sample at a controlled strain rate on a single shear plane (ASTM International, 2008). To give a description of the mechanics behind the direct shear test, a cylindrical or rectangular soil sample is encased in a box Subsequently, a normal force, *P*, applied to the top of the shear box followed by a shear force, *S*, which pushes the top of the box across the box. This causes the soil to soil sample to shear along the plane defined between the upper and bottom boxes (George et

al. 1964; Das, 1994; Holtz and Kovacs, 1982). Other equipment used in these tests involves the use of simple torsional vane shear device (Sibley and Yamane, 1966; Das, 1994; Holtz and Kovacs, 1982; Dunn et al. 1980).

It has been shown that changes in soil cohesion can be predicted through shear deformations based on moisture content of the tested soil sample. Working with two undisturbed residual soils obtained from natural hillslopes in Mt. Kanozan, Japan, Matsushi and Matsukura (2006) showed that the cohesive strength of an unsaturated soil can be estimated as an exponential function of the moisture concentration of the soil. This function was determined from the variables obtained from basic direct shear tests with subsequent regression analyses. Through direct shear tests, changes in soil particle and pore orientations during drained and undrained direct shear tests have been shown to be an indication of cohesiveness in sandy silt-clay soils (Cetin and Soylemez, 2003; Cetin, 1999). From the results obtained from working with artificially prepared natural clay soil samples collected from Adana basin and eastern Taurides, Turkey, Cetin and Soylemez (2003) showed that the orientation pattern of the soil particles and pores changed before and after shearing. These changes in orientation pattern, indicated by angles (0^o and 5^o) to the horizontal, were shown to be correlated with the failure plane of the soil. The study concluded that failure of the cohesive sandy silt-clay soils occurred at 15 ml/g shear deformation under undrained tests and 13-15 ml/g shear deformation under drained tests.

Other studies have used shear tests to determine shear behavior of carbonate sands under static and cyclic loading (Al-Douri and Poulos, 1992), to determine shear strength of geomembrane/cohesive soil interfaces in landfills (Fishman and Pal, 1994), to estimate *In Situ* soil strength and strength angle on shear-Normal gage (McNeill and Green, 2008),

to estimate changes in clay swelling and shear strength properties of different compacted soil specimens (Attom et al. 2001), to evaluate the shear strength of lime/fly ash slurry stabilized soil (Borden and Baez, 1991), to evaluate the performance deformation behavior of geosynthetic-reinforced soil structures (Ketchart and Wu, 2002), and to investigate the structural stability of a reinforcement-sand-clay system (Bo et al. 2006). Accurate interpretation of soil shear tests is pivotal to the conclusion of the failure surface of the soil sample therefore, the need to determine the cohesion and frictional angle of the soil (Kryzhanovskii et al. 1986; Cavallaro et al. 2004). The results presented in these studies are indications to the fact that direct shear tests can be used to determined the shear deformations in cohesive soil samples, which can be used as an indication of the level of resistance of such soils against dust generation.

Unconfined compression test is employed to determine the compressive strength of undisturbed, remolded, polymer stabilized, or treated cohesive soil samples using a strain-controlled application of axial load (ASTM International, 2008). The main purpose of this test is to determine the unconfined compressive strength (qu), which is then used to calculate the unconsolidated undrained shear strength of the cohesive soil under unconfined conditions (Hird and Chan, 2007; Matsuoka et al. 2002). . According to the ASTM standard, the unconfined compressive strength (qu) is defined as the compressive stress at which an unconfined cylindrical specimen of soil will fail in a simple compression test. In addition, in this test method, the unconfined compressive strength is taken as the maximum load attained per unit area, or the load per unit area at 15 ml/g axial strain, whichever occurs first during the performance of a test.

Studies have also shown that the unconfined compressive strengths of soil samples indicate potential resistance of such soils to deformations resulting from constant loading and unloading activities on top of the soil surface. The performance soil stabilization by polymers or other soil reinforcement products as well as residual unsaturated soils have been determined of unconfined compression tests (Iasbik et al. 2003; Nishimura and Fredlund, 2000). In an investigation to compare the unconfined compression strengths of silty soil and kaolin, Nishimura and Fredlund (2000) demonstrated a relationship between the soil-water characteristics and soil suction between the samples. From the results of the soil-water characteristic curve, it was concluded that the unconfined compressive strength of the samples increased with slightly with increasing suctions. The results of their study also indicated that the failure plane of the soil samples was horizontal in the residual state of unsaturation (Nishimura and Fredlund, 2000; Nishimura and Fredlund, 1999).

In a similar research study focused on determining the unconfined compression strength of soft aged clays, Ohta et al (1989) worked with clay sample collected 22 sites in Japan. By carrying out a stability analysis from results obtained from measurement of residual effective stress in undisturbed samples, they showed that unconfined compression strength analysis can be used to determine the factor of safety of using soft aged clay as materials in embankments and additives in stabilizing foundations (Ohta et al. 1989). The mixing of soft clay with stabilizing agents as a means of improving the engineering functionality of soils has been investigated by Hird and Chan (2007). Other investigations in this area have shown a relationship between tensile and compressive strengths of compacted soils using silty clay samples (Peters and Leavell, 1988), a

comparison between the microstructure, strength, and consolidation properties of Ariaka clay deposits obtained from samplers in Japan (Shogaki, 2005), a shear and interface strength of clay at very low effective stress (Pederson et al. 2003), and a measurement of soil layer strengths and stress-strain behavior of unsaturated soils using unconfined compression methods (Dawidowski et al. 2001; Matsuoka et al. 2002). Typical values of shear strength of cohesive soils are shown in Table 3.

Table 3: Typical values of shear strength of cohesive soil

Consistency of clay	Shear Strength (Half of Unconfined Compressive Strength) (lb/ft^2)
Very soft	<250
Soft	250-500
Medium	500-1,000
Stiff	1,000-2,000
Very stiff	2,000-4,000
Hard	>4,000

Source: Liu and Evett, 2003.

CHAPTER 5: MECHANISMS OF DUST GENERATIONS FROM EXPOSED SOILS

5.1 Introduction

Dust generation from exposed soils occurs mainly due to mechanical disturbance of the granular materials in the soil matrix. Such disturbance can occur in the form of pulverization and abrasive actions on the surface soil by wheels, tires, and blades of moving automobiles. Also, the dust particles can also entrapped by the turbulent action of winds over the exposed surface soil thereby mobilizing the particulates in air. Other activities on surface soils that can lead to dust emission include drilling and blasting, crushing, loading and unloading of finished goods (Young, 2006; Zobeck and Pelt, 2006; Singer et al. 2003). For a better understanding of the mechanics behind dust generation from both vehicular and wind actions, it is important to discuss some of the models developed from studies in these areas.

5.2 Models of vehicle-induced dust generation

Studies have been performed to investigate the problem of dust generation by vehicular traffic. In a study to show the transport pattern of vehicle-generated fugitive dust, Veranth et al. (2003) developed analytical models from a field study conducted at the Dugway Proving Ground, Tooele County, Utah. By creating a uniform dust cloud using a 1994 Ford pickup truck on a graded road, the authors were able to measure dust concentration using seven portable DustTrak analyzers with PM_{10} inlets. From the data collected in this study, horizontal flux of dust was developed as a product of the dust

concentration multiplied by the wind speed integrated from ground level to the top of the dust cloud (Veranth et al. 2003). Equation 72 shows the mass flux per length of road passing through a plane at constant distance from the road,

$$F_{dust} = \int_{z=\infty}^{z=\infty} \int_{t=0}^{t=t_{max}} C(x,z,t)u(x,z,t)\mathbf{d}t\mathrm{d}z \quad (72)$$

where C is the dust concentration (mg m^{-3}) and u (m s^{-1}) is the wind component perpendicular to the y, z plane, and t_{max} is the trip interval or other averaging time. A vertical dust concentration model was also developed to show a vertical change in dust concentration using a Gaussian distribution derived from Goossens (1985) as shown in equation 73,

$$C(z) = C_{\mathrm{ref}} \left(\frac{z}{z_{ref}}\right)^{-Q} \quad (73)$$

where C_{ref} is the dust concentration measured at height z_{ref} and Q is the fitting parameter.

Similar studies carried by Watson et al. (2001), who developed a TRAKER (vehicle-based method for measuring road dust emissions) to investigate a vehicle-based road dust emissions in Treasury Valley, Idaho, Chen et al. (1999), who used particle systems, computational fluid dynamics, and behavioral simulation techniques to simulate dust behavior in real time. The following equations show the mathematical models developed from these studies;

$$\theta = C_{C,S,T} * e^{-c_2 s} \quad (74)$$

where θ is the dust emission potential (g/vkt m/s^{-1}), $C_{C,S,T}$ is a constant that is specific to the county under study, setting (urban or rural), and time of the year (winter or summer), s is the traffic speed, and c_2 is a positive empirical constant (Watson et al. 2001).

$$\frac{P_h}{\rho_{air}} + gh + \frac{1}{2}V_h^2 = \frac{P0}{\rho_{air}} \quad (75)$$

Where p_h and V_h are the pressure (N/m^2) and velocity (m/s) at height h (m), and p_0 (N/m^2) is the pressure on the ground (Chen et al. 1999).

Different studies have been carried out to investigate the problem of wind-induced dust generation and numerical models have been developed from such studies as well. In a study conducted in the southern Great Plains of west Texas at the United States Department of Agriculture, Agriculture Research Service (USDA-ARS), Wind Erosion and Water Conservation Research Unit field station in Big Spring, Texas, Zobeck and Pelt (2006) demonstrated a detailed analysis on three dust storm dates (March 4, 18 and 27, 2003). Working with different saltation/creep samplers located at towers cited in relation to eroding open fields, these authors were able to monitor suspended dust using aerosol monitors mounted on the towers at heights of 2, 5, and 10 m. From results obtained at mean wind speeds of 2 ms^{-1} observed over a period of 240 to 395 min long, different flux equations were applied and modified to determine the horizontal mass flux at the soil surface. Equations 76, 77, and 78 show the derivation of the horizontal mass flux,

$$F_V = \frac{u^* k(C_b - C_t)}{ln\left(\frac{z_t}{z_b}\right)} \tag{76}$$

where F_V is the vertical flux (mg $m^{-2}min^{-1}$), u is the wind speed (ms^{-1}), k is von Karman's dimensionless constant (0.4), C_b and C_t are the concentrations (mg m^{-3}) of PM_{10} at the bottom of and top DustTraks respectively, and z_b and z_t are the heights of bottom and top DustTraks, respectively (Zobeck and Pelt, 2006; Kaimal and Finnigan, 1994).

$$F_h(z) = F_{z=0}\left(1 + \frac{z}{\beta}\right)^{-2} \tag{77}$$

$$F_h(z)^{-0.5} = F_{z=0}^{-0.5}\left(1 + \frac{z}{\beta}\right) \tag{78}$$

where $F_h(z)$ (mg $m^{-2}min^{-1}$) the horizontal mass flux at height z (m) is, $F_{z=0}$ is the horizontal mass flux at the soil surface ($kg \cdot m^{-2}/s$), and β is a scale height parameter (dimensionless).

Similar studies by Rice et al. (1996), who investigated wind erosion of crusted soil sediments using 12 m long wind tunnel with a cross-section area of 0.5 x 0.5 m, Singer et al. (2003), who assessed the PM_{10} and $PM_{2.5}$ dust generation potential of soils and sediments in the Southern Aral Sea Basin, Uzbekistan, and Miller and Woodbury (2003), who tested simple protocols to determine agricultural dust generation potentials from cattle feedlot soil and surface samples in 6000-head-capacity, open-air beef cattle feedlot at the USDA Agricultural Research Service, U.S. Meat Animal Research Center located in south-central Nebraska. These studies all show that wind action is a significant contributor to dust generation especially in exposed soil surfaces therefore the need to develop appropriate technologies to combat this problem. As part of the solution, use of dust suppressants has been suggested (Pulugurtha and James, 2006). There is a lack of research in the use of biopolymer as dust suppressants therefore the main focus of this present research study, which is investigating the use of extracellular polysaccharides produced by *Arthrobacter viscosus* to improve the strength of soils thereby effectively reducing the potential of dust generation from such soils due to failure and cracking.

CHAPTER 6: EXPRIMENTATION

6.1 Experiment Design

To determine the soil strengthening effects of the direct application of EPS and the injection of microbial broth to the three different soils used in this research (including silty clay, sandy clay, and sandy silty clay of different plasticities), the following three important tests were carried out,

a) Unconfined compression tests: these test were typically performed to determine unconfined compressive strength of the treated cohesive (based on their clay content) soil samples in the remolded condition using a strain-controlled application of the axial load of 5000 lbs. Since exposed surface soils are under unconfined conditions. The essence of this test was to numerically quantify the deformation index (derived in equation 29) for each soil type, this can be used as a measurement of potential dust formation from these soils under stresses from anthropogenic and natural activities.

b) Direct shear tests: these tests were typically performed to determine the shear strength of the EPS-amended cohesive soil samples using computerized direct shear equipment. These tests were performed at three different normal stresses of 34.47 kN/m^2 (5 psi), 68.95 kN/m^2 (10 psi), and 103.42 kN/m^2 (15 psi), in order to determine the cohesion C and angle of internal friction $Ø$ for each soil. Soils generally fail by shear and depending on the magnitude of this

failure, soils can disintegrate into particles under heavy stresses thereby facilitating the transportation of such particles by wind action as dusts. Therefore, the feasibility of dusting from soils can be estimated based on the level of cohesion and frictional resistance obtained from each EPS-amended soil sample was used in this research. These results of these tests will be used in chapter 8 to compute the coefficient of soil failure (from equation 33) and friability indices (from equation 37),

c) Liquid content tests (mini-desiccation tests): desiccation tests were performed to essentially quantify the amount of liquid remaining in each soil after a certain period of time. For the purpose of this research, liquid content determination was performed at a relative humidity of 36 % and temperature of 37 ^{o}C for 72 hours in an oven. The reason behind these tests is that dusting occurs mostly in dry fine-grained soils such as silty clay soils therefore, a reduction in the rate of liquid loss from such soils as a result of EPS treatment is significant whereas increased liquid loss increases the chances of dusting.

Generally, the initial focus of the experimental design in this research was on monitoring the growth pattern of *Arthrobacter viscosus* in Haggstrom and sterilized soil media, the quantification of the EPS produced by the microorganism in both media, and the characterization of the soil for accurate interpretation and explanation of observed interactions between *Arthrobacter viscosus*, EPS, and the soil. A specialized method of soil sterilization through gamma irradiation was performed in collaboration with the Radiation Science & Engineering Center at Penn State University, University Park, PA. All other experiments and analyses were carried out using laboratory equipment available

at the Global Institute of Energy and Environmental Systems (GIEES), geotechnical and geoenvironmental laboratories at the Department of Civil and Environmental Engineering, and other laboratories at the University of North Carolina, Charlotte, USA.

To ensure reproducibility of the results obtained from this study, tests were performed in triplicate as indicated in Table 4. To determine the appropriate concentrations of the EPS and microbial broth to be used in the field test simulation using a sandbox, various pilot tests were carried out at the initial stage of this study. With the stated objective of this research being investigation of the soil stabilization capacity of EPS produced by the microorganism, *Arthrobacter viscosus*, it was necessary to determine its growth pattern in both liquid and solid media therefore, the test performed with Haggstrom media and sterilized soil. Since the successful growth of this microorganism in both liquid and solid media correlates with its ability to produce EPS, it was also necessary to determine the concentration the EPS produced within a 14 day interval. This formed the basis for the EPS quantification tests, which involved measuring the dry weight of the EPS produced at each 24 hour period in the 14 day interval.

Further experiments were performed to investigate the relationships among the aqueous concentration of EPS, microbial broth and the sorption of EPS molecules on various mixed fractions of the silty clay soil. These tests were performed at five different concentration levels of the EPS solution and microbial broth with the whole silty clay soil (SCSoil) and its two selected mixed fractions; sandy silty clay soil (SSCSoil) and sandy clay soil (SDCSoil). The sorption tests also allowed the determination of the concentration of EPS produced in the soil by the microorganisms, especially in the test

involving the direct application of microbial broth to the soil to initiate *in situ* EPS production.

As an indirect method of determining the stability of EPS treated soil against potential failures that can result in dust generation, geotechnical tests involving direct shear and unconfined compressive strength determinations, were performed to analyze the behavior of the soil samples under both shear stress and normal stress respectively. These tests were also performed in triplicate and at three different loads to determine the cohesion and angles of internal friction of the soil samples. This experimental design also allowed the appraisal of the changes in the moisture concentration of the different soil mixes as manifestations of their interactions with the aqueous EPS solution and microbial broth of different concentrations. It was assumed that more moisture will be retained in soil samples with more EPS concentration, added directly or produced *in situ* by the microbe in broth. It was also assumed that increase in cohesion will be achieved in soils with more EPS concentrations as a result of increased resistance to desiccation and failures under stress with time. To evaluate these assumptions, soil samples were desiccated after the geotechnical tests and the distribution of the EPS molecules in the desiccated soil samples were examined using fluorescence microscopy. The overall design of the experiments performed in this study is shown in Table 4.

6. 2 Materials and their sources

6.2.1 Microorganism and culture conditions

A strain of *Arthrobacter viscosus* ATCC® 19584, which produces a viscous extracellular polysaccharide (Figure 19), was obtained from the American Type Culture Collection, Manassas, VA. To initiate the process of growing the microorganism in the laboratory for the production of extracellular polysaccharides, two main media were initially prepared following appropriate protocols on the product label namely, Difco™ nutrient broth (8 g/l) and Difco™ yeast mold agar (41 g/l) obtained from ATCC.

The frozen microbial pellet was initially rehydrated using 1.0 ml of yeast mold broth pipetted from a 6 ml solution of the broth, which was obtained from ATCC as well. Following the recommendations of ATCC, the rehydrated *Arthrobacter viscosus* was then grown on yeast mold agar (YMA) plates at 28 ^{o}C and incubated for 72 hours in complete darkness. At the end of the 72 hour period, the plates were maintained at 4 ^{o}C until used. To maintain good viability of the microorganisms and their ability to produce extracellular polysaccharides, they were transferred once every two weeks to new YMA plates. As a proactive measure to an eventual death or loss of the microorganisms growing in the plates, microbial cells growing in the yeast mold broth were harvested, lyophilized, and stored at -80^{o}C.

6.2.2 Preparation of growth medium

A Haggstrom liquid growth medium was prepared, which consists of 1.0 g/l peptone, 1.0 g/l yeast extract, 0.1 g/l NH_4Cl, 0.6 g/l Na_2HPO_4, 0.4 g/l KH_2PO_4, 0.2 g/l $MgSO_4.7H_2O$. The medium also contained trace elements of 0.036 µM $FeSO_4.7H_2O$, 0.097 µM H_3BO_3, 0.017 µM $CoCl_2.6H_2O$, 0.08 µM $CuSO_4.5H_2O$, 0.019 µM $MnSO_4.H_2O$, and 0.008 µM $ZnSO_4.7H_2O$. The medium was then brought to a pH of 8.5 with 10 N KOH and sterilized using autoclave at 121 ^{o}C for 20 mins. The medium was prepared in two parts: the first part contained all the necessary components for the medium except the carbon source, and the second part contained the carbon source added after autoclaving. The carbon source, glucose, was added at a final concentration of 3.0% (wt/vol.).

6.2.3 Inoculum preparation

Nutrient broth medium was prepared at 8 g/l, and actively growing cells of *Arthrobacter viscosus* from a YMA plate were inoculated into a 500 ml pre-sterilized glass flask containing 300 ml of the broth. The liquid cultures were incubated for 72 hours in a Barnstead Lab-line incubator-shaker model Max^{Q}4000.

Table 4: Experiment Design for this Research

MICROBIAL GRWOTH IN NUTRIENT MEDIA	MICROBIAL GROWTH IN STERILE SOIL	BATCH EPS PRODUCTION BY MICROBE IN STERILE SOIL					SOIL MIXES	SOIL CHARACTERISTICS TEST				BIOKINETIC PROCESSES AND INTERACTIONS				FIELD SIMULATION WITH SANDBOXES AND SOIL TREATMENT			SOIL STRENGTH DETERMINATION						FM IMAGING		
																			DIRECT SHEAR TEST			UNCONFINED		DESICCATION TESTS			
1	1	20 mL/g Microbe	40% Microbe	60% Microbe	80% Microbe	100 mL/mL Microbe	SOIL MIXES	Grain Size Distribution Test	Moisture Concentration Determination	Atterberg Limits	FM	EPS Concentration	Microbial Concentration	DI water (Control)	Batch Sorption with TGA	SCSoil HZDRES/01	SDCSoil HZDRES/02	SSCSoil HZDRES/03	SCSoil	SDCSoil	SSCSoil	SCSoil	SDCSoil	SSCSoil	SCSoil	SDCSoil	SSCSoil
																									EPS Concentration	Microbial Concentration	DI water (Control)
																			3 x 15 x 3			42 x 3					
	Soil Sterilization by Gamma Irradiation	3	3	3	3	3	SCSoil	1	1	1	1	C_0	MC_0	WC_0	3	5	5	5	42			135			3	3	3
												C_1	MC_1	WC_1	3												
												C_2	MC_2	WC_2	3												
												C_3	MC_3	WC_3	3												
												C_4	MC_4	WC_4	3												
												C_5	MC_5	WC_5	3												
		3	3	3	3	3	SDCSoil	1	1	1	1	C_0	MC_0	WC_0	3	5	5	5	42			135			3	3	3
												C_1	MC_1	WC_1	3												
												C_2	MC_2	WC_2	3												
												C_3	MC_3	WC_3	3												
												C_4	MC_4	WC_4	3												
												C_5	MC_5	WC_5	3												
		3	3	3	3	3	SSCSoil	1	1	1	1	C_0	MC_0	WC_0	3	5	5	5	42			135			3	3	3
												C_1	MC_1	WC_1	3												
												C_2	MC_2	WC_2	3												
												C_3	MC_3	WC_3	3												
												C_4	MC_4	WC_4	3												
												C_5	MC_5	WC_5	3												

Note:

Silty Clay Soil is denoted by SCSoil
Sandy Clay Soil is denoted by SDCSoil
Silty Sandy Clay Soil is denoted by SSCSoil
Fluorescence Microscopy is denoted by FM
Extracellular Polysaccharide is denoted by EPS

C_0 = Deionized water
C_1 = 5 ml/g soil EPS Concentration
C_2 = 10 mL/g soil EPS Concentration
C_3 = 15 ml/g soil EPS Concentration
C_4 = 20 mL/g soil EPS Concentration
C_5 = 25 mL/g soil EPS Concentration

MC_0 = Deionized water
MC_1 = 5 ml/g soil Microbe Concentration
MC_2 = 10 mL/g soil Microbe Concentration
MC_3 = 15 ml/g soil Microbe Concentration
MC_4 = 20 mL/g soil Microbe Concentration
MC_5 = 25 mL/g soil Microbe Concentration

WC_0 = Water content
WC_1 = 5 % soil Water Content
WC_2 = 10 % soil Water Content
WC_3 = 15 % soil Water Content
WC_4 = 20 % soil Water Content
WC_5 = 25 % soil Water Content

After the incubation period, different volumes of the liquid cultures were used to inoculate different volumes of the Haggstrom medium to investigate the production rate of extracellular polysaccharides by the microorganisms.

6.2.4 Growth determination for microorganism in liquid media

An actively growing colony from the YMA plate was placed into 100 ml nutrient broth and incubated in the shaker at 150 rpm for 24 hours. After the 24 hour period, 10 µl of the incubated broth was withdrawn and transferred into a newly sterilized 100 ml nutrient broth and incubated on a shaker as well. The cell density of the sample was determined from the optical density at 650 nm (OD_{650}) using a spectrophotometer. The OD readings were compared with a control sample to determine the growth curve of the microorganism over a 16 hour period.

6.3 Batch EPS production

Experiments in shaker flasks to monitor the production rate of EPS by different volumes of the liquid culture containing the microorganisms were conducted in 500 ml conical flasks containing 300 ml Haggstrom and inoculated nutrient broth medium. The different volumes, in ml, of the inoculated nutrient broth medium that were used include 20, 40, 60, 80, 100, 120, 140, 160, 180, and 200. The final solutions in the shaker flasks were made up to 300 ml with the Haggstrom medium. The flasks were capped with perforated aluminum foil, which permits passive aeration, and incubated at 28 ^{o}C at a shaking speed of 150 rpm in darkness for 14 days in the Barnstead Lab-line incubator-shaker model Max^{Q}4000, shown in Figure 8. In order to check the reproducibility of the experimental results, all batch productions of EPS were repeated at three times.

(a)

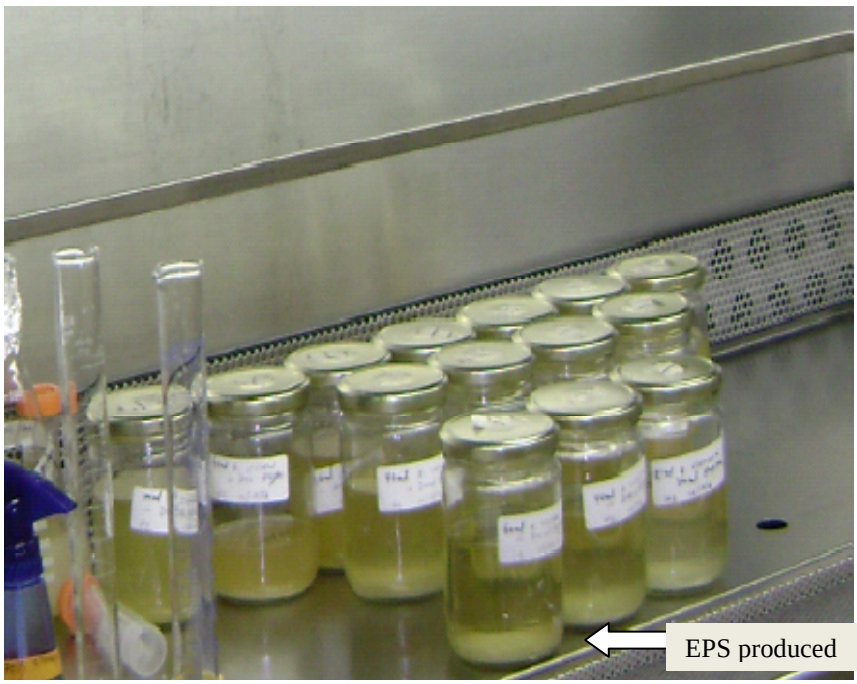

(b)

Figure 8: (a) Incubator-shaker with EPS production media (b) EPS produced in Haggstrom

6.4 Analytical Method: EPS extraction

During the batch production of EPS, 10 ml samples were withdrawn from the 300 ml Haggstrom/nutrient broth liquid samples at 24 hr intervals using sterilized polystyrene pipettes. All the withdrawn samples were centrifuged immediately to separate cells from the liquid medium. Samples were centrifuged at 15,000 rpm, for 60 mins at 4 ^{o}C to destroy and precipitate any suspended cells as well the produced EPS. To determine the concentration of EPS production occurring in each shaker flask, the precipitated EPS was lyophilized after the decantation of the supernatant. After a 24 hour period, the produced EPS with the suspended bacterial cells was quantified by dry-weight determination.

6.5 Thermogravimetric Analyses (TGA) of EPS

Thermogravimetric analysis (TGA) is a procedure that measures the amount and rate of change in the mass of a heated sample based on time and temperature under a controlled environment. These measurements were used to determine the thermal and oxidative stability of the biopolymer as well as its composition. In summary, TGA measurements are used for the following measurements: a) compositional analysis of multi-component materials or blends, b) thermal stabilities, c) oxidative stabilities, d) product life estimation, e) decomposition kinetics of materials, f) effects of reactive atmospheres on materials, g) filler concentration of materials, and h) moisture and volatiles concentration (Sichina, 2008).

To determine the thermal stability of the EPS produced in the Haggstrom/nutrient broth medium by the microorganism, the EPS produced from the different volumes of microbial broth in the batch production was analyzed using the TGA. In order to check the reproducibility of the TGA results, all TGA analyses of EPS were repeated at three

times. As shown in Figure 13, the TA instrument Q500 thermal analyzer used in this study recorded the thermographs with ultra purified nitrogen gas and air as the carrier gas. EPS samples produced from the batch production tests were freeze-dried at high pressure overnight and placed in platinum pans for the TGA analyses. The temperature of TGA was increased from ambient to 900 ^{o}C at a heating rate of 20 ^{o}C per minute. Using the Universal Analysis software, analyses of the plots of weight (%) versus temperature (^{o}C) were performed.

6.6 Soil sample collection and characterization

The soil sample used for this research study was collected at a road construction site on the intersection between East Stonewall Street and South College Street in downtown Charlotte, NC. The ongoing construction to expand these roads was intended to accommodate the future increase in traffic due to the construction of the NASCAR Hall of Fame near South College Street in Charlotte. In order to obtain a good representation of soil sample within this area, samples were collected at different locations on the road construction site using plastic containers and thoroughly mixed onsite. Under this condition, the samples were subsequently transported to the laboratory as disturbed specimens.

Prior to the treatment of the soil samples and the tests for their shear strengths and unconfined compression strengths, the following standard tests for soil characterization were performed:

i) Grain-size characterization of the soil samples using both mechanical and hydrometer analyses,

j) Determination of the liquid limits of the soil samples,

k) Determination of the plastic limits and plasticity indices of the soil samples,

l) Determination of the specific gravity of the soil samples, and

m) Determination of the moisture concentration of soil samples using the conventional oven method.

The standard test method for the grain-size analysis of the soil samples was performed following ASTM D422, the determination of the liquid limit, plastic limit, and plasticity index of the samples (Atterberg limits) were performed following ASTM 4318, the specific gravity of the sample were determined following ASTM D854, and the determination of the moisture concentration of the samples performed following ASTM D2216.

6.7 Preparation of different soil mixes

For the purpose of this experiment, it was important to prepare three different soil mixes from the different soil particle sizes determined through sieving of the samples. Sieve analysis was carried out following ASTM 422, which separated the soil sample into a series of fractions. Soil fractions passing to sieve No. 40 were collected as sand while soil fractions passing to sieve No. 200 were collected as clay and silt with clay samples collected in the pan. Subsequently, soil mixes including silty clay soil (SCSoil), designated as HZDRES/01, sandy clay soil (SDCSoil), designated as HZDRES/02 and sandy silty clay (SSCSoil), designated as HZDRES/03 were prepared at ratios of 3:1, 3:1, 1:1:1 respectively. In terms of percentage compositions of the soil samples, silty clay soil contained 65 % silt, 21.5 % clay, and 13.5 % loam; sandy clay soil contained 65 % sand, 21.5 % clay, and 13.5 % loam; sandy silty clay contained 30 % silt, 30 % sand, 30 %

clay, and 10 % loam. As a safety measure against the inhalation of an excessive concentration of dust generated during this procedure, adequate respirators and eye goggles were used for protection. Table 5 shows the different classification of fine-grained soils as used in this research and Figure 9 shows the specific classification of the soil used in this research based on plasticity index and liquid limit.

Further determination of the Atterberg limits of these different soil mixes was carried out for proper classification using ASTM D 2487 as standard for soil classification for engineering purposes. Table 5 and Figure 6 show the criteria that were used to classify these soil types.

6.8 Measurement of specific surface area

Using a Beckman Coulter SA 3100 equipment that is available in GIEES laboratory at UNCC, the specific surface areas of the soil samples were measured. Prior to the loading of the three different soil samples into the sample tubes, the weight of each empty sample tube was measured and labeled according to the soil types. Subsequently, 3 g of each soil type was poured into the sample tubes and the weight of each soil containing tube was measured as well. Sample tubes were loaded into the port and outgassed for 240 minutes at a temperature of 300 ^{o}C. Upon the completion of the outgassing process, samples were weighed again and loaded back into the port for analysis using the COULTER SA-VIEW^{TM} Software. In this analysis, liquid nitrogen was used as the carrying gas regulated at 12 psig. The BET surface area analyses for the three different soils were in the range of 8 and 8.4 m^2/g. These tests were carried out in triplicates and data points were computed as mean values.

6.9 Soil sterilization

In order to monitor the growth of the microorganisms in soil samples along with the rate of EPS production in the absence of other competing microorganisms in the soil, soil samples were sterilized using gamma irradiation. Soil sterilization was performed at the Radiation Science & Engineering Center at Penn State University. This sterilization method was used in order to preserve the nutrient status of the soil sample while eliminating any other microorganisms present in the sample.

6.10 Determination of the microbial growth rate using batch tests

To determine the growth pattern of the microorganisms in soil, an overnight culture of nutrient broth containing *Arthrobacter viscosus* was used to inoculate the soil samples. In performing these tests, 50 g of each soil mix was poured into a 50 ml centrifuge tube and 10 ml of the nutrient broth was added to the soil samples. To monitor the microbial growth rate, samples were collected from different depths of the tube within a 16 hour period. The collected samples were diluted 6-fold using Phosphate buffered saline (PBS). The diluted samples were subsequently cultured on YMA plates for 24 hours and from the counting of the visible colonies (multiplying by the number of dilutions), the microbial growth rate in soil were determined.

6.11 Batch tests determination of the concentration of EPS produced in sterilized soil

To determine the EPS production rate in the sterilized samples, an overnight culture of nutrient broth containing *Arthrobacter viscosus* was used to inoculate the soil samples at different concentrations to determine the optimum volume needed for maximum EPS production. In carrying out these tests, 50 g of each soil mix was poured into a 50 ml centrifuge tube and 10 ml of the nutrient broth was added to the soil samples.

To monitor the EPS production rate, samples were collected from different depths of the tube in between a 24 hour period. The collected samples were subsequently analyzed using the TGA.

6.12 Construction of sandboxes for soil tests

As shown in Figure 10a and 10b, the sandboxes used for this study were constructed in the using an external dimension of 15.24 cm (6") by 7.62 cm (3") and internal dimensions of 6.451 am (2.54") by 6.451 cm (2.54"). Three different sandboxes were constructed using the following guidelines: the internal compartments contained three sections for each treatment divided into 15 subsections for replicate treatments giving a total of 45 compartments for each sandbox. The materials used for the construction of the sandboxes include 5.08 cm (2") by 10.16 cm (4") wood, fiber glass sheets, acrylic sheets, fiber glass resin, screws, nails, and other miscellaneous hardware.

6.13 Soil sample introduction into the sandboxes

For the purpose of this experiment, it was predetermined that the depth of surface soil on which dust generation mainly occurs is up to 10 cm. To simulate this depth in the sandboxes, 500 g was poured into each subcompartment and mixed. The whole set up was agitated to ensure proper settling of the soil samples and leveling of the top layer of the soil, simulating what can be obtained in the field. As a safety measure against the inhalation of an excessive concentration of dust generated during this procedure, adequate respirators and eye goggles were used for protection as well. A trowel was used to turn the soil to ensure proper mix. To ensure proper aeration and material homogeneity, the samples were allowed to stand for 24 hours before treatments were applied.

Table 5: Soil classification chart for fine-grained soils

Criteria for Assigning Group Symbols and Group Names Using Laboratory Tests		Soil Classification Group Symbol	Group Name
Fine-grained soils: 50% or more passing the No. 200 sieve			
Silt and Clays inorganic	PI > 7 and plots on or above "A" line	CL	Lean clay [K, L, M]
	PI < 4 or plots below "A" line	ML	Silt [K, L, M]
Liquid limit less than 50 organic	Liquid limit – oven dried / Liquid limit – not dried < 0.75	OL	Organic Clay [K, L, M,N] / Organic silt [K, L, M, O]
Silt and Clays inorganic	PI plots on or above "A" line	CH	Fat clay [K, L, M]
	PI plots below "A" line	MH	Elastic Silt [K, L, M]
Liquid limit 50 or more organic	Liquid limit – oven dried / Liquid limit – not dried < 0.75	OH	Organic Clay [K,L, M,N] / Organic silt [K, L, M, Q]

Note:
[K] if soils contain 15 to 20 % plus No. 200, add "with sand" or "with gravel as necessary.
[L] if soil contains ≥ 30 % plus No. 200, predominantly sand, add, "sand" to group name.
[M] if soil contains ≥ 30 % plus No. 200, predominantly gravel add, "gravelly" to group name.
[N] PI ≥ 4 and plots on or above "A" line.
[O] PI < 4 and plots below "A" line.
[P] PI plots on or above "A" line.
[Q] PI plots below "A" line.

Source: ASTM International, 2008

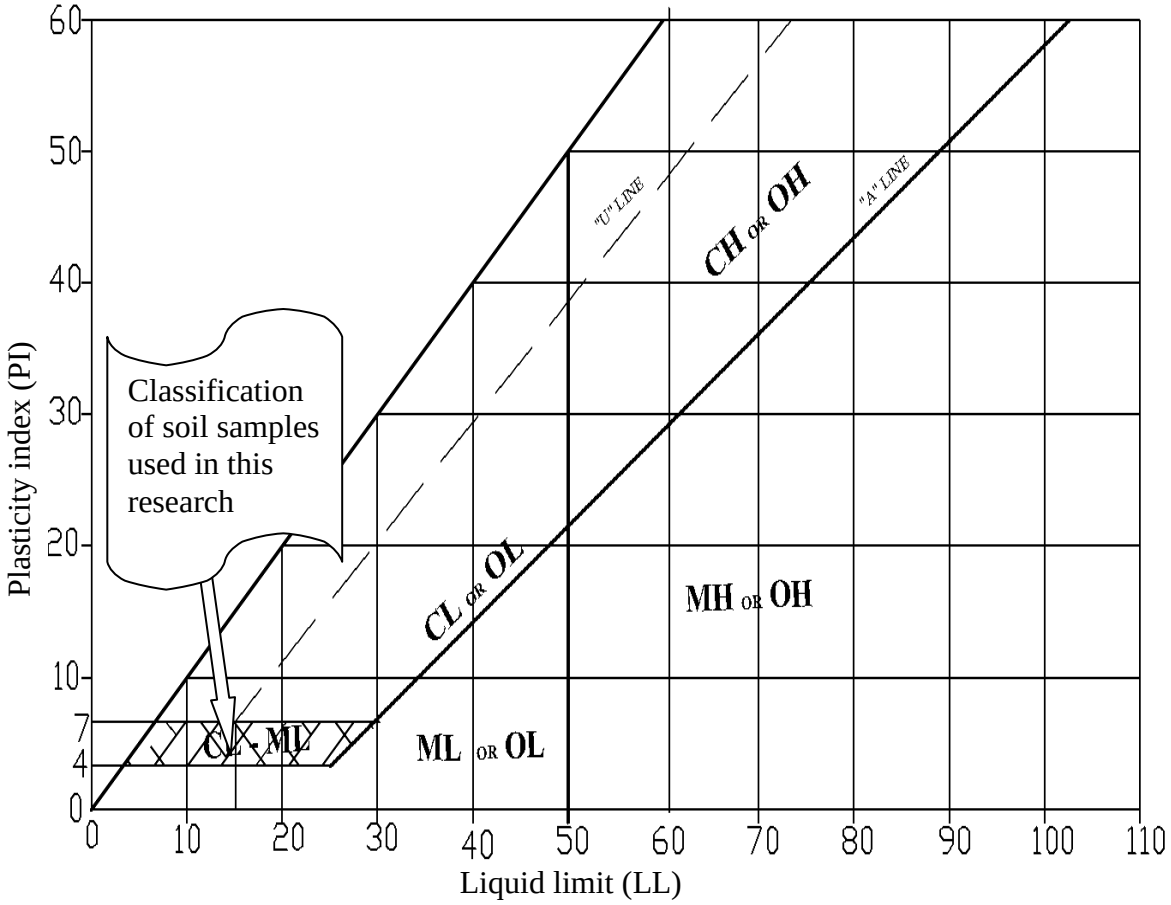

Figure 9: Plasticity Chart: for classification of fine-grained soil and fine-grained fraction of coarse-grained soils (ASTM International, 2008)

Figure 10a: Soil samples in sandboxes for different treatments

Figure 10b: Sandboxes with different soils before treatments

6.14 Treatment of soil samples in sandboxes (field treatment simulation)

A total of 75 sub-compartments measuring 5.161 cm (2.032") by 5.161 cm (2.032") and 9.906 cm (3.9") deep were used for each of the soil sample mixes; silty-clay soil, sandy-clay soil, and silty-sandy-clay soil (raw mix). Treatment of soil samples in the sandboxes involved the application of three the stabilizing materials used in this research. In terms of factorial analysis, the experimental set up consisted of two factors: three treatments (Extracellular polysaccharide-Culture Media (EPS-CM), Microbial broth with cells, and DI water). Five replicates were prepared for each treatment, and treatment with water was used as a control. In summary, 225 sub-compartments containing soil sample mixes were treated.

The first treatment involved a direct application of different concentrations of extracted EPS to achieve different moisture concentrations in the samples. The summary of the set up is as follows:

- 2.5 liters of EPS in 500 g of soil for 5 mL/g EPS-CM soil treatment
- 5 liters of EPS in 500 g of soil for 10 mL/g EPS-CM soil treatment
- 7.5 liters of EPS in 500 g of soil for 15 mL/g EPS-CM soil treatment
- 10 liters of EPS in 500 g of soil for 20 mL/g EPS-CM soil treatment
- 12.5 liters of EPS in 500 g of soil for 25 mL/g EPS-CM soil treatment

The second treatment involved the application of different concentrations of microbial broth (containing *Arthrobacter viscosus*) to achieve different moisture concentrations in the samples. This treatment was set up to indirectly monitor *In situ* production of EPS by the microorganism in soil. The summary of the set up is as follows:

- 2.5 liters of microbial broth with cells in 500 g of soil for 5 mL/g soil treatment
- 5 liters of microbial broth with cells in 500 g of soil for 10 mL/g soil treatment
- 7.5 liters of microbial broth with cells in 500 g of soil for 15 mL/g soil treatment
- 10 liters of microbial broth with cells in 500 g of soil for 20 mL/g soil treatment
- 12.5 liters of microbial broth with cells in 500 g of soil for 25 mL/g soil treatment

The third treatment (control) involved the application of different concentrations of water to achieve different moisture concentrations in the samples. Figure 11 shows the set up of the treated samples and the summary of the set up is as follows:

- 2.5 liters of water in 500 g of soil for 5 mL/g soil treatment
- 5 liters of water in 500 g of soil for 10 mL/g soil treatment
- 7.5 liters of water in 500 g of soil for 15 mL/g soil treatment
- 10 liters water in 500 g of soil for 20 mL/g soil treatment
- 12.5 liters water in 500 g of soil for 25 mL/g soil treatment.

6.15 Sample collection from sandboxes

After the determination of soil strength parameters at 0 day, a 24 hour period was allowed for the treatment samples to stand. This was to enable the microorganisms to adjust to the new environment and to allow the treatments to infiltrate through the soil layers. For day 1 sampling, after the expiration of 24 hours, the first set of samples were collected from three replicates at an average depth of 3 cm for direct shear strength and unconfined compression strength tests while the other two replicates were sampled for EPS sorption tests and imaging of EPS distribution using fluorescence microscopy in soil respectively. Subsequent sampling of the treated soil continued at different intervals of 48

Figure 11: Setup of treated soil samples in sandboxes

Figure 12: Soil samples after treatments in sandboxes

hours for day 2 sampling at an average depths of 6 cm, 72 hours for day 3 sampling at an average depth of 9 cm. An average of 125 g of soil samples was collected at each sampling time for the geotechnical tests while samples for the TGA analysis and soil imaging for EPS were collected by direct penetration of 13 ml sterile tubes into the soil at average depths of 3 cm, 6 cm, and 9 cm.

These experiments were performed under ambient room temperature of 26 ^{o}C. The following relationships were obtained from these experiments: cohesion among the different soil types at different EPS, microbial broth, and water concentrations; unconfined strengths among the different soil types based on EPS-CM, microbial broth, water contents, and time, angle of internal friction among the different soil types based on soil treatment, shear strength among the soil types based on treatment, liquid loss among the soil types based on treatment, and fluorescence image analysis of the soil samples based on treatment and time. At this point, it is important to note that these investigations were performed as an indirect measurement of the propensity to form dusts as a result of the deformation or failure of these different soils under exposed conditions and different loads or activities.

6.16 Direct shear strength determination of treated soils

The direct shear test for soil samples were performed under consolidated drained conditions following ASTM D3080 standard. This test was performed with the following objectives; to estimate the angle of internal friction ($\emptyset$) and cohesion (C) from plots with different normal loads for different soils under drained conditions, to determination the shear parameters for over and normally consolidated samples, to control the stress and strain rates, and to compute the residual shear by prescribing a slow rate of shear with a

maximum displacement limit. As shown in Figure 13, the equipment used for these tests was the S2220 DigiShear™ Automated Direct Shear System.

6.17 Unconfined compression strength determination of treated soils

These tests were performed on the soil samples to determine their unconfined compressive strengths as treated and remolded cohesive soil samples. These tests were also carried out under consolidated and undrained following the ASTM D2166 standard. As shown in Figure 13, the equipment used for these tests was the Digital Tritest 50 BS 1377-7.

6.18 Soil desiccation tests based on moisture relationships with sample treatments

Using the oven method, the determination of the moisture concentrations of the treated samples was performed following ASTM D2216 standard. Under this method, treated soil samples used in the direct shear and unconfined compression tests were weighed under wet conditions before placing them in an oven. After a 24 hour period in the oven, the weights of the soil samples were measured and the moisture concentrations of the samples were determined by simple computations.

6.19 EPS sorption determination on treated samples

Soil samples collected with the 13 mL sterile tubes were used to determine the concentration of EPS sorbed to the treated samples at different depths and sampling times. To achieve this objective, TGA analyses was performed on each of the samples. The instrument used, TA Instrument TGA Q500 series is shown in Figure 14. In these analyses, different concentrations of the samples were placed in the platinum pans of the TGA equipment and each test was run at a mode (TGA 1000 ^{o}C) and test (ramp). This experimental mode and test procedures were designed to heat the sample at a constant

Figure 13a: Direct shear strength testing instrument used in this research

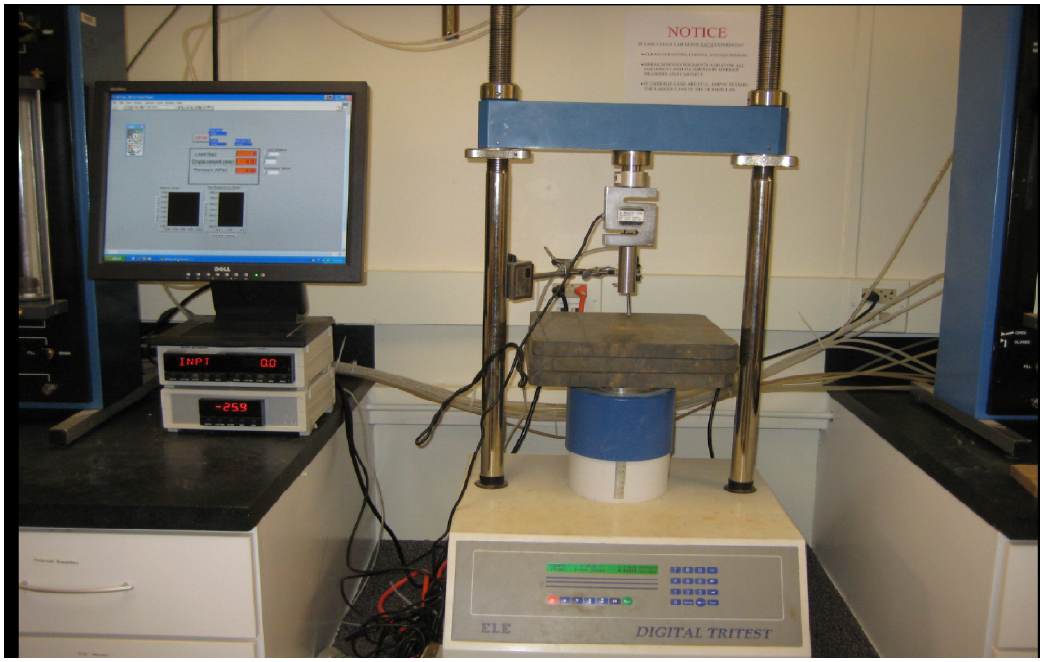

Figure 13b: Unconfined compressive strength testing instrument used in this research

Figure 14: TGA analysis instrument used in this research

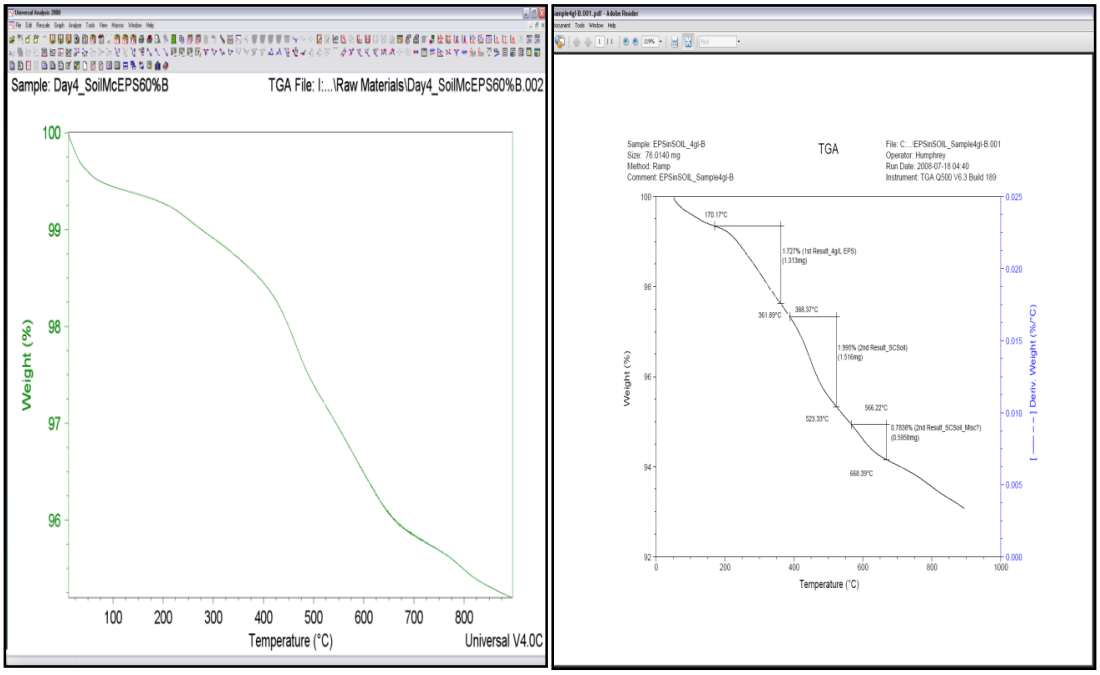

Figure 15: Screen shots of universal analysis 2000 results

rate of 20 ^{o}C and were to determine the thermal stability and composition of the samples over a broad temperature range. The final temperature was set at 900 ^{o}C and at a flow rate of 60 mL/min using ultra high purity nitrogen. The analyses of the peaks were carried out using a universal analysis 2000 software (Figure 15).

6.20 Imaging EPS distribution in treated samples by fluorescent microscopy

To visualize the spatial distribution of EPS in treated soil samples under a fluorescent microscope, a modified version of the protocol prescribed by Priester et al. (2007) and Rodriguez and Bishop (2007) was followed. Soil samples were incubated at 37 ^{o}C for 72 h. After the incubation period, 40 mg of soil was weighed out and mixed with 1 mL of phosphate buffer solution (PBS) containing ethidium bromide (EtBr) using 2 mL centrifuge tubes. The samples were mixed thoroughly using a vortex mixer. The solutions were then centrifuged for 60 mins at 37 ^{o}C and 5000 rpm. The supernatant was withdrawn and discarded using a pipette. This was followed by an addition of another 1 mL PBS/EtBr solution and centrifugation was repeated with supernatant discarded (Bonaventura et al. 2006; Kolari, 2003). Pellets of the soil sample were mounted on a slide and covered with a slip for viewing under the fluorescent microscope and EPS fluorescence was observed at 488 nm using Olympus model BX51 fluorescence microscope, shown in Figure 16.

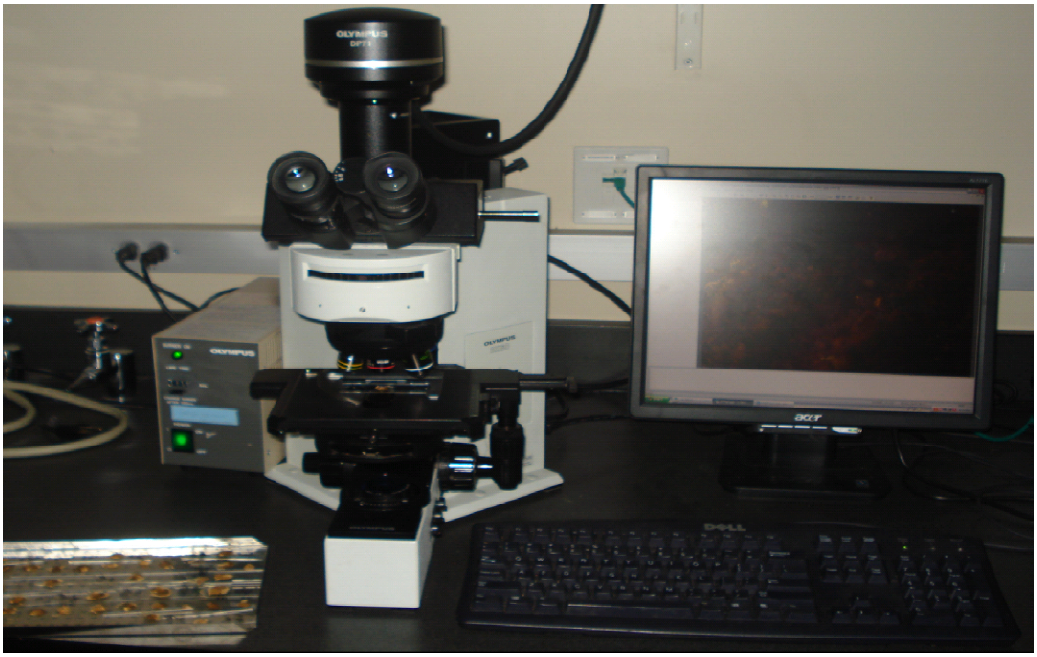

Figure 16: Olympus model BX51 fluorescence microscope (Olympus, USA)

6.21 Statistical analyses

In order to determine the significance of the different parameters evaluated and the data obtained in this study, statistical analyses were performed. Using Microsoft Excel, correlation analyses were carried out in order to examine the effects on the different levels of EPS produced in Haggstrom media and the three soil types. Similarly, two-way analyses of variance ANOVA were carried out using SAS to determine the significance of cohesion in all soils based on the different soil treatments tested. Error bars in the results of EPS production in Haggstrom media and soils, and the comparison of soil strength parameters indicate standard deviations while error bars in empirical results of deformation indices, friability, coefficient of failure, comparisons of effective porosities, and quantification of EPS produced indicate standard error of means.

CHAPTER 7: EXPERIMENTAL RESULTS AND ANALYSIS

7.1. Characteristics of soil

The soils used in this research have been identified as piedmont residual soils and their behavioral characteristics have been well documented. These soils are predominant in the southeastern to the mid-Atlantic regions of the U.S and are the primary foundation bearing soils mainly found in many cities within this region including Atlanta, Charlotte, Philadelphia, Washington DC, and Baltimore (Finke et al., 1999; Hoyos Jr. and Macari, 1999). Residual soils are formed from the weathering of rocks and the mineralogy and behavior of these soils mainly depends on the nature of the parent materials as well as other factors such as climate, age, and topography of the area (Mohamedzein and Aboud, 2006; Townsend, 1985; Pitts and Kannan, 1987). The mineralogy of residual in North Carolina has been documented as well. Data obtained from X-ray diffraction of residual soil samples by Leith and Craig (1965) showed that the minerals that occur frequently in these soils include kaolinite, vermiculite, illite, quartz, mica, feldspar, amphiboles and montmorillonite. Residual soils have also been shown to be composed of mainly clay, fine silt, and coarse silt fractions therefore the different soil types used in this research.

The different soil types silty clayof soil (SCSoil); sandy clay soil (SDCSoil); and sandy silty clay soil (SSCSoil) were classified based on the American Society for Testing and Materials (ASTM) classification system designated D 2487, also known as the Unified Soil Classification System (USCS). As shown in Figure 17, the grain size

distribution curve indicates significant contents of silt and clay fractions relative to the coarse fractions. The specific surface areas, particle density, and bulk density, and porosity of the soil samples were also determined and as expected, the specific surface area decreases in the following order: silty clay soil > sandy silty clay soil > sandy clay soil. No major differences were observed between the particle and bulk densities of the soil samples while the porosities decreased in the following order: sandy clay soil > sandy silty clay soil > silty clay soil. The actual data of these results are summarized in the Table 6. The data obtained from the grain size analysis was used to plot a semi-logarithmic graph, which was analyzed to determine the Atterberg Limits as shown in Figure 17 and 18.

Table 6: Characteristic of soil sample used in this research

Soil Type	Silty clay Soil	Sandy clay soil	Sandy silty clay soil
Moisture content (%)	2	2	2
Liquid Limit (%)	17	17	17
Plastic Limit (%)	11	8	11
Plasticity Index (%)	6	9	6
Specific Surface Area (m^2/g)	8.40 ± 1.34	8.12 ± 1.41	8.20 ± 1.37
Particle Density (g/m^3)	2.45	2.50	2.46
Bulk Density (g/cm^3)	2.120	1.956	2.007
Initial Porosity (%)	13.47	21.01	18.40

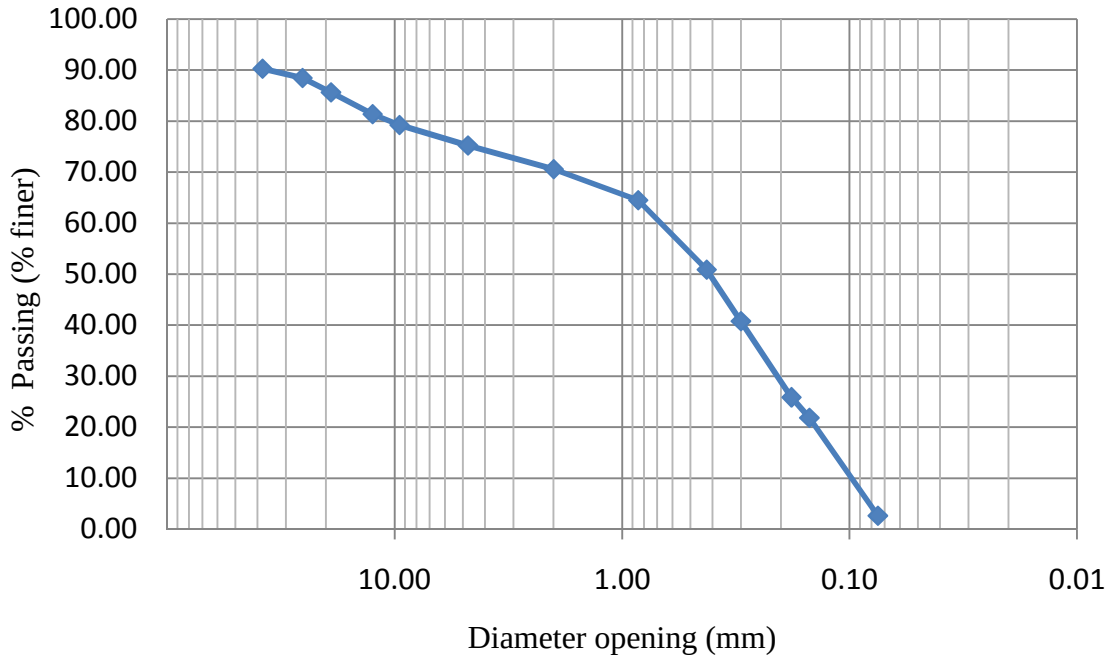

Figure 17: Graph showing grain size distribution of soil sample

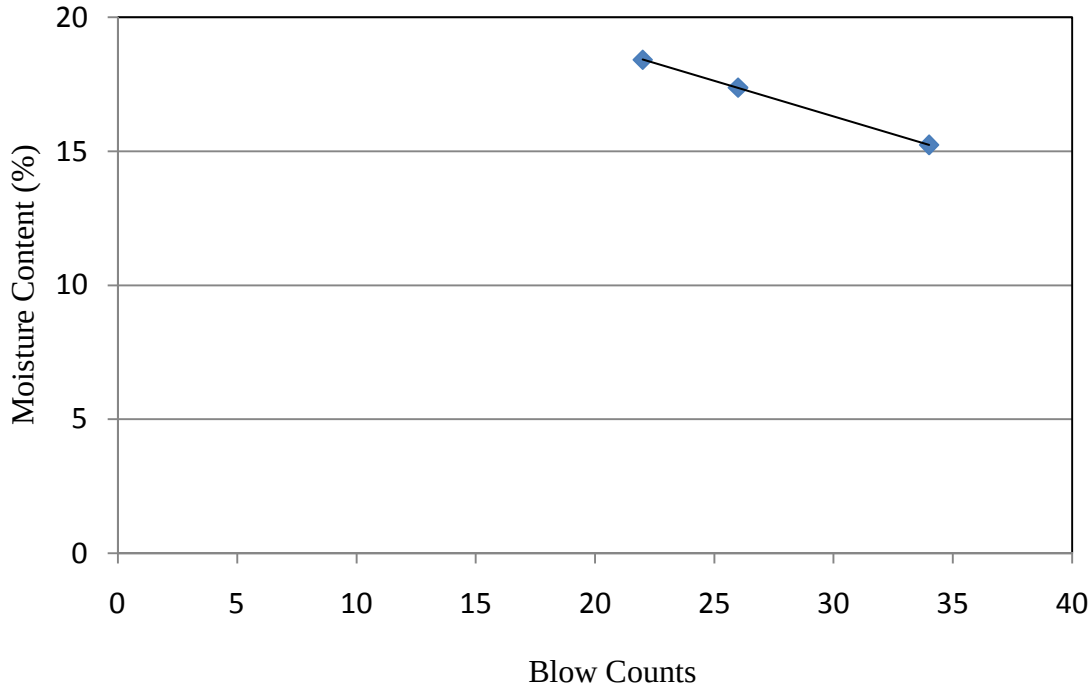

Figure 18: Graph showing Atterberg limits

7.2 Growth curve of *Arthrobacter viscosus*

An initial growth of the *Arthrobacter viscosus* was observed in the yeast mold agar plates, which showed the microorganism growing as opalescent viscous colonies as shown in Figure 19. Prior to initiating a batch production of EPS using *A. viscosus* in liquid media using glucose as carbon source, the growth curve was monitored within a 24 hr period. In performing this test, turbidity measurements were used to determine the cell density and EPS production was determined from dry weight measurements of lyophilized broth samples collected at hourly intervals.

As illustrated in Figure 20, the results obtained indicate that *A. viscosus* undergoes a growth curve in the following order: lag phase, environmental acclimatization period, occurs in the first 3 hr: log phase, period of increased cell productions, occurs within a 10 hr period: and a stationary phase, period of no further cell increments, occurs from the 13 hr onwards. The EPS production estimation shows a trend of increasing concentrations from 0.50 to 4.00 mg/mL, which continues after the stationary phase of the microorganism from Figure 20 as well. Report from previous studies show that EPS production measured at intervals of 7, 9, and 16 hr culture cycle remained constant at the 16 hr due the complete utilization of the nutrients in media therefore, cell growth and/or EPS production can be further facilitated by adding a carbon source (Bergmaier et al. 2003; Gandhi et al. 1997). The result obtained in this study shows a correlation between cell growth of *A. viscosus* and EPS production.

7.3 Batch fermentation and quantification of EPS production in Haggstrom media

The production of EPS in liquid media was investigated using different concentrations of microbial broth in Haggstrom media. The objective of this test was to determine the optimum concentration of the broth to be used for a large scale production of the EPS needed for soil stabilization.

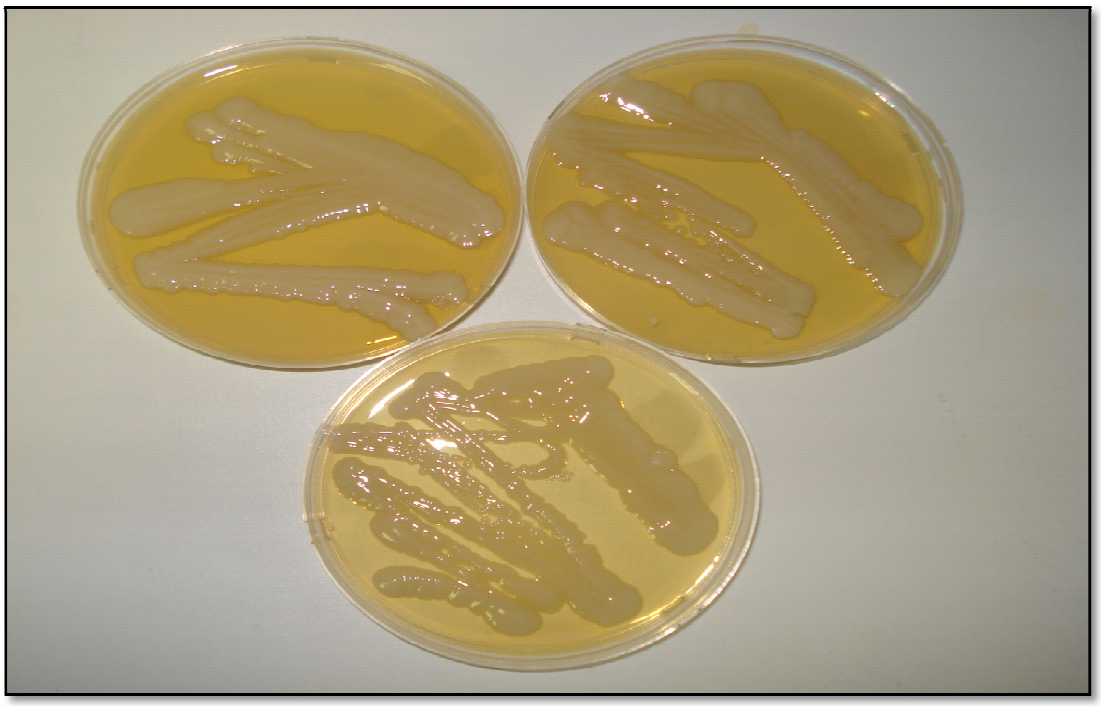

Figure 19: *Arthrobacter viscosus* growing in yeast mold agar plates

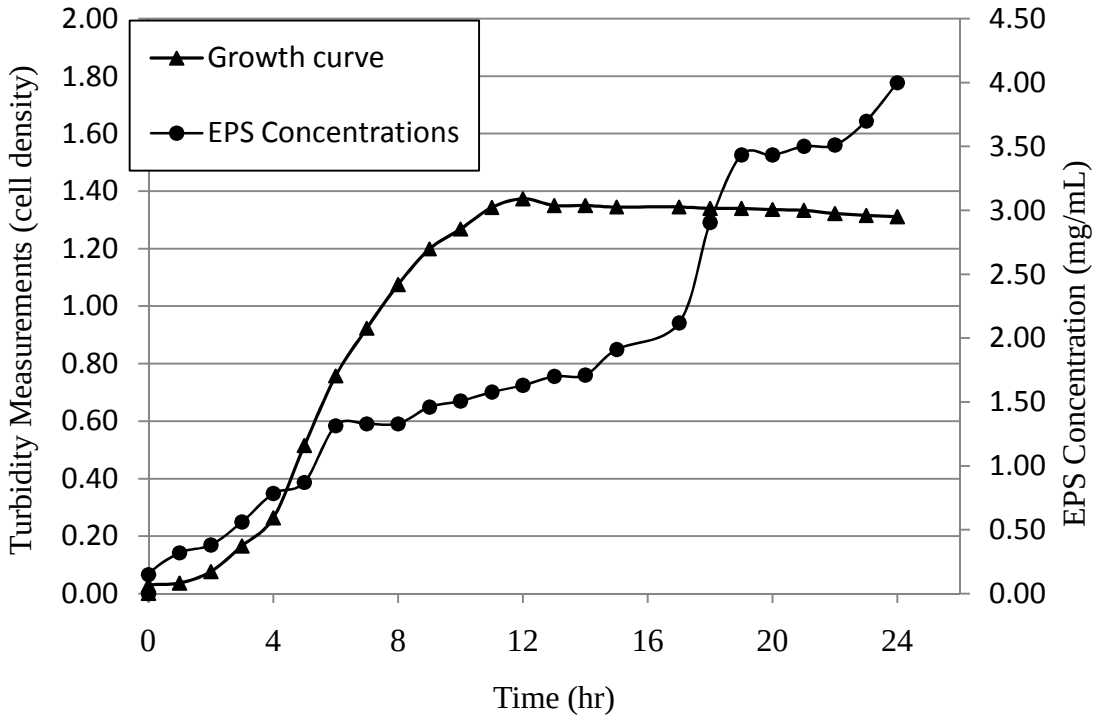

Figure 20: Growth curves of *Arthrobacter viscosus* with EPS production

soil treatments. Following the modified protocol developed from the methods described by Lopez et al. (2003) and Novak et al. (1992), batch fermentation was carried out at a constant temperature of 28 ^{0}C and pH of 8.5 using 3 % (w/v) of glucose as carbon source. The characterization of EPS based on carbon used has been documented. According to Novak et al. (1992), Knutson et al. (1979), Jeanes et al. (1973), and Bodie et al. (1985), EPS produced by *Arthrobacter viscosus* with glucose as carbon source contains 28.7 % glucose, 30 % galactose, 18 % mannuronic acid, and 24 % acetyl. The percentage total weight and average molecular mass have been determined as 101 % and 900 kDa (1494.48 e^{-18} mg). Results obtained by Lopez et al. (2003) also showed that increased production of EPS occurred at a controlled pH of 8 and constant temperature of 28 ^{o}C in a bioreactor. The results obtained in this study showed that the rate and quantity of EPS produced varied with time and microbial broth concentrations.

The experiments were performed using 500 ml-shaken round-bottomed glass bottles containing a total volume 300 ml of microbial broth and Haggstrom media. A constant shaking speed of 150 rpm was maintained to ensure homogeneity in the media. Three different experiments were performed and the average of EPS concentrations was plotted with time. The most important variable in these experiments was the microbial broth concentrations. Under these conditions, crude EPS concentration of 3.5 g/mL of Haggstrom media was observed within 72 hours in the media containing 100 and 80 ml/mL microbial broth while a total of 2.5 g, 2.3 g, and 2 g were obtained from 60, 40, and 20 ml/mL broths respectively. Since it was expected that increase in microbial growth will result in increased production of EPS in media, the experiments were further monitored for 336 hours (14 days) following the recommendations of Novak et al.

(1992). As shown in Figures 21 and 22, the results obtained in this study showed that the EPS production pattern was shown to occur in a nonlinear manner with time however, with the focus of this research centered on estimating the highest yield of EPS after 336 hours; it was observed that maximum EPS production of 13 g/mL occurred at 240 hours with 100 ml/mL broth, 12 g/mL at 336 hours with 80 ml/mL broth, 12.5 g/mL at 288 hours with 60 ml/mL broth, 10 g/mL at 288 hours with 40 ml/mL broth, and 10.5 g/mL at 288 hours with 20 ml/mL broth.

These results indicate that the addition of glucose as a carbon source enhances the production of EPS by *Arthrobacter viscosus*. The amount of the microbial broth used can also be correlated with the EPS production due to the nutrient concentration in the media. However, studies have shown that *Arthrobacter viscosus* can produce a significant amount of EPS even in the absence of adequate nutrients. The reported amount of EPS produced in the 20 ml/mL broth compared with the 40 ml/mL broth in this study confirms this. A significant decrease in EPS concentration, 7.5 mg/mL and 8.5 mg/mL observed in the 100 ml/mL broth and 80 ml/mL respectively as well those observed at lower broth concentrations respectively can be attributed to the adverse effect of a lower pH in the media. The negative effects of low pH in the growth media have been reported by Novak et al. (1992) and Lopez et al. (2002).

However, in this study, no measures were taken to control the pH to allow for the natural process of pH fluctuations that occur based on different environmental factors, which is the case on exposed surface soils. For the purposes of this study, 60 ml/mL broth was chosen to be the optimum concentration for a large scale production of the EPS needed for soil treatment. This was based on the observation steady increase in EPS production after 336 hrs compared to other broth concentrations used in this research.

However, the results of the EPS production pattern using these different broth concentrations are inconclusive due to the cyclical pattern observed. Therefore, 60 ml/mL broth cannot be concluded as the optimum concentration needed for effective EPS production.

7.4 Batch EPS production in soil

As stated earlier in the methodology of EPS treatment of various soils used in this research, one approach adopted was to allow the microorganism to produce the EPS in situ by applying it directly to the soil as microbial broth. To investigate the practicality of this approach, the production of EPS by *A.* viscosus in the different soil types used in this research was monitored over a 72 hr period using different microbial broth concentrations. It was assumed that more EPS will be produced in soils with higher concentrations of microbial broth. To monitor the amount of EPS produced in each soil at different time intervals, soil samples treated with the microbial broth were collected, lyophilized, and analyzed with thermogravimetric analysis instrument (TGA). The objective of this analysis was to quantify EPS in each soil based on the rate of change in weight of the samples as a function of temperature in a controlled environment.

From Figures 23 and 24, the results obtained in this study show that the EPS decomposes at about 355.58 ^{o}C, silty clay soil at 518.29 ^{o}C, sandy clay soil at 520.81 ^{o}C, and sandy silty clay soil at 509. 49 ^{o}C. Data shown in Figure 25 shows that optimum EPS production occurred between 48 and 72 hr in silty clay soil with the highest EPS concentration of 3.8 mg/g soil observed at microbial broth concentration of 20 mL/g of soil. Figure 26 and 27 show different nonlinear patterns of EPS production in both sandy silty clay and sandy clay soils with highest EPS amount of 2.5 mg/g soil and 3.3 mg/g soil occurring in both soils respectively. A decline in the amount of EPS produced in the

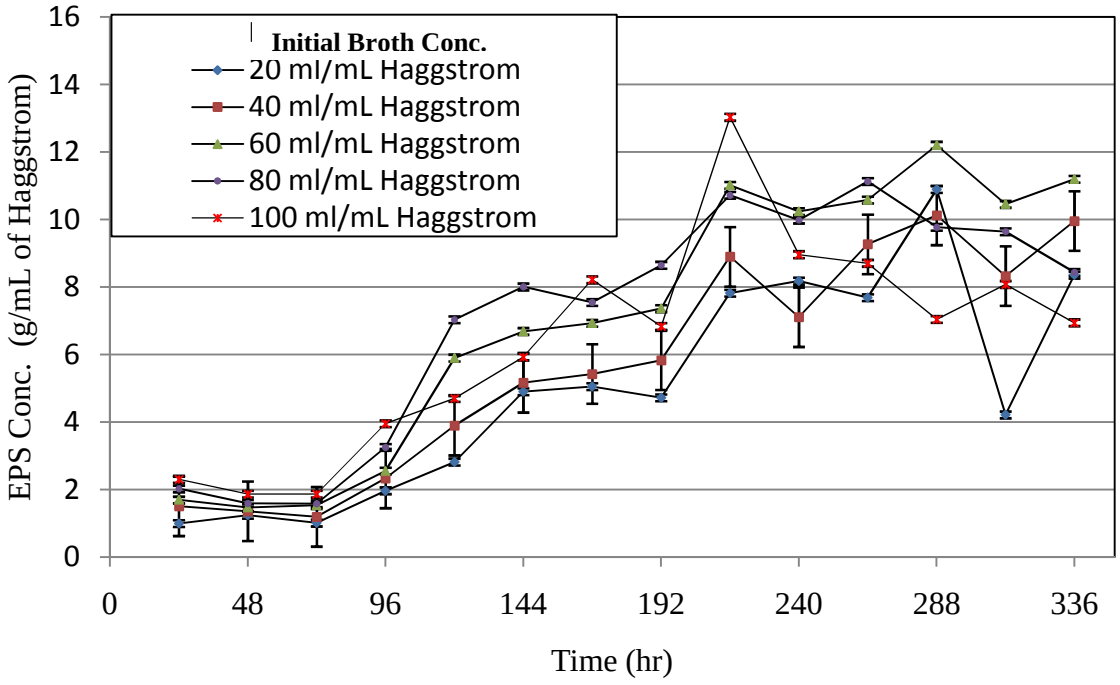

Figure 21: 336 hr EPS production curve by *A. viscosus* in Haggstrom media

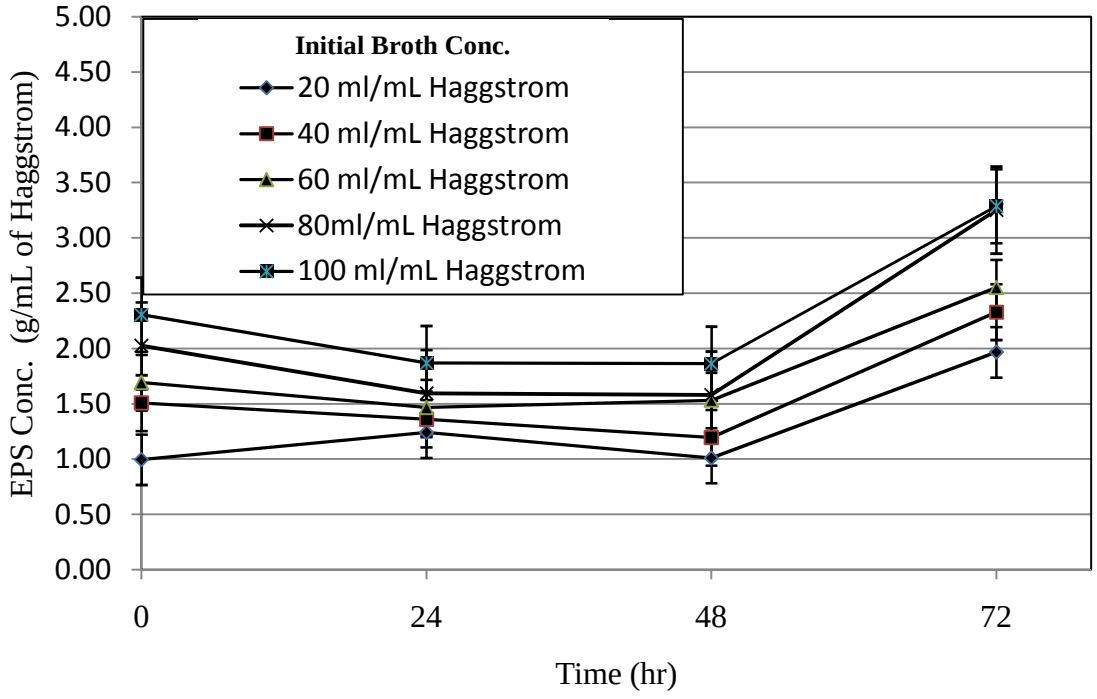

Figure 22: 72hr EPS production curve by *A. viscosus* in Haggstrom media

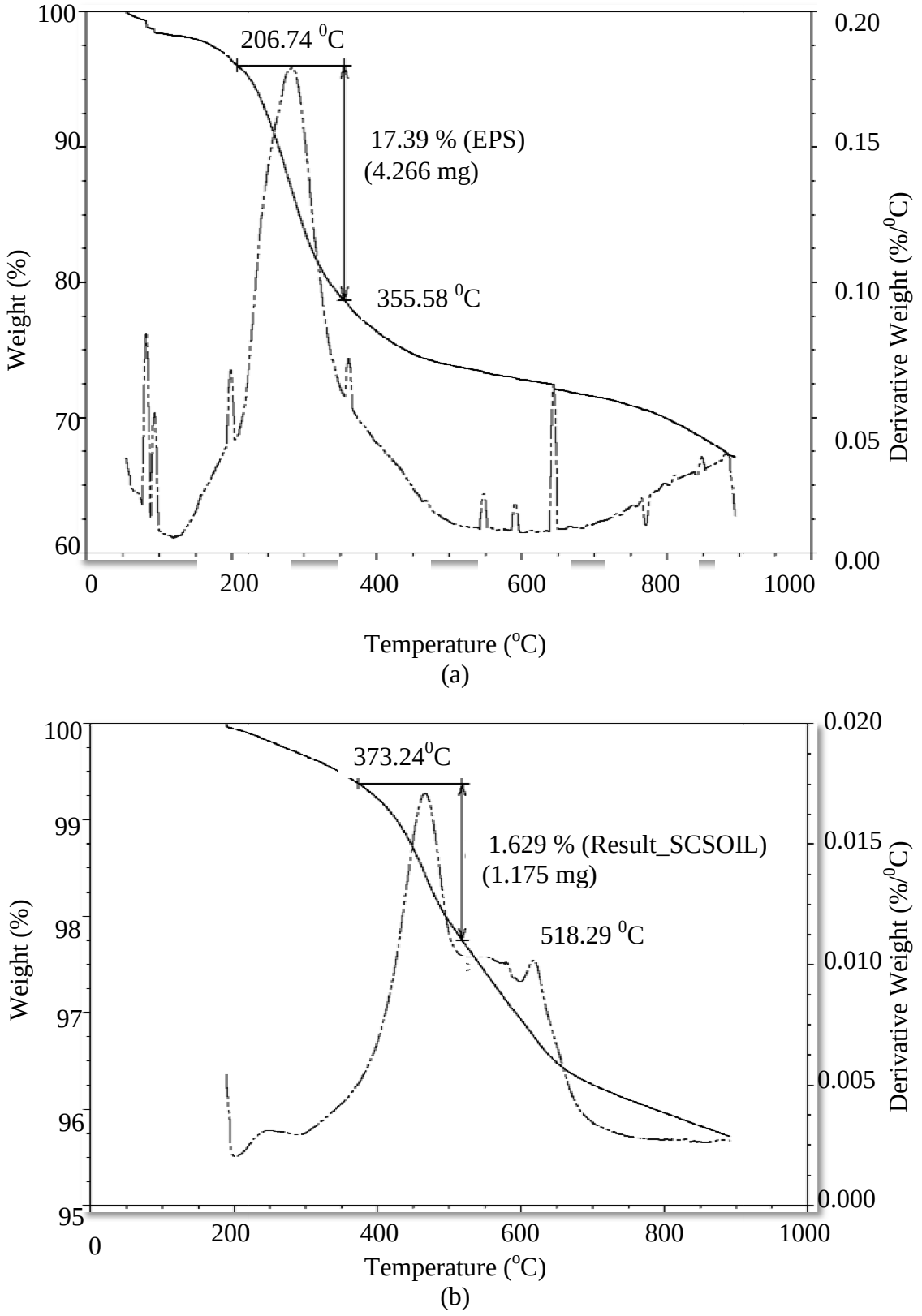

Figure 23: TGA plots (a) EPS; (b) Silty clay soil

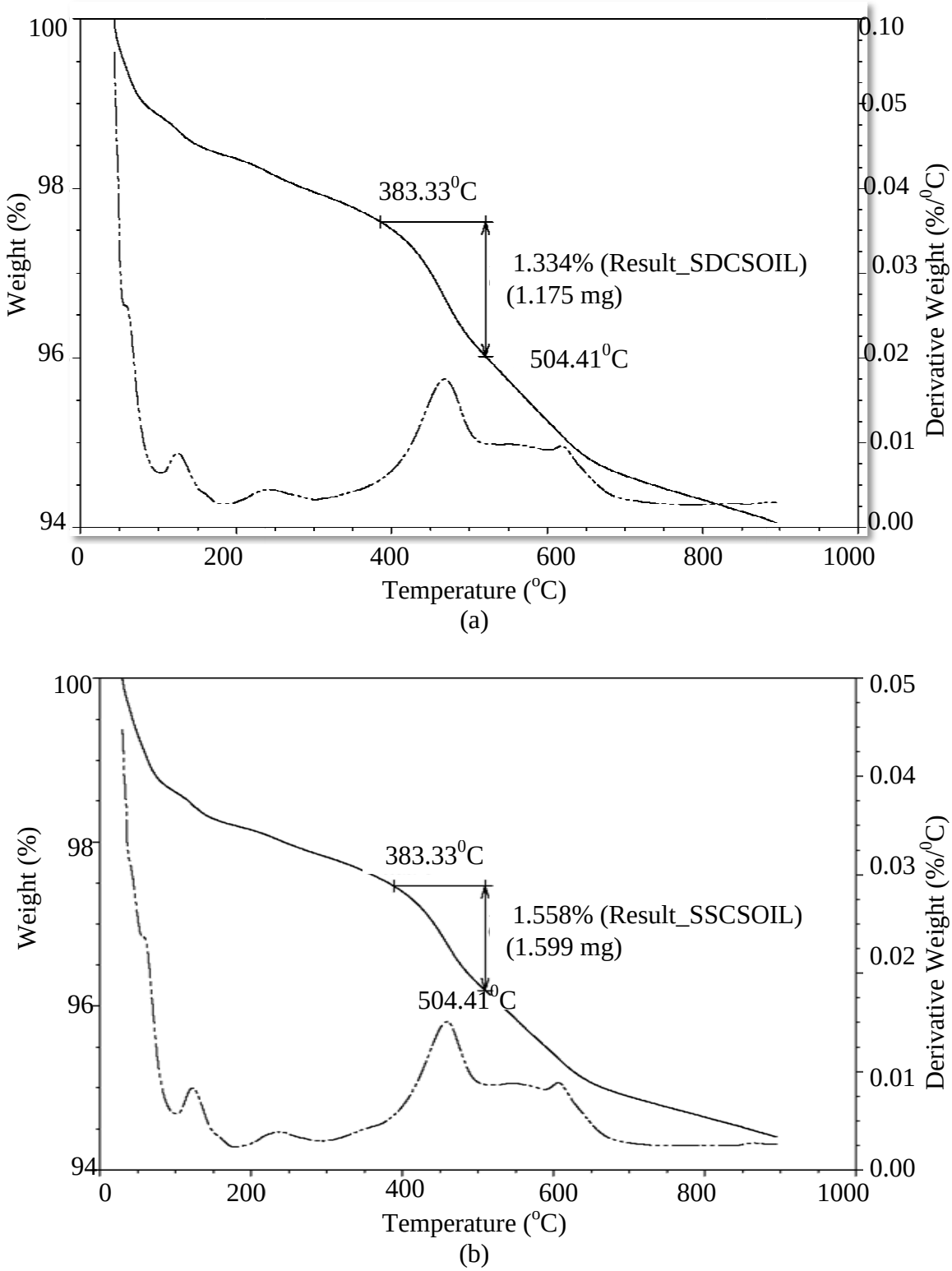

Figure 24: TGA plots of (a) sandy clay soil and (b) sandy silty clay soil

soil samples was observed with time and subsequent increases could be correlated with the complexity of population dynamics of the microorganism in soil and available nutrients (Schmidt, 1987). Another explanation of the observed trend in the EPS production in soil can be the available surface area for microbial adhesion and EPS adhesion.

Further monitoring of EPS production by *A. viscosus* in all three soils showed that the ability of the bacteria to produce this biopolymer is enhanced by a greater surface area as seen in the production curve in Figure 28. The results also showed that optimum EPS productions occurred intermittently at 48 hr and 120 hr. The observed decline in the mass of EPS produced has been explained by the decomposition of biopolymers in soil (Martens and Frankenberger, 1992). These authors reported a rapid decomposition of monosaccharide fractions of the produced biopolymer resulting in the decrease of the overall amount of the biopolymer. In addition, this trend can also be explained based on the fact that as EPS is produced in soil, it occupies the intergranular pore space but as it grows, it enters more into the intragranular pore spaces such that it becomes available for burning when analyzed with TGA thereby reducing the amount observed in the soil sample (Inyang, 2008).

Conversely, the rates of EPS production in sandy clay and sandy silty clay soil indicates a less significant production of the biopolymer, which can be attributed to the presence of more intergranular pore spaces in sandy clay and sandy silty clay soils. The presence of these intergranular pores spaces makes more O_2 available but makes it difficult for the more cells of *A. viscosus* to attach to the soil particles thereby inhibiting their ability to generate more EPS. Similar results were reported by Vandevivere and Baveye (1992), which concluded that EPS production in a sandy soil column was not significant due to the inability of the inoculated strains to form colonies in the soil column. Another factor that has been reported to influence the effectiveness of microbes to produce biopolymers in soil is the moisture content of the soil. According to Cosentino et al. (2006), the dryness and wetness of a soil sample affects the respiration of inhabitant

microbes in the soil and could affect their ability to produce extracellular polysaccharides.

With this in mind, the abundance of intergranular spaces in sandy clay and sandy silty clay soil samples is most likely to result into increased liquid loss, which could account for less microbial metabolic activities. This hinders the successful production of EPS in such soils as indicated in the results of this study. In comparing this with the silty clay soil, a reduced number of intergranular pore spaces reduce a significant liquid loss thereby providing more moisture for increased microbial activities leading to greater EPS production (Caire et al. 2000). Other authors have also confirmed that in clayey soil samples, visible EPS quantities can be observed to form compartments with and among the clay particles (Lunsdorf et al. 2000; Kumar et al. 2007). The formation of these EPS compartments with soil samples tend to enhance the binding of the clay particles thereby increasing their stability and the distribution of the EPS can be observed in the soil using microbiological stains as will be reported in this present research as well. These results, as confirmed by Robb (1984), indicate the significance of biopolymers in the adhesion dynamics of the bacterial cells to solid surfaces.

Research has shown that the roughness of the soil surface is essential in the initial process of biofilms development (Loosdrecht et al. 1989). Since EPS are the main components of biofilms (Flemming et al. 2007; Hilger et al. 2000; Zhang et al. 1999), it has been documented that the fundamental process contributing to biofilm development in soil matrix could be from the combined effects of a) transport of organic molecules and microbial cells to the wetted soil surface, b) adhesion of organic molecules to the wetted soil surface resulting in a conditioned soil surface, c) adhesion of microbial cells to the conditioned soil surface, d) metabolic activities by the attached microbial cells inducing the adhesion of more cells and associated materials, and e) detachment of portions of the biofilms (Characklis, 1984). These factors explain the different amounts of EPS produced in the different soils in this research.

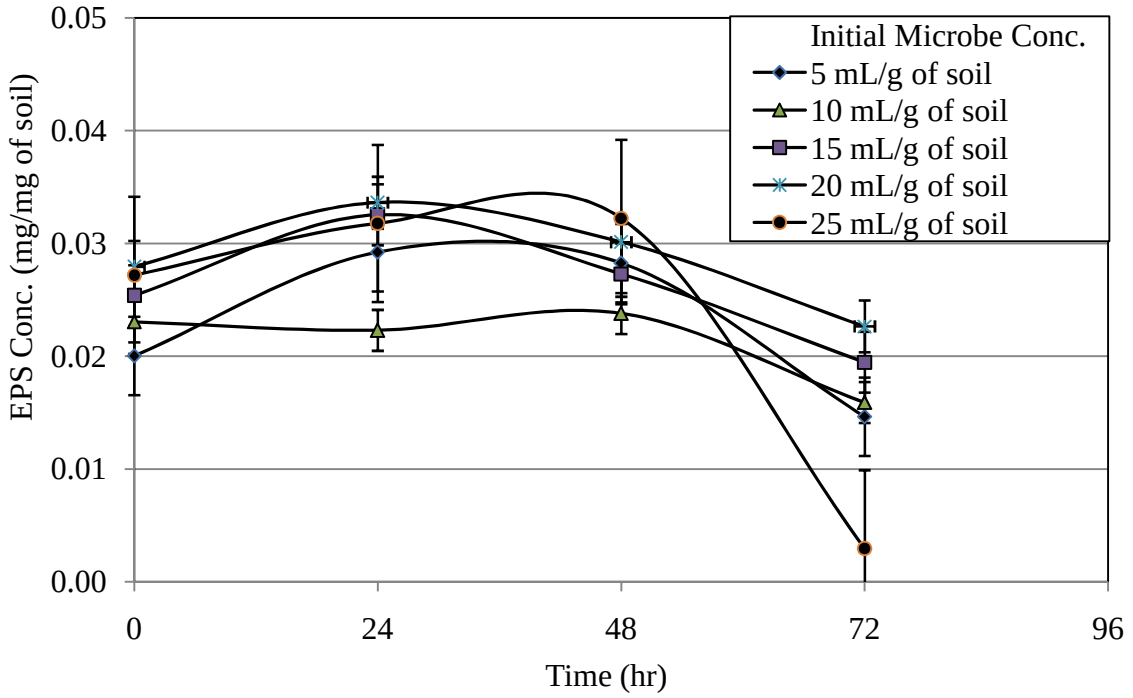

Figure 25: EPS production curve in silty clay soil

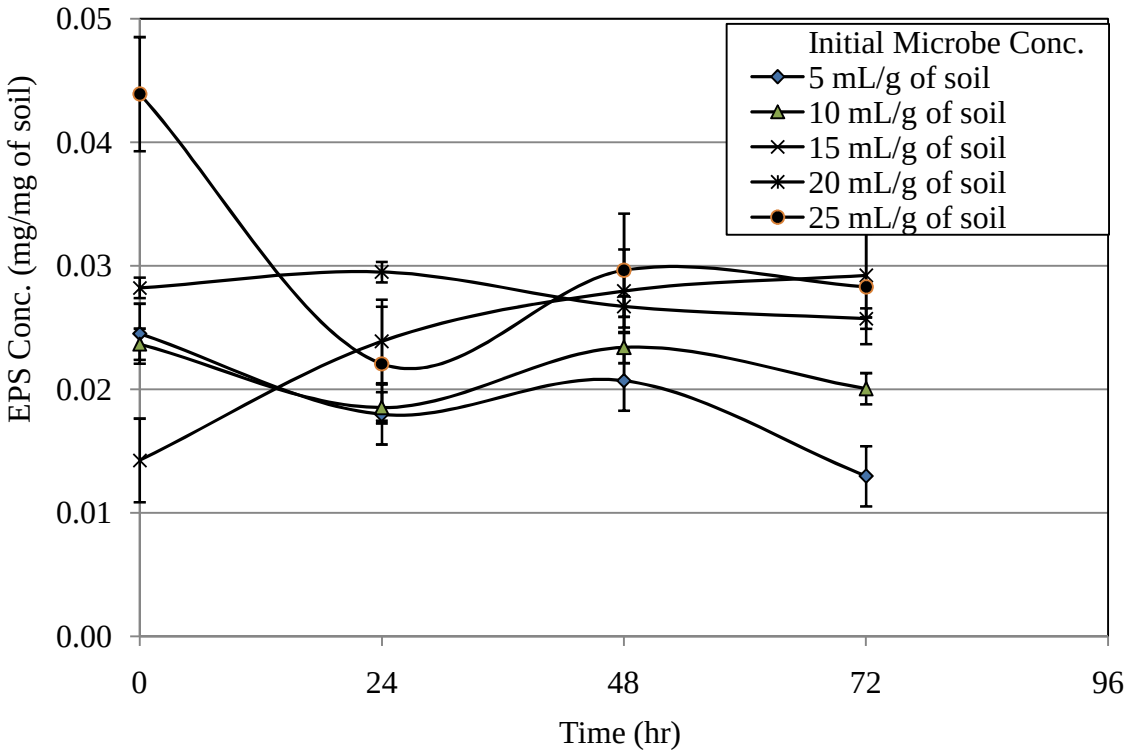

Figure 26: EPS production curve in sandy silty clay soil

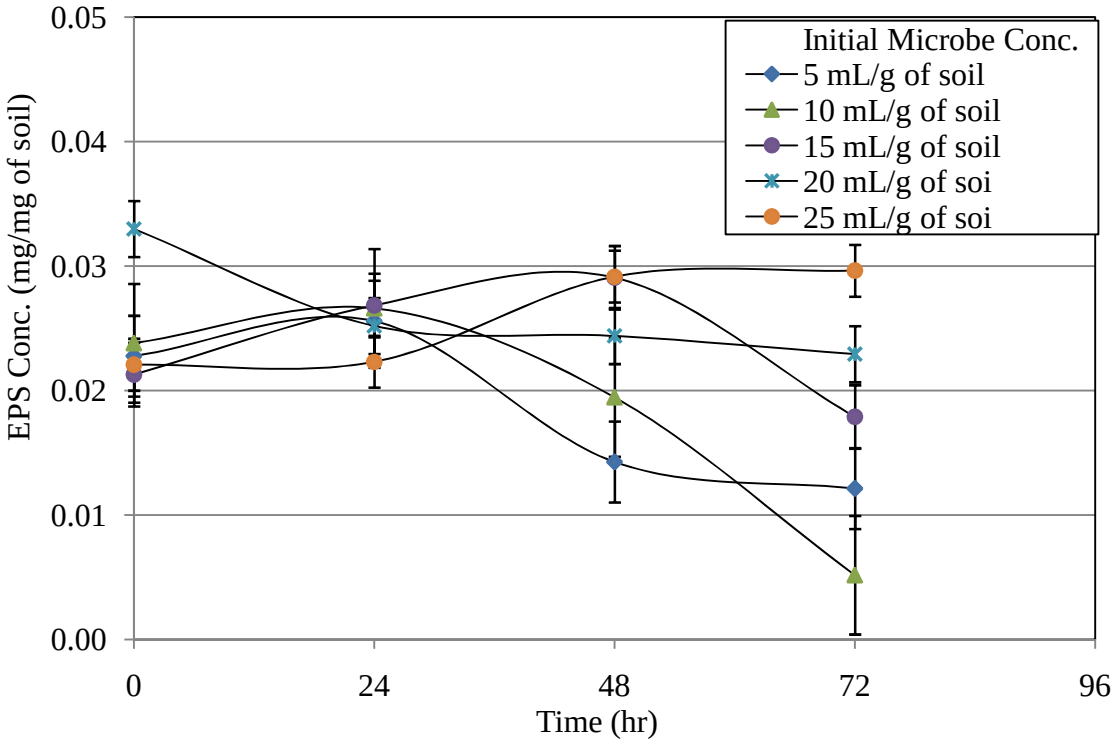

Figure 27: EPS production curve in sandy clay soil

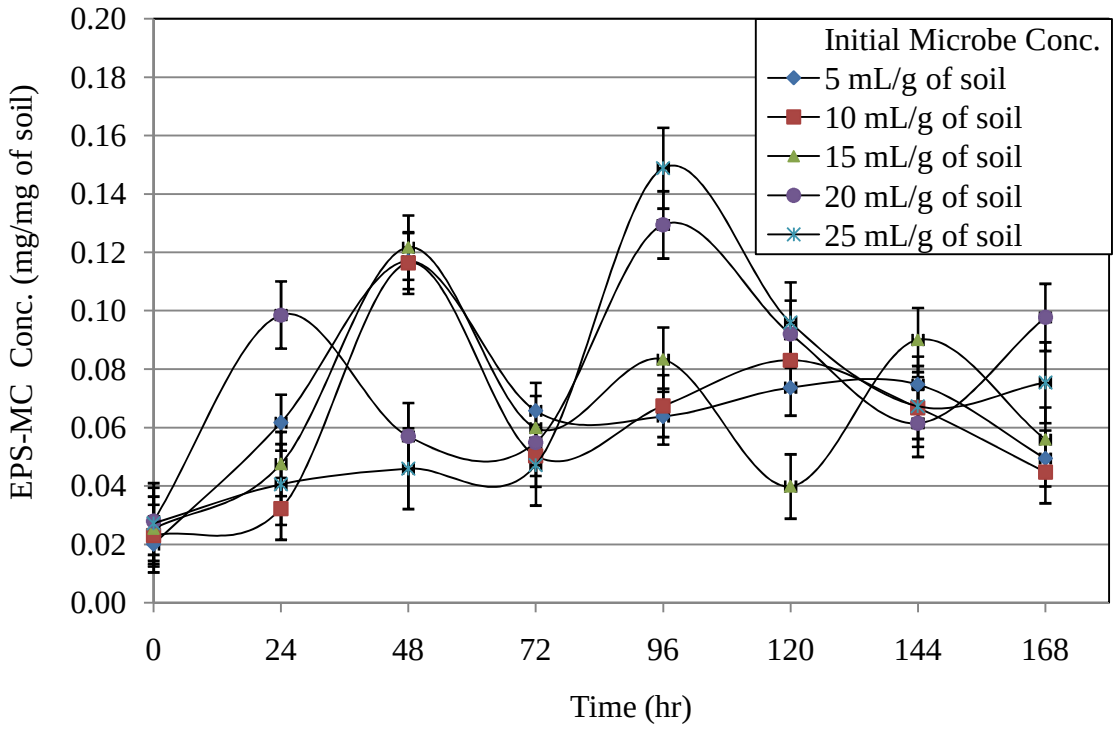

Figure 28: 7-day EPS production curve in silty clay soil

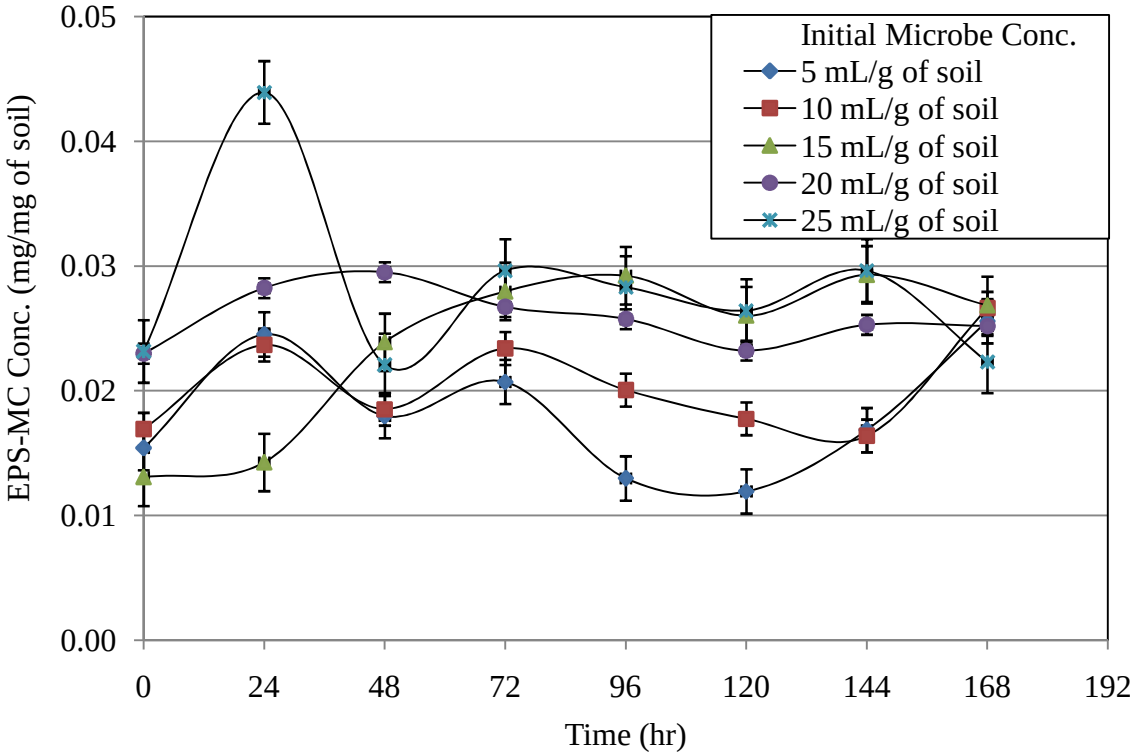

Figure 29: 7-day EPS production curve in sandy silty clay soil

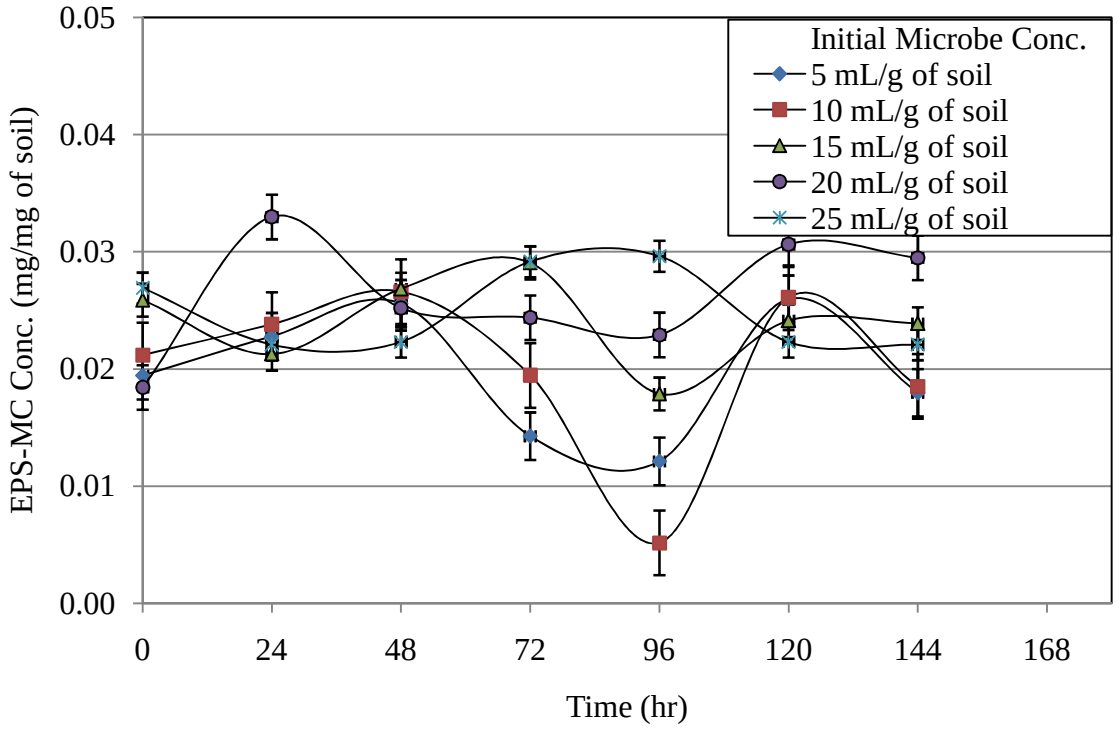

Figure 30: 7-day EPS production curve in sandy clay soil

7.5 Analysis of treated soils in sandboxes

To accomplish the main goal of this research, which is to monitor and compare the strengthening effects of EPS-CM in treated and untreated soil samples, it was necessary to simulate a natural environment. The soil strengthening effects of direct application of extracted EPS-CM to soil, indirect application of EPS through in situ production by applied microbial broth, and control samples treated with deionized water were compared. The soil strength parameters measured in this research include unconfined compressive strengths and shear strengths. Although it has been reported that soil strength decreases with increasing water content (Favaretti, 1995), soil liquid content is essential to the resistance of exposed soil to cracking under due to stress. Therefore, desiccation tests were performed to determine the effects of soil treatment with EPS on liquid loss with time.

7.5.1 Determination of unconfined compressive and shear strength

Results from unconfined compression and direct shear tests in soils were computed to show the strain at failure based on different soil types and treatments. A general trend of decreasing strain with increasing concentration of treatment and a trend of increasing strain with time was observed in most samples. Figures 31 and 32 show the soil samples under unconfined compression and direct shear tests. As represented in Figure 33, silty clay soil treated with EPS-CM showed a range of maximum deformation of 0.34 to 0.20 from day 1 to day 3 at EPS-CM concentration of 5 mL/g of soil. At higher EPS-CM concentrations, these values tend to increase and decrease with time indicating variations in this soil behavior with time. On the other hand, in the sandy silty clay and sandy clay soil, an opposite trend was observed as shown in Figure 34 and 35. The maximum deformation was shown to occur at day 3 while decreasing between day 1 and 2 but the results showed a decrease in deformation with increasing EPS-CM

concentrations as well. In summary, the lowest deformation results of 0.25 occurred at day 3 in silty clay soil with 25 mL/g EPS-CM, 0.18 at day 3 in sandy silty clay soil treated with 25 mL/g EPS-CM, and 0.15 at day 1 in sandy clay soil treated with 25 mL/g EPS-CM.

In comparing these results with control samples, no definite pattern of soil deformation was observed. However, maximum deformations ranging from 0.20 to 0.25 were observed between day 1 and day 3 in all the soil types and the soils exhibited fluctuations and increments between water contents and times of treatment. These inconsistent variations in soil deformation as shown in Figures 36, 37, and 38, show water treatment in soil does not exhibit a consistent pattern of soil deformation improvement. It also proves that EPS-CM treatment of soil samples can be used as a variable in determining the amount of deformation occurring in soil samples at different times.

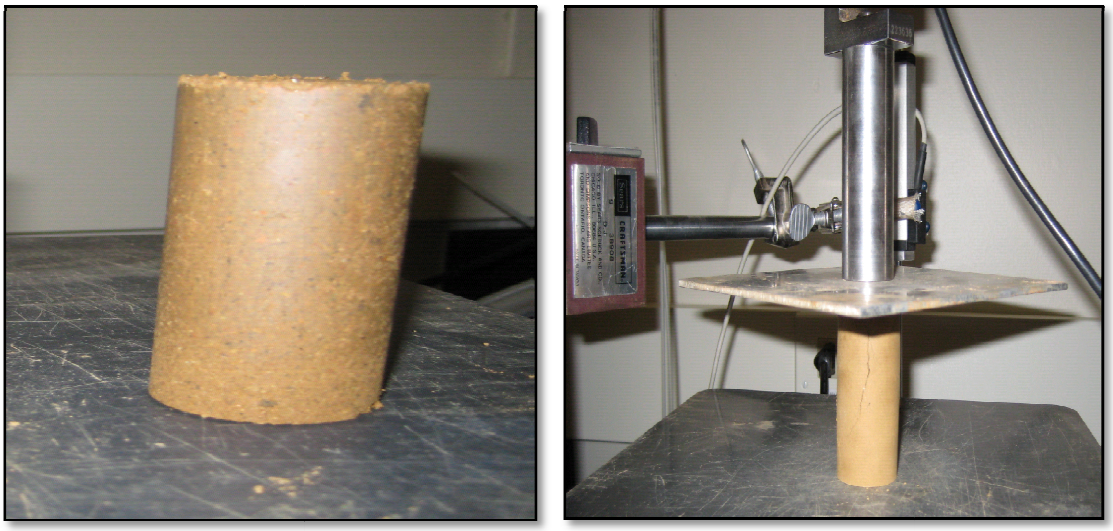

(a) (b)

Figure 31: Unconfined compression (a) prepared sample; (b) sample under deformation

(a)

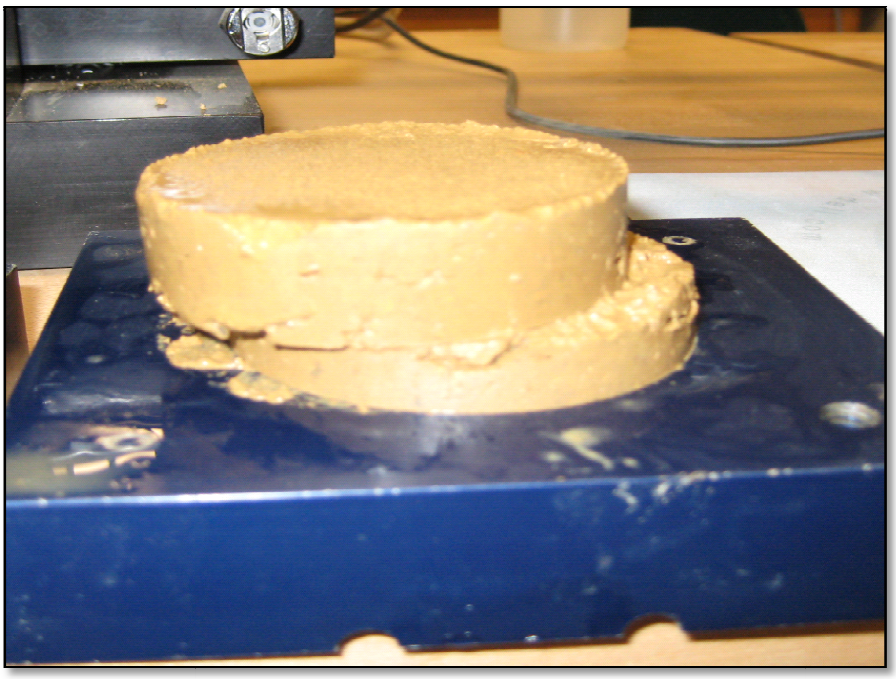

(b)

Figure 32: Direct shear (a) slightly sheared sample; (b) completely sheared sample

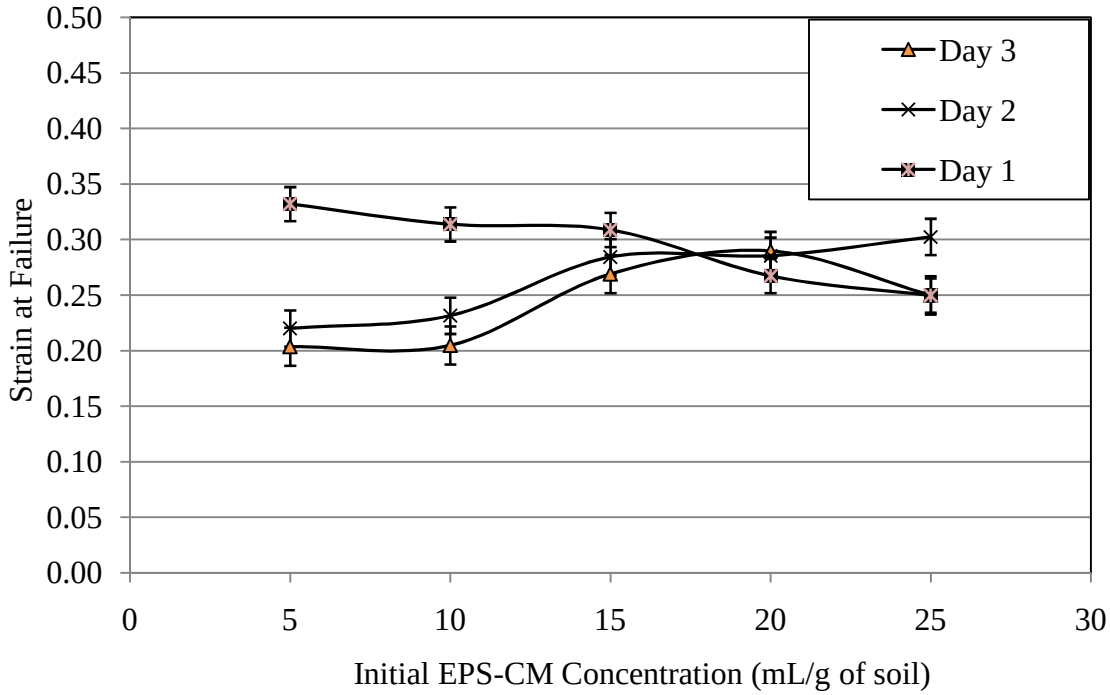

Figure 33: Deformation pattern in silty clay soil based on EPS-CM concentration with time

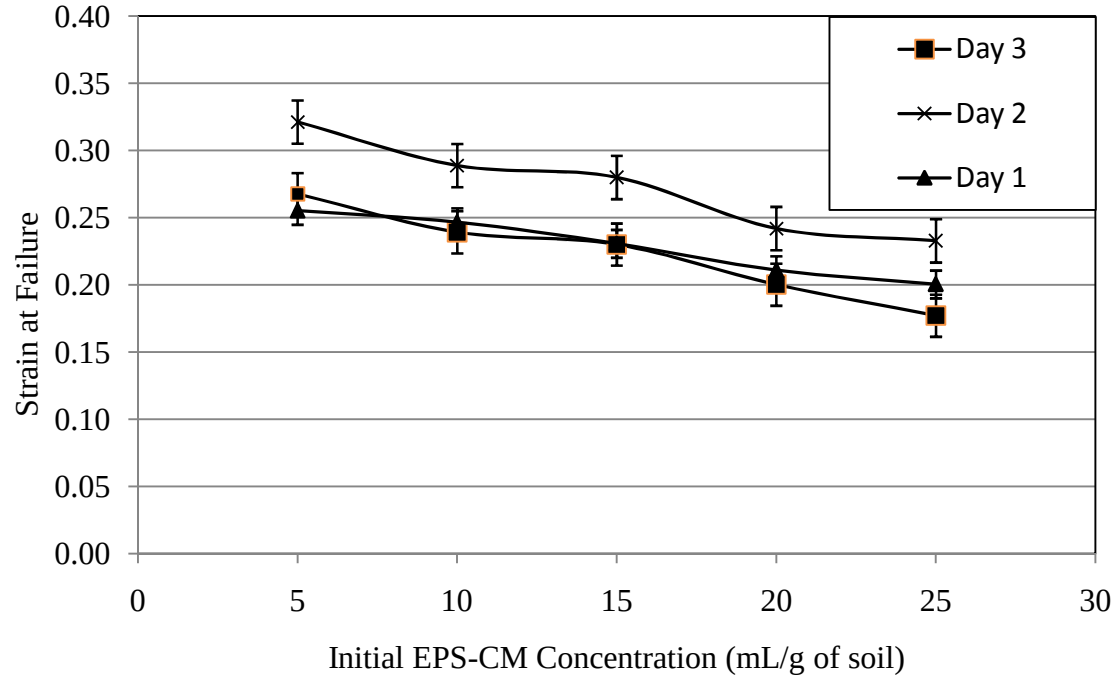

Figure 34: Deformation pattern in sandy silty clay soil based on EPS-CM conc. with time

In comparing results obtained in the different soil types, it can be inferred that the least deformation of 0.15 observed in sandy silty clay and sandy clay soil show that the roughness of soil surface (based on sand content) is significant in the adhesion of the EPS-CM in these soils. A lower EPS-CM content in these may mean a lower liquid retention therefore, less deformation by unconfined compressive stress. In order to verify this result, a comparison of liquid loss with treatment and time was performed, which is discussed in the next section. It can also be concluded that the amount of clay content, which is significantly higher in the silty clay soil, contributes to the greater surface area of the soil allowing more EPS-CM adhesion therefore, more liquid retention. More liquid retention reduces the compressive strength of soils as shown in these results.

7.5.2 Determination of liquid loss based on soil treatments

To compare the effects of soil treatments with time, soils treated with initial concentrations of EPS, microbial broth, and water were desiccated for 72 hours. From the results obtained in these test, it was shown that a general trend of decreasing liquid loss with time occurred most of the samples. Consistent with the expected results in this research, Figure 39 shows that liquid losses in EPS-CM treated silty clay soils occurred the least at higher concentrations of the EPS-CM and the initial liquid content of 16% occurred at the maximum EPS-CM treatment of 25 mL/g of soil compared to 14 % and 11 % observed in both broth treated and control samples (Figures 41, 46, and 47). Soil samples containing EPS-CM by direct application (Figures 39, 42, and 45) or induced by microbial concentrations (Figures 42, 45, and 48) show lower feasibility of drying during desiccation when compared to control samples (Figures 43, 46, and 49). Generally, silty clay samples showed

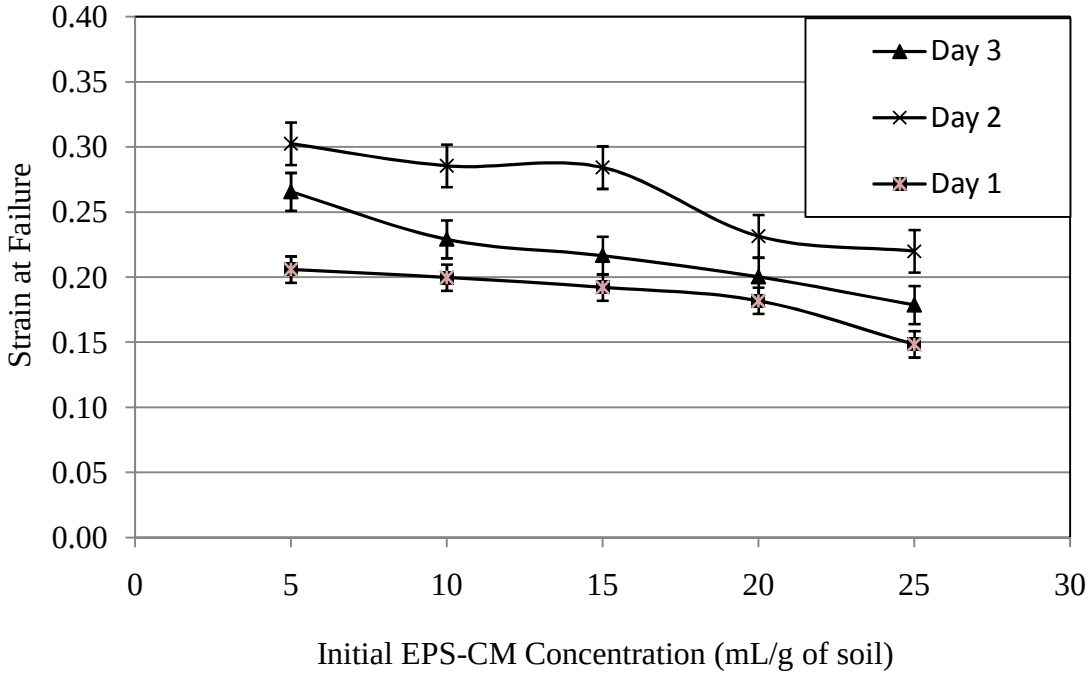

Figure 35: Deformation pattern in sandy clay soil based on EPS-CM concentration with time

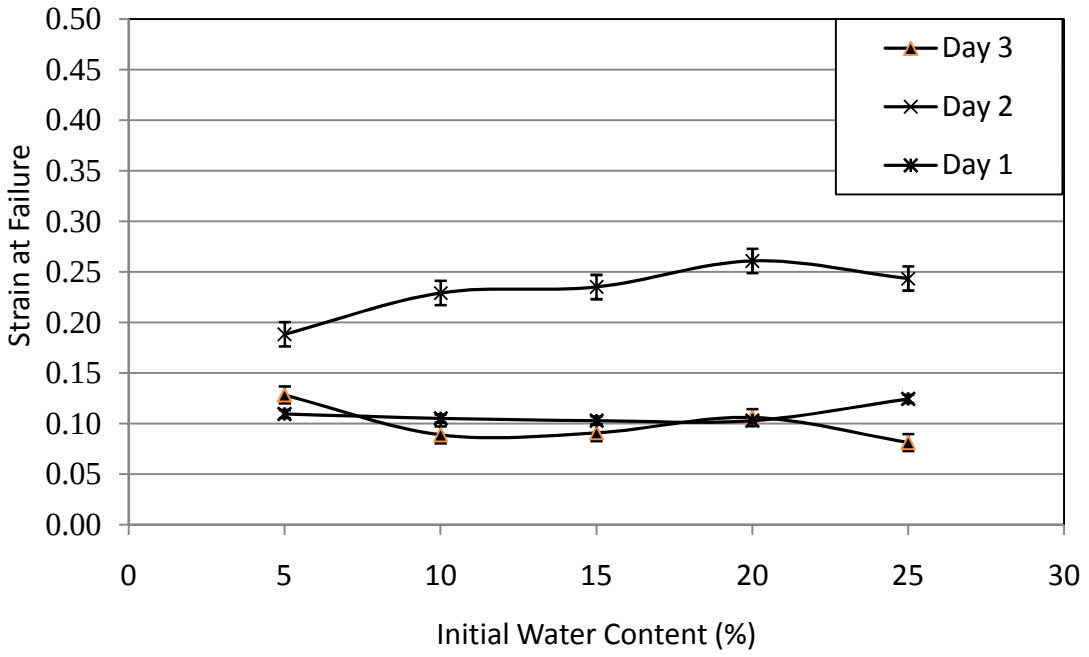

Figure 36: Deformation pattern in silty clay soil based on water content with time

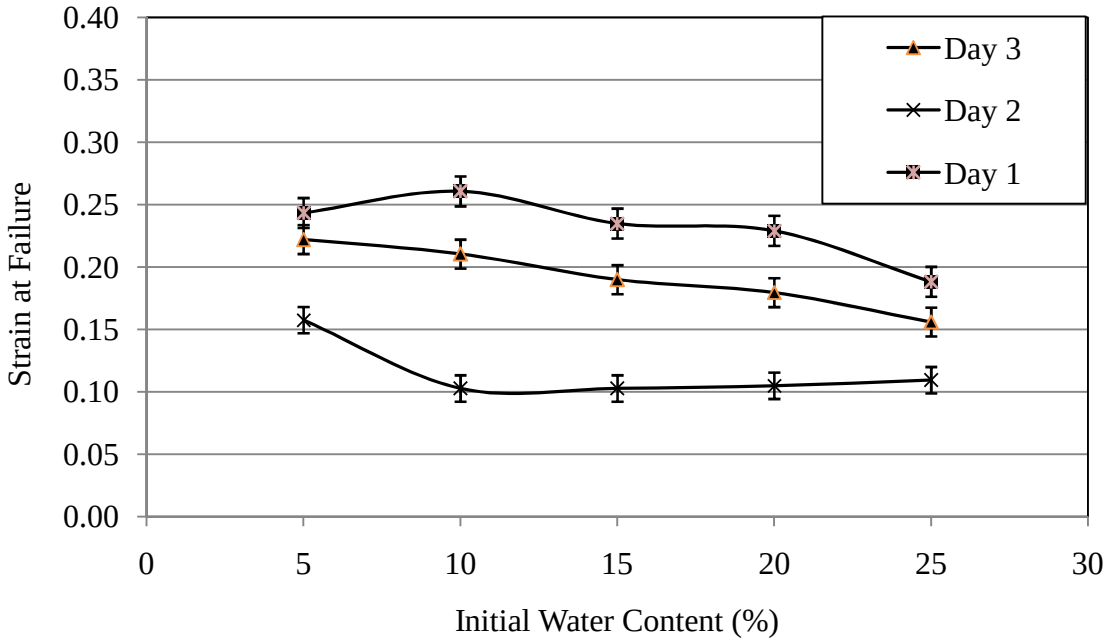

Figure 37: Deformation pattern in sandy silty clay soil based on water content with time

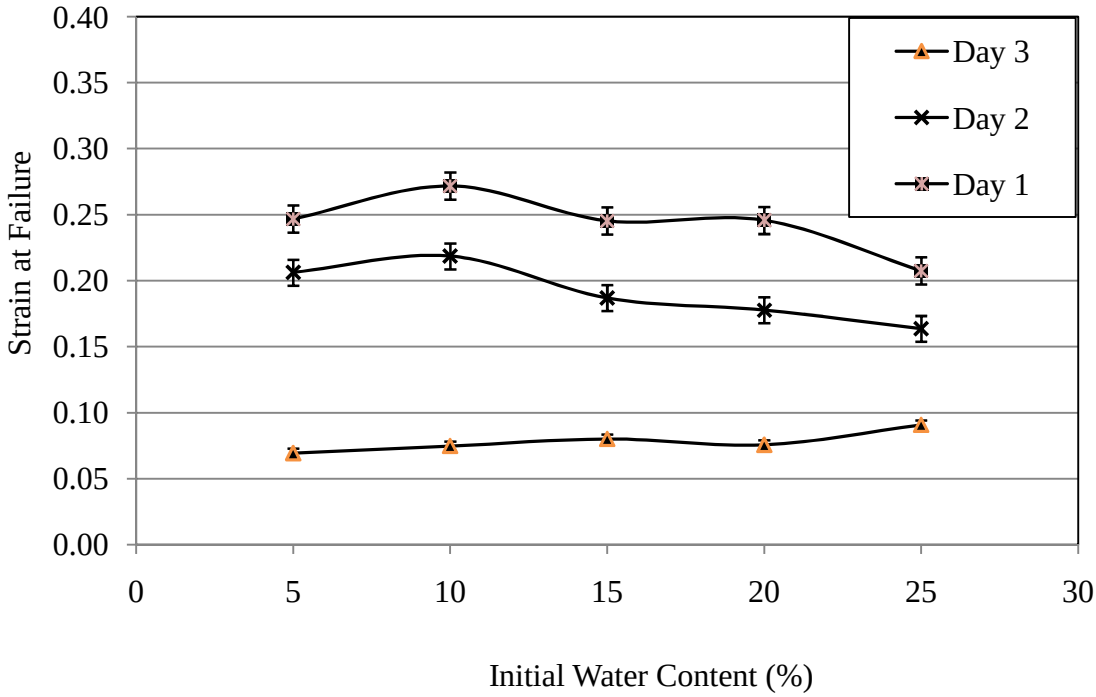

Figure 38: Deformation pattern in sandy clay soil based on water content with time

greater resistance to desiccation than sandy silty clay and sandy clay soils therefore, the least desiccation occurred in the following order; silty clay soil < sand clay soil < sandy silty clay soil.

7.5.3 Comparisons of strength parameters

A major component of this research was a summation and analysis of the results from the unconfined compressive tests and direct shear tests in order to determine a relationship between cohesion, angle of internal friction, and shear strength of these soils. It was postulated in the proposal of this research that increased cohesion in the soil could be achieved with EPS treatment, which will in turn increase the shear strength of the soil. Subsequently, increased shear strength of the soil means a reduction in the propensity of each treated soil to generate dust. As a general observation in EPS treated soils, increase in cohesion occurred with a decrease in the angle of internal friction and an increase in the shear strength of the soils. For microbial treated and control soil samples, cohesion remained relatively constant with a decrease in shear strengths and angles of internal friction.

Focusing mainly on the soil strength and cohesion values obtained, Figure 50 shows that soil strength increased from 37 to 45 kN/m^2 while cohesion increased from 15 to 28 kN/m^2 at increasing EPS concentrations for silty clay soil with slight decrease occurring at EPS concentrations of 20 and 25 mL/g of soil. In sandy silty clay soil (Figure 51), the soil strength obtained was 48 kN/m^2 while the cohesion was 27 kN/m^2, and for sandy clay soil (Figure 52), soil strength obtained was 42 kN/m^2 and cohesion was 24 kN/m^2. In comparing these values with soil samples treated with microbial broth and DI water, soil strength decreased from 37 to 28 kN/m^2 in silty clay soil while cohesion remained constant at approximately 15 kN/m^2 (Figures 53, 54 and 55). As shown in Figure 56, 57, and 58, similar results were obtained for water treated sandy silty clay and sandy clay soils as well.

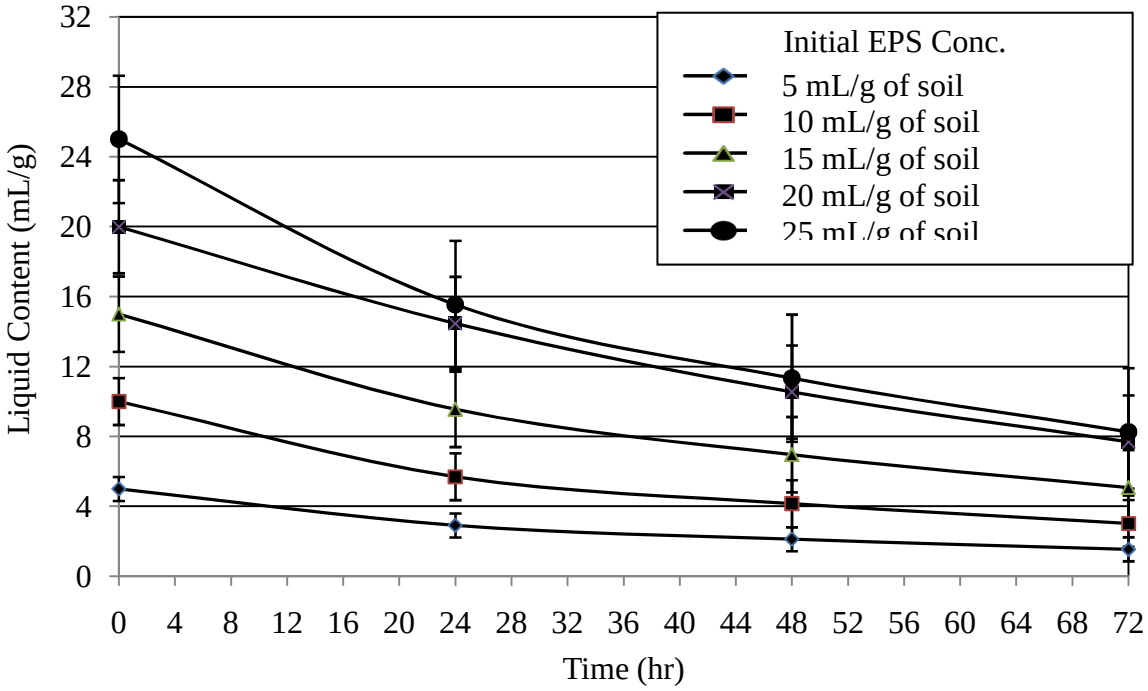

Figure 39: Liquid content with time during desiccation of silty clay soil containing EPS-CM at various concentrations

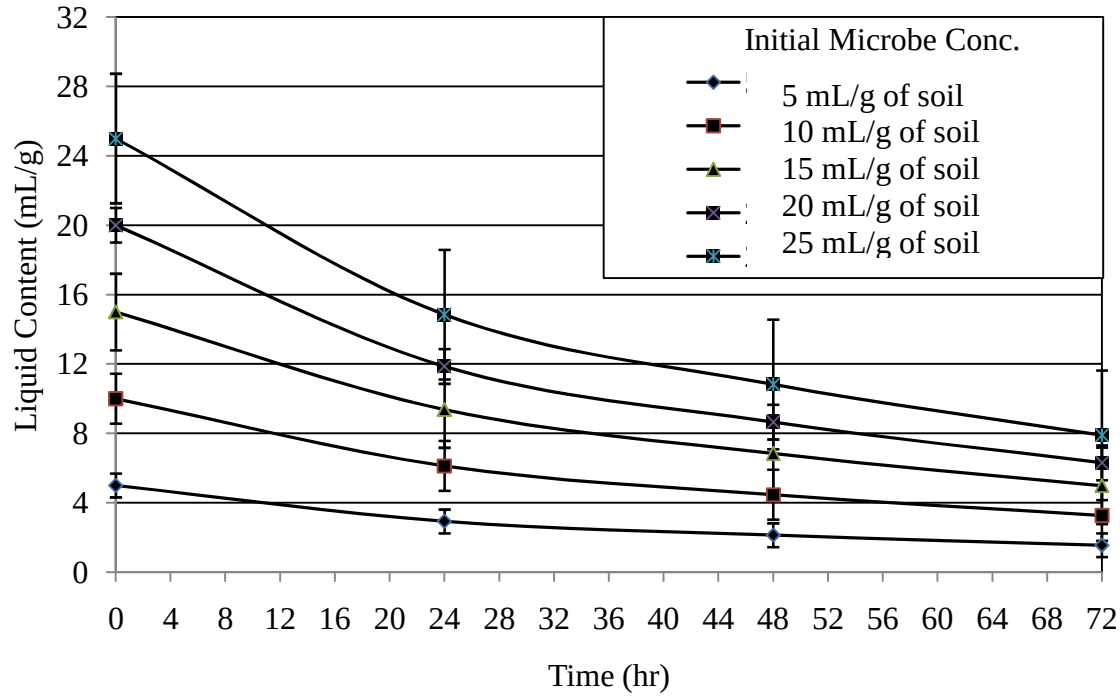

Figure 40: Liquid content with time during desiccation of silty clay soil containing microbe at various concentrations

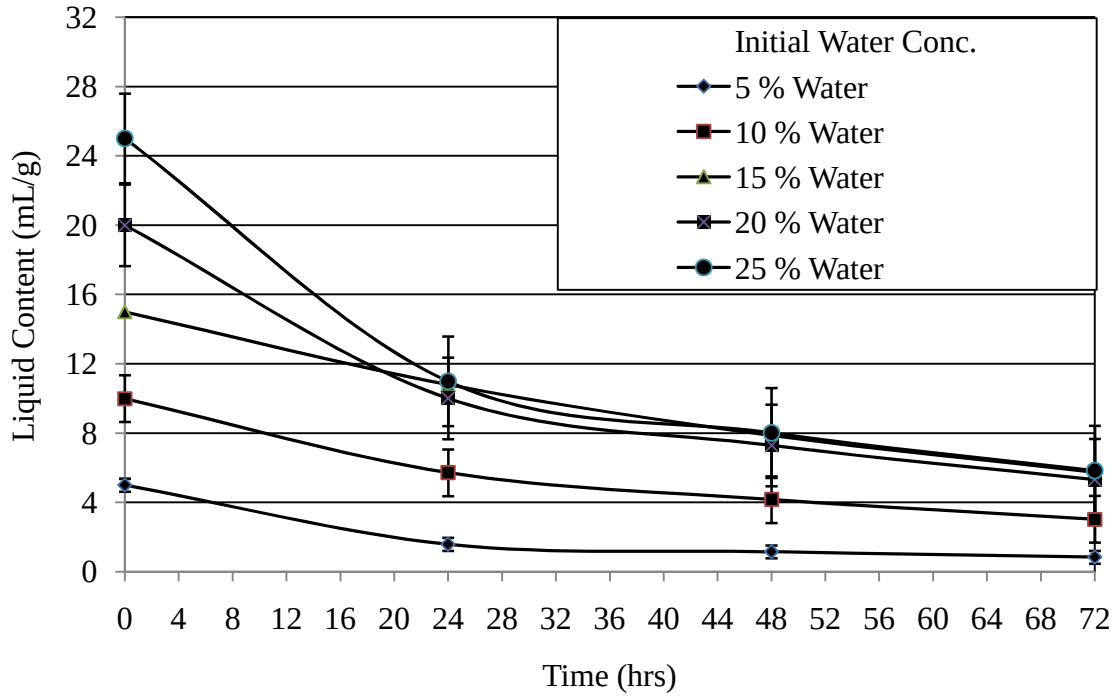

Figure 41: Liquid content with time during desiccation of silty clay soil containing water at various concentrations

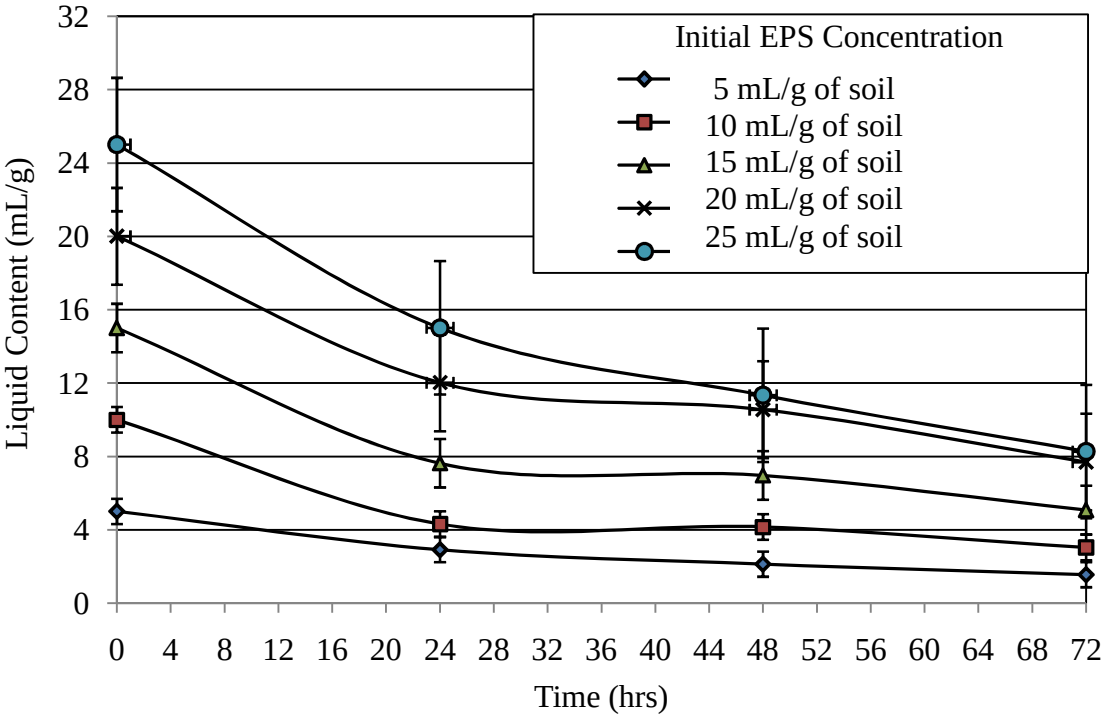

Figure 42: Liquid content with time during desiccation of sandy silty clay soil containing EPS at various concentrations

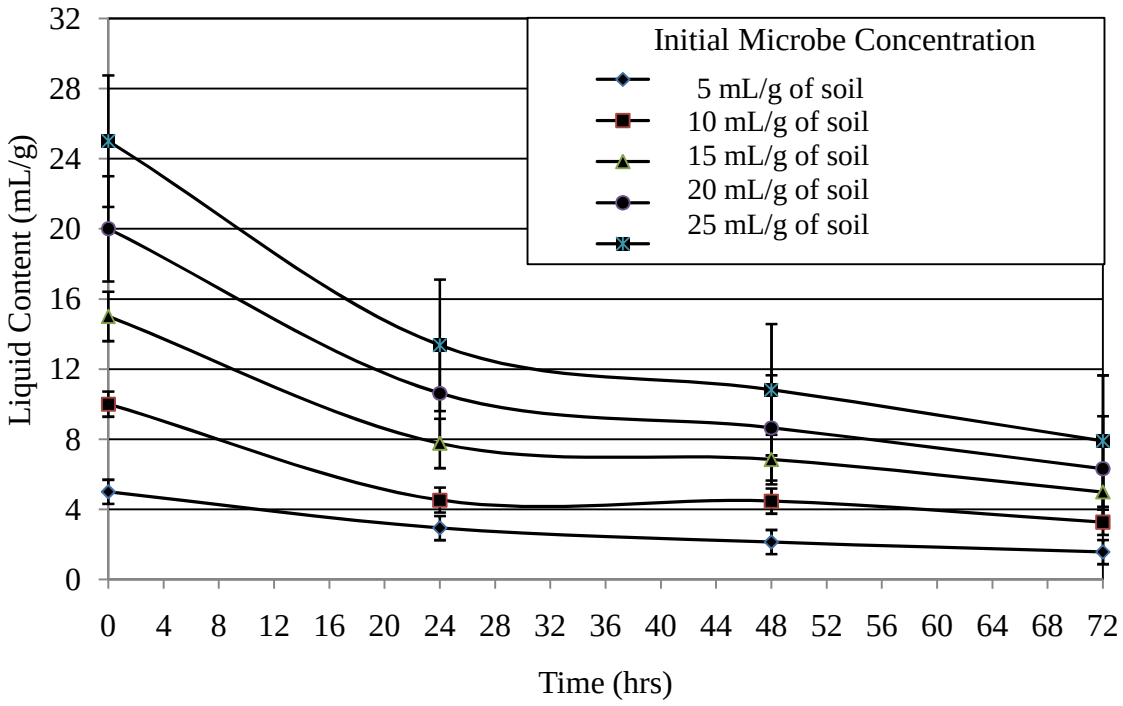

Figure 43: Liquid content with time during desiccation of sandy silty clay soil containing microbe at various concentrations

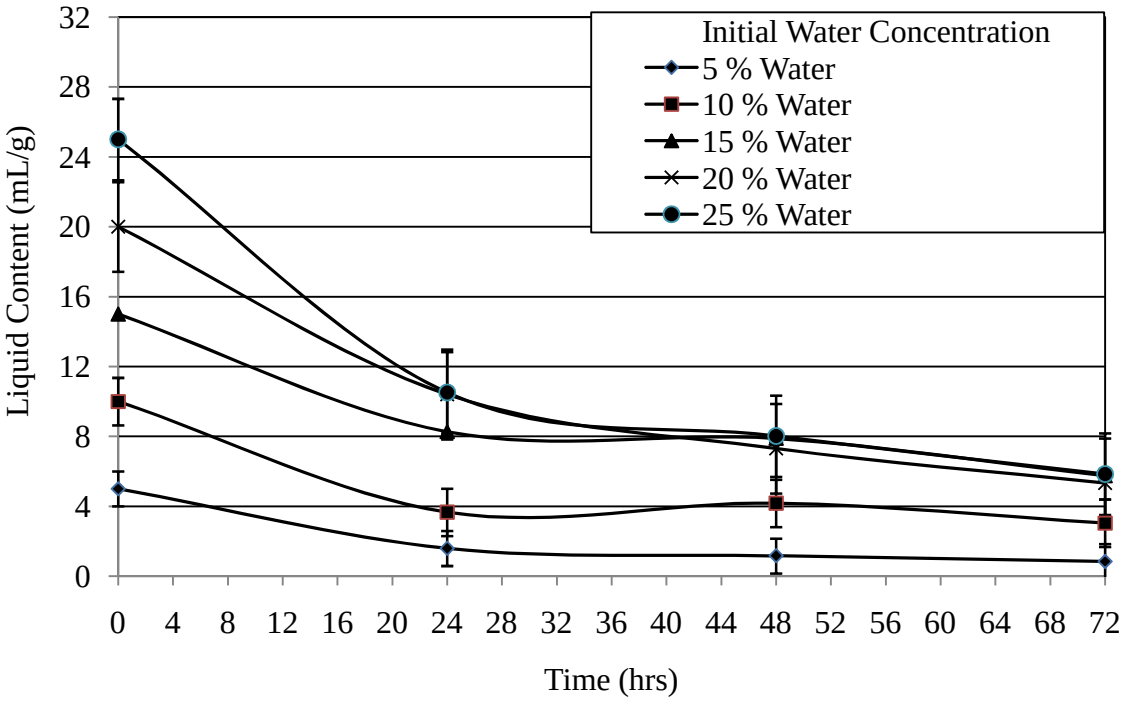

Figure 44: Liquid content with time during desiccation of sandy silty clay soil containing water at various concentrations

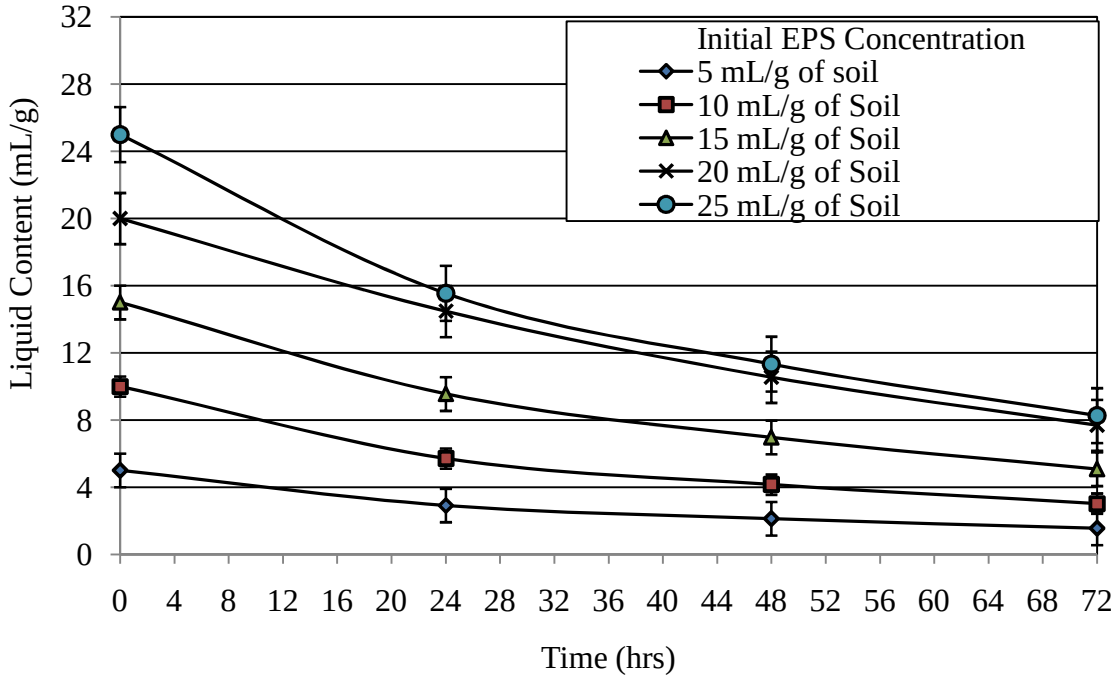

Figure 45: Liquid content with time during desiccation of sandy clay soil containing EPS-CM at various concentrations

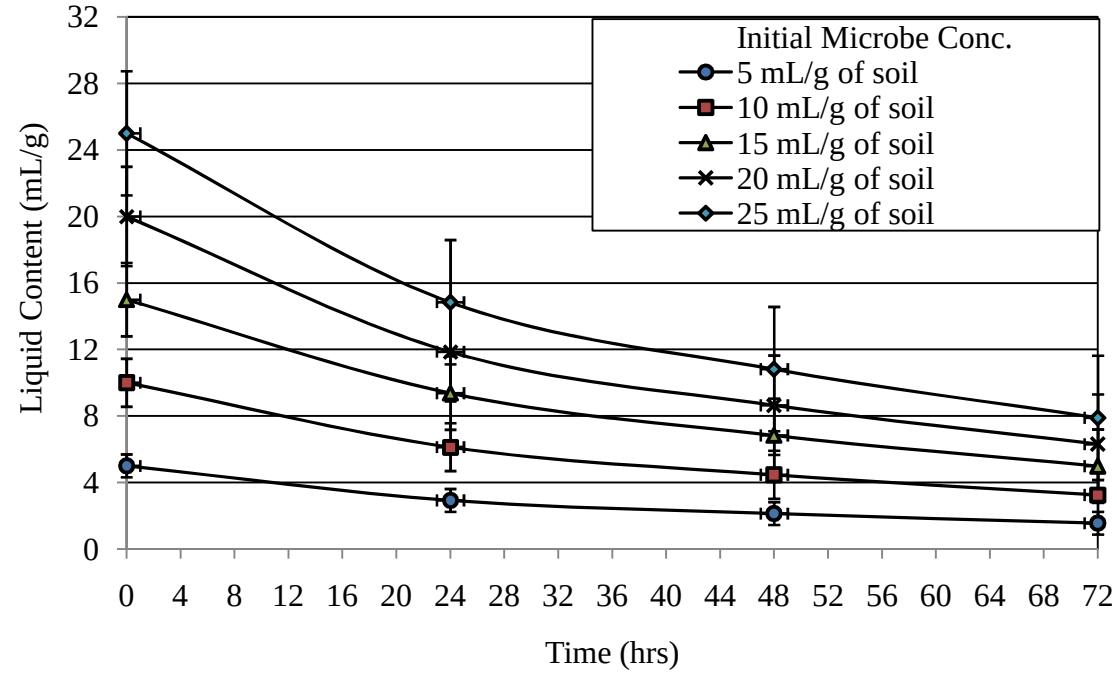

Figure 46: Liquid content with time during desiccation of sandy clay soil containing microbe at various concentrations

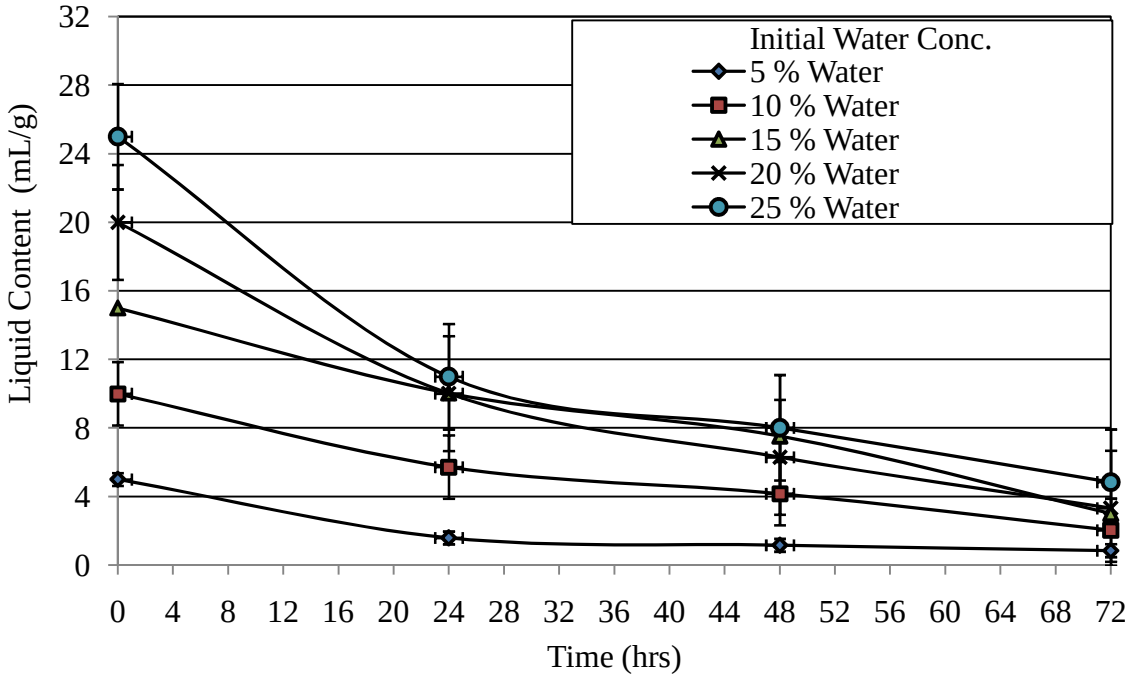

Figure 47: Liquid content with time during desiccation of sandy clay soil containing water at various concentrations

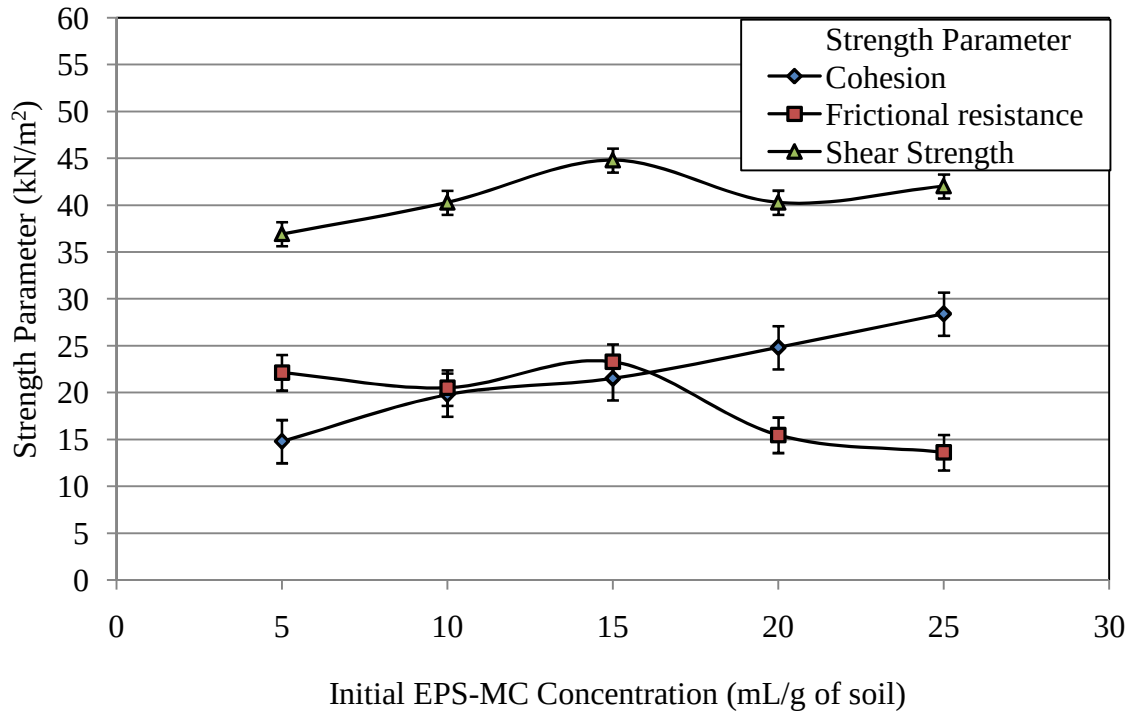

Figure 48: Strength comparisons in silty clay soil with EPS-CM treatment

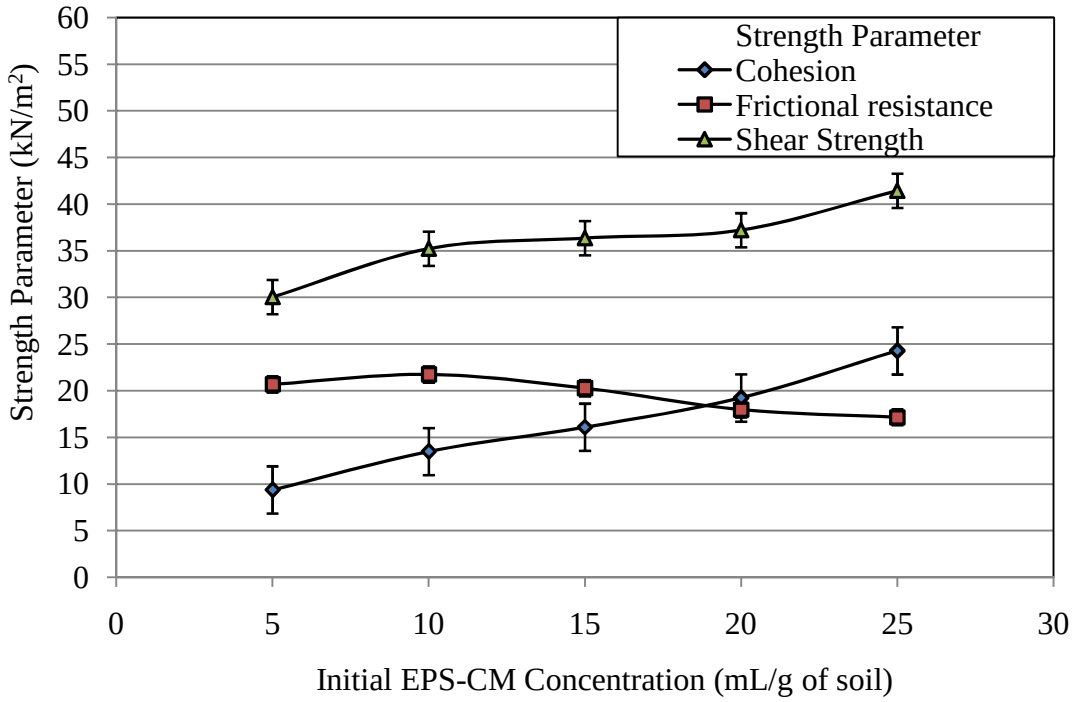

Figure 49: Strength comparisons in sandy clay soil with EPS-CM treatment

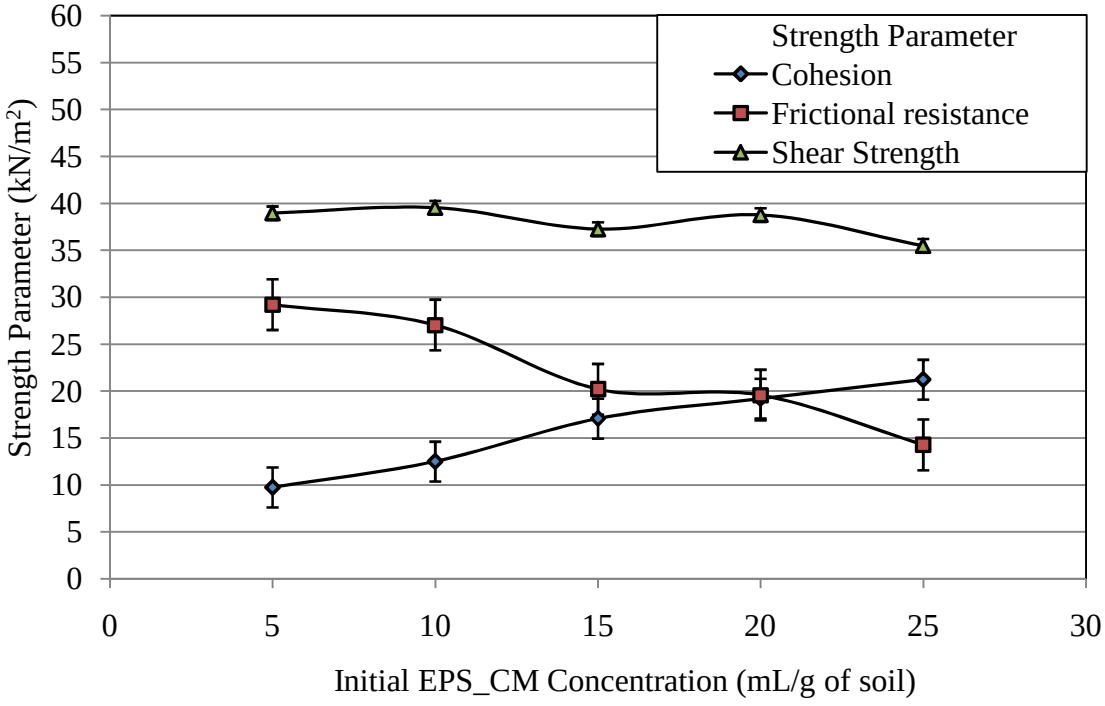

Figure 50: Strength comparisons in sandy silty clay soil with EPS-CM treatment

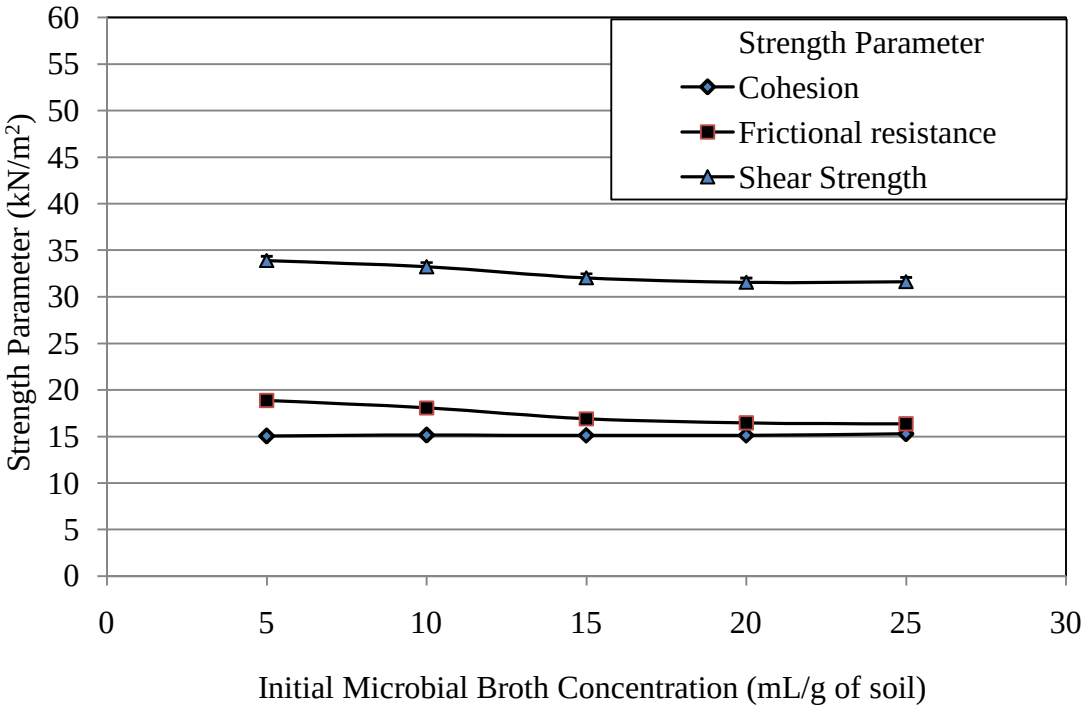

Figure 51: Strength comparisons in silty clay soil with microbe treatment

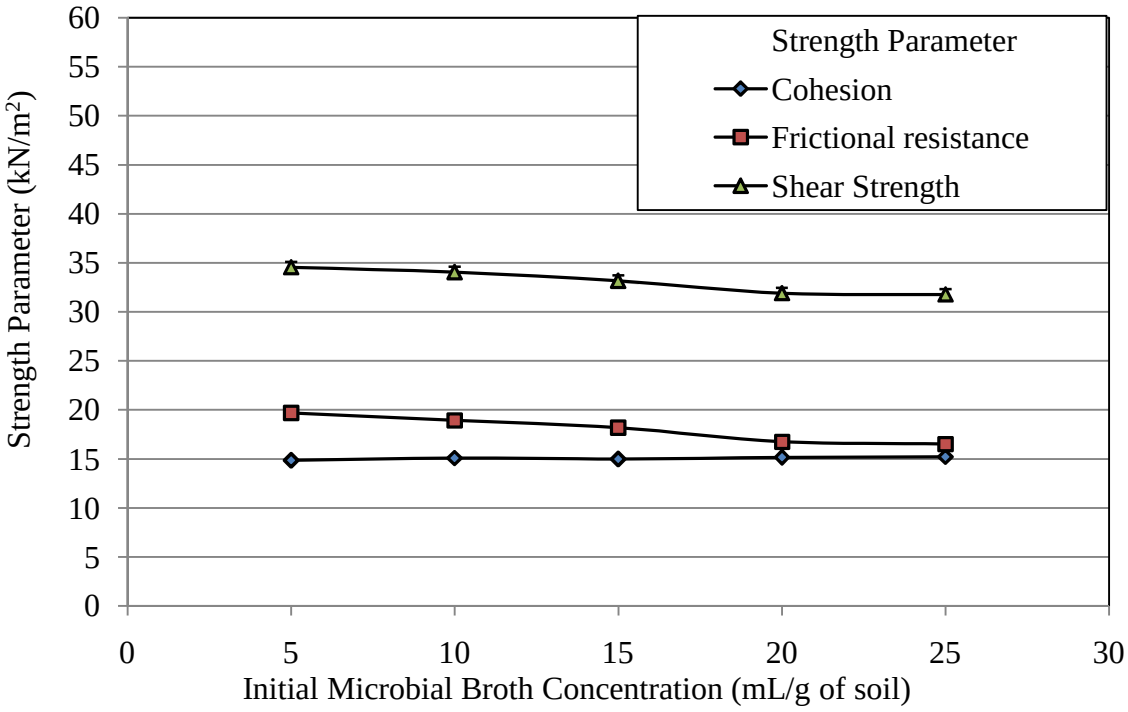

Figure 52: Strength comparisons in sandy clay soil with microbe treatment

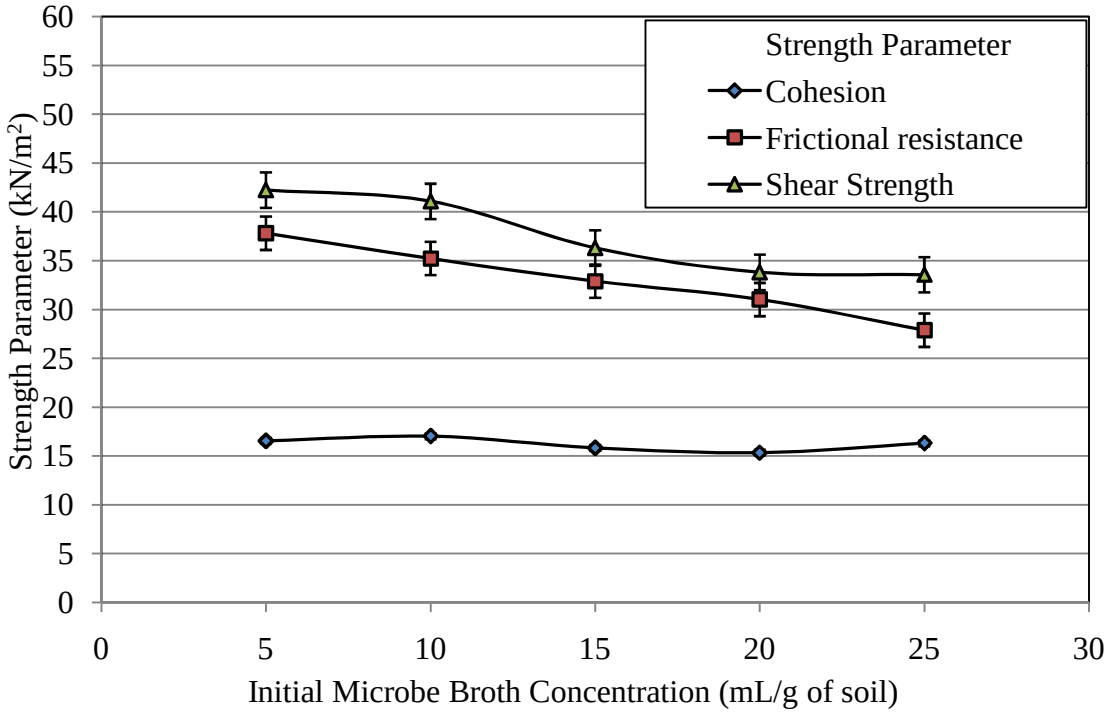

Figure 53: Strength comparisons in sandy silty clay soil with microbe treatment

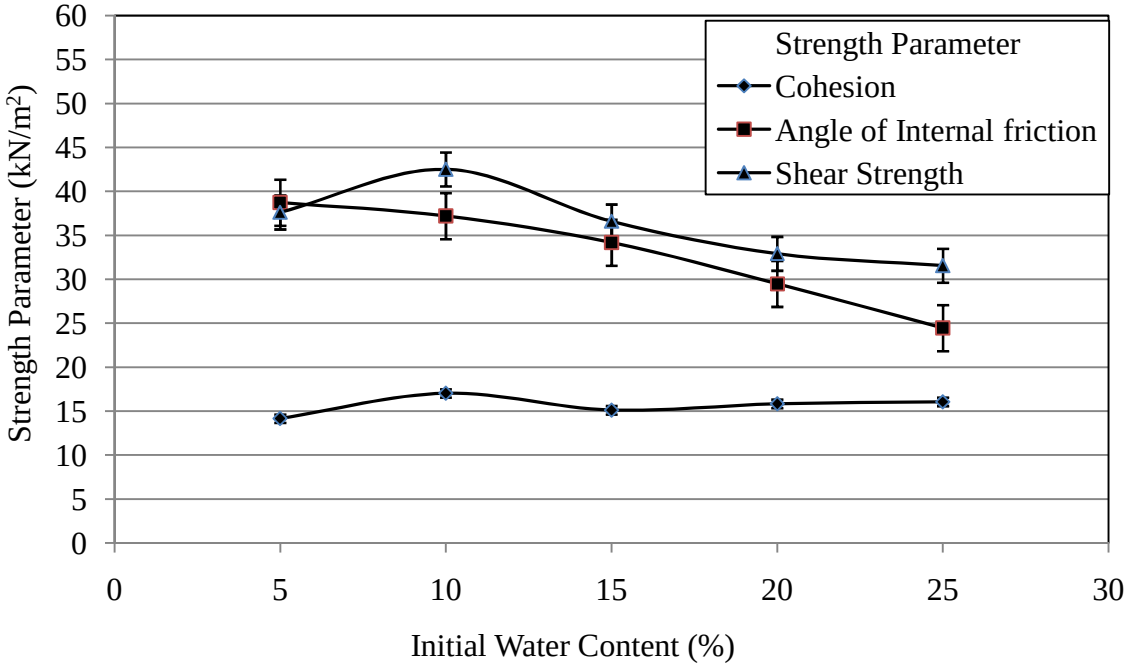

Figure 54: Strength comparisons in silty clay soil with water

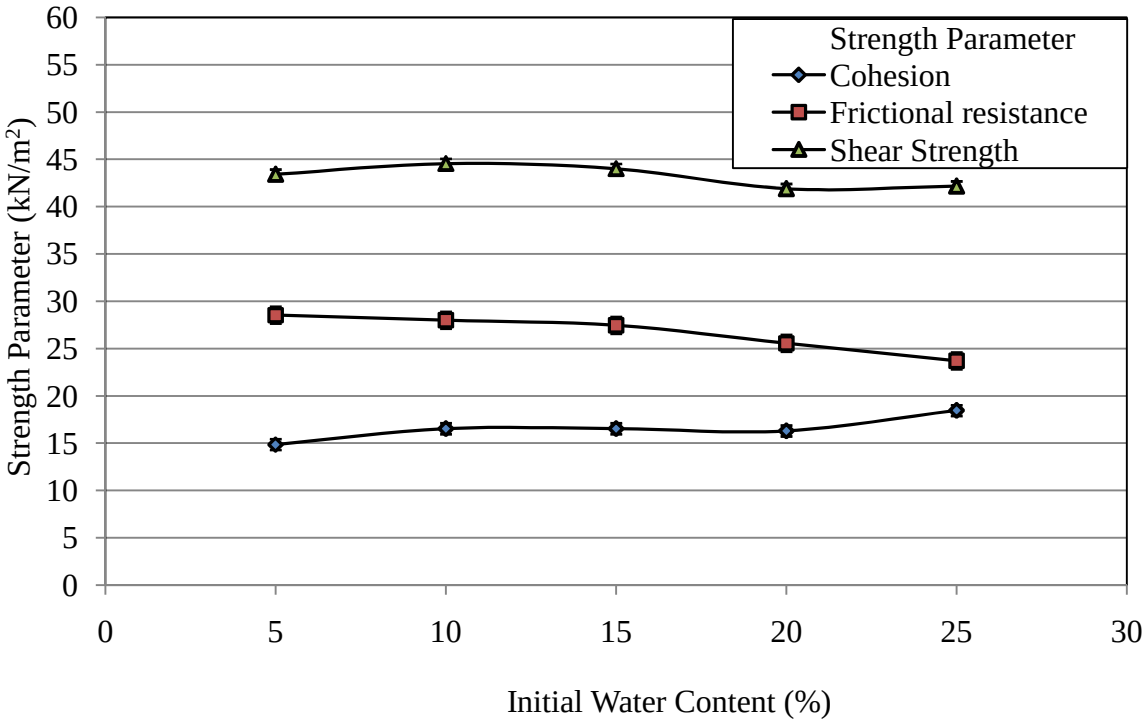

Figure 55: Strength comparisons in sandy clay soil with water

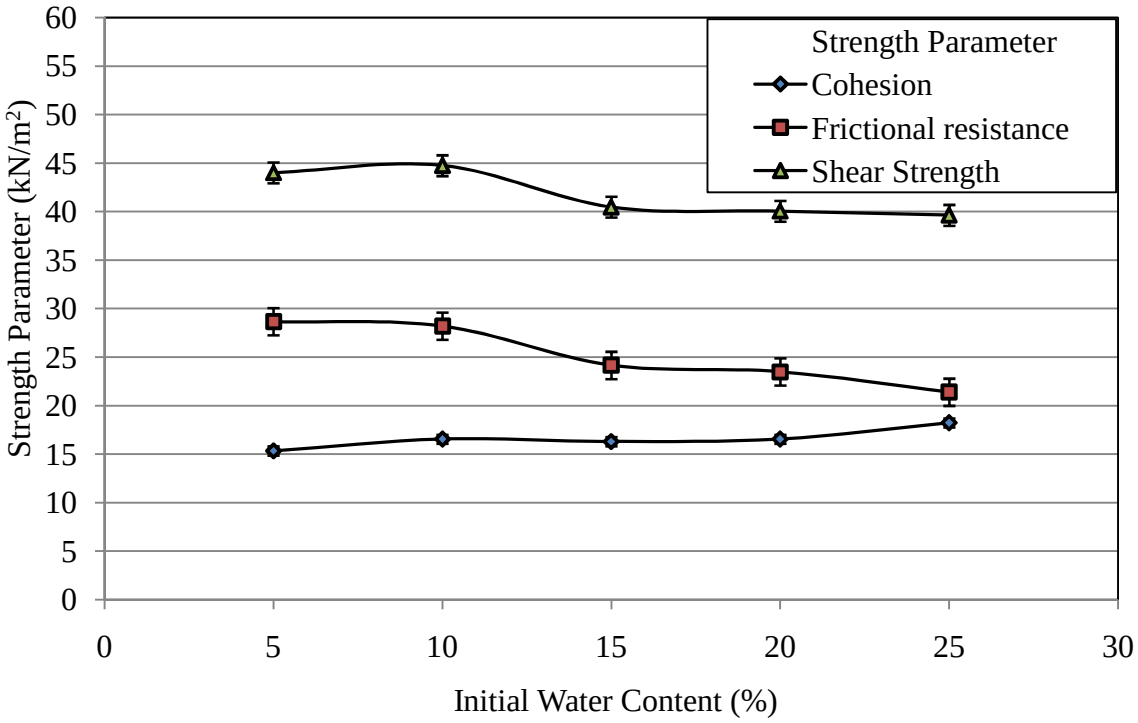

Figure 56: Strength comparisons in sandy silty clay soil with water

7.5.4 Fluorescence imaging of treated and untreated soil samples

Fluorescence microscopy of various segments of the treated and untreated soil samples was performed at 24 hr intervals for 72 hr to show the spatial distribution of EPS-CM in all the soils treated with EPS solution (5 to 25 mL/g), microbial broth (5 to 25 mL/g), and the control samples. Part of the objective of these tests was to show the ability of the *Arthrobacter viscosus* to produce EPS in the soil under laboratory conditions as well. Using a magnification of 4x, images of raw EPS and soil samples are presented in Figure 57.

As presented in Figures 58, 60, and 62 it can be observed that at higher EPS-CM concentrations, soil particles form visible aggregates as s result of the EPS-CM flocculation over the particles. It can also be seen that no EPS-CM flocculation occurs in control samples (Figures 58 – 63 p, q, and r) and in soils treated with microbial broth, it is can be inferred that enough EPS is produced to enhance soil aggregation (Figures 59, 61, 63).

From these results, it is evident that a good a spatial distribution of EPS-CM in the soil samples can mainly be achieved by a direct application of the extracted EPS-CM into the soil rather than applying the microbial broth. This is because there are many other factors in the soil that can inhibit the effective production of EPS in the soil by *A. viscosus* despite their ability to survive in unfavorable environment therefore, genetically engineering the microorganism might be necessary to achieve a meaningful results but there are caveats associated with this process.

Similar to the results obtained in this research, previous studies by Farrell et al. (1967) have shown that the amount of water content in soil affects the axial strain under compression and computations from measured stress-strain relationships can be used to

estimate the deformation. The treatment of soil samples with EPS-CM and microbial broth in this present research was aimed at improving the water retention capacity of the soil with the hope that increase water content in the soil will result in decreased deformation.

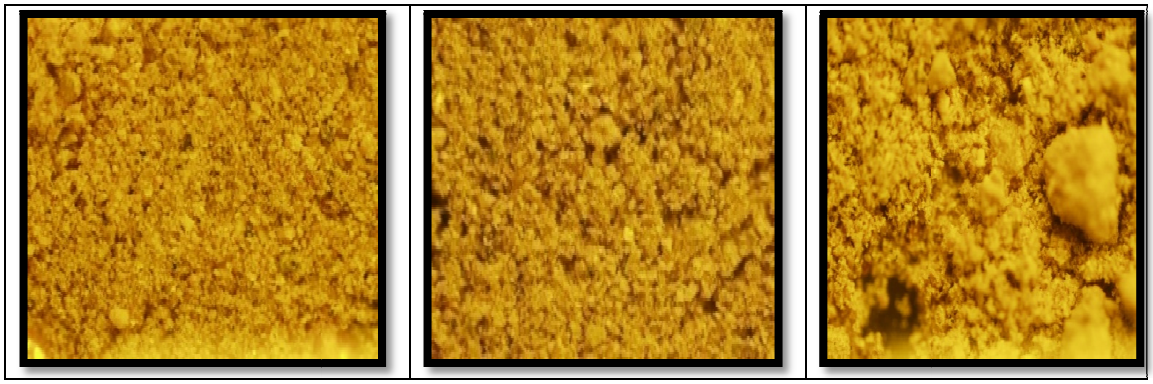

(a) Untreated SCSoil (b) Untreated SSCSoil (c) Untreated SDCSoil

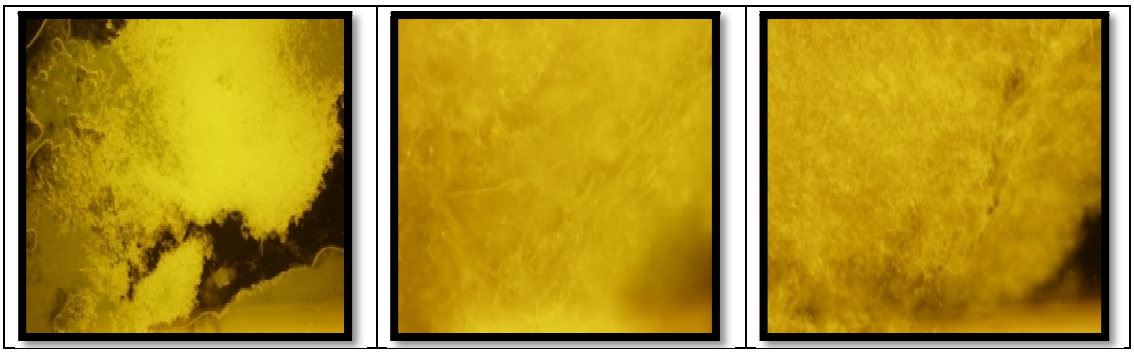

(d) Moist EPS (e) EPS @ 10x magnification (f) EPS @ 4x magnification

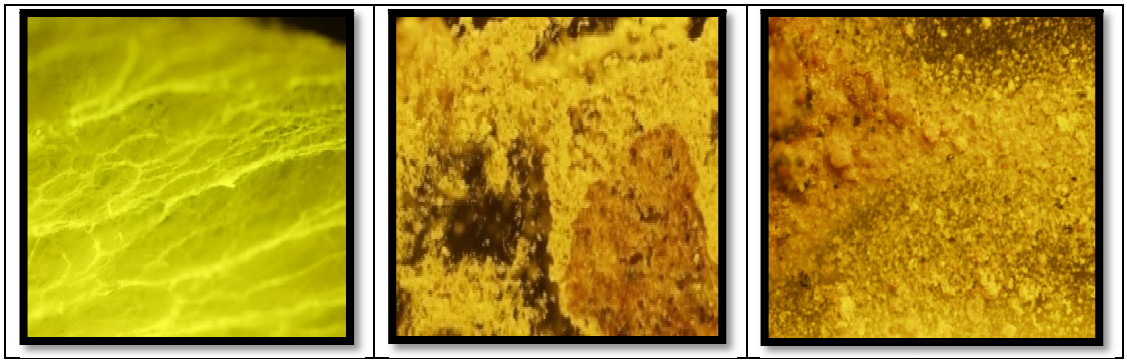

(g) EPS strands (h) Raw EPS in test soil (i) Moist untreated soil under light

Figure 57: Fluorescence microscope images of test samples

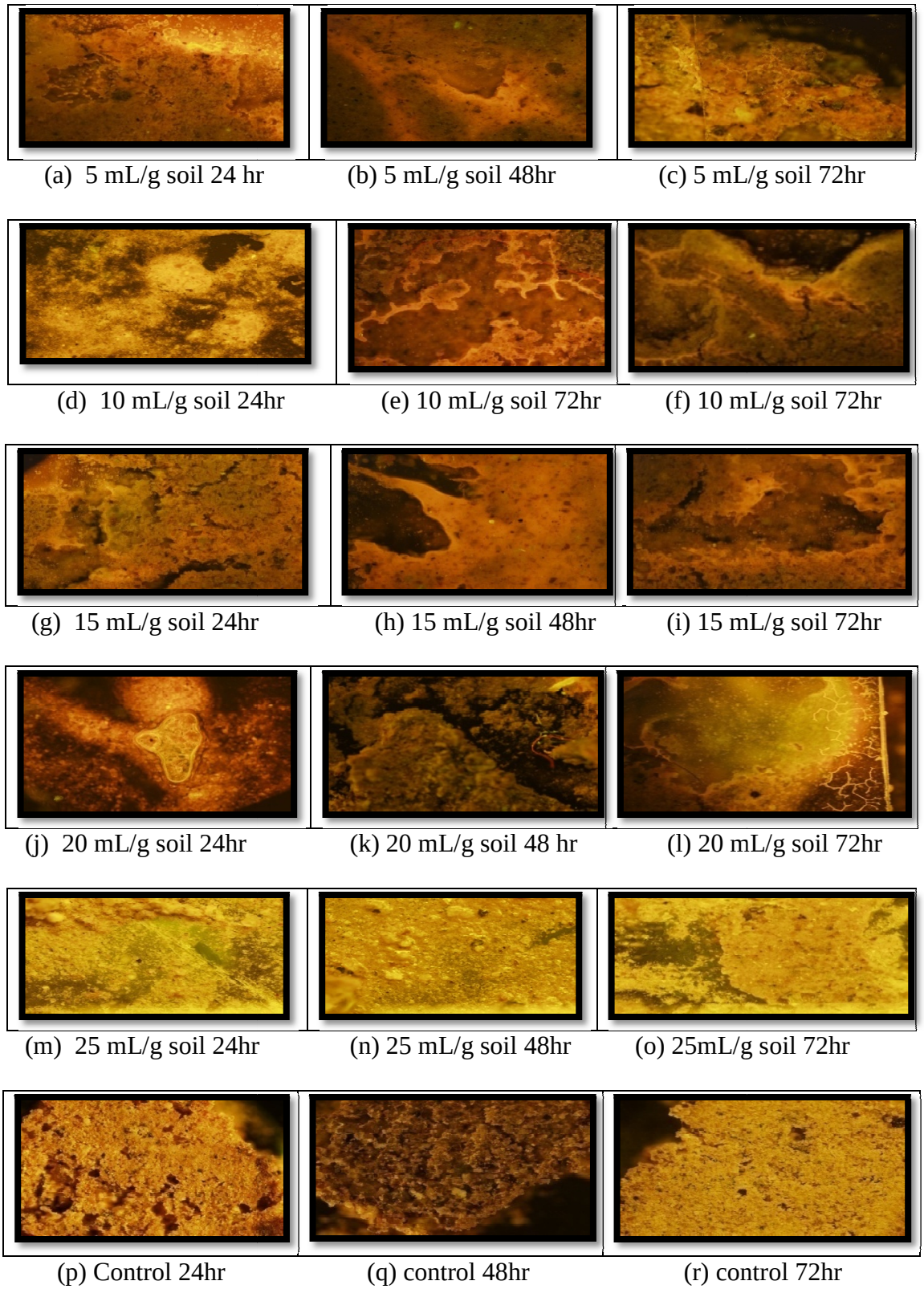

Figure 58: Fluorescence microscope images of silty soil samples treated with EPS

(a) 5 mL/g soil 24 hr (3.09) (b) 5 mL/g soil 48hr (4.79) (c) 5 mL/g soil 72hr (3.11)

(d) 10 mL/g soil 24hr (2.43) (e) 10 mL/g soil 48hr (6.3) (f) 10 mL/g soil 72hr (2.4)

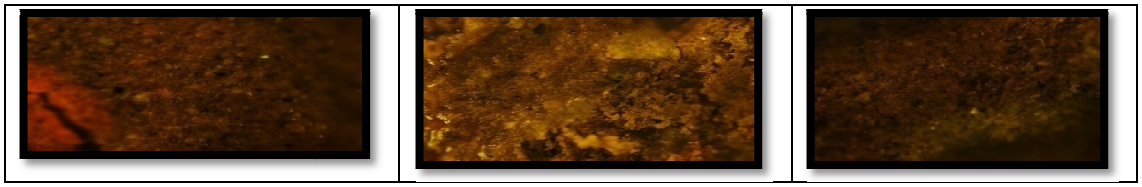

(g) 15 mL/g soil 24hr (4.7) (h) 15 mL/ microbe 48hr (7.7) (i) 15 mL/g soil 72hr (4.9)

(j) 20 mL/g soil 24hr (3.3) (k) 20 mL/g soil 48 hr (2.7) (l) 20 mL/g soil 72hr (3.5)

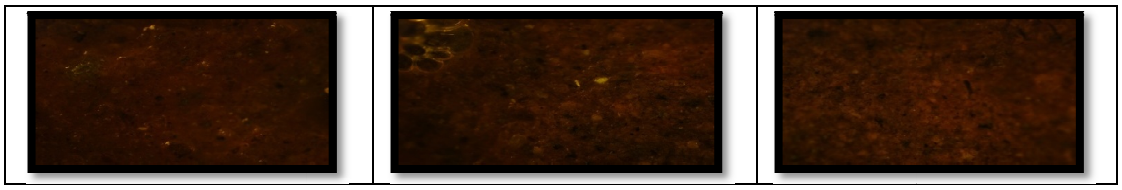

(m) 25 mL/g soil 24hr (1.9) (n) 25 mL/g soil 48hr (2.8) (o) 25mL/g soil 72hr (2.0)

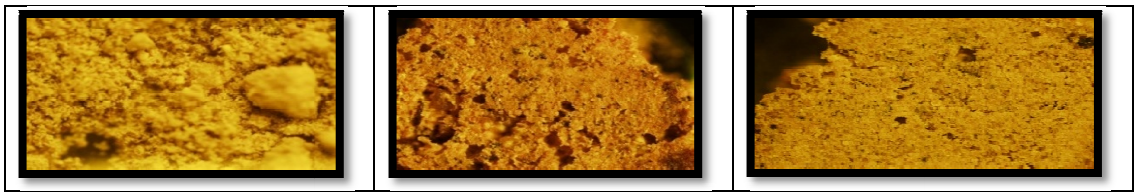

(p) Control 24hr (q) control 48hr (r) control 72hr

Figure 59: Fluorescence microscope images of silty clay soil samples treated with microbe; Numbers in parenthesis indicate EPS concentration (mg/mg of soil) measured at time *t*.

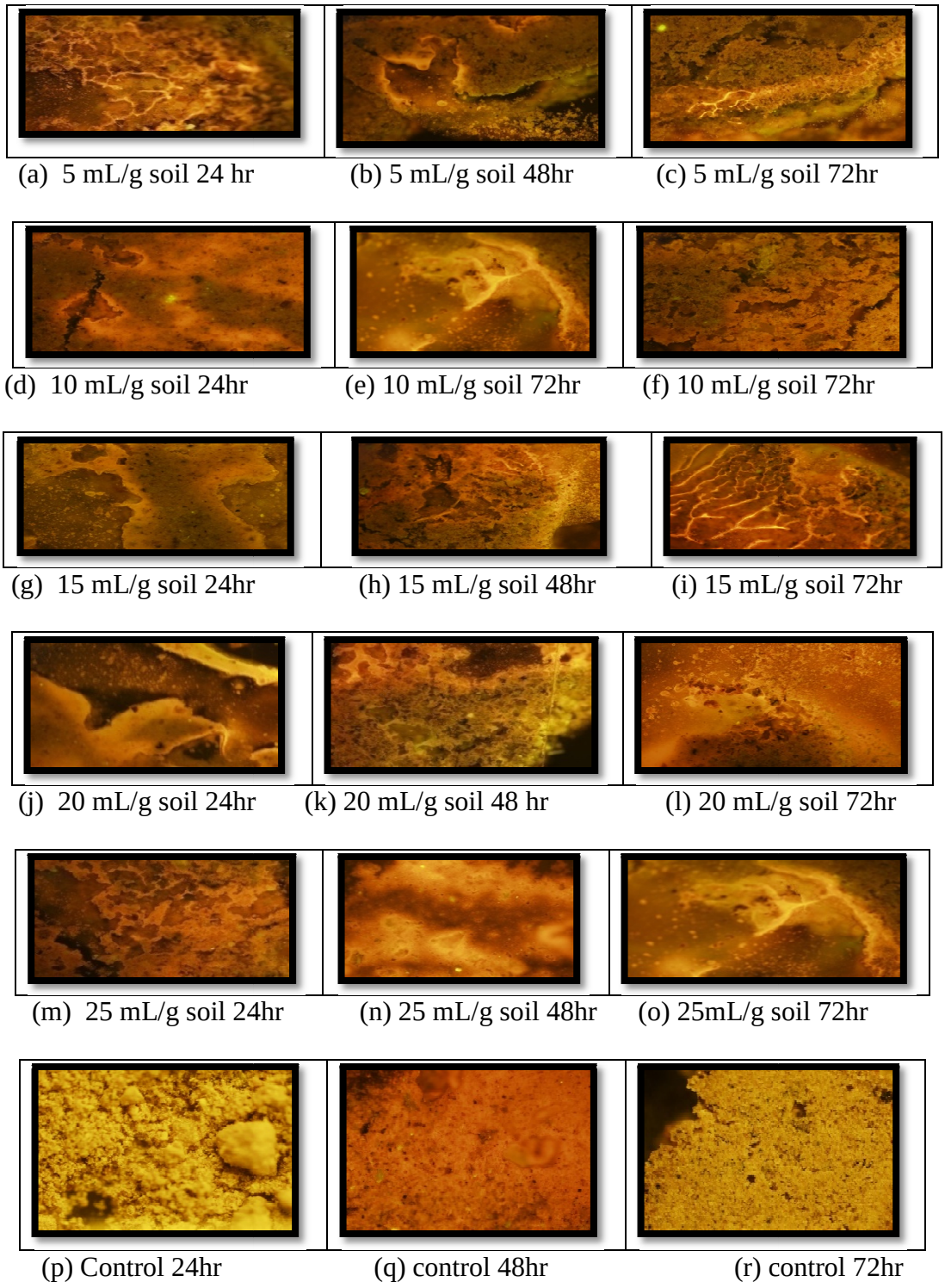

Figure 60: Fluorescence microscope images of sandy clay soil samples treated with EPS

(a) 5 mL/g soil 24 hr (1.5) (b) 5 mL/g soil 48hr (2.5) (c) 5 mL/g soil 72hr (1.8)

(d) 10 mL/g soil 24hr (1.3) (e) 10 mL/g soil 72hr (2.3) (f) 10 mL/g soil 72hr (2.0)

(g) 15 mL/g soil 24hr (1.6) (h) 15 mL/g soil 48hr (1.6) (i) 15 mL/g soil 72hr (2.1)

(j) 20 mL/g soil 24hr (1.4) (k) 20 mL/g soil 48 hr (3.3) (l) 20 mL/g soil 72hr (1.8)

(m) 25 mL/g soil 24hr (1.7) (n) 25 mL/g soil 48hr (1.7) (o) 25mL/g soil 72hr (1.4)

(p) Control 24hr (q) control 48hr (r) control 72hr

Figure 61: Fluorescence microscope images of sandy clay soil samples treated with microbe. Numbers in parenthesis indicate EPS concentration (mg/mg of soil) measured at time *t*

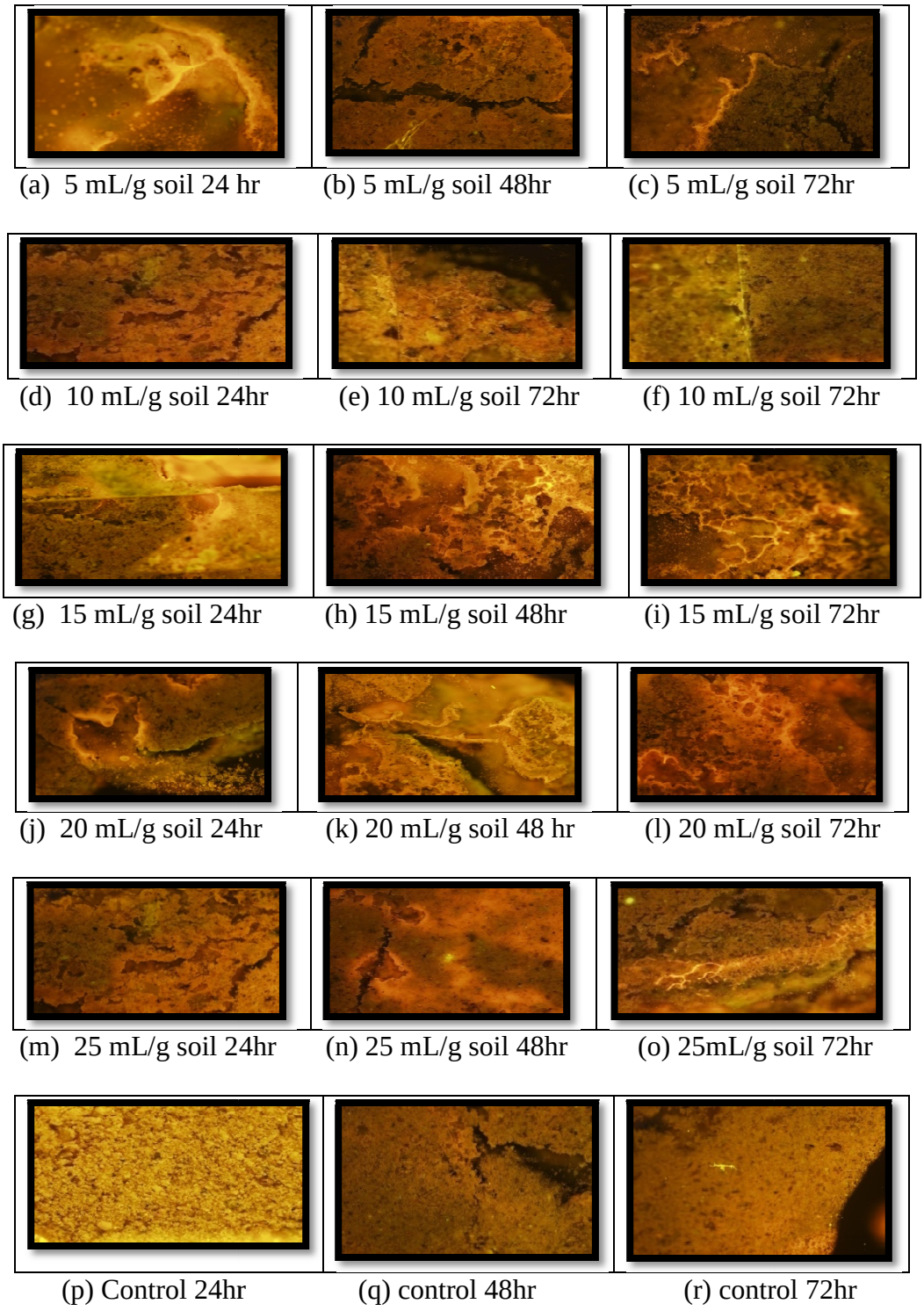

Figure 62: Fluorescence microscope images of sandy silty clay soil samples treated with EPS_CM

(a) 5 mL/g soil 24 hr (2.7) (b) 5 mL/g soil 48hr (1.0) (c) 5 mL/g soil 72hr (1.4)

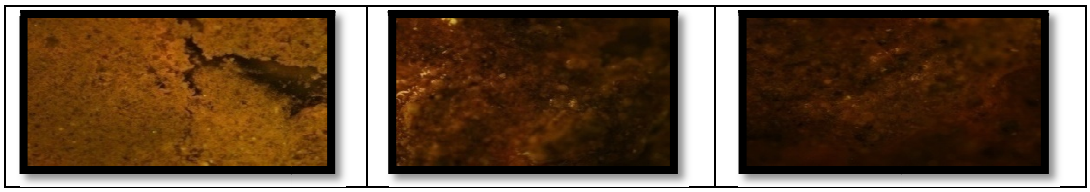

(d) 10 mL/g soil 24hr (1.8) (e) 10 mL/g soil 72hr (1.7) (f) 10 mL/g soil 72hr (1.5)

(g) 15 mL/g soil 24hr (1.2) (h) 15 mL/g soil 48hr (1.4) (i) 15 mL/g soil 72hr (1.8)

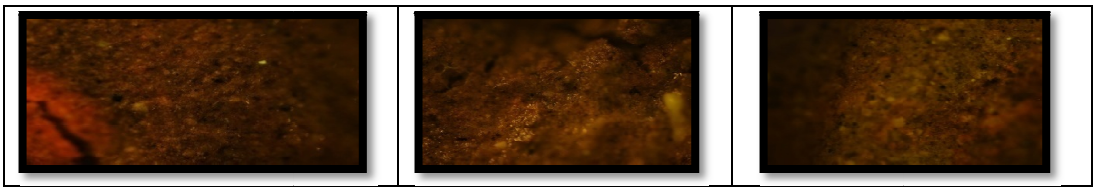

(j) 20 mL/g soil 24hr (1.6) (k) 20 mL/g soil 48 hr (2.5) (l) 20 mL/g soil 72hr (1.5)

(m) 25 mL/g soil 24hr (2.1) (n) 25 mL/g soil 48hr (1.7) (o) 25mL/g soil 72hr (1.7)

(p) Control 24hr (q) control 48hr (r) control 72hr

Figure 63: Fluorescence microscope images of sandy silty clay soil samples treated with microbe. Numbers in parenthesis indicate EPS-CM concentration (mg/mg of soil) measured at time *t*

The results so far confirm this theory while it also shows that unconfined compressive strength of soils decreases with increasing amount of water content. Therefore, it was necessary to determine the threshold at which increased amount of EPS-CM resulted in decreased compressive strength and results obtained show that this occurs after soil treatment with more than 15 mL/g of EPS-CM in soil. This result is consistent with previous work on sediment stability (Yallop et al. 2000), where a positive correlation between the amount of biofilms and sediment stability was obsereved. Previous studies by Causarano (1993) reported a decrease in soil compressive strength with increasing water content of 15 g/100g of soil as well. On the other, an explanation for the slight improvement in soil strength observed in soil samples treated with microbial broth could the adhesion of the bacterial EPS-CM to the soil intergranular surfaces, which enhances that soil resistance to deformation (Dade et al. 1990).

Soil cohesion, which is one of the critical component in the results obtained in this research, has been reported to be function of volumetric water content as well (Matsushi and Matsukura, 2006; Mohan et al. 1999; Abu-Hejleh and Znidarcic, 1999; Francois and Royer-Carfagni, 2005). In their effort to establish a relation between changes in soil cohesion with moisture content in sand soil and silt soil, Matsushi and Matsukura (2006) were able to show that increase in moisture content resulted in shear strength decrease, and hence, a decrease in cohesive strength. Similar conclusions were reported by Bonala and Reddy (1999). However, Karalis (2003) has shown that water loss in soft cohesive soils produces in loss of cohesion in soils. It has been reported that soil friability, another component of this research similar to soil strength (Watts and Dexter 1998; Dexter, 2004), depends on soil water content, plasticity, and aggregation. Results obtained from the relationship between soil treatment and liquid loss can be used

to predict the friability index of each soil, which can be correlated with the potential of dust generation as well.

CHAPTER 8: CONSISTENCY OF OBTAINED RESULTS WITH CONCEPTUAL MODEL

In chapter 2, models were developed to describe the results of EPS production in soil by *A. viscosus* and its effect on soil porosity. In chapter 7, experimental results of the relationship between soil treatment and soil strength parameters such as cohesion, frictional resistance, strain, and shear strength were obtained from geotechnical tests. To further analyze these experimental results using the conceptual models developed in chapter 2, more comparisons between these soil strength parameters, were carried out to determine their relationships based on soil types and treatments. These experimental results are consistent with the theoretical results of these models. In the following sections, the relationships between these soil strength parameters will be explored.

8.1 The comparisons of strength parameters and effective porosity with time in silty clay soil

The experimental result of the relationship between frictional resistance, cohesion, and effective porosity in silty clay soil is shown in Figure 66 and 67. In comparing the frictional resistance in the soil sample with time based on treatment, the result shows that this strength parameter decreases with time and concentration with treatment and this is in agreement with Figure 1 and 2. At 24 hr, the frictional resistance decreased from 27 kN/m^2 at 5 mL/g microbial content to 13 kN/m^2 at 25 mL/g microbial content; at 48 hr, the frictional resistance decreased from 22 kN/m^2 at 5 mL/g microbial content to 14 kN/m^2 at 25 mL/g treatment of soil; at 72 hr, the frictional resistance

decreased from 18 kN/m^2 at 5 mL/g microbial content to 13 kN/m^2 at 25 mL/g microbial content. In the determination of the soil cohesion based on treatment and time, it is shown that increased microbial content, which means increased EPS production, resulted in increased cohesion.

In the determination of effective porosity in silty clay soil with time, it is shown that effective porosity generally decreases with increasing time and microbial content in soil. This can be attributed to the gradual increase in the amount of EPS produced in the soil by the microorganisms. As already reported in this research, the continuous production of EPS in the soil matrix by *A. viscosus* with time, results in the filling up of intergranular pores in the soil. This in effect, reduces the effective porosity of the soil. From this result, it can be inferred that a reduction in the number of intergranular pores will mean more compaction in the soil, which will ultimately increase the cohesion in the soil as indicated.

8.2 The comparisons of strength parameters and effective porosity with time in sandy clay soil

The experimental result of the relationship between frictional resistance, cohesion, and effective porosity in sandy clay soil are shown in Figure 65 and 66. In comparing the frictional resistance in the soil sample with time based on treatment, the result shows that this strength parameter decreases with time and concentration with treatment as well. At 24 hr, the frictional resistance decreased from 26 kN/m^2 at 5 mL/g microbial content to 13 kN/m^2 at 25 mL/g microbial content; at 48 hr, the frictional resistance decreased from 23 kN/m^2 at 5 mL/g microbial content to 18 kN/m^2 at 25 mL/g

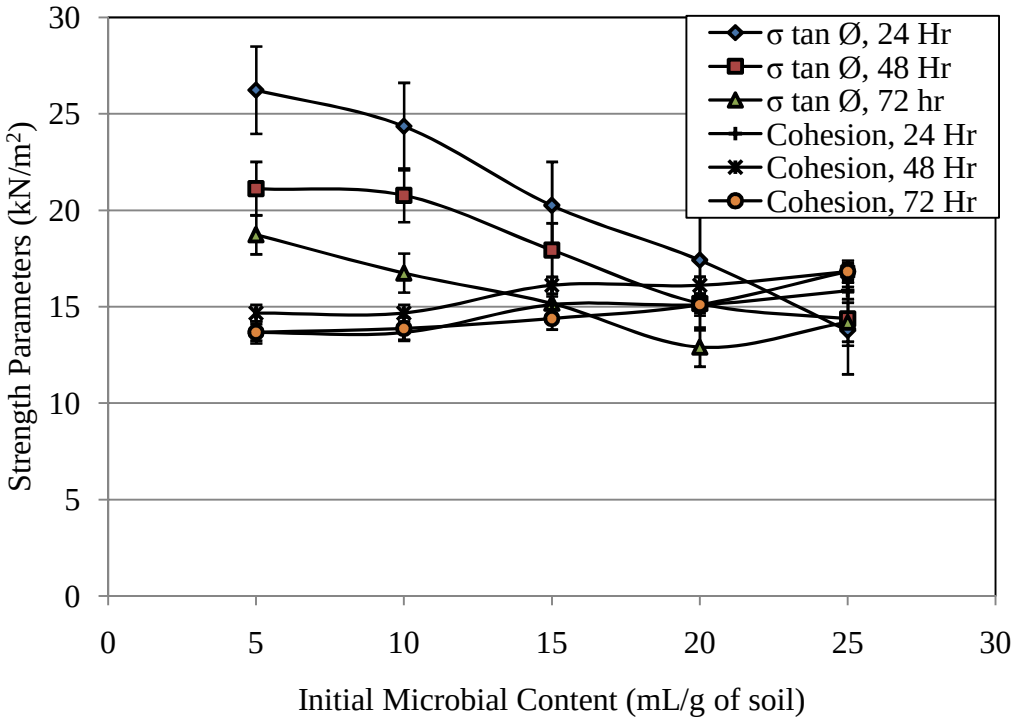

Figure 64: Comparing strength parameters in silty clay soil based on microbial induced EPS-CM

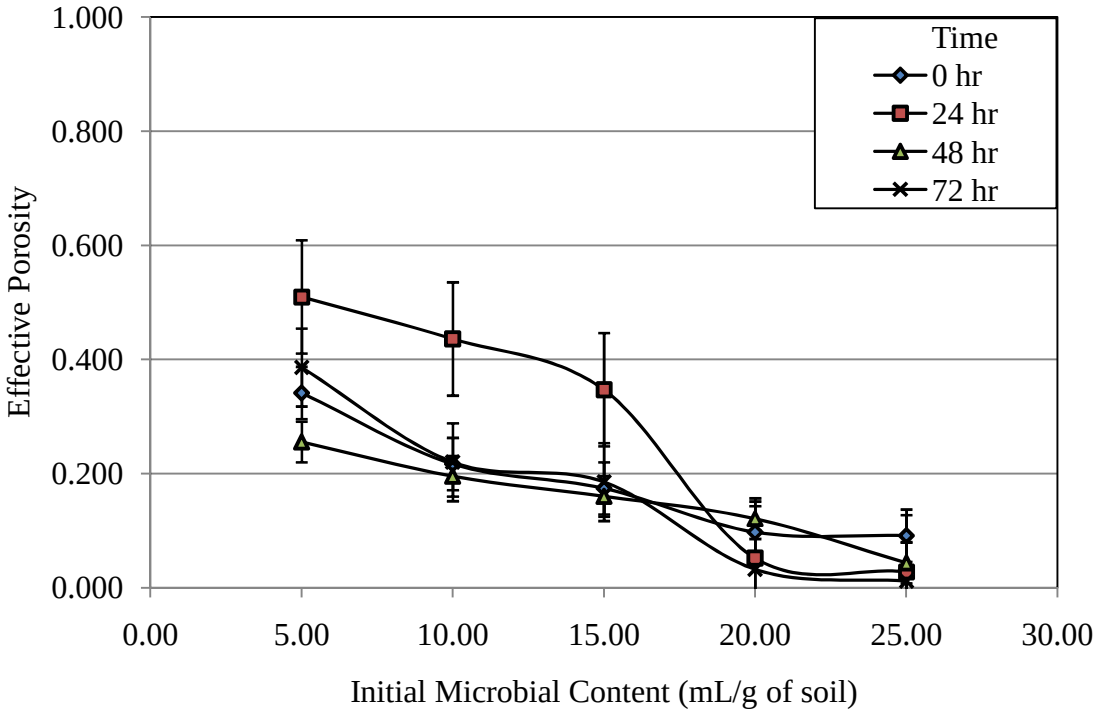

Figure 65: Change in effective porosity in silty clay soil with time

treatment of soil; at 72 hr, the frictional resistance decreased from 18 kN/m^2 at 5 mL/g microbial content to 8 kN/m^2 at 25 mL/g microbial content. In the determination of the soil cohesion based on treatment and time, it is shown that increased microbial content resulted in increased cohesion as well. This theoretical result is consistent with the experimental result shown in Figure 51. Contrary to the expectations in this research, production of EPS in sandy clay soil by *A. viscosus*, which in turn affected the cohesion, frictional resistance, and effective porosity in the soil, indicates the versatility of these microorganisms in their effective adhesion to the soil particle surface for biofilm production for a short period of time. However, a sustained EPS production and soil effective porosity reduction in these soils over a long period of time was not feasible as indicated in the effective porosity at 48 hr. The observed decreased in effective porosity can be attributed to the minimal increase in the amount of EPS produced in the soil by the microorganisms as well.

8.3 The comparisons of strength parameters and effective porosity with time in sandy silty clay soil

The experimental result of the relationship between frictional resistance, cohesion, and effective porosity in sandy silty clay soil are shown in Figure 68 and 69. In comparing the frictional resistance in the soil sample with time based on treatment, the result shows that this strength parameter decreases with time and concentration with treatment as well. At 24 hr, the frictional resistance decreased from 28 kN/m^2 at 5 mL/g microbial content to 17 kN/m^2 at 25 mL/g microbial content; at 48 hr, the frictional resistance decreased from 23 kN/m^2 at 5 mL/g microbial content to 18 kN/m^2 at 25 mL/g treatment of soil; at 72 hr, the frictional resistance decreased from 18 kN/m^2 at 5 mL/g microbial content to 8 kN/m^2 at 25 mL/g microbial content. In the determination of the

soil cohesion based on treatment and time, it is shown that increased microbial content resulted in increased cohesion as well. This theoretical result is consistent with the experimental result shown in Figure 52. As shown in Figures 70 and 71, the production of EPS in sandy silty clay soil by *A. viscosus*, which in turn affected the cohesion and frictional resistance in the soil, also indicates that the ability of these microorganisms to thrive under unfavorable conditions in these soils through their adhesion mechanism to the soil particle surface for EPS production for a short period on time. Again, a sustained EPS production and soil effective porosity reduction in these soils over a long period of time was not feasible as indicated in the increased effective porosity at 48 hr. These results are also consistent with the hypothetical relationships developed in chapter 2 (Figure 2).

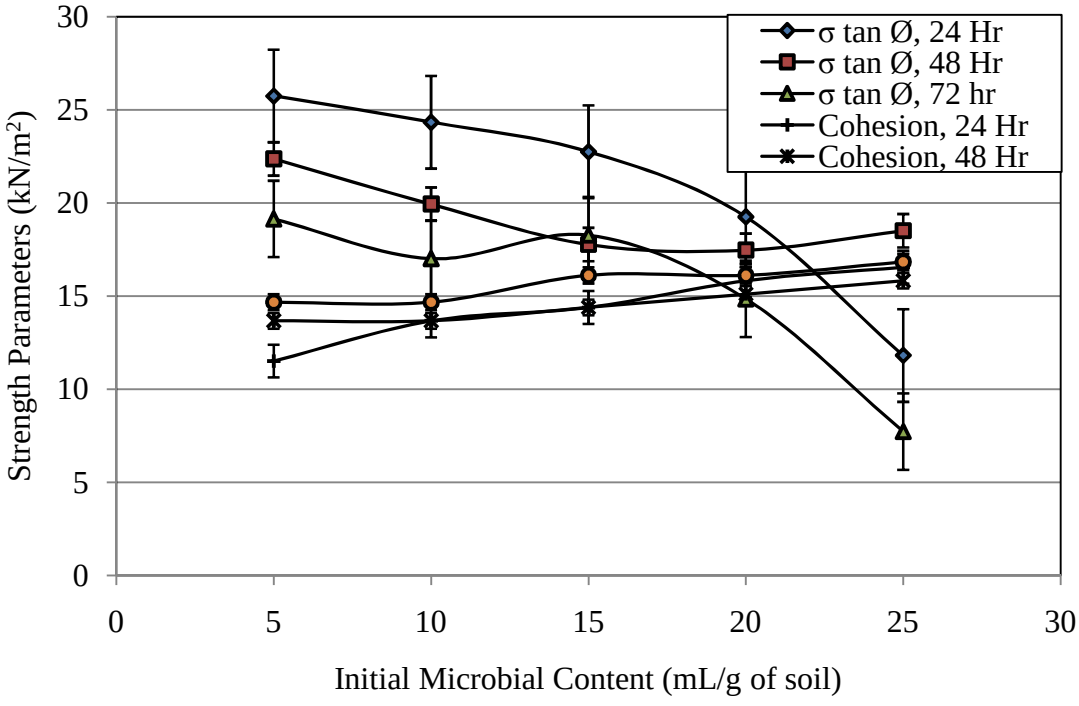

Figure 66: Comparing strength parameters in sandy clay soil based on microbial induced EPS

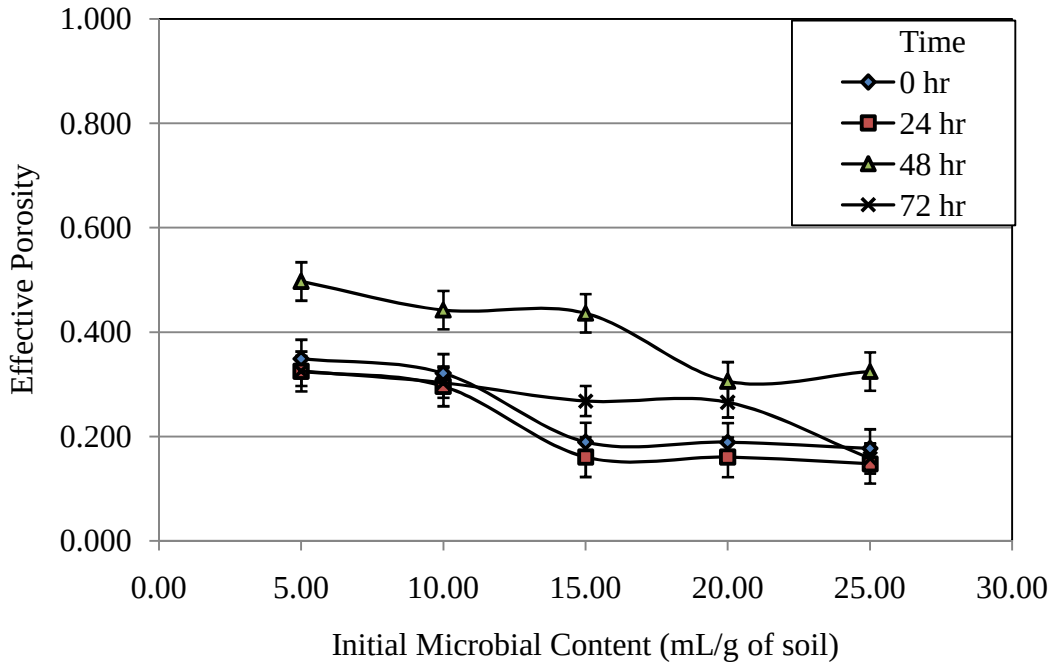

Figure 67: Change in effective porosity in sandy clay soil with time

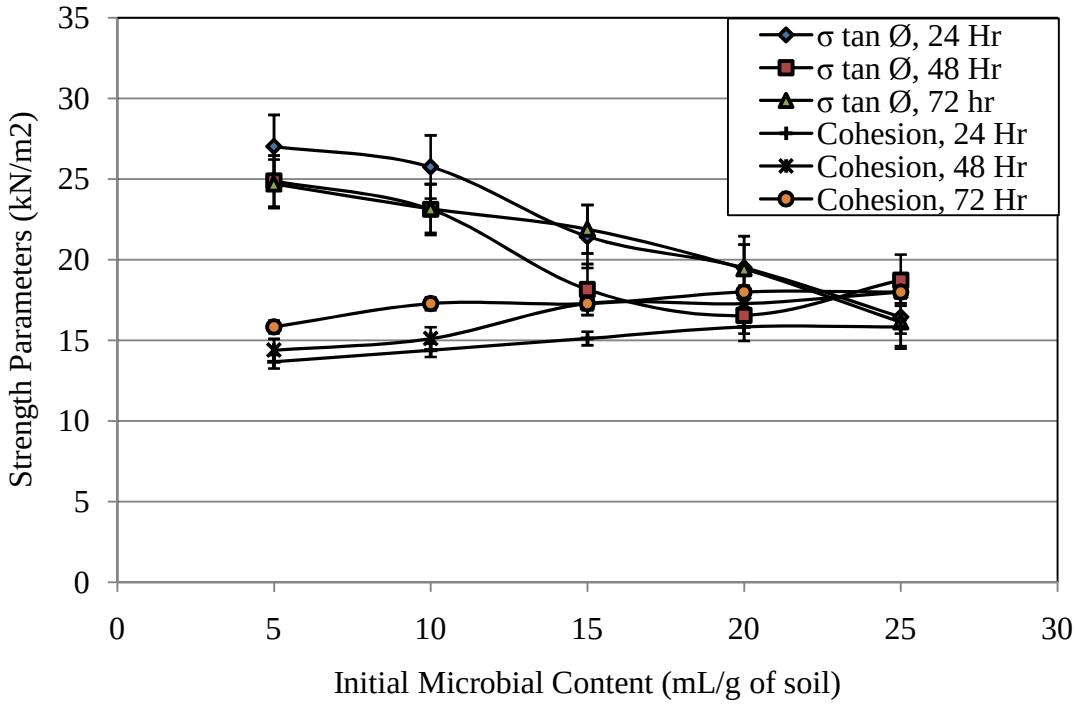

Figure 68: Comparing strength parameters in sandy silty clay soil based on microbial induced EPS

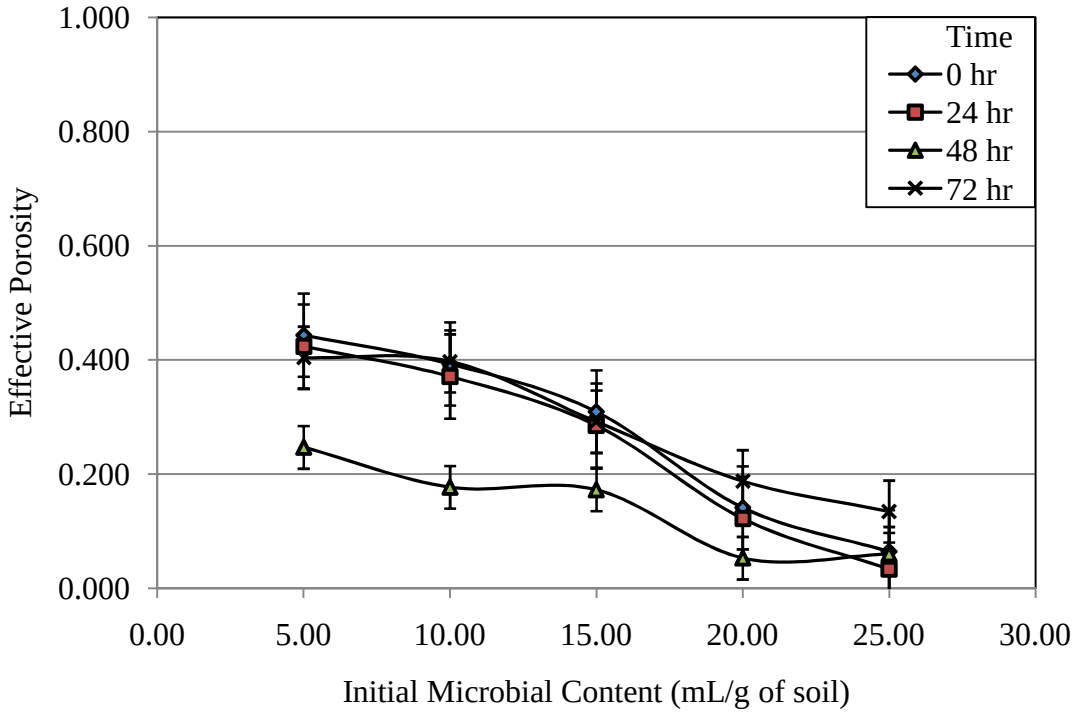

Figure 69: Change in effective porosity in sandy silty clay soil with time

8.4 Quantitative estimation of EPS production

As part of the objectives of this research, it important to quantitatively estimate the amount of EPS produced in each soil with time based on equation 51 developed in chapter 2, this can be applied using the growth constants determined from the 7-day monitoring of EPS production in each soil. From the data obtained, the calculated amounts of EPS produced in each soil based on time are shown in Figures 70, 73, and 75. In the silty clay soil, EPS production at different time intervals indicates a continuous increase in production after 96 hr with increasing EPS concentration in the range of 1.1 to 1.4 mg/mg of soil obtained. This can be attributed to the available surface area in the soil that enhances the adhesion of the microorganism hence, promoting EPS production and sorption. This follows the observations of Bos et al. (1999), Loosedrecht et al. (1990), and Flemming et al. (2007), which concluded that the tendency of the microorganisms to

attach to surfaces increases their ability to form biofilms (composed mainly of EPS), which in the case of soil, creates bridges between soil particles and the EPS (shown in Figure 59 to 62). Conversely, soil samples with increased pore spaces such as the sandy clay and sandy silty clay soils used in this research creates little or no surface areas for bacterial adhesion. This in effect, affects the ability of the microorganism to remain in the soil for a long period of time thereby reducing the amount of EPS that can be produced in such soils. The evidence of this phenomenon is shown in Figure 72 and 74 where the calculated concentrations of EPS in the range of 0.9 to 1.1 mg/mg of soil are obtained with a decreasing trend observed with increasing time. A comparison between the calculated and measured EPS concentration as shown in Figure 71, 73, and 75, indicates that a direct measurement of the EPS produced yields values that give a better picture of the trend of EPS production in the soil samples.

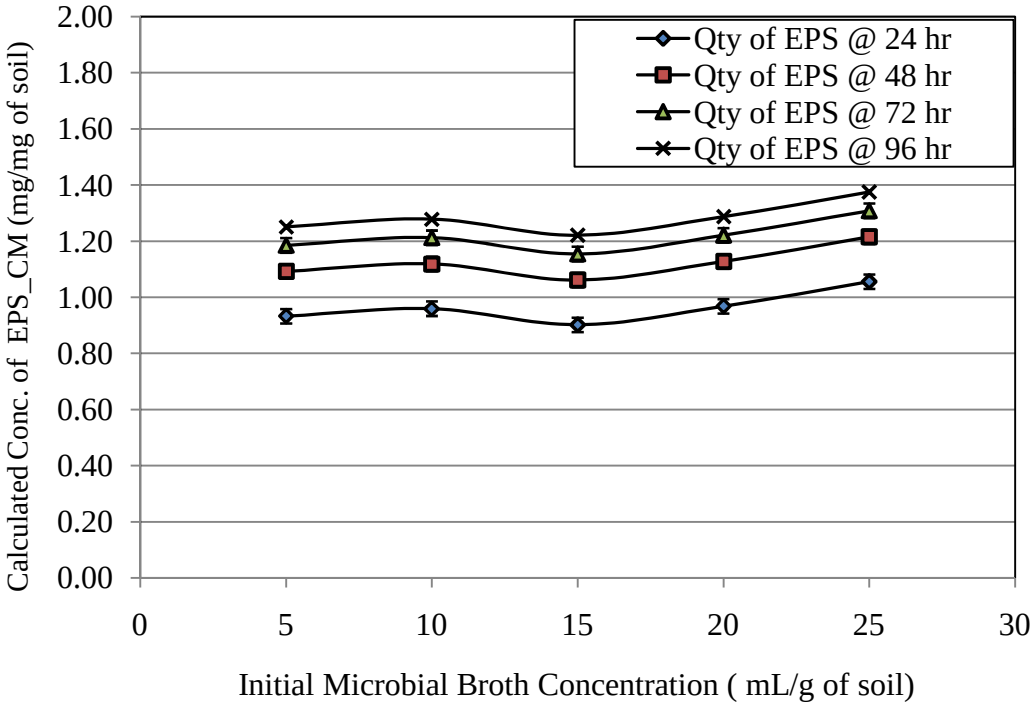

Figure 70: Theoretical quantification of in silty clay soil using based on time

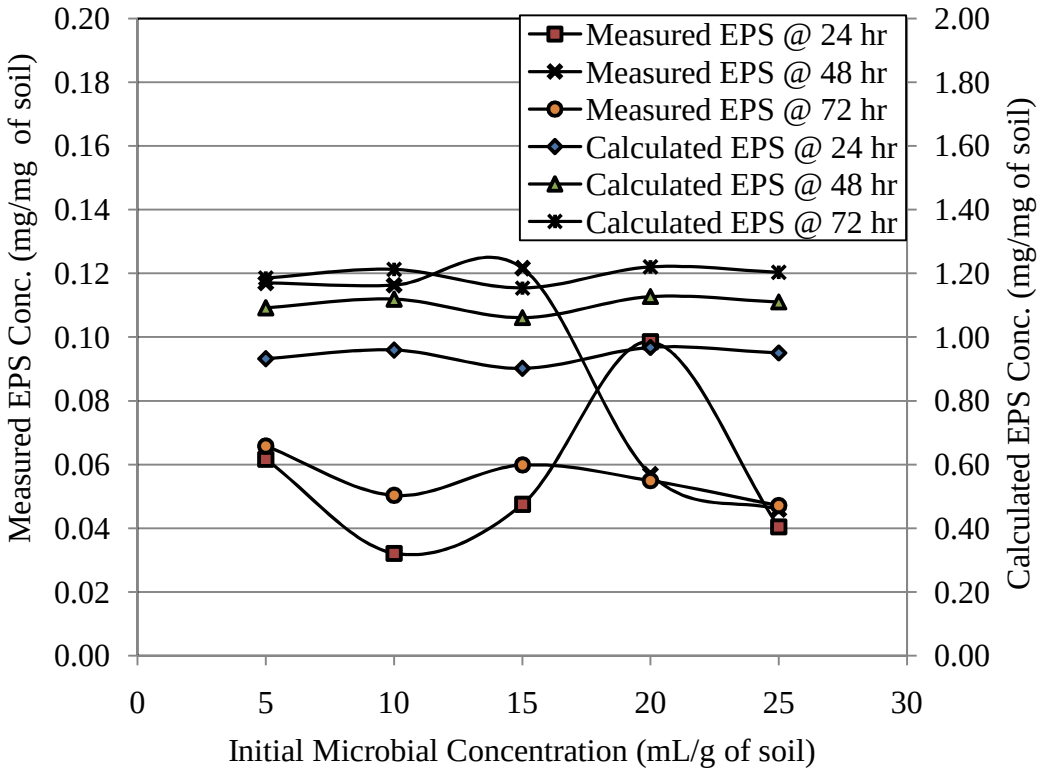

Figure 71: A comparison between measured and calculated EPS-CM concentrations in SCSoil

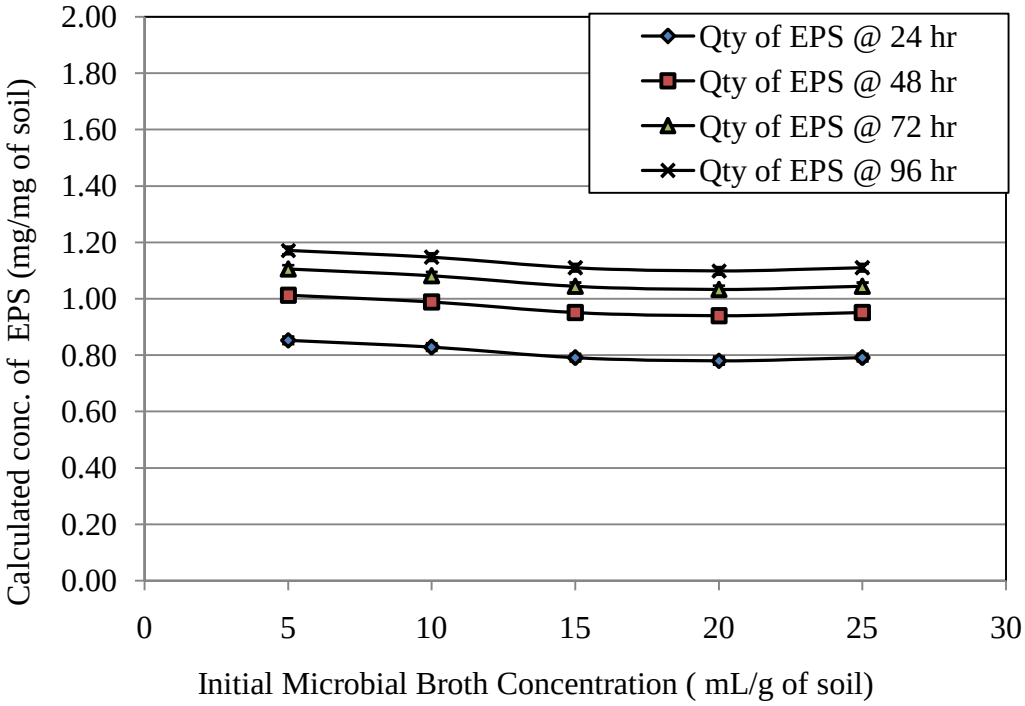

Figure 72: Theoretical quantification of in sandy clay soil based on time

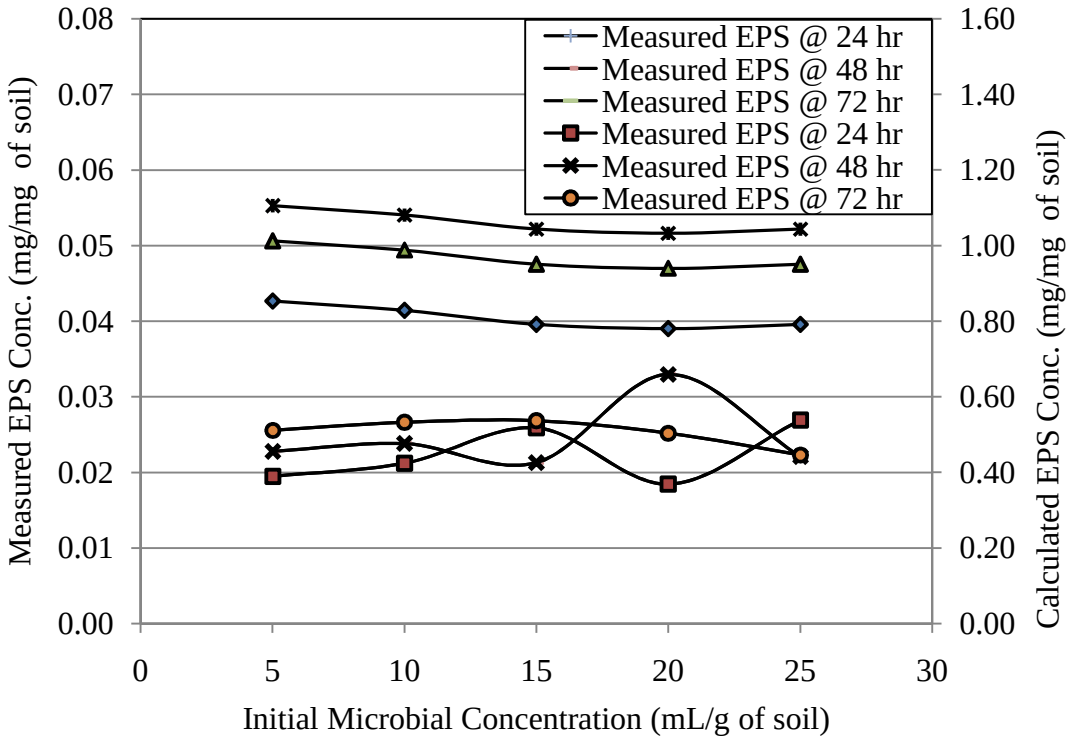

Figure 73: A comparison between measured and calculated EPS-CM concentrations in SDCSoil

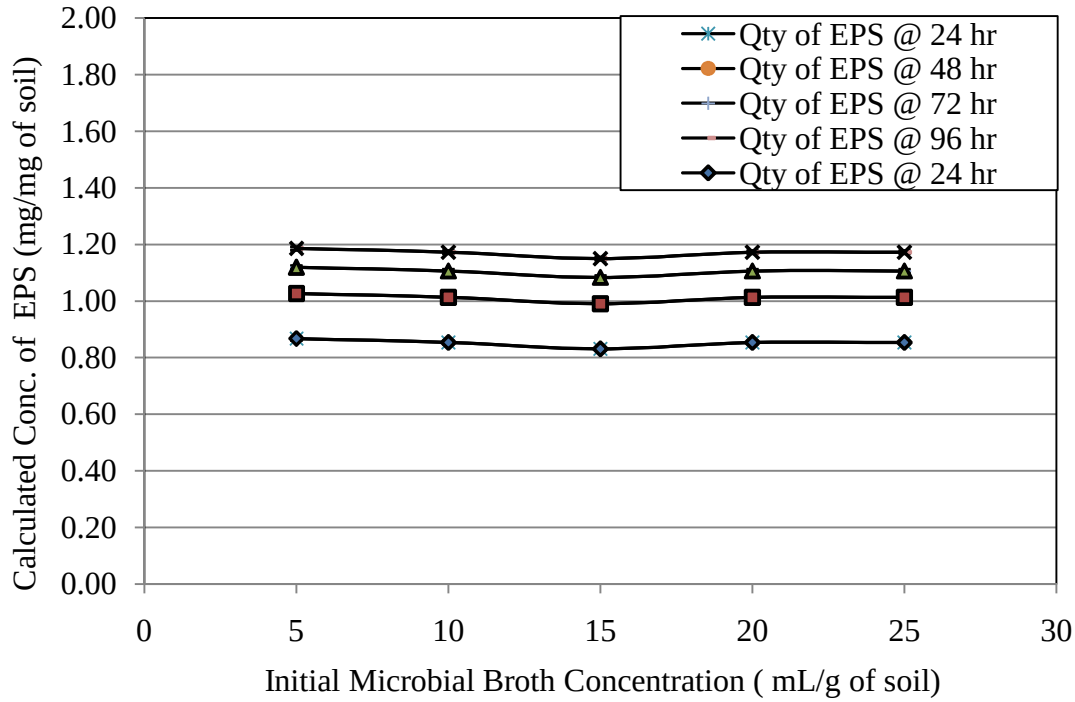

Figure 74: Theoretical quantification of in sandy silty clay soil based on time

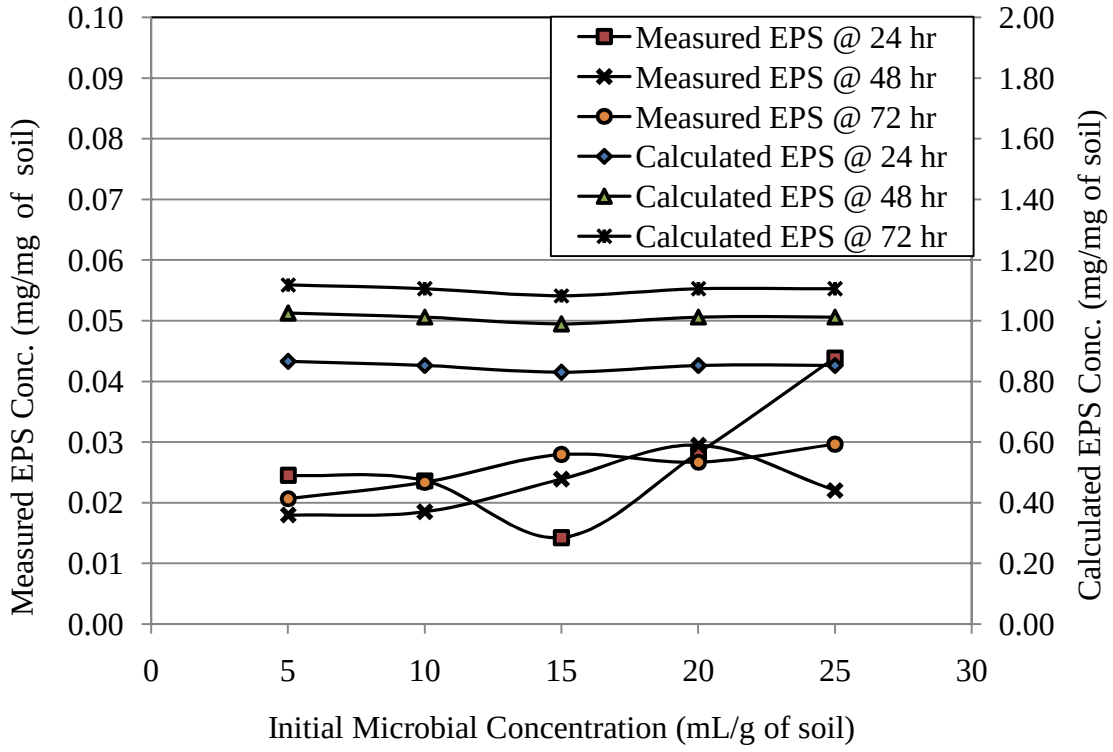

Figure 75: A comparison between measured and calculated EPS concentrations in SSCSoil

8.5 Determination of the adhesion energy of EPS-CM to soil surfaces

Another objective in this research was to quantitatively determine the adhesion energy of *Arthrobacter viscosus* to the different soils based on the initial microbial broth added surface areas. Using equation 56 developed in chapter 2, the adhesion energy of *A. viscosus* in each soil was determined to be in the range of -2.85 kJ/m^2 to -2.39 kJ/m^2. These results are mostly in agreement with those estimated by Loosdrecht et al. (1989) who reported adhesion Gibbs energy of -2.5 kJ/m^2 and -1.9 kJ/m^2 for *Arthrobacter globiformis* and *Arthrobacter* strain 177 respectively. The adhesion energy observed in these microorganisms has also been widely attributed to their biopolymer producing ability (Loosedrecht et al. 1987; Palmer et al. 2007; Stenstrom, 1989; Imam and Gould, 1990; Loosedrecht et al. 1989; Loosedrecht et al. 1990; Loosedrecht et al. 2002). From the results obtained, the relationships between the adhesion energy of EPS and soil treatment are shown in Figure 76, 77, and 78.

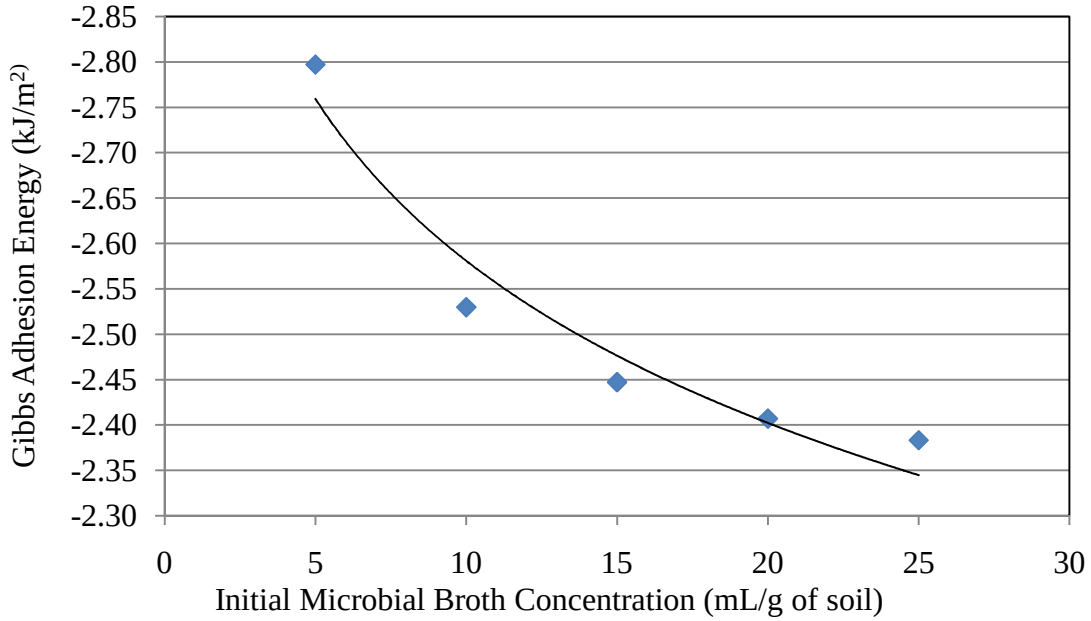

Figure 76: Trend of adhesion Gibbs energy of *Arthrobacter viscosus* in silty clay soil

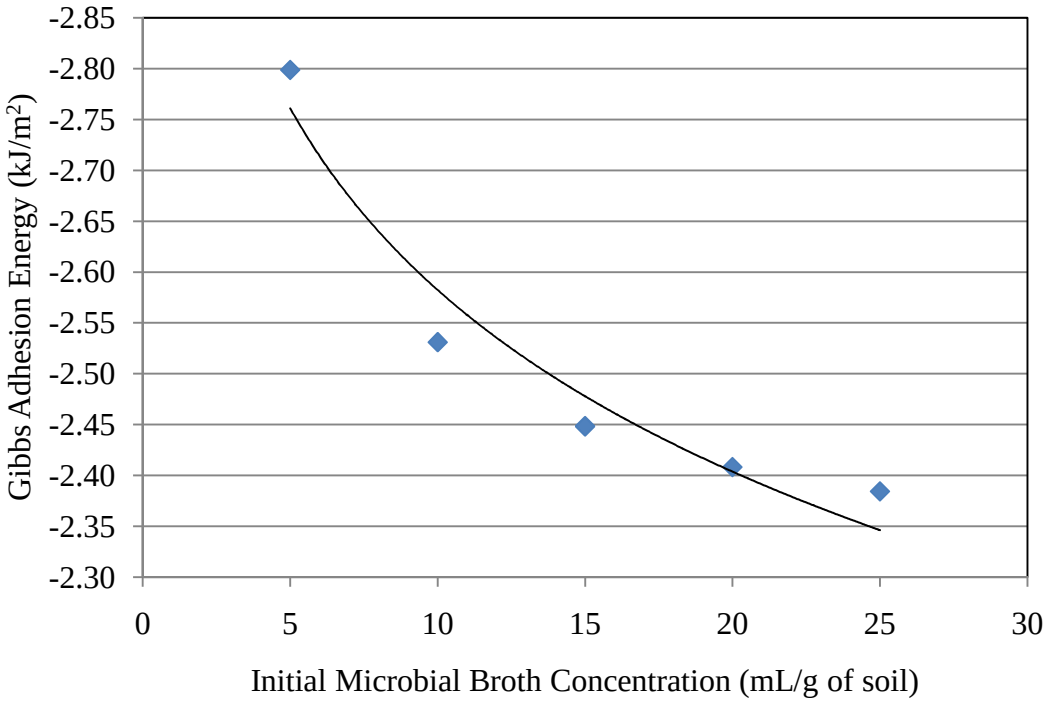

Figure 77: Trend of adhesion Gibbs energy of *Arthrobacter viscosus* in sandy clay soil

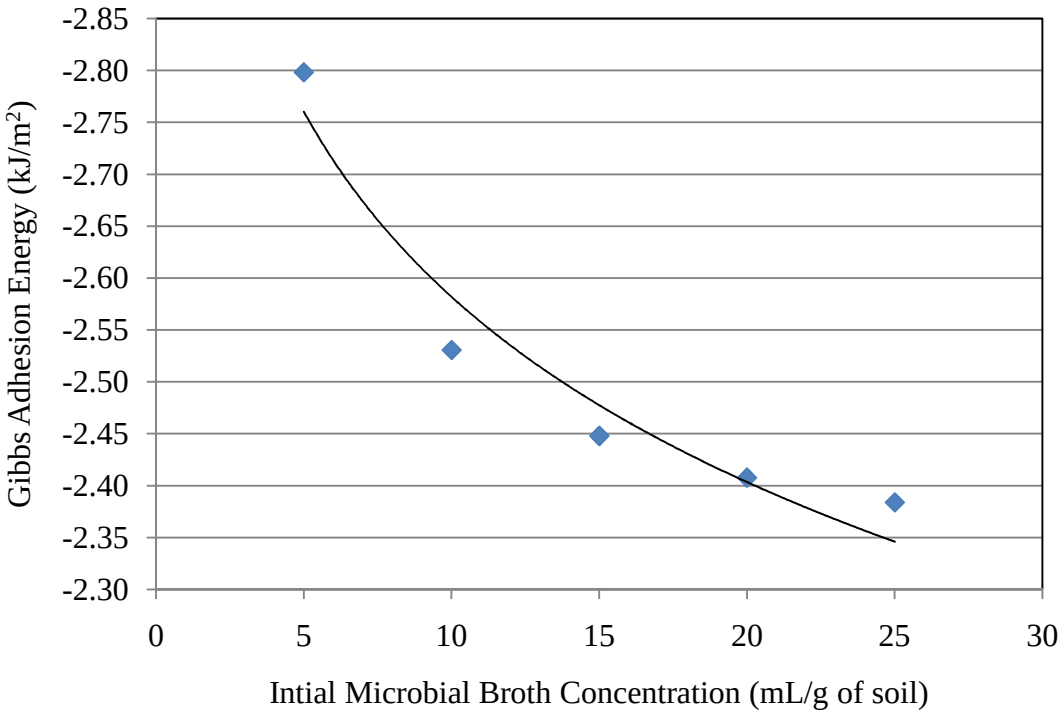

Figure 78: Trend of adhesion Gibbs energy of *Arthrobacter viscosus* in sandy silty clay soil

8.6 Determination of deformation indices of EPS-CM amended soil samples

In order to test the hypotheses presented in this research with respect to the expected increase in soil resistance to deformation based on the EPS-CM treatment, the deformation index of each soil was determined based on the EPS-CM concentration and cohesion observed in each soil. These indices were quantitatively determined using equation 29 developed in chapter 2 and the result is shown in Figure 76. This result follows the pattern of the hypothetical relationships shown in Figure 5, which indicates that an increase in the deformation resistance indices occurs with time based on the EPS-CM concentration and cohesion. In the silty clay soil, it is shown (Figure 79) that a deformation resistance index D_N in the range of 401 to 1500 can be obtained based on initial microbial concentrations of 5 to 25 ml/g of soil. This result also shows that while the production and/or use of EPS-CM in silty clay soils improve their resistance to deformation, this resistance is not infinite and it expected to fail at some point. In sandy

clay and sandy silty clay soils there is a moderate increase in the regime values but are still not significant compared to the silty clay soil.

8.7 Determination of coefficient of soil failure

In addition to the determination of deformation index, equations 31, 32, and 33 developed in chapter 2 determine a dimensionless coefficient of failure μ that indicates the susceptibility of soils to failure due to decreasing shear strength, cohesion, frictional resistance, and EPS-CM concentration in each soil. In all the three soil samples used in this research, it is shown that this coefficient decreases with increasing EPS-CM concentration. As shown in Figure 80, the initial coefficient of failure is lower for silty clay soil (0.18) compared to sandy clay soil (0.23) and sandy silty clay soil (0.21) but generally, this coefficient decreases to about 0.07 in all three soils treated with EPS-CM. The smaller this number, the less susceptible the soil is to potential failure due to stress, therefore the less likely to form dust.

8.8 Determination of friability indices

Following the modification made on the equation developed by Utomo and Dexter (1981) that the friability of soils based on their aggregate strength and volume, equation 37 developed in chapter 2 has been used to quantify the friability index of each soil based on their EPS-CM content, shear strength, bulk volume, and estimated cohesion. As shown in Figure 81, the friability indices of the three soils used in this research decreases with increasing microbial broth concentration hence, increasing EPS production. This is in agreement with the Figure 6 that showed a hypothetical relationship between these parameters. Based on the data obtained, a low friability index indicates a less propensity of the soil sample to fail under stress leading to dusting. The result also shows that friability in silty clay soil is lower (0.008 to 0.001) for silty clay soil compared to sandy clay (0.0105 to 0.003) and sandy silty clay (0.009 to 0.002) soils.

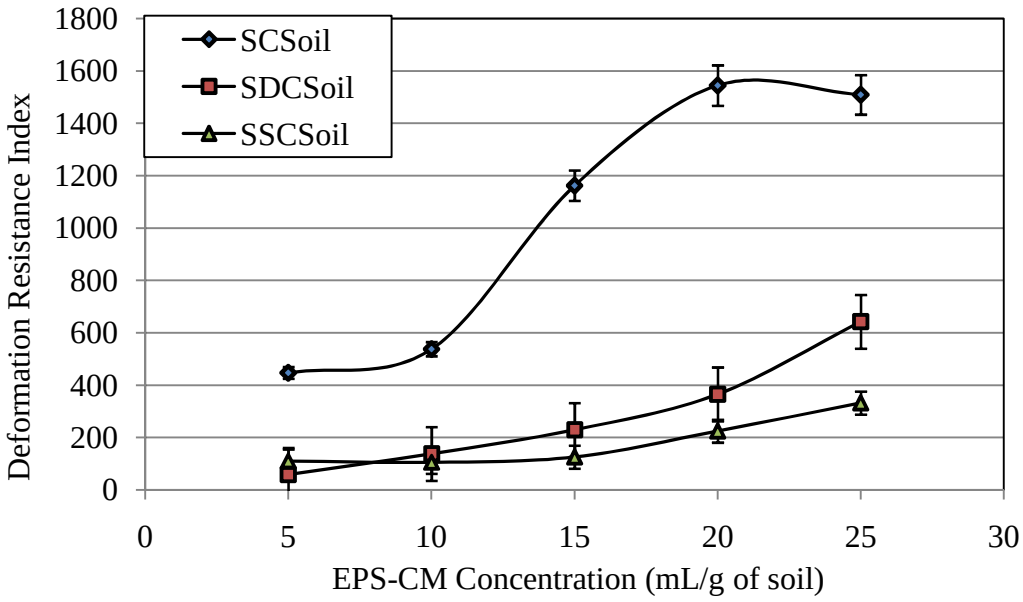

Figure 79: A comparison of the deformation resistance index of the EPS-CM amended soils

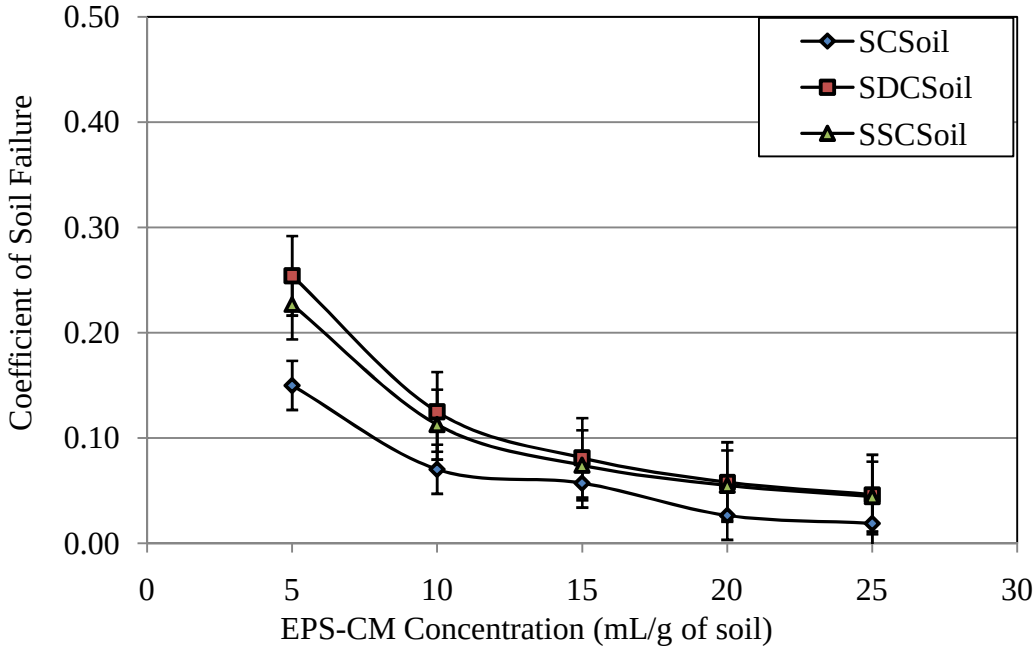

Figure 80: A comparison of the coefficient of failure of the EPS-CM amended soils

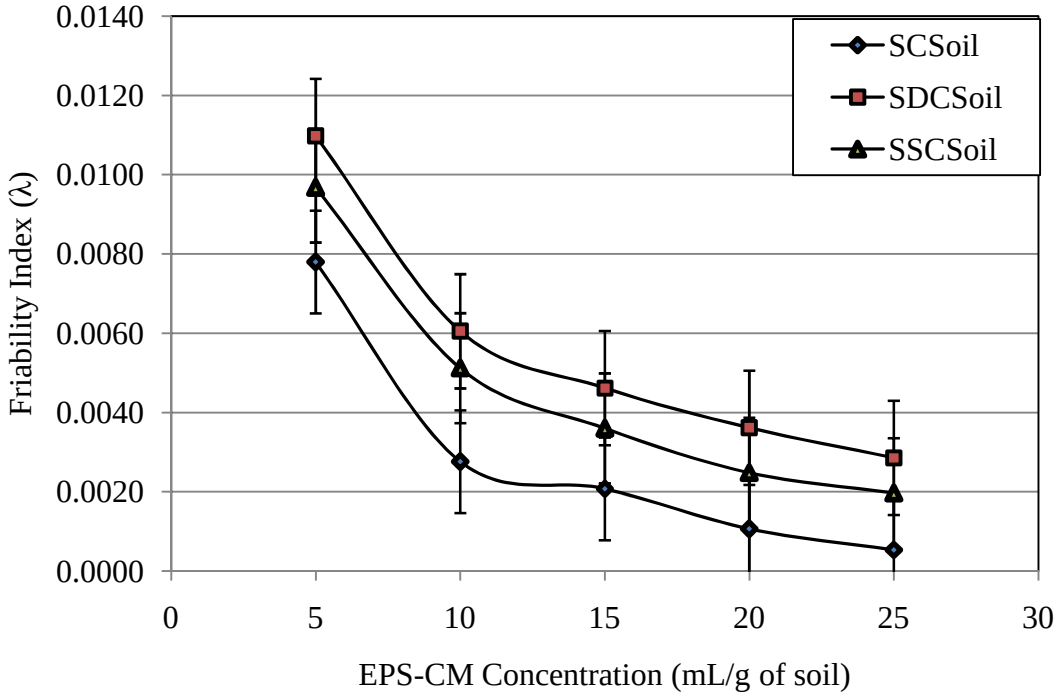

Figure 81: A comparison of the friability indices of the EPSMC amended soil samples

8.9 Statistical Analyses

Based on a significance level of 0.6, Table 7 shows that the correlation between all broth volumes and the EPS produced in the Haggstrom media were significant at all times except at 240 hr, 264 hr, and 336hr. The correlation between all broth volumes and the EPS produced in the silty clay soil was significant at all times except at 24 hr, 120 hr, and 144 hr (Table 8). The correlation between all broth volumes and the EPS produced in sandy clay soil was significant at all times except at 24 hr, 48 hr, and 144 hr (Table 9) while the correlation between all broth volumes and the EPS produced in the sandy silty clay soil were significant at all times (Table 10).

Based on ANOVA testing for significance at $P \leq 0.05$, cohesion was significant in silty clay soil based on control and EPS-CM treatments while broth treatment showed no significance (Table 11). Conversely, no significance was observed between cohesion and the treatments in sandy clay soil (Table 12). In sandy silty clay soil, significances were

observed between cohesion, broth treatments, and EPS-CM treatments while no significance was observed between the control and cohesion (Table 13).

Further correlation analyses between cohesion and desiccation in all three soils indicate that the relationships between these two factors are significant as shown in Tables 14, 15, and 16. From these results, it can be inferred that the amount of broth (with bacterial cells) used in combination with Haggstrom media plays a significant role in the quantity of EPS produced. Similarly, the cohesion and desiccation observed in the different soil types are dependent on the type of soil stabilization treatment applied in such soils.

Table 7: Correlation results showing the significant effect of EPS produced in Haggstrom media based on time. Values ≥ 0.6 indicate significance.

Correlation Factors Broth (with cells) vs. Mean EPS	Significance
24 hr	0.989
48 hr	0.977
72 hr	0.984
96hr	0.977
120 hr	0.661
144 hr	0.617
168 hr	0.983
192 hr	0.746
216 hr	0.960
240 hr	0.543
264 hr	0.441
288 hr	0.669
312 hr	0.596
336 hr	0.420

Table 8: Correlation results showing the significant effect of EPS produced in silty clay soil based on time. Values ≥ 0.6 indicate significant results

Correlation Factors Broth (with cells) vs. Mean EPS	Significance
24 hr	0.145
48 hr	0.863
72 hr	0.694
96hr	0.956
120 hr	0.377
144 hr	0.286
168 hr	0.758

Table 9: Correlation results showing the significant effect of EPS produced in sandy clay soil based on time. Values ≥ 0.6 indicate significant results

Correlation Factors Broth (with cells) vs. Mean EPS	Significance
24 hr	0.503
48 hr	0.258
72 hr	0.694
96hr	0.854
120 hr	0.882
144 hr	0.140
168 hr	0.649

Table 10: Correlation results showing the significant effect of EPS produced in sandy silty clay soil based on time. Values ≥ 0.6 indicate significant results

Correlation Factors Broth (with cells) vs. Mean EPS	Significance
24 hr	0.634
48 hr	0.649
72 hr	0.929
96hr	0.848
120 hr	0.883
144 hr	0.838
168 hr	0.694

Table 11: Results of analysis of variance ANOVA indicating the significance of cohesion *C* in silty clay soil based on treatments. Values ≤ 0.05 indicate significant results

Source	DF	ANOVA SS	Mean Square	FValue	Pr > F
Control	4	663.7842563	165.9460641	17.95	0.0001
Broth content	4	282.8989067	70.7247267	1.90	0.1864
EPS-CM content	4	260.4006012	65.1001503	0.87	0.0516

Table 12 Results of analysis of variance ANOVA indicating the significance of cohesion *C* in sandy clay soil based on treatments. Values ≤ 0.05 indicate significant results

Source	DF	ANOVA SS	Mean Square	FValue	Pr > F
Control	4	12.90324103	3.22581026	1.95	0.1789
Broth content	4	270.4339646	67.6084911	1.15	0.3864
EPS-CM content	4	0.20112648	0.05028162	2.11	0.1547

Table 13: Results of analysis of variance ANOVA indicating the significance of cohesion *C* in sandy silty clay soil based on treatments. Values ≤ 0.05 indicate significant results

Source	DF	ANOVA SS	Mean Square	FValue	Pr > F
Control	4	12.90324103	3.22581026	1.95	0.1789
Broth content	4	469.0236498	117.2559124	3.32	0.0563
EPS-CM content	4	0.25509103	0.06377276	4.46	0.0252

Table 14: Correlation results showing the significant effects of cohesion on desiccation in silty clay soil based on time and treatment. Values ≥ 0.6 indicate significant results

Correlation Factors Cohesion vs. EPS-CM	Significance
24 hr	0.978
48 hr	0.845
72 hr	0.961

Table 15: Correlation results showing the significant effects of cohesion on desiccation in sandy silty clay soil based on time and treatment. Values ≥ 0.6 indicate significant results

Correlation Factors Cohesion vs. EPS-CM	Significance
24 hr	0.964
48 hr	0.950
72 hr	0.998

Table 16: Correlation results showing the significant effects of cohesion on desiccation in sandy clay soil based on time and treatment. Values ≥ 0.6 indicate significant results

Correlation Factors Cohesion vs. EPS-CM	Significance
24 hr	0.977
48 hr	0.845
72 hr	0.961

CHAPTER 9: CONCLUSIONS AND FUTURE WORK

9.1 Practical significance of the results

In field applications of dust control technologies, an important component is the cost effectiveness and the environmental sustainability of such technologies. In this present capital driven economy, cost is usually associated and quantified in terms of material acquisition and heavy road equipment supply. Little or no attention is paid to the environmental cost of applying of harmful chemical dust suppressants to exposed soils, which is their potential to degrade into more toxic substances that can contaminate both aquatic and terrestrial environments. Furthermore, the use of extracellular polysaccharide as alternative to chemical dust suppressants is one technology that has been shown to involve less expensive equipment and materials for large scale production and application. Currently, biopolymers are daily produced in huge amounts by microorganisms in aerobic digesters of waste water treatment plants and in bioreactors. So it is possible to set up a bioreactor with a good amount of *Arthrobacter viscosus* as the main microorganism thereby, enabling them to produce enough EPS that can be extracted and applied as dust suppressants and erosion control additives. The practicality of this approach in terms of cost and implementation is obtainable.

9.2 Conclusions

Models and indices for predicting the effectiveness of EPS in stabilizing surface soils against dust generation have been developed. The application of these models can

be an effective tool in the determination of the amount of EPS or microbial broth needed to stabilize a defined area of exposed soil as well the amount of stability that can be achieved based on the soil type. The use of EPS as an alternative biopolymer to other synthetic dust suppressants and the so called “biodegradable polymers” has three major advantages:

1. The environmental hazards arising from the use of synthetic dust suppressants are removed.
2. Large scale production of EPS is feasible as evidenced in WWTP and bioreactors.
3. This technology promises to be cost effective.

These advantages make the use extracellular polysaccharides in surface soil stabilization more attractive and safe. Based on the pilot tests, data obtained through field simulation tests performed in the laboratory, and data analyses in this research, the following conclusions are made.

1. Based on the cyclical production pattern of EPS in the Haggstrom media and the different soils, no conclusion can be made on the microbial broth concentration required for optimum EPS production. However, results indicate that EPS production in soil by *A. viscosus* is more efficient in silty clay soils than sandy clay and sandy silty clay soils.
2. The amounts of EPS produced in both Haggstrom and soils by varying amounts of broth (with cells) indicate that a relationship exists in these parameters.
3. A direct application of EPS-CM to the soil samples showed a better

correlation between soil strength parameters such as cohesion, frictional resistance, shear strength, strain at failure, and desiccation compared to direct application microbial broth (with cells) and the control.

4. From the results of unconfined compression and direct shear tests, increased cohesions from 37 to 45 kN/m^2 occurs in EPS amended silty clay soil compared to maximum cohesions of 27 kN/m^2 and 24 kN/m^2 obtained for sandy clay and sandy silty clay soils. Compared to control samples, little increases of 15 kN/m^2 or no increased cohesions are obtained.
5. Generally, frictional resistance decreases with increasing concentrations of microbial broth/EPS.
6. In unconfined testing of soils treated with EPS/microbial broth, a general trend of decreasing strain with increasing concentration of soil treatment and a trend of increasing strain with time is obtainable.
7. In silty clay soil treated with EPS a deformation of 0.34 to 0.20 from day 1 to day 3 at EPS concentration 0f 5 mL/g of soil but at higher EPS concentrations, these values tend to increase and decrease with time indicating variations in this soil behavior with time. Lowest deformation of 0.25 occurs in silty clay soils treated with 25 mL/g soil of EPS compared to sandy clay and sandy silty clay soils. Therefore, lower deformation indices are obtained in silty clay soils compared to sandy clay and sandy silty clay soils.
8. Effective porosity in EPS/microbial broth amended silty clay soil continues to decrease with time due to continued EPS production by *A. viscosus* while changes in effective porosity with time in sandy clay and sandy silty clay is

not consistent therefore increases with time.

9. Deformation resistance indices increase in silty clay, sandy clay, and sandy silty clay based on EPS treatment but this index is more significant in silty clay soil samples compared to sandy samples.
10. Friability indices decrease in silty clay, sandy clay, and sandy silty clay based on EPS treatment but this index is more significant in silty clay soil samples compared to sandy samples.
11. For a drying duration of 72 hours (at temperature of 37 ^{o}C and relative humidity of 34 %), EPS amended silty clay soils retained 5 % more liquid with time under desiccation tests compared to sandy clay and silty clay soils.

Generally, it is known that silty clay soil samples are more likely to form dusts than sandy clay and sandy silty clay soils. However, these results show that silty clay soils amended with EPS-CM through both direct injection of EPS producing microbes and direct EPS-CM application display more resistance to desiccation and failure under stress therefore, are less likely for form dusts compared to the other soil types. Again, failure of the EPS amended soils can be defined in terms of maximum strength based on secant or tangent moduli of elasticity, which will be the focus of subsequent analyses of further study. In this study, a 14 day monitoring of EPS production in Haggstrom and soil media was not enough to draw a meaningful conclusion on the optimum broth (with cells) concentration required for optimum EPS. Furthermore, EPS in soil is subject to various environmental factors that lead to their degradation, which was not monitored in this research. More studies are needed in these areas as well. The experimental results suggest that EPS stabilization of soil against dust generation is dependent on various soil

stresses pertinent to typical Civil and Environmental Engineering works. Finally, the use of the method developed in this study following field verification may yield more accurate estimates of dust generation potentials of different soils, and thus need further investigation.

9.3 Future work

The use of EPS as a surface soil stabilization material is still a simulated experiment performed in the laboratory for now; more research is needed to investigate the possibility of a large scale production of this biomaterial for real time applications. For this technique to be successful, a genetically modified *Arthrobacter viscosus* may need to be developed to ensure maximum EPS production both in the field and in liquid media.

Since this is fermentation process, appropriate technologies is needed to control the odor emanating from the production of this biopolymer in liquid media. The use of a respirator is not enough protection from this strong odor. Wearing a canister may seem a little bit extreme therefore, the construction of a large ventilation system over the EPS production media should be considered. This will undoubtedly affect the cost of production but the environmental benefits will offset this.

The amount of EPS produced in soil has been quantitatively investigated in this research using different microbial broth concentrations; the second phase of this quantification process should involve monitoring the degradation process of EPS in soil with time and this will require using new technologies as well. The following journal articles are expected to come out of this research,

1) A conceptual model of soil strength changes due to secretions of EPS by soil

microbes.

2) Cyclical persistence of *Arthrobacter viscosus* in soil as an indicated by EPS fluctuations.
3) Using desiccation of EPS-amended clayey soils as an index of potential dust suppression.
4) Scaling of the effects of microbial activities on soil strength and stability: A review.

REFERENCES

Acea, M. J., Prieto-Fernandez, A., Diz-Cid, N. (2003). "Cyanobacteria inoculation of heated soils: effect on microorganisms of C and N cycles and on chemical composition in soil surface". *Soil Bio. & Biochem. 35*, 513-524.

Allen, M.S., Welch, K.T., Prebyl, B.S., Baker, D.C., Meyers, A.J., Sayler, G.S. (2004). "Analysis and glycosyl composition of the exopolysaccharide isolated forms the floc-forming wastewater bacterium *Thauera* sp. MZ1T". *Environmental Microbiology 6*, 780 -790.

Al-Shayea, N.A. (2001). "The combined effect of clay and moisture content on the behavior of remolded unsaturated soils." *Engineering Geology 2*, 319-342.

ASTM, International. (2008). "Standard test method for direct shear test under consolidated drained conditions". *ASTM, International*, D 3080 – 04.

ASTM, International. (2008). "Standard test method for laboratory determination of water (moisture) content of soil and rock my mass". *ASTM, International*, D 2216–05.

ASTM, International. (2008). "Standard test method for liquid limit, plastic limit, and plasticity index of soils". *ASTM, International*, D 4318 – 05.

ASTM, International. (2008). "Standard test method for particle-size analysis of soils". *ASTM, International*, D422 – 63.

ASTM, International. (2008). "Standard test method for specific gravity of soil solids by water pycnometer". *ASTM, International*, D 854 – 06.

ASTM, International. (2008). "Standard test method for unconfined compressive strength of cohesive soil". *ASTM, International*, D 2166 – 06.

Atiş, C.D. (2004). "Carbonation-porosity-strength model for fly ash concrete". *Journal of Materials in Civil Engineering 16*, 91-94.

Azeredo, J., Lazarova, V., Oliveira, R. (1999). "Methods to extract the exopolymeric matrix from biofilms: A comparative study". *Water Science and Technology 39*, 243-250.

Azeredo, J., Visser, J., Oliveira, R. (1999). "Exopolymers in bacterial adhesion: interpretation in terms of DLVO and XDLVO theories". *Coll. and Surfaces B: Biointerfaces 14*, 141-148.

Bader, F. B. (1982). "Kinetics of double-substrate limited growth". In Bazin, M. J. (Ed.), Microbial population dynamics. CRC Press, Boca Raton, FL. USA.

Baker, L.R. (1988). "Areal measurement of topography". *Surface Topography 1,* 207-213.

Balkwill, D. L., Boone, D. R. (1997). "Identity and diversity of microorganisms cultured from subsurface environments". In Amy, P. S. and Haldeman, D. L. (Eds.), The microbiology of the terrestrial deep subsurface. CRC Press LLC, Boca Raton, NY. pp. 105-117.

Banu, N. A., Singh, B., Copeland, L. (2004). "Soil microbial biomass and microbial biodiversity in some soils from New South Wales, Australia". *Australian Journal of Soil Research 42,* 777-782.

Barbaro, S.E., Trevors, J.T., Inniss, W.E. (2001). "Effects of low temperature, cold shock, and various carbon sources on esterase and lipase activities and exopolysaccahride production by a psychrotrophic *Acinetobacter* sp". *Can. Journal of Microbiology 47,* 194-205.

Barry, P. V., Stott, D.E., Turco, R. F., Bradford, J. M. (1991). "Organic polymers' effect on soil shear strength and detachment by single raindrops". *Soil Sci. Soc. of Am. J. 55,* 799-804.

Basheva, E.S., Gurkov, T.D., Christov, N.C., Campbell, B. (2006). "Interactions in oil/water/oil films stabilized by β-lactoglobulin; role of the surface charge". *Colloids and Surfaces A: Physiochem. Eng. Aspects 282-283,* 99-108.

Behrens, S.H. (1998). "Aggregation in charge-stabilized colloidal suspensions revisited". *Langmuir 14,* 1951-1954.

Béjar, V., Llamas, I., Calvo, C., Quesada, E. (1998). "Characterization of exopolysaccharides produced by 19 halophilic strains of the species *Halomonas eurihalina*". *Journal of Biotechnology 61,* 135-141.

Ben-Hur, M., and Letey, J., and Shainberg, I. (1990). "Polymer effects on erosion under laboratory rainfall simulator conditions". *Soil Science Society of America Journal 54,* 1092-1095.

Ben-Hur, M. (2006). "Using synthetic polymers as soil conditioners to control runoff and soil loss in arid and semi-arid regions – a review". *Australian Journal of Soil Research 44,* 191-204.

Bergmaier, D., Champagne, C.P., Lacroix, C. (2003). "Exopolysaccharide production during batch cultures with free and immobilized *Lactobacillus rhamnosus* RW-9595M". *Journal of Applied Microbiology 95,* 1049-1057.

Bhattacharjee, S., Ko, C.H., Elimelech, M. (1998). "DLVO interaction between rough surfaces". *Langmuir 14,* 3365-3375.

Bishop, A.W., Blight, G.E., (1963). "Some aspects of effective stress in saturated and partly saturated soils". *Géotechnique 13*, 177–197.

Blessing, G.V., Eitzen, D.G. (1988). "Surface roughness sensed by ultrasound". *Surface Topography 1,* 23-267.

Blume, E., Bischoff, M., Reichert, J. M., Moorman, T., Konopka, A., Turco, R. F. (2002). "Surface and subsurface microbial biomass, community structure and metabolic activity as a function of soil depth and season". *Appl. Soil Ecol. 20*, 171-181.

Bodie, E.A., Schwartz, R.D., Catena, A. (1985). "Production and characterization of a polymer from *Arthrobacter* sp.". *Applied and Environmental Microbiology 50,* 629-633.

Bogner, J.E., Miller, R.M., Spokas, K. (1995). "Measurement of microbial biomass and activity in landfill soils". *Waste Management & Research 13,* 137-147.

Bollander, P. (1999a). "Dust palliative selection and application guide". Project Report. 9977-1207-SDTDC. San Dimas, CA: United States Department of Agriculture. 20 p.

Bonaventura, G.D., Pompillo, A., Picciani, C., Iezzi, M. et al. (2006). Biofilm formation by the emerging fungal pathogen *Trichosporon asahii*: Development, architecture, and antifungal resistance. *Antimicrobial Agents and Chemotherapy 50*, 3269-3276.

Bonet, R., Simon-Pujol, M.D., Congregado, F. (1993). "Effects of nutrients on exopolysaccharide production and surface properties of *Aeromonas salmonicida*". *Applied and Environmental Microbiology 59,* 2437-2441.

Bos, R., Van der Mei, H.C., Busscher, H.J. (1999). "Physico-chemistry of initial microbial adhesive interactions – its mechanisms and methods for study". *FEMS Microbiology Reviews 23*, 179-230.

Boulton, J.W., Lepage, M., Jordan, M. (2007). "Fugitive and wind-blown dust: creative solutions to asesss and control fugitive and wind-blown dust emissions at industrial facilities". *Emerging Issues 3.* Retrieved September 21, 2008 from www.rwdi.com.

Boyd, R.D., Verran, J. (2002). "Use of the atomic force microscope to determine the effect of substratum surface topography on the bacterial adhesion". *Langmuir 18,* 2343-2346.

Briones, A. A. and Uehara, G. (1977). "Soil elastic constants: II. Application to analysis of soil cracking". *Soil Sci. Soc. of Am. J. 41*, 26-29.

Brockman, F. J., and Murray, C. J. (1997). "Microbiological heterogeneity in the terrestrial subsurface and approaches for its description". In Amy, P. S. and Haldeman, D. L. (Eds.), The microbiology of the terrestrial deep subsurface. CRC Press, Boca Raton, FL.

Brockman, F. J., and Murray, C. J. (1997). "Microbiological heterogeneity in the terrestrial subsurface and approaches for its description". In Amy, P. S. and Haldeman, D. L. (Eds.), The microbiology of the terrestrial deep subsurface. CRC Press, Boca Raton, FL.

Brown, R.B. (2003). "Soil texture". *University of Florida: IFAS Extension SL29,* 1-8.

Campos, L.C., Su, M.F.J., Graham, N.J.D., Smith, S.R. (2002). "Biomass development in slow sand filters". *Water Research 36,* 4543-4551.

Cerning, J., Renard, C.M.G.C., Thibault, J.F., Bouillanne, C., Landon, M., Desmazeaud, M., Topisirovic, L. (1994). "Carbon source requirements for exopolysaccharide production by *Lactobacillus casei* CG11 and partial structure analysis of the polymer". *Applied and Environmental Microbiology 60,* 3914-3919.

Chen, J.X., Fu, X., Wegman, E.J. (1999). "Real-time simulation of dust behavior generated by fast traveling vehicle". *ACM Transactions on Modeling and Computer Simulation 9,* 81-104.

Chen, X., Stewart, P.S. (2002). "Role of electrostatic interactions in cohesion of bacterial biofilms". *Appl Microbiol Biotechnol 59,* 718-720.

Chenu, C. (1993). "Clay- or sand-polysaccharide associations as models for the interface between micro-organisms and soil; water related properties and microstructure". *Geoderma 56,* 143-156.

Chenu, C., Stotzky, G. (2002). "Interactions between microorganisms and soil particles: an overview". In Huang, P. M., Bollag, J. M., and Senesi, N. (Eds.), Interactions of soil particles and microorganisms: impact on the terrestrial ecosystem. John Wiley & Sons, Ltd, West Sussex: England. pp. 1-39.

Congregado, F., Estañol, I., Espuny, M.J., Fusté, M.C., Manresa, M.A., Marqués, A.M., Guinea,J., Simon-Pujol, M.D. (1985). "Preliminary studies on the production and composition of the extracellular polysaccharide synthesized by Pseudomonas sp. ESP-5028". *Biotechnology Letters 7,* 883-888.

Cosentino, D., Chenu, C., Bissonnais, Y.L. (2006). "Aggregate stability and microbial community dynamics under drying-wetting cycles in a silt loam soil". *Soil Biology & Biochemistry 38,* 2053-2062.

Costerton, J.W., Stewart, P.S., Greenberg, E.P. (1999). "Bacterial biofilms: a common cause of persistent infections". *Science 284,* 1318-1322.

Costerton, W.J., Wilson, M. (2004). "Introducing *Biofilms*". *Biofilms 1,* 1-14.

Cunningham, A.B., Characklis, W.G., Abedeen, F., Crawford, D. (1991). "Influence of biofilm accumulation on porous media hydrodynamics". *Environ. Sci. Technol. 25,* 1305-1311.

Daniels, J.L., Cherukuri, R. (2005). "Influence of biofilm on barrier material performance". *Practice Periodical of Hazardous, Toxic, and Radioactive Waste Management 9,* 245-252.

Daniels, J.L., Cherukuri, R. and Ogunro, V.O. (2009) "Consolidation and Strength Characteristics of Biofilm Amended Barrier Soils" *Appropriate Technologies for Environmental Protection in the Developing World*; Yanful, Ernest K. (Ed.), Hardcover, ISBN: 978-1-4020-9138-4, pp. 265-279.

Daniels, J.L., Cherukuri, R., Hilger, H.A., Oliver, J.D. and Bin, S. (2005). "Engineering Behavior of Biofilm Amended Earthen Barriers Used in Waste Containment" *Management of Environmental Quality, An International Journal*, 16 (6), 691-704.

Daniels, J.L., Taylor, G. and Hilger, H.A. (2006). "Shear strength of a landfill cover soil as a function of methane exposure and biofilm production" International Conference on Infrastructure Development and the Environment, Abuja, Nigeria, September 10-15, 2006.

De Brouwer, J.F.C., Ruddy, G.K., Jones, T.E.R., Stal, L.J. (2002). "Sorption of EPS to sediment particles and the effect on the rheology of sediment slurries". *Biogeochemistry 61,* 57-71.

De Brouwer, J.F.C., Ruddy, G.K., Jones, T.E.R., Stal, L.J. (2005). "Biogenic stabilization of intertidal sediments: the importance of extracellular polymeric substances produced by benthic diatoms". *Microbial Ecol. 49,* 501-512.

De Brouwer, J.F.C., Stal, L.J. (2001). "Short-term dynamics in microphytobenthos distribution and associated extracellular carbohydrates in surface sediments of an intertidal mudflat". *Marine Ecology Progress Series 218,* 33-44.

De Brouwer, J.F.C., Wolfstein, K., Ruddy, G.K., Jones, T.E.R., Stal, L.J. (2005). "Biogenic stabilization of intertidal sediments: The importance of extracellular polymeric substances produced by benthic diatoms". *Microbial Ecology 49,* 501-512.

De Caire, G.Z., De Cano, M.S., Palma, R.M., De Mulé, C.Z. (2000). "Changes in soil enzyme activities following additions of cyanobacterial biomass and exopolysaccharide". *Soil Biology & Biochemistry 32*, 1985-1987.

De Boer, W., Klein Gunnewiek, P.J.A., Parkinson, D., 1996. Variability of N mineralization and nitri®cation in a simple, simulated microbial forest soil community. *Soil Biology & Biochemistry 28*, 203-211.

Decho, A.W., Visscher, P.T., Reid, R.P. (2005). "{roduction and cycling of natural microbial exopolymers (EPS) within a marine stromatolite". *Palaeogeography, Palaeoecology 219,* 71-86.

DeFlaun, M. F., Oppenheimer, S. R., Streger, S., Condee, C. W., Fletcher, M. (1999). "Alterations in adhesion, transport, and membrane characteristics in an adhesion-deficient pseudomonad". *Appl. & Environ. Microbio. 65*, 759-765.

DeFlaun, M. F., Oppenheimer, S. R., Streger, S., Condee, C. W., Fletcher, M. (1999). "Alterations in adhesion, transport, and membrane characteristics in an adhesion-deficient pseudomonad". Applied and Environmental Microbiology 65, 759-765.

Degeest, B., Vaningelgem, F., De Vuyst, L. (2001). "Microbial physiology, fermentation kinetics, and process engineering of heteropolysaccharide production production by lactic acid bacteria". *International Dairy Journal 11,* 747-757.

Den Blanken, J.G. (1983). "Mathematical description of the microbial activity in a batch system of activated carbon, phenol, and *Arthrobacter* strain 381". In McGuire, M.J., Suffet, I.H. (Eds.), Treatment of water by granular activated carbon. American Chemical Society, Washington, D.C., USA. pp. 202-355.

Dennis, J.L. and Turner, J.P. (1998). "Hydraulic conductivity of compacted soil treated with biofilm", ASCE Journal of Geotechnical and Geoenvironmental Engineering 124, 120-127.

Dexter, A.R., Kroesbergen, B. (1985). "Methodology for determination of tensile strength of soil aggregates". *Journal of Agricultural Engineering Research 31*, 139-147.

Dexter, A.R. (2004). "Soil physical quality: Part II. Friability, tillage, tilth and hard-setting". *Geoderma 120*, 215- 225.

Drayton, R.S., Wilde, B.M., Harris, J.H.K. (1992). "Geographical information system approach to distributed modelling". *Hydrological Processes 6,* 361-368.

Dubey, S. K., Tripathi, A. K., Upadhyay, S. N. (2006). "Exploration of soil bacterial communities for their potential as bioresource". *Biores.Technol. 97,* 2217-2224.

Dubey, S. K., Tripathi, A. K., Upadhyay, S. N. (2006). "Exploration of soil bacterial communities for their potential as bioresource". Bioresource Technology 97, 2217-2224.

Dueñas, M., Munduate, A., Perea, A., Irastorza, A. (2003). "Exopolysaccharide production by *Pediococcus damnosus* 2.6 in a semidefined medium under different growth conditions". *International Journal of Food Microbiology 87*, 113-120.

Eginton, P.J., Gibson, H., Holah, J., Handley, P.S., Gilbert, P. (1995). "The influence of substratum properties on the adhesion of bacterial cells". *Colloids and Surfaces B: Biointerfaces 5,* 153-159.

Epps, A. and Ehsan, M. (2002). "Laboratory study of dust palliative effectiveness". *Journal of Materials in Civil Engineering 14,* 427-435.

Evans, E.A., Calderwood, D.A. (2007). "Forces and bond dynamics in cell adhesion". *Science 316,* 1148-1153.

Fierer, N., Schimel, J. P., Holden, P. A. (2003). "Variations in microbial community composition through two soil depth profiles". *Soil Biol. & Biochem. 35,* 167-176.

Fierer, N., Schimel, J. P., Holden, P. A. (2003). "Variations in microbial community composition through two soil depth profiles". Soil Biology and Biochemistry 35, 167-176.

Fiessinger, F., Mallevialle, J., Benedek, A. (1983). "Interaction of adhesion and bioactivity in full-scale activated-carbon filters: The mont valerian experiment". In McGuire, M.J., Suffet, I.H. (Eds.), Treatment of water by granular activated carbon. American Chemical Society, Washington, D.C., USA. pp. 202-319.

Findlay, R.H., White, D.C. (1983). "Polymeric beta-hydroxyalkanoates from environmental samples and *Bacillus megaterium*". *Applied and Environmental Microbiology 45,* 71-78.

Fredlund, D.G. and Rahardjo, H. (1993). Soil mechanics for unsaturated soils. Wiley Publishers. NY, USA.

Gamar, L., Blondeau, K., Simonet, J.M. (1997). "Physiological approach to extracellular polysaccharide production by *Lactobacillus rhamnosus* strain C83". *Journal of Applied Microbiology 83,* 281-287.

Gamar-Nourani, L., Blondeau, K., Simonet, J.M. (1998). "Influence of culture conditions on exopolysaccharide production by *Lactobacillus rhamnosus* strain C83". *Journal of Applied Microbiology 85,* 664-672.

Gandhi, H.P., Ray, R.M., Patel, R.M. (1997). "Exopolymer production by *Bacillus* species". *Carbohydrate Polymers 34*, 323-327.

Gasdorf, H. J., Benedict, R. G., Cadmus, M. C., Anderson, R. F., Jackson, R. W. (1965). "Polymer producing species of Arthrobacter". *J. of Bacteriology 99*, 147-150.

Gasdorf, H.J., Benedict, R.G., Cadmus, M.C., Anderson, R.F., Jackson, R.W. (1965). "Polymer producing species of *Arthrobacter*". *Journal of Bacteriology 90,* 147-150.

Gay, C. and Leibler, L. (1999). "On stickiness". *Physics Today 52*, 48-52.

Gay, C., Leibler, L. (1999). "On stickiness: The behavior of tacky materials is difficult to quantify, involving as it does such dynamic phenomena as meniscus instability, cavitation, and the formation of filaments". *American Institute of Physics,* 48-52.

Gillies, J.A., Watson, J.G., Rogers, C.F., Chow, J.C. (2007). "For presentation at the air & waste management association's 90th annual meeting & exhibition, June 8-13, 1997, Toronto,Ontario, Canada". *PM10 emissions and dust suppressant efficiencies on an unpaved road, merced county, CA*, 1-10.

Gonsalves, k. E., Patel, S. H., Chen, X. (1991). "Development of potentially degradable mateirials for marine applications. Ll. Polypropylene-starch blends". *J. of Appl. Poly. Sci. 43*, 405-415.

Görner, T., de Donato, P., Ameil, M.-H., Montarges-Pelletier, E., Lartiges, B.S. (2003). "Activated sludge exopolymers: separation and identification using size exclusion chromatography and infrared micro-spectroscopy". *Water Research 37*, 2388-2393.

Grayston, S. J., Griffith, G. S., Mawdsley, J. L., Campbell, C. D., Bardgett, R. D. (2001). "Accounting for variability in soil microbial communities of temperate upland grassland ecosystems". *Soil Biol. & Biochem. 33*, 533-551.

Grayston, S. J., Griffith, G. S., Mawdsley, J. L., Campbell, C. D., Bardgett, R. D. (2001). "Accounting for variability in soil microbial communities of temperate upland grassland ecosysytems". Soil Biology and Biochemistry 33, 533-551.

Guibard, G., Tixier, N., Boujou, A., Baudu, M. (2003). "Relation between extracellular polymers' composition and its ability to complex Cd, Cu, and Pb". *Chemosphere 52,* 1701-1710.

Guibaud, G., Comte, S., Bordas, F., Dupuy, S., Baudu, M. (2005). "Comparison of the complexation of extracellular polymeric substances (EPS), extracted from activated sludges and produced by pure bacteria strains, for cadmium, lead and nickel". *Chemosphere 59*, 629-638.

Hansen, L. H., Ferrari, B., Sorensen, A. H., Veal, D., Sorensen, S. J. (2001). "Detection of oxytetracycline production by streptomyces rimosus in soil microcosms by combining whole-cell biosensors and flow cytometry". *Appl. & Environ. Microbio. 67*, 239-244.

Hansen, L. H., Ferrari, B., Sorensen, A. H., Veal, D., Sorensen, S. J. (2001). "Detection of oxytetracycline production by streptomyces rimosus in soil microcosms by combining whole-cell biosensors and flow cytometry". Applied and Environmental Microbiology 67, 239-244.

Hayashi, H., Tsuneda, S., Hirata, A., Sasaki, H. (2001). "Soft particle analysis of bacterial cells and its interpretation of cell adhesion behaviors in terms of DLVO theory". *Coll. & Surfaces B: Biointerfaces 22*, 149-157.

Heithoff, D.M., Mahan, M.J. (2004). "*Vibrio cholera* biofilms: stuck between a rock and a hard place". *Journal of Bacteriology 186*, 4835-4837.

Hilger, H.A., Liehr, S.K., Barlaz, M.A. (1999). "A model to assess biofilm exopolymer effects on methane oxidation in landfill cover soil". *Seventh International Waste Management and Landfill Symposium 99*, 411-417.

Hill, G. T., Mitkowski, N. A., Aldrich-Wolfe, L., Emele, L. R., Jurkonie, D. D., Ficke, A. et al. (2000). "Methods for assessing the composition and diversity of soil microbial communities". *Appl. Soil Ecol. 15*, 25-36.

Hill, G. T., Mitkowski, N. A., Aldrich-Wolfe, L., Emele, L. R., Jurkonie, D. D., Ficke, A. et al. (2000). "Methods for assessing the composition and diversity of soil microbial communities". Applied Soil Ecology 15, 25-36.

Hossain, F. (2004). "Activated sludge bulking: A review of causes and control strategies". *IE (I) Journal-EN 85,* 1-6.

Howsam, P. (1990). Microbiology in civil engineering. In Cullimore, D.R. (Ed.), Microbes in civil engineering environments: Introduction. E.&F.N. Spon. London, UK. http://www.uwsp.edu/geo/faculty/hefferan/Geol320/mohrsstress.htm. Class 4: Mohr's circle. 5 July 2007. pp. 1-10.

Hu, C., Liu, Y., Paulsen, B.S., Petersen, D., Klaveness, D. (2003). "Extracellular carbohydrate polymers from five desert soil algae with different cohesion in the stabilization of fine sand grain". *Carbohydrate Polymers 54*, 33-42.

Imam, S. H. and Gould, J. M. (1990). "Adhesion of an amylolytic *Arthrobacter* sp. to starch-containing plastic films". *Applied and Environmental Microbiology, 56,* 872-876.

Inyang, I. and Bae, S. (2006). “Impacts of dust on environmental systems and human health”. *Journal of Hazardous Materials 132,* 5-6.

Inyang, I. (2008). Personal communication.

Jeanes, A., Knutson, C. A., Pittsley, J. E., Watson, P. R. (1965). “Extracellular polysaccharide produced from glucose by *Arthrobacter viscosus* NRRL B-1973: chemical and physical characterization”. *Journal of Appl. Poly. Sci. 9,* 627-638.

Jeanes, A., Knutson, C. A., Pittsley, J. E., Watson, P. R. (1965). “Extracellular polysaccharide produced from glucoe by *Arthrobacter viscosus* NRRL B-1973: chemical and physical characterization”. Juornal of Applied Polymer Science 9, 627-638.

Jjemba, P. K., Kinkle, B. K., Shann, J. R. (2006). “In-situ enumeration and probing of pyrene-degrading soil bacteria”. *FEMS Microbial Ecol. 55,* 287-298.

Jjemba, P. K., Kinkle, B. K., Shann, J. R. (2006). “In-situ enumeration and probing of pyrene-degrading soil bacteria”. FEMS Microbial Ecology 55, 287-298.

Jolly, L., Vincent, S.J.F., Duboc, P., Neeser, J.R. (2002). “Exploiting exopolysaccharides from lactic acid bacteria”. *Antonie van Leewenhoek 82,* 367-374.

Juo, A.S.R., Franzluebbers, K. (2003). Tropical soils: properties and management for sustainable agriculture. Oxford University Press, Inc. New York, NY., USA. pp. 267-273.

Kachlany, S.C., Levery, S.B., Kim, J.S., Reuhs, B.L., Lion, L.W., Ghiorse, W.C. (2001). “Structure and carbohydrate analysis of the exopolysaccharide capsule of *Pseudomonas putida* G7”. *Environmental Microbiology 3,* 774-784.

Kang, S., Hoek, E.M.V., Choi, H., Shin, H. (2006). “Effect of membrane surface properties during the fast evaluation of cell adhesion”. *Separation Science and Technology 41,* 1475-1487.

Katsikogianni, M., Spiliopoulou, I., Dowling, D.P., Missirlis, Y.F. (2006). “Adhesion of slime producing *Staphylococcus epidermidis* strains to PVC and diamond-like carbon/silver/fluorinated coatings”. *J Mater Sci: Mater Med 17,* 679-689.

Keyes, F.G., Collins, S.C. (1932). “The pressure variation of the heat function as a direct measure of the van der waals forces”. *Proc. N.A.S. 18,* 328-333.

Kinkel, L. L., Nordheim, E. V., Andrews, J. H. (1992). “Microbial community analysis in incompletely or destructively sampled systems”. *Microbial Ecol. 24,* 227-242.

Kinkel, L. L., Nordheim, E. V., Andrews, J. H. (1992). “Microbial community analysis in incompletely or destructively sampled systems”. Microbial Ecology 24, 227-242.

Koch, A. L. (2001). "Oligotrophs versus copiotrophs". *Bioessays 23,* 657-661.

Kolari, M. (2003). Attachment mechanisms and properties of bacterial biofilms on non-living surfaces. Academic Dissertation in Microbiology, University of Helsinki, Finland.

Kommedal, R., Bakke, R., Stoodley, P. (2001). "Modelling production of extracellular polymeric substances in a *Pseudomonas aeruginosa* chempstat culture". *Water Science and Technology 43,* 129-134.

Konrad, J.-M and Ayad, R. (1997). "An idealized framework for the analysis of cohesive soils undergoing desiccation". *Can. Geotech. J.* 34, 477-488.

Kruyt, N.P., Rothenburg, L. (2006). "Shear strength, dilatancy, energy and dissipation in quasi static deformation of granular materials". *J. Stat. Mech.,* 07021-07034.

Kuhns, H., Gillies, J., Watson, J., Etyemezian, V., Green, M., Pitchford, M. (2008). "Vehicle-based road dust emissions measurements". Retrieved January 27, 2008 from http://www.epa.gov/ttn/chief/conference/ei12/fugdust/kuhns.pdf.

Kumar, A.S., Mody, K., Jha, B. (2007). "Bacterial exopolysaccharides – a perception". *Journal of Basic Microbiology 47,* 103-117.

La Rosa, G., De Carolis. E., Sali. M., Papacchini. M., Riccardi. C., Mansi. A., (2006). "Genetic diversity of bacterial strains isolated from soils, contaminated with polycyclic aromatic hydrocarbons, by 16S rRNA gene sequencing and amplified fragment length polymorphism fingerprinting". Microbiological Research 161,150-157.

Lane, D.D., Baxter, T.E., Cuscino, T., Cowherd, Jr., C. (1984). "Use of laboratory methods to quantify dust suppressant effectiveness". *Society of Mining Engineers of AIME 274, 2001-2004.*

Lange, S.R., Bhushan, B. (1988). "Use of two-and-three-dimensional noncontact surface profiler for tribology applications". *Surface Topography 1,* 277-289.

Laspidou, C.S., Rittmann, B.E. (2002). "Non-steady state modeling of extracellular polymeric substances, soluble microbial products, and active and inert biomass". *Water Research 36,* 1983-1992.

Lee, W.Y., Park, Y., Ahn, J.K., Ka, K.H., Park, S.Y. (2007). "Factors influencing the production of endopolysaccharide and exopolysaccharide from *Ganoderma applanatum*". *Enzyme and Microbial Technology 40,* 249-254.

Leon-Morales, C.F., Leis, A.P., Strathmann, M., Flemming, H.C. (2004). "Interactions between laponite and microbial biofilms in porous media: implications for colloid transport and biofilm stability". *Water Research 38,* 3614-3626.

Leon-Morales, C.F., Leis, A.P., Strathmann, M., Flemming, H.C. (2004). "Interactions between laponite and microbial biofilms in porous media: implications for colloid transport and biofilm stability". *Water Research 38,* 3614-3626.

Li, J., Luan, Z., Zhu, B., Gong, X., Dangcong, P. (2002). "Effects of colloidal organic matter on nitrification and composition of extracellular polymeric substances in biofilms". *Journal of Chemical Technology and Biotechnology 77,* 1333-1339.

Li, S.Y., Lellouche, J.-P., Shabtai, Y., Arad, S.M. (2001). "Fixed carbon partitioning in the red microalga *Porphyridium* sp. (Rhodophyta)". *J. Phycol. 37,* 289-297.

Li, X.G., Cao, H.B., Wu, J.C., Zhong, F.L., Yu, K.T. (2002). "Enhanced extraction of extracellular polymeric substances from biofilms by alternating current". *Biotechnology Letters 24,* 619-621.

Liu C. and Evett, J. B. Soil properties: testing, measurement, and evaluation. 5th ed. Prentice Hall, Upper Saddle River, NJ. USA.

Loosdrecht, M.C.M. van, Lyklema, J., Norde, W., Schraa G., Zehnder, A.J.B. (1987). "The role of bacterial cell wall hydrophobicity in adhesion". *Applied and Environmental Microbiology 53,* 1893-1897.

Loosdrecht, M.C.M. van, Lyklema, J., Norde, W., Zehnder, A.J.B. (1989). "Bacterial adhesion: A physicochemical approach". *Microbial Ecology 17,* 1-15.

Loosdrecht, M.C.M. van, Lyklema, J., Norde, W., Zehnder, A.J.B. (1990). "Influences of interfaces on microbial activity". *Microbiological Reviews 17,* 75-87.

Loosdrecht, M.C.M. van, Heijnen, J.J., Eberl, H., Kreft, J., Picioreanu, C. (2002). "Mathematicalmodeling of biofilm structures". *Antonie van Leeuwenhoek 81,* 245-256.

Lopez, E., Ramos, I., Sanromán, M.A. (2003). "Extracellular polysaccharides production by *Arthrobacter viscosus*". *Journal of Food Engineering 60,* 463-467.

Lui, Y.Q. (2004). "The effects of extracellular polymeric substances on the formation and stability of biogranules". *Applied Microbiology & Biotechnology 65,* 143-148.

Lünsdorf, H., Erb, R.W., Abraham, W.-R., Timmis, K.N. (2000). "Clay hutches': a novel interaction between bacteria and clay minerals". *Environmental Microbiology 2,* 161-168.

Mal, D., Sinha, S., Dutta, T., Mitra, S., Tarafdar, S. (2007). "Formation of crack patterns in clay films: Desiccation and relaxation". *Journal of the Physical Society of Japan 76*, 014801-1-14801-5.

Malik, M., Nadler, A., Letey, J. (1991). "Mobility of polyacrylamide and polysaccharide polymer through soil materials". *Soil Technology 4*, 255-263.

Marder, M. and Fineberg, F. (1996). "How things break: solid fail through the propagation of cracks, whose speed is controlled by instabilities at the smallest scales". American Institute of Physics. Retrieved April 25, 2007 from http:// chaos.ph.utexas.edu/ ~marder/ fracture/ phystoday/ how_things_break/how_things break.html.

Martens, D.A., Frankenberger, Jr., W.T. (1992). "Decomposition of bacterial polymers in soil and their influence on soil structure". *Biology and Fertility of Soils 13*, 65-73.

Mayer, C., Moritz, R., Kirschner, C., Borchard, W., Maibaum, R. et al. (1999). "The role of intermolecular interactions: studies on model systems for bacterial biofilms". *Inter. J. of Biol. Macromol. 26*, 3-16.

Mayer, C., Moritz, R., Kirschner, C., Borchard, W., Maibaum, R. et al. (1999). "The role of intermolecular interactions: studies on model systems for bacterial biofilms". International Journal of Biological Macromolecules 26, 3-16.

Mazover, A., König, C.S., Holland, D. (2005). "Introduction of tensile strength to sea-ice modeling". *Center for Atmosphere and Ocean Science*. New York University. pp. 1-19.

McSwain, B.S., Irvine, R.L., Hausner, M., Wilderer, P.A. (2005). "Composition and distribution of extracellular polymeric substances in aerobic flocs and granular sludge". *Applied and Environmental Microbiology 71*, 1051-1057.

McSwain, B.S., Irvine, R.L., Hausner, M., Wilderer, P.A. (2005). "Composition and distribution of extracellular polymeric substances in aerobic flocs and granular sludge". *Applied and Environmental Microbiology 71*, 1051-1057.

Miller, D. N., and Woodbury, B.L. (2003). "Simple protocols to determine dust potentials from cattle feedlot soil and surface samples". *Journal of Environmental Quality 32*, 1634-1640.

Mills, A. L., Powelson, D. K. (1996). "Bacterial interactions with surfaces in soils". In Fletcher, M (Ed.), Bacterial adhesion: molecular and ecological diversity. Wiley-Liss, Inc. New York. pp. 25-57.

Mills, A. L., Powelson, D. K. (1996). "Bacterial interactions with surfaces in soils". In Fletcher, M (Ed.), Bacterial adhesion: molecular and ecological diversity. Wiley-Liss, Inc. New York, NY. pp. 25-57.

Miyazaki, T. (2006). Water flow in soils. CRC Press. Baco Raton, FL. USA.

Monokrousos, N., Papatheodorou, E. M., Diamantopoulos, J. D., Stamou, G. P. (2004). "Temporal and spatial variability of soil chemical and biological variables in a Mediterranean shrubland". Forest Ecology and Management 202, 83-91.

Morvan, H., Gloaguen, V., Vebret, L., Joset, F., Hoffmann, L. (1997). "Structure-function investigations on capsular polymers as a necessary step for new biotechnological applications: The case of the cyanobacteria *Mastigocladus laminosus*". *Plant Physiol. Biochem 35,* 671-683.

Muirhead, R.W., Collins, R.P., Bremer, P.J. (2006). "Interaction of *Escherichia coli* and soil particles in runoff". *Applied and Environmental Microbiology 72,* 3406-3411.

Munkholm, L.J., Kay, B.D. (2002). "Effect of water regime on aggregate-tensile strength, rupture energy, and friability". *Soil Sci. Soc. of Am. J. 66,* 702-709.

Munkholm, L.J., Schjønning, P., Kay, B.D. (2002). "Tensile strength of soil cores in relation to aggregate strength, soil fragmentation and pore characteristics". *Soil & Tillage Research 64,* 125-135.

Nakahara, A., Matsuo, Y. (2006). "Imprinting memory into paste to control crack formation in drying process". *J. Stat. Mech.,* 07016-07027.

Nam, T.K., Timmons, M.B., Montemagno, C.D., Tsukuda, S.M. (2000). "Biofilm characteristics as affected by sand size and location in fluidized bed vessels". *Aquacultural Engineering 22,* 213-224.

Nannipieri, P., Ascher, J., Ceccherini, M. T., Landi, L., Pietramellara, G., Renella, G. (2003). Microbial diversity and soil functions. European Journal of Soil Science, December 2003, 54, 655–670.

Nemergut, D. R., Costello, E. K., Meyer, A. F., Pescador, M. Y., Wieintraub, M. N., and Schmidt, S. K. (2005). "Structure and function of alpine and arctic soil microbial communities'. *Res .in Microbio. 156,* 775-784.

Nemergut, D. R., Costello, E. K., Meyer, A. F., Pescador, M. Y., Wieintraub, M. N., and Schmidt, S. K. (2005). "Structure and function of alpine and arctic soil microbial communities". Research in Microbiology 156, 775-784.

Olofsson, A.C., Hermansson, M., Elwing, H. (2003). "*N*-Acetyl-L-Cysteine growth, extracellular polysaccharide production, and bacterial biofilm formation on solid surfaces". *Applied and Environmental Microbiology 69,* 4814-4822.

Omoike, A., Chorover, J., Kwon, K.D., Kubicki, J.D. (2004). "Adhesion of bacterial exopolymers to α-FeOOH: Inner-sphere complexation of phosphodiester groups". *Langmuir 20,* 11108-11114.

Ong, L.C., Lin, Y.H. (2003). "Metabolite profiles and growth characteristics of *Rhizobium meliloti* cultivated at different specific growth rates". *Biotechnol. Prog. 19,* 714-719.

Or, D., Phutane, S., Dechesne, A. (2007). "Extracellular polymeric substances affecting pore scale hydrologic conditions for bacterial activity in unsaturated soils". *Vadose Zone J. 6,* 298-305.

Ortega-Morales, B.O., Santiago-Garcia, J.L., Chan-Bacab, M.J., Moppert, X., Miranda-Tello, E. (2007). "Characterization of extracellular polymers synthesized by tropical intertidal biofilm bacteria". *Journal of Applied Microbiology 102,* 254-264.

Osanna, P.H., Durakbasa, N.M. (1988). "Comprehensive analysis of workpiece geometry using the co-ordinate measurement technique". *Surface Topography 1,* 135-141.

Otero, A., Vincenzini, M. (2004). "*Nostoc* (Cyanophyceae) goes nude: Extracellular polysaccharides serve as a sink for reducing power under unbalanced C/N metabolism". *J. Phycol. 40,* 74-81.

Ozol, M.A. (1978). "Chapter 35—Shape, surface, texture, surface area, and coatings". American Society for Testing and Materials. Philadelphia, Pa., USA. pp. 585-628.

Palmer, J., Flint, S., Brooks, J. (2007). Bacterial cell adhesion, the beginning of a biofilm. *Journal Industrial Microbiology Biotechnology 34,* 577-588.

Papatheodorou, E. M., Argyropoulou, M. D., Stamou, G. P. (2004). "The effects of large- and small-scale differences in soil temperature and moisture on bacterial functional diversity and the community of bacterivorous nematodes". *Appl. Soil Ecol. 25,* 37-49.

Park, H., and Schumacher, R. (2005). "New method to characterize microbial diversity using flow cytometry". *J. of Industrial. Microb. Biotech.32,* 94-102.

Park, H., and Schumacher, R. (2005). "New method to characterize microbial diversity using flow cytometry". Journal of Industrial Microbial Biotechnology 32, 94-102.

Park, Y. S., Kim, D. S., Park, T. J., Song, S. K. (2000). "Effect of extracellular polymeric substances (EPS) on the adhesion of activated sludge". *Bioprocess Eng. 22,* 1-3.

Paul, E. A., and Clark, F. E. (1996). Soil microbiology and biochemistry. Academic Press. San Diego, CA. USA.

Pfiffner, S.M., McInerney, M.J., Jenneman, G.E., Knapp, R.M. (1986). "Isolation of halotolerant, thermotolerant, facultative polymer-producing bacteria and characterization of the exopolymer". *Applied and Environmental Microbiology 51*, 1224-1229.

Philippis, R.D., Vincenzini, M. (1998). "Exocellular polysaccharides from cyanobacteria and their possible applications". *FEMS Microbiology Reviews 22*, 151-175.

Priester, J.H., Horst, A.M., Van De Werfhorst, L.C., Saleta, J. L., et. al. (2007). Enhanced visualization of microbial biofilms by staining and environmental scanning electron microscopy. *Journal of Microbiological Methods 68*, 577-587.

Priester, J.H., Olson, S.G., Webb, S.M., Neu, M.P., Hersman, L.E., Holden, P.A. (2006). "Enhanced exopolymer production and chromium stabilization in *Pseudomonas putida* unsaturated biofilms". *Applied and Environmental Microbiology 72*, 1988-1996.

Prince, J. L., and Dickinson, R. B. (2003). "Kinetics and forces of adhesion for a pair of capsular/uncapsulated staphylococcus mutant strains". *Langmuir 19*, 154-159.

Pulurgurtha, S.S. and James, D. (2006). "Estimating windblown PM-10 emissions from vacant urban land using GIS". *Journal of Hazardous Materials 132*, 47-57.

Radić, T., Kraus, R., Fuks, D., Radić, J., Pečar, O. (2005). "Transparent exopolymeric particles' distribution in the northern Adriatic and their relation to microphytoplankton biomass and composition". *Science of the Total Environment 353*, 151-161.

Rajabipour, F., Weiss, J., Shane, J.D., Mason, T.O., Shah, S.P. (2005). "Procedure to interpret electrical conductivity measurements in cover concrete during rewetting". *Journal of Materials in Civil Engineering 17*, 586-594.

Ramamurthy, T. (2001). "Shear strength response of some geological materials in triaxial compression". *International Journal of Rock Mechanics & Mining Sciences 38*, 683-697.

Reddy, K. (2008). "Engineering properties of soils based on laboratory testing". Retrieved January 26, 2008 from http://www.uic.edu/classes/cemm/cemmlab/Title.pdf.

Rice, M.A., Willets, B.B., McEwan, I.K. (1996). Wind erosion of crusted soil sediments. *Earth Surface Processes and Landforms 21*, 279-293.

Robb, I. D. (1984). "Stereo-biochemistry and function of polymers. In Marshall, K. C. (Ed.), Microbial adhesion and aggregation". Springer-Verlag, New York, NY. pp. 39-49.

Robb, I. D. (1984). “Stereo-biochemistry and function of polymers. In Masrshall, K. C. (Ed.), Microbial adhesion and aggregation”. Springer-Verlag, New York, NY. pp. 39-49.

Roberson, E.B., Firestone, M.K. (1992). “Relationship between desiccation and exopolysaccharide production in a soil *Pseudomonas* sp.”. *Applied and Environmental Microbiology 58*, 1284-1291.

Rodríguez, S.J., Bishop, P.L. (2007). “Three-dimensional quantification of soil biofilms using image analysis”. *Environmental Engineering Science 24,* 96-103.

Rosazak, D.B., Colwell, R.R. (1987). “Survival strategies of bacteria in the natural environment”. *Microbiological Reviews 51,* 365-379.

Rutter, P. R., Dazzo, F. B., Freter, R., Gingell, D., Jones, G. W., et al., (1984). “Mechanisms of adhesion. Group report”. In Marshall, K. C. (Ed.), Microbial adhesion and aggregation. Springer-Verlag, NY. pp. 5-19.

Rutter, P. R., Dazzo, F. B., Freter, R., Gingell, D., Jones, G. W., et al., (1984). “Mechanisms of adhesion. Group report”. In Marshall, K. C. (Ed.), Microbial adhesion and aggregation. Springer-Verlag, New York, NY. pp. 5-19.

Sadhukhan, S., Majumder, S.R., Mal, D., Dutta, T., Tarafdar, S. (2007). “Desiccation cracks on different substrates: simulation by a spring network model”. *J. Phys.: Condens. Matter*, *19,* 356206-356216.

Schneider, U., Steckroth, A., Rau, N., Hübner, G. (1988). “An approach to the evaluation of surface profiles by separating them into functionally different parts”. *Surface Topography 1,* 71-83.

Sekar, R., Venugopalan, V.P., Satpathy, K.K., Nair, K.V.K., Rao, V.N.R. (2004). “Laboratory studies on adhesion of microalgae to hard substrates”. *Hydrobiologica 512,* 109-116.

Sharma, P.K. and Rao, K.H. (2003). “Adhesion of *Paenibacillus polymyxa* on chalcopyrite and pyrite: surface thermodynamics and extended DLVO theory”. *Coll. & Surfaces B: Biointerfaces 29,* 21-38.

Sharma, P.K., Rao, K.H. (2003). “Adhesion of *Paenibacillus polymyxa* on chalcopyrite and pyrite: surface thermodynamics and extended DLVO theory”. *Colloids and Surfaces B: Biointerfaces 29,* 21-38.

Shein, E.V., Polyanskaya, L.M., Devin, B.A. (2002). “Transport of microorganisms in soils: Physiochemical approach and mathematical modeling”. *Eurasian Soil Science 35,* 500-508.

Sheng, G.P., Yu, H.Q., Yu, Z. (2005). "Extraction of extracellular polymeric substances from the photosynthetic bacterium *Rhodopseudomonas acidohila*". *Appl Microbiol Biotechnol 67,* 125-130.

Shingel, K.I. (2004). "Current knowledge on biosynthesis, biological activity, and chemical modification of the exopolysaccharide, pullulan". *Carbohydrate Research 339,* 447-460.

Sichina, W.J. (2008). "Characterization of polymers using TGA". Retrieved October 15, 2008 from http://depts.washington.edu/mseuser/Equipment/RefNotes/TGA_Notes.pdf.

Sivapullaiah, P.V., Lakshmi K. H., Madhu, K.K. (2003). "Geotechnical properties of stabilized Indian red earth". Geotechnical and Geological Engineering 21: 399–413, 2003.

Singer, A., Zobeck, T., Poberezsky, L., Argaman, E. (2003). "The PM_{10} and $PM_{2.5}$ dust generation of soil/sediments in the southern Aral Sea basin, Uzbekistan". *Journal of Arial Environments 54,* 705-728.

Smith, J. L., Halvorson, J. J., Bolton, H. (2002). "Soil properties and microbial activity across a 500 m elevation gradient in a semi-arid environment". *Soil. Bio. & Biochem. 34,* 1749-1757.

Smith, J. L., Halvorson, J. J., Bolton, H. (2002). "Soil properties and microbial activity across a 500 m elevation gradient in a semi-arid environment". Soil Biology and Biochemistry 34, 1749-1757.

Snyder, V.A. and Miller, R. D. (1985). "Tensile strength of unsaturated soil". *Soil Sci. Soc. of Am. J. 49,* 58-65.

Sohlenius, B., and Bostrom, S. (1999). "Effects of climate change on soil factors and metazoan microfauna (nematodes, tardigrades and rotifiers) in a Swedish tundra soil – a soil transplantation experiment". *Appl. Soil Ecol. 12,* 113-128.

Sohlenius, B., and Bostrom, S. (1999). "Effects of climate change on soil factors and metazoan microfauna (nematodes, tardigrades and rotifiers) in a Swedish tundra soil – a soil transplantation experiment". Applied Soil Ecology 12, 113-128.

Sojka, R. E., Entry, J. A., Orts, W. J., Morishita, D. W., Ross, C. W., Home, D. J. (2005). "Synthetic and bio-polymer use for runoff water quality management in irrigated agriculture". *Water Sci. Technol. 51,* 107-115.

Song, J.F. (1988). "Random profile precision roughness calibration specimens". *Surface Topography 1,* 303-314.

Staats, N., Stal, L.J., Mur, L.R. (2000). "Exopolysaccharide production by the epipelic diatom *Cylindrotheca closterium:* effects of nutrient conditions". *Journal of Experimental Marine Biology and Ecology 249,* 13-27.

Stefanov, W. L. (2003). "Identification of fugitive dust generation, transport, and deposition areas using remote sensing". *Environmental and Engineering Geoscience 9,* 151-165.

Stenstrom, T. A. (1989). Bacterial hydrophobicity, an overall parameter for the measurement of adhesion potential to soil particles. *Applied and Environmental Microbiology 55,* 142-147.

Stevens, T. O., and Holbert, B. S. (1995). "Variability and dependence of bacteria in terrestrial subsurface samples: implications for enumeration". *Journal of Microbiological Methods 21,* 283-292.

Swanton, S. W. (1995). "Modelling colloid transport in groundwater; the production of colloid stability and retention behavior". *Advances in Colloid and Interface Science 54,* 129-208.

Taylor, I.S., Patterson, D.M., Mehlert, A. (1999). "The quantitative variability and monosaccharide composition of sediment carbohydrates associated with intertidal diatom assemblages". *Biogeochemistry 45,* 303-327.

Thomas, T.R. (1988). "Surface roughness: The next ten years". *Surface Topography 1,* 3-9.

Thomas, T.R., Thomas, A.P. (1988). "Fractals and engineering surface roughness". *Surface Topography 1,* 143-152.

Tolhurst, T. J., Black, K. S., Shayler, S. A., Mather, S., Black, I., Baker, K., Paterson, D. M. (1999). "Measuring the in situ erosion shear stress of intertidal sediments with the cohesive strength meter (CSM)". *Estuarine Coastal and Shelf Sci. 49,* 281-294.

Torino, M.I., Mozzi, F., Font de Valdez, G. (2005). "Exopolysaccharide biosynthesis by *Lactobacillus helveticus* ATCC 15807". *Applied Microbiology and Biotechnology 68,* 259-265.

Tunlid, A., and White, D. C. (1992). "Biochemical analysis of biomass, community structure, nutritional status, and metabolic activity of microbial communities in soil". In Stotzky, G. and Bollag, J. (Eds.), Soil biochemistry. Marcel Dekker, Inc. New York. pp. 229-262.

Underwood, G.J.C., Boulcott, M., Raines, C.A. (2004). "Environmental effects on exopolymer production by marine benthic diatoms: Dynamics, changes in composition, and pathways of production". *J. Phycol 40,* 293-304.

USEPA. (2002). "Potential environmental impacts of dust suppressants: avoiding another times beach". An Expert Panel Summary. EPA/600/R-04/031, May 30-31.

Valentin, C., Bresson, L.M. (1997). "Soil crusting". In Lal, R., Blum, W.H., Valentine, C., Stewart, B.A. (Eds.), Methods for assessment of soil degradation. CRC Press LLC. Boca Raton, Fl., USA. pp. 89-93.

Valk, A.van der. (2006). The biology of freshwater wetlands. Oxford University Press. New York, USA.

Vandevivere, P., Baveye, P. (1992). "Effect of bacterial extracellular polymers on the saturated hydraulic conductivity of sand columns". *Applied and Environmental Microbiology 58,* 1690-1698.

Vandewalle, N., Lumay, G., Gerasimov, O., Ludewig, F. (2007). "The influence of grain, shape, friction and cohesion on granular compaction dynamics". *The European Physical Journal E 22*, 241-248.

Van der Aa, B.C. and Dufrene, Y.F. (2002). "In situ characterization of bacterial extracellular polymeric substances by AFM". *Colloids and Surfaces B: Biointerfaces 23,* 173–182.

Varnam, A. H., and Evans, M. G. (2000). Environmental microbiology. Manson Publishing, Inc. London, UK.

Veranth, J. M., Pardyjak, E.R., Seshadri, G. (2003). "Vehicle-generated fugitive dust transport: analytic models and field study". *Atmospheric Environment 37,* 2295-2303.

Waldrop, M. P. and Firestone, M. K. (2006). "Response of microbial community composition and function to soil climate change". *Microbial Ecol. 52,* 716-724.

Walker, S.L. (2005). "The role of nutrient presence on the adhesion kinetics of *Burkholderia cepacia* G4g and ENV435g". *Colloids and Surfaces B: Biointerfaces 45,* 181-188.

Wang, L., Wang, X., Mohammad, L., Abadie, C. (2005). "Unified method to quantify aggregate shape angularity and texture using fourier analysis". *Journal of Materials in Civil Engineering 17,* 498-504.

Watson, W., Woods, A. (1988). "The 3-D representation of engineering surfaces". *Surface Topography 1*, 165-182.

Watts, C.W., Dexter, A.R. (1998). "Soil friability: theory, measurement and the effects of management and organic carbon content". *European Journal of Soil Science 49,* 73-84.

Wesenberg-Ward, K.E., Tyler, B.J., Sears, J.T. (2005). "Adhesion and biofilm formation of *Candida albicans* on native and pluronic-treated polystyrene". *Biofilms 2,* 63-71.

Wu, J., Cheung, P.C.K., Wong, K., Huang, N. (2004). "Studies on submerged fermentation of *Pleurotus tuber-regium* (Fr.) singer. Part 2: effect of carbon-to-nitrogen ration of the culture medium on the content and composition of the mycelia dietary fibre". *Food Chemistry 85,* 101-105.

Wuertz, S., Spaeth, R., Hinderberger, A., Griebe, T., Flemming, H.-C., and Wildere, P.A. (2001). "A new method for extraction of extracellular polymeric substances from biofilms and activated sludge suitable for direct quantification of sorbed metals". *Water Science and Technology 43,* 25-31.

Yallop, M.L., Paterson, D.M., Wellsbury, P. (2000). "Interrelationships between rates of microbial production, exopolymer production, microbial biomass, and sediment stability in biofilms of intertidal sediments". *Microbial Ecol. 39,* 116-127.

Yang, Z., Weiss, W.J., Olek, J. (2006). "Water transport in concrete damaged by tensile loading and freeze-thaw cycling". *Journal of Materials in Civil Engineering 18,* 424-434.

Yi, T., Harper, Jr., W.F. (2007). "The effect of biomass characteristics on the partitioning and sorption hysteresis of 17α-ethinylestradiol". *Water Research 41,* 1543-1553.

Zhang, T.C., Bishop, P.L. (1994). "Evaluation of tortuosity factors and effective diffusivities in biofilms". *Water Research. 28,* 2279-2287.

Zhang, X., Bishop, P.L., Kinkle, B.K. (1999). "Comparison of extraction methods for quantifying extracellular polymers in biofilms". *Water Science and Technology 39,* 211 218.

Zobeck, T.M, and Pelt, R.S.V. (2006). "Wind-induced dust generation and transport mechanics on bare agricultural field". *Journal of Hazardous Materials 132,* 26-38.

APPENDIX A: TGA ANALYSIS GRAPHS

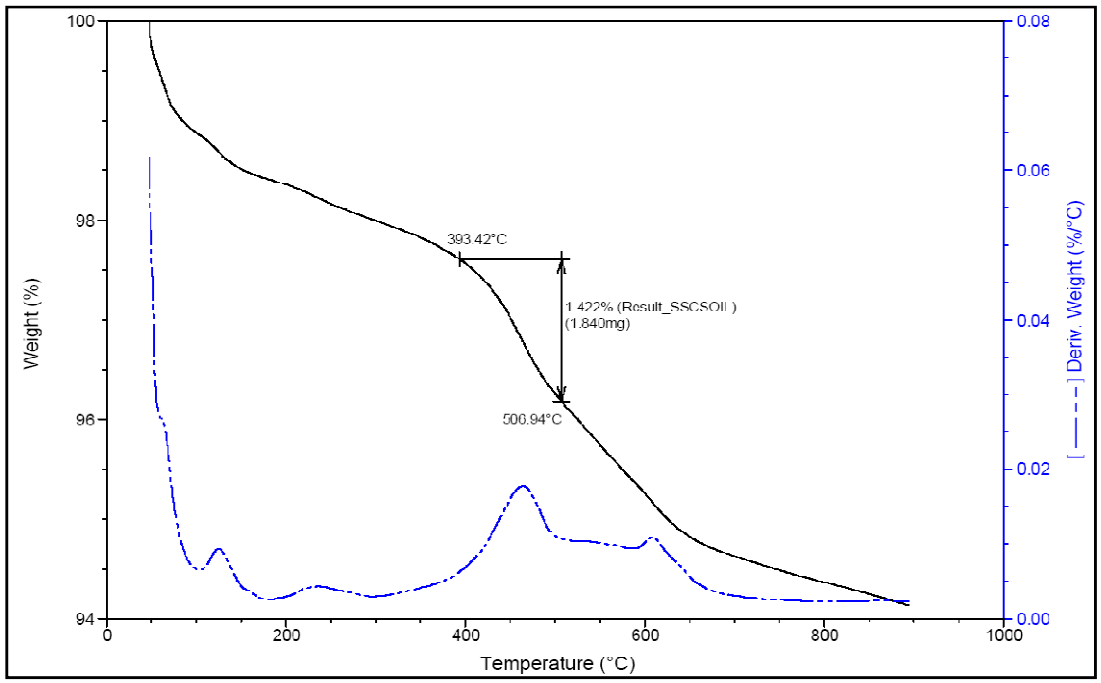

(a)

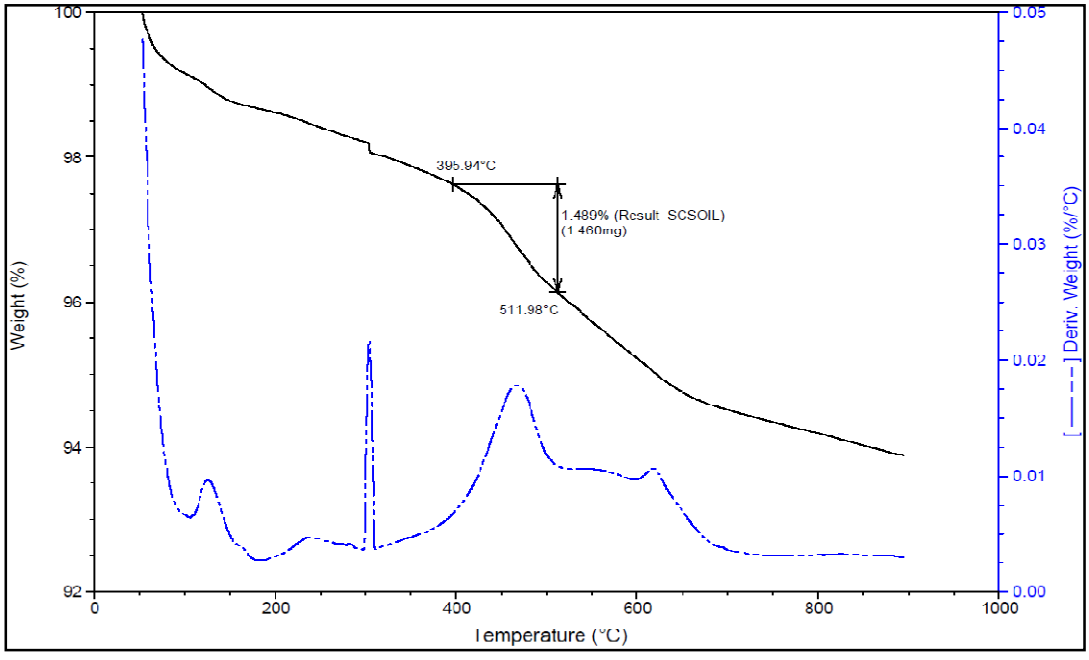

(b)

TGA results showing (a) Sandy silty clay soil; (b) Silty clay soil

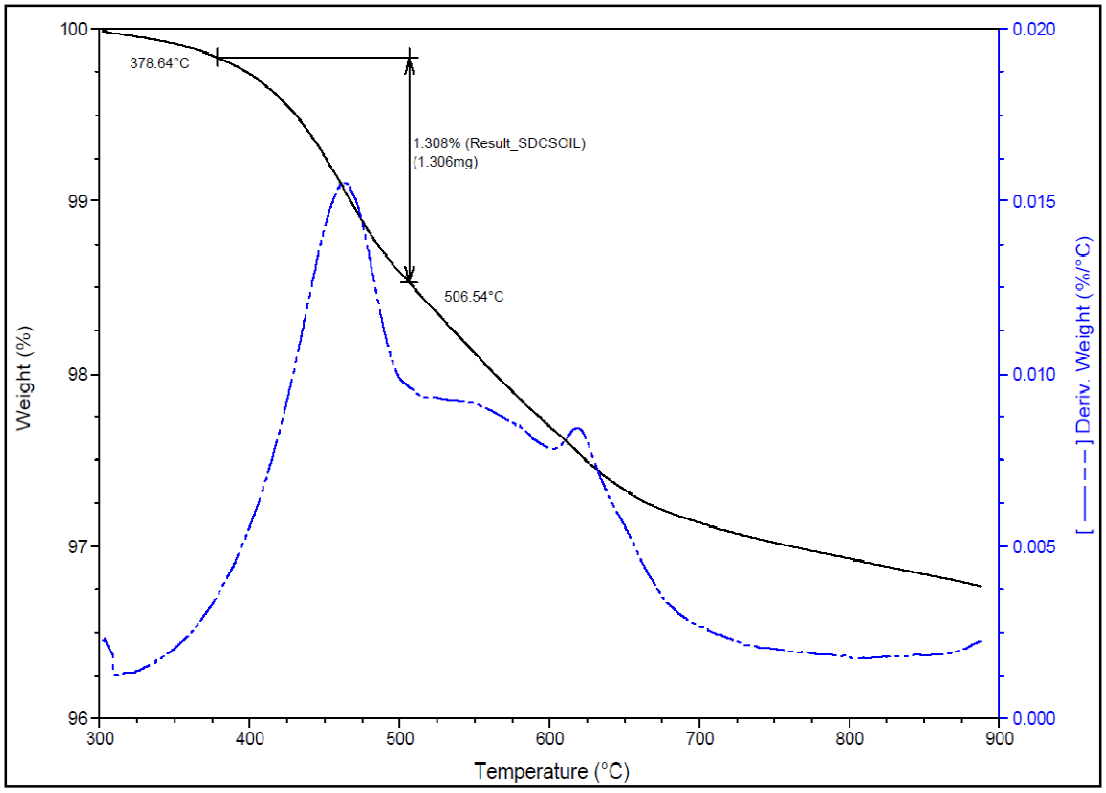

(a)

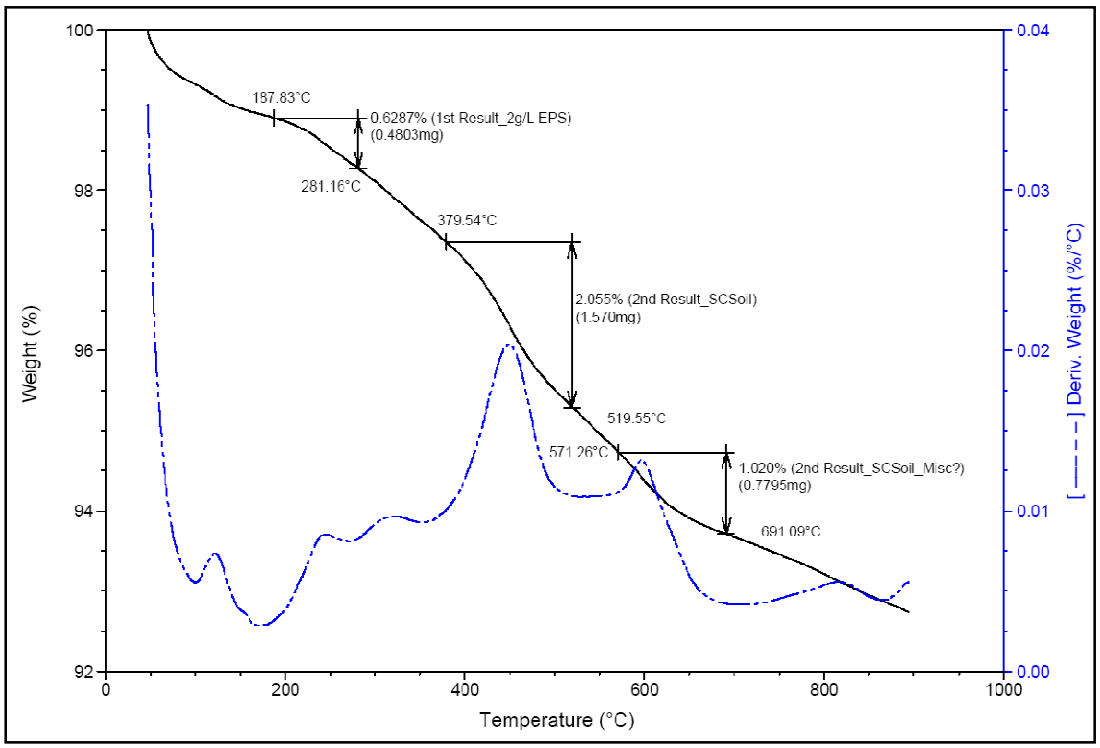

(b)

Figure TGA results showing (a) Sandy clay soil; (b) 2 g/L EPS in soil

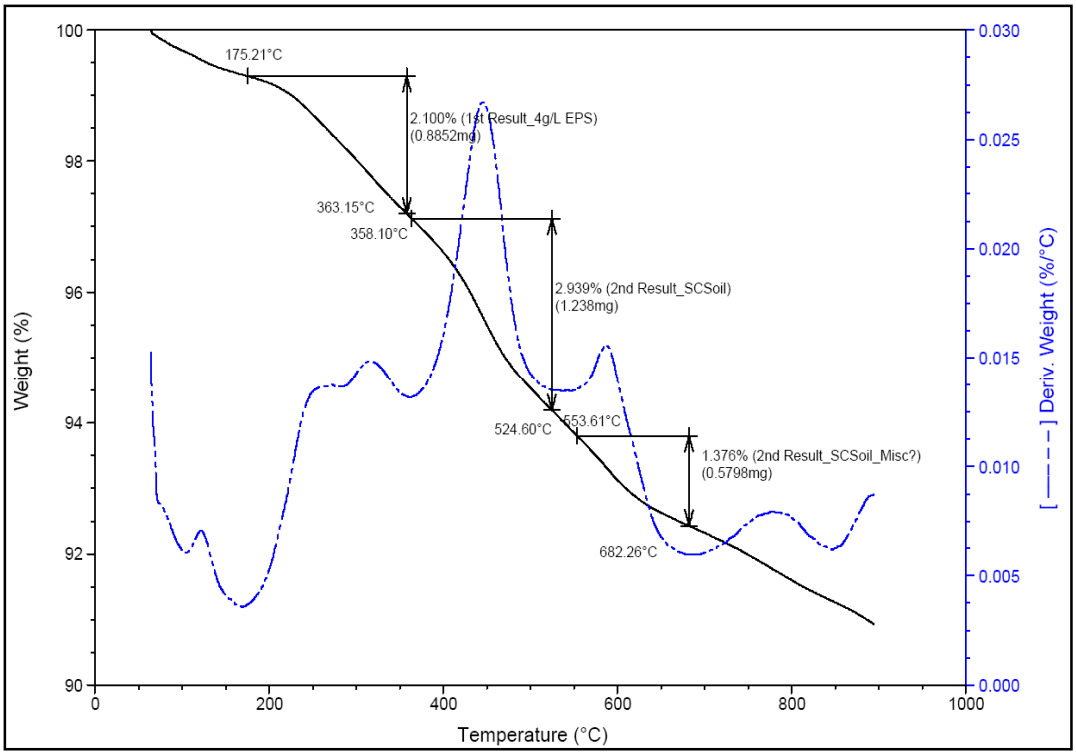

(a)

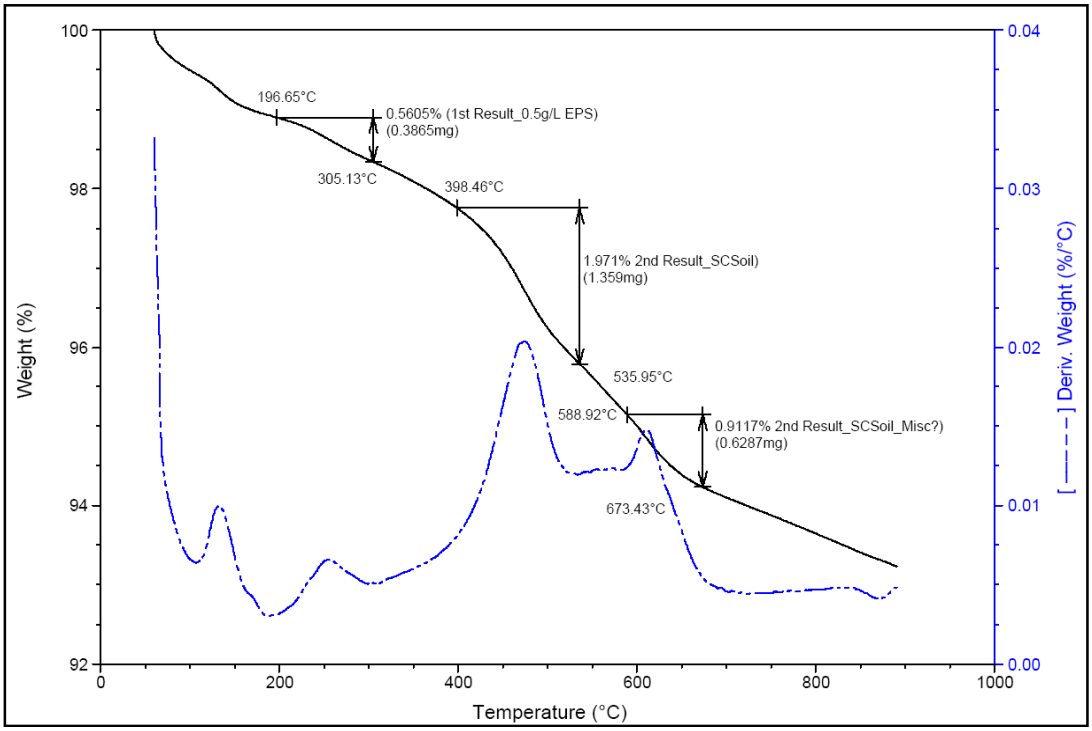

(b)

TGA results showing (a) 4 g/L EPS in soil; (b) 0.5 g/L EPS in soil

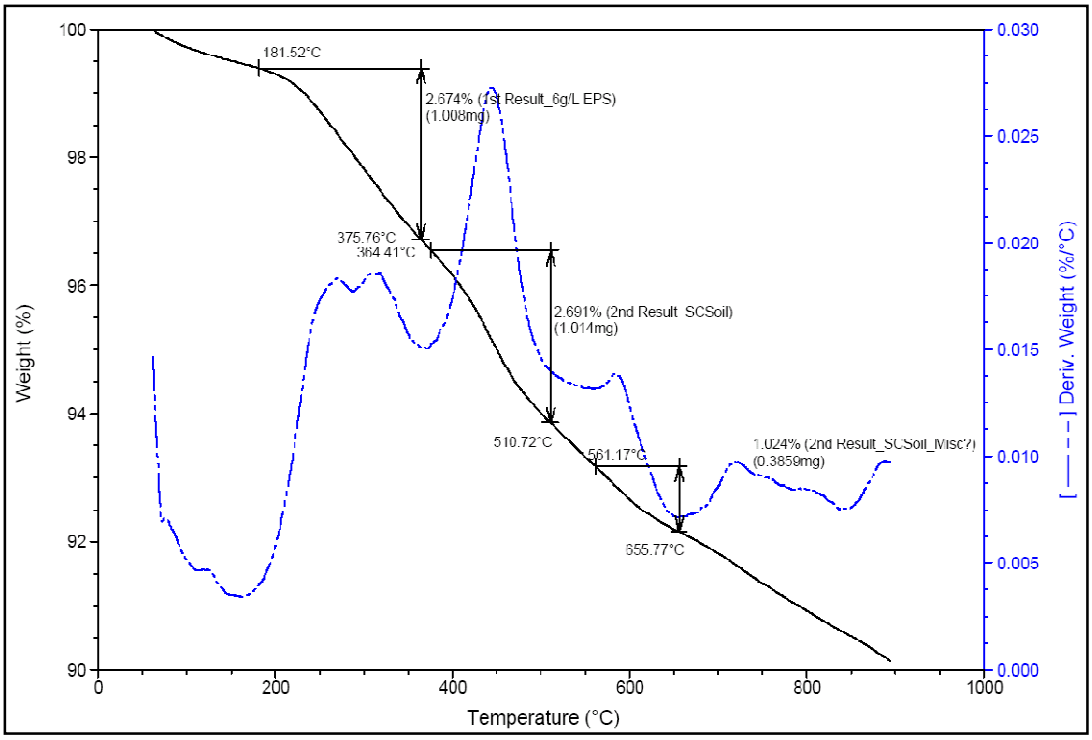

(a)

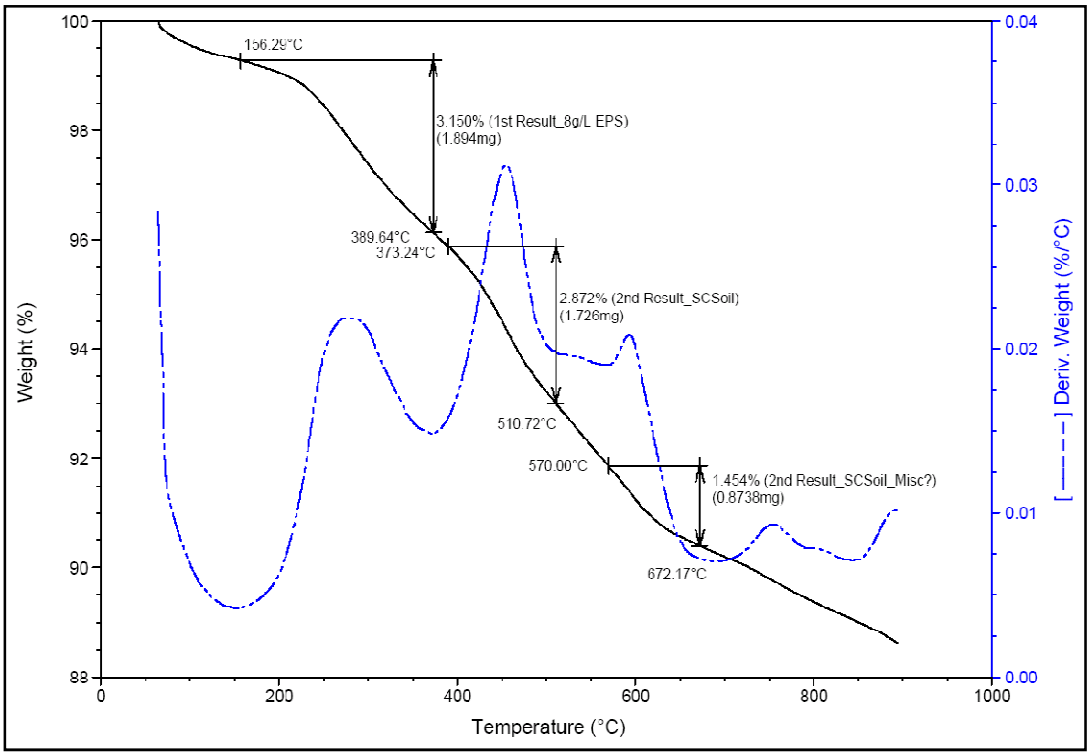

(b)

TGA results showing (a) 6 g/L EPS in soil; (b) 8 g/L EPS in soil

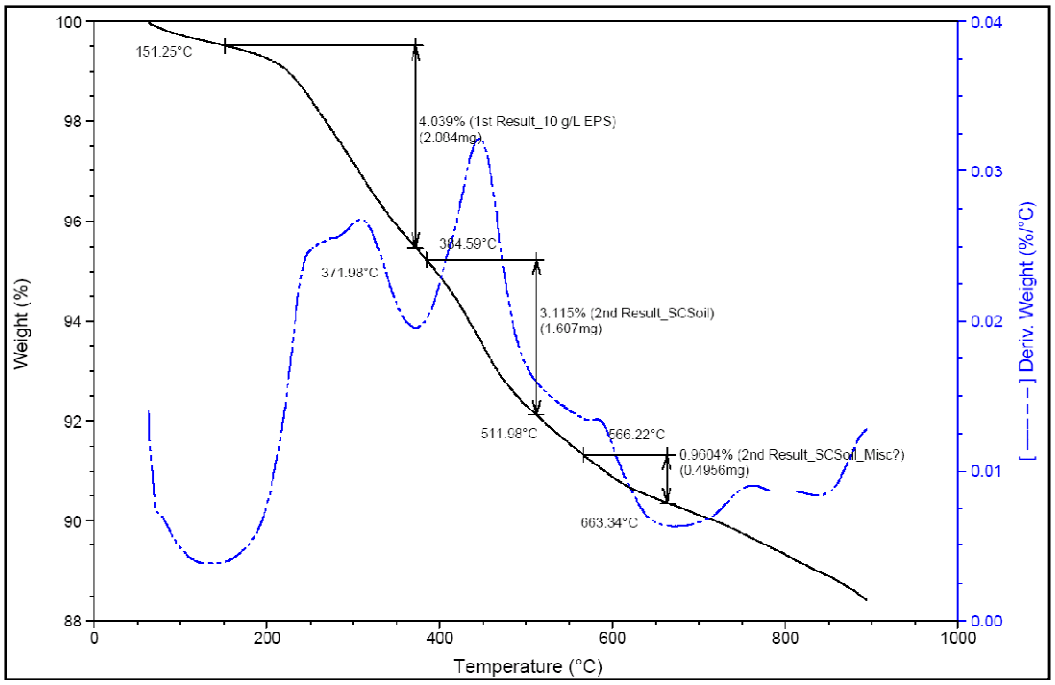

(a)

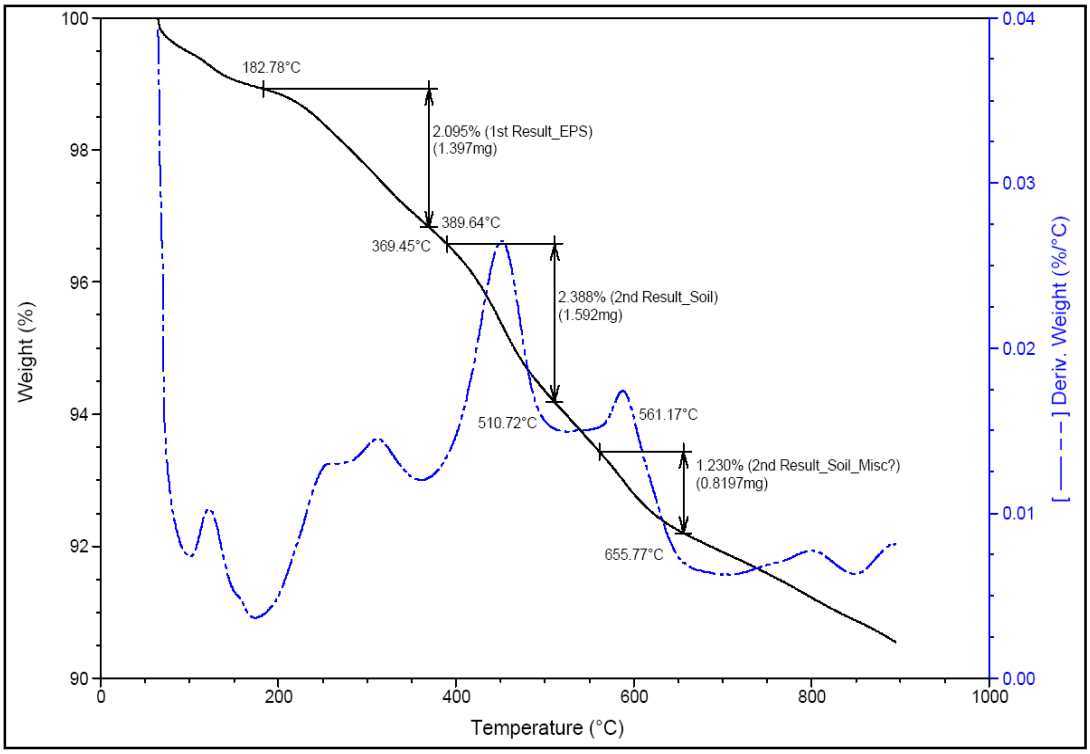

(b)

TGA results showing (a) 4 g/L EPS in soil; (b) 0.5 g/L EPS in soil

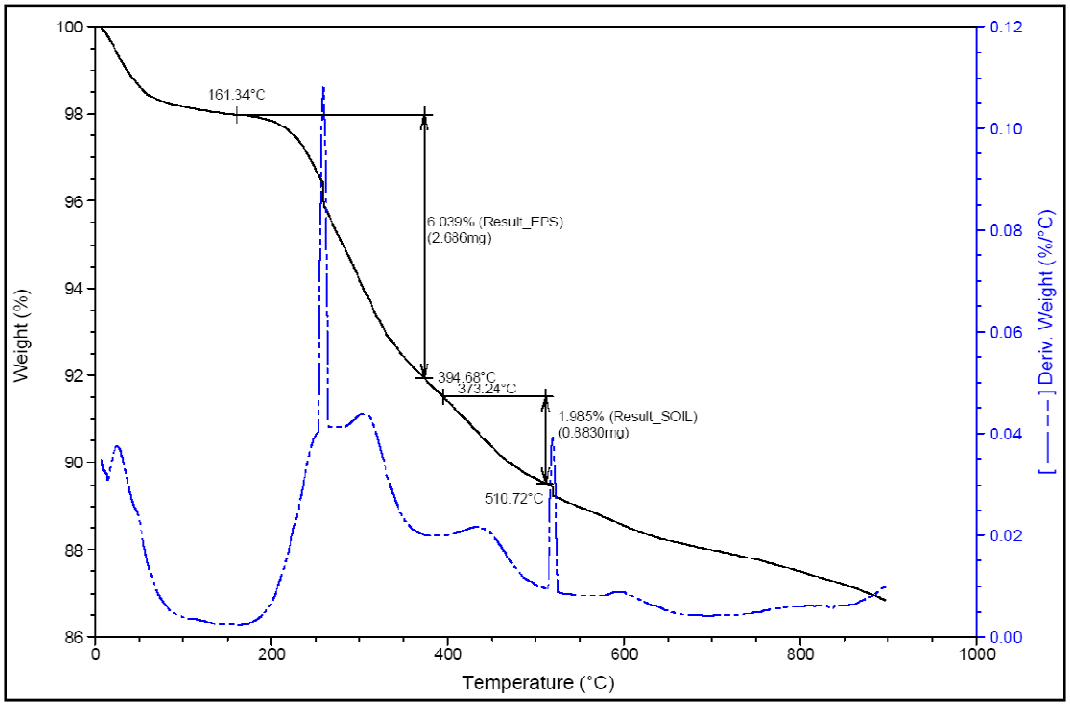

(a)

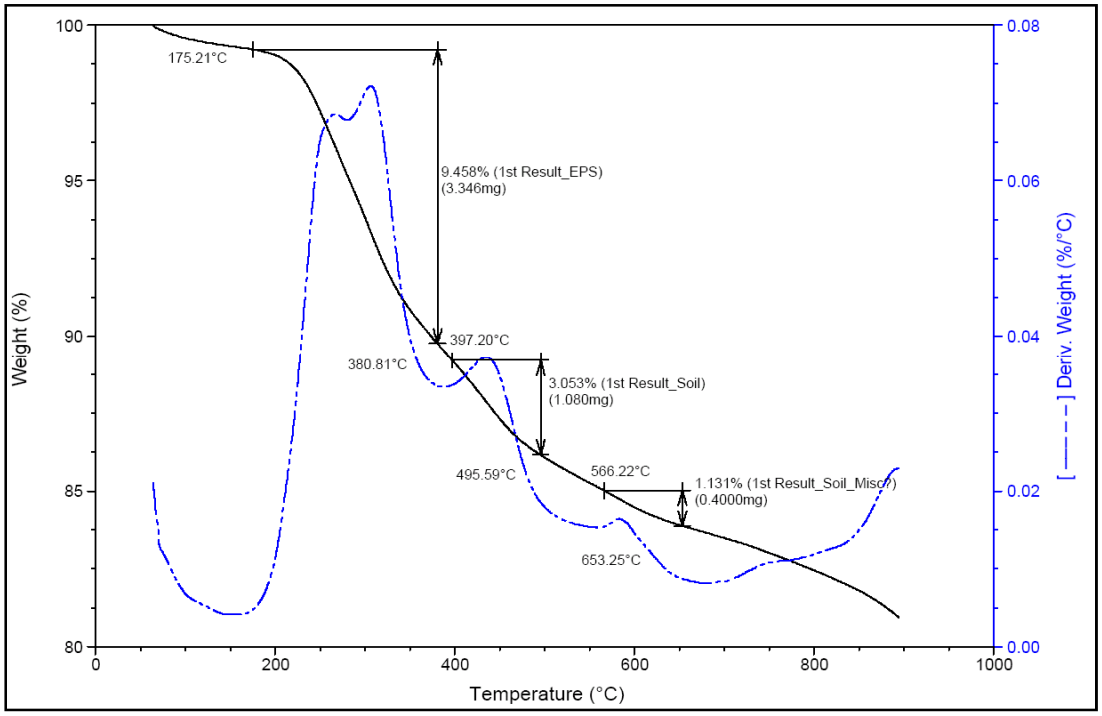

(b)

TGA results showing (a) 40 g/L EPS in soil; (b) 80 g/L EPS in soil

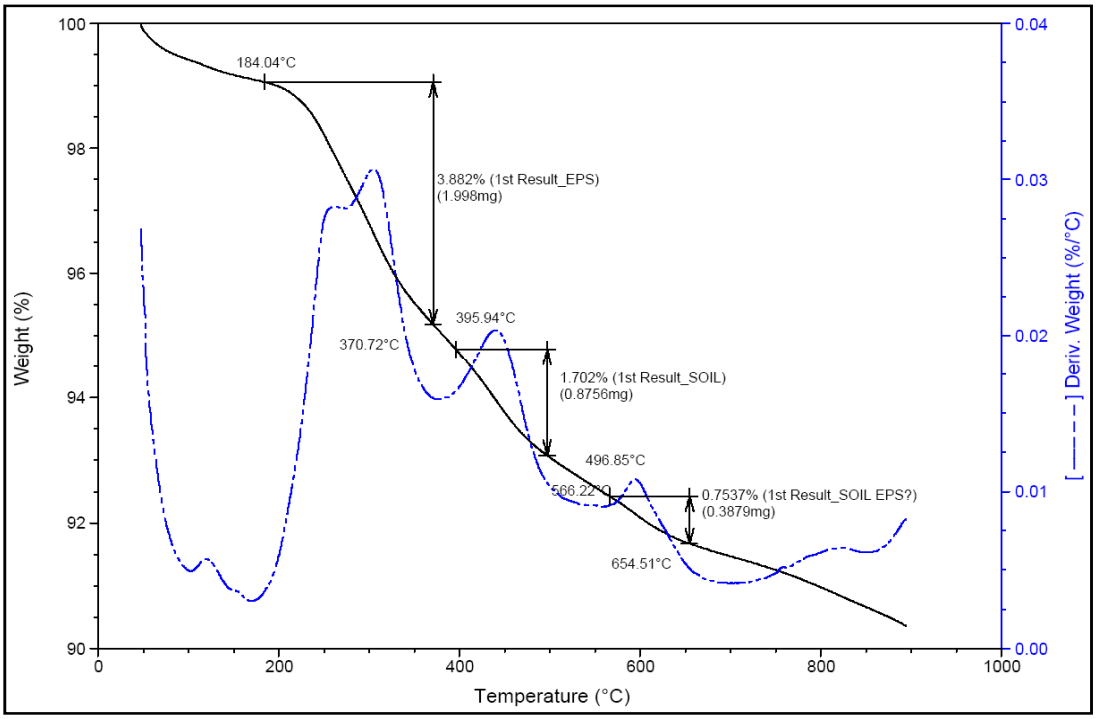

(a)

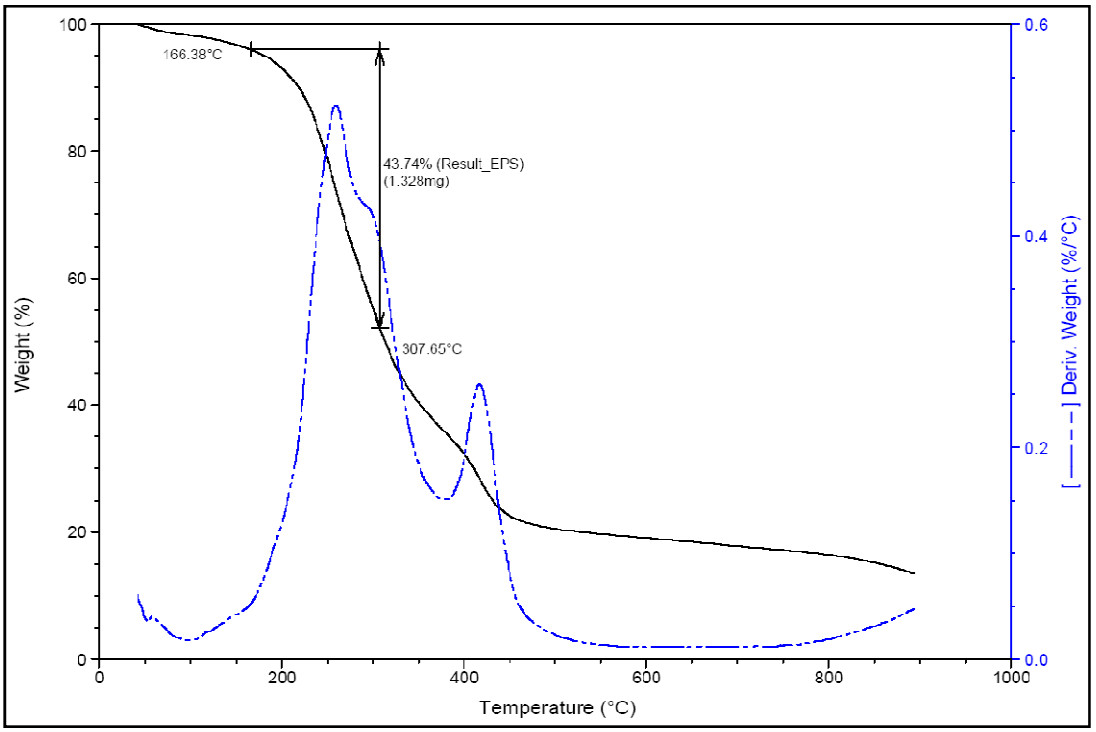

(b)

TGA results showing (a) 100 g/L EPS in soil; (b) 40 % broth production of raw EPS

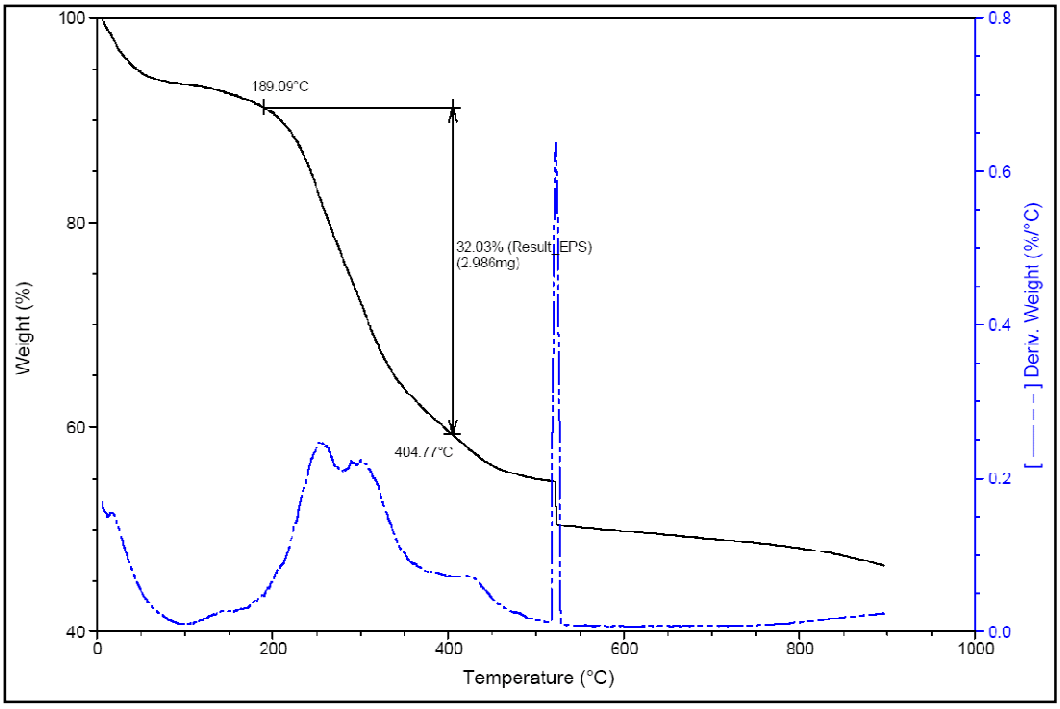

(a)

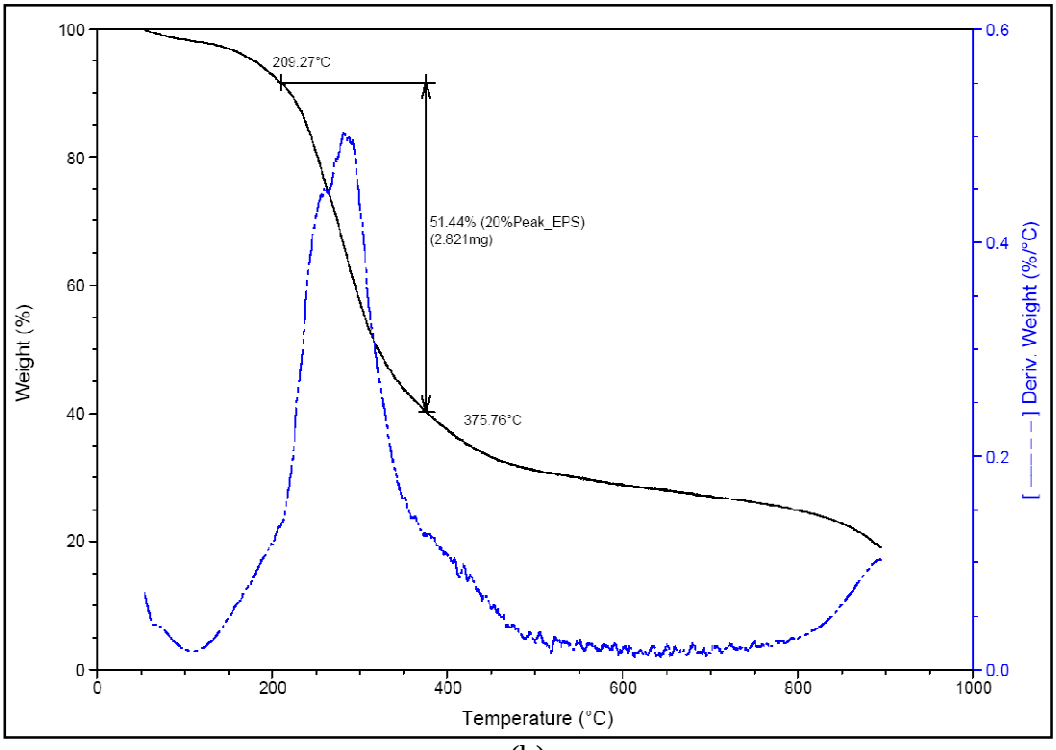

(b)

TGA results showing (a) 10 % broth production of raw EPS; (b) 20 % broth production of raw EPS

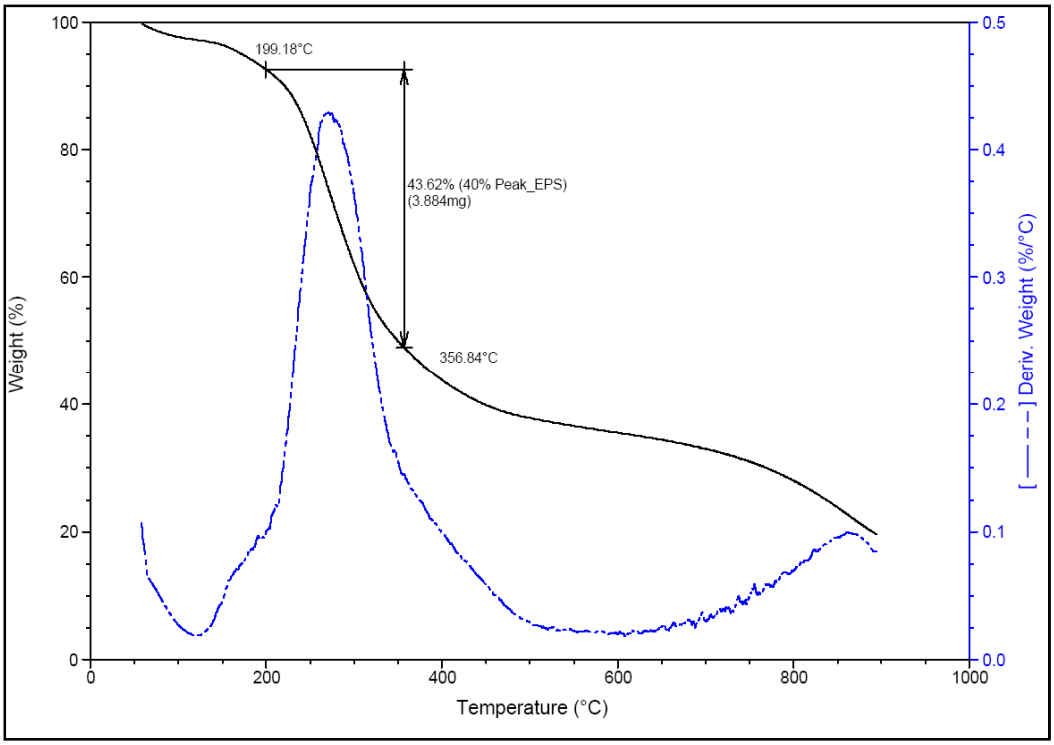

(a)

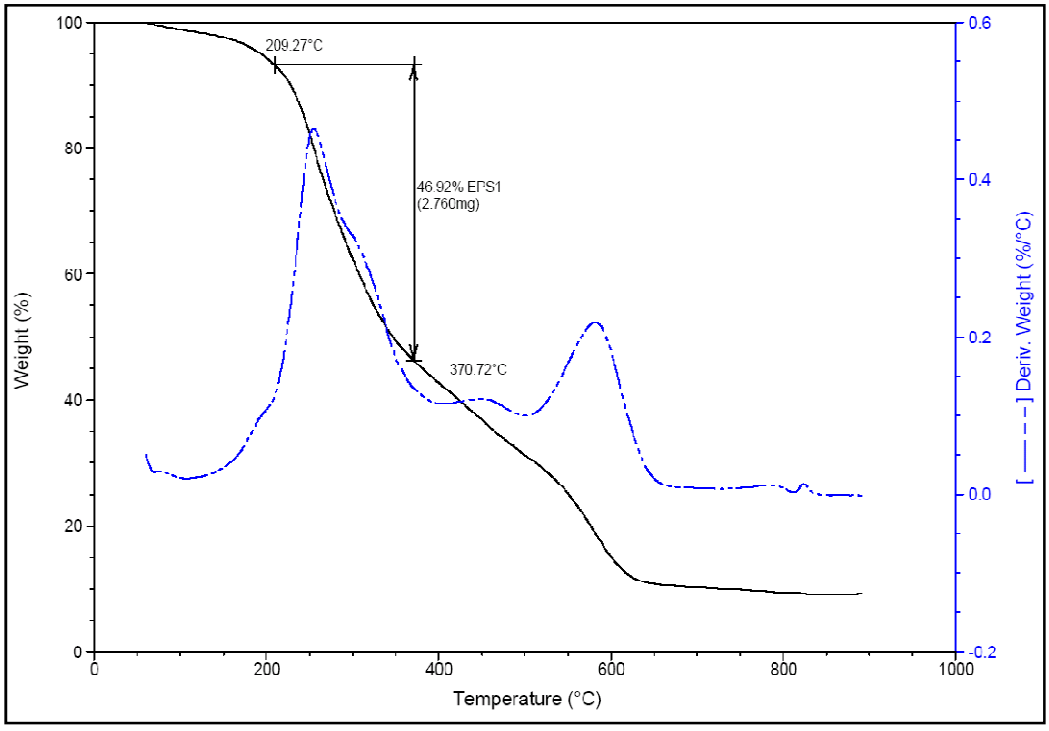

(b)

TGA results showing (a) 40 % broth production of raw EPS; (b) 60 % broth production of raw EPS

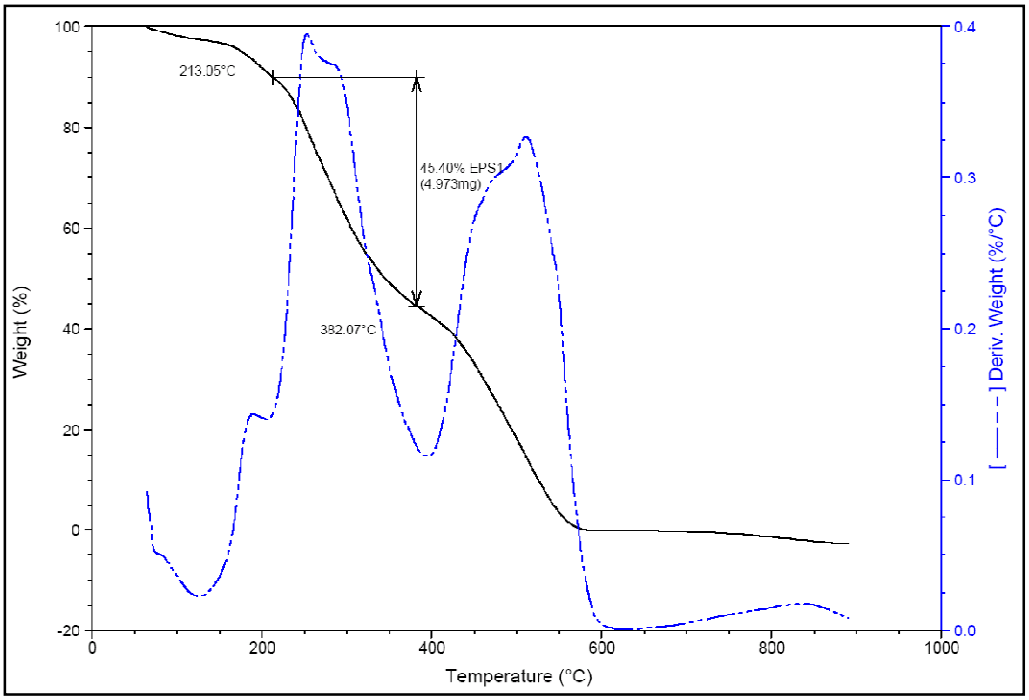

(a)

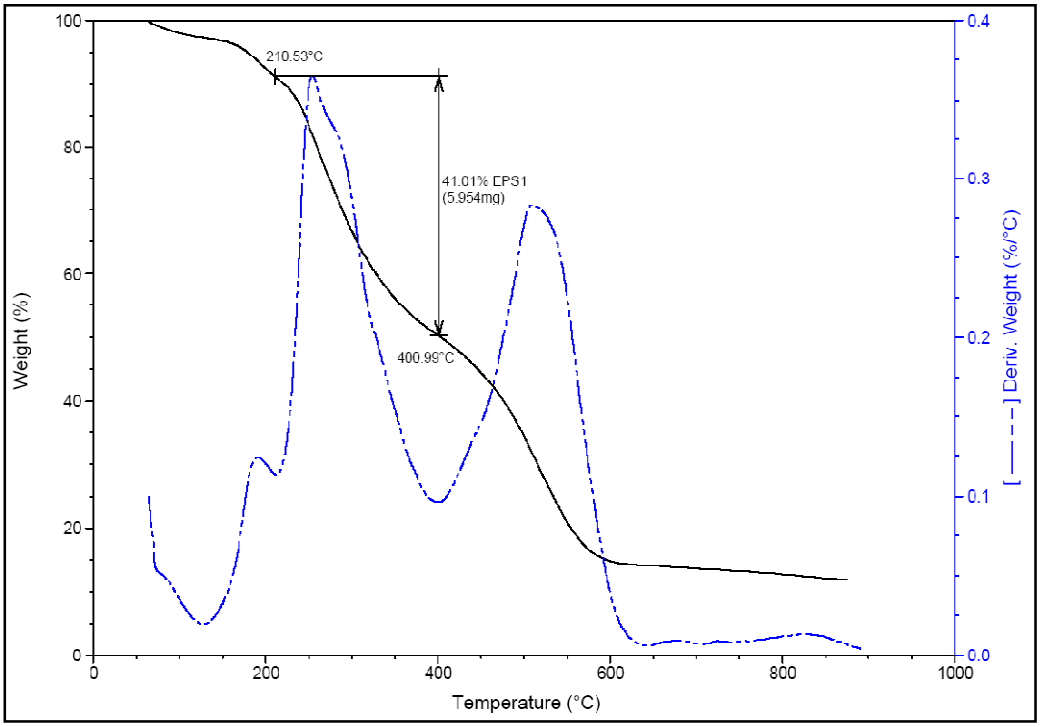

(b)

TGA results showing (a) 80 % broth production of raw EPS; (b) 100 % broth production of raw EPS

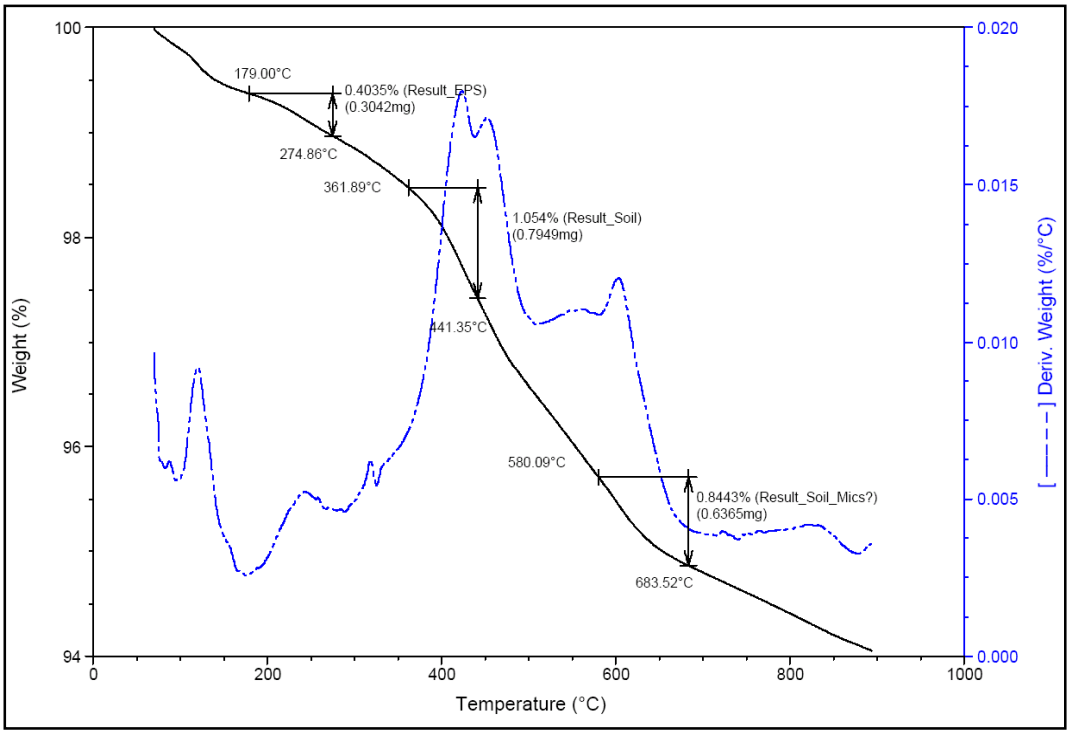

(a)

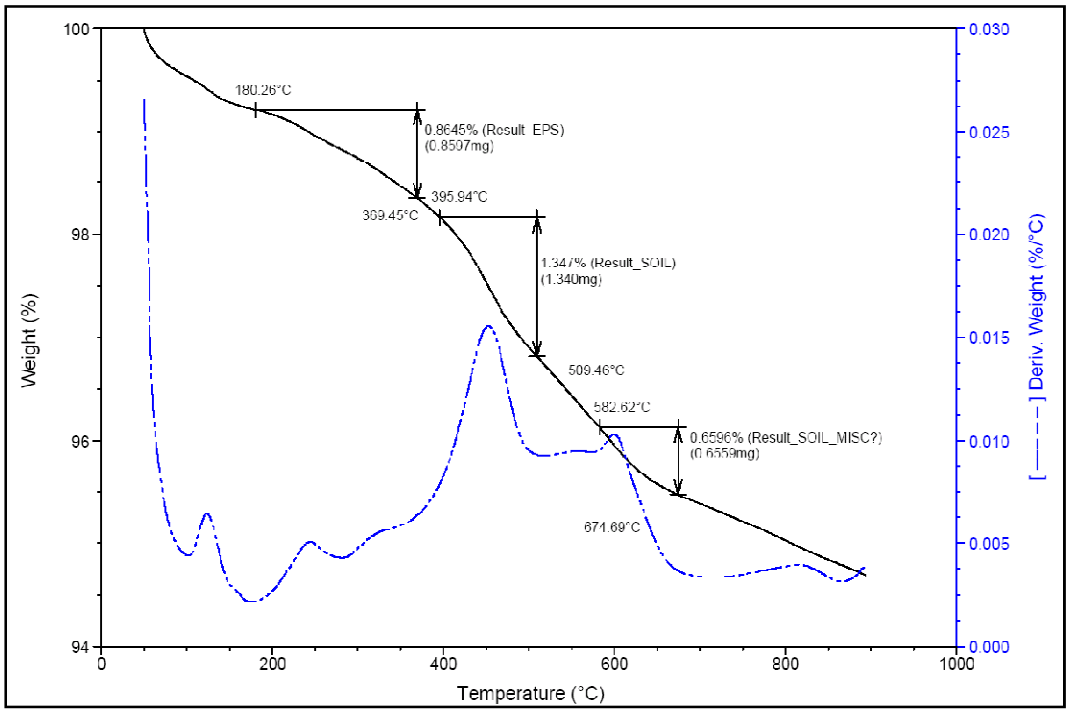

(b)

TGA results: (a) 10 % broth production of EPS in soil; (b) 20 % broth productions of EPS in soil

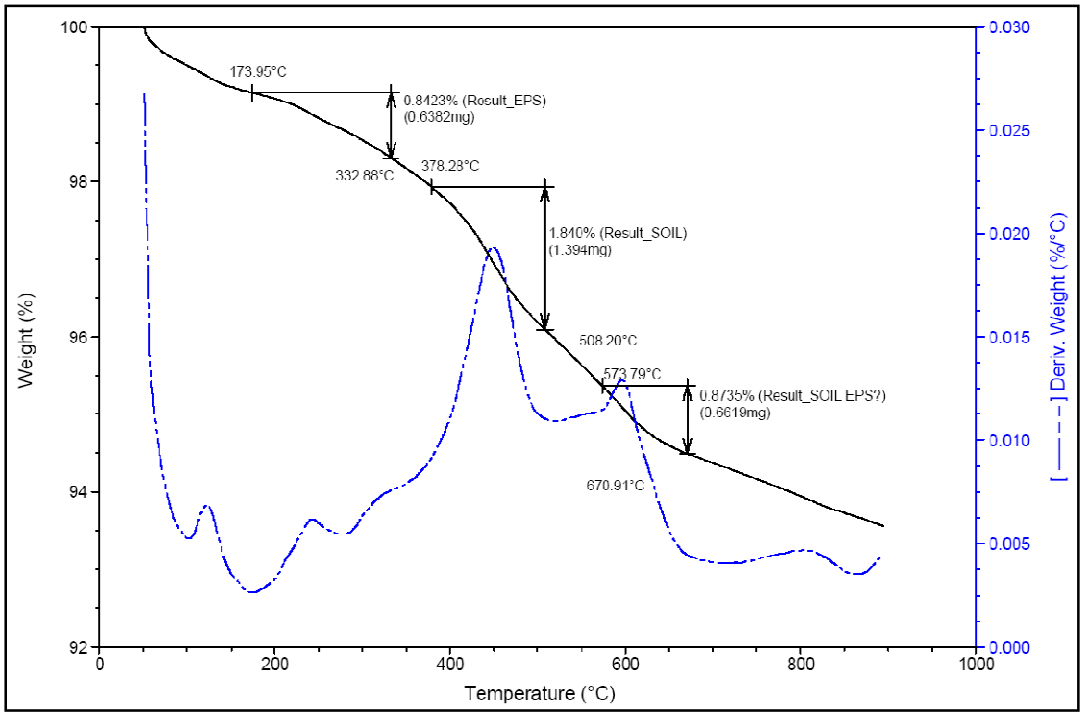

(a)

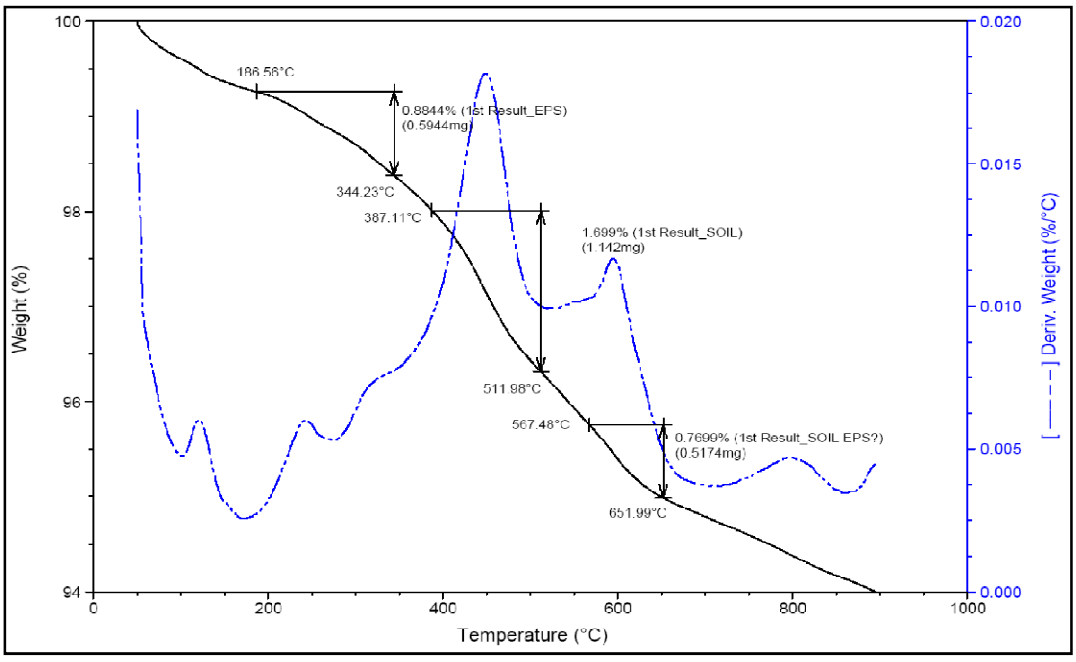

(b)

TGA results: (a) 30 % broth production of EPS in soil; (b) 40 % broth productions of EPS in soil

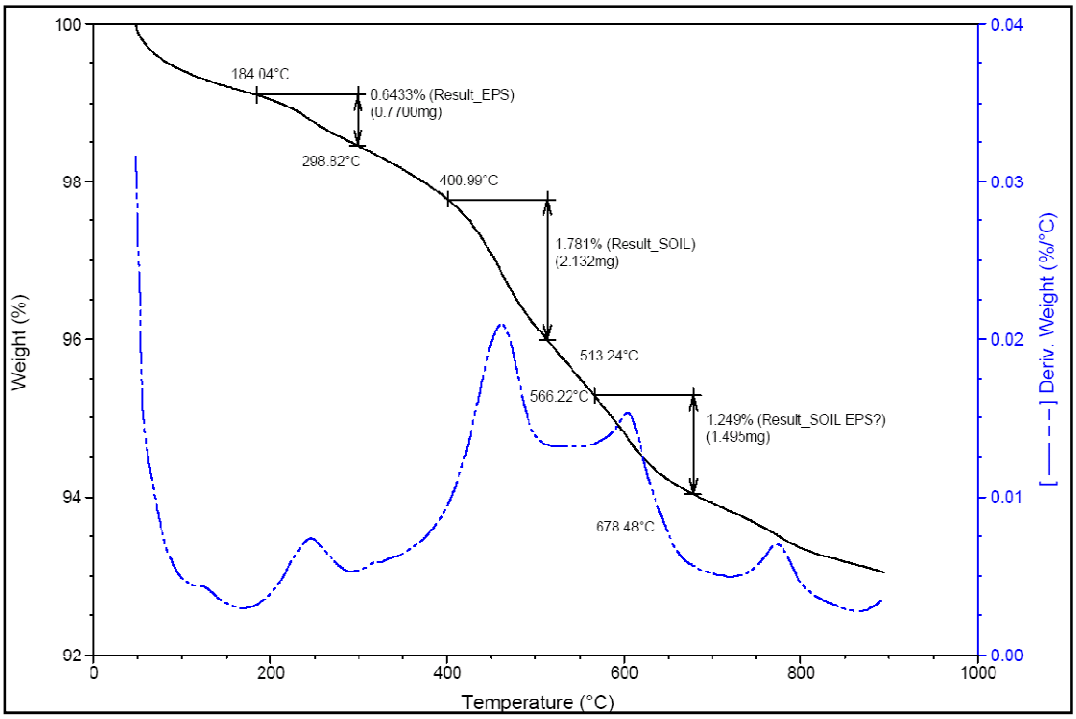

(a)

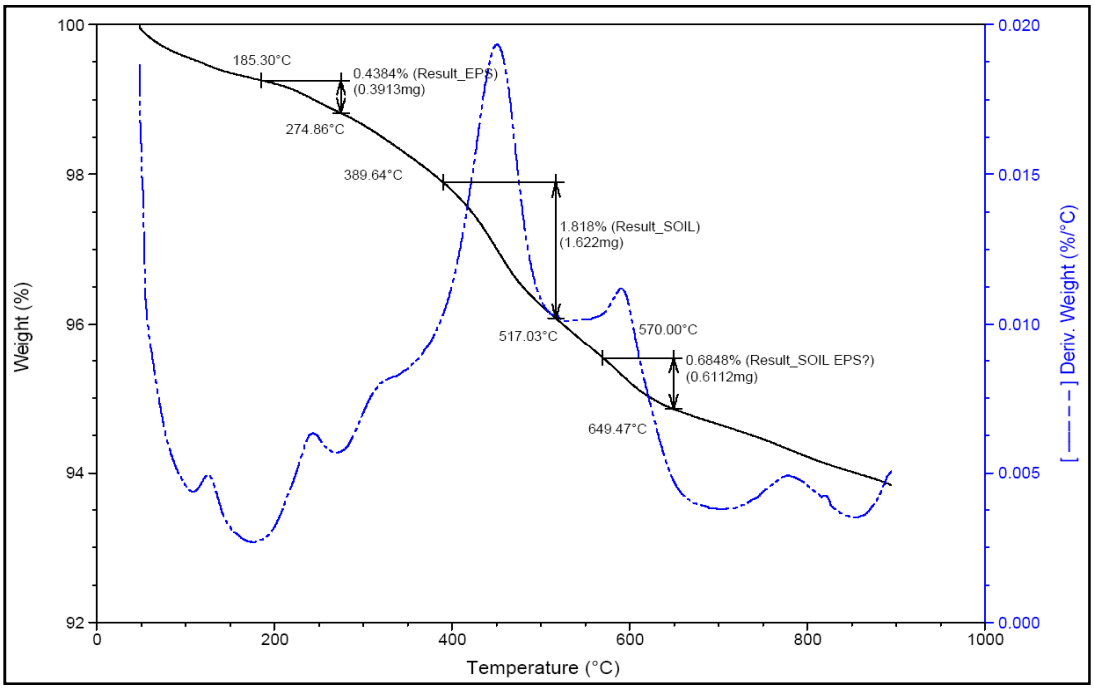

(b)

TGA results: (a) 50 % broth production of EPS in soil; (b) 60 % broth productions of EPS in soil

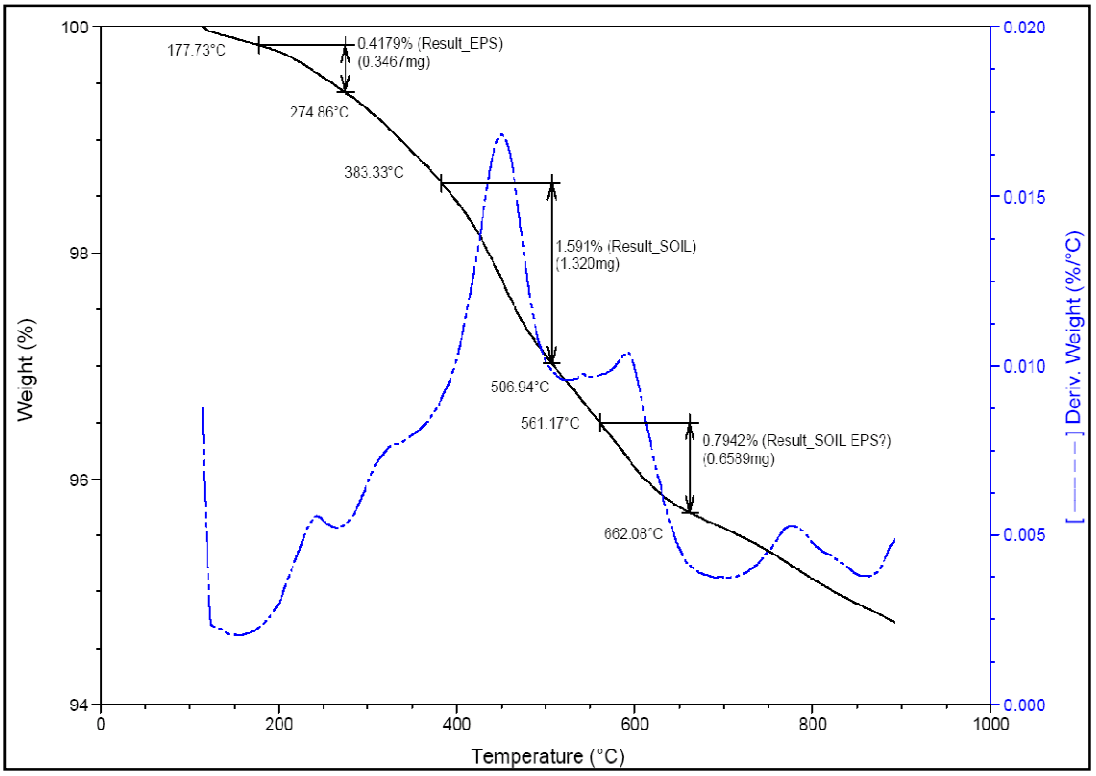

(a)

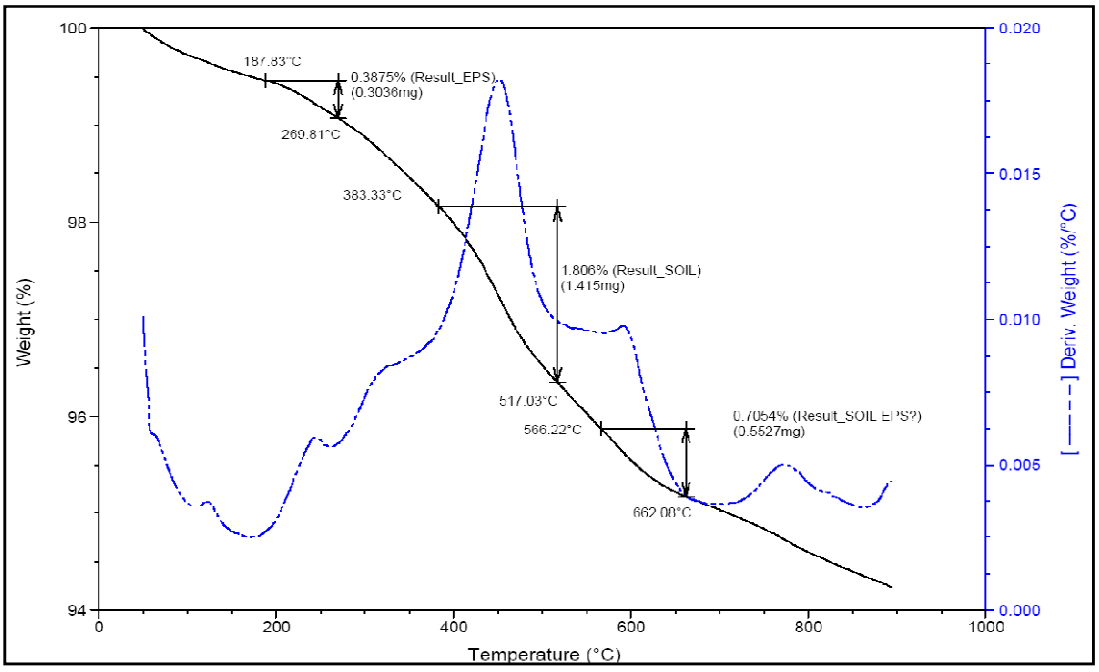

(b)

TGA results (a) 70 % broth production of EPS in soil; (b) 80 % broth productions of EPS in soil

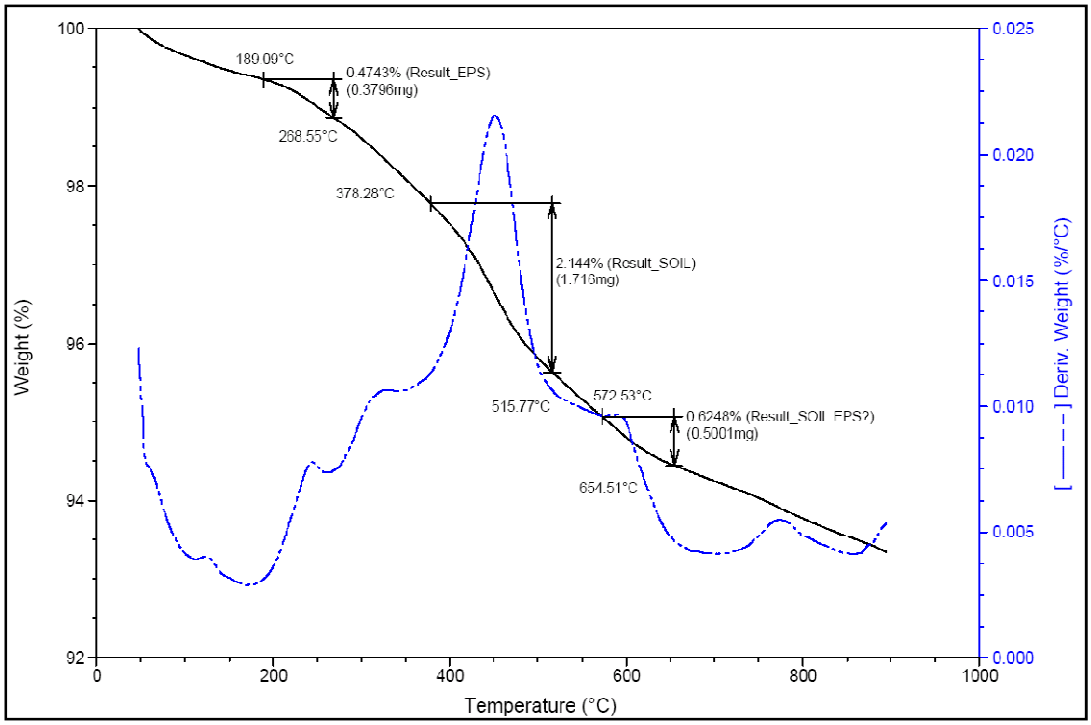

(a)

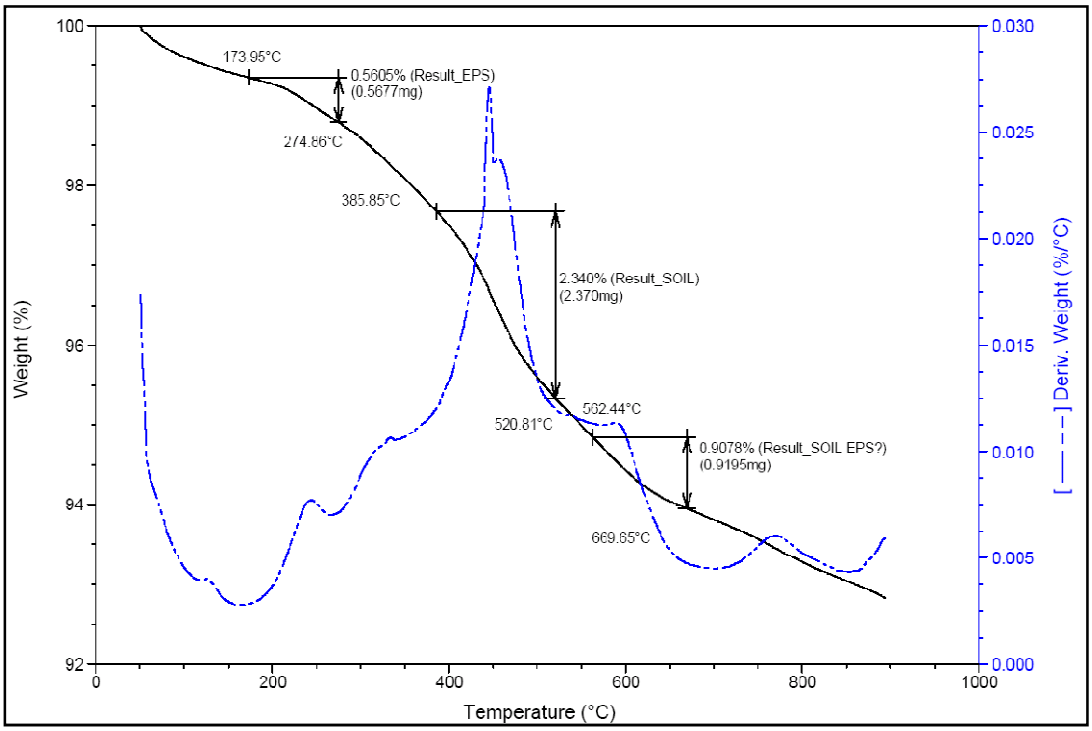

(b)

TGA results: (a) 90 % broth production of EPS in soil; (b) 100 % broth productions of EPS in soil

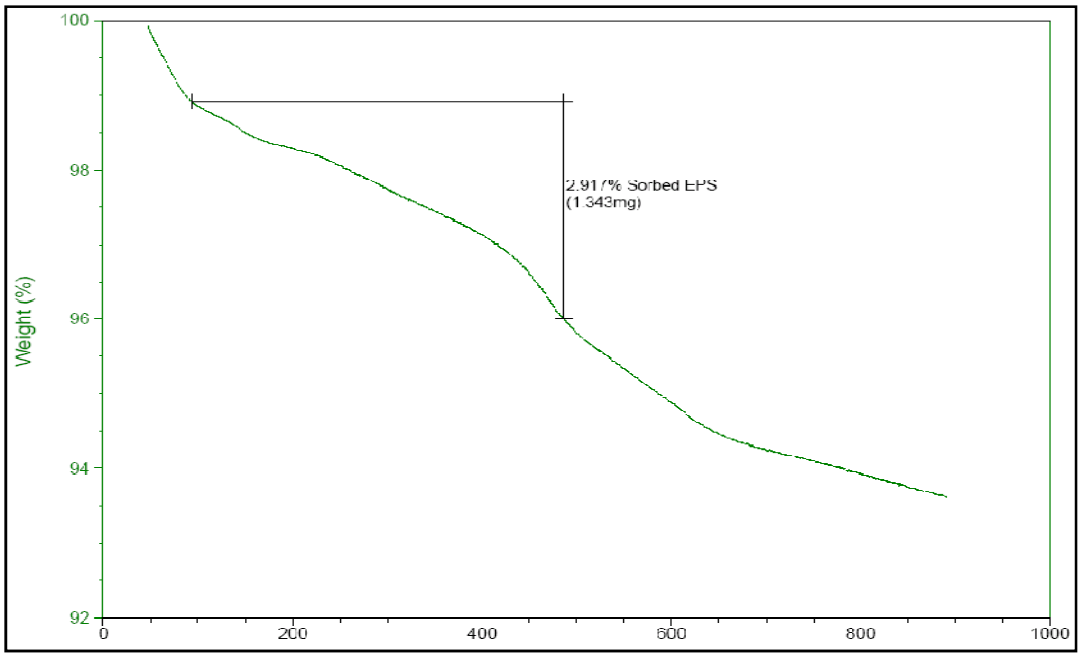

(a)

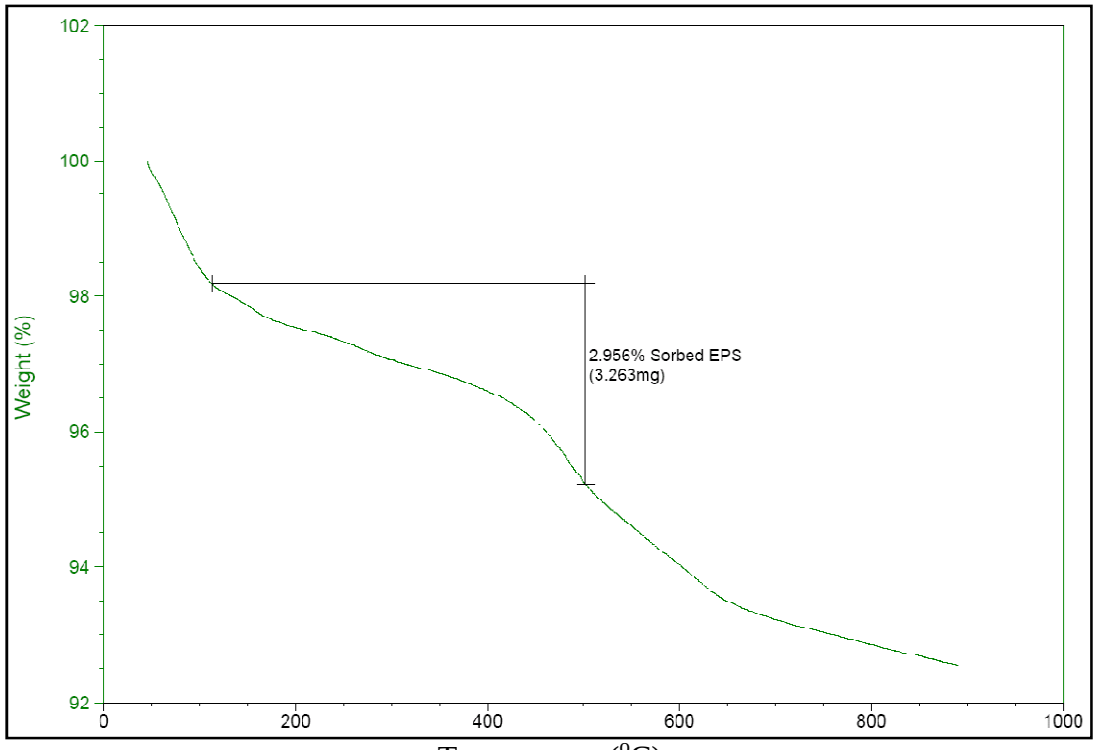

(b)

TGA results showing (a) 25 % EPS in sandy clay soil; (b) 25 % EPS in silty clay soil

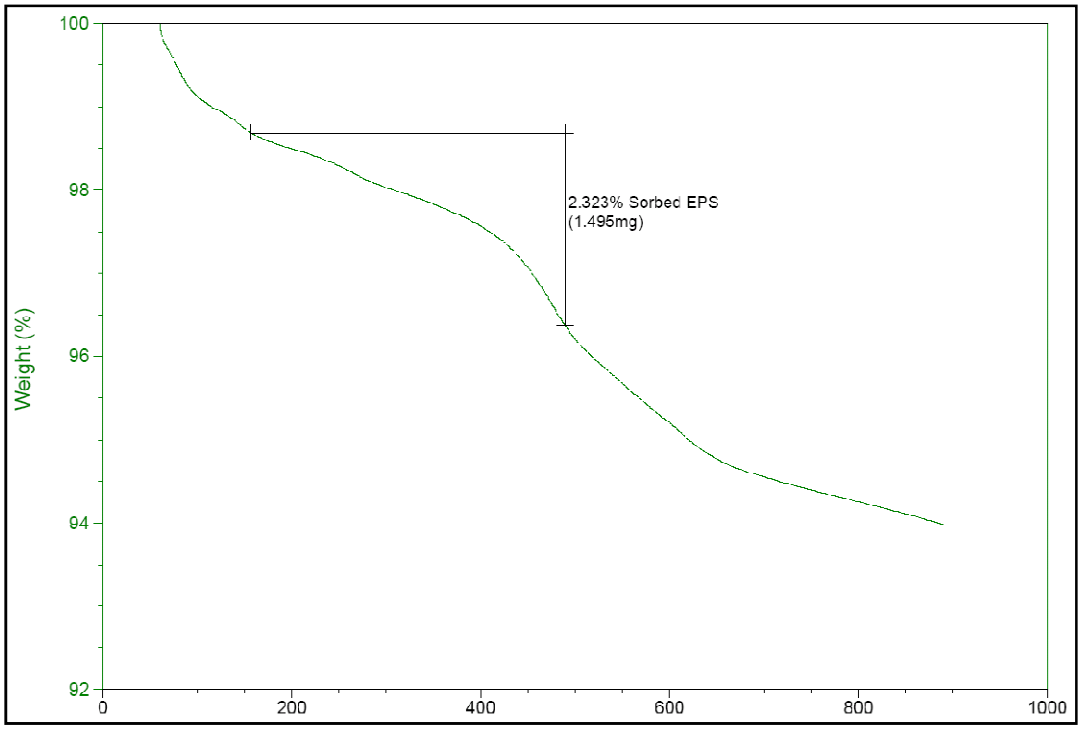

(a)

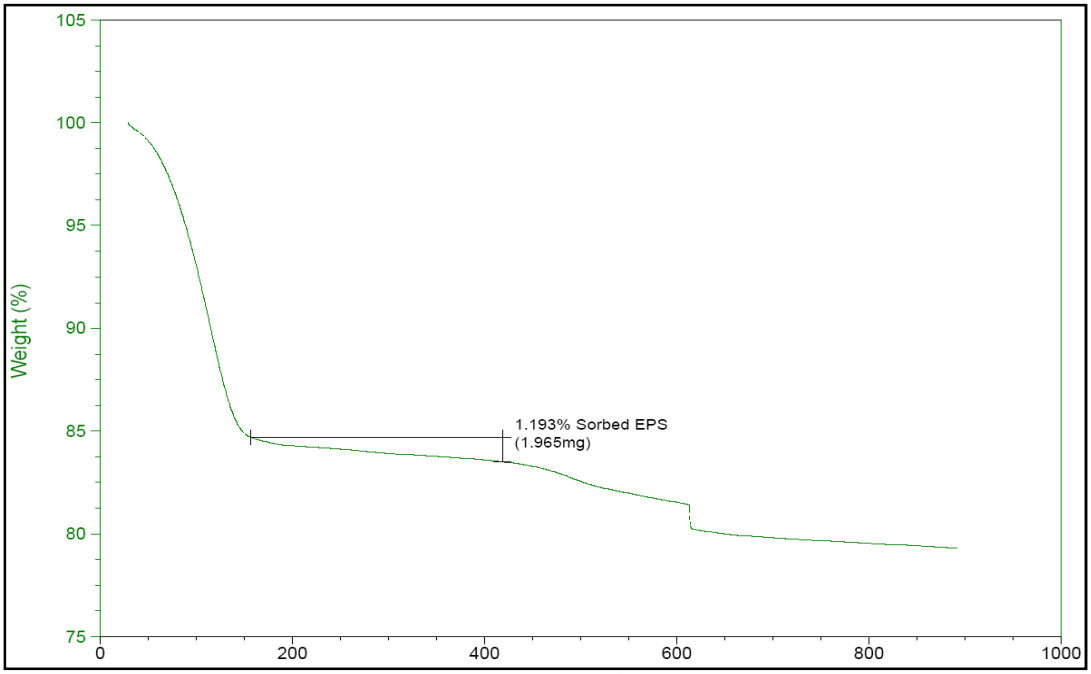

(b)

TGA results showing (a) 20 % EPS in Sandy silty clay soil; (b) 5 % EPS in Sandy silty clay soil

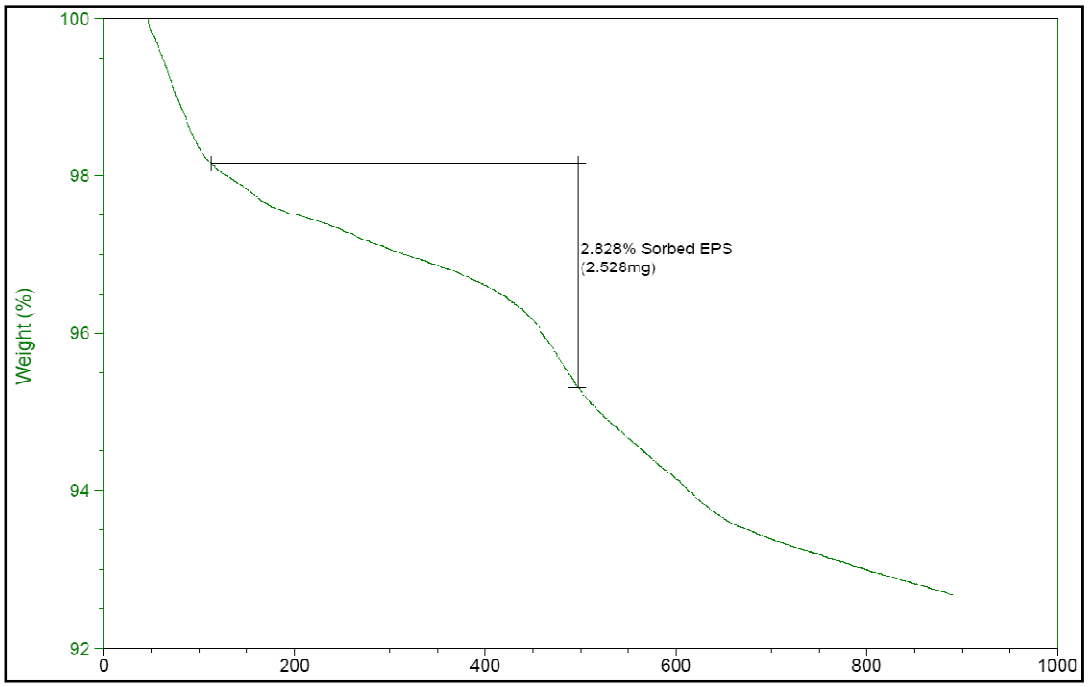

(a)

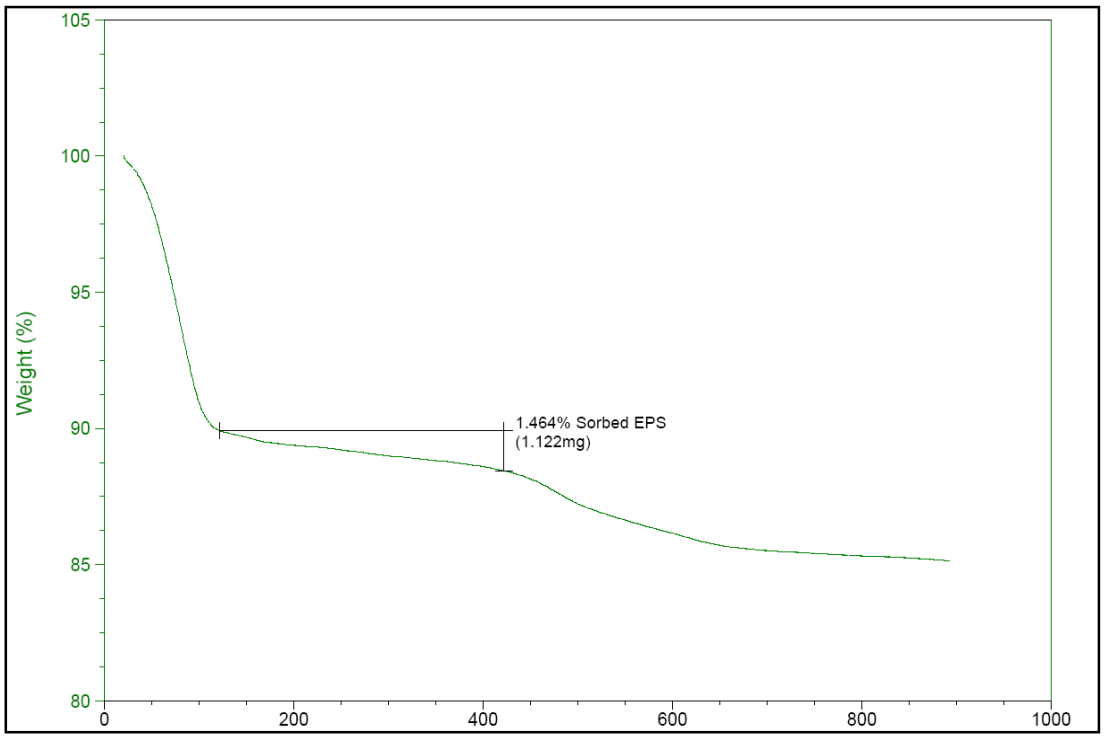

(b)

TGA results showing (a) 25 % EPS in Sandy silty clay soil; (b) 5 % EPS in silty clay soil

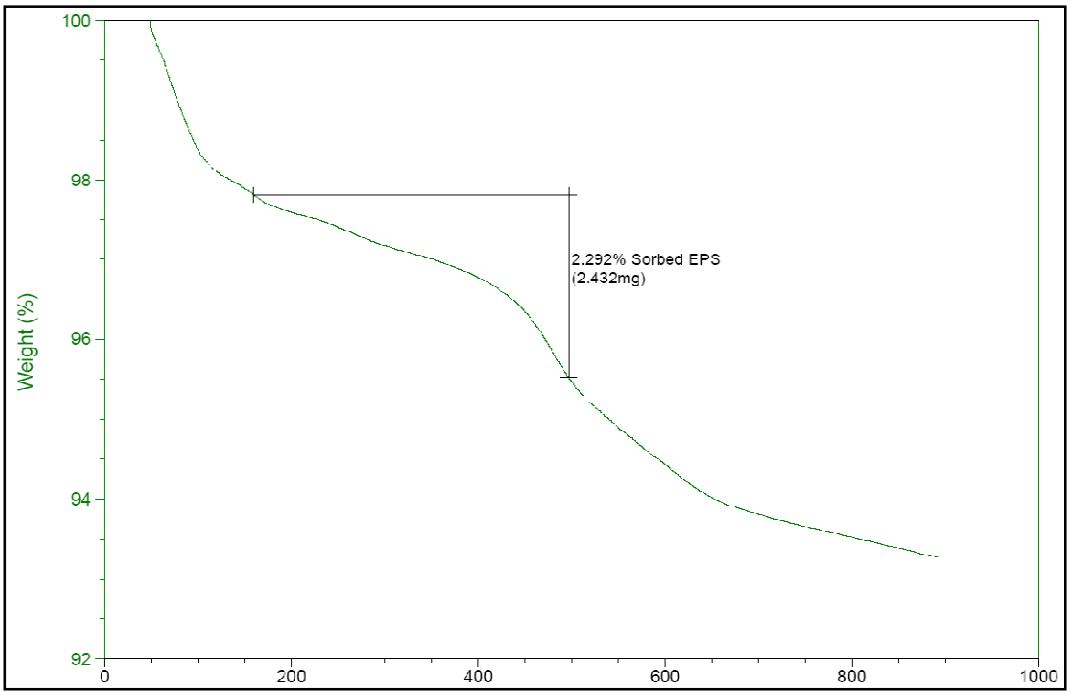

(a)

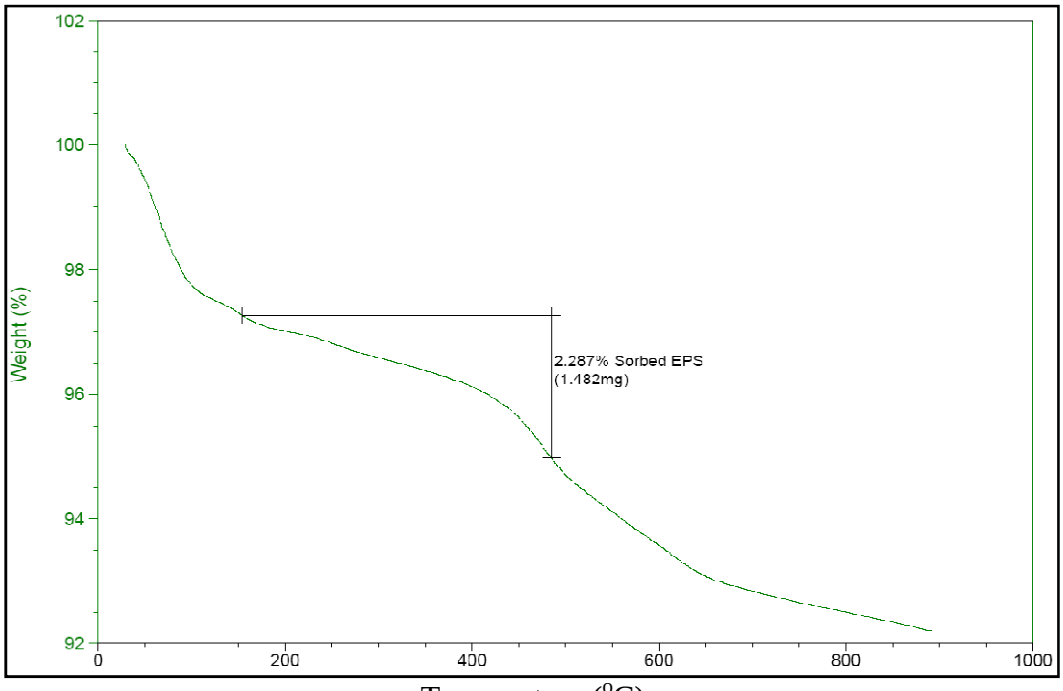

(b)

TGA results showing (a) 20 % EPS in sandy clay soil; (b) 20 % EPS in silty clay soil

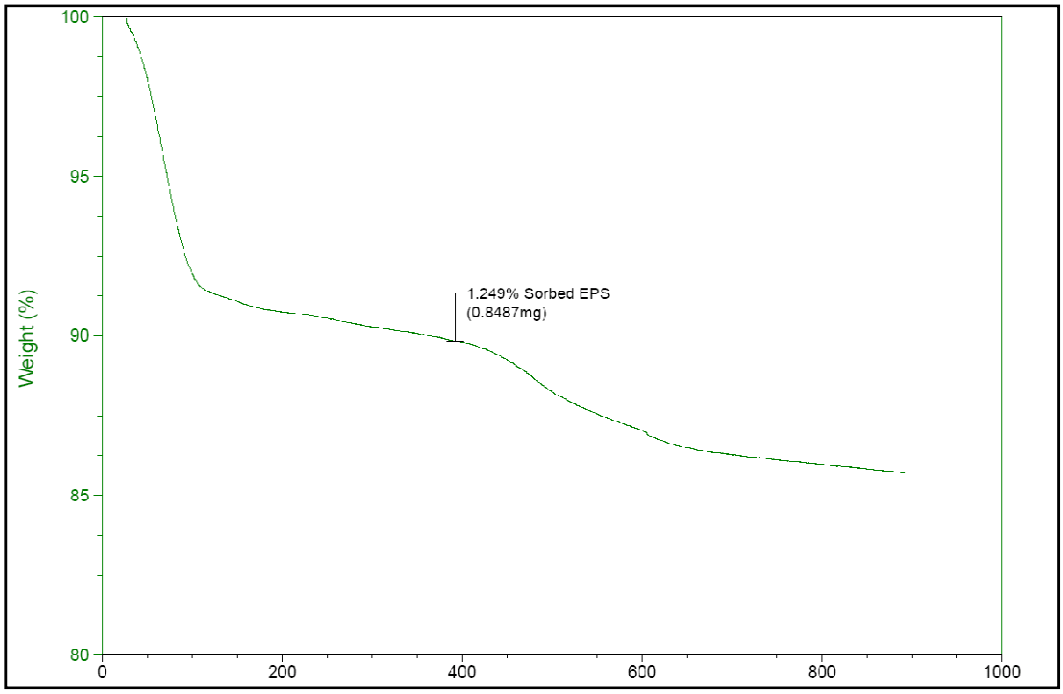

(a)

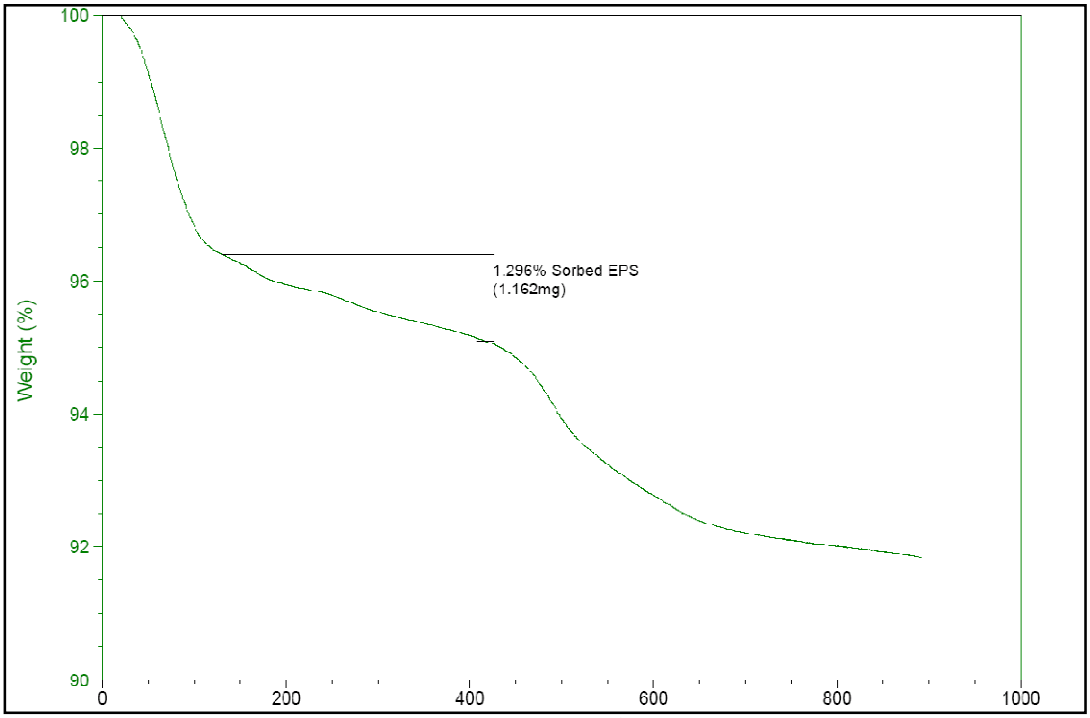

(b)

TGA results showing (a) 5 % EPS in sandy clay soil; (b) 25 % EPS in Sandy silty clay soil

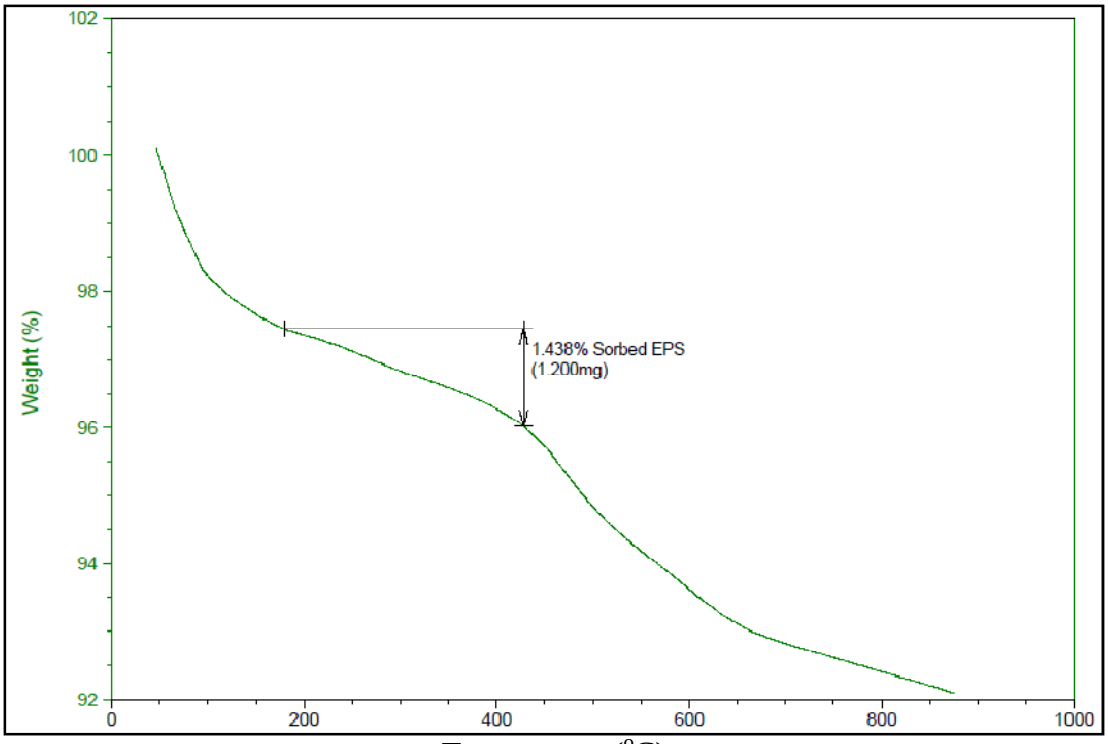

(a)

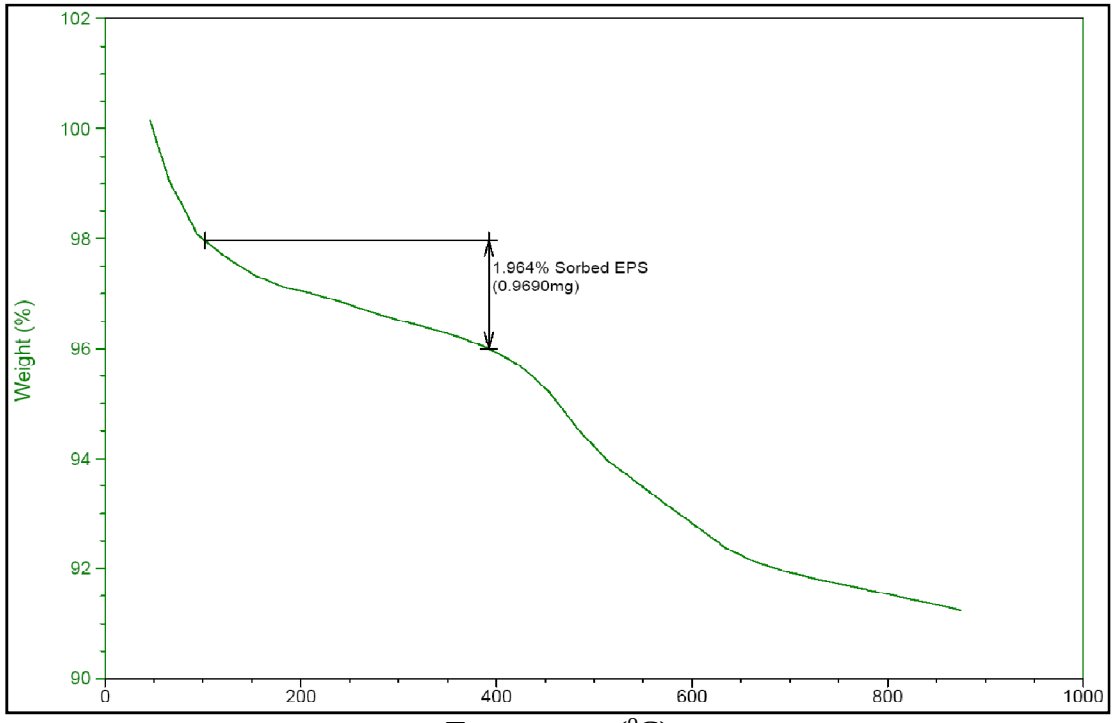

(b)

TGA results showing (a) 10 % EPS in silty clay soil; (b) 10 % EPS in sandy clay soil

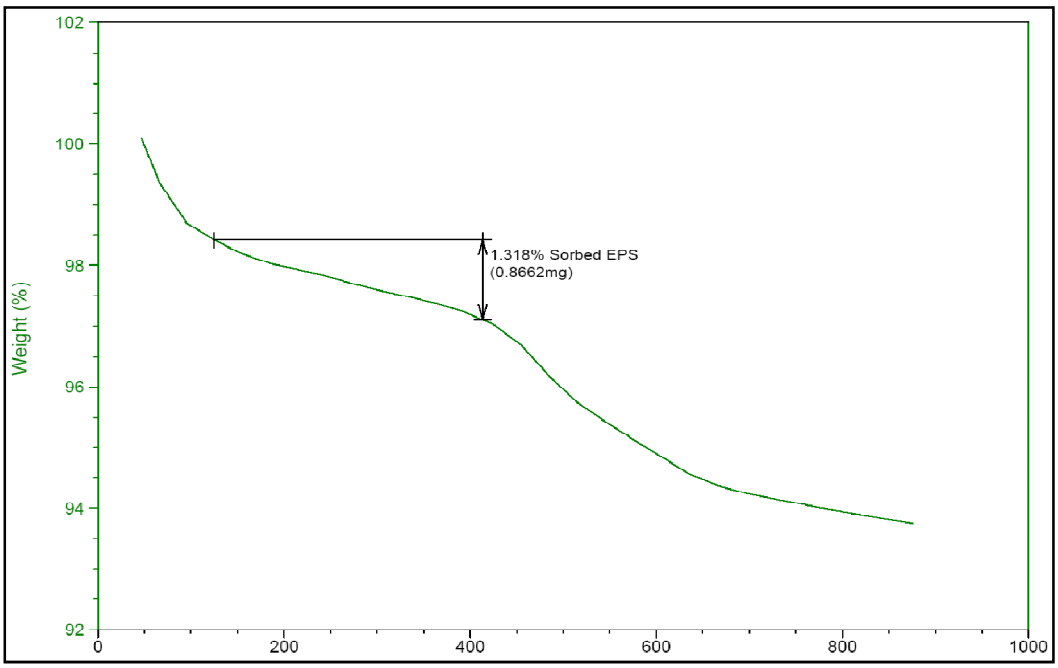

(a)

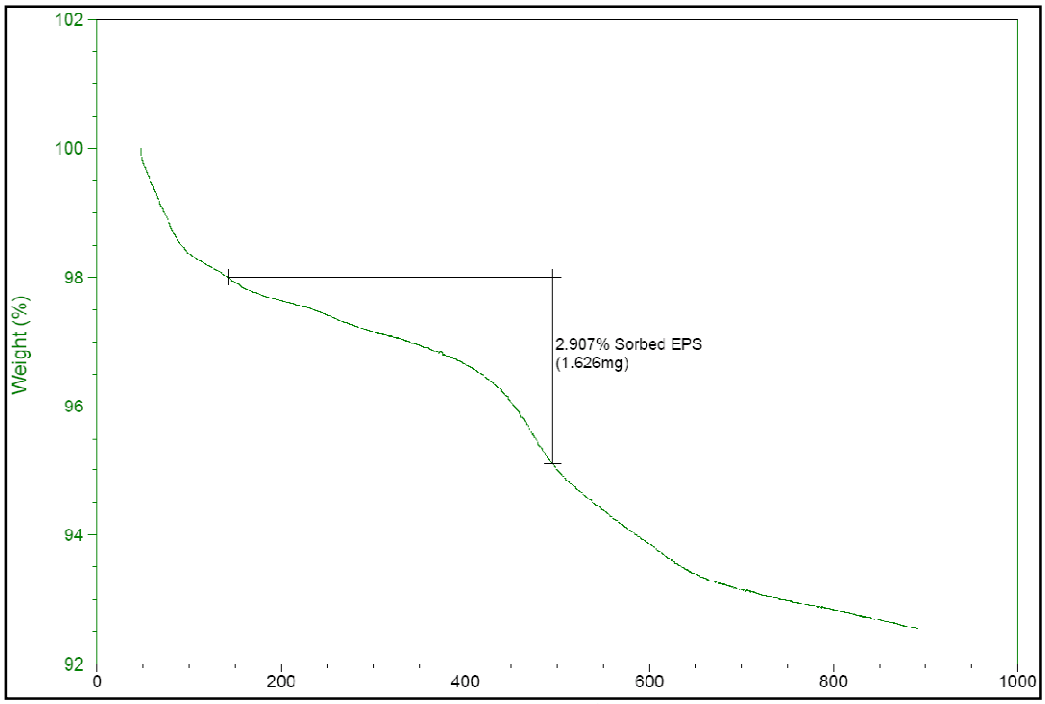

(b)

TGA results showing (a) 10 % EPS in Sandy silty clay soil; (b) 15 % EPS in sandy clay soil

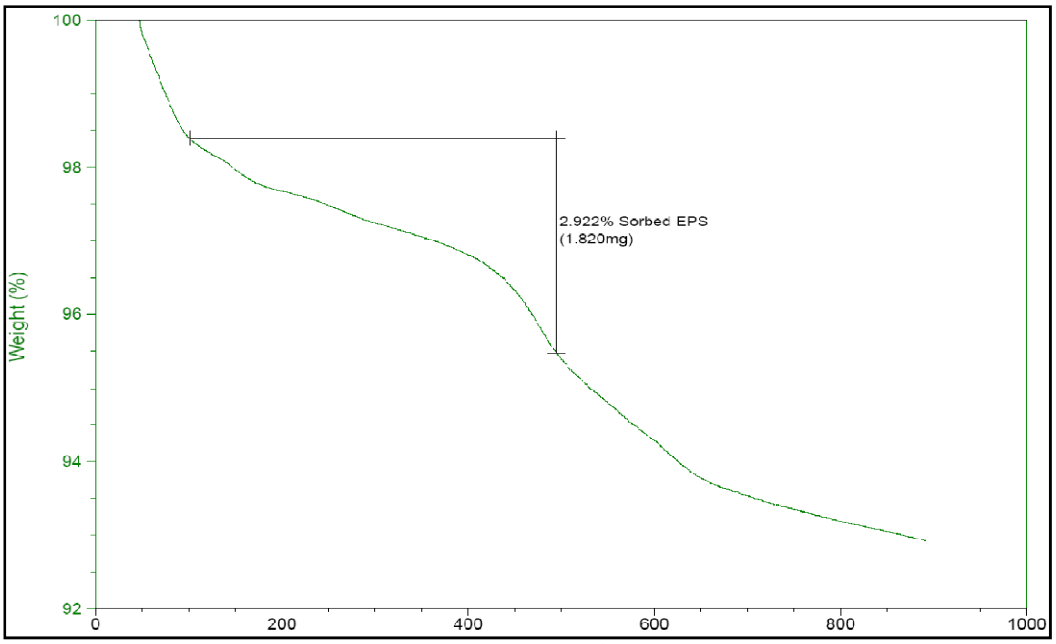

(a)

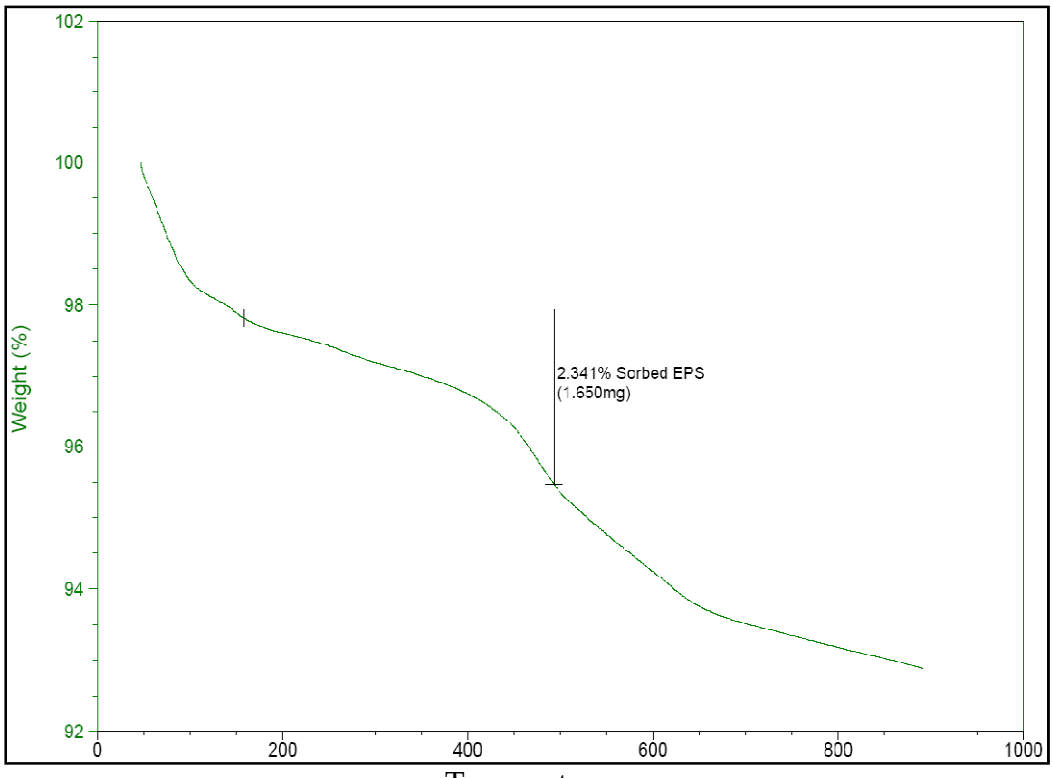

(b)

TGA results showing (a) 15 % EPS in Sandy silty clay soil; (b) 15 % EPS in silty clay soil

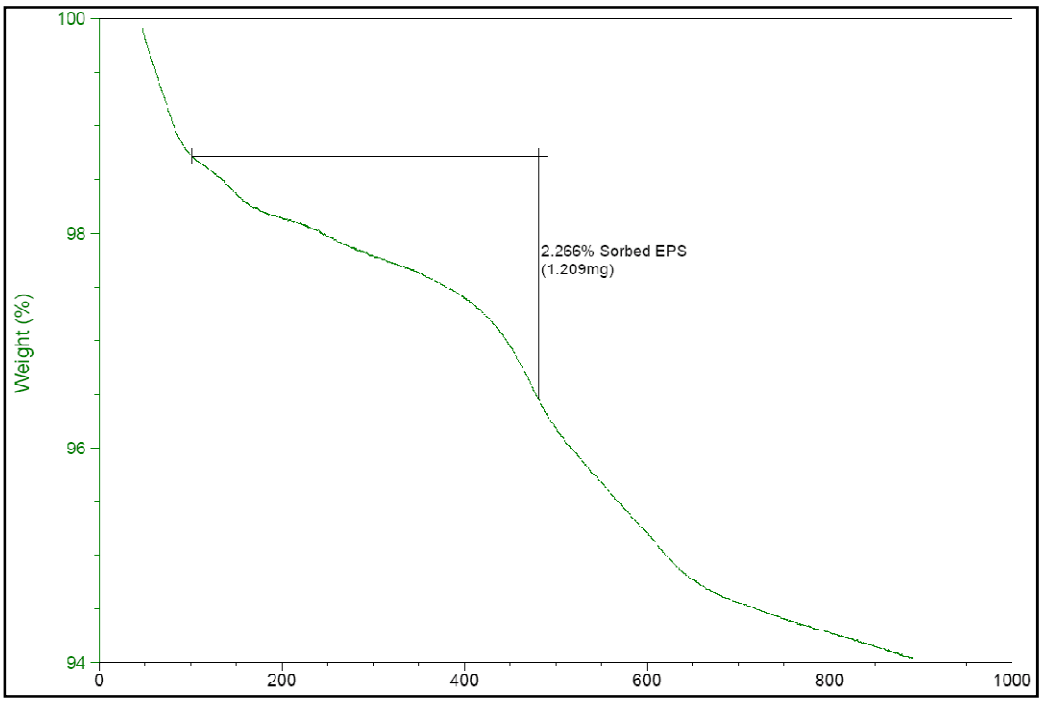

(a)

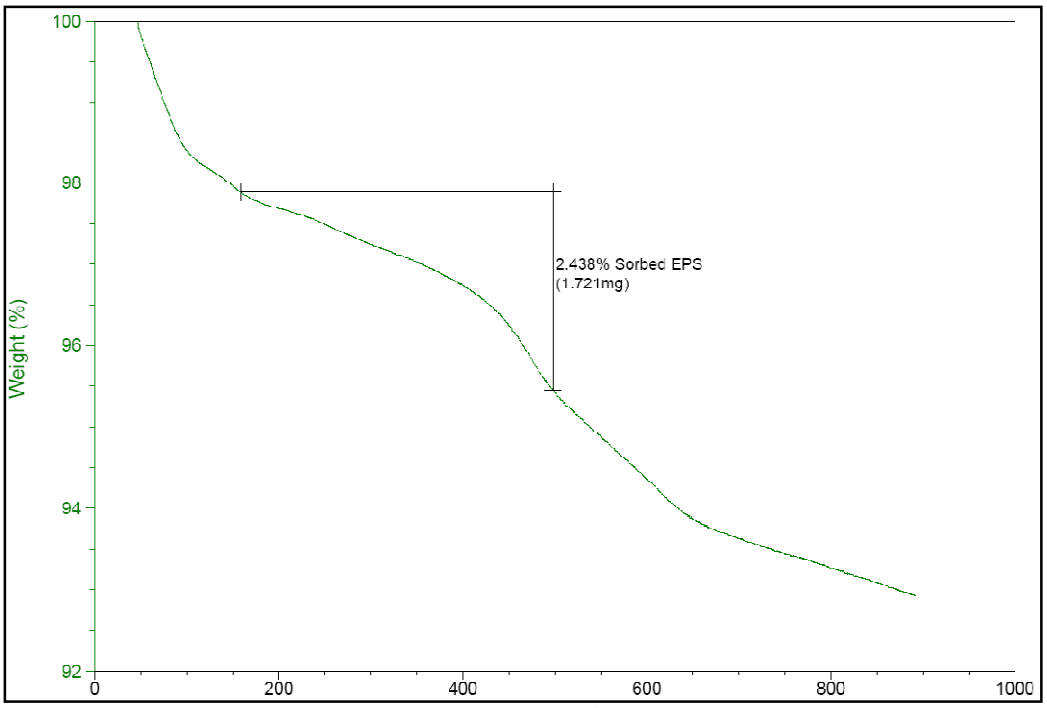

(b)

TGA results showing (a) 20 % EPS in silty clay soil; (b) 20 % EPS in sandy clay soil

APPENDIX B: GRAPHS OF UNCONFINED COMPRESSION TESTS FOR SILTY CLAY SOIL

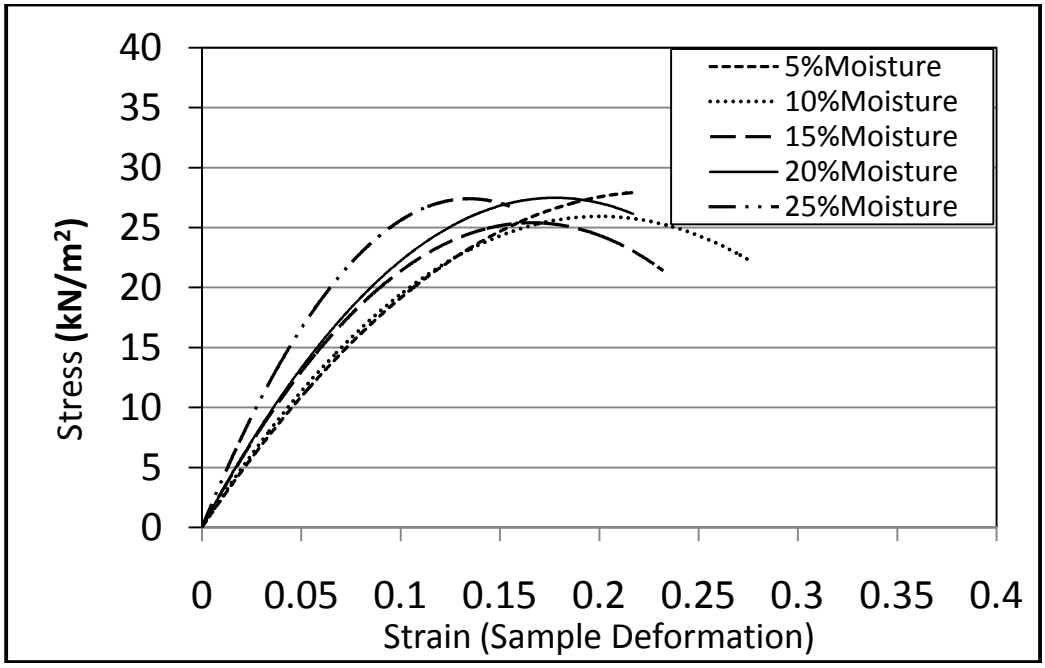

Unconfined compression result of silty clay soil treated control at day 10

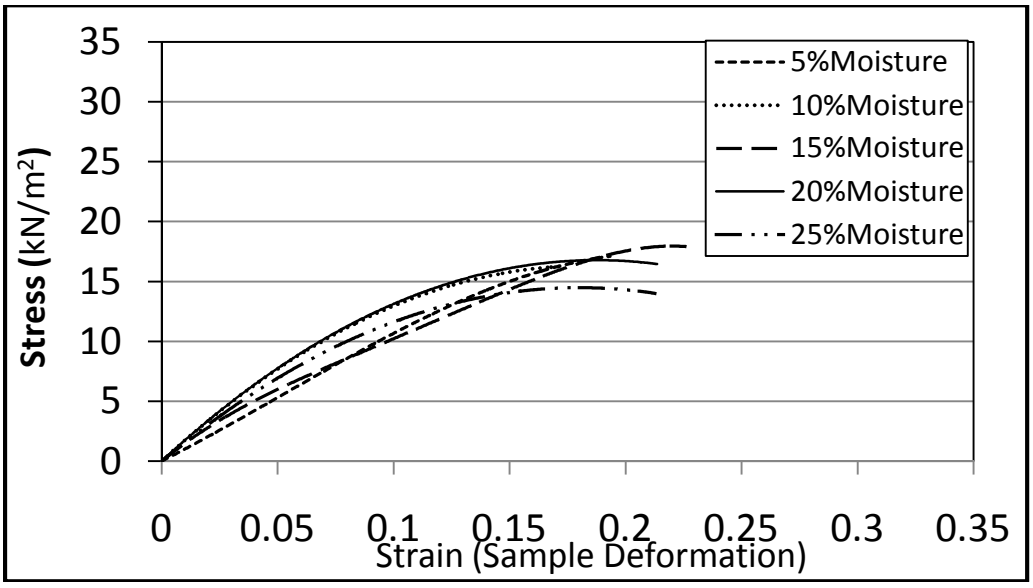

Unconfined compression result of silty clay soil treated control at day 12

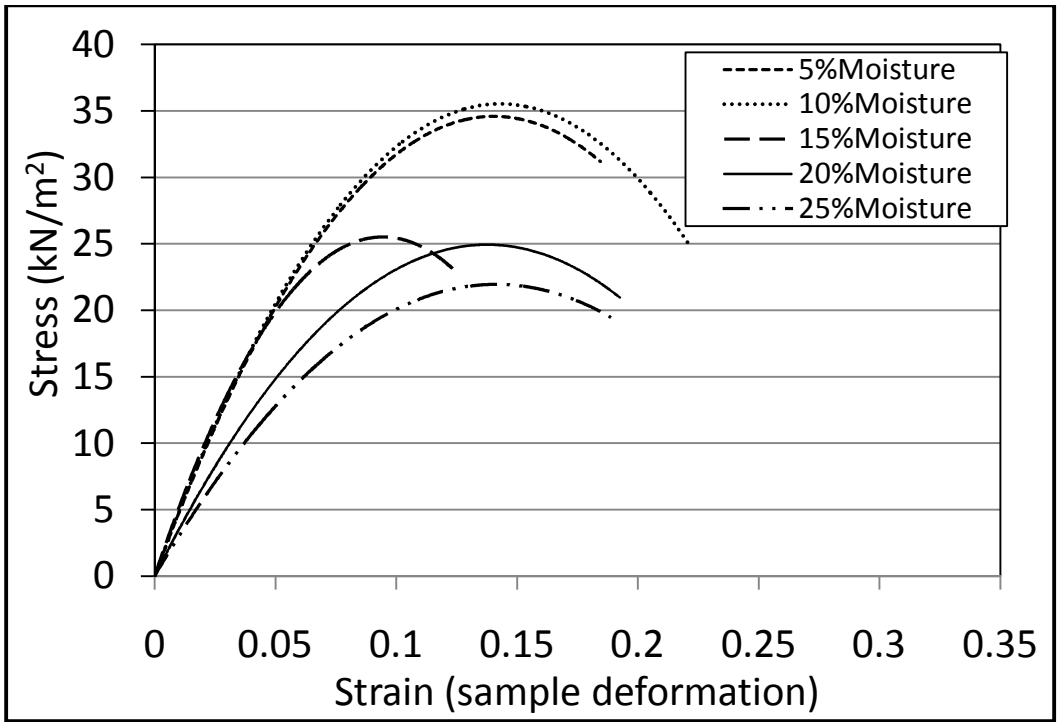

Unconfined compression result of silty clay soil treated control at day 11

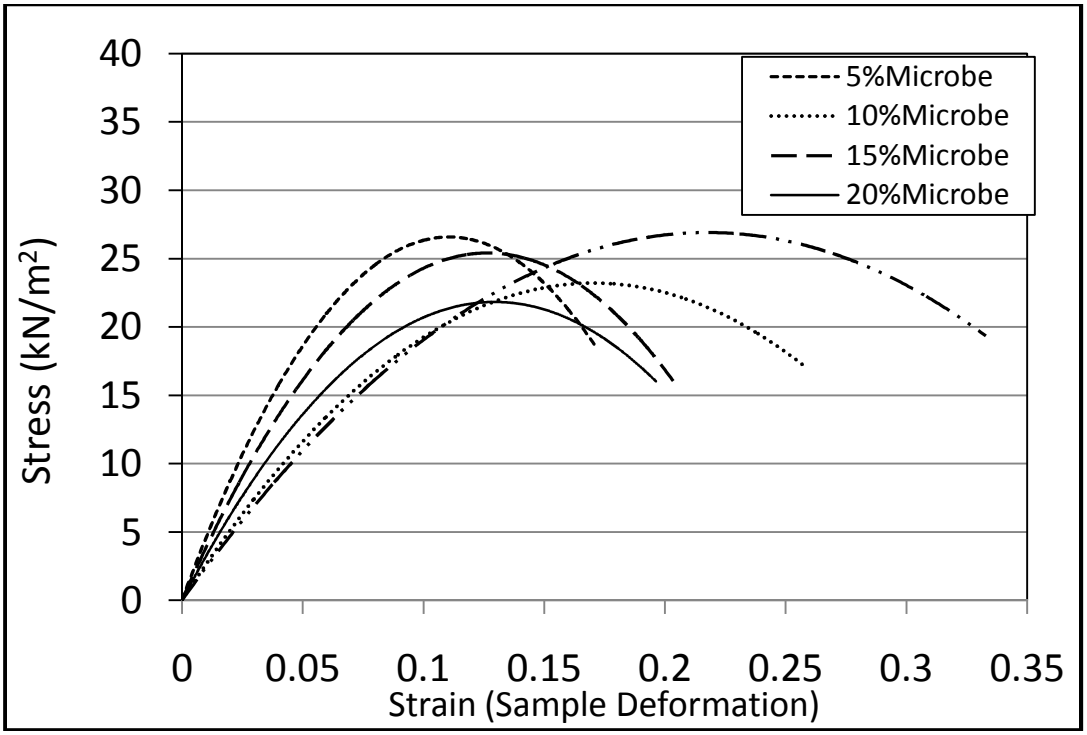

Unconfined compression result of silty clay soil treated with microbe at day 4

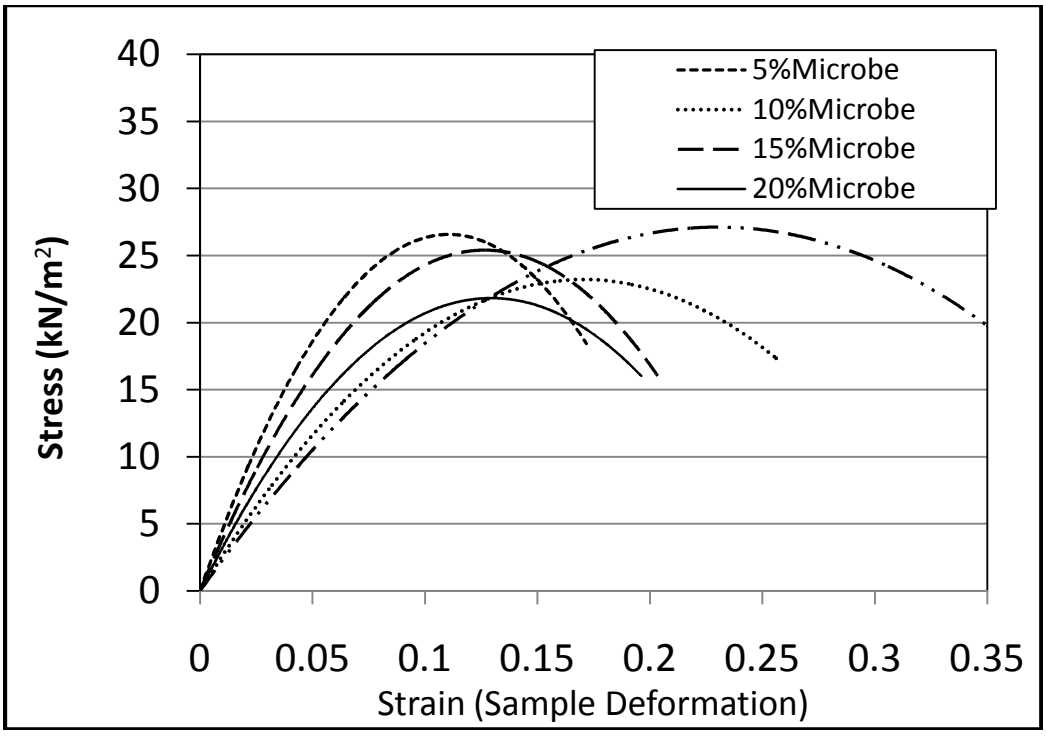

Unconfined compression result of silty clay soil treated with microbe at day 3

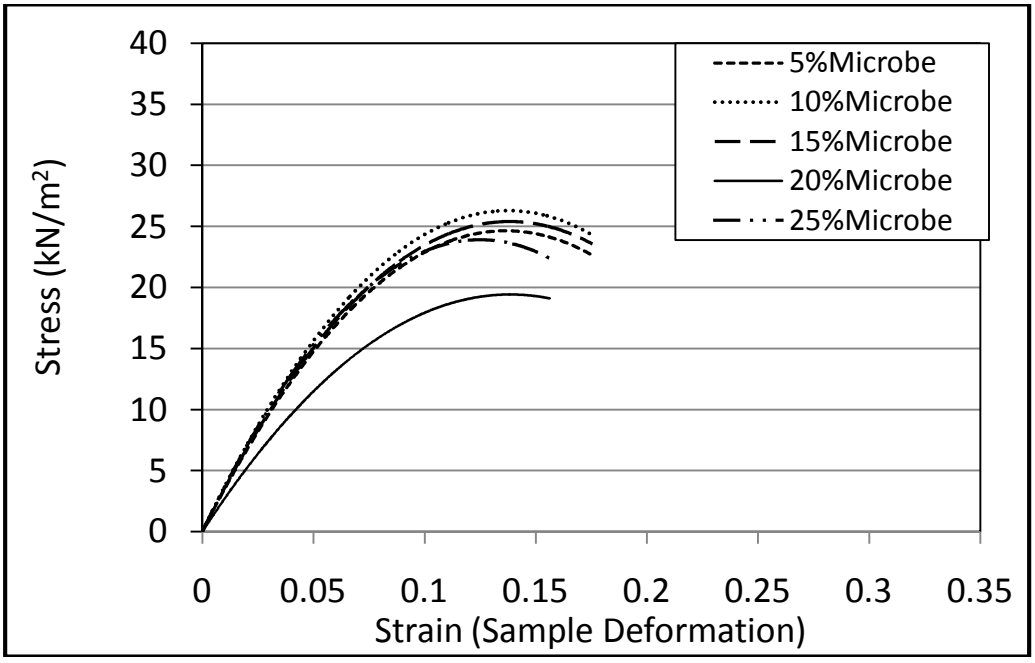

Unconfined compression result of silty clay soil treated with microbe at day 2

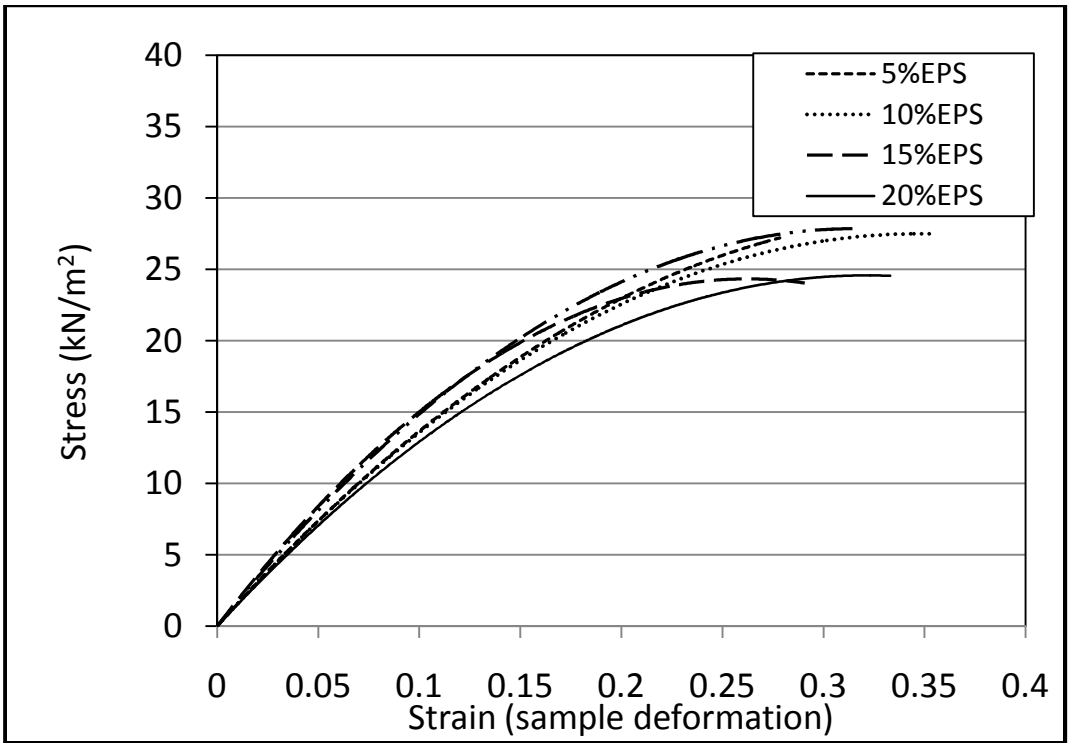

Figure Unconfined compression result of silty clay soil treated with EPS at day 5

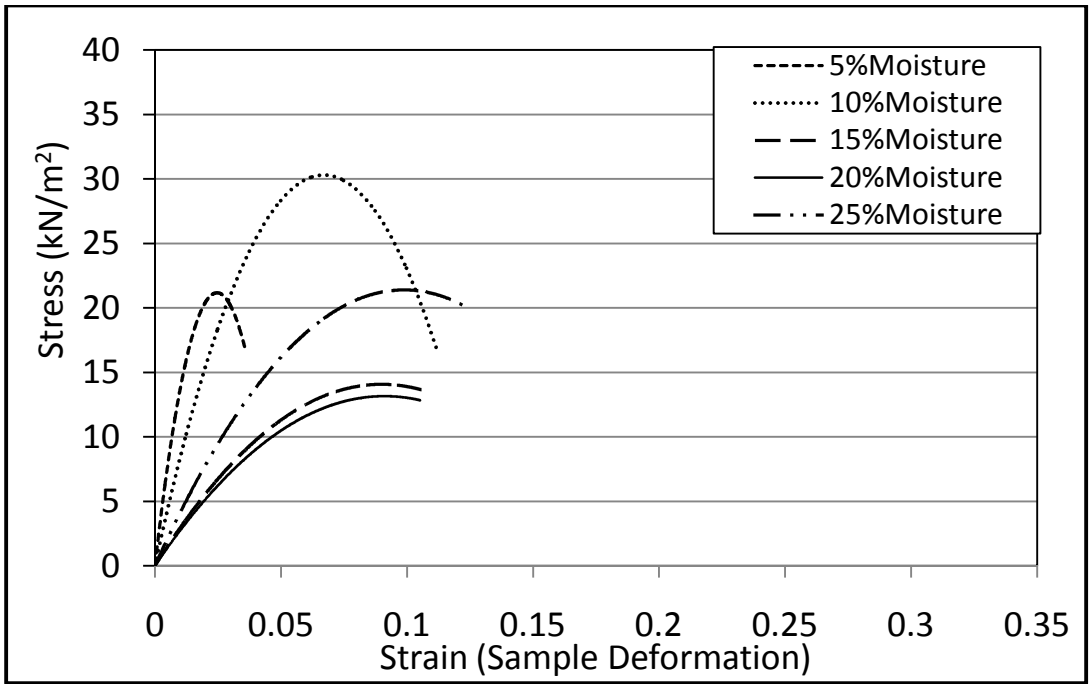

Figure Unconfined compression result of silty clay soil treated control at day 9

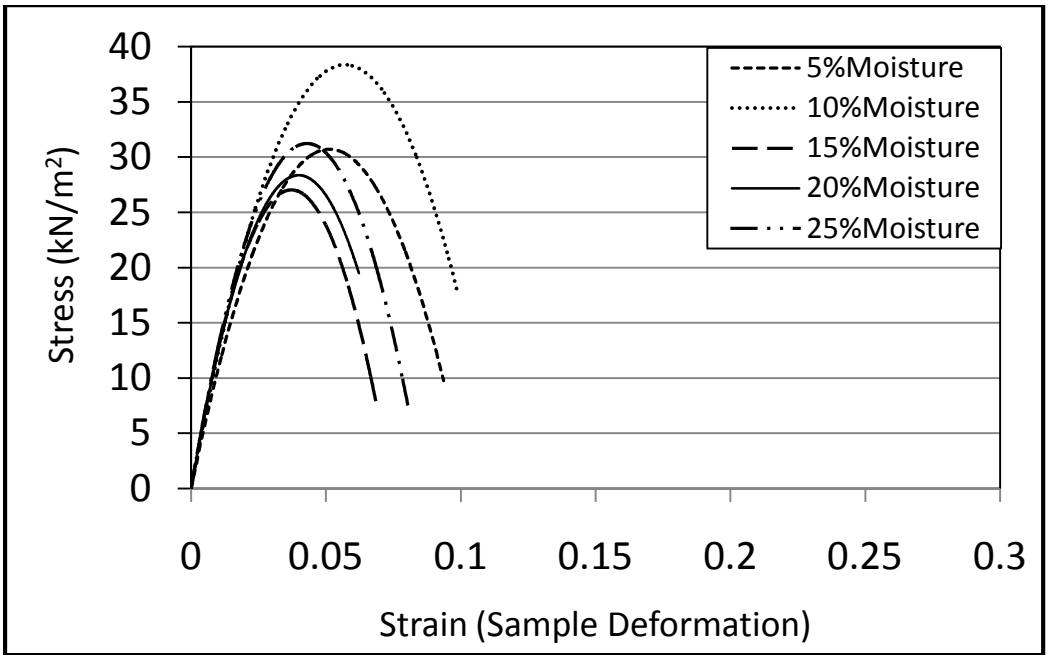

Unconfined compression result of silty clay soil treated control at day 8

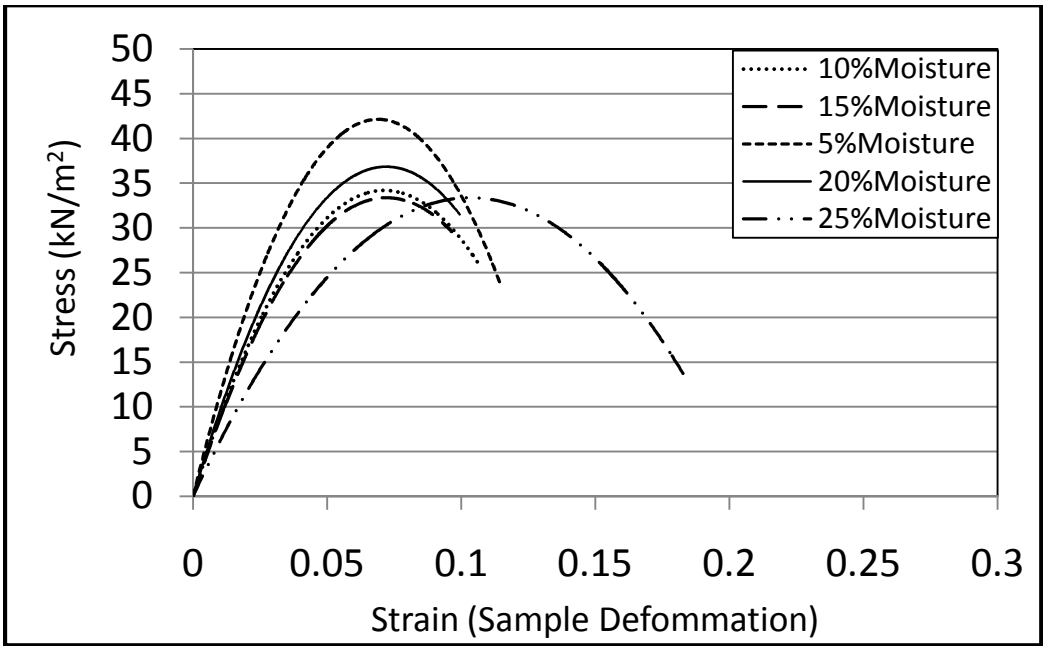

Unconfined compression result of silty clay soil treated control at day 7

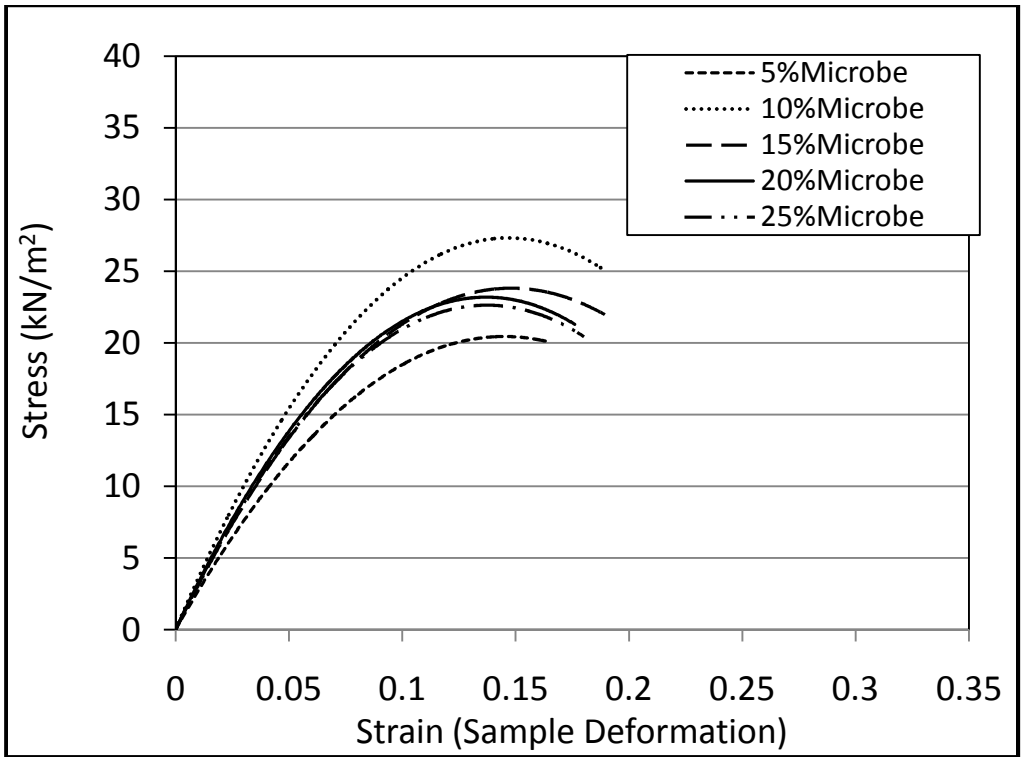

Unconfined compression result of silty clay soil treated with microbe at day 14

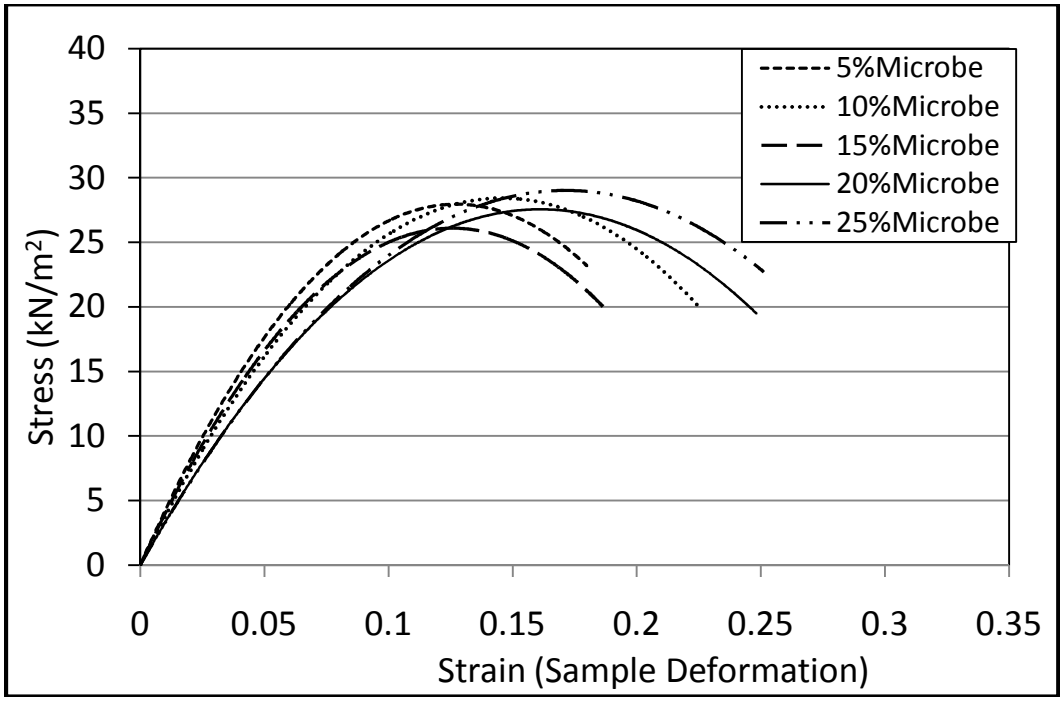

Unconfined compression result of silty clay soil treated with microbe at day 10

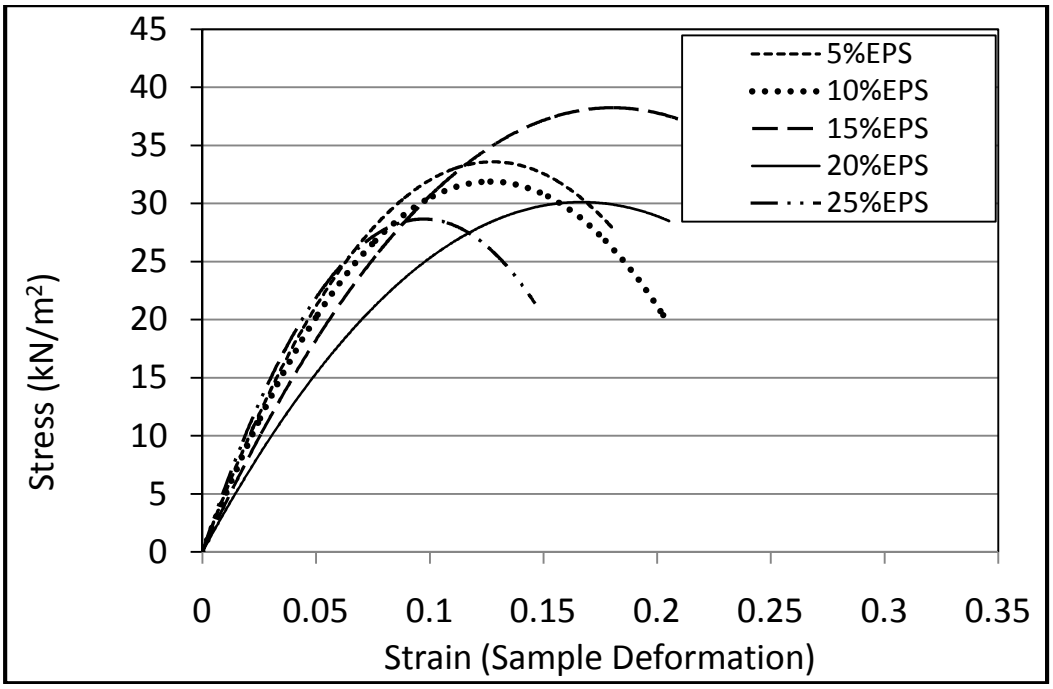

Unconfined compression result of silty clay soil treated with EPS at day 9

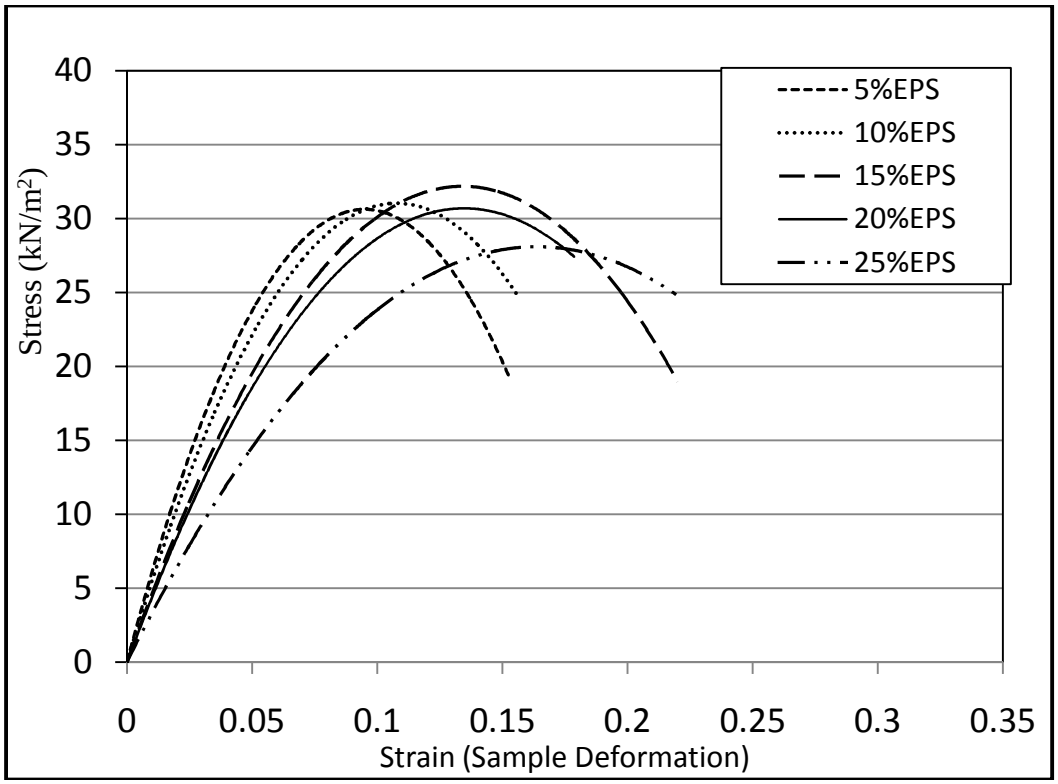

Unconfined compression result of silty clay soil treated with EPS at day 8

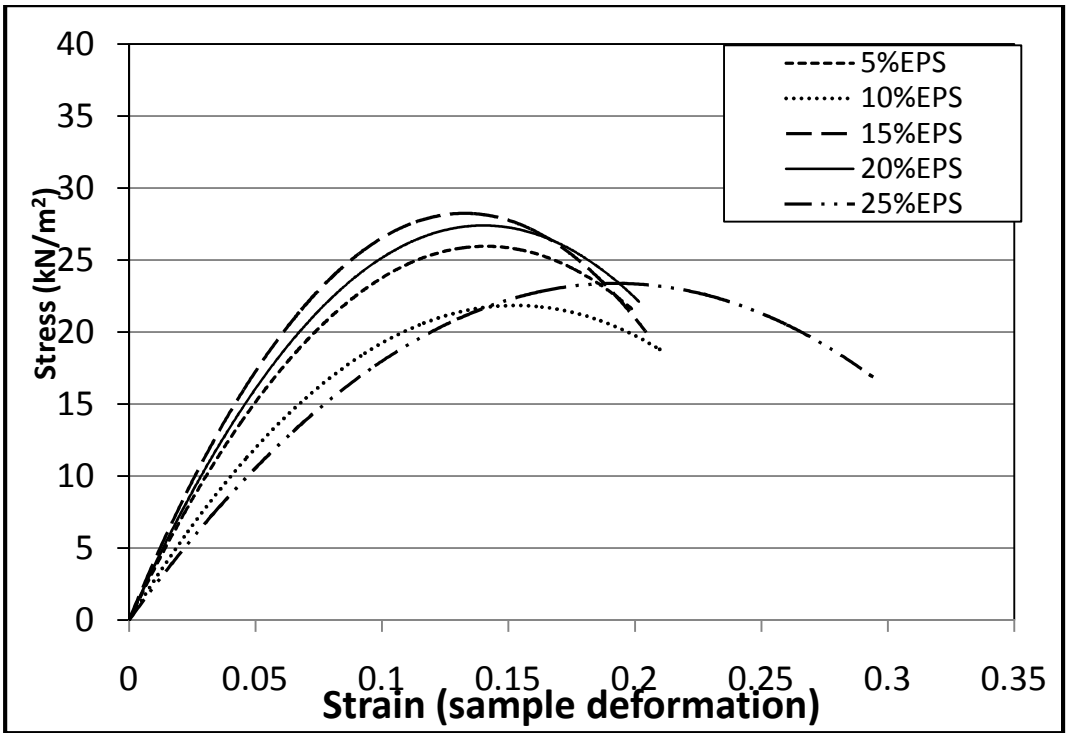

Unconfined compression result of silty clay soil treated with EPS at day 7

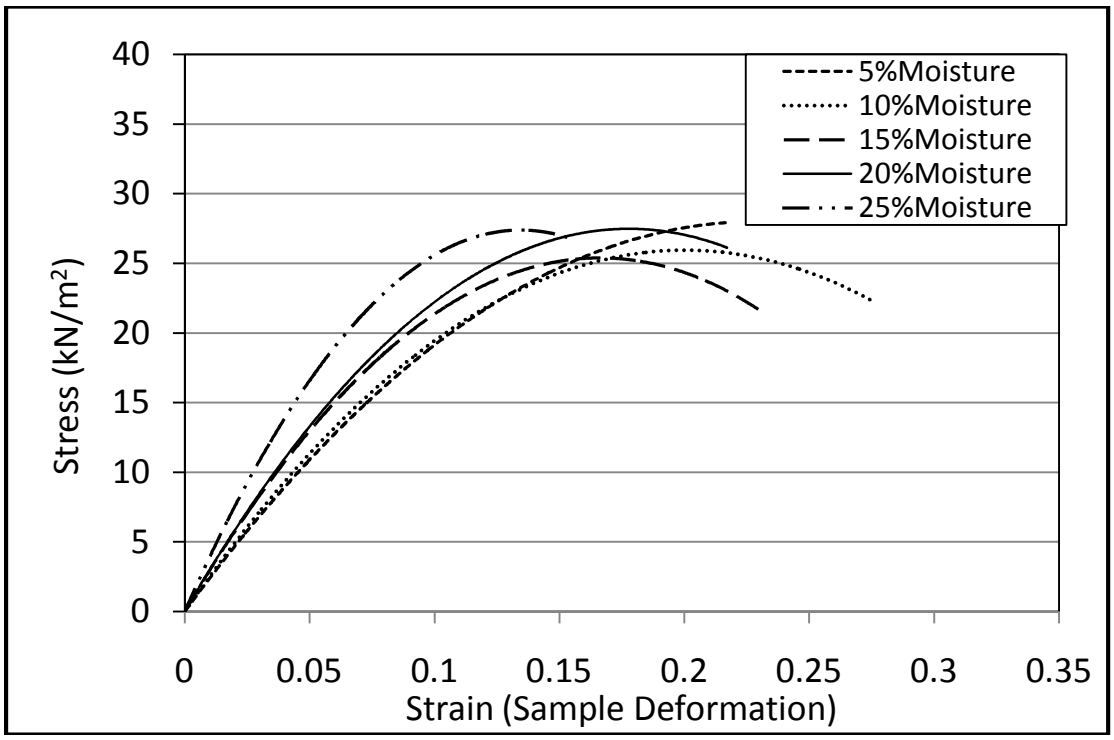

Unconfined compression result of silty clay soil treated control at day 14

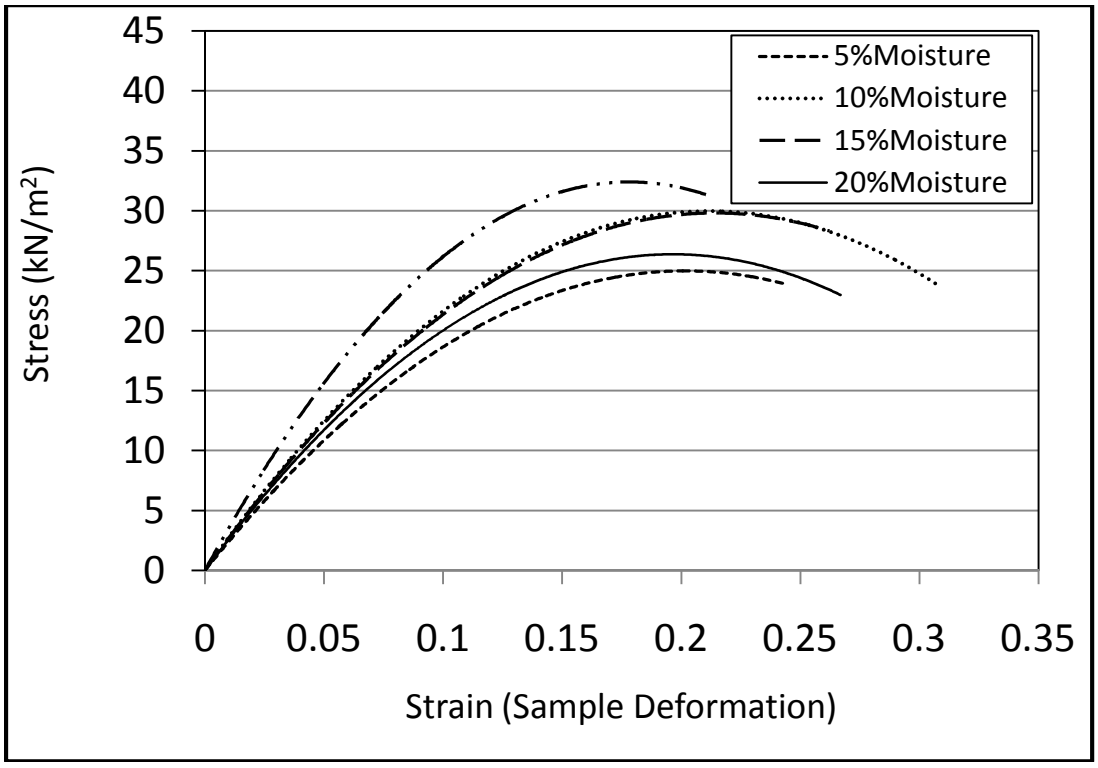

Unconfined compression result of silty clay soil treated control at day 13

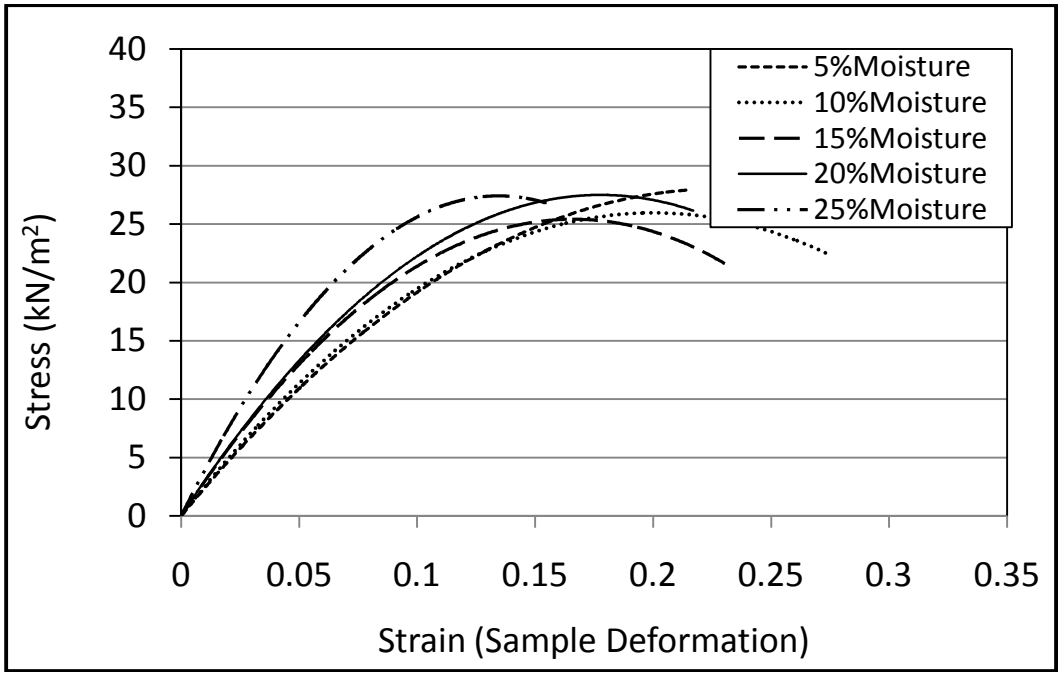

Unconfined compression result of silty clay soil treated control at day 6

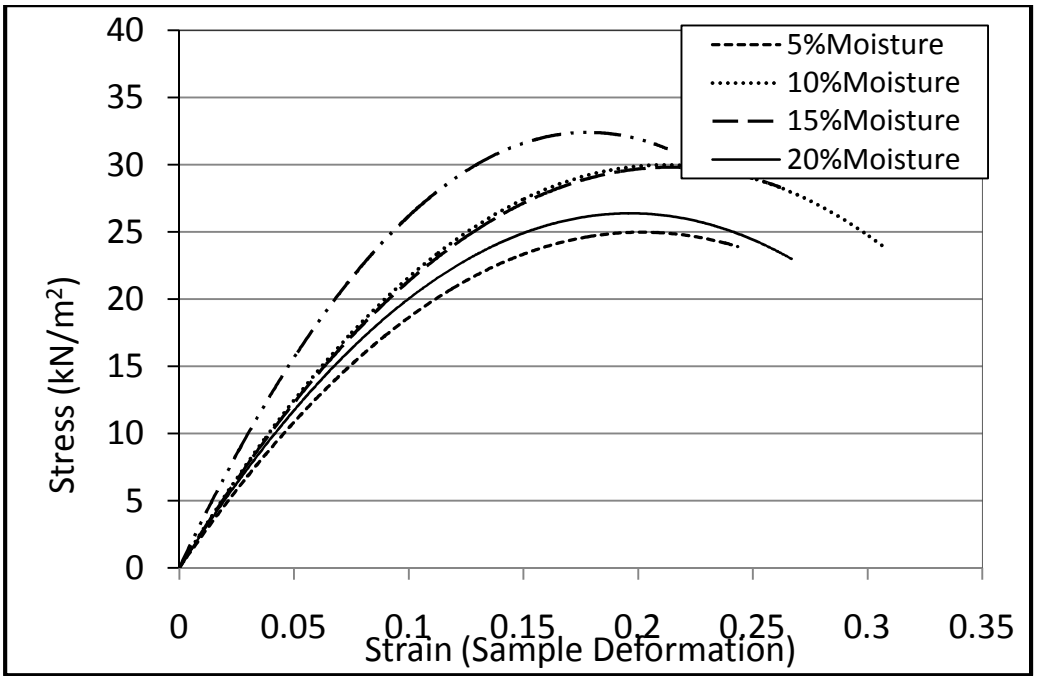

Unconfined compression result of silty clay soil treated control at day 5

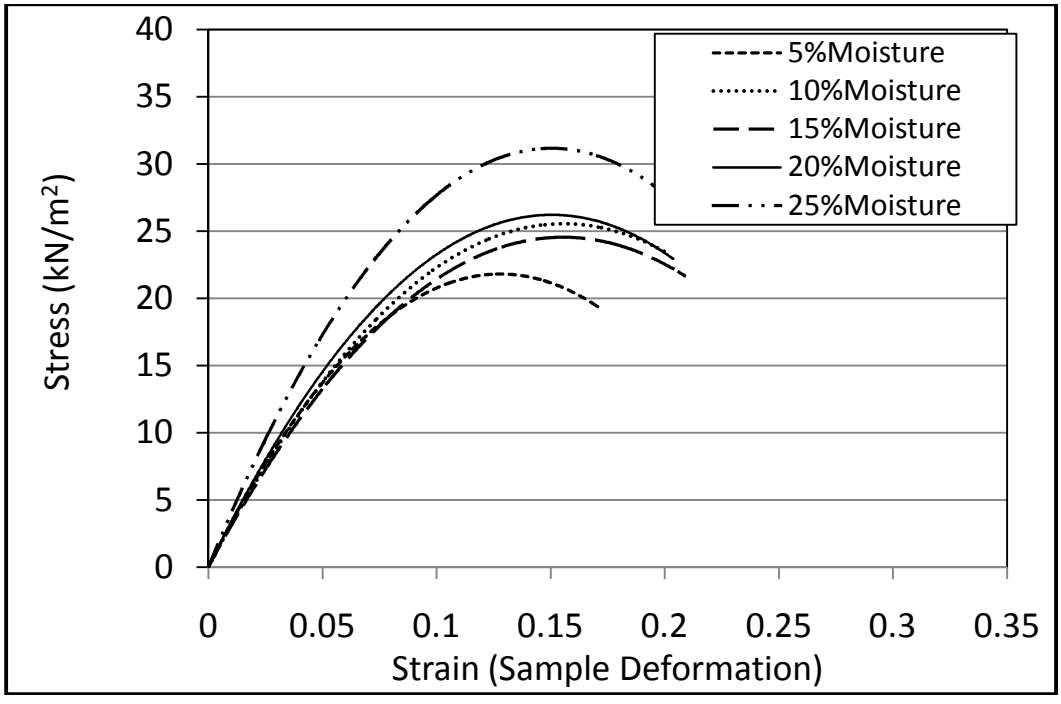

Unconfined compression result of silty clay soil treated control at day 4

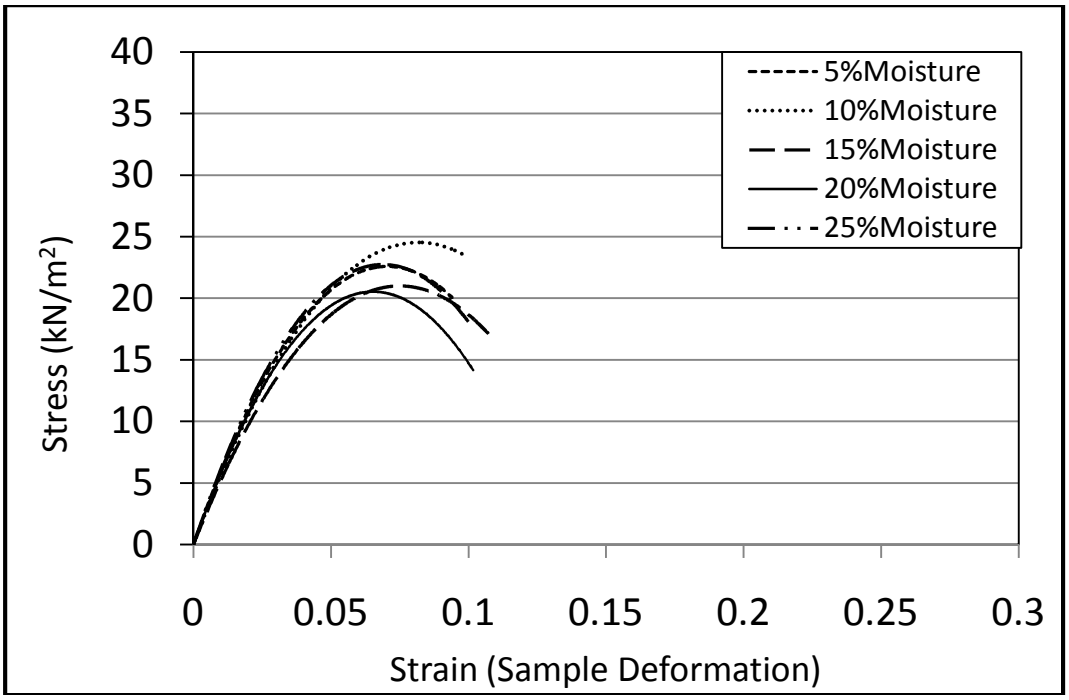

Unconfined compression result of silty clay soil treated control at day 3

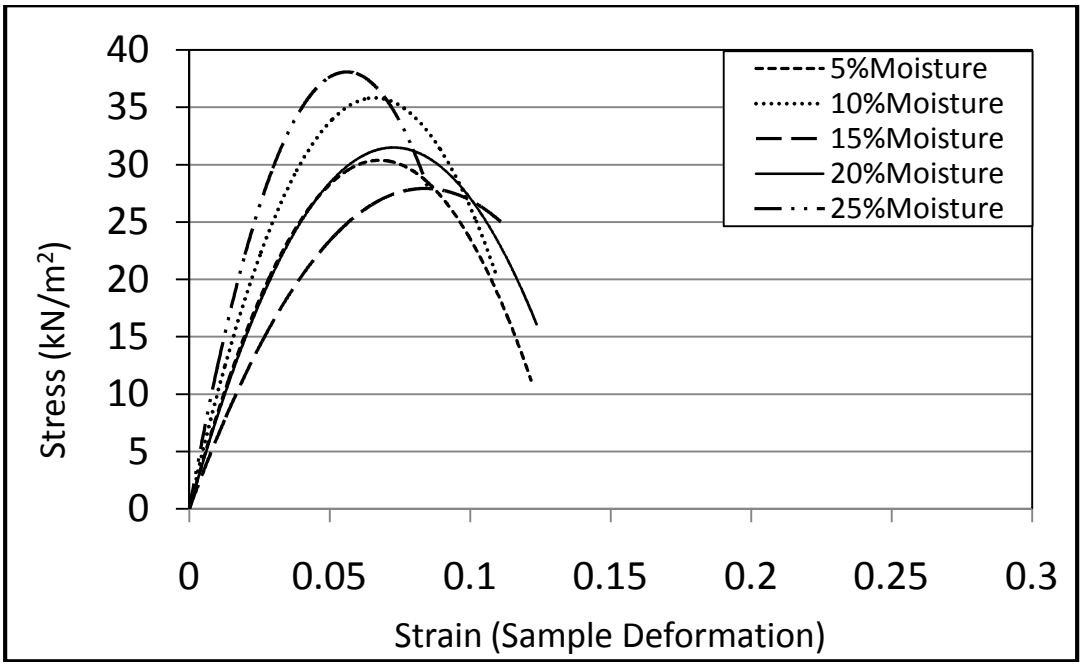

Unconfined compression result of silty clay soil treated control at day 2

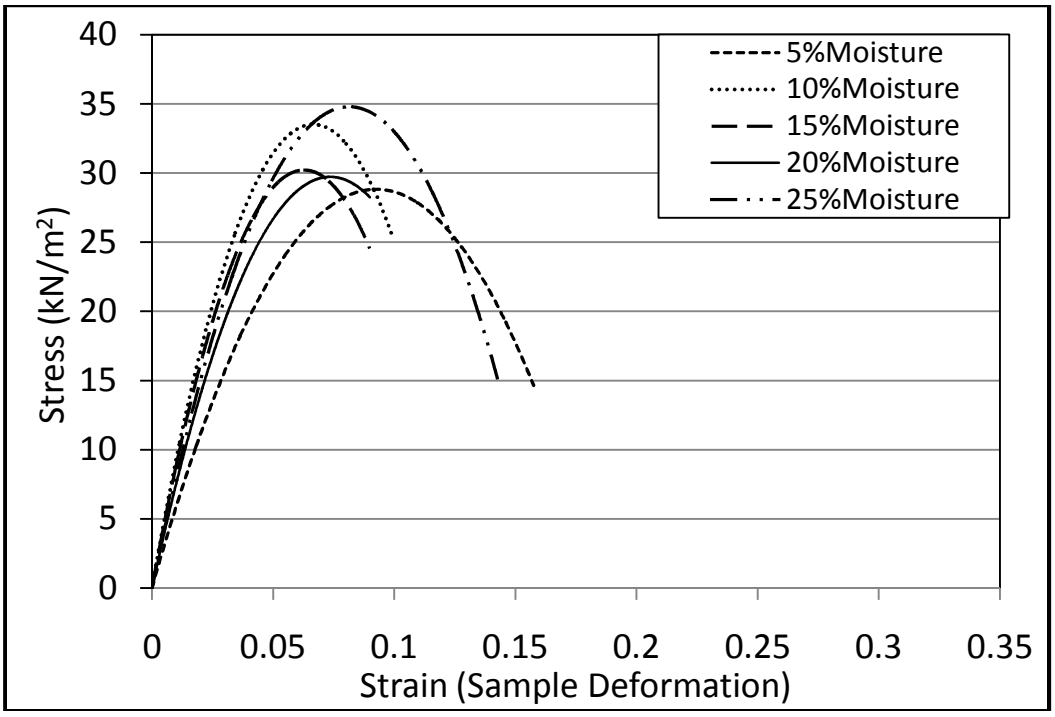

Unconfined compression result of silty clay soil treated control at day 1

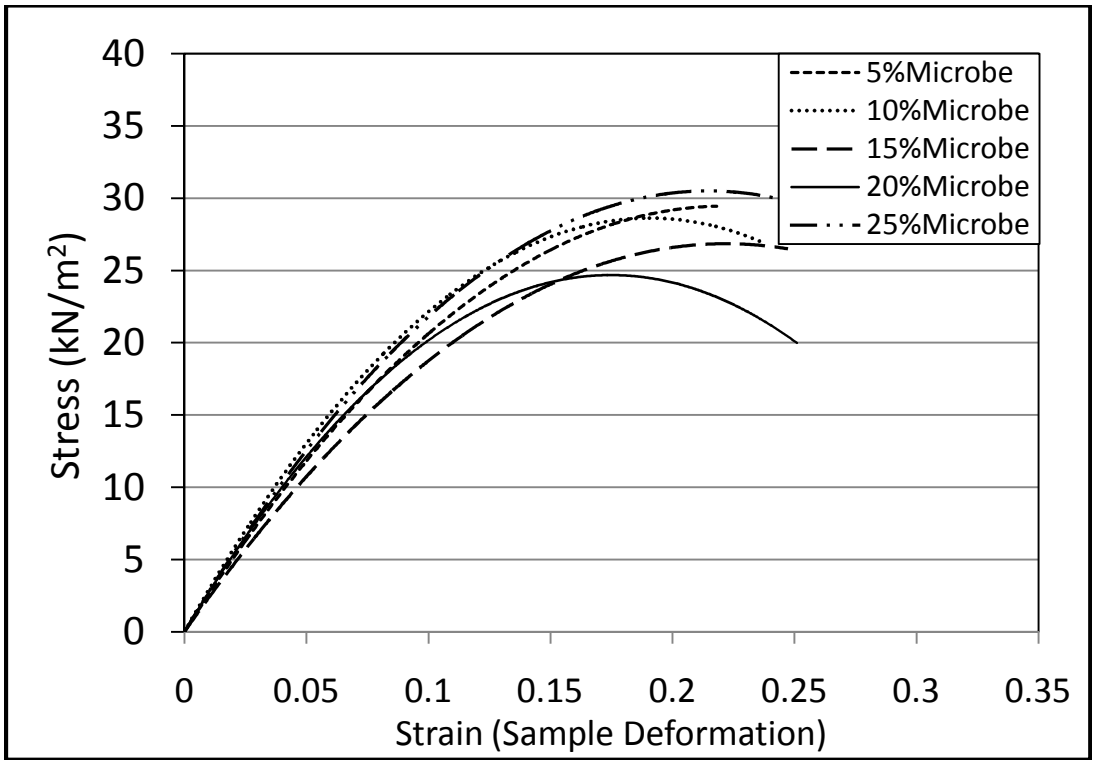

Unconfined compression result of silty clay soil treated with microbe at day 13

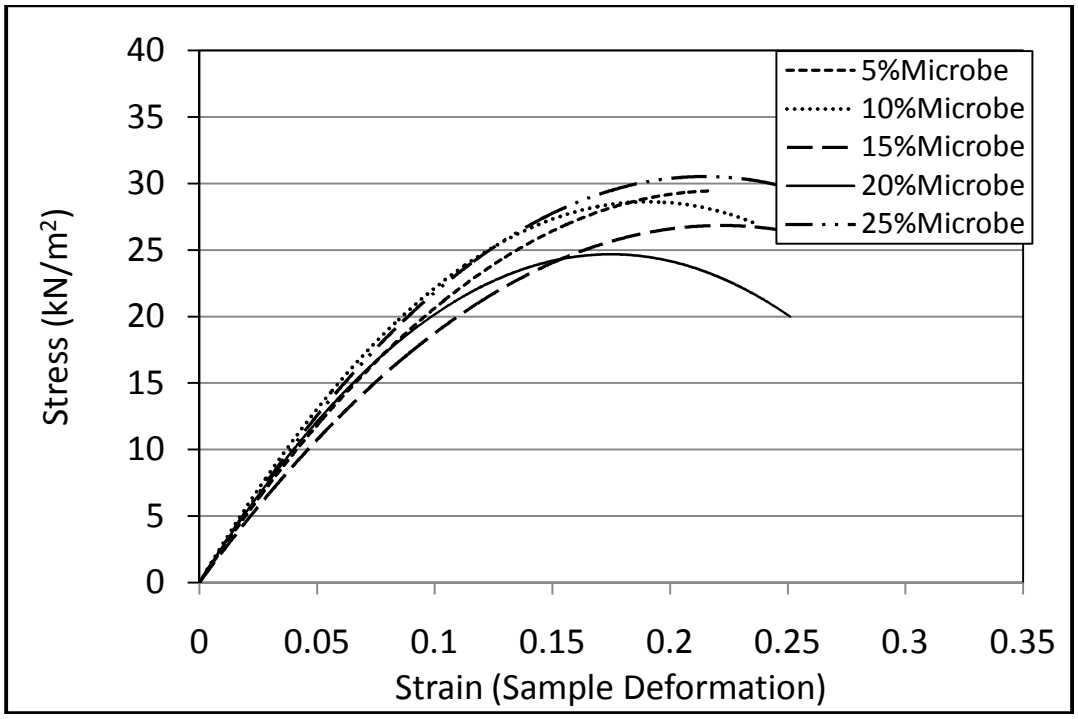

Unconfined compression result of silty clay soil treated with microbe at day 12

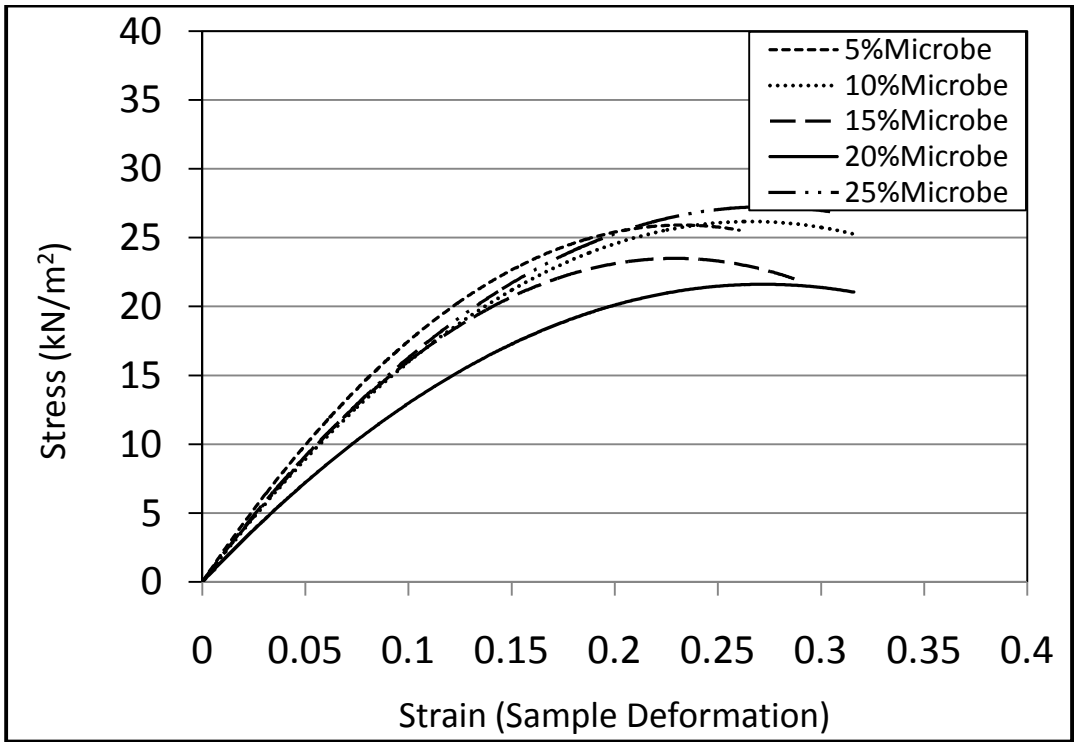

Unconfined compression result of silty clay soil treated with microbe at day 11

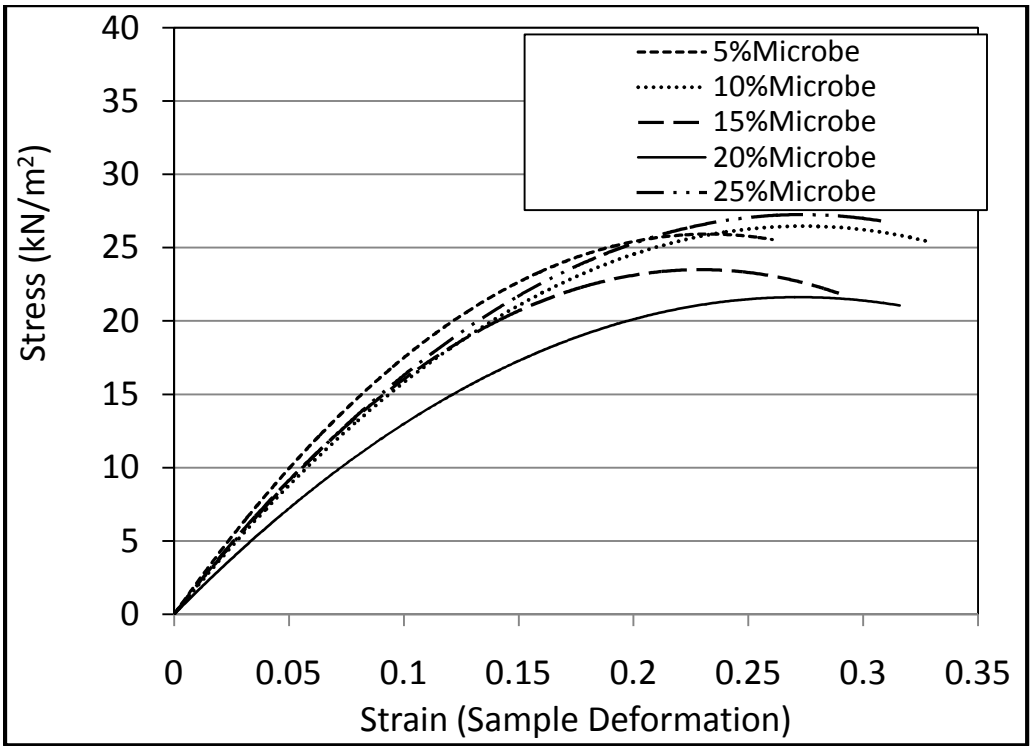

Unconfined compression result of silty clay soil treated with microbe at day 9

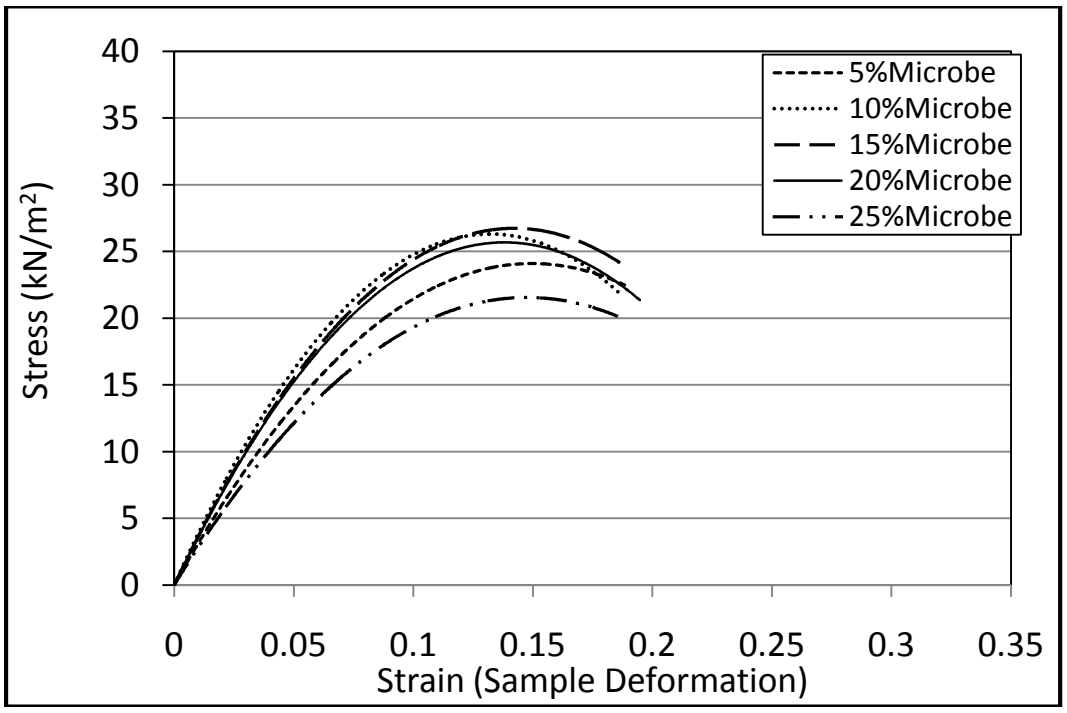

Unconfined compression result of silty clay soil treated with microbe at day 8

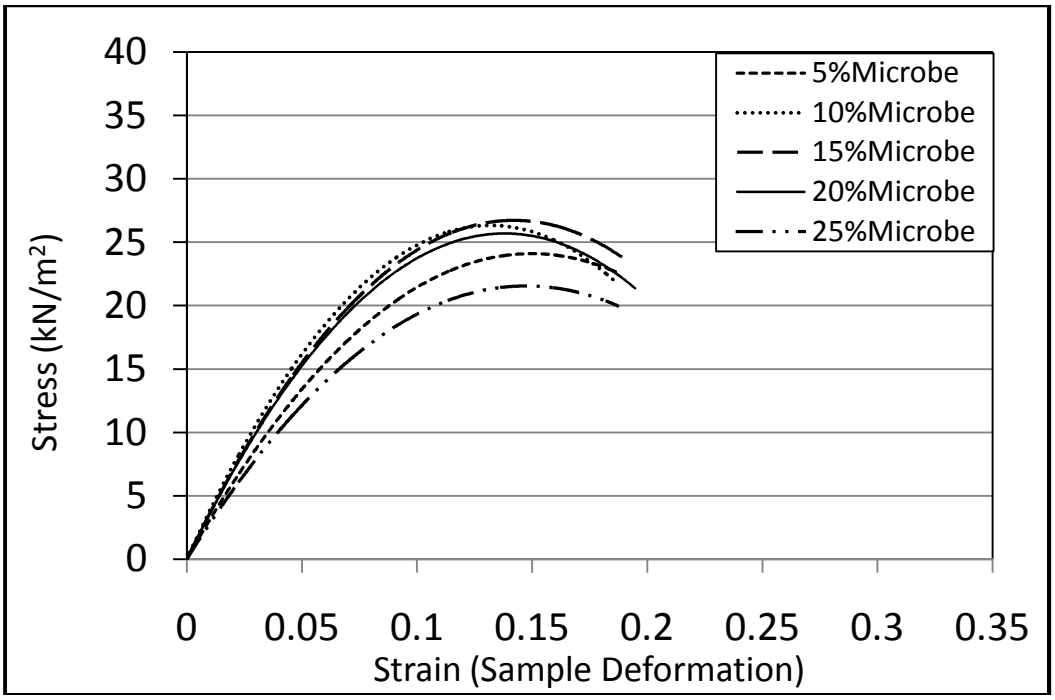

Unconfined compression result of silty clay soil treated with microbe at day 7

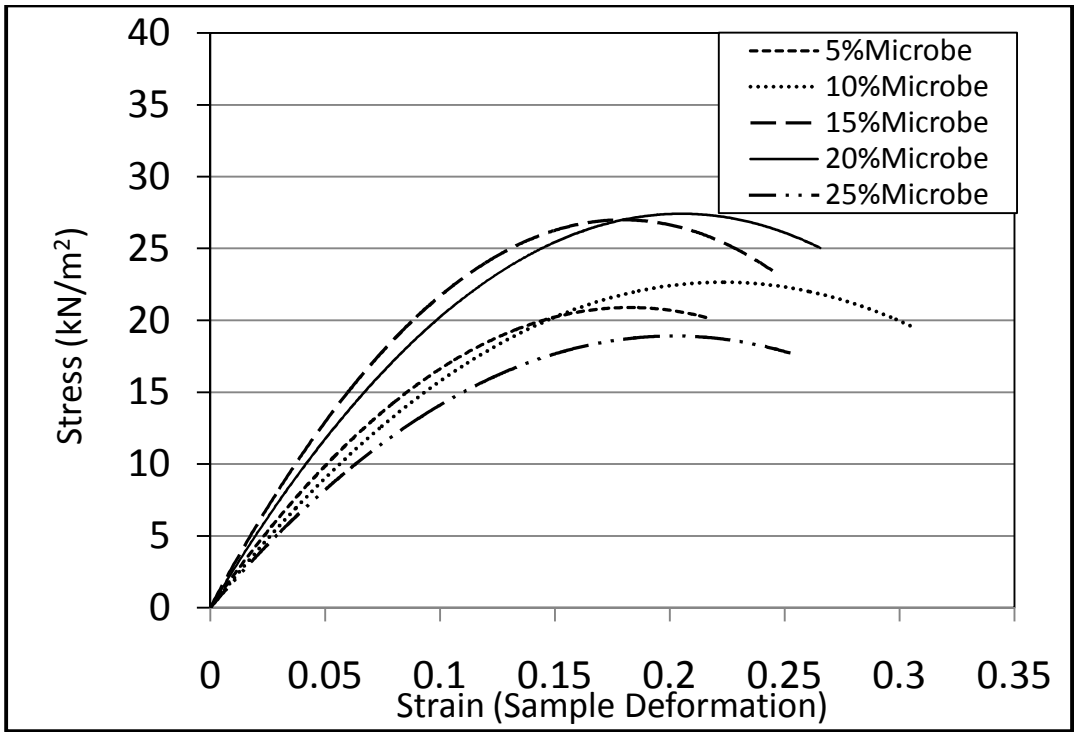

Unconfined compression result of silty clay soil treated with microbe at day 6

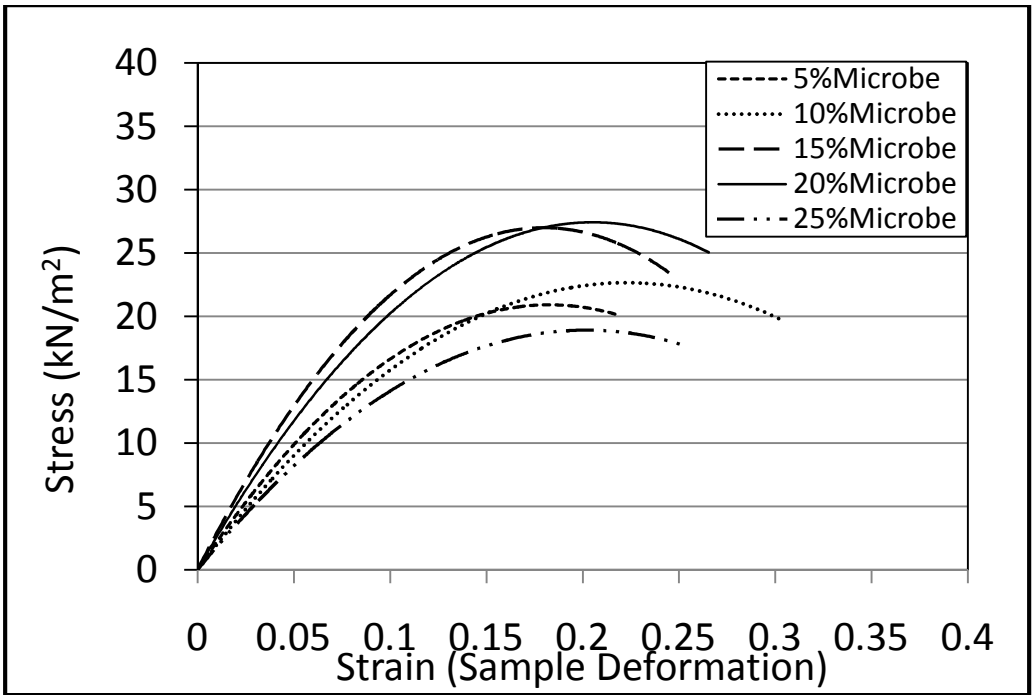

Unconfined compression result of silty clay soil treated with microbe at day 5

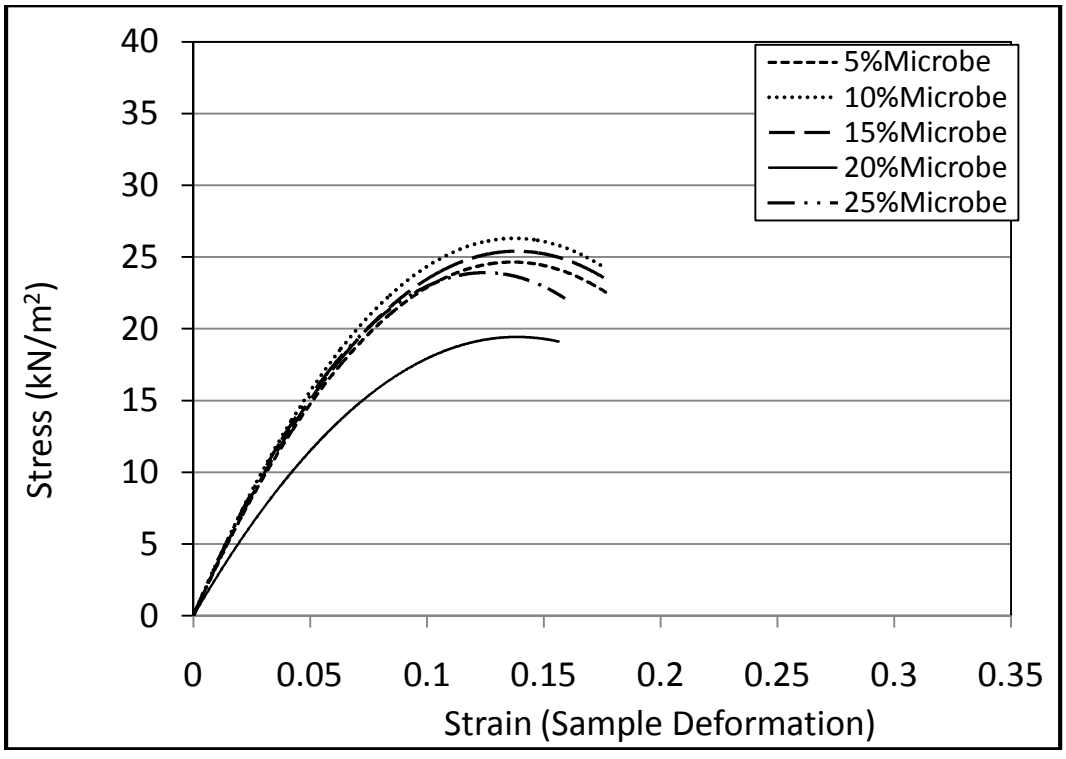

Unconfined compression result of silty clay soil treated with microbe at day 1

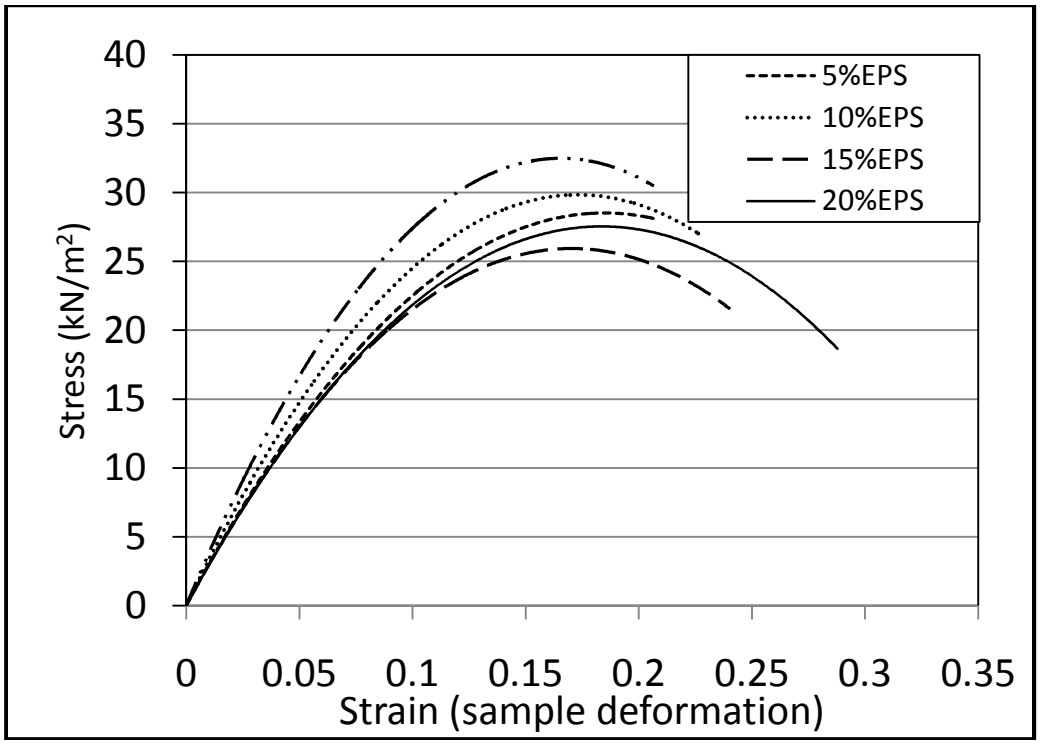

Unconfined compression result of silty clay soil treated with EPS at day 14

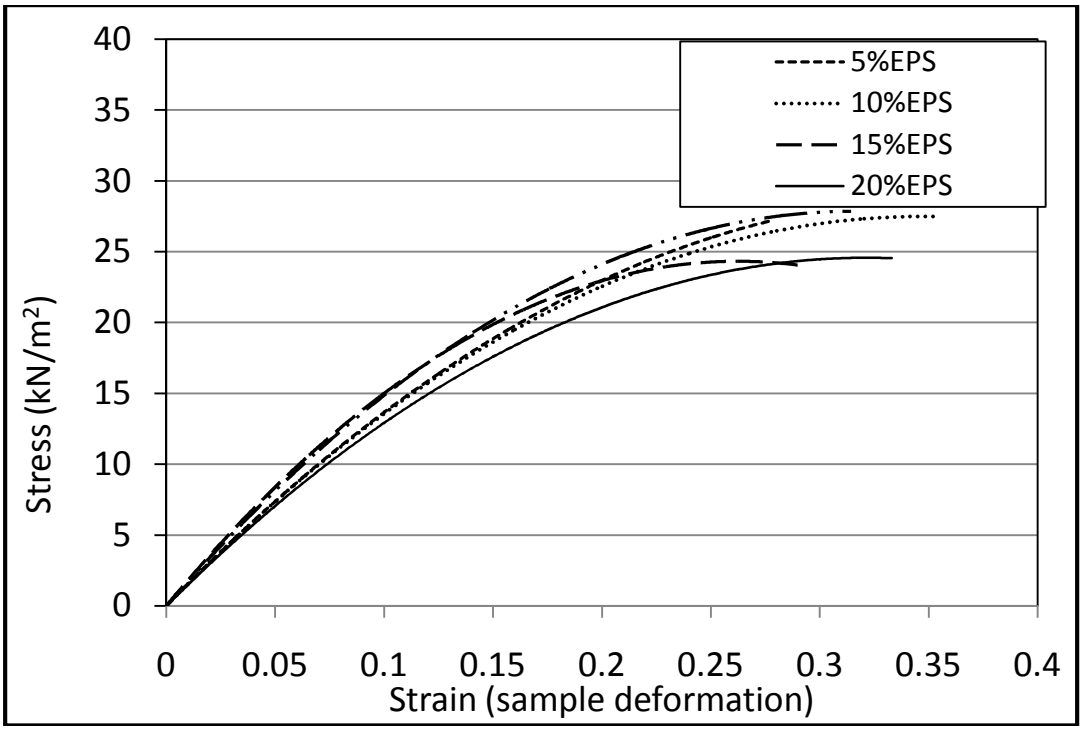

Unconfined compression result of silty clay soil treated with EPS at day 13

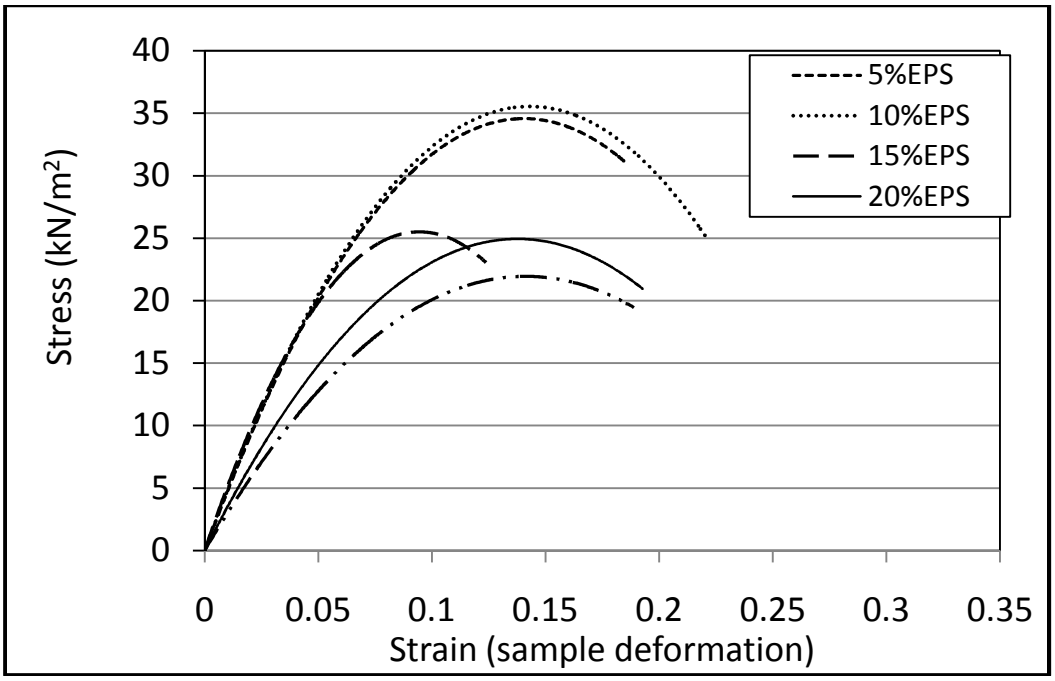

Unconfined compression result of silty clay soil treated with EPS at day 12

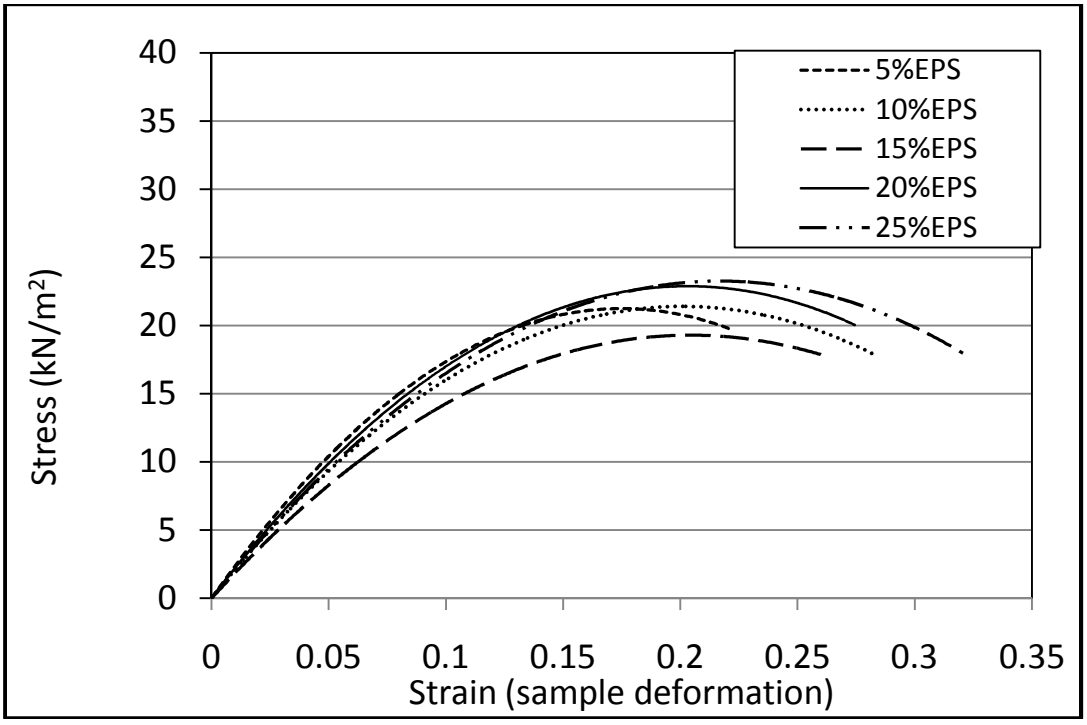

Unconfined compression result of silty clay soil treated with EPS at day 11

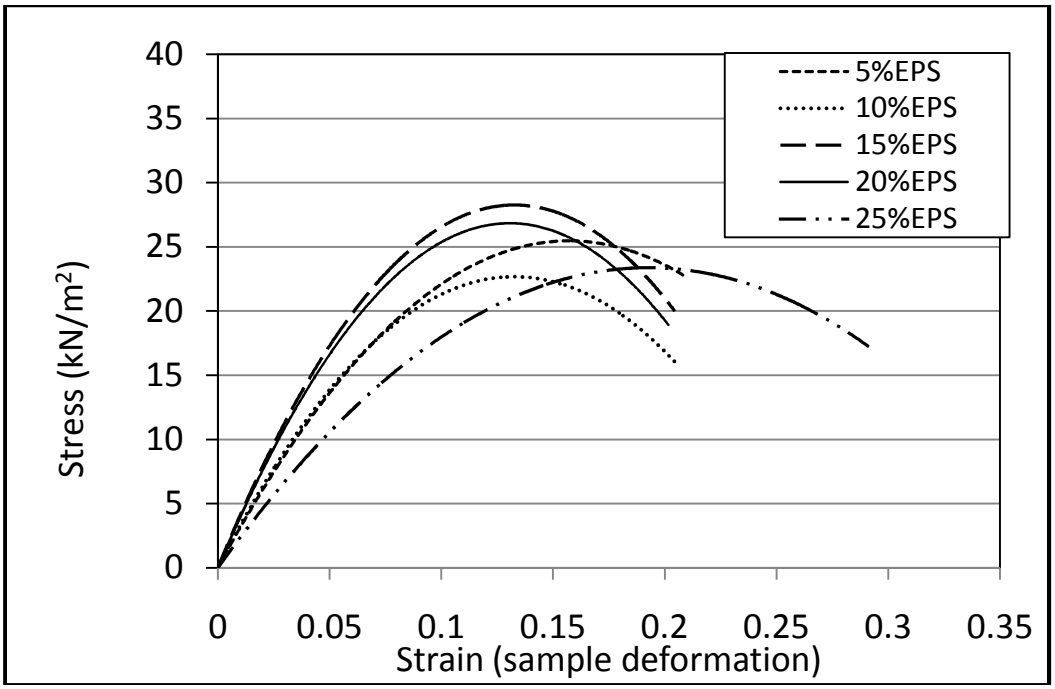

Unconfined compression result of silty clay soil treated with EPS at day 10

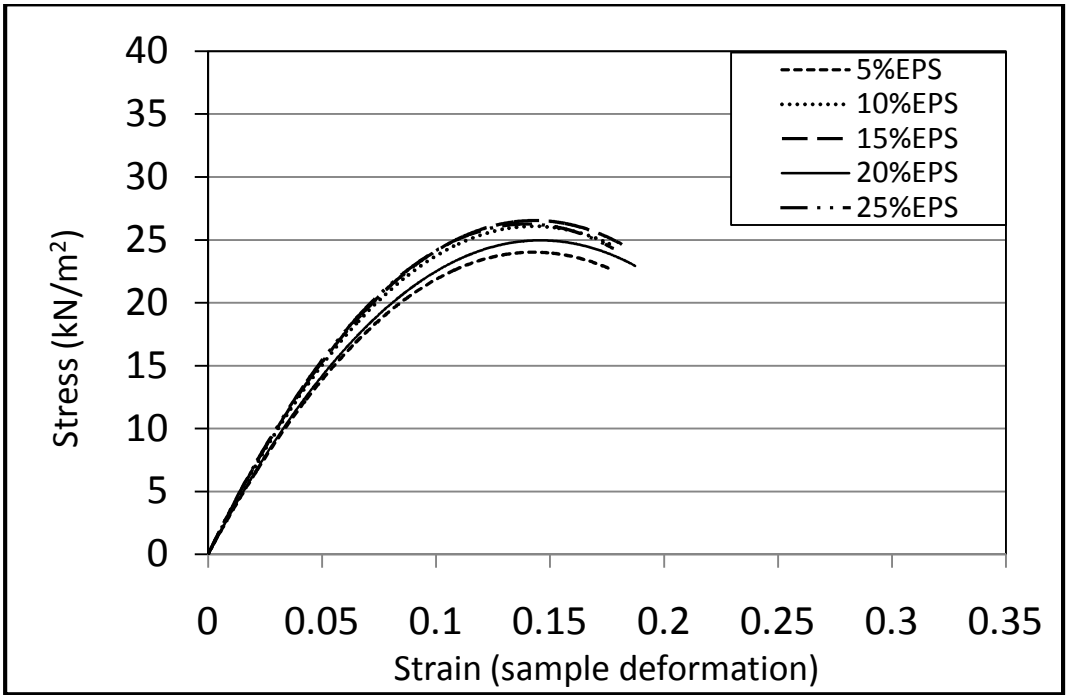

Unconfined compression result of silty clay soil treated with EPS at day 4

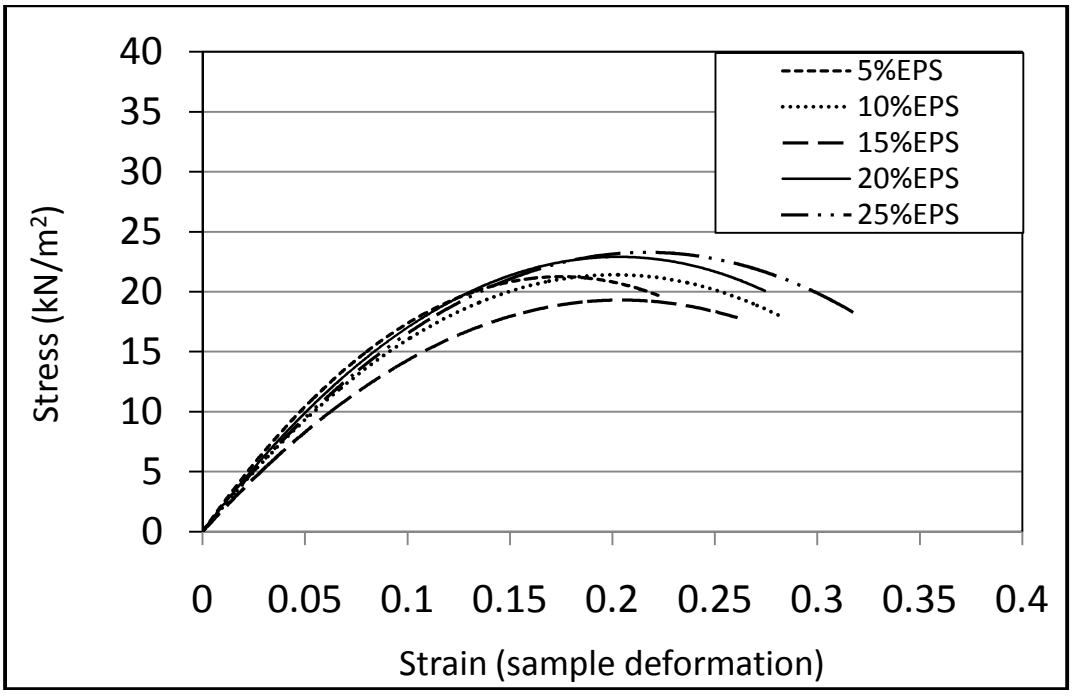

Unconfined compression result of silty clay soil treated with EPS at day 3

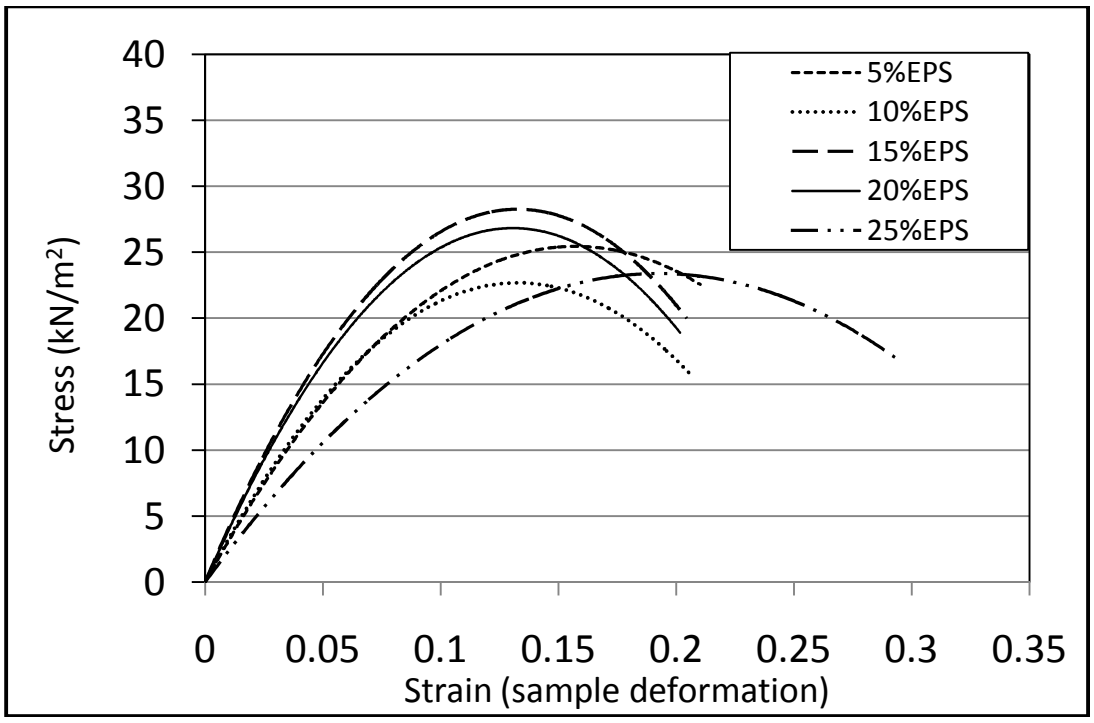

Unconfined compression result of silty clay soil treated with EPS at day 2

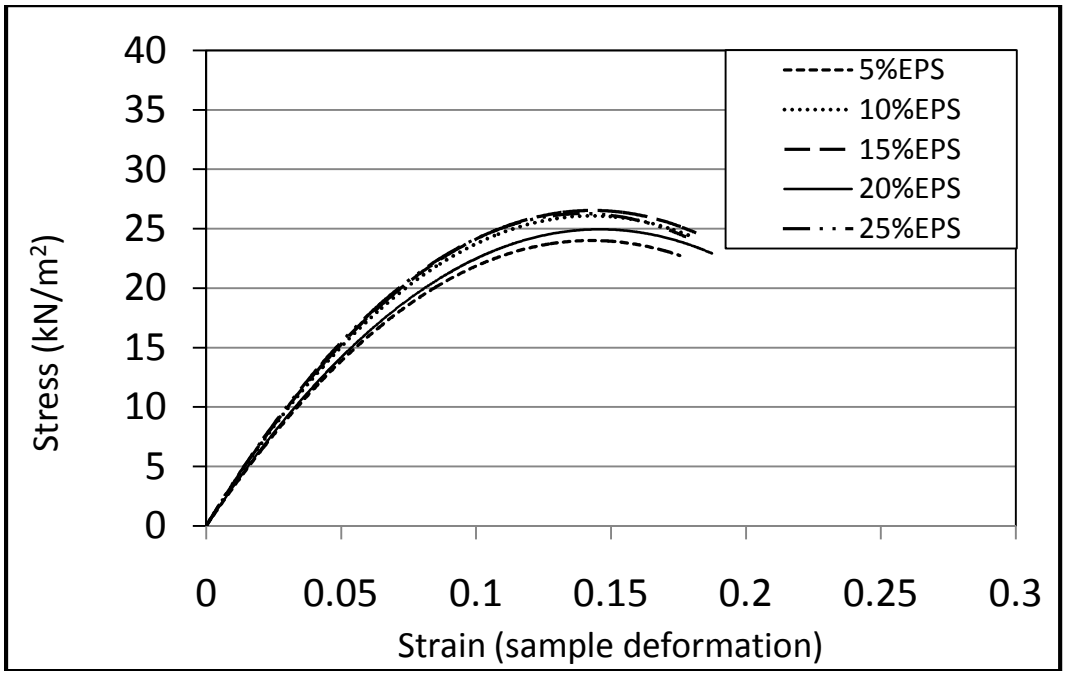

Unconfined compression result of silty clay soil treated with EPS at day 1

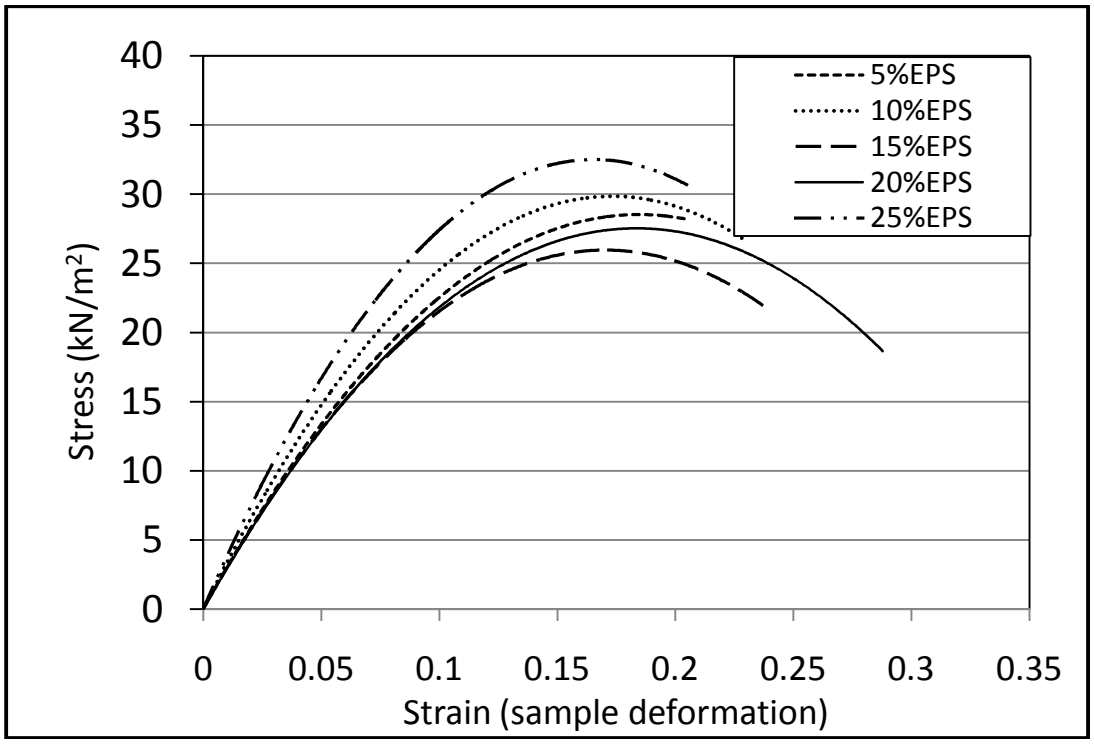

Unconfined compression result of silty clay soil treated with EPS at day 6

APPENDIX C: GRAPHS OF UNCONFINED COMPRESSION TESTS FOR SANDY CLAY SOIL

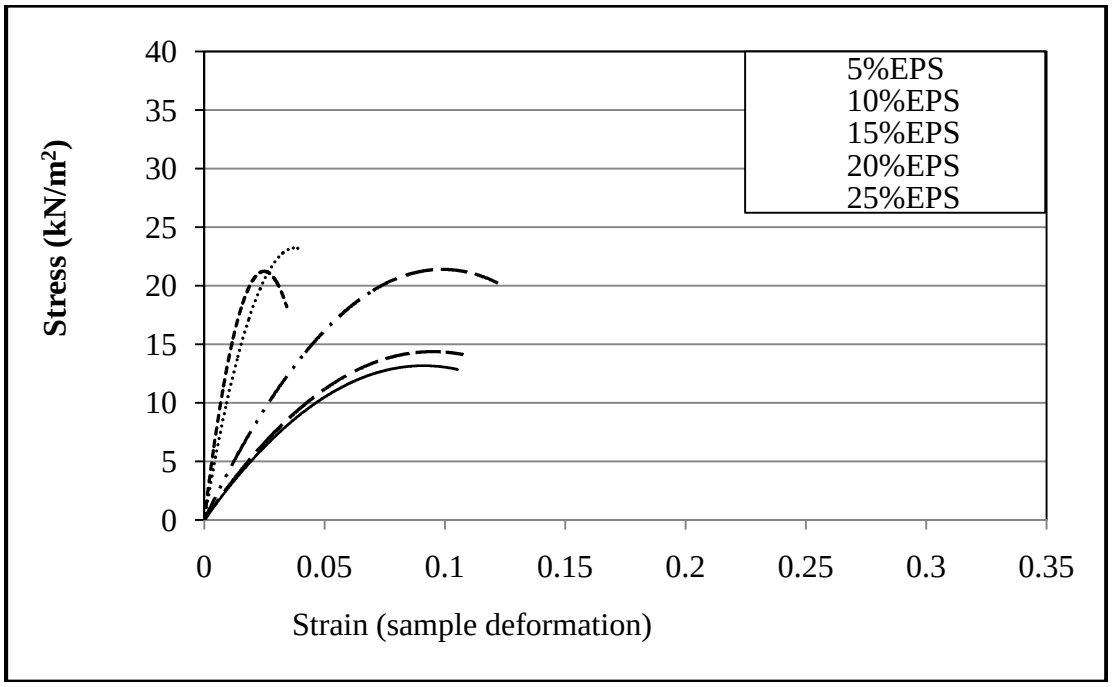

Unconfined compression result of sandy clay soil control sample at day 10

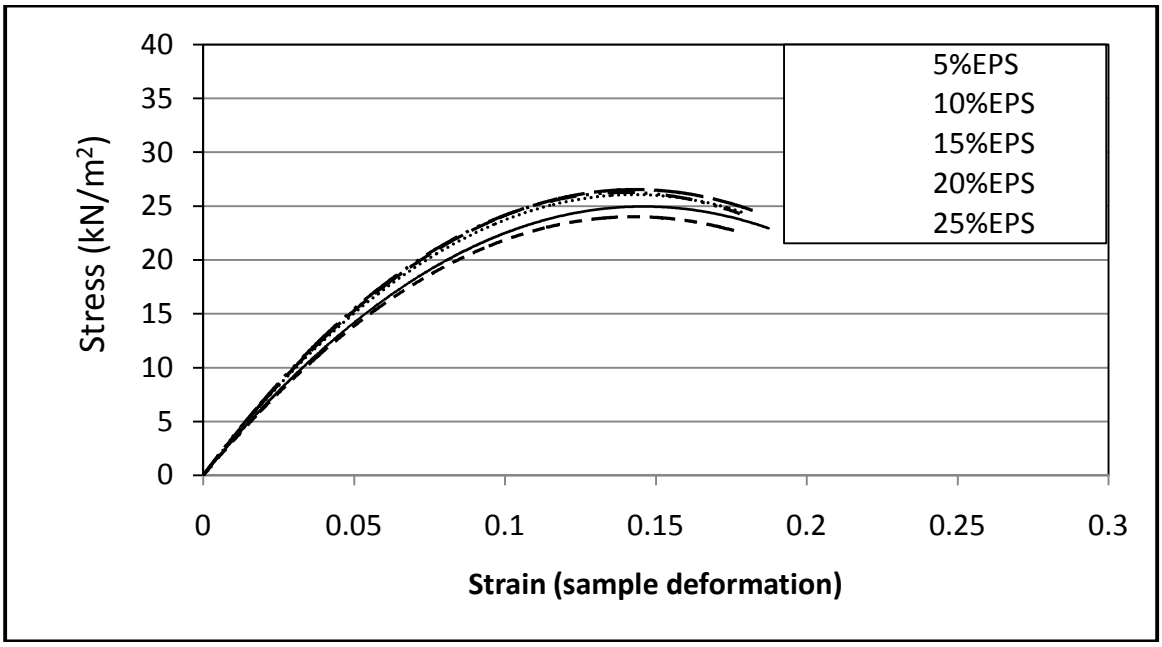

Unconfined compression result of sandy clay soil treated with EPS at day 1

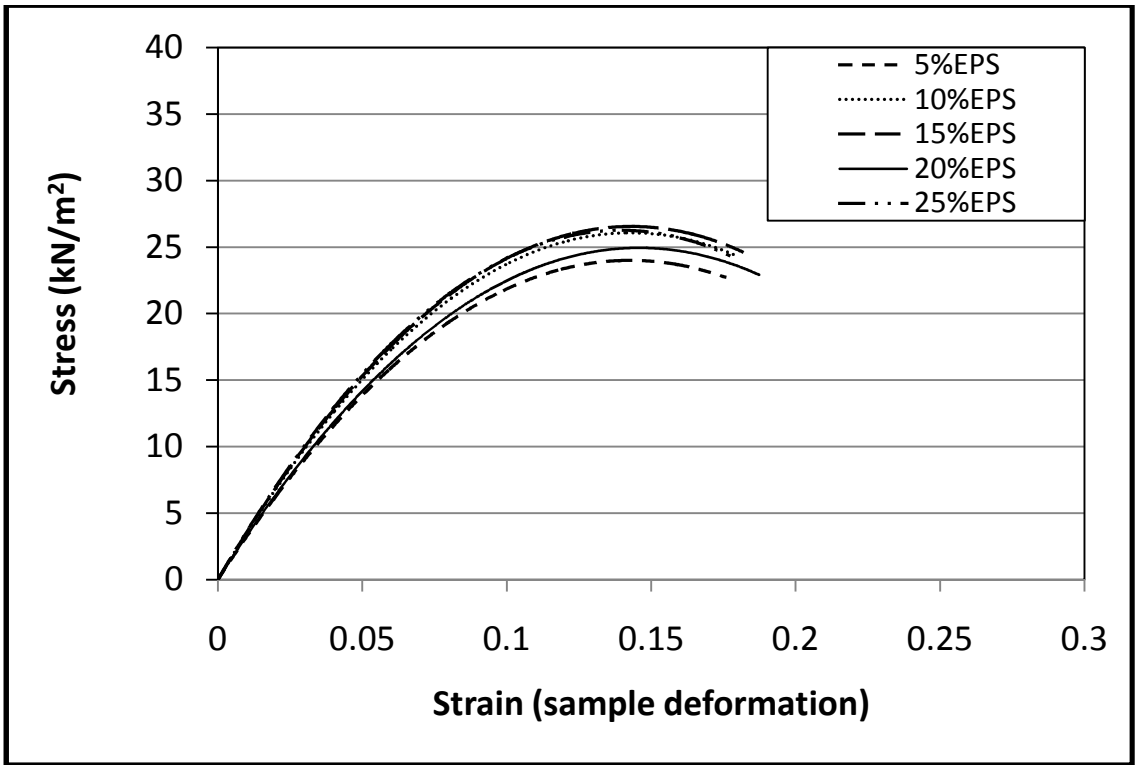

Unconfined compression result of sandy clay soil treated with EPS at day 3

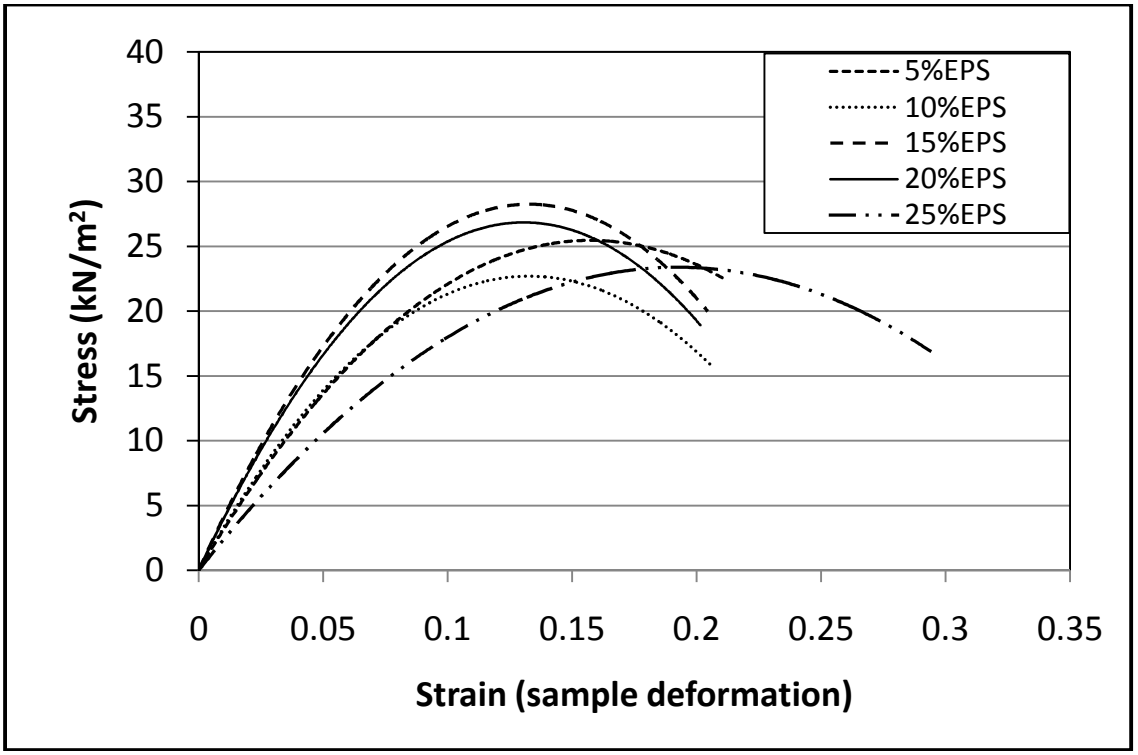

Unconfined compression result of sandy clay soil treated with EPS at day 3

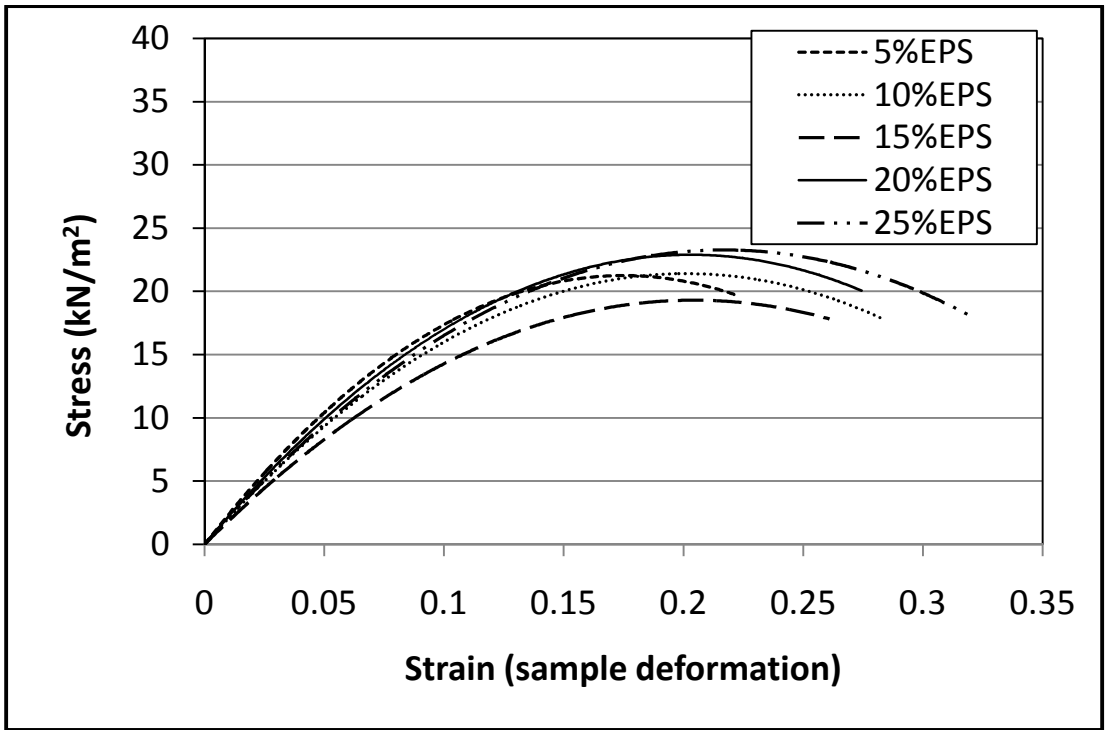

Unconfined compression result of sandy clay soil treated with EPS at day 4

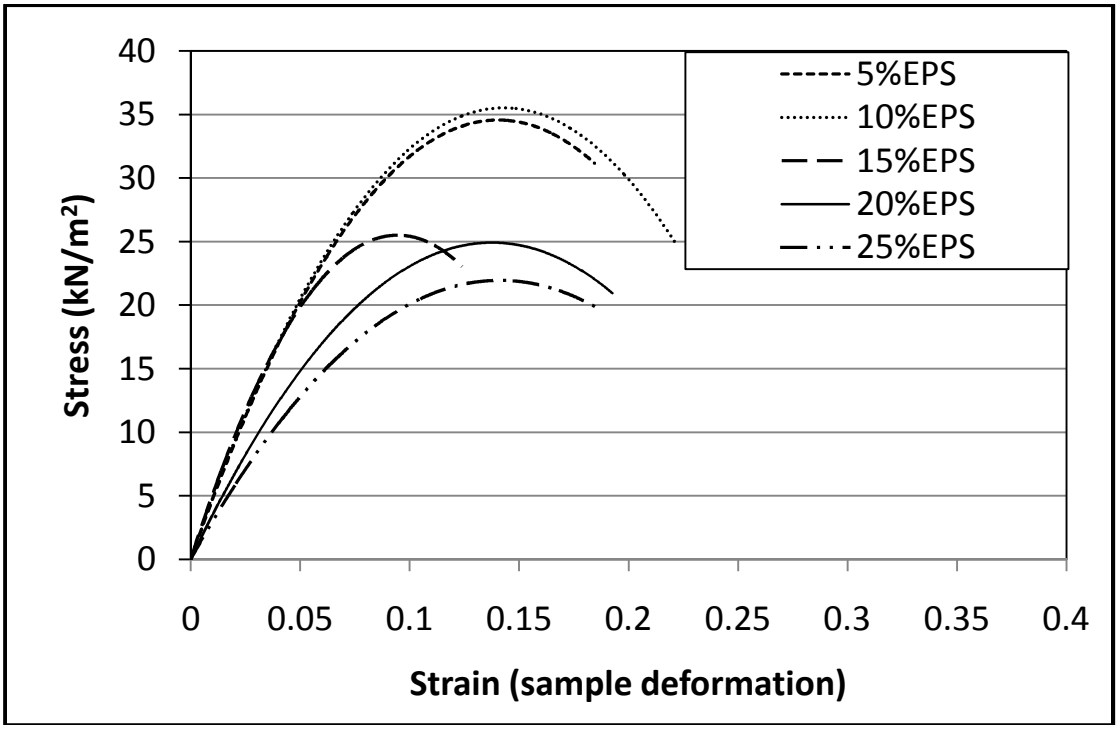

Unconfined compression result of sandy clay soil treated with EPS at day 5

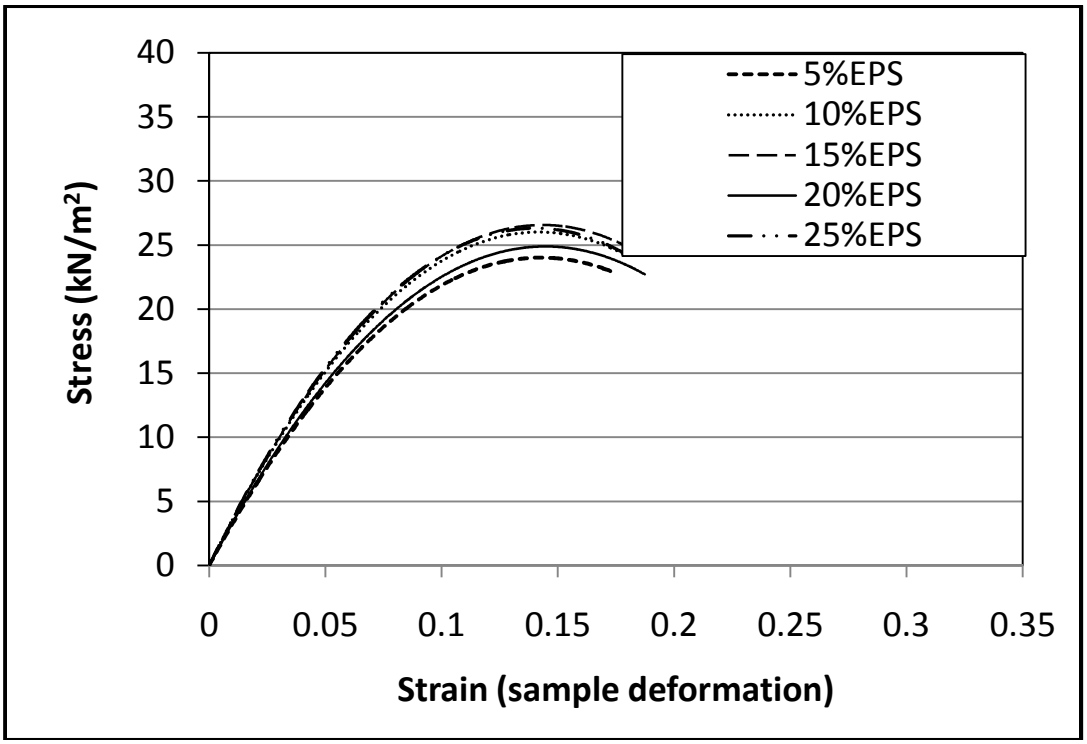

Unconfined compression result of sandy clay soil treated with EPS at day 6

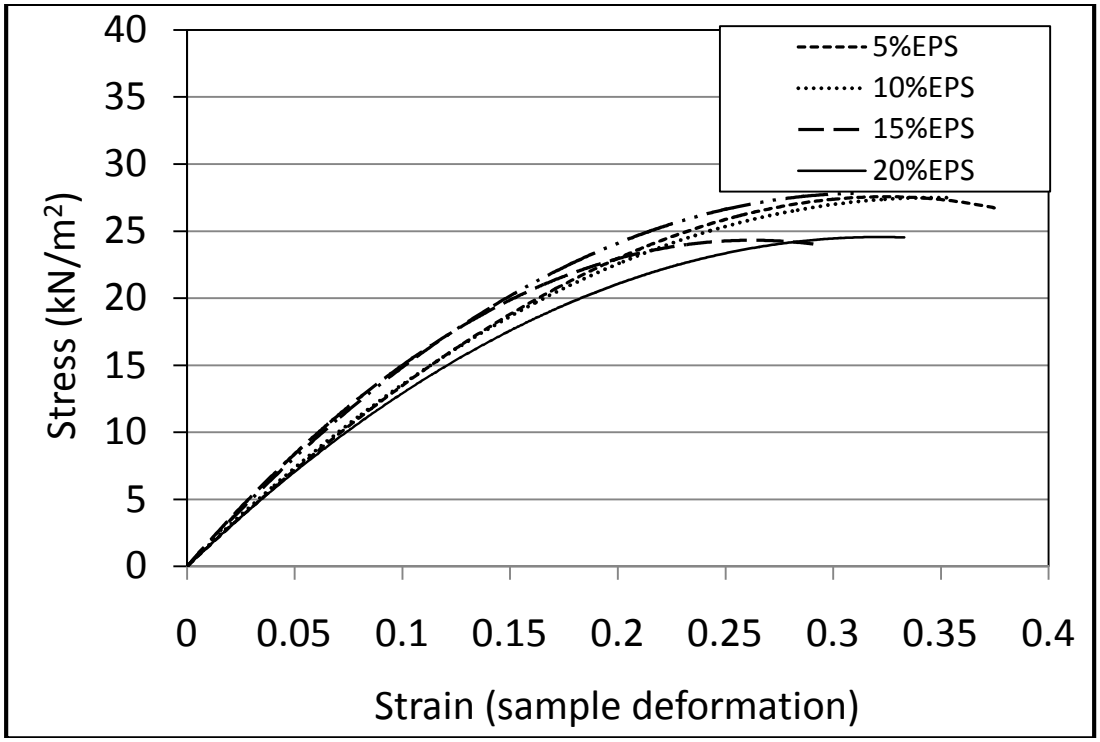

Unconfined compression result of sandy clay soil treated with EPS at day 7

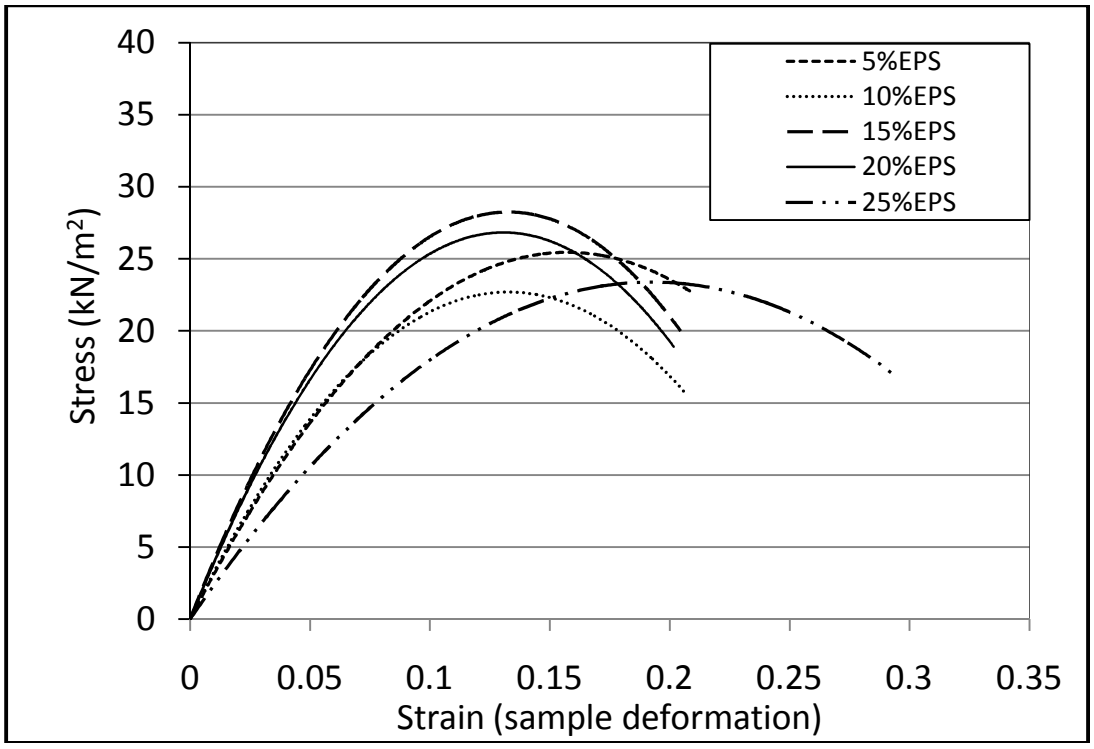

Unconfined compression result of sandy clay soil treated with EPS at day 8

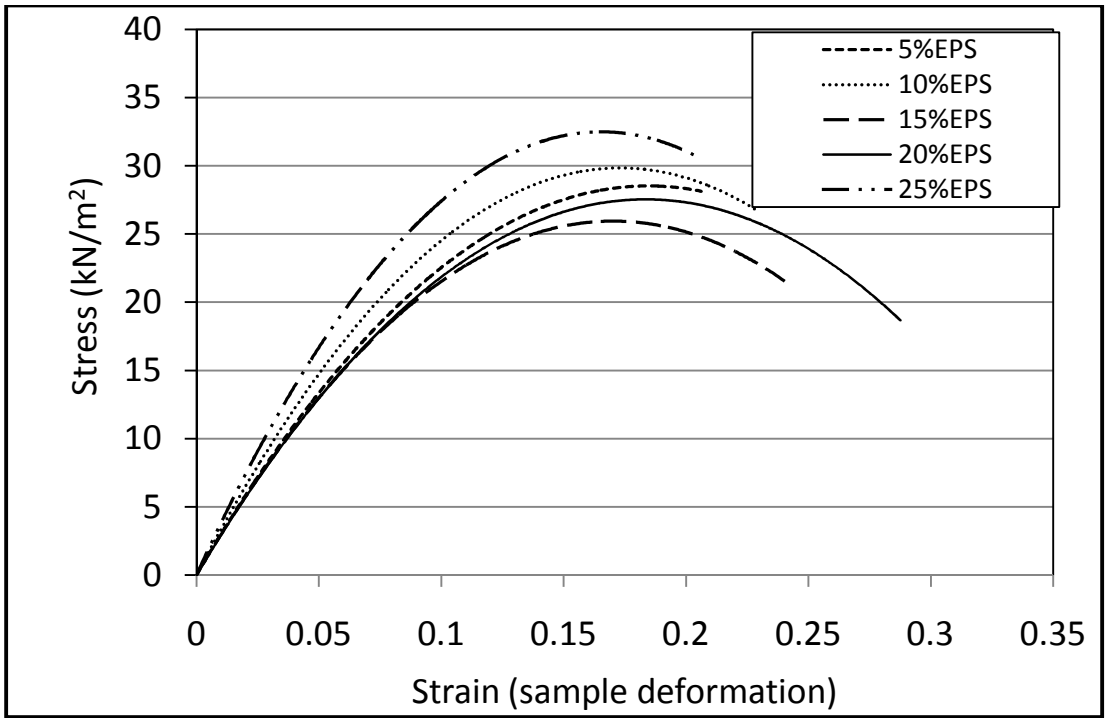

Unconfined compression result of sandy clay soil treated with EPS at day 9

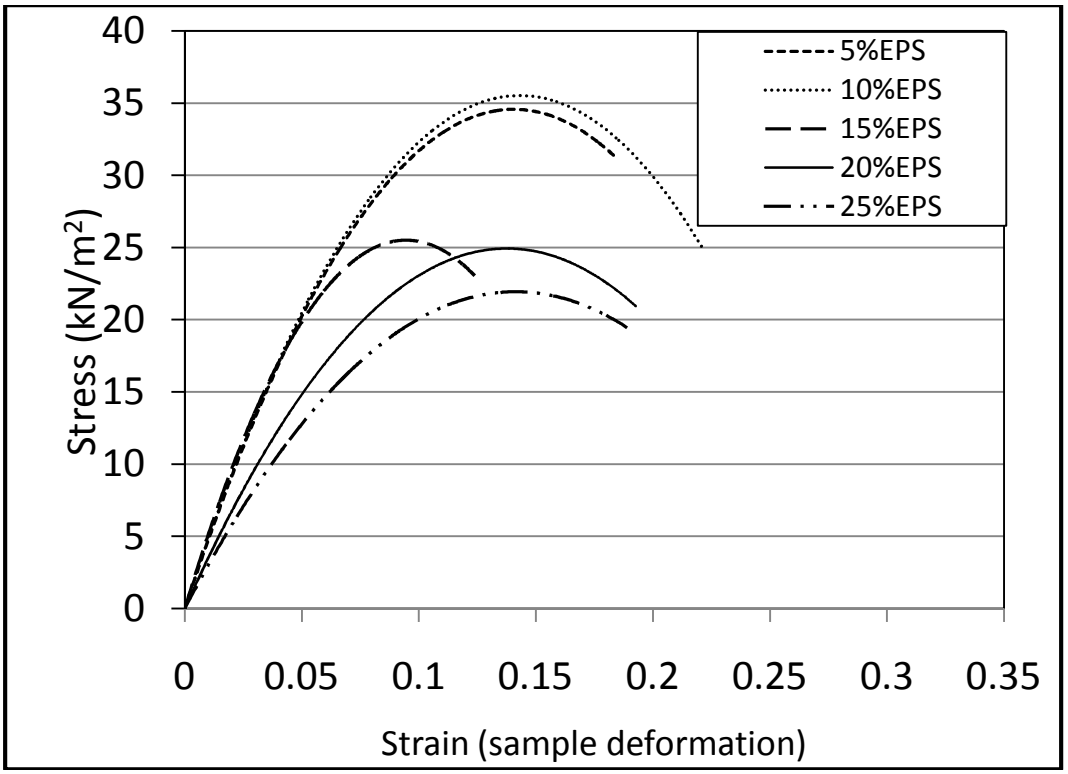

Unconfined compression result of sandy clay soil treated with EPS at day 10

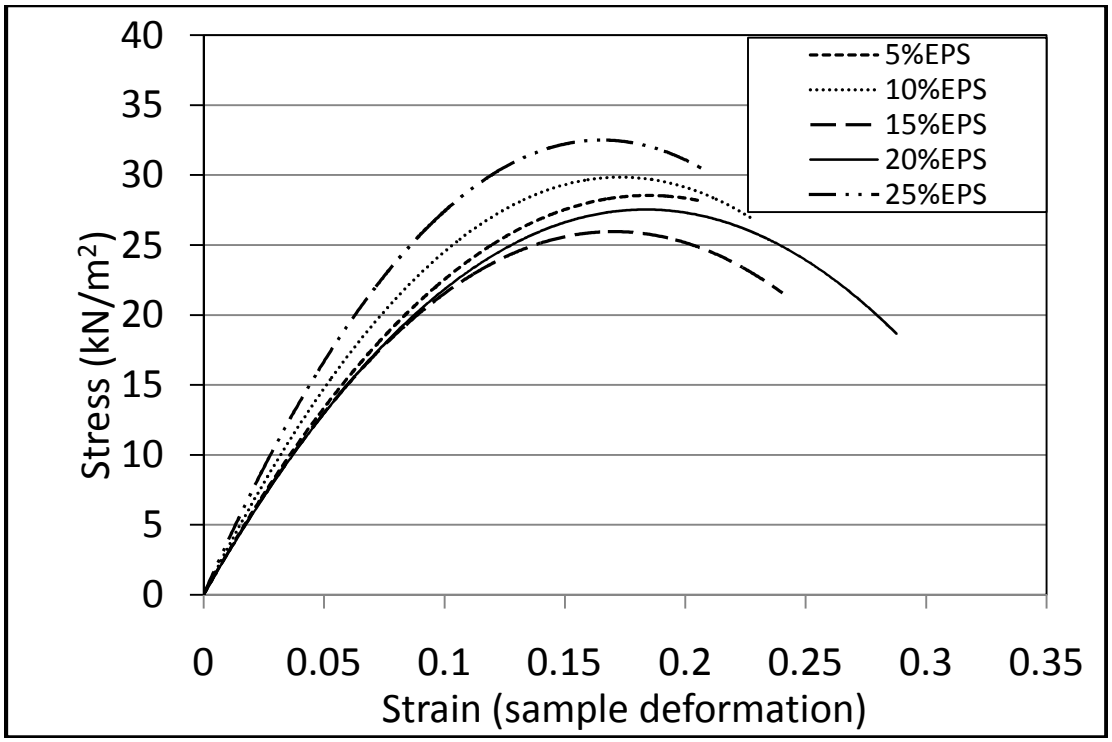

Unconfined compression result of sandy clay soil treated with EPS at day 11

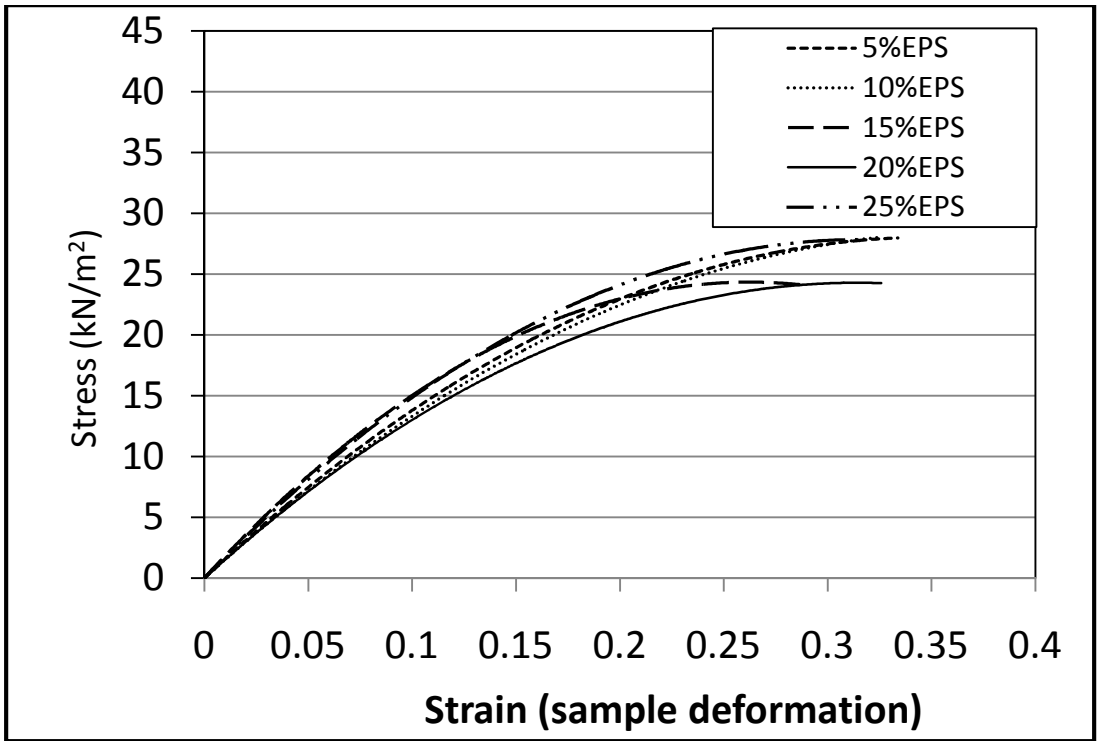

Unconfined compression result of sandy clay soil treated with EPS at day 12

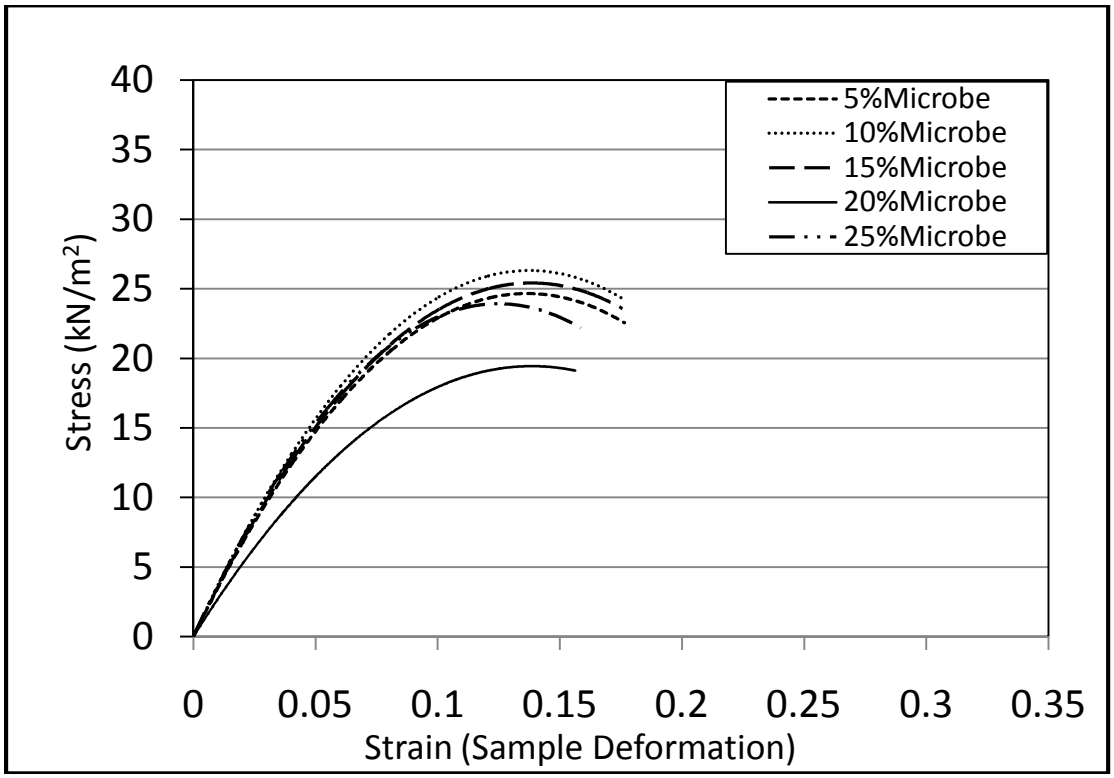

Unconfined compression result of sandy clay soil treated with EPS at day 12

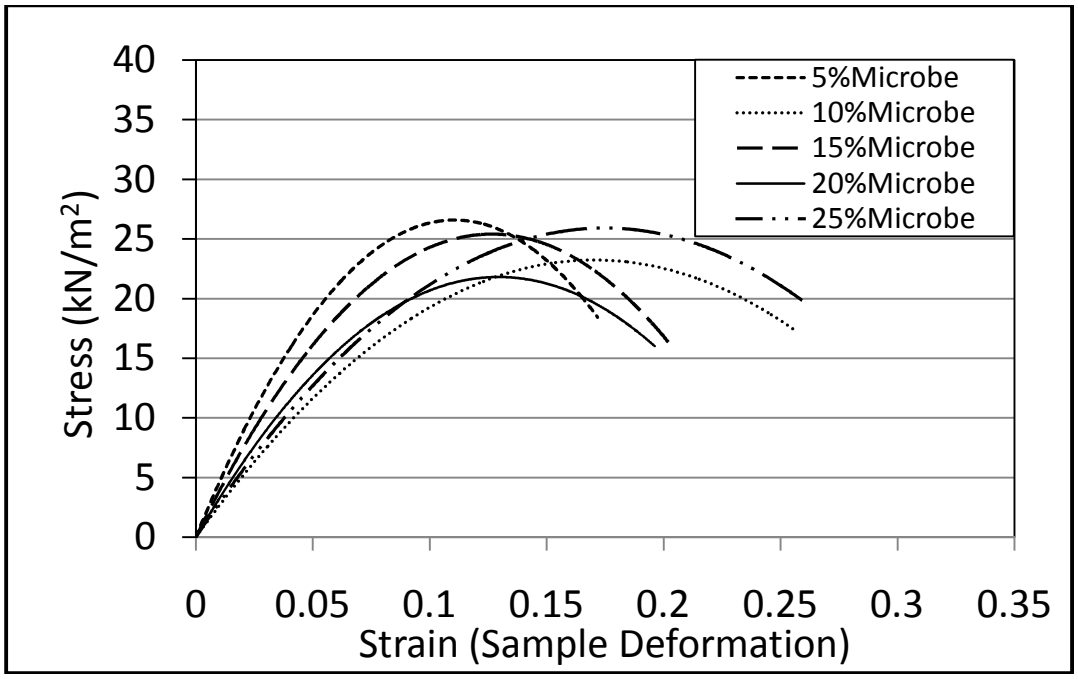

Unconfined compression result of sandy clay soil treated with microbe day 2

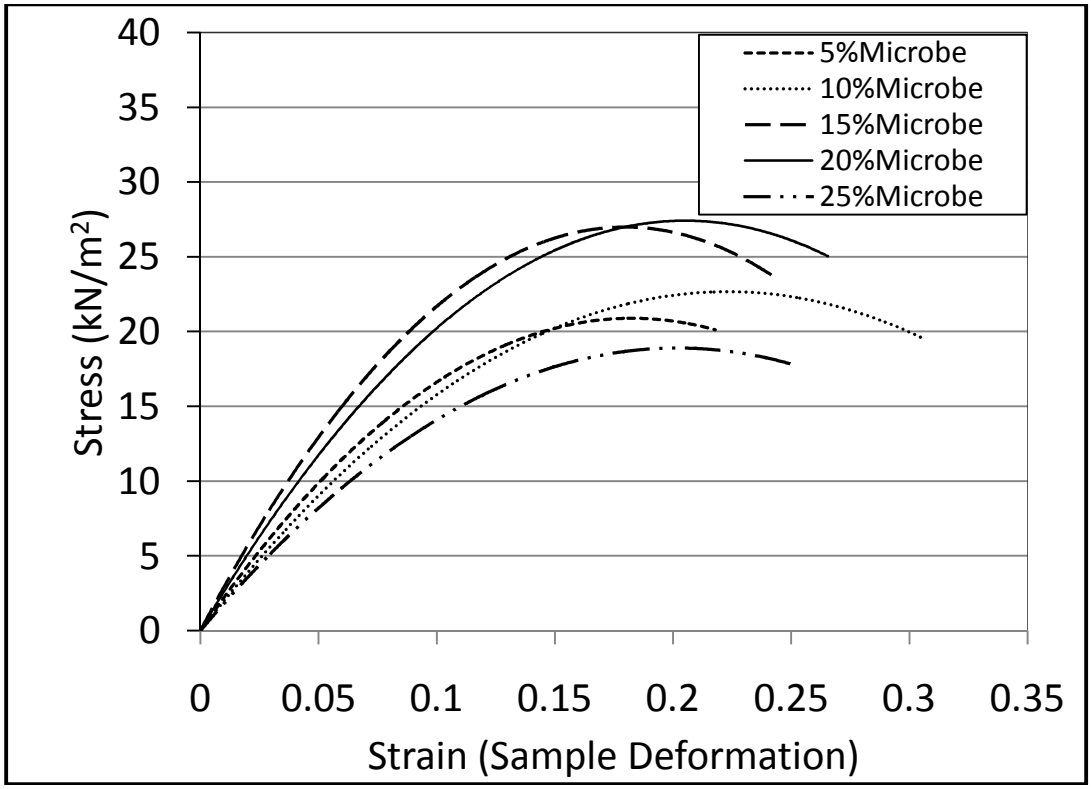

Unconfined compression result of sandy clay soil treated with microbe day 3

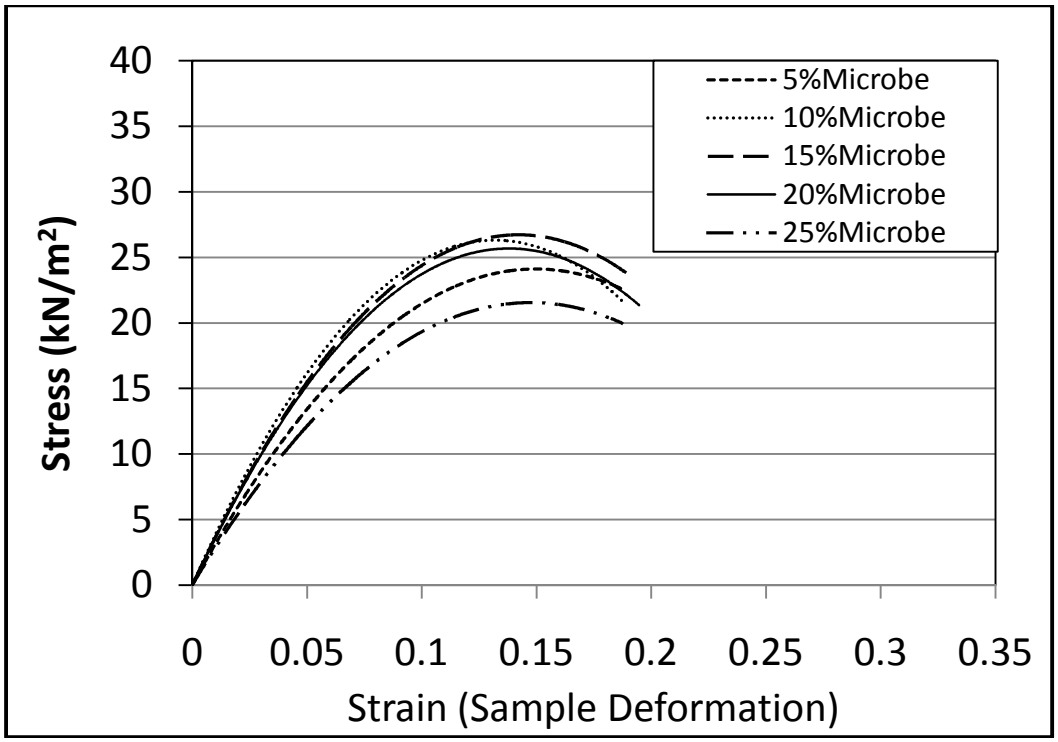

Unconfined compression result of sandy clay soil treated with microbe day 4

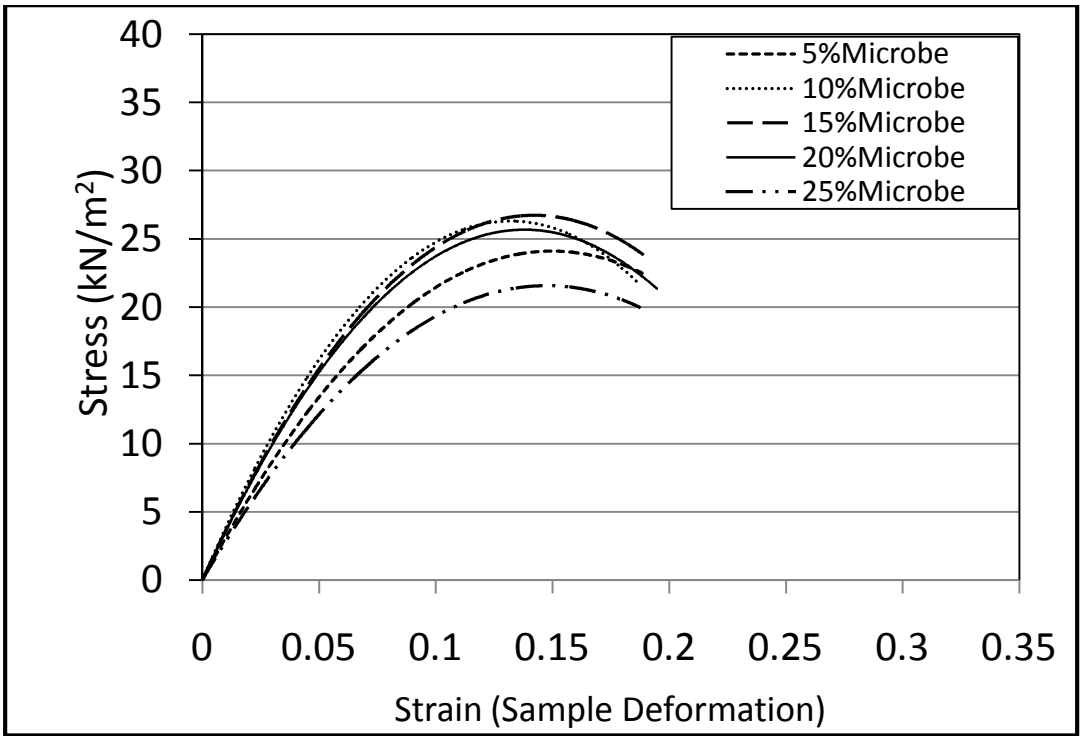

Unconfined compression result of sandy clay soil treated with microbe day 5

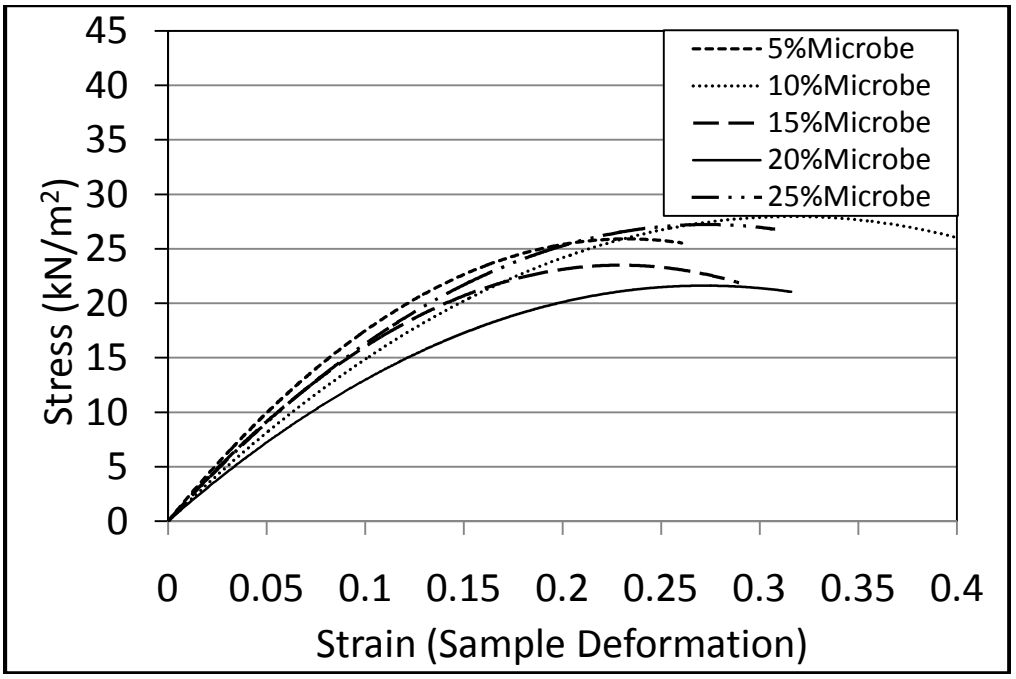

Unconfined compression result of sandy clay soil treated with microbe day 6

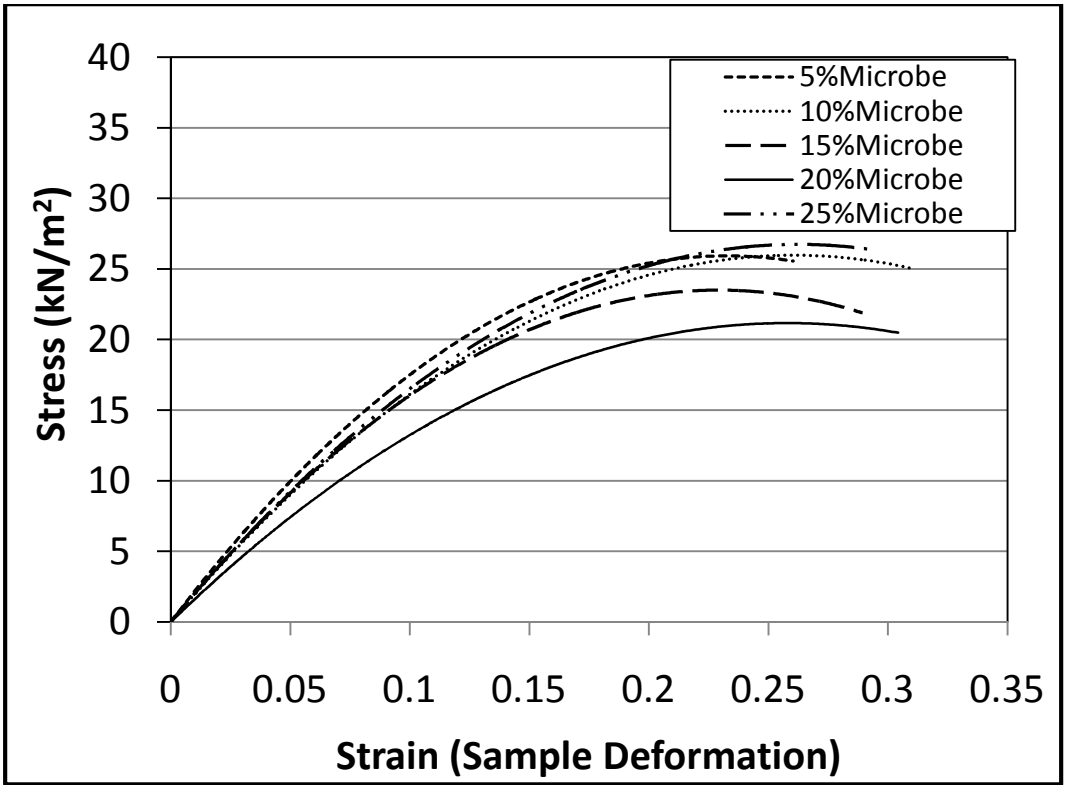

Unconfined compression result of sandy clay soil treated with microbe day 7

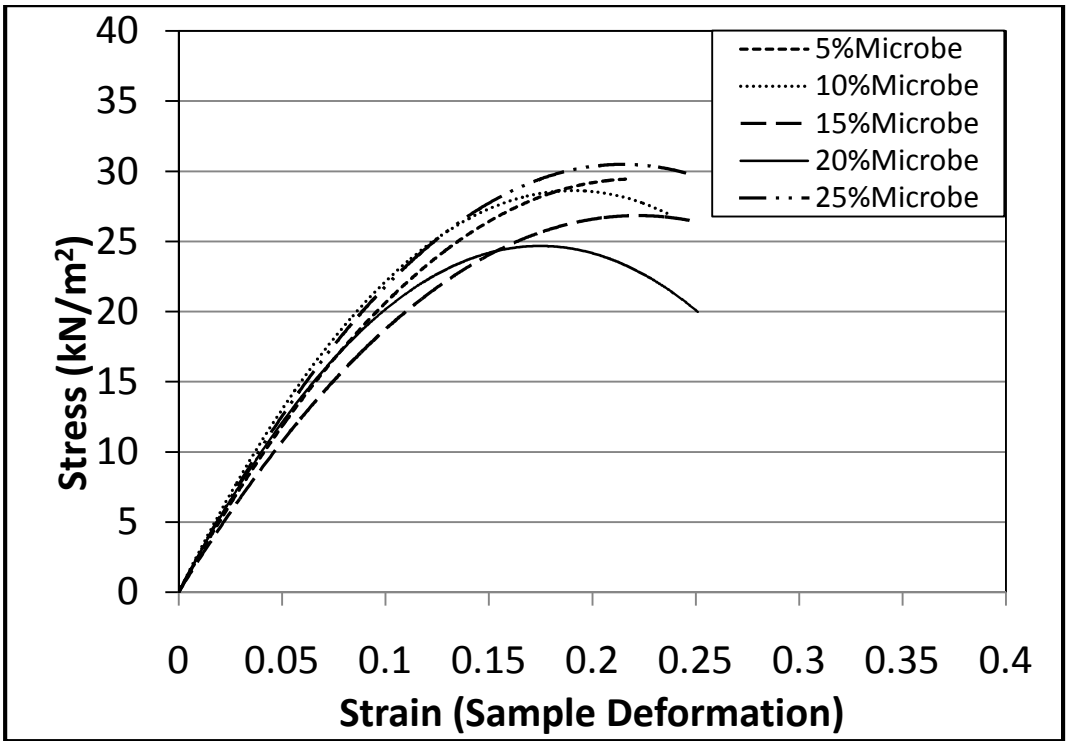

Unconfined compression result of sandy clay soil treated with microbe day 8

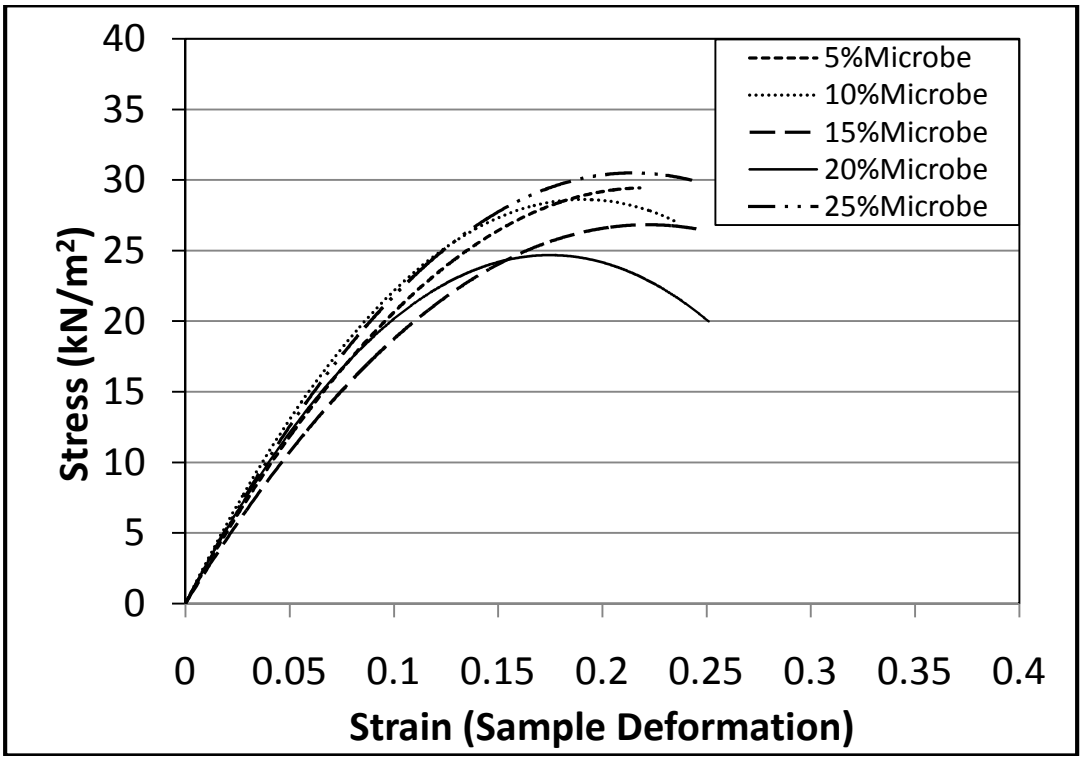

Unconfined compression result of sandy clay soil treated with microbe day 9

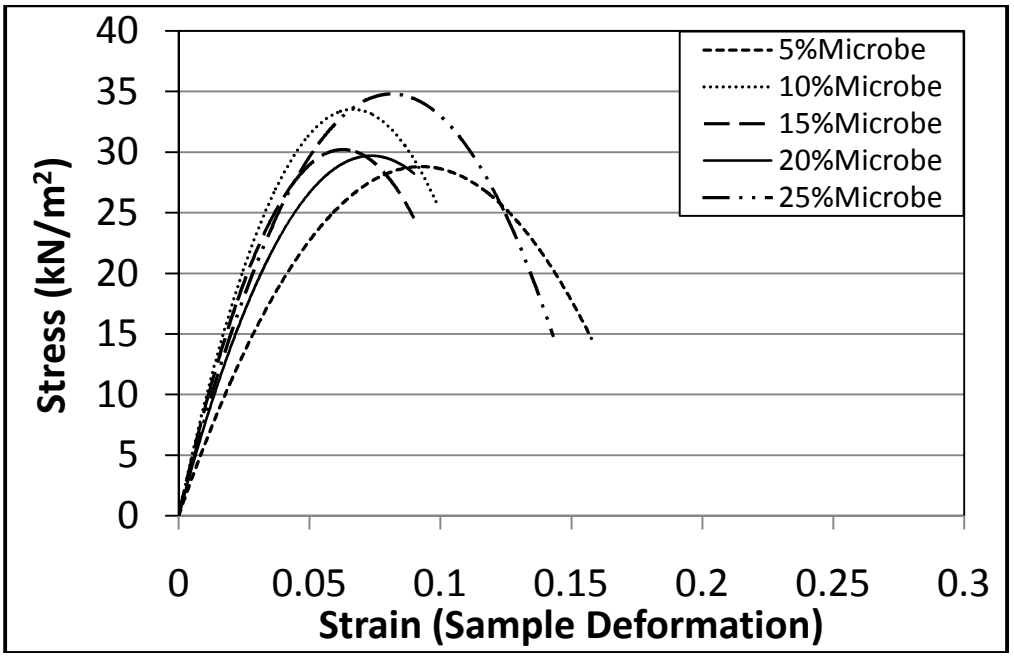

Unconfined compression result of sandy clay soil treated with microbe day 14

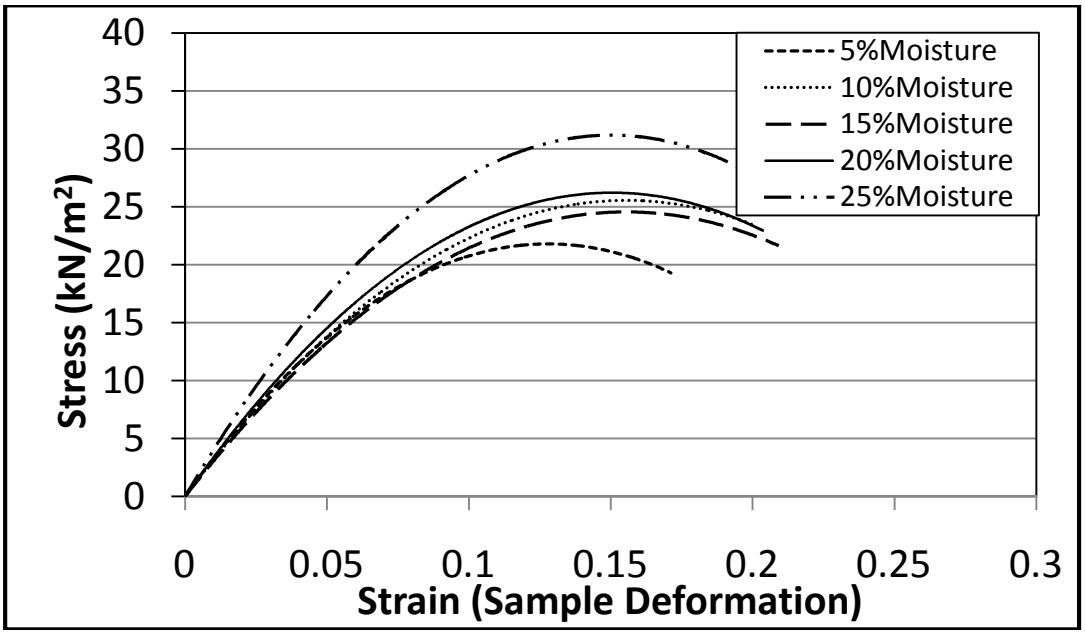

Unconfined compression result of sandy clay soil treated control day 2

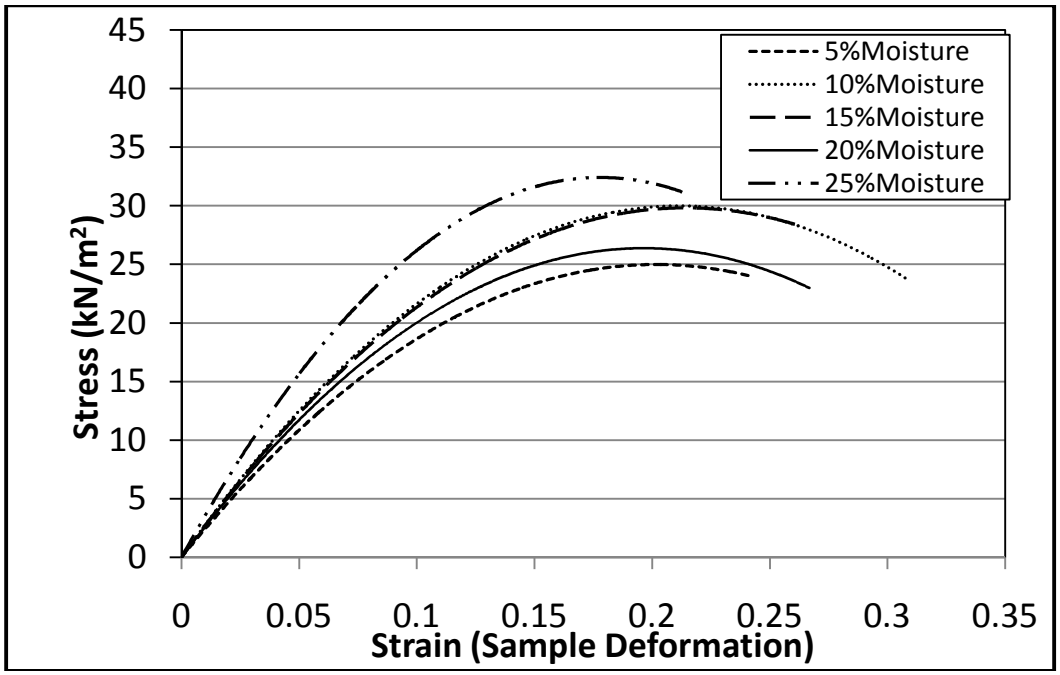

Unconfined compression result of sandy clay soil control day 3

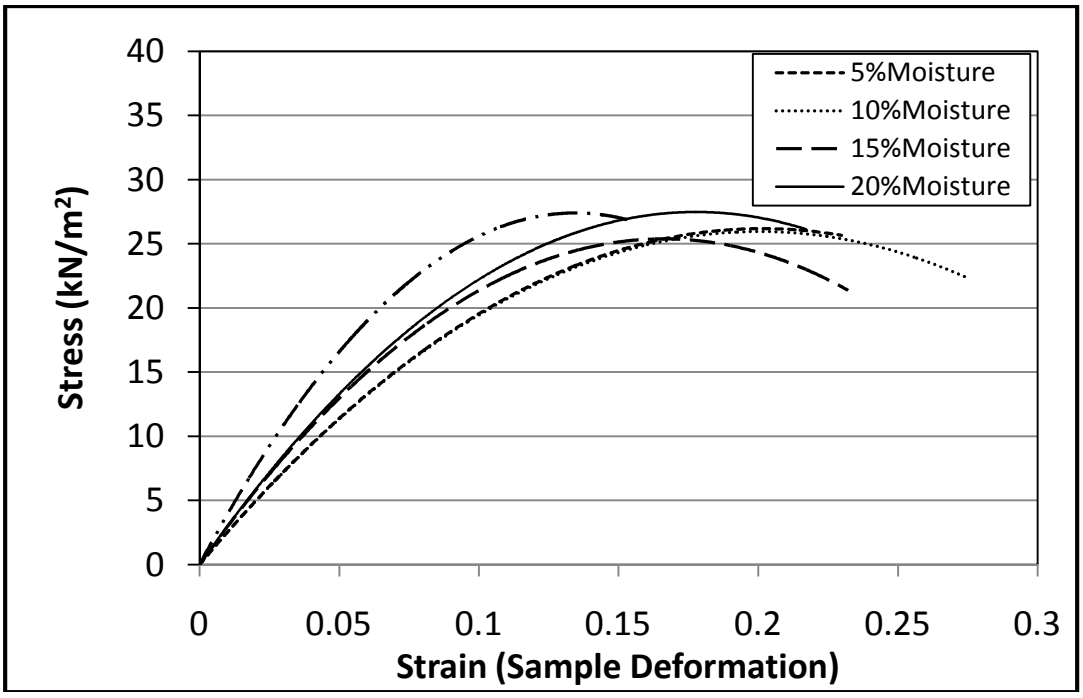

Unconfined compression result of sandy clay soil control day 4

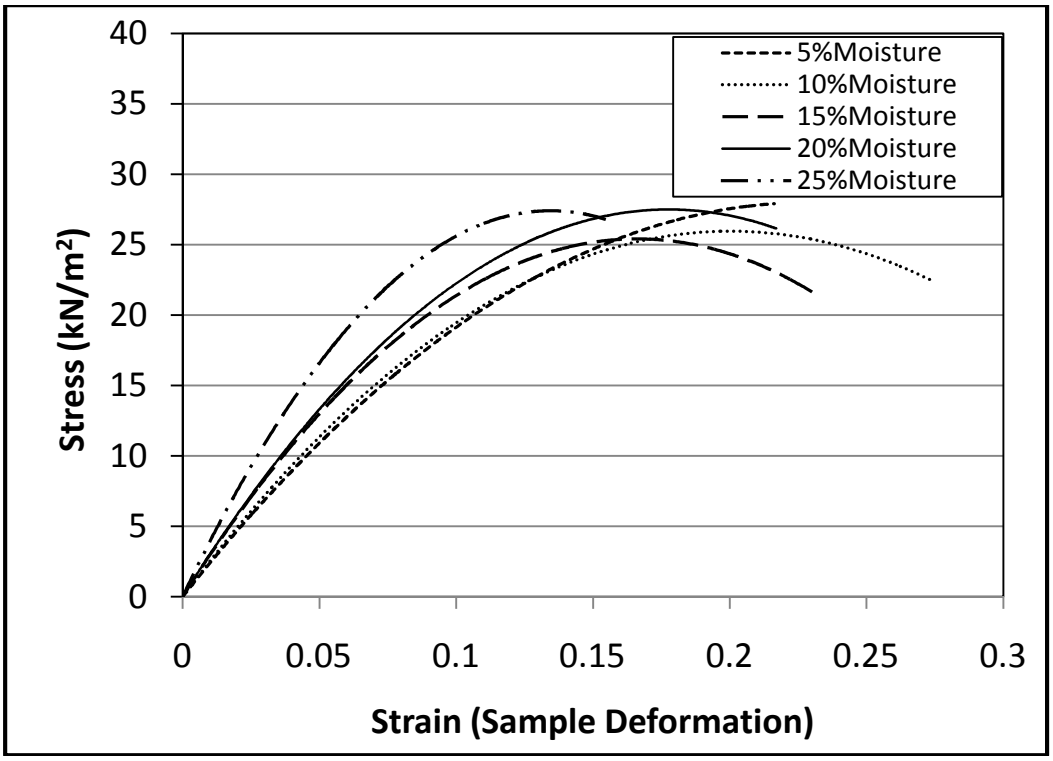

Unconfined compression result of sandy clay soil control day 5

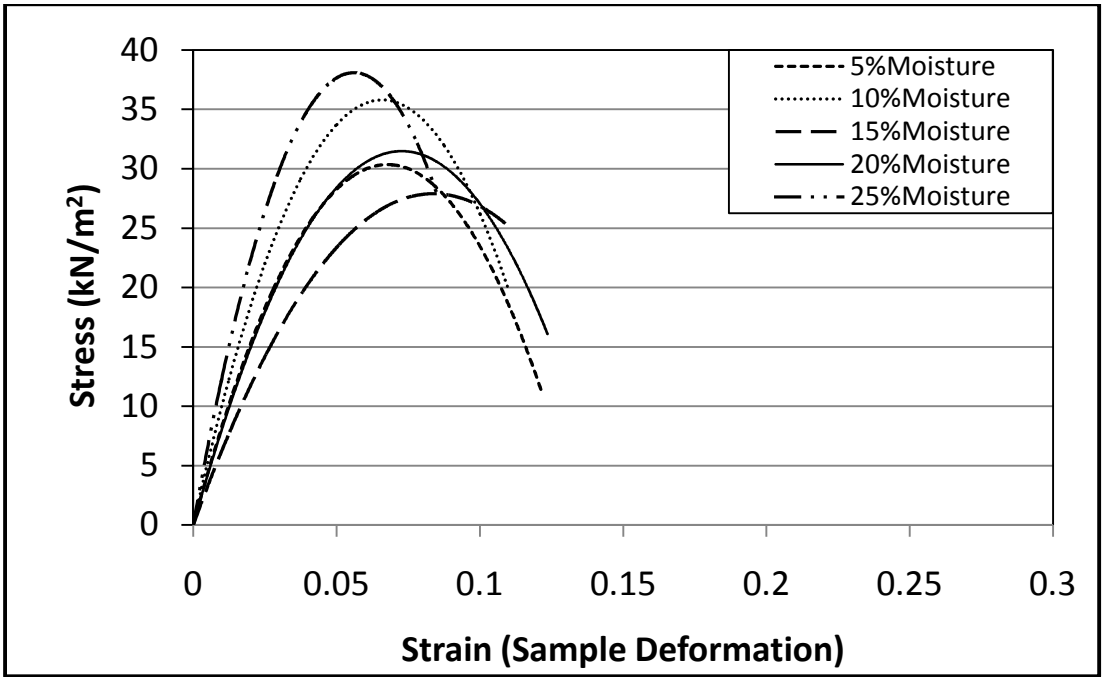

Unconfined compression result of sandy clay soil control day 11

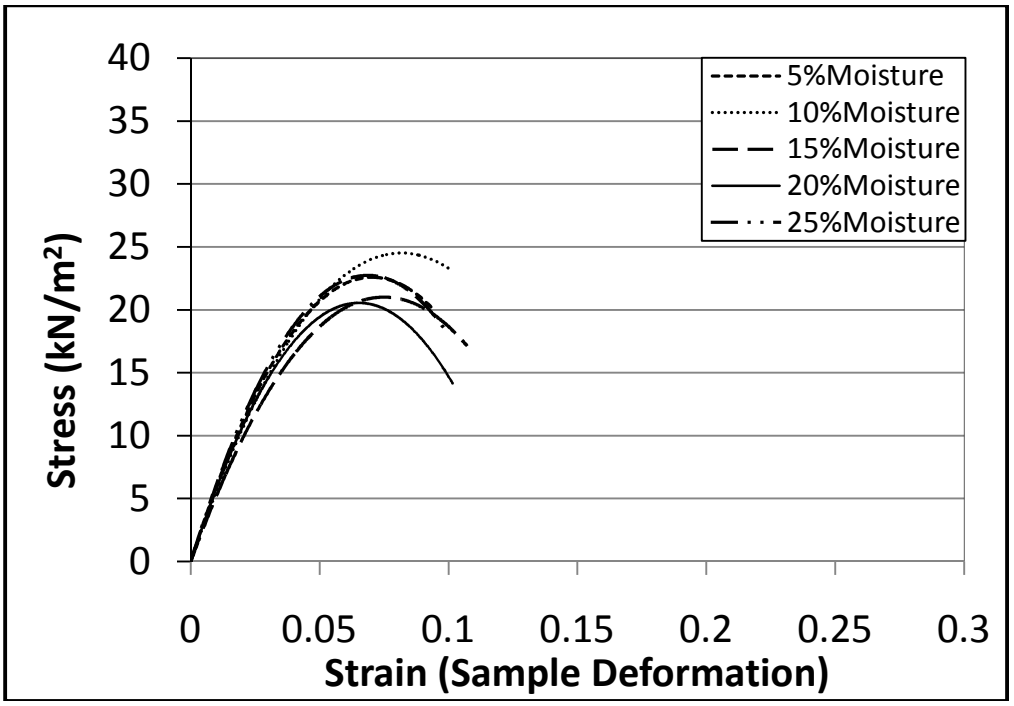

Unconfined compression result of sandy clay soil control day 12

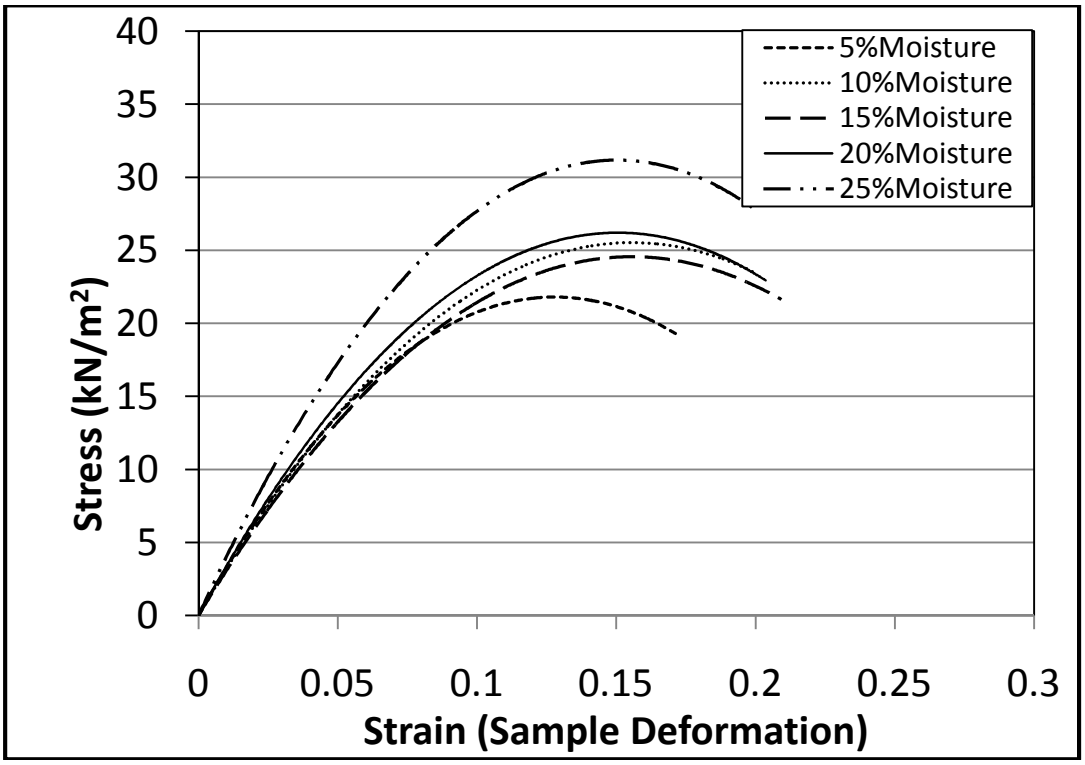

Unconfined compression result of sandy clay soil control day 13

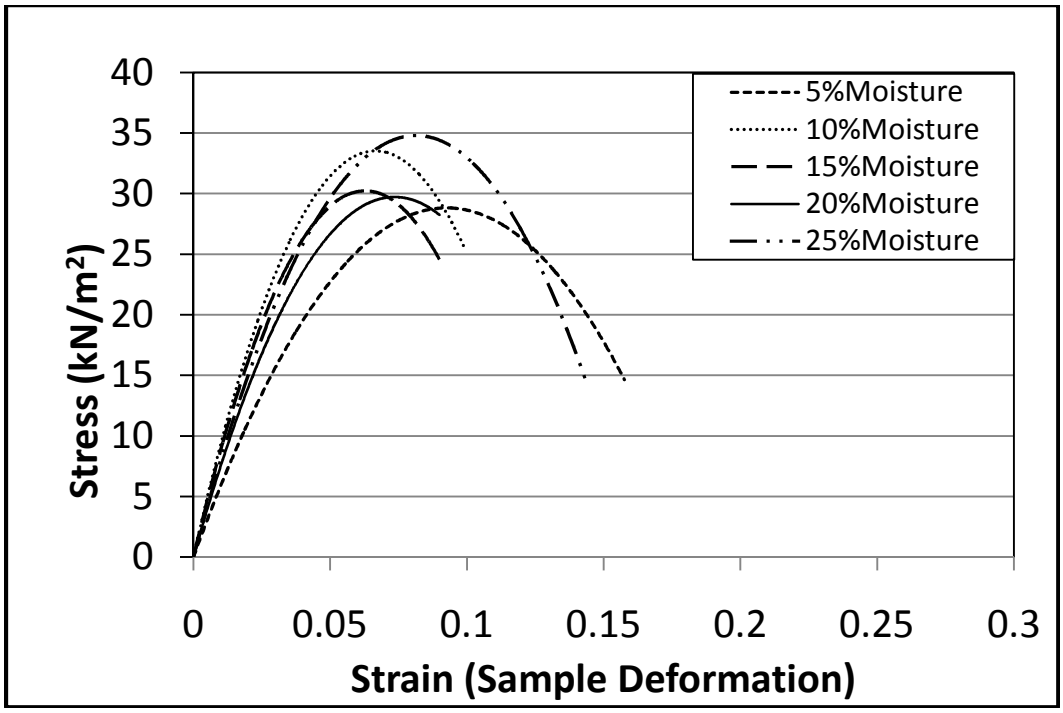

Unconfined compression result of sandy clay soil control day 14

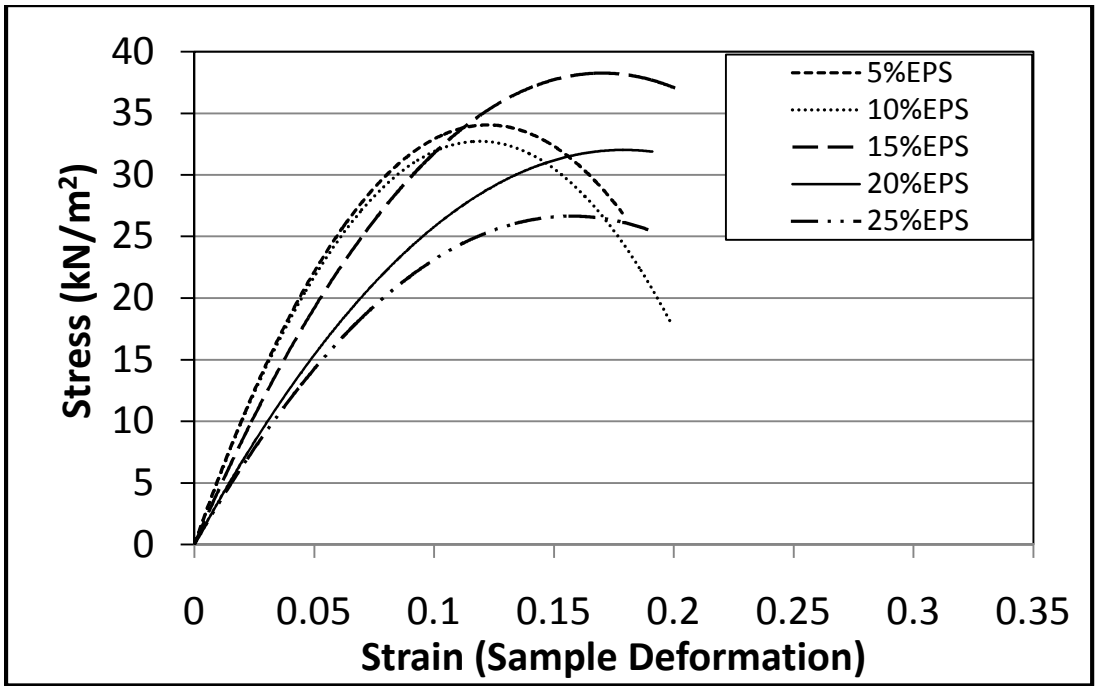

Unconfined compression result of sandy clay soil treated with EPS day 13

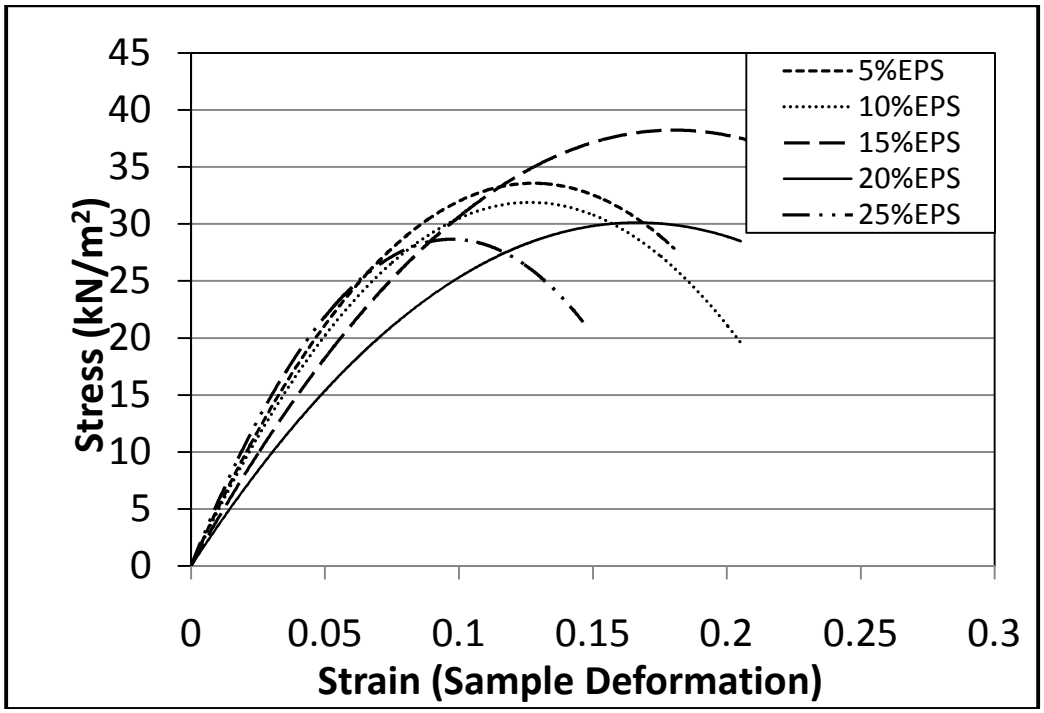

Unconfined compression result of sandy clay soil treated with EPS day 14

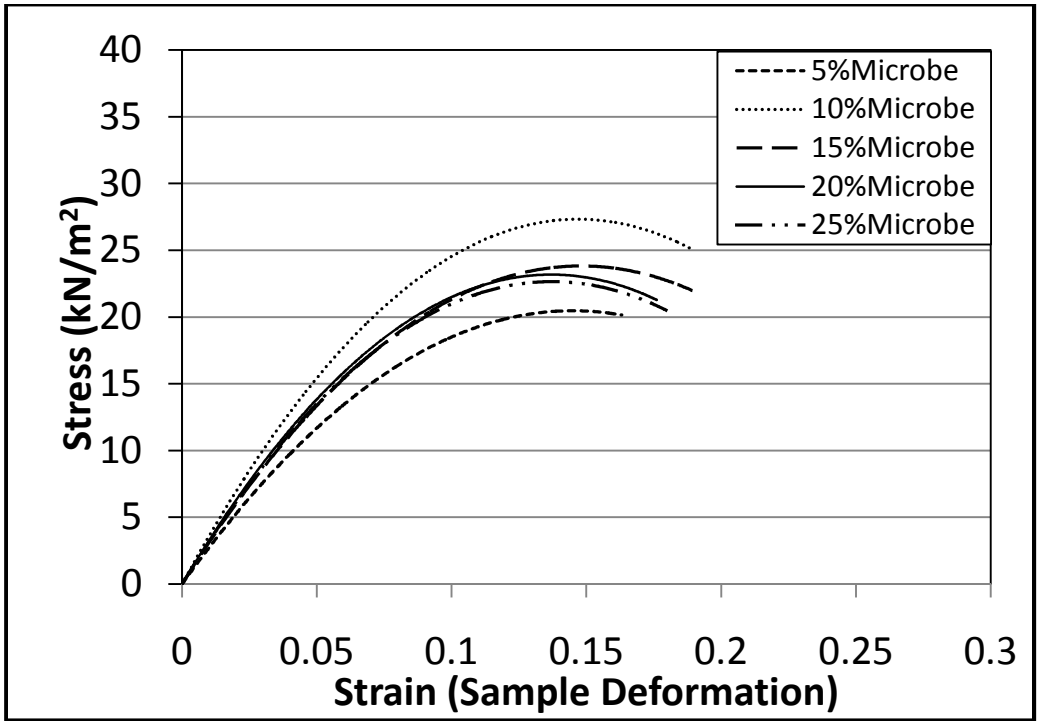

Unconfined compression result of sandy clay soil treated with microbe day 10

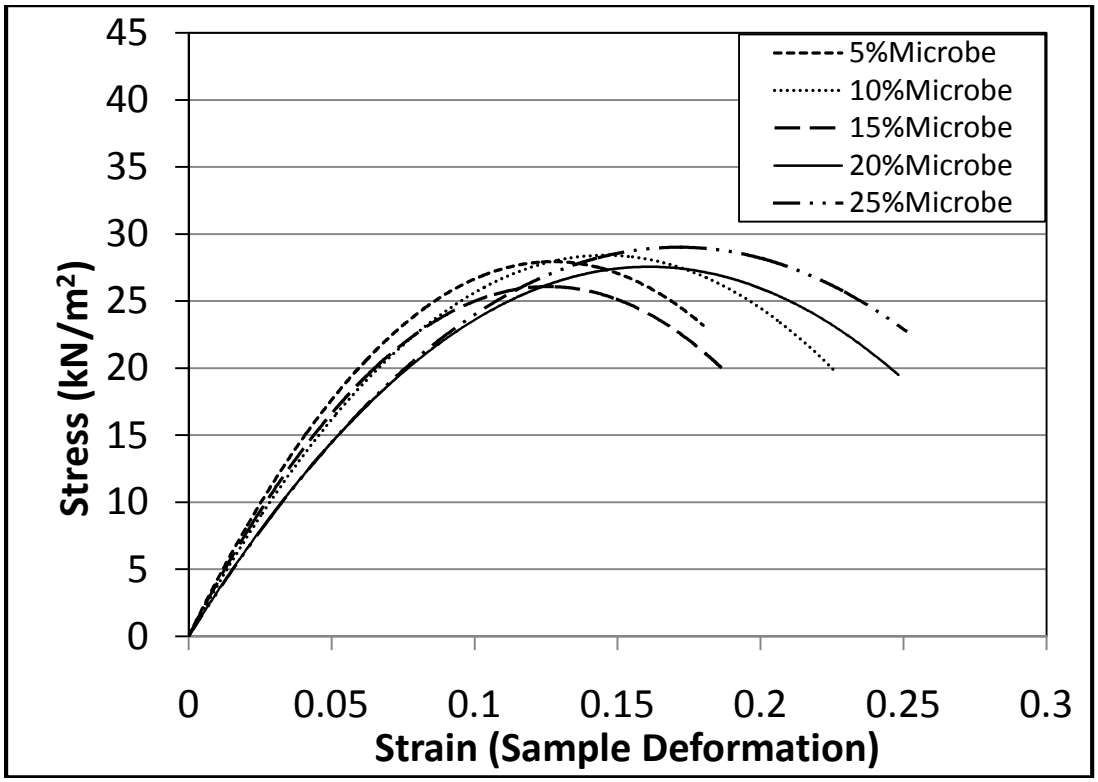

Unconfined compression result of sandy clay soil treated with microbe day 11

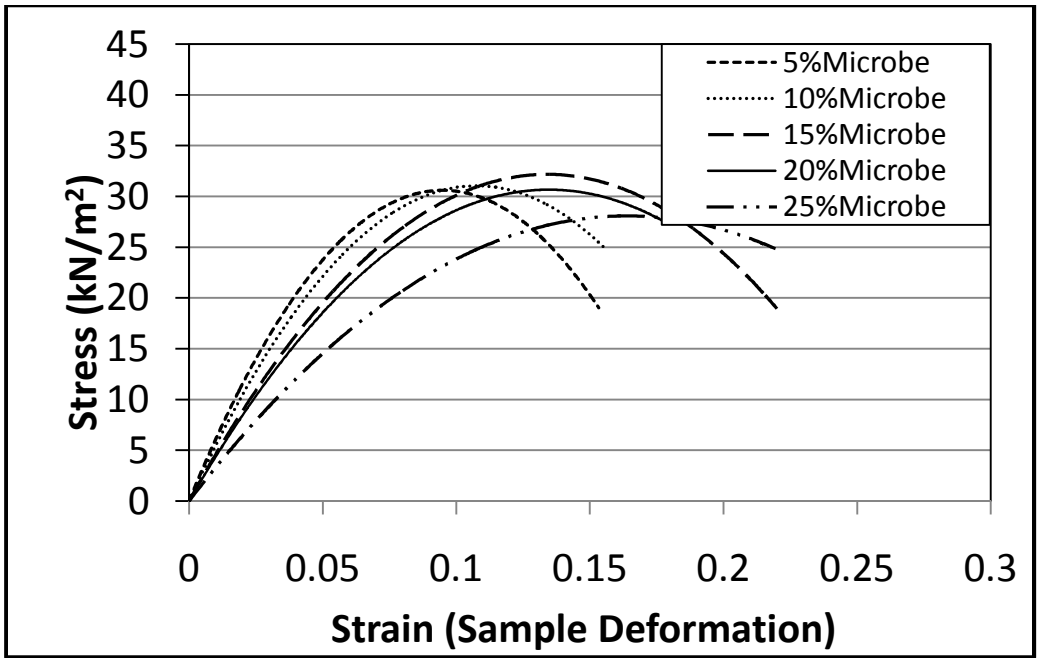

Unconfined compression result of sandy clay soil treated with microbe day 12

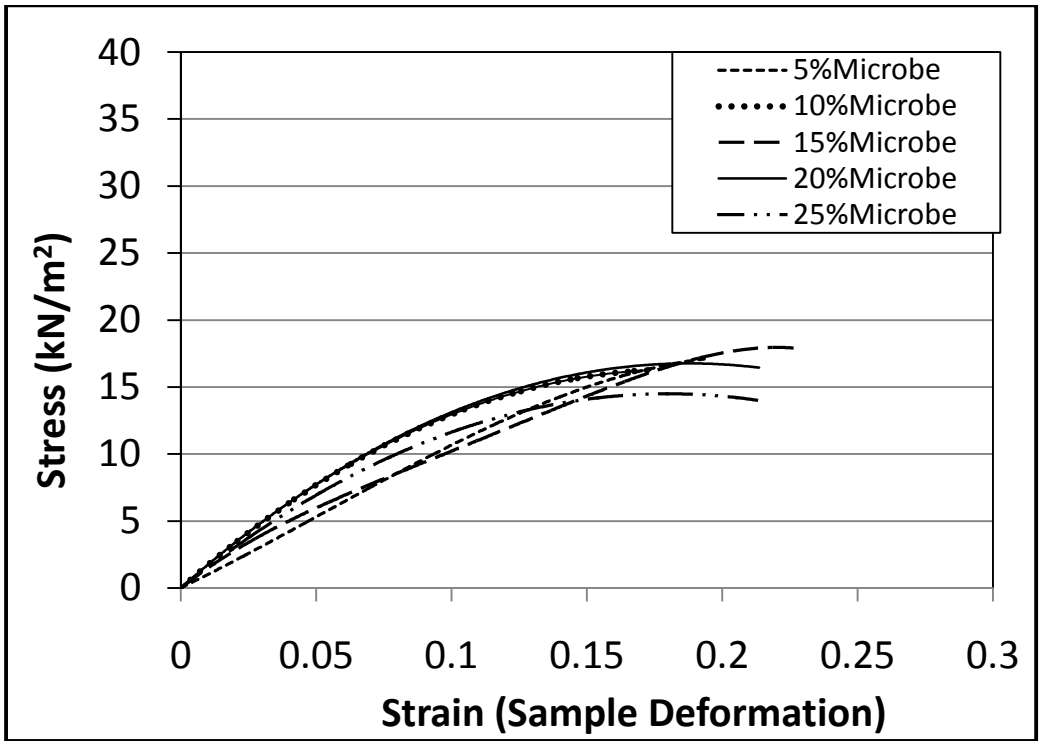

Unconfined compression result of sandy clay soil treated with microbe day 13

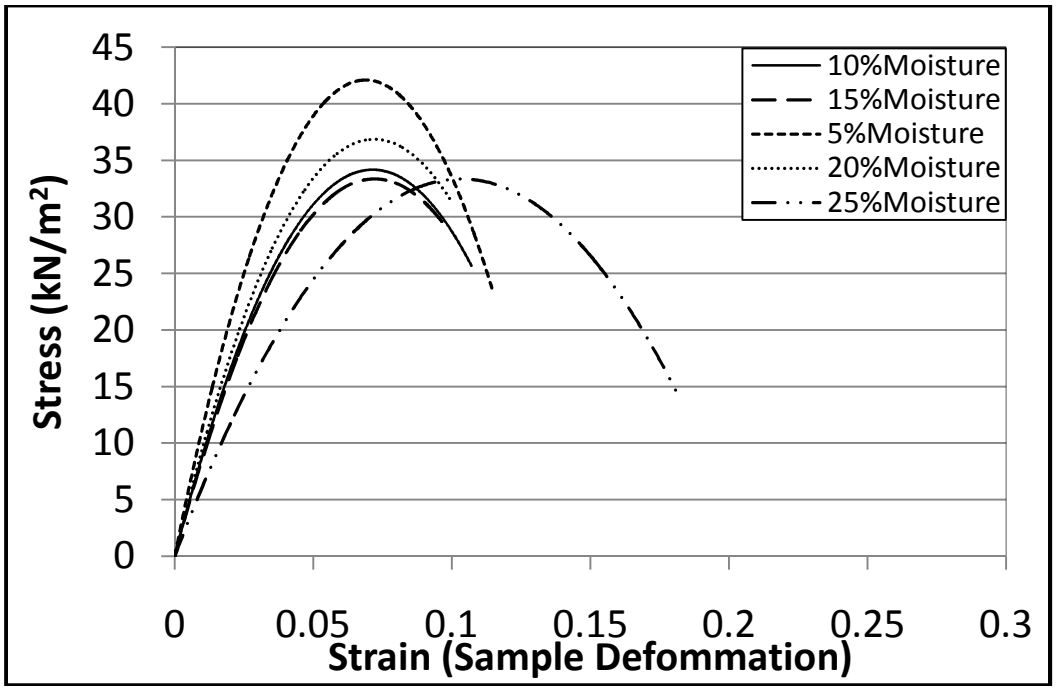

Unconfined compression result of sandy clay soil treated control samples day 6

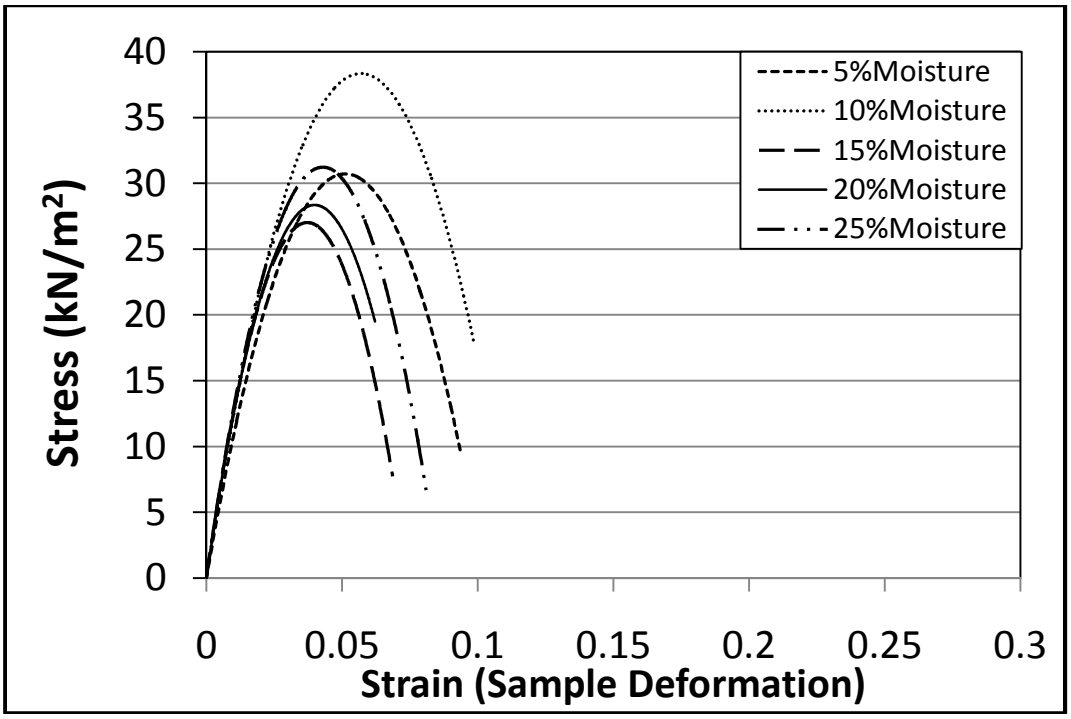

Unconfined compression result of sandy clay soil treated control samples day 7

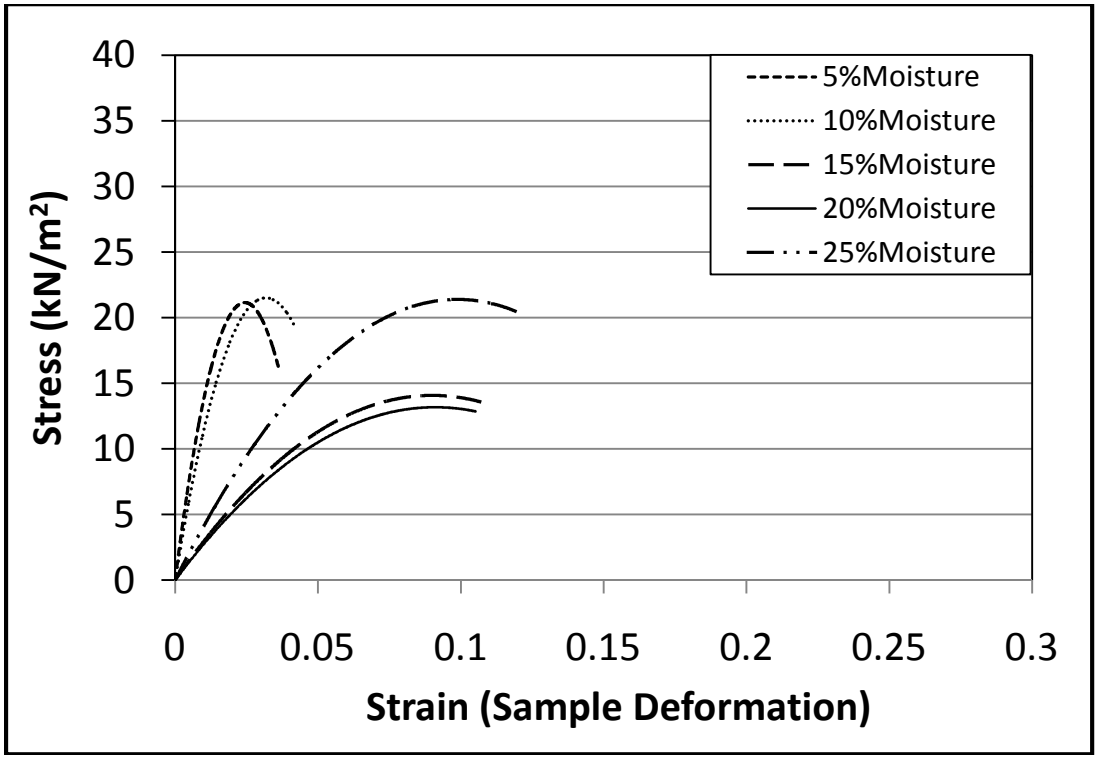

Unconfined compression result of sandy clay soil treated with microbe day 8

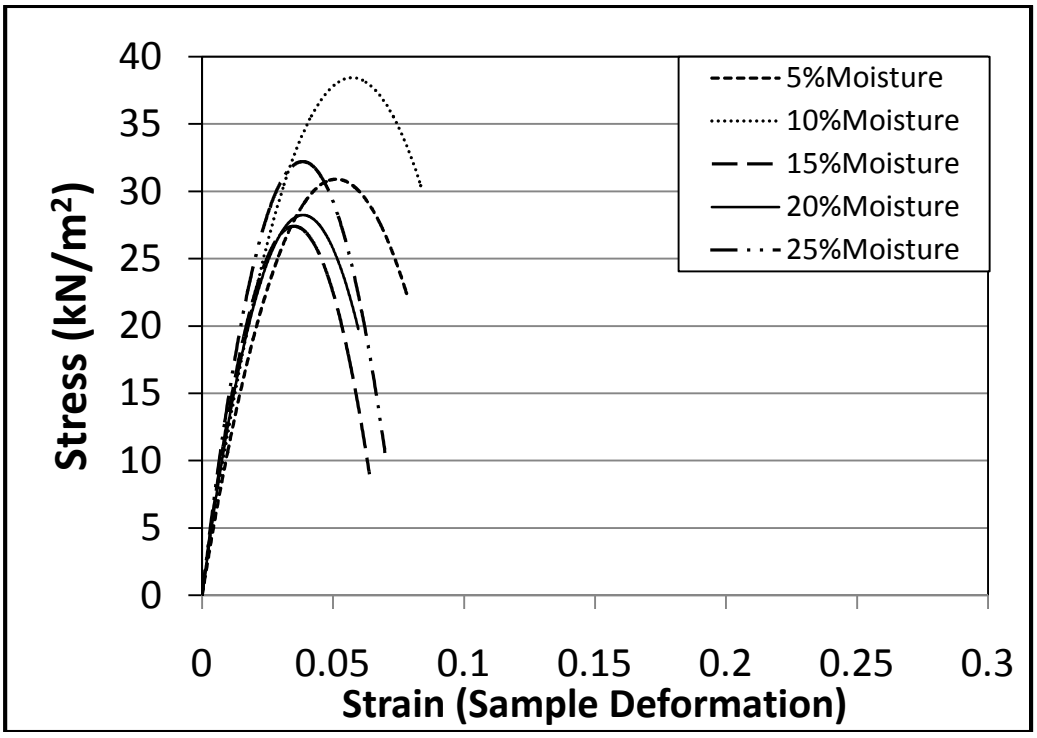

Unconfined compression result of sandy clay soil control samples day 9

APPENDIX D: GRAPHS OF UNCONFINED COMPRESSION TESTS FOR SANDY SILTY CLAY SOIL

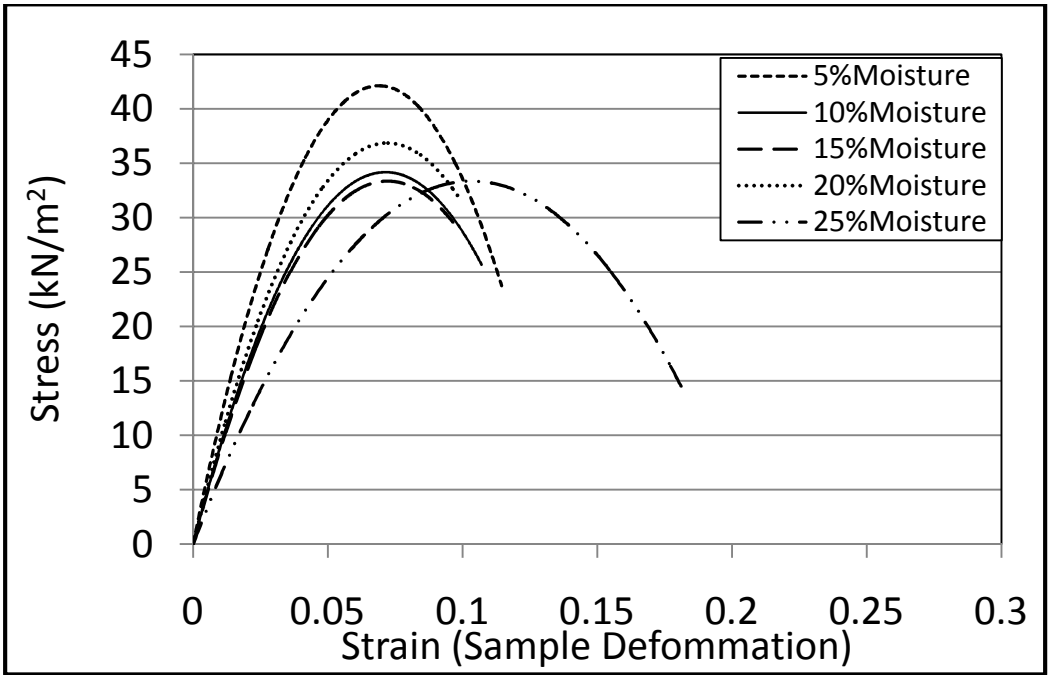

Unconfined compression result of Sandy silty clay soil control day 12

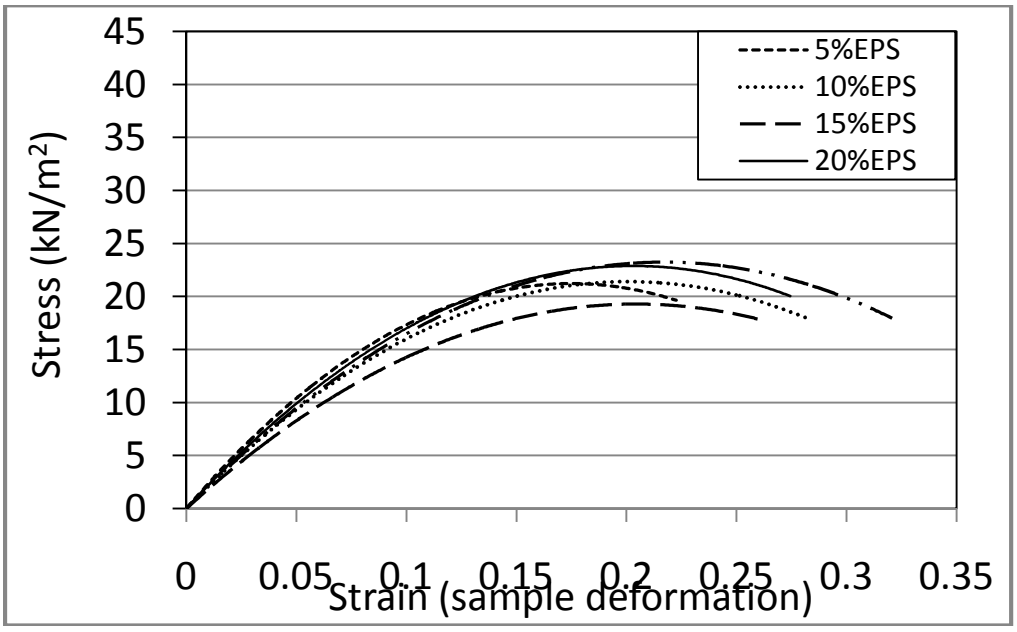

Unconfined compression result of Sandy silty clay soil treated with EPS at day 6

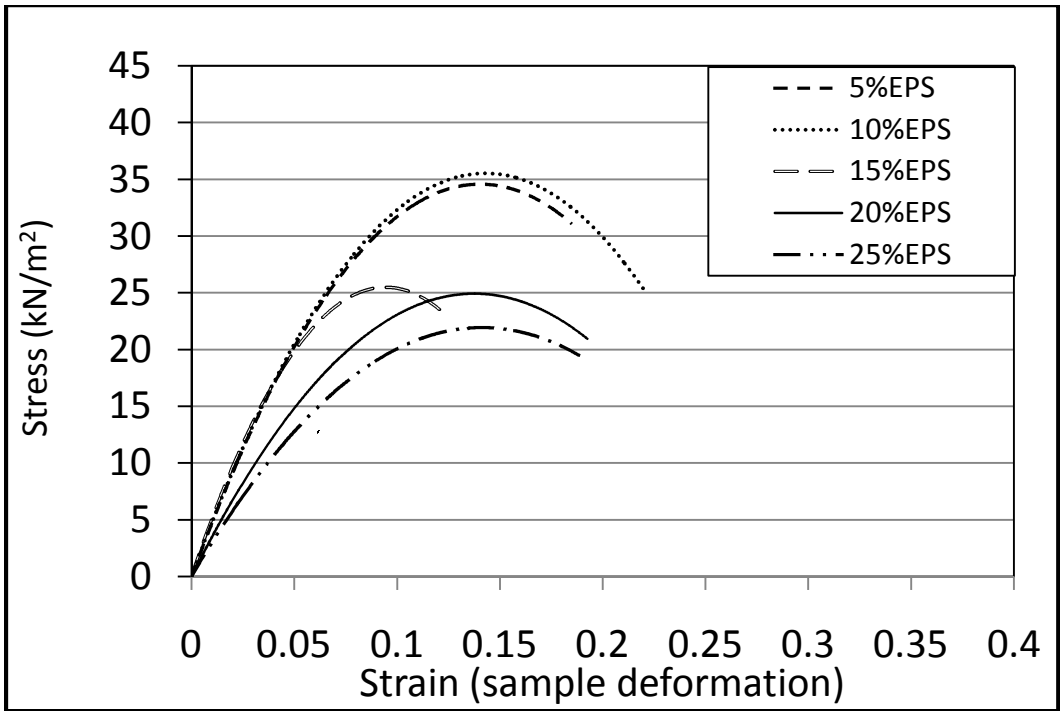

Unconfined compression result of Sandy silty clay soil treated with EPS at day 1

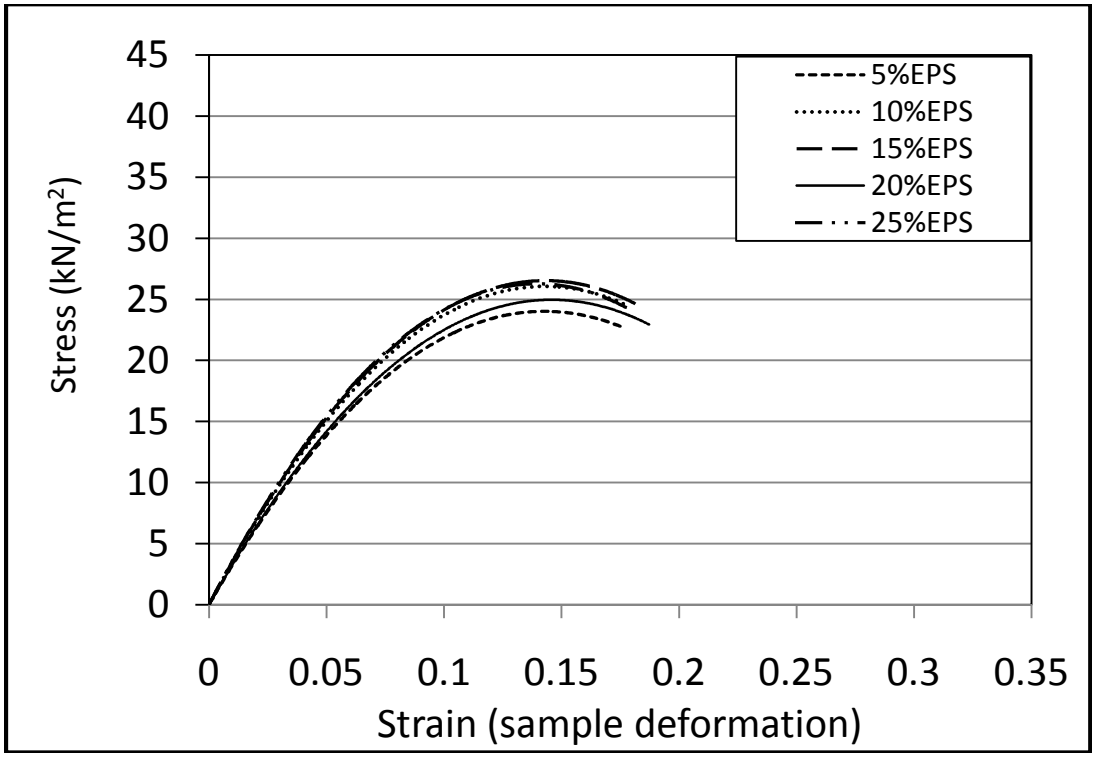

Unconfined compression result of Sandy silty clay soil treated with EPS at day 4

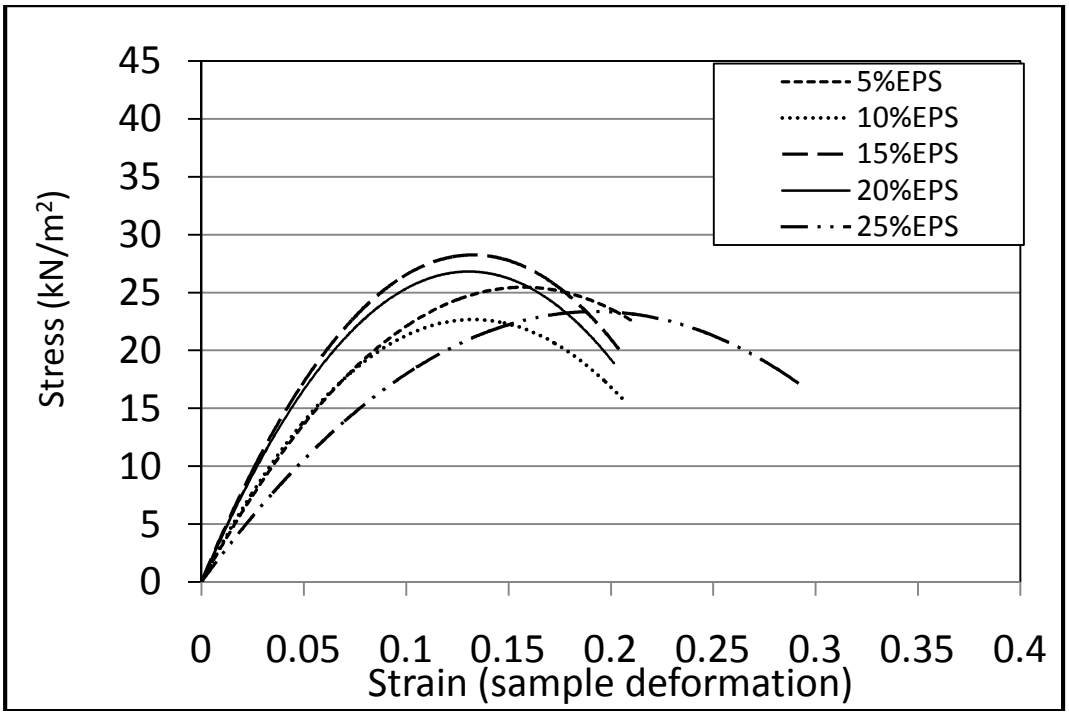

Unconfined compression result of Sandy silty clay soil treated with EPS at day 5

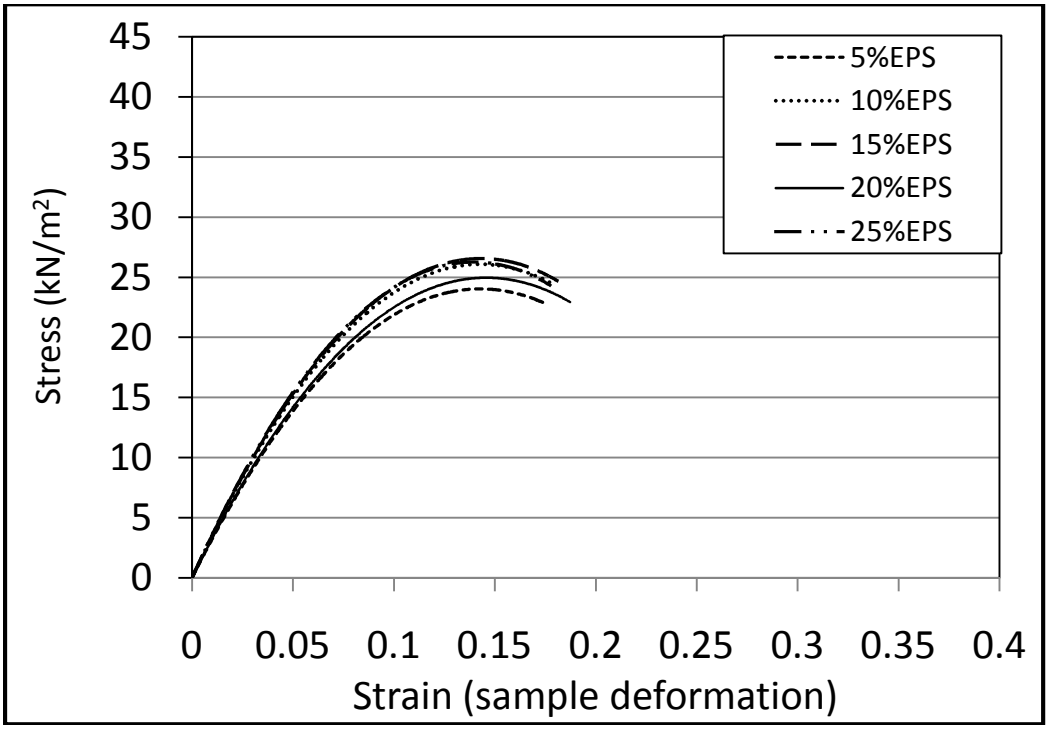

Unconfined compression result of Sandy silty clay soil treated with EPS at day 7

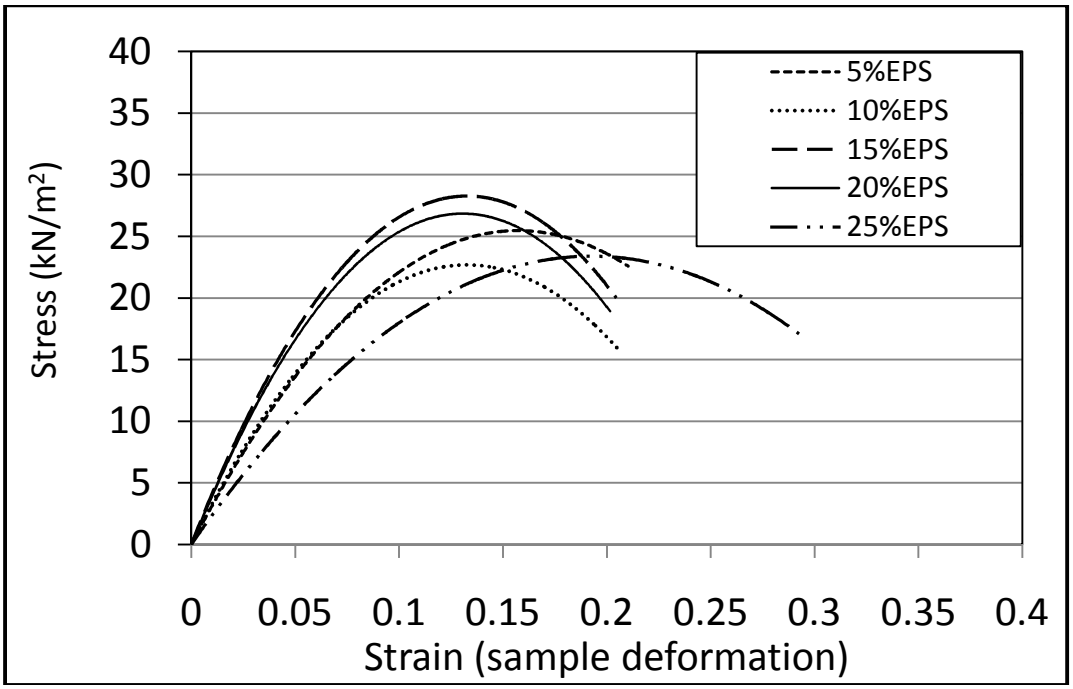

Unconfined compression result of Sandy silty clay soil treated with EPS at day 8

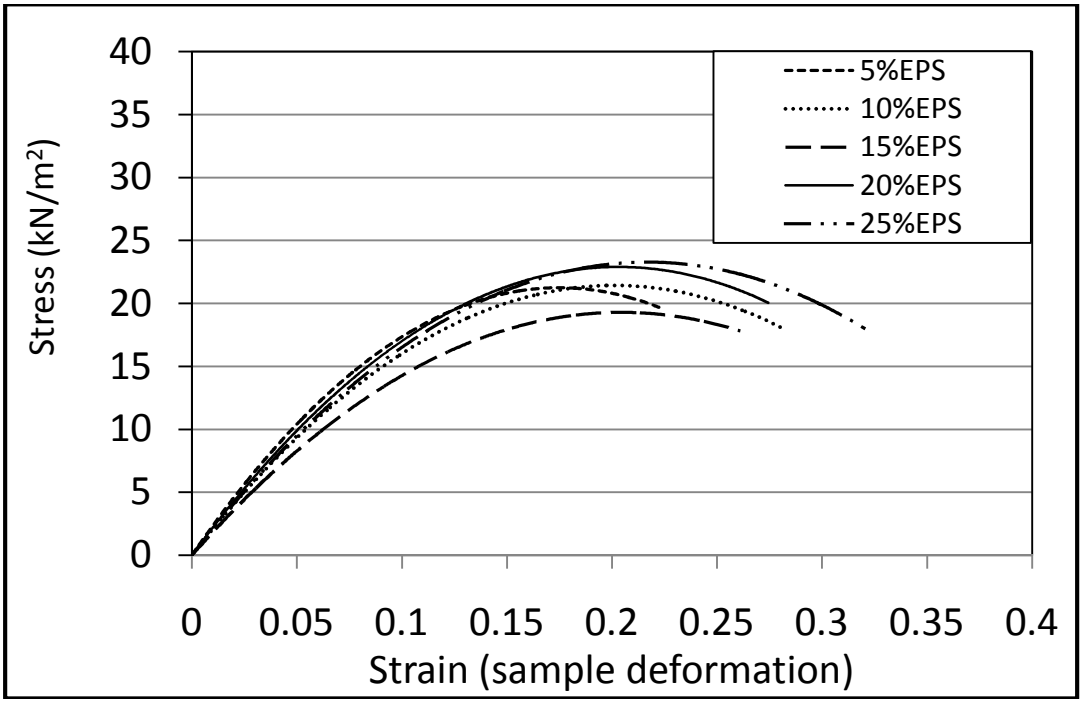

Unconfined compression result of Sandy silty clay soil treated with EPS at day 9

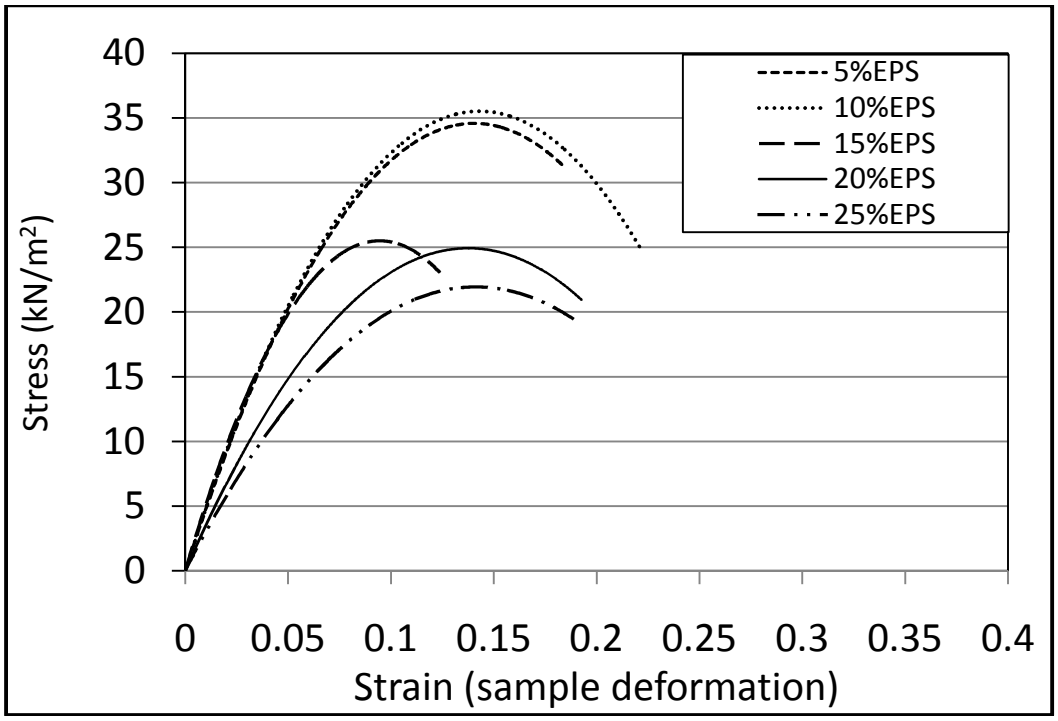

Unconfined compression result of Sandy silty clay soil treated with EPS at day 10

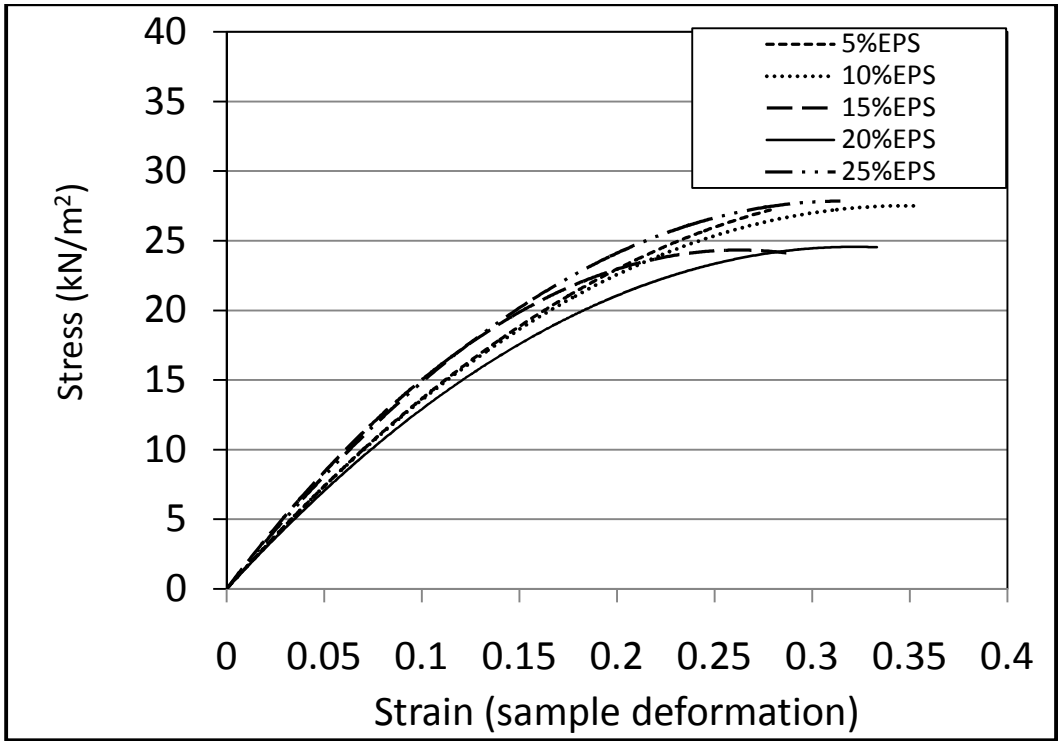

Unconfined compression result of Sandy silty clay soil treated with EPS at day 11

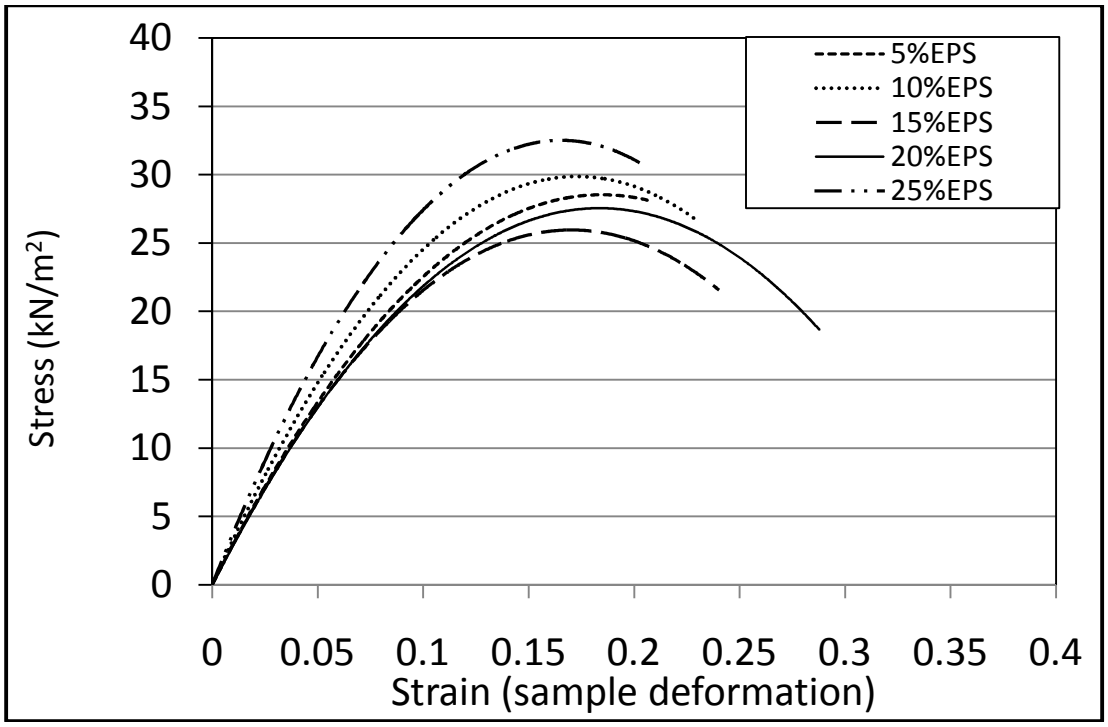

Unconfined compression result of Sandy silty clay soil treated with EPS at day 12

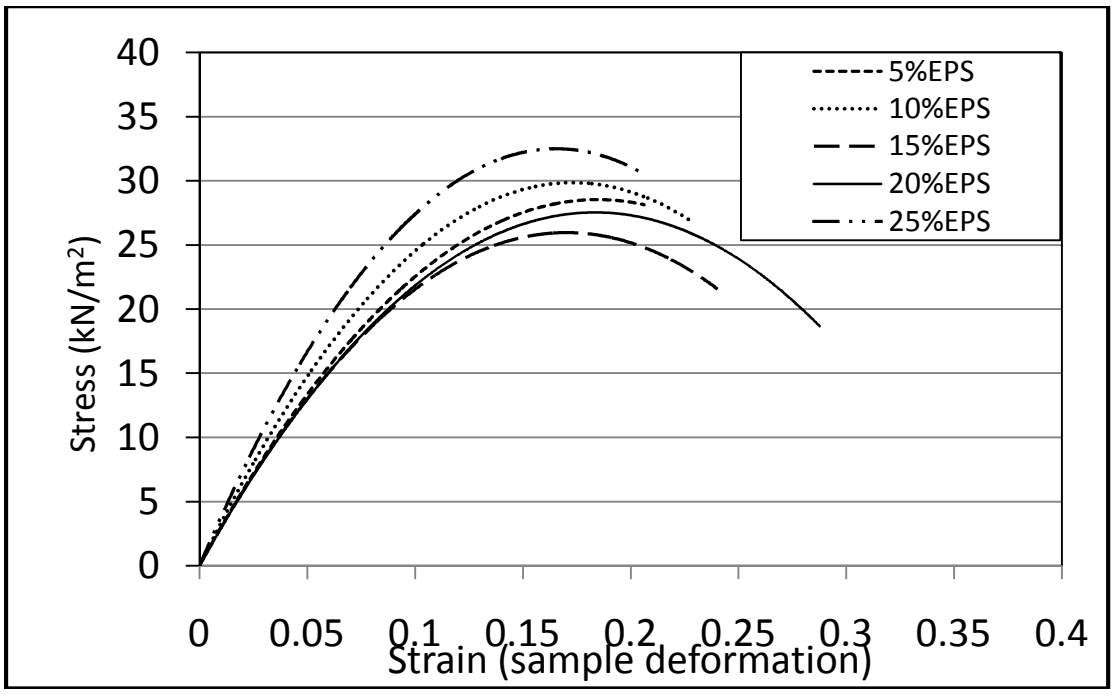

Unconfined compression result of Sandy silty clay soil treated with EPS at day 3

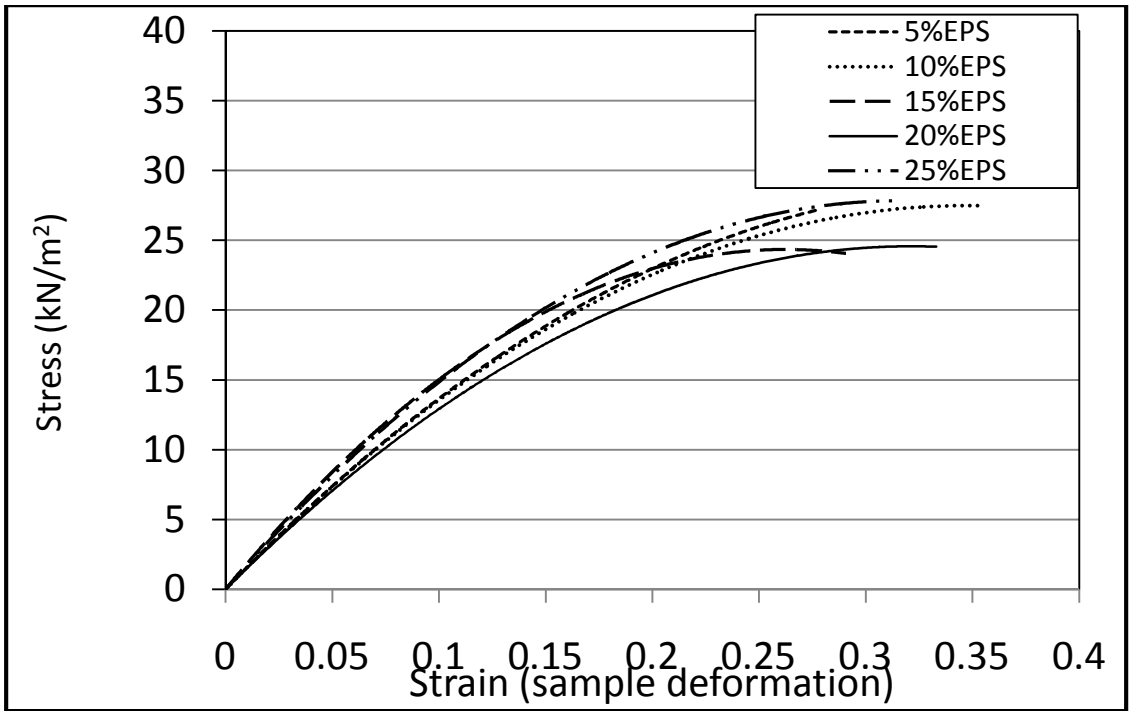

Unconfined compression result of Sandy silty clay soil treated with EPS at day 2

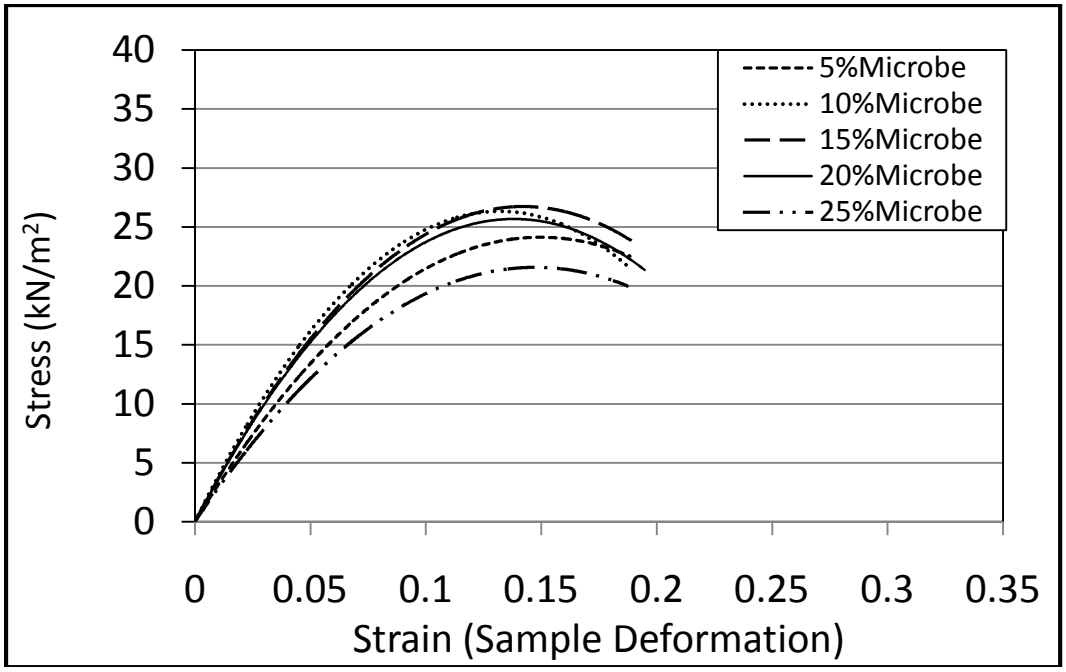

Unconfined compression result of Sandy silty clay soil treated with microbe at day 1

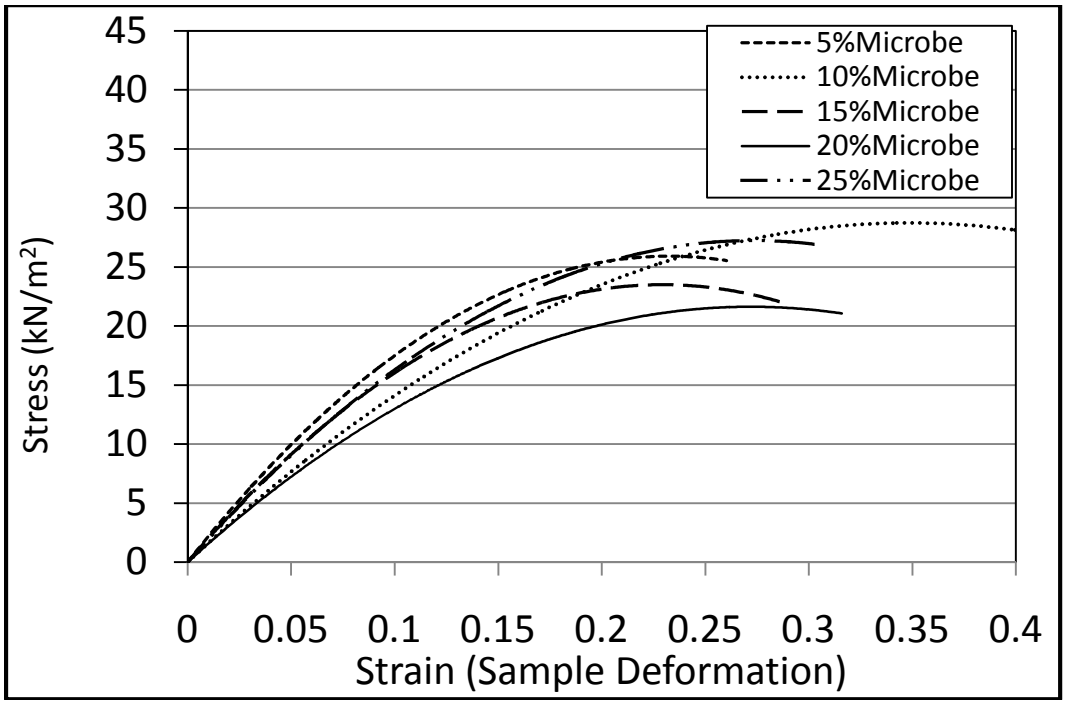

Unconfined compression result of Sandy silty clay soil treated with microbe at day 2

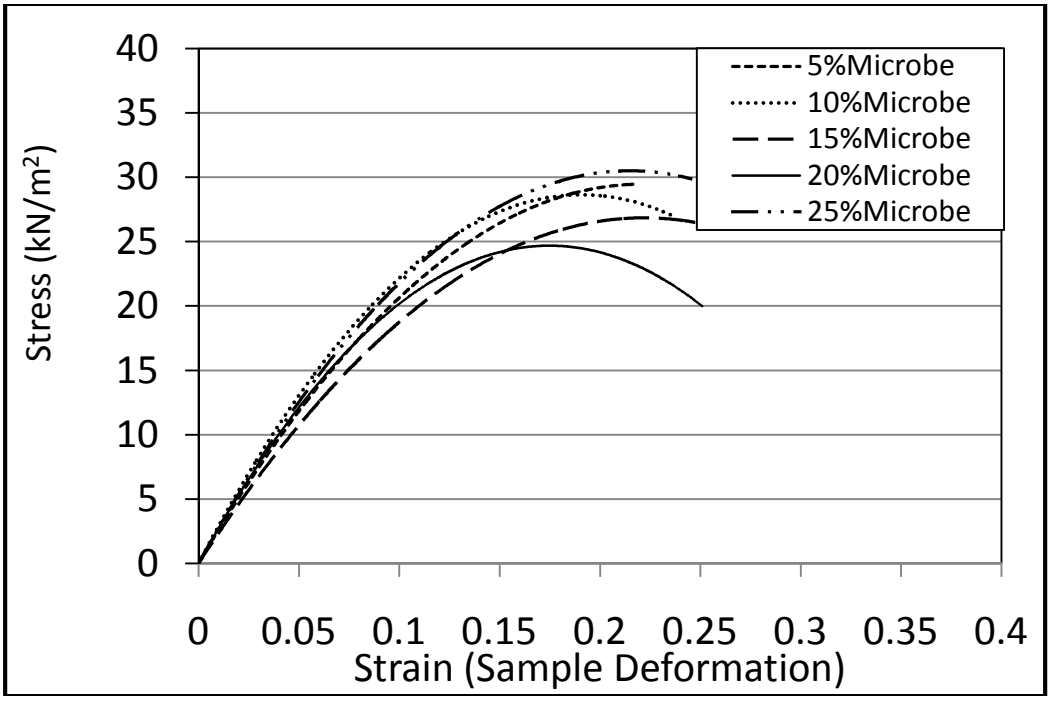

Unconfined compression result of Sandy silty clay soil treated with microbe at day 3

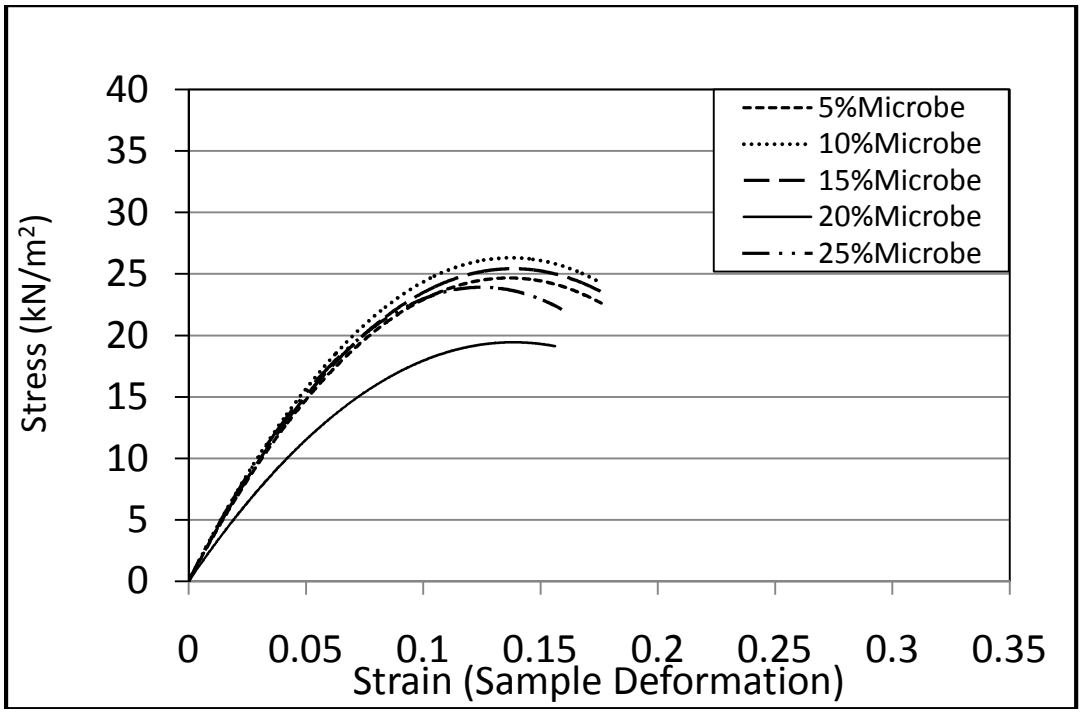

Unconfined compression result of Sandy silty clay soil treated with microbe at day 4

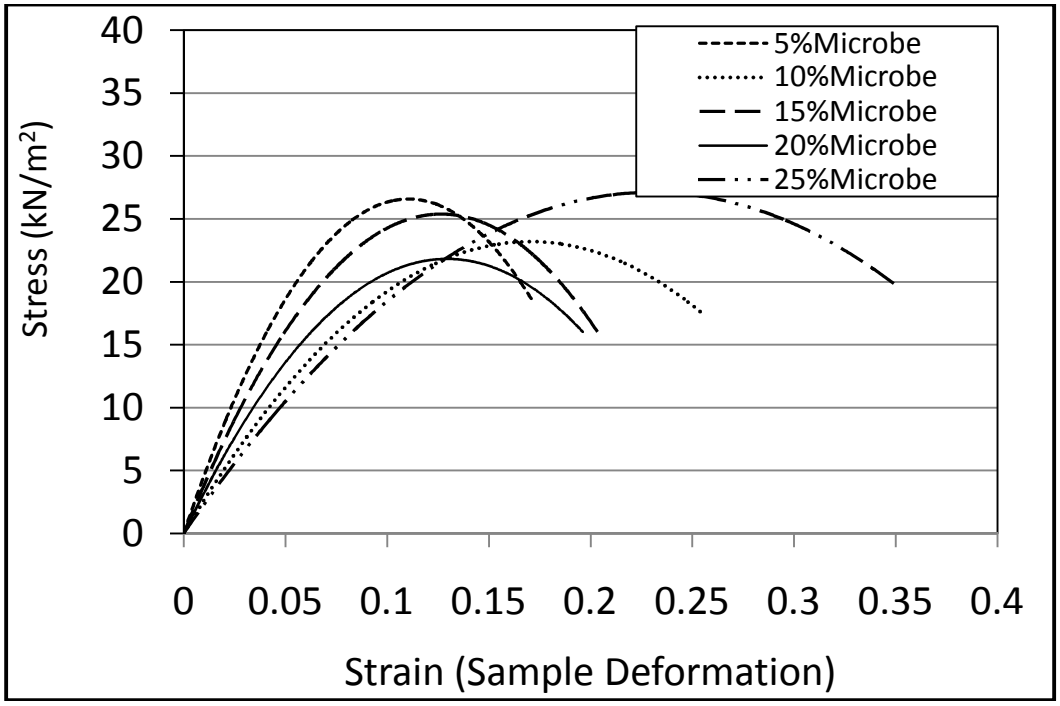

Unconfined compression result of Sandy silty clay soil treated with microbe at day 5

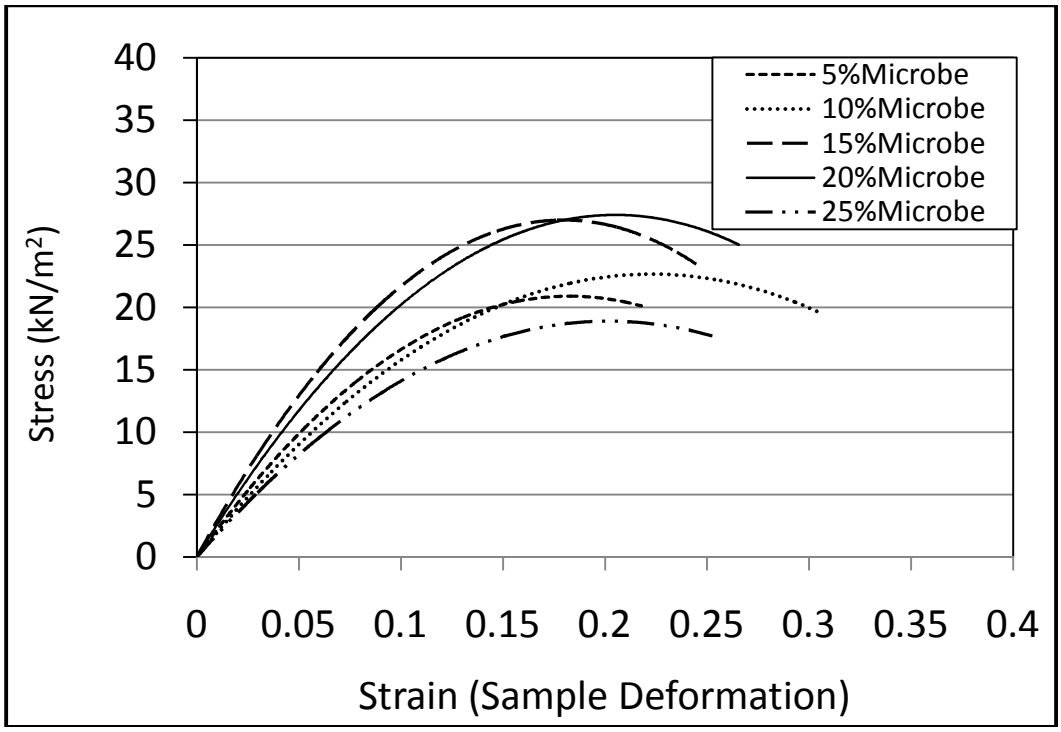

Unconfined compression result of Sandy silty clay soil treated with microbe at day 6

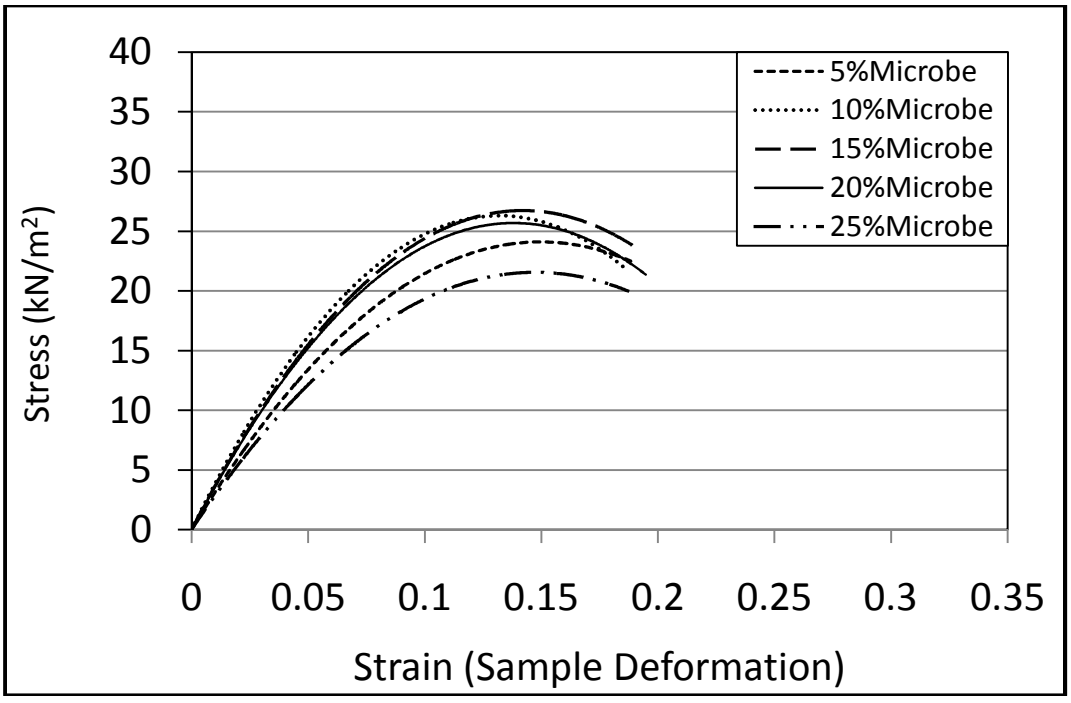

Unconfined compression result of Sandy silty clay soil treated with microbe at day 7

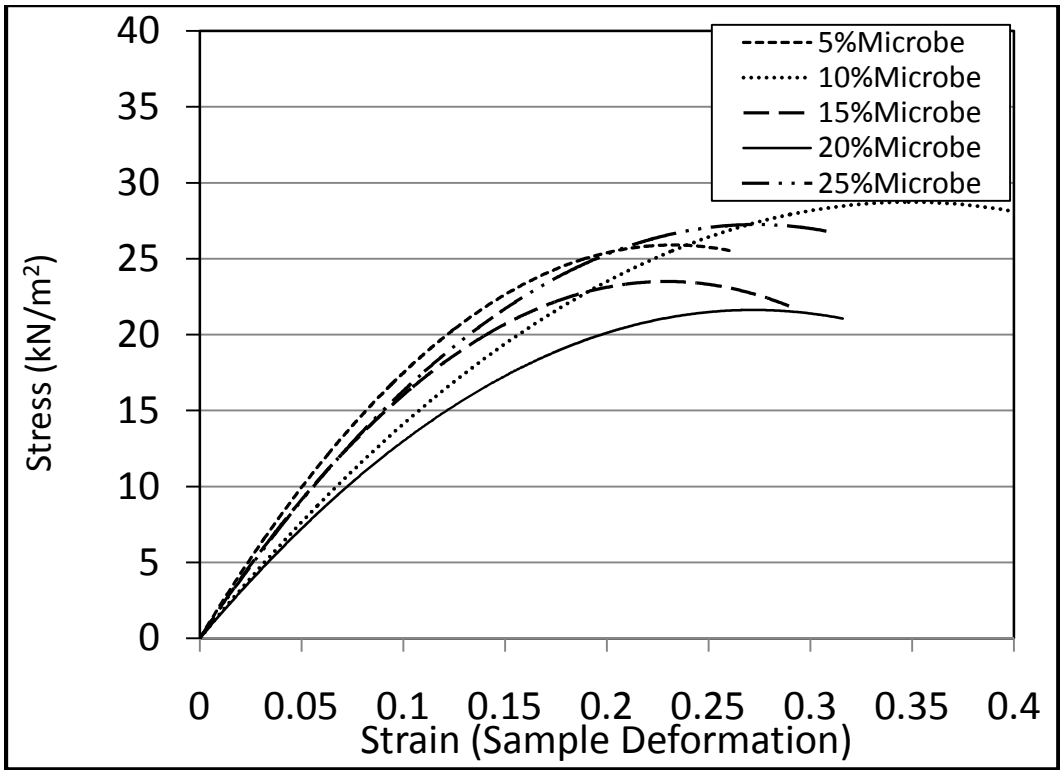

Unconfined compression result of Sandy silty clay soil treated with microbe at day 8

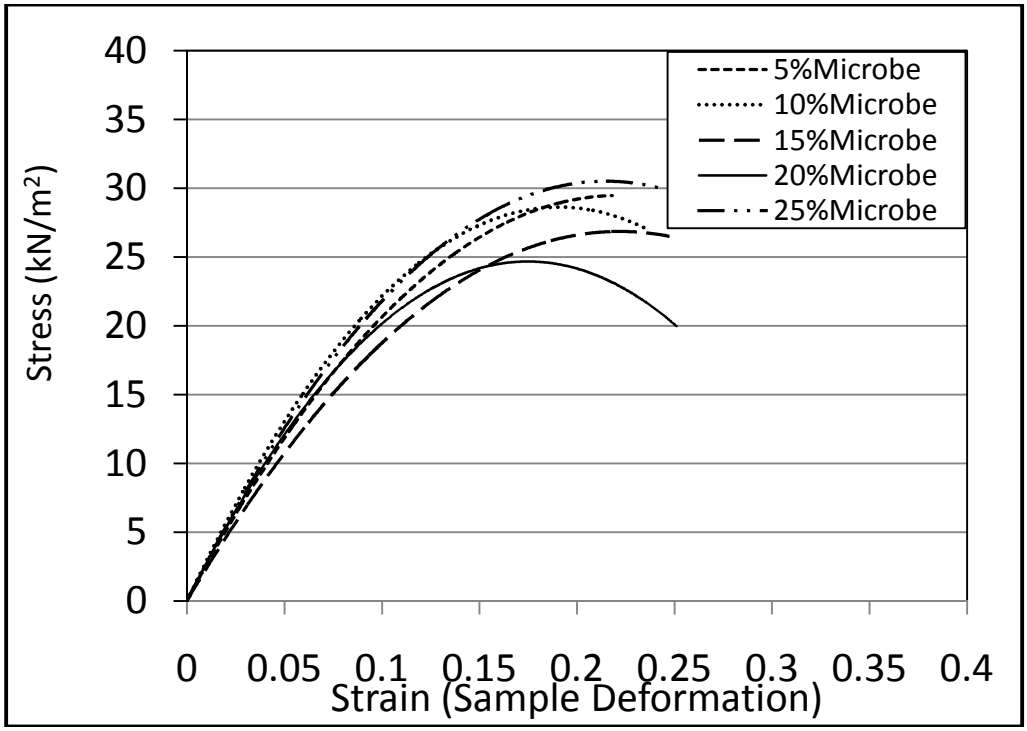

Unconfined compression result of Sandy silty clay soil treated with microbe at day 9

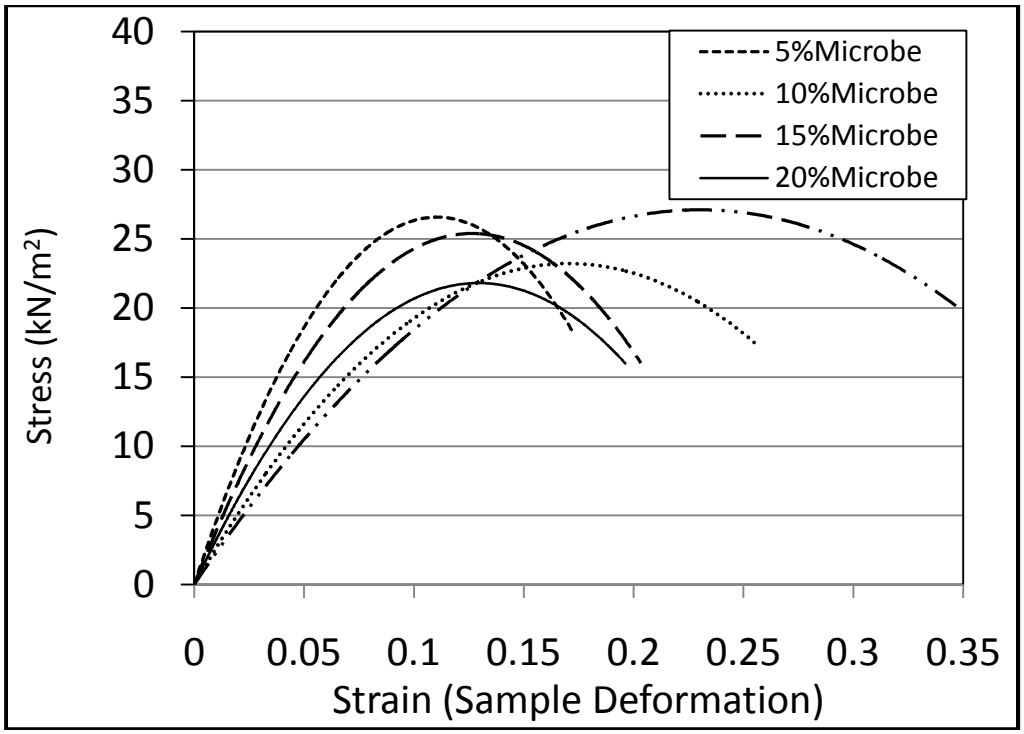

Unconfined compression result of Sandy silty clay soil treated with microbe at day 13

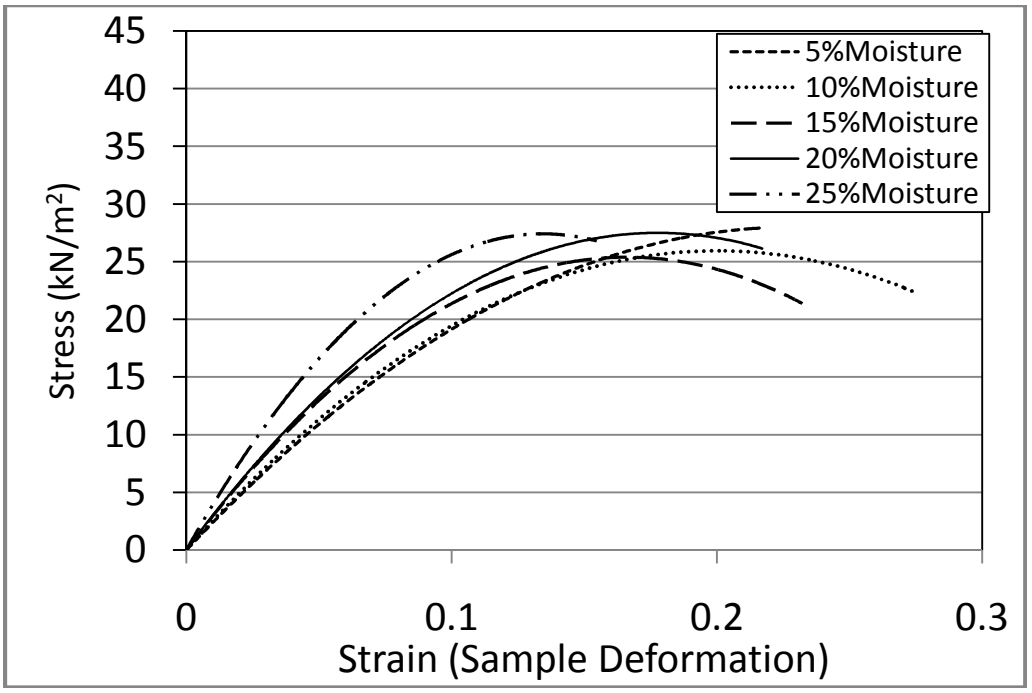

Unconfined compression result of Sandy silty clay soil treated with microbe at day 14

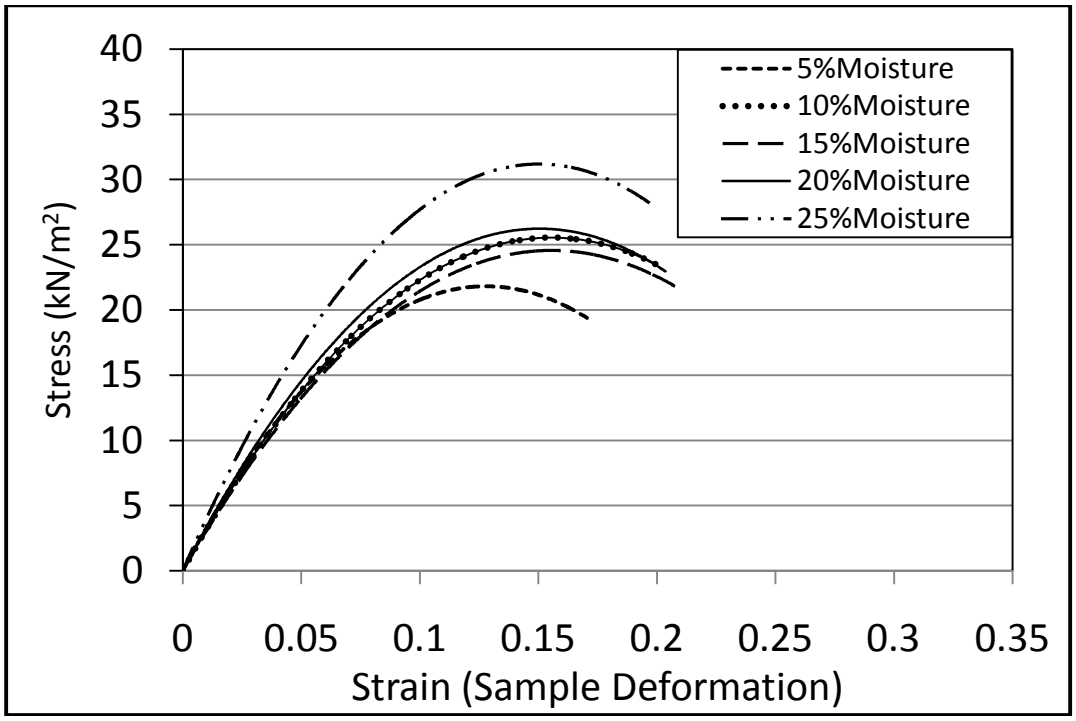

Unconfined compression result of Sandy silty clay soil treated control at day 1

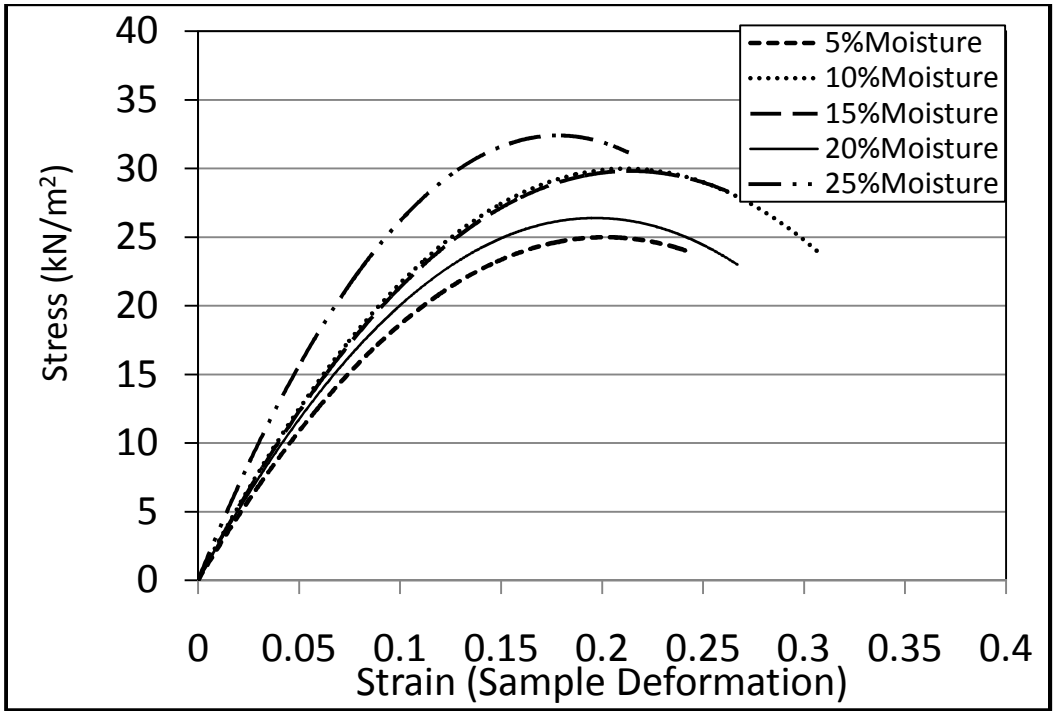

Unconfined compression result of Sandy silty clay soil treated control at day 2

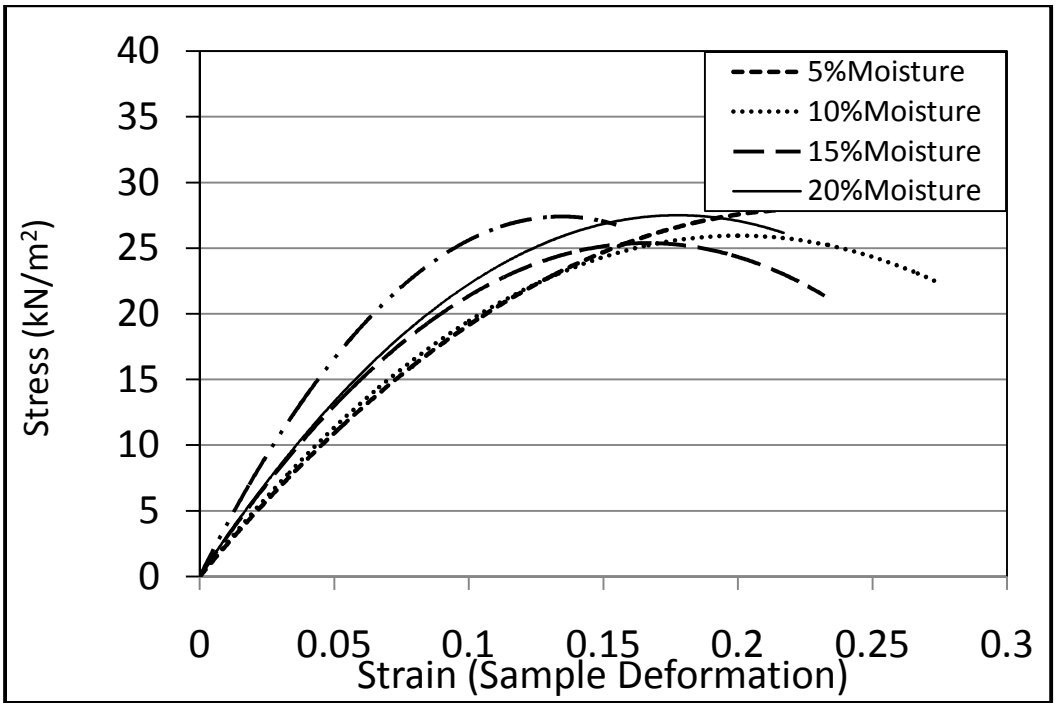

Unconfined compression result of Sandy silty clay soil treated control at day 3

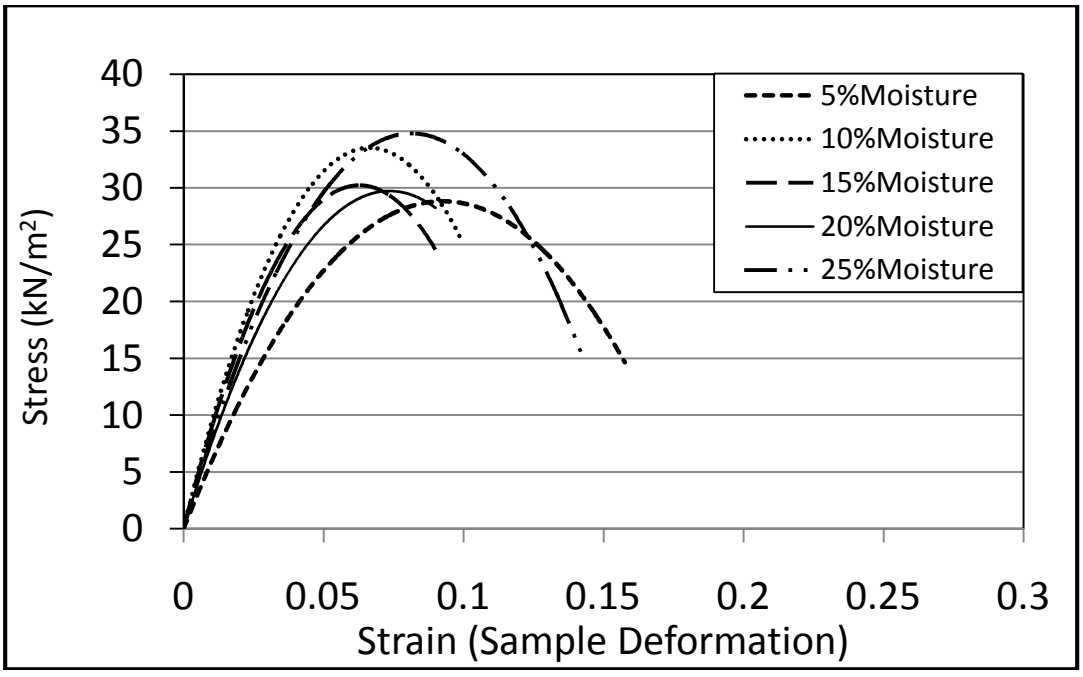

Unconfined compression result of Sandy silty clay soil treated control at day 4

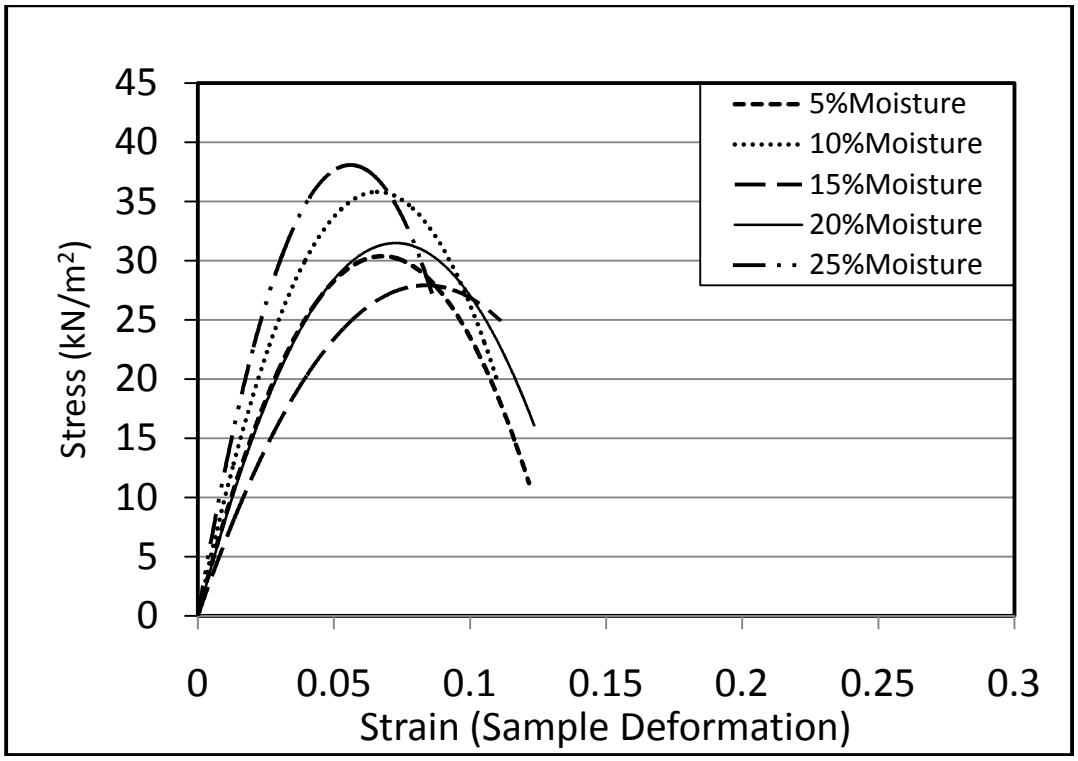

Unconfined compression result of Sandy silty clay soil treated control at day 5

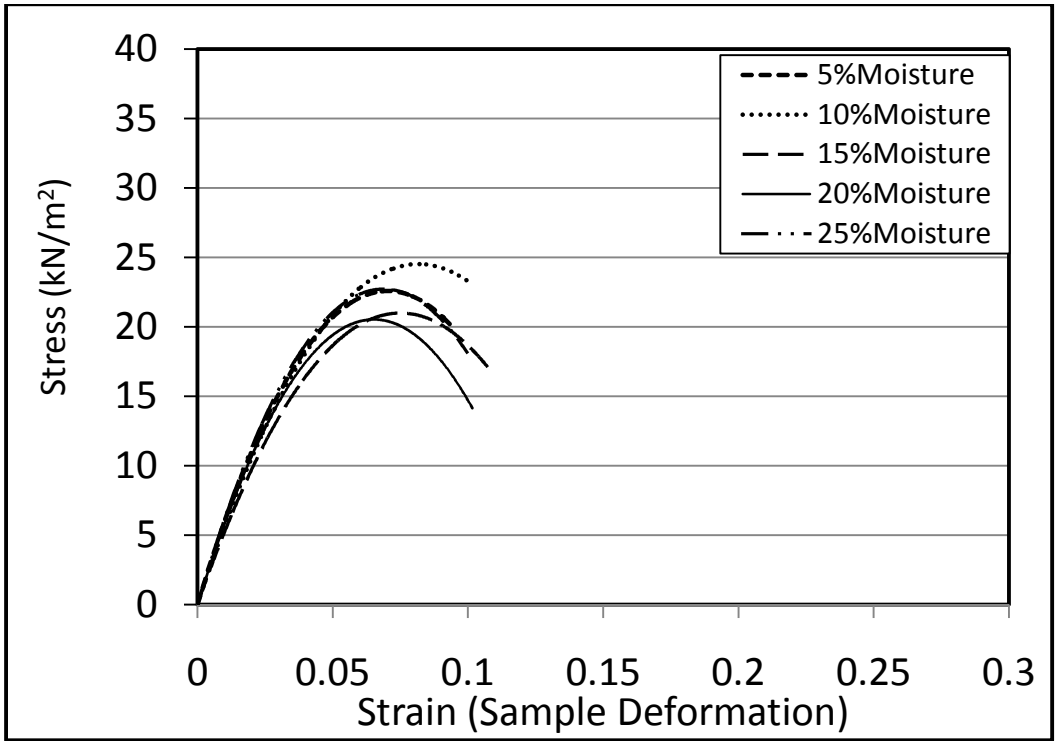

Unconfined compression result of Sandy silty clay soil treated control at day 6

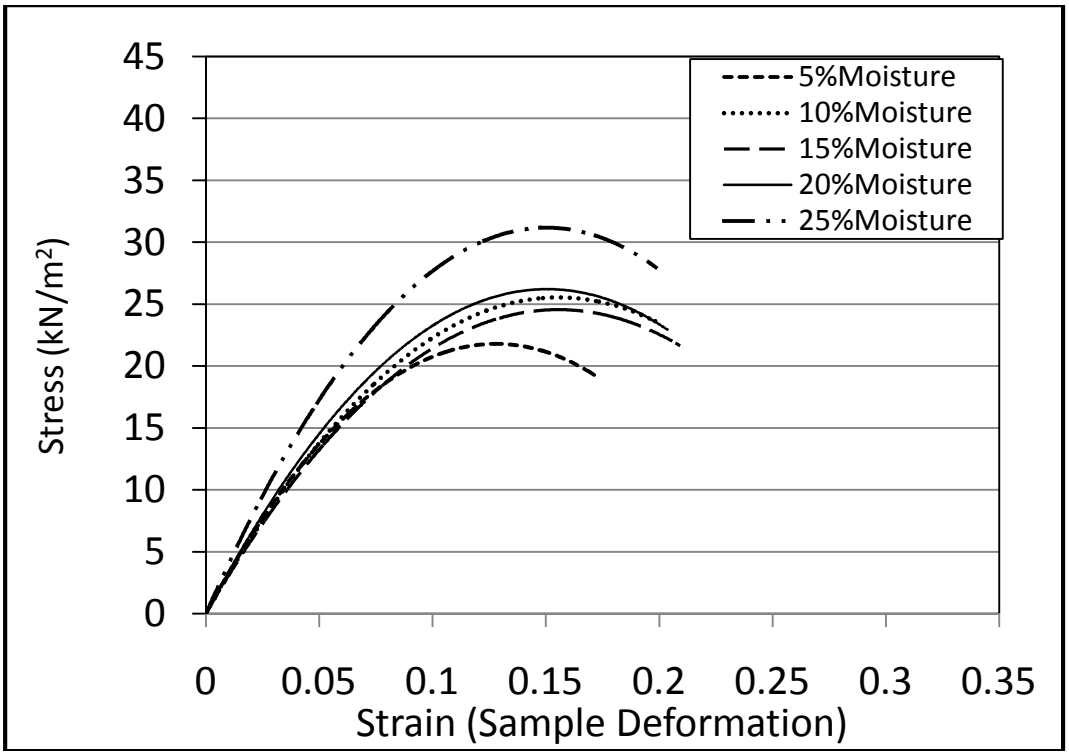

Unconfined compression result of Sandy silty clay soil treated control at day 7

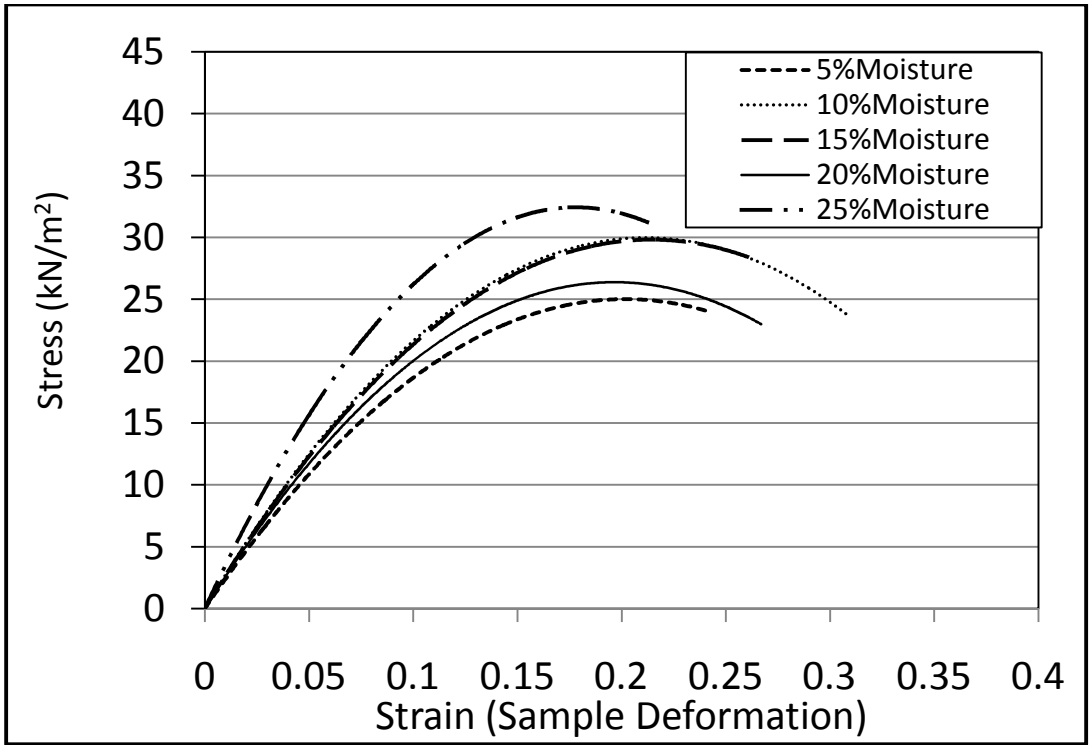

Unconfined compression result of Sandy silty clay soil treated control at day 8

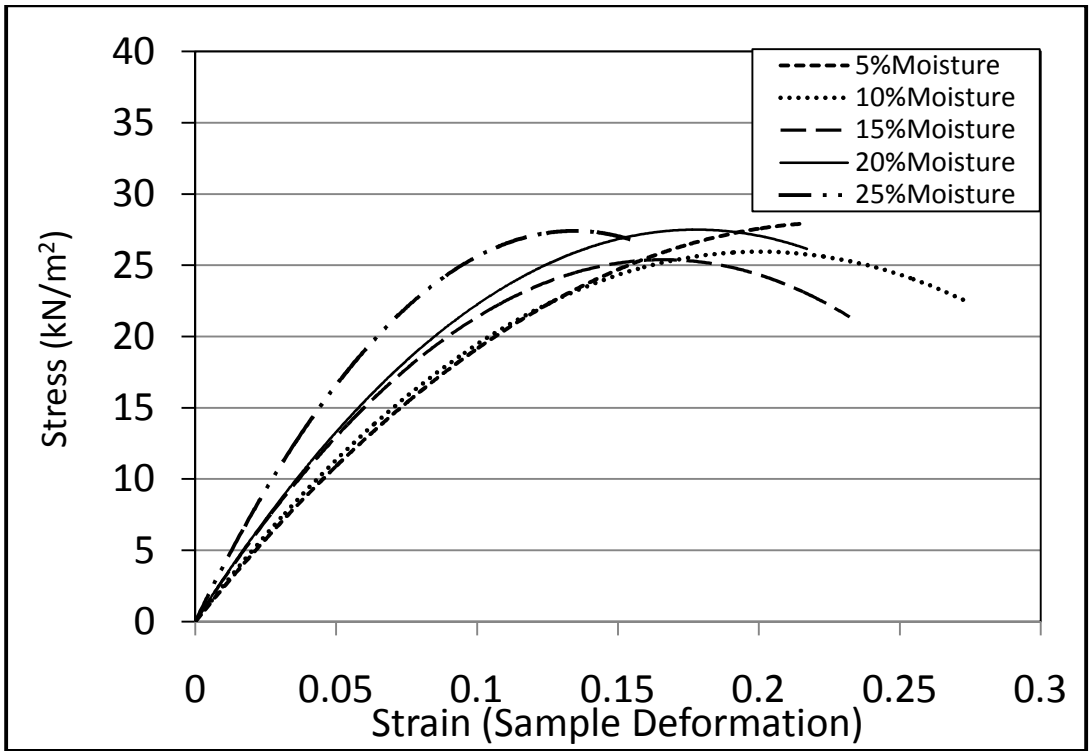

Unconfined compression result of Sandy silty clay soil treated control at day 9

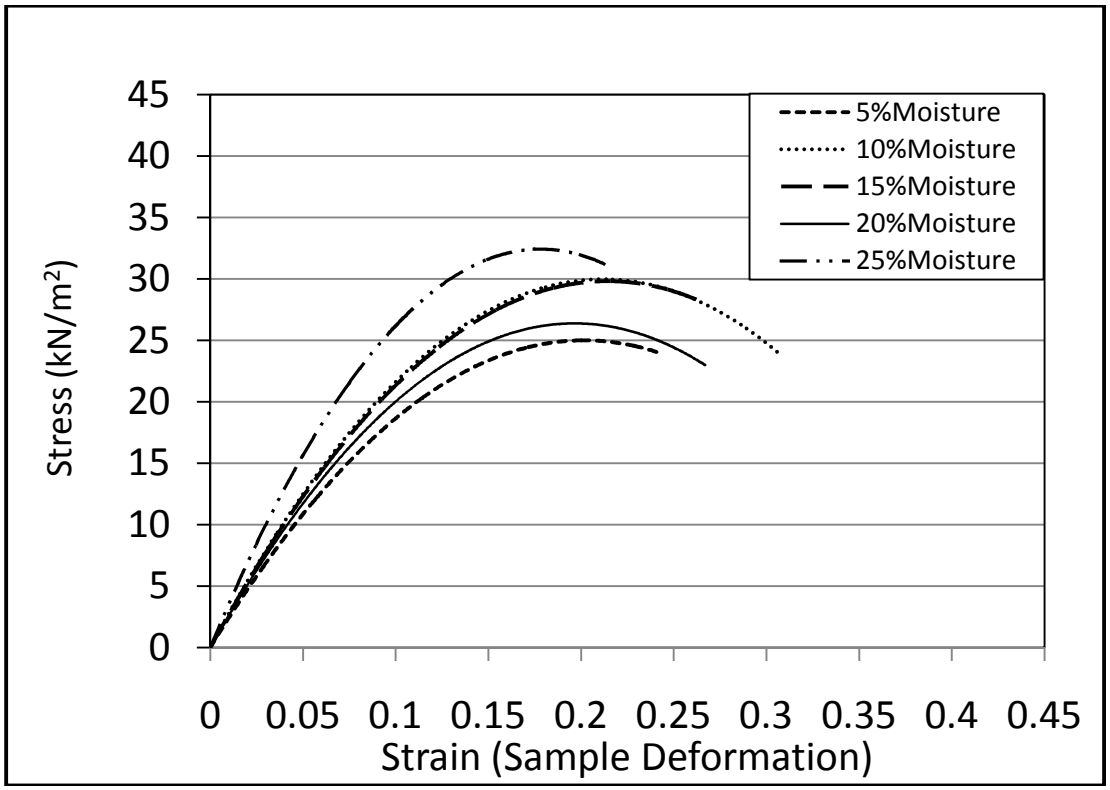

Unconfined compression result of Sandy silty clay soil treated control at day 13

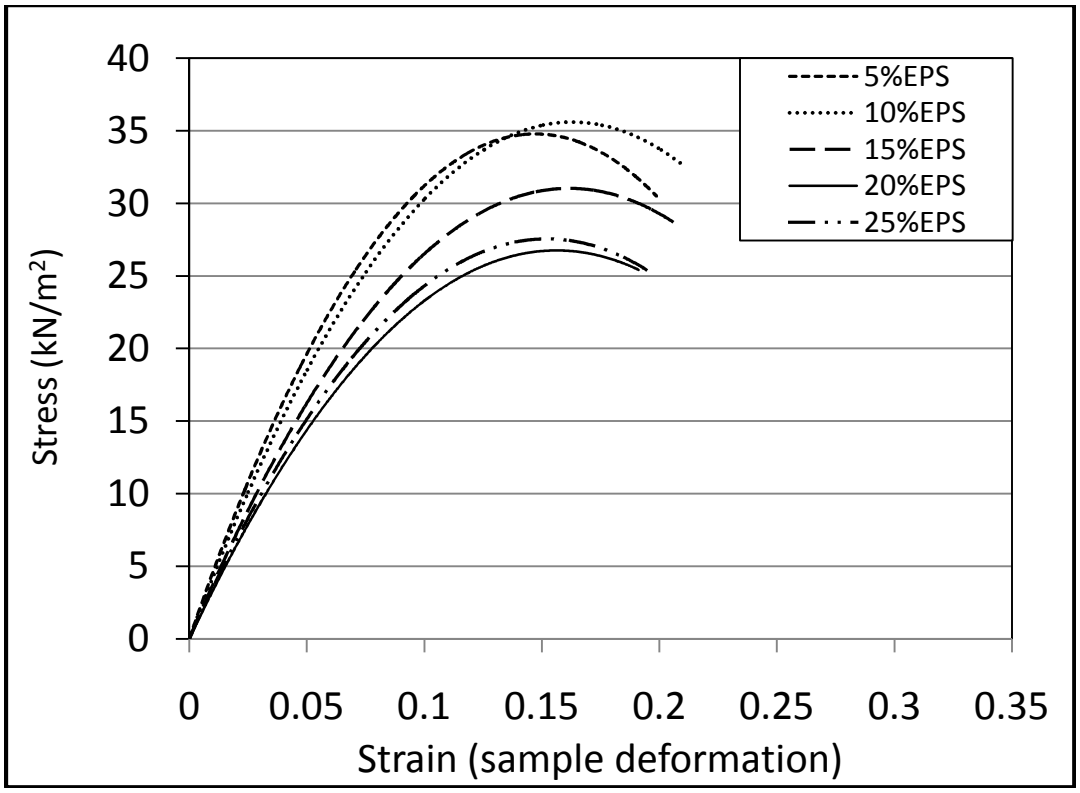

Unconfined compression result of Sandy silty clay soil treated with EPS at day 13

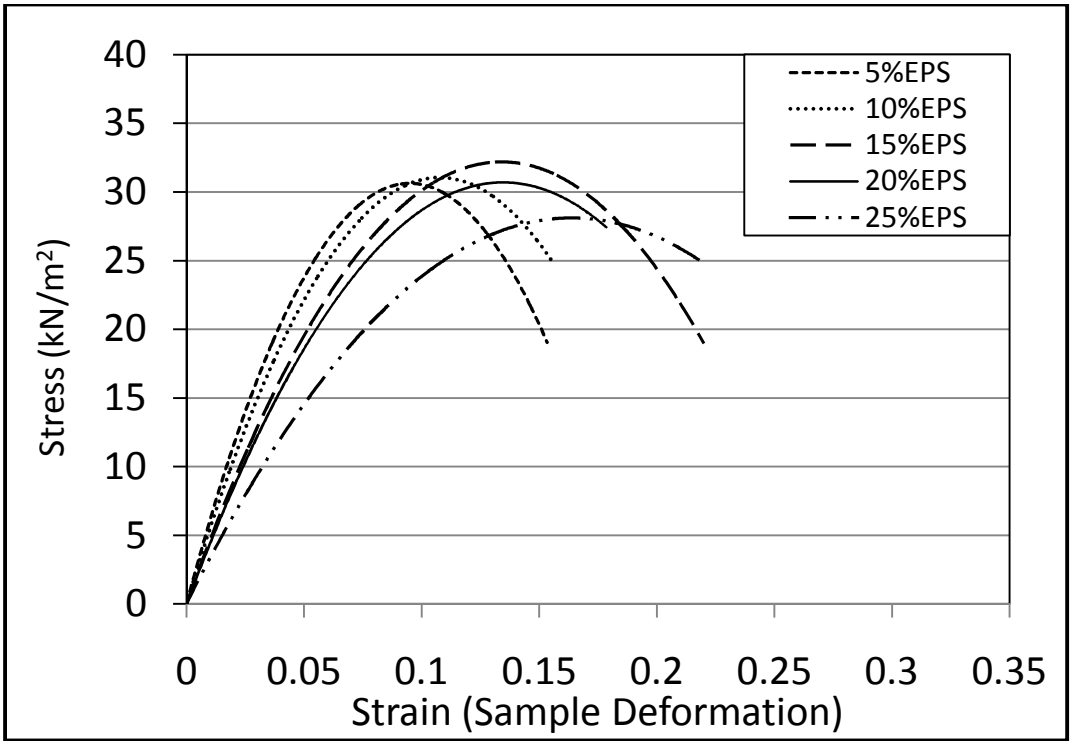

Unconfined compression result of Sandy silty clay soil treated with EPS at day 14

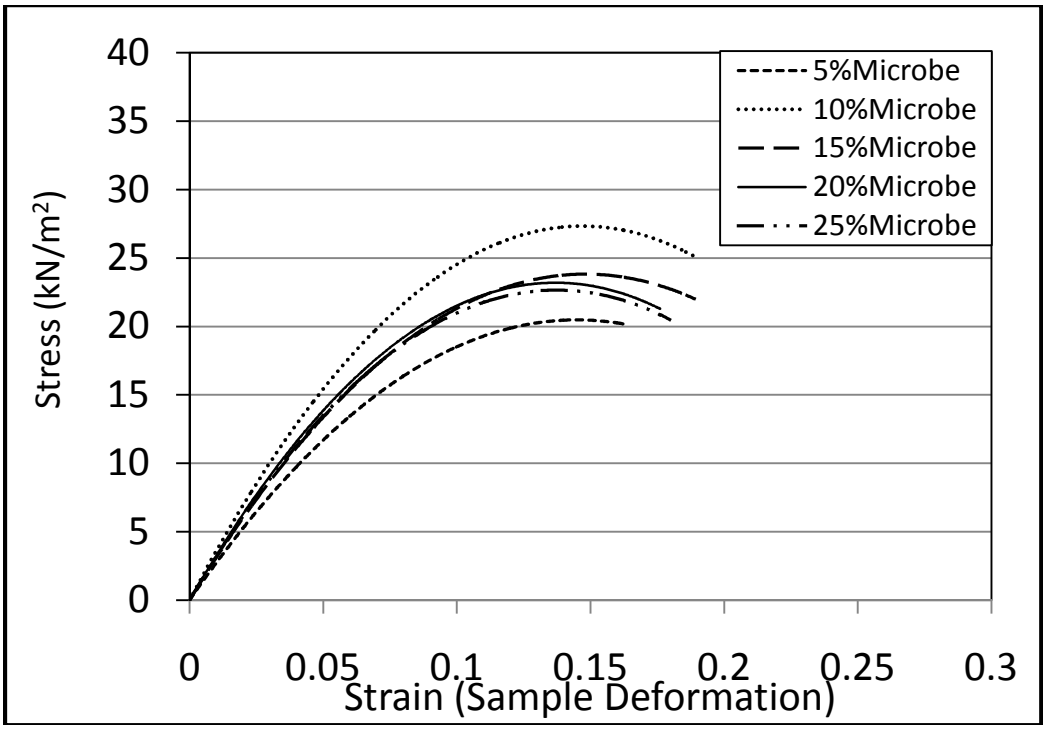

Unconfined compression result of Sandy silty clay soil treated microbe at day 10

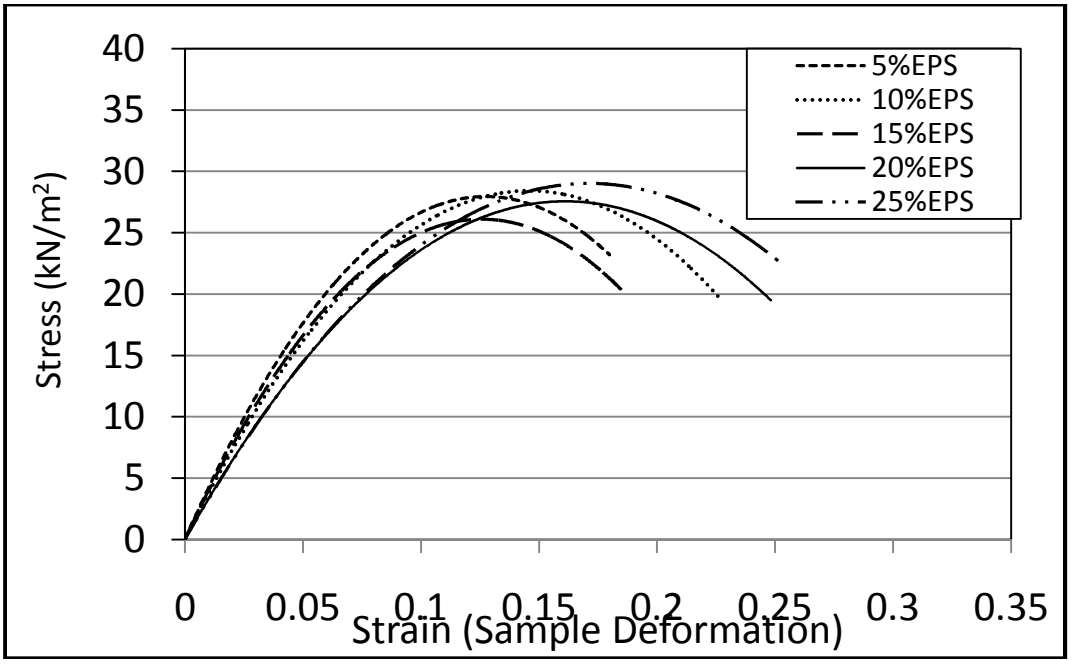

Unconfined compression result of Sandy silty clay soil treated with microbe at day 11

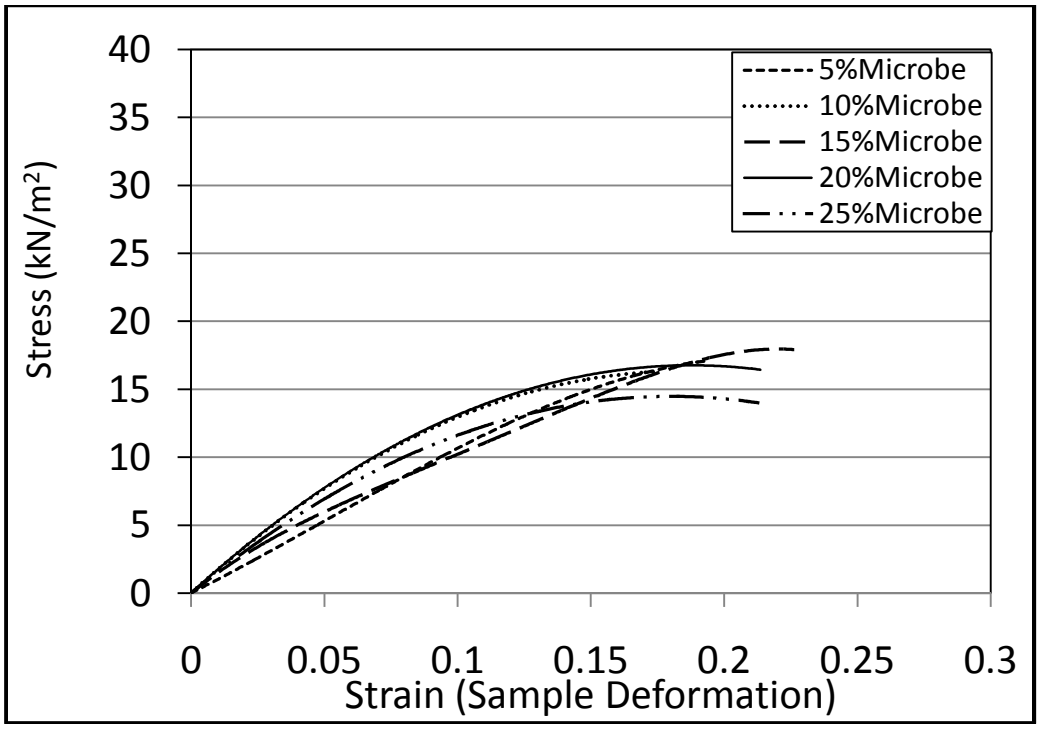

Unconfined compression result of Sandy silty clay soil treated with microbe at day 12

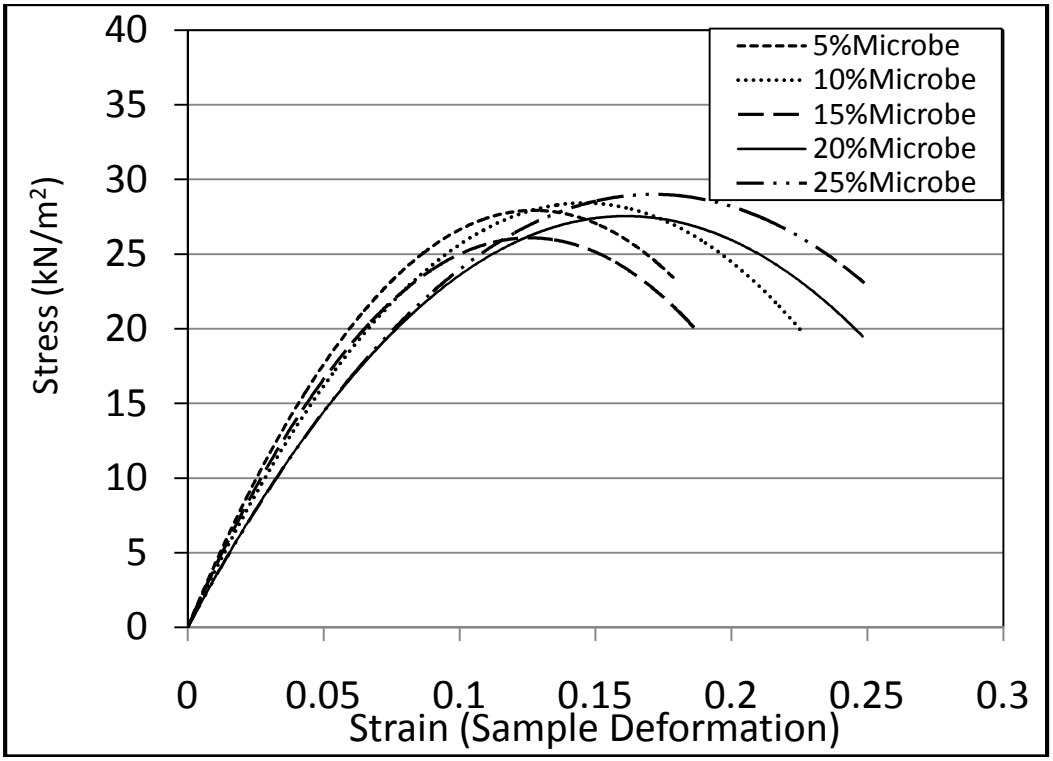

Unconfined compression result of Sandy silty clay soil treated with microbe at day 14

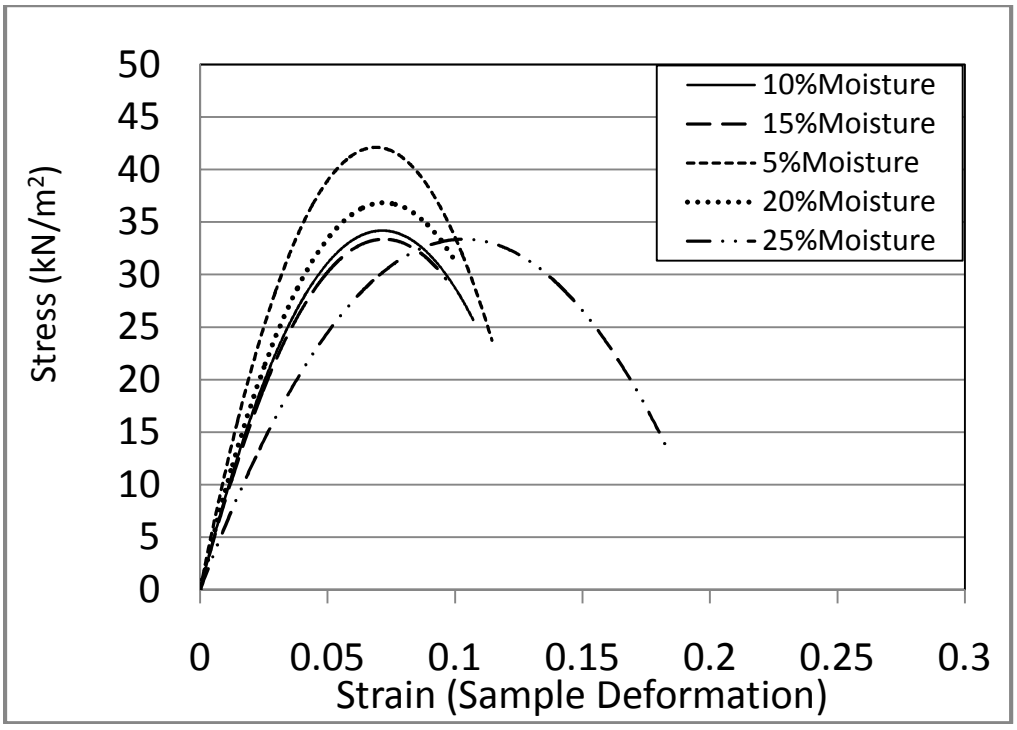

Unconfined compression result of Sandy silty clay soil treated control at day 10

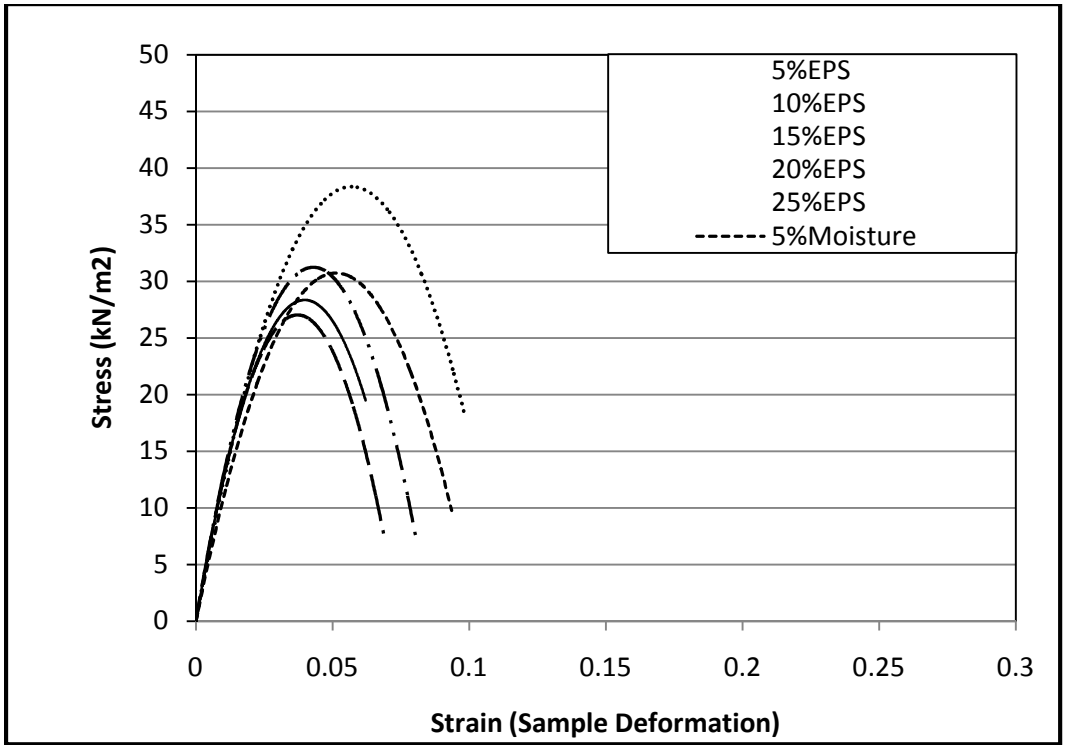

Unconfined compression result of Sandy silty clay soil treated control at day 11

APPENDIX E: GRAPHS OF SHEAR STRENGTH TESTS ON SOILS

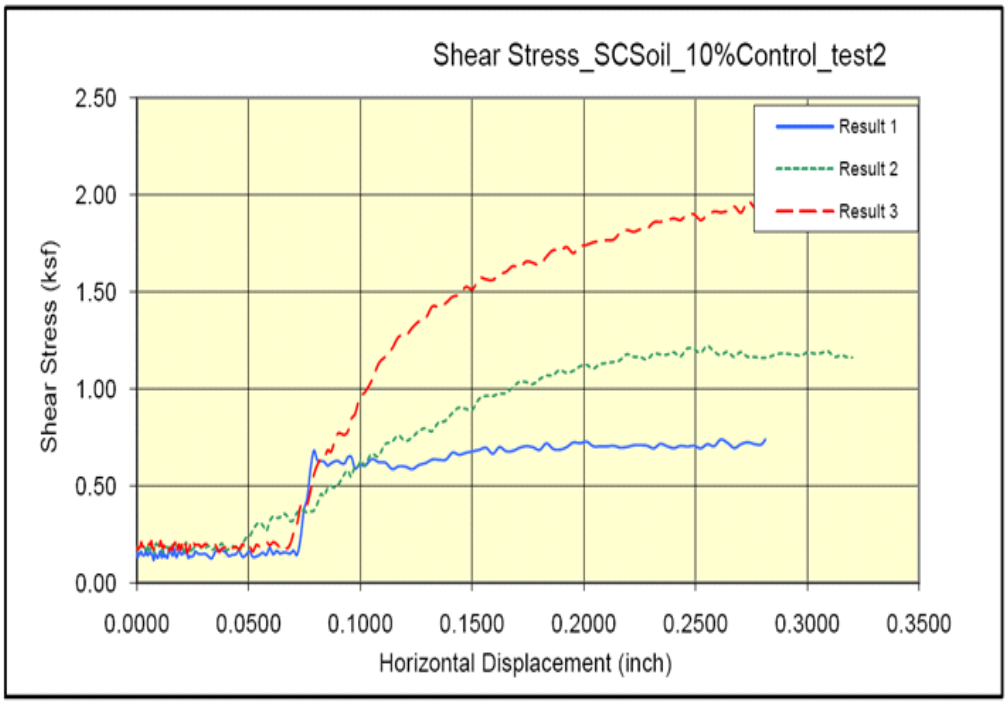

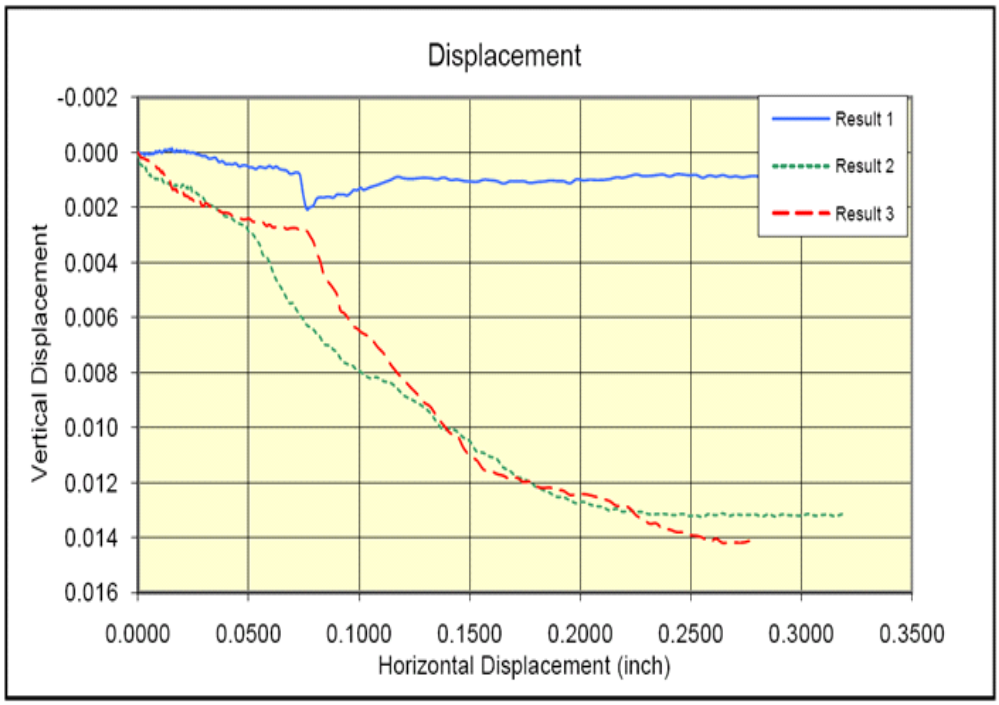

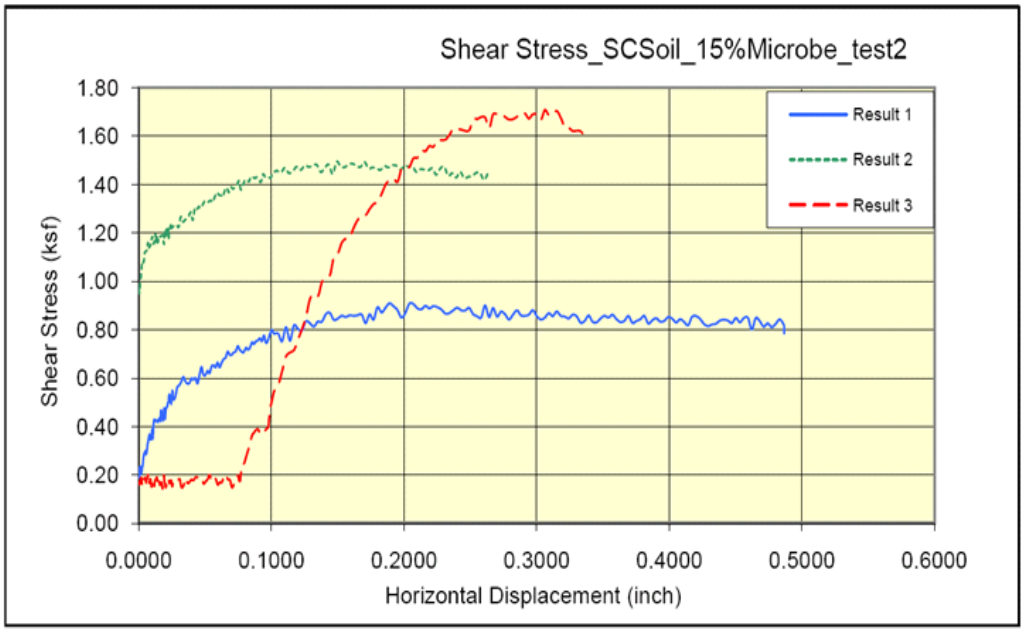
Shear Stress_SCSoil_15%Microbe_test2
Shear Stress (ksf)
1.80
1.60
1.40
1.20
1.00
0.80
0.60
0.40
0.20
0.00
0.0000
0.1000
0.2000
0.3000
0.4000
0.5000
0.6000
Horizontal Displacement (inch)
Result 1
Result 2
Result 3

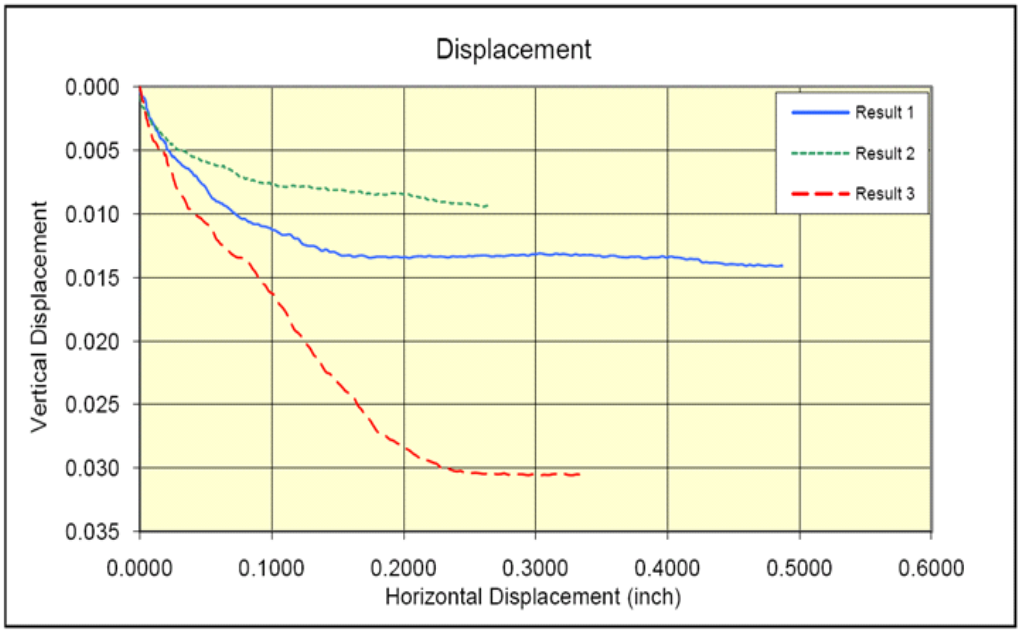
Displacement
Vertical Displacement
0.000
0.005
0.010
0.015
0.020
0.025
0.030
0.035
0.0000
0.1000
0.2000
0.3000
0.4000
0.5000
0.6000
Horizontal Displacement (inch)
Result 1
Result 2
Result 3

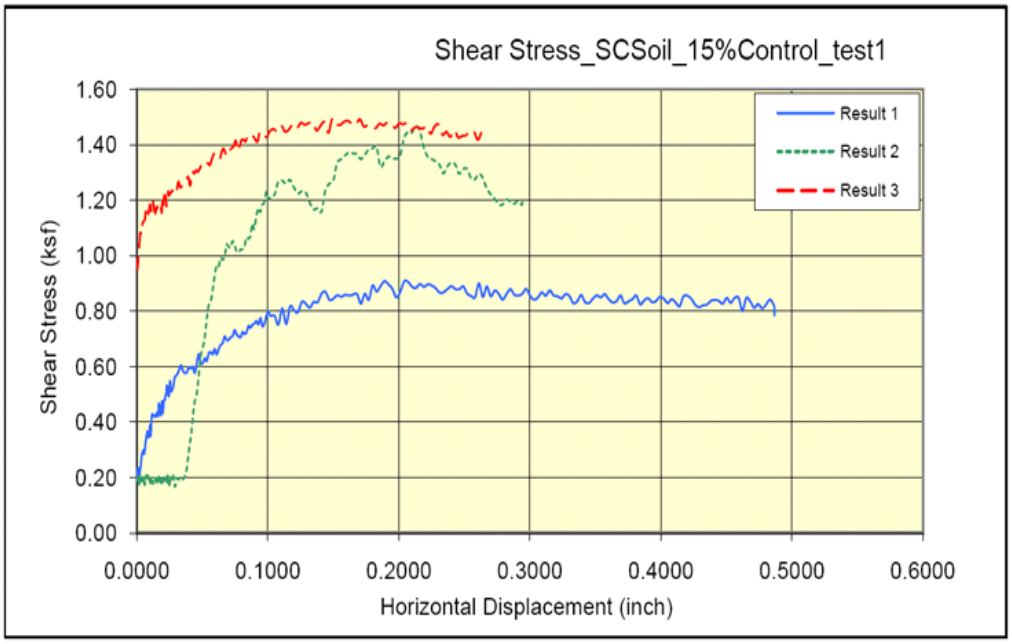
Shear Stress_SCSoil_15%Control_test1
Shear Stress (ksf)
1.60
1.40
1.20
1.00
0.80
0.60
0.40
0.20
0.00
0.0000
0.1000
0.2000
0.3000
0.4000
0.5000
0.6000
Horizontal Displacement (inch)
Result 1
Result 2
Result 3

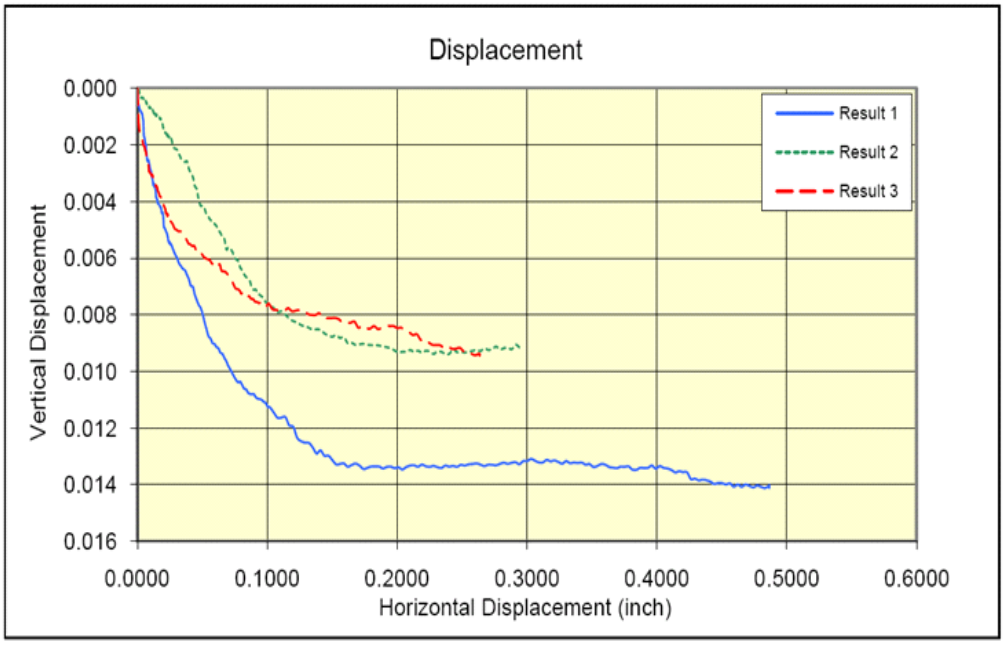
Displacement
Vertical Displacement
0.000
0.002
0.004
0.006
0.008
0.010
0.012
0.014
0.016
0.0000
0.1000
0.2000
0.3000
0.4000
0.5000
0.6000
Horizontal Displacement (inch)
Result 1
Result 2
Result 3

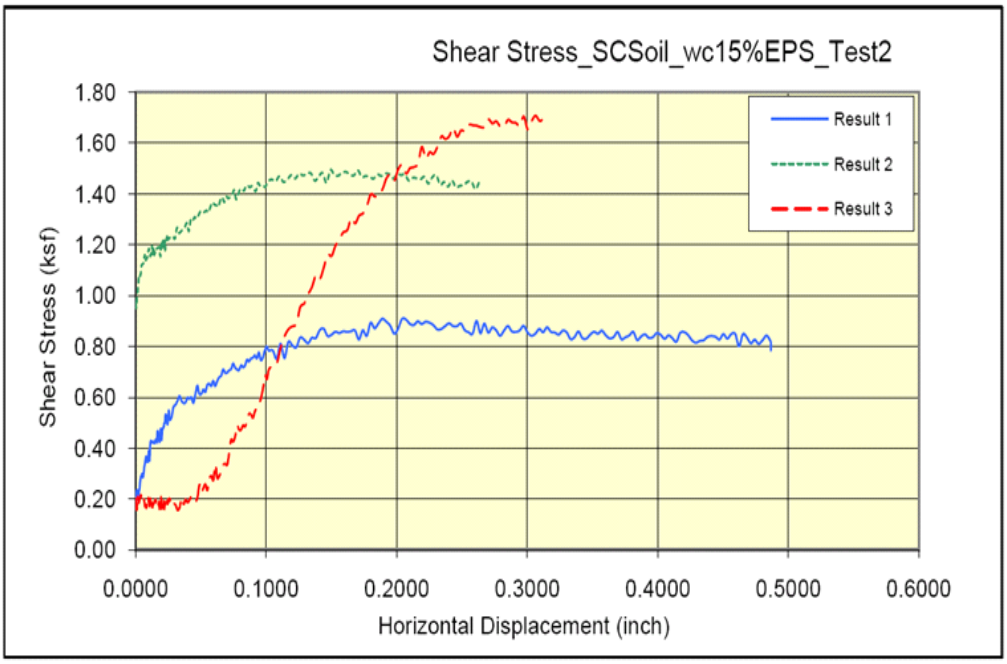
Shear Stress_SCSoil_wc15%EPS_Test2
Result 1
Result 2
Result 3
Shear Stress (ksf)
1.80
1.60
1.40
1.20
1.00
0.80
0.60
0.40
0.20
0.00
0.0000
0.1000
0.2000
0.3000
0.4000
0.5000
0.6000
Horizontal Displacement (inch)

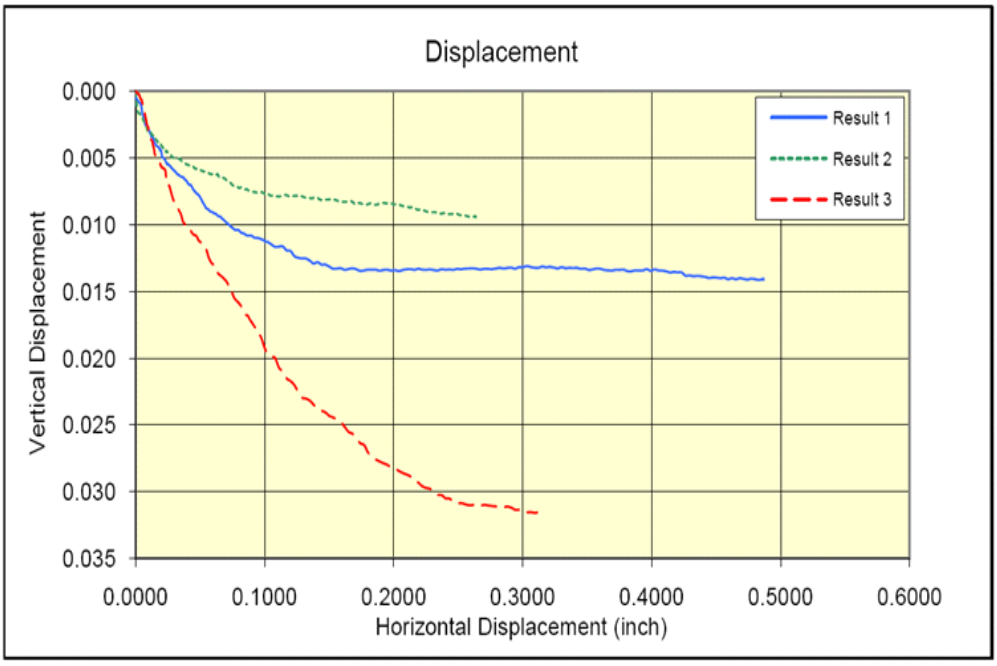
Displacement
Result 1
Result 2
Result 3
Vertical Displacement
0.000
0.005
0.010
0.015
0.020
0.025
0.030
0.035
0.0000
0.1000
0.2000
0.3000
0.4000
0.5000
0.6000
Horizontal Displacement (inch)

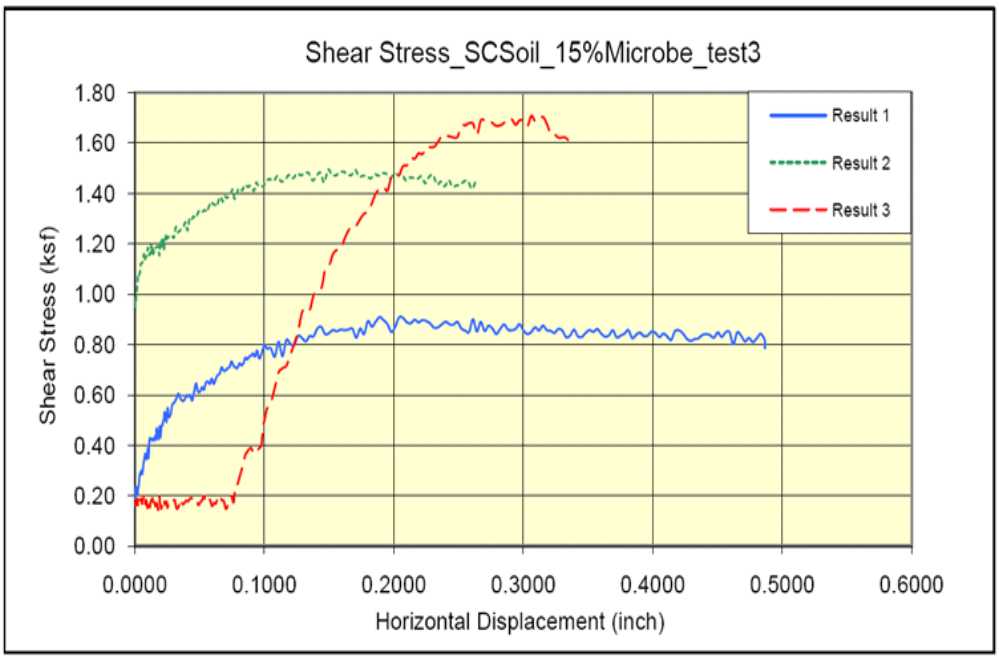
Shear Stress_SCSoil_15%Microbe_test3
Shear Stress (ksf)
1.80
1.60
1.40
1.20
1.00
0.80
0.60
0.40
0.20
0.00
0.0000
0.1000
0.2000
0.3000
0.4000
0.5000
0.6000
Horizontal Displacement (inch)
Result 1
Result 2
Result 3

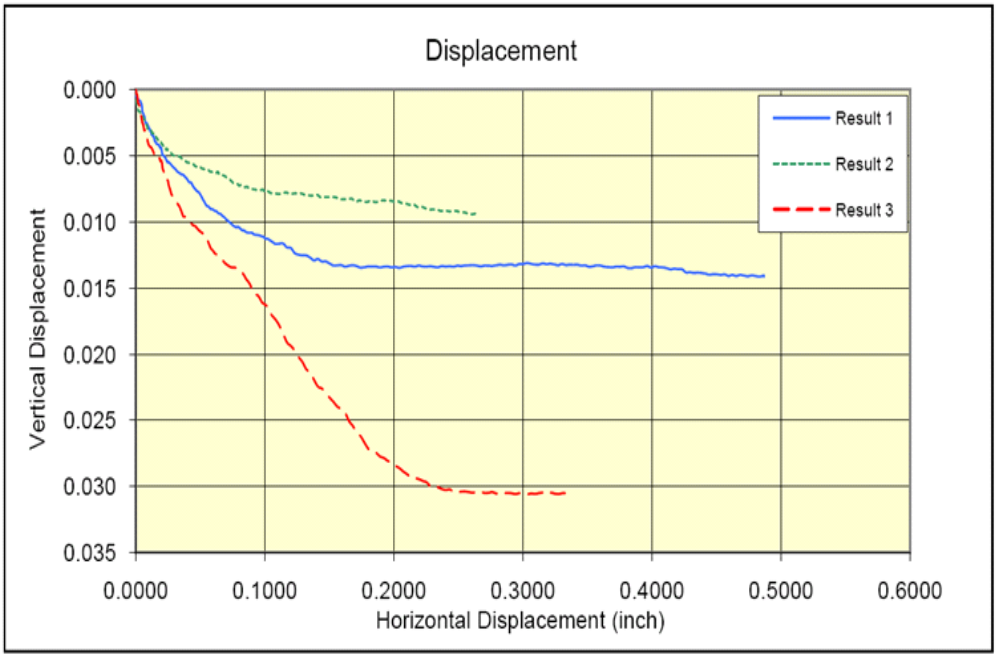
Displacement
Vertical Displacement
0.000
0.005
0.010
0.015
0.020
0.025
0.030
0.035
0.0000
0.1000
0.2000
0.3000
0.4000
0.5000
0.6000
Horizontal Displacement (inch)
Result 1
Result 2
Result 3

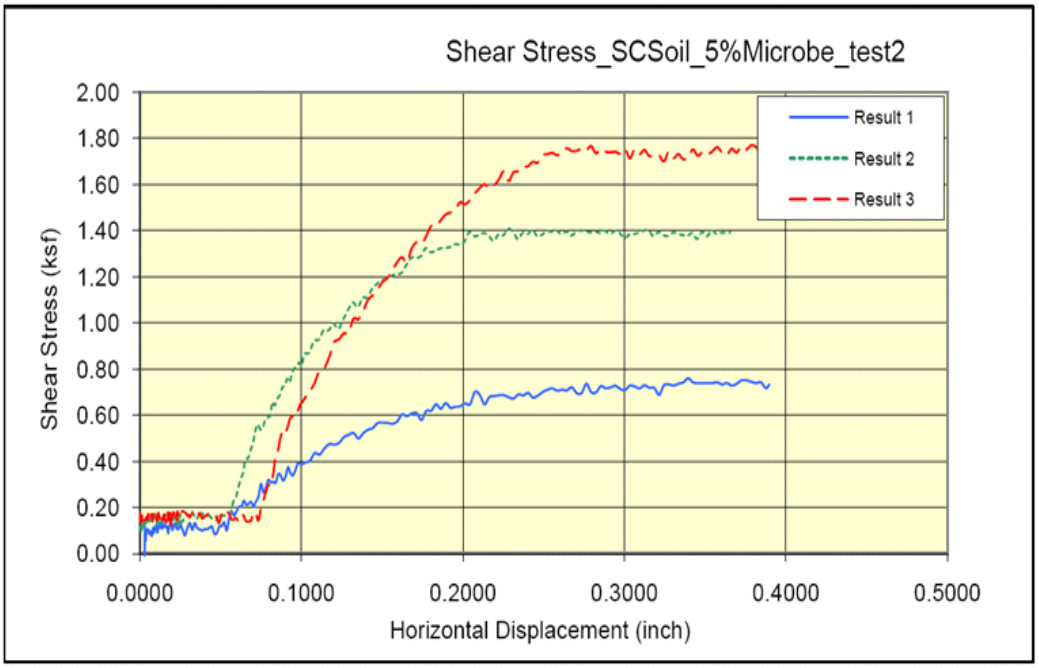
Shear Stress_SCSoil_5%Microbe_test2
Shear Stress (ksf)
2.00
1.80
1.60
1.40
1.20
1.00
0.80
0.60
0.40
0.20
0.00
0.0000
0.1000
0.2000
0.3000
0.4000
0.5000
Horizontal Displacement (inch)
Result 1
Result 2
Result 3

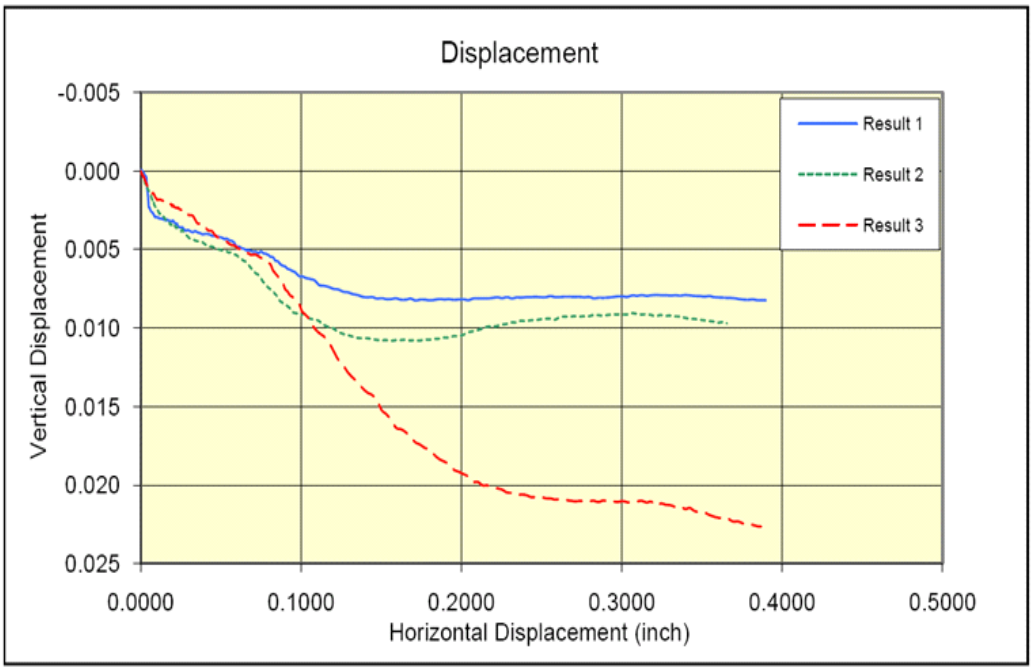
Displacement
Vertical Displacement
-0.005
0.000
0.005
0.010
0.015
0.020
0.025
0.0000
0.1000
0.2000
0.3000
0.4000
0.5000
Horizontal Displacement (inch)
Result 1
Result 2
Result 3

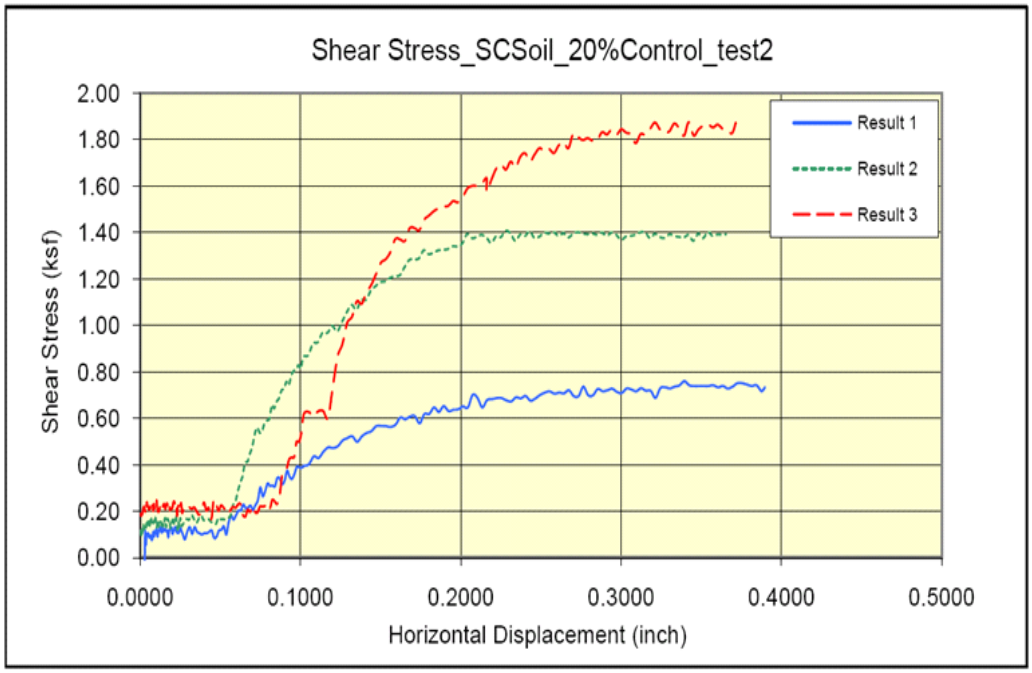
Shear Stress_SCSoil_20%Control_test2
Shear Stress (ksf)
2.00
1.80
1.60
1.40
1.20
1.00
0.80
0.60
0.40
0.20
0.00
0.0000
0.1000
0.2000
0.3000
0.4000
0.5000
Horizontal Displacement (inch)
Result 1
Result 2
Result 3

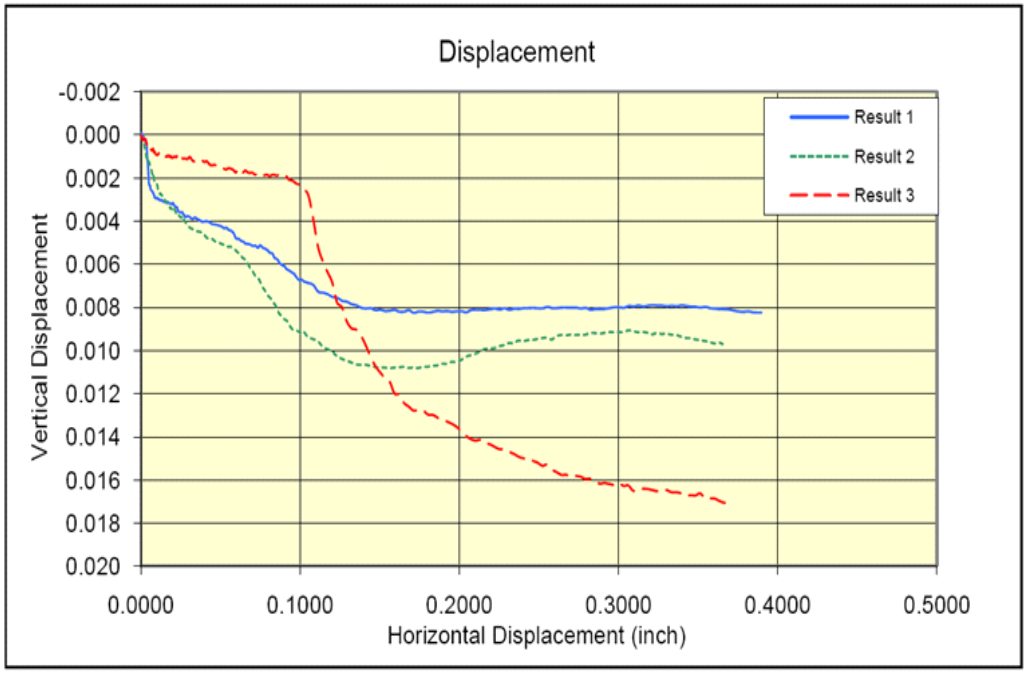
Displacement
Vertical Displacement
-0.002
0.000
0.002
0.004
0.006
0.008
0.010
0.012
0.014
0.016
0.018
0.020
0.0000
0.1000
0.2000
0.3000
0.4000
0.5000
Horizontal Displacement (inch)
Result 1
Result 2
Result 3

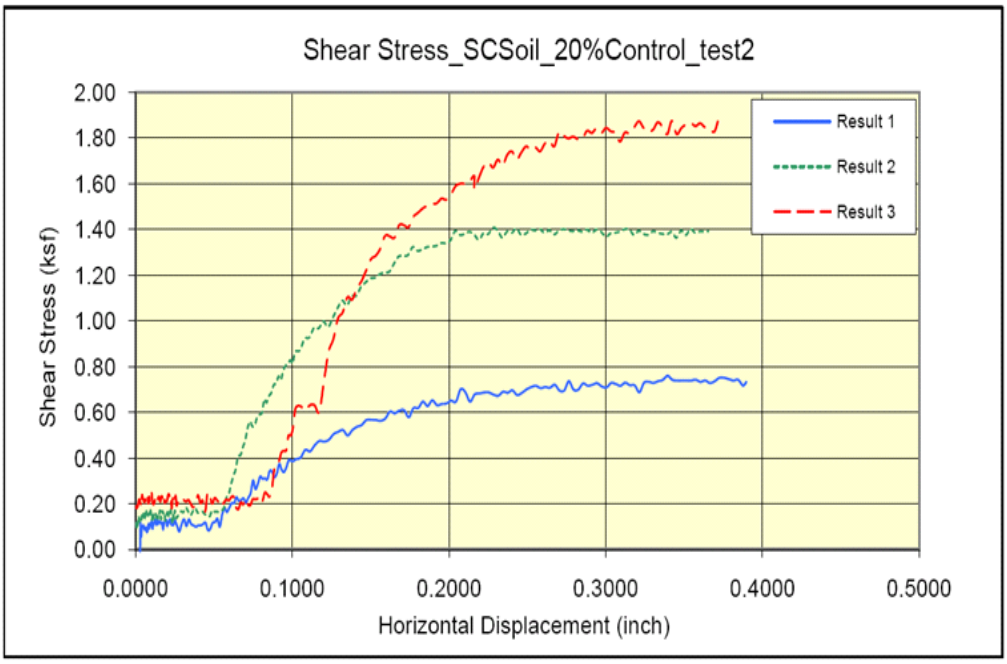
Shear Stress_SCSoil_20%Control_test2
Shear Stress (ksf)
2.00
1.80
1.60
1.40
1.20
1.00
0.80
0.60
0.40
0.20
0.00
0.0000
0.1000
0.2000
0.3000
0.4000
0.5000
Horizontal Displacement (inch)
Result 1
Result 2
Result 3

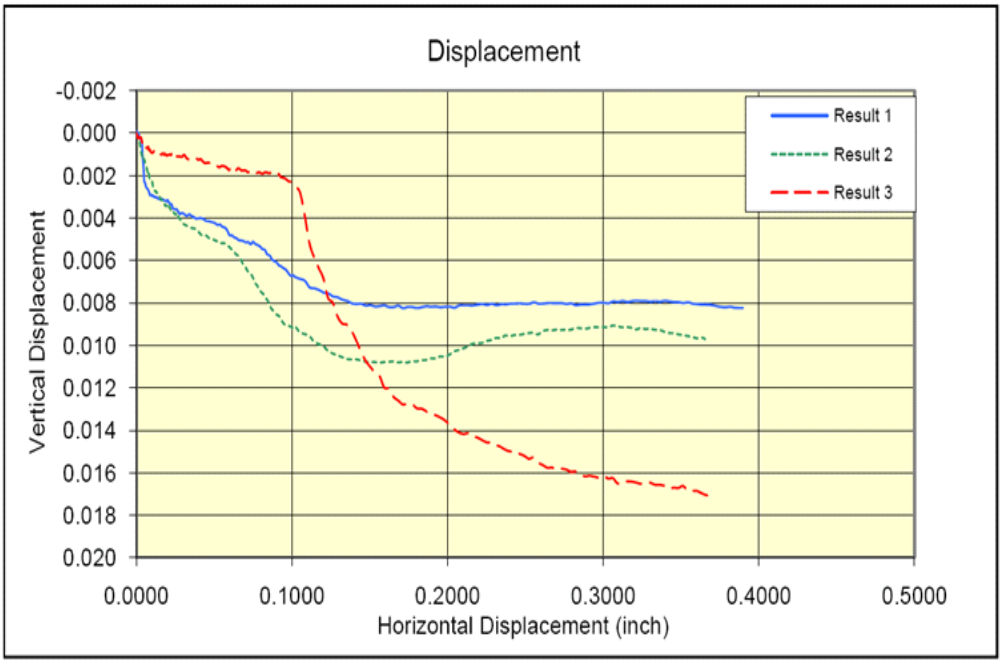
Displacement
Vertical Displacement
-0.002
0.000
0.002
0.004
0.006
0.008
0.010
0.012
0.014
0.016
0.018
0.020
0.0000
0.1000
0.2000
0.3000
0.4000
0.5000
Horizontal Displacement (inch)
Result 1
Result 2
Result 3

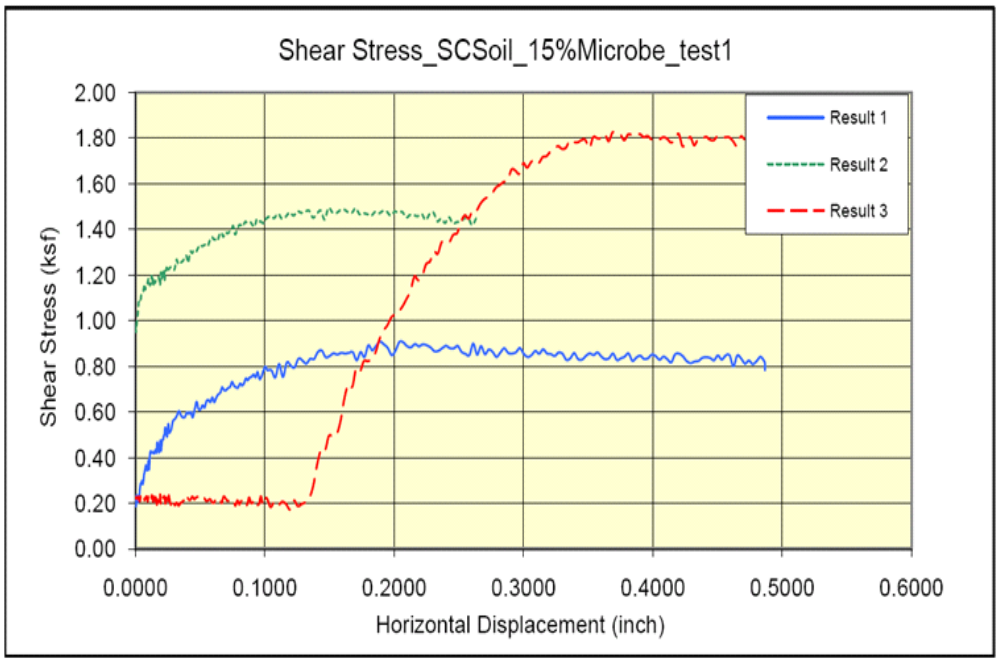
Shear Stress_SCSoil_15%Microbe_test1
Shear Stress (ksf)
2.00
1.80
1.60
1.40
1.20
1.00
0.80
0.60
0.40
0.20
0.00
0.0000
0.1000
0.2000
0.3000
0.4000
0.5000
0.6000
Horizontal Displacement (inch)
Result 1
Result 2
Result 3

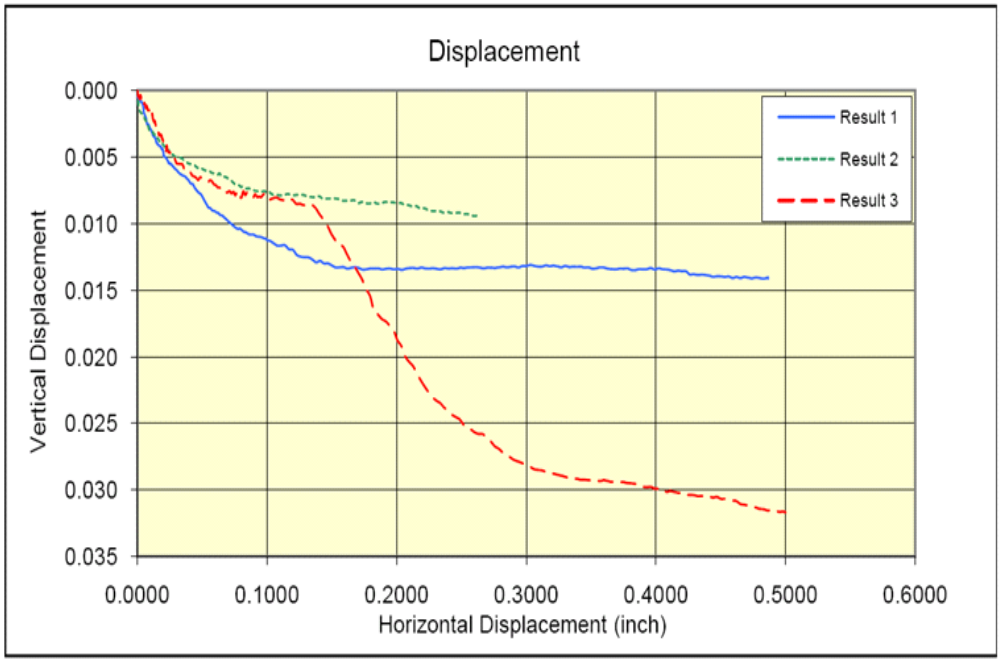
Displacement
Vertical Displacement
0.000
0.005
0.010
0.015
0.020
0.025
0.030
0.035
0.0000
0.1000
0.2000
0.3000
0.4000
0.5000
0.6000
Horizontal Displacement (inch)
Result 1
Result 2
Result 3

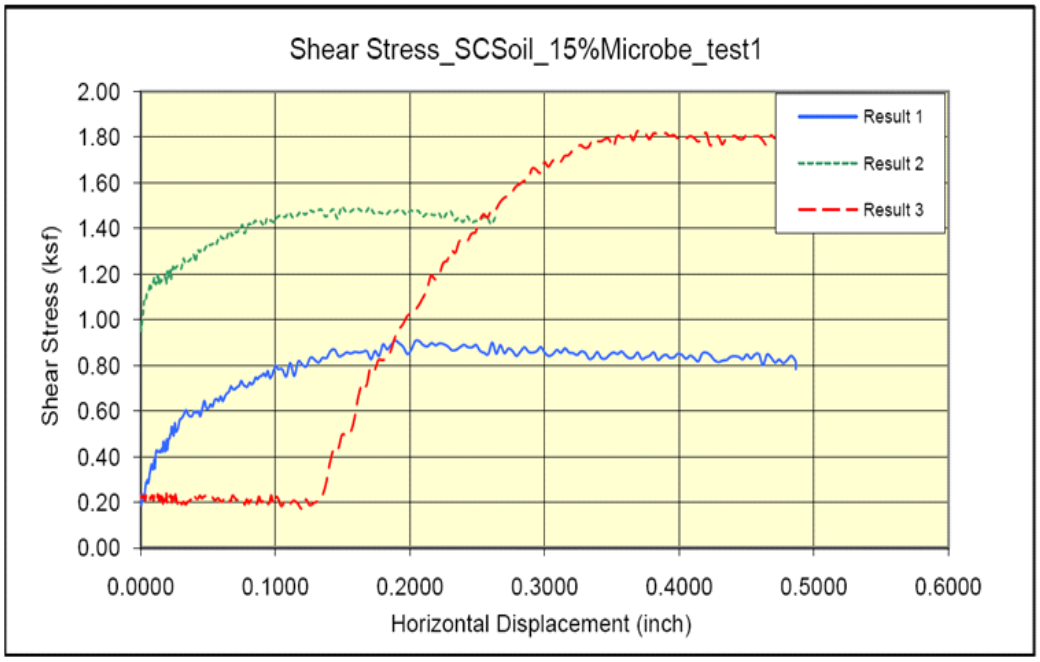
Shear Stress_SCSoil_15%Microbe_test1
Shear Stress (ksf)
2.00
1.80
1.60
1.40
1.20
1.00
0.80
0.60
0.40
0.20
0.00
0.0000
0.1000
0.2000
0.3000
0.4000
0.5000
0.6000
Horizontal Displacement (inch)
Result 1
Result 2
Result 3

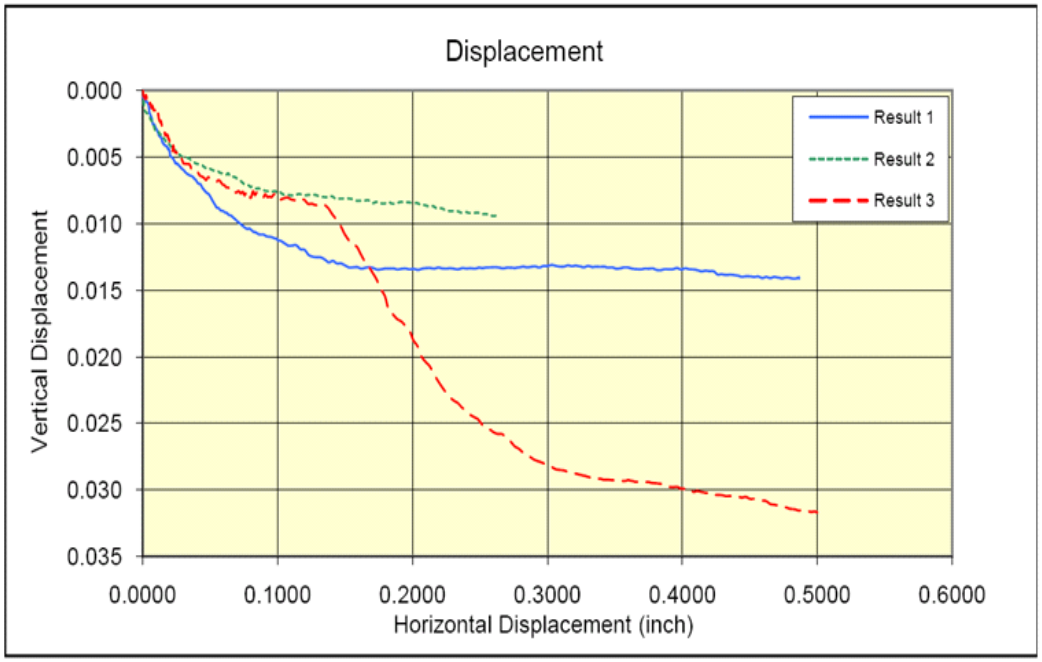
Displacement
Vertical Displacement
0.000
0.005
0.010
0.015
0.020
0.025
0.030
0.035
0.0000
0.1000
0.2000
0.3000
0.4000
0.5000
0.6000
Horizontal Displacement (inch)
Result 1
Result 2
Result 3

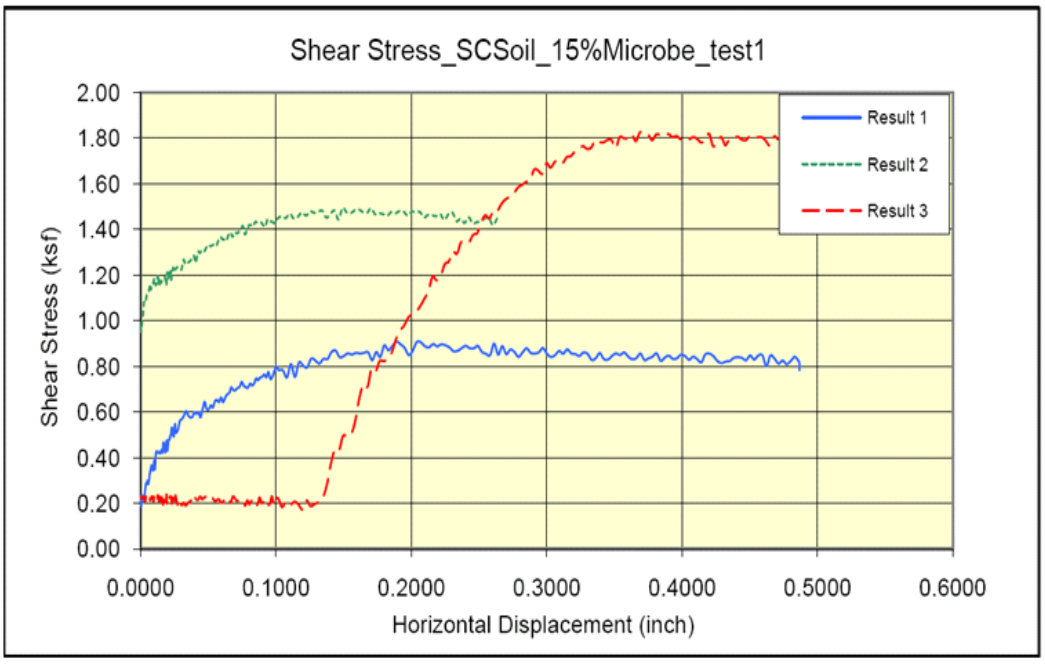
Shear Stress_SCSoil_15%Microbe_test1
Shear Stress (ksf)
2.00
1.80
1.60
1.40
1.20
1.00
0.80
0.60
0.40
0.20
0.00
0.0000
0.1000
0.2000
0.3000
0.4000
0.5000
0.6000
Horizontal Displacement (inch)
Result 1
Result 2
Result 3

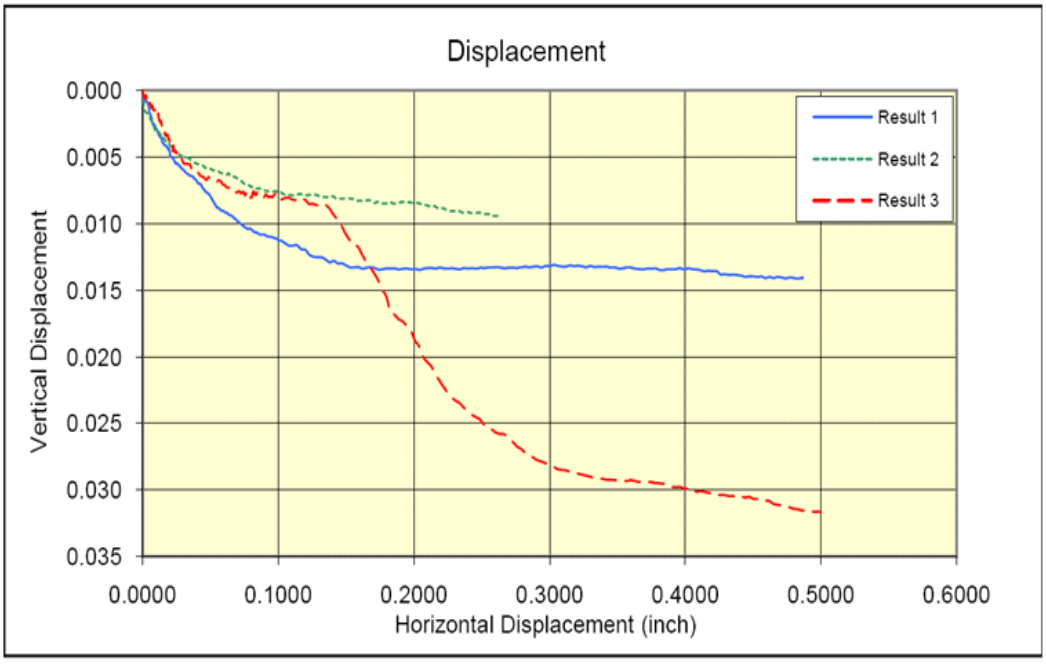
Displacement
Vertical Displacement
0.000
0.005
0.010
0.015
0.020
0.025
0.030
0.035
0.0000
0.1000
0.2000
0.3000
0.4000
0.5000
0.6000
Horizontal Displacement (inch)
Result 1
Result 2
Result 3

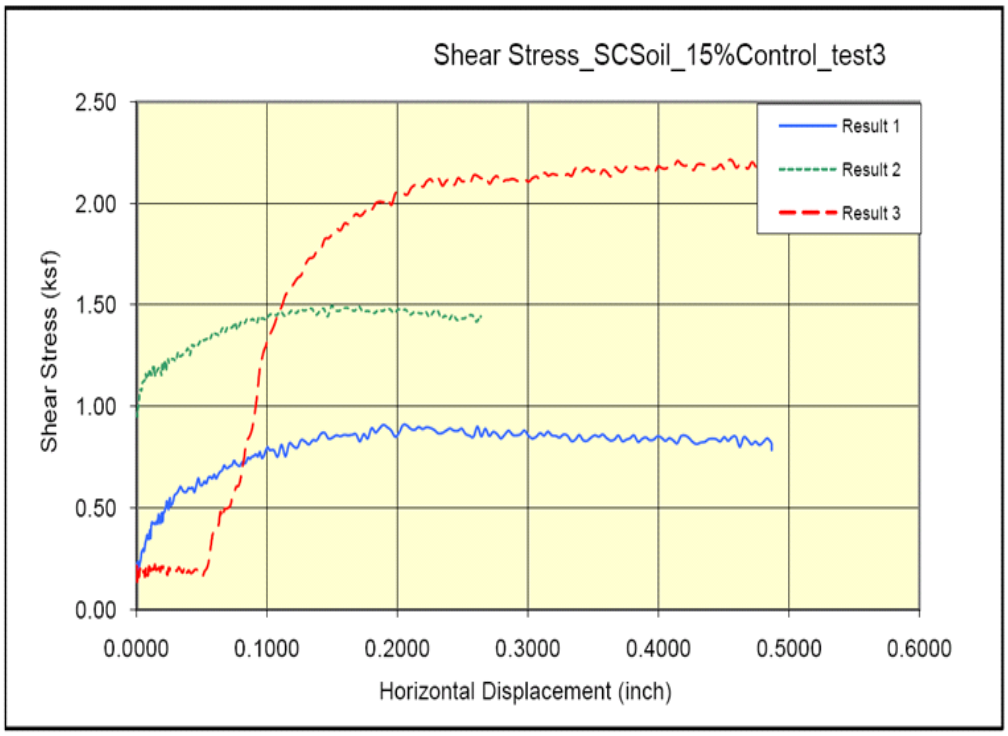
Shear Stress_SCSoil_15%Control_test3
Shear Stress (ksf)
2.50
2.00
1.50
1.00
0.50
0.00
0.0000
0.1000
0.2000
0.3000
0.4000
0.5000
0.6000
Horizontal Displacement (inch)
Result 1
Result 2
Result 3

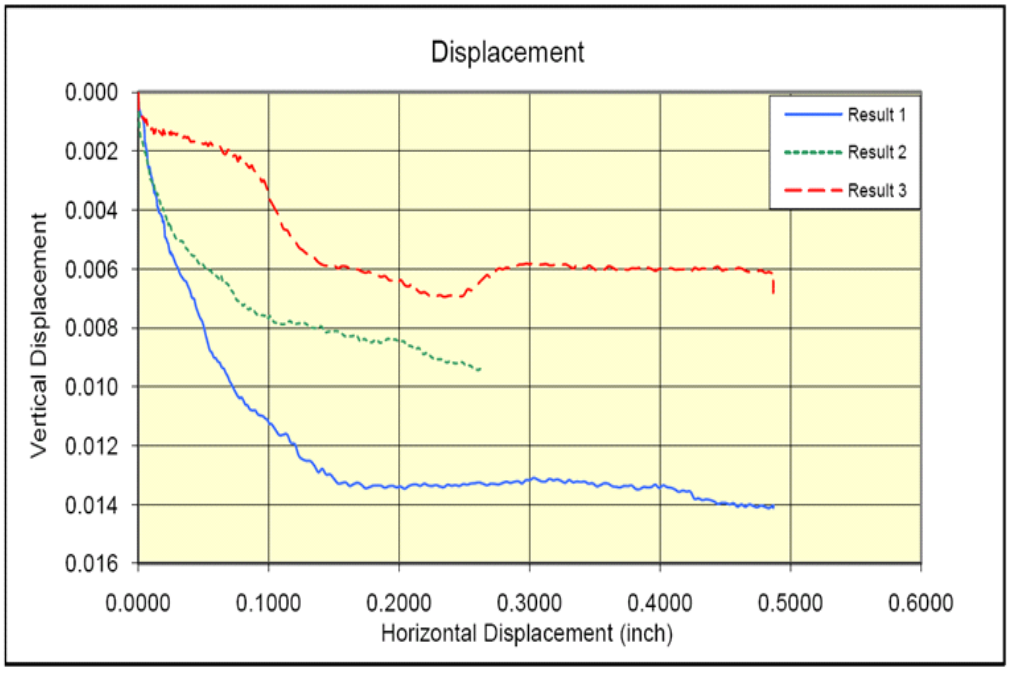
Displacement
Vertical Displacement
0.000
0.002
0.004
0.006
0.008
0.010
0.012
0.014
0.016
0.0000
0.1000
0.2000
0.3000
0.4000
0.5000
0.6000
Horizontal Displacement (inch)
Result 1
Result 2
Result 3

f

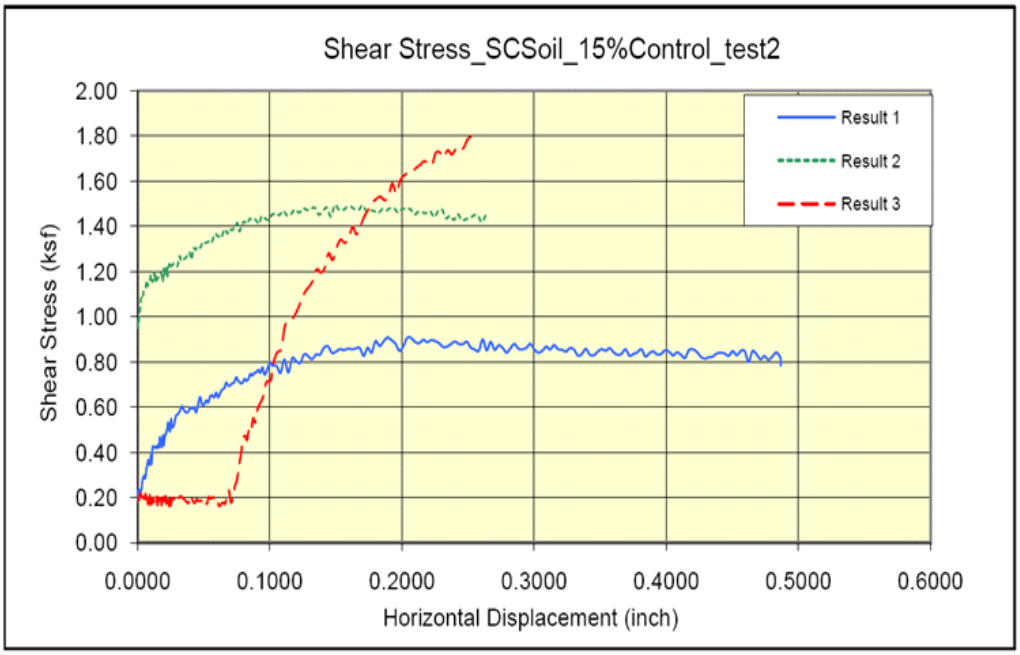
Shear Stress_SCSoil_15%Control_test2
Shear Stress (ksf)
2.00
1.80
1.60
1.40
1.20
1.00
0.80
0.60
0.40
0.20
0.00
0.0000
0.1000
0.2000
0.3000
0.4000
0.5000
0.6000
Horizontal Displacement (inch)
Result 1
Result 2
Result 3

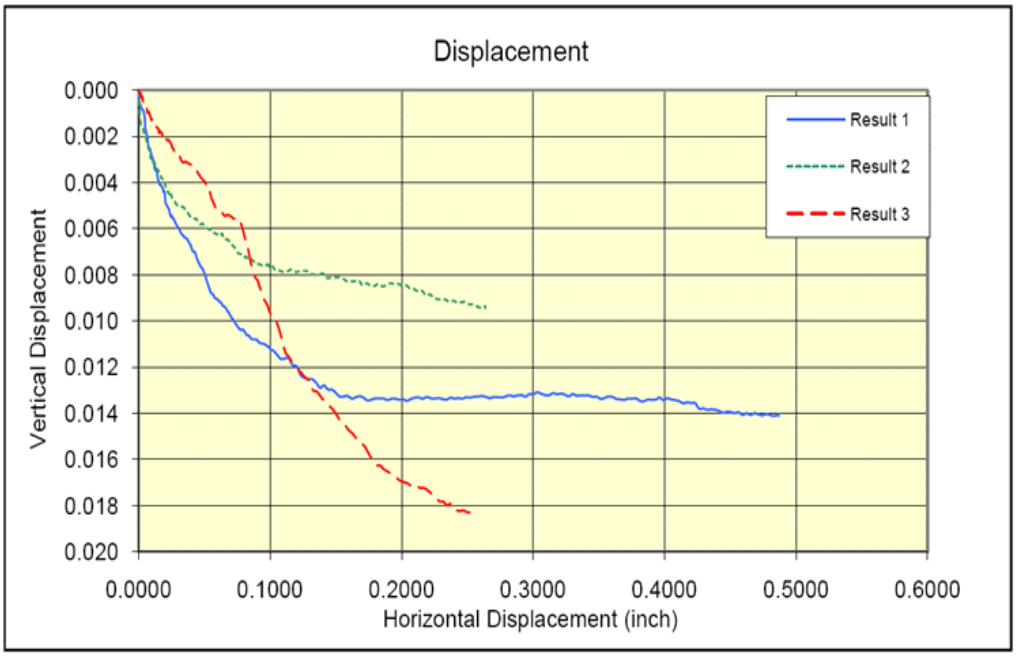
Displacement
Vertical Displacement
0.000
0.002
0.004
0.006
0.008
0.010
0.012
0.014
0.016
0.018
0.020
0.0000
0.1000
0.2000
0.3000
0.4000
0.5000
0.6000
Horizontal Displacement (inch)
Result 1
Result 2
Result 3

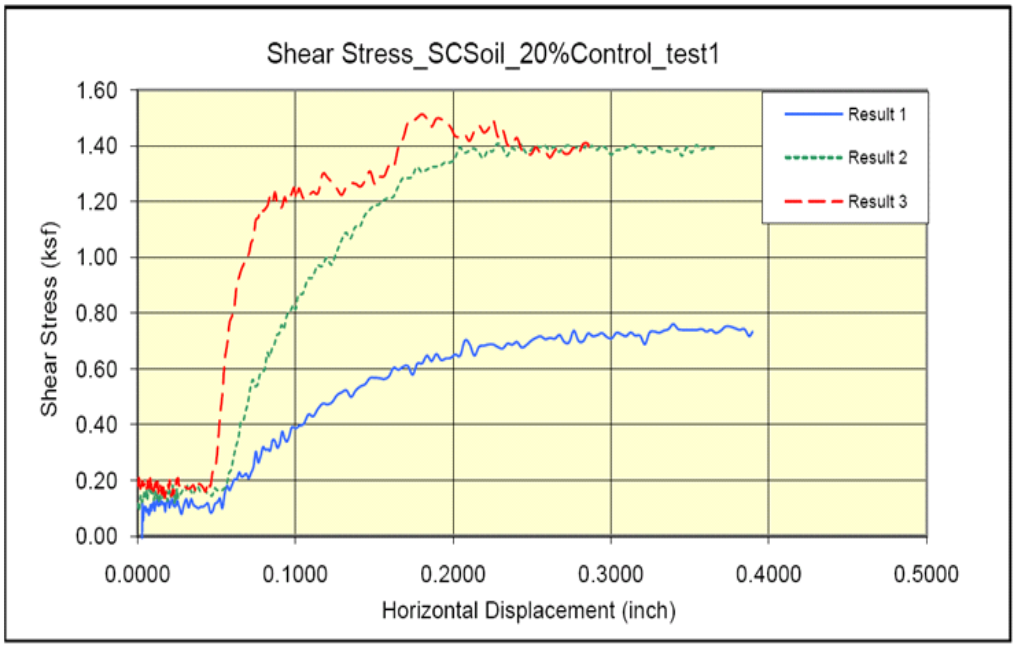
Shear Stress_SCSoil_20%Control_test1
Shear Stress (ksf)
1.60
1.40
1.20
1.00
0.80
0.60
0.40
0.20
0.00
0.0000
0.1000
0.2000
0.3000
0.4000
0.5000
Horizontal Displacement (inch)
Result 1
Result 2
Result 3

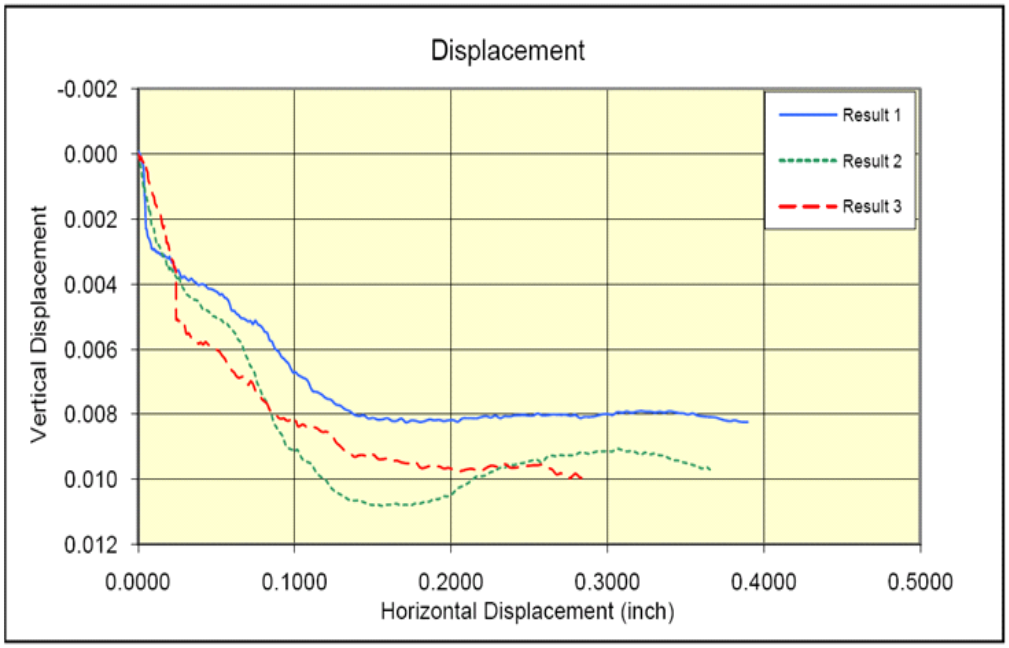
Displacement
Vertical Displacement
-0.002
0.000
0.002
0.004
0.006
0.008
0.010
0.012
0.0000
0.1000
0.2000
0.3000
0.4000
0.5000
Horizontal Displacement (inch)
Result 1
Result 2
Result 3

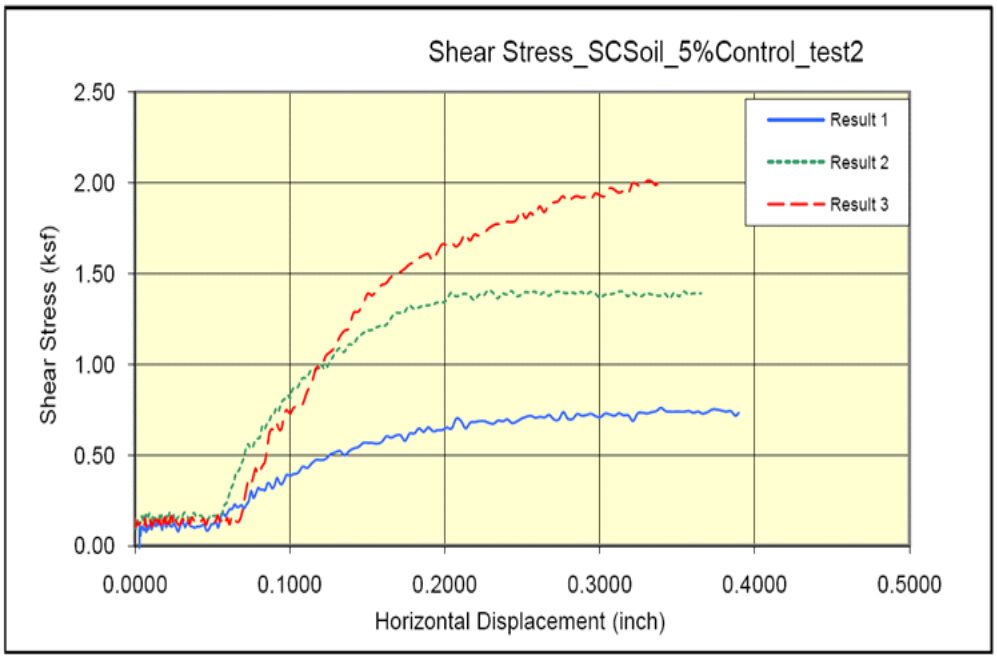
Shear Stress_SCSoil_5%Control_test2
Result 1
Result 2
Result 3
Shear Stress (ksf)
2.50
2.00
1.50
1.00
0.50
0.00
0.0000
0.1000
0.2000
0.3000
0.4000
0.5000
Horizontal Displacement (inch)

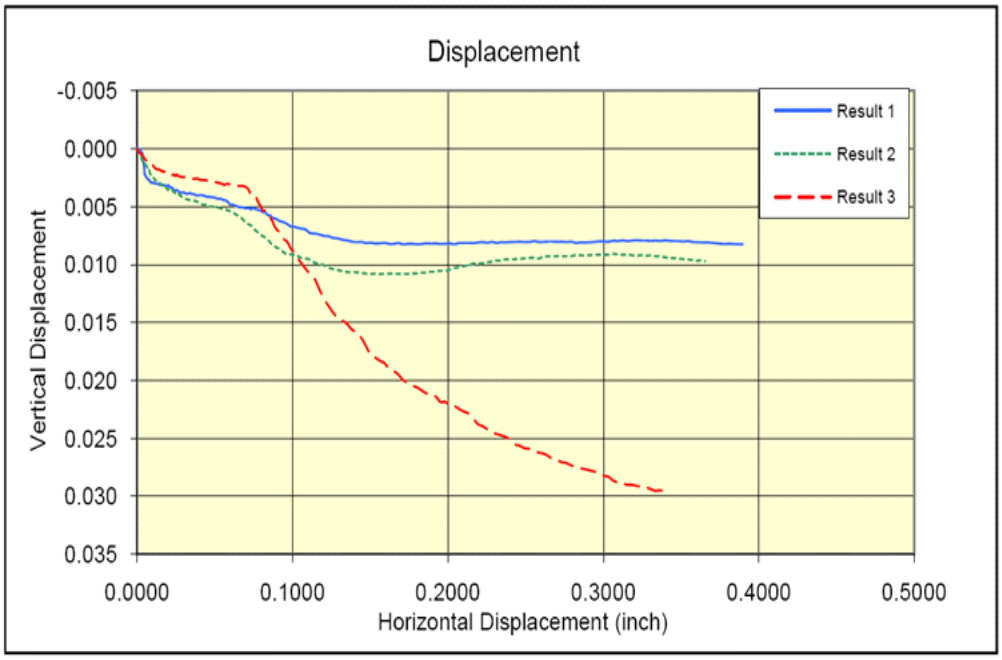
Displacement
Result 1
Result 2
Result 3
Vertical Displacement
-0.005
0.000
0.005
0.010
0.015
0.020
0.025
0.030
0.035
0.0000
0.1000
0.2000
0.3000
0.4000
0.5000
Horizontal Displacement (inch)

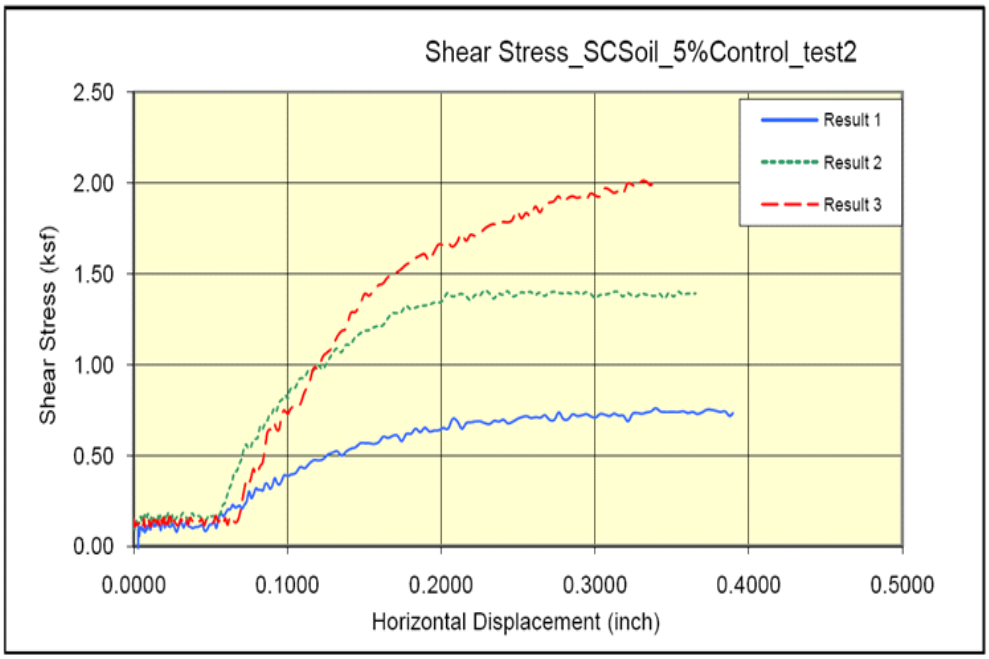
Shear Stress_SCSoil_5%Control_test2
Result 1
Result 2
Result 3
Shear Stress (ksf)
2.50
2.00
1.50
1.00
0.50
0.00
0.0000
0.1000
0.2000
0.3000
0.4000
0.5000
Horizontal Displacement (inch)

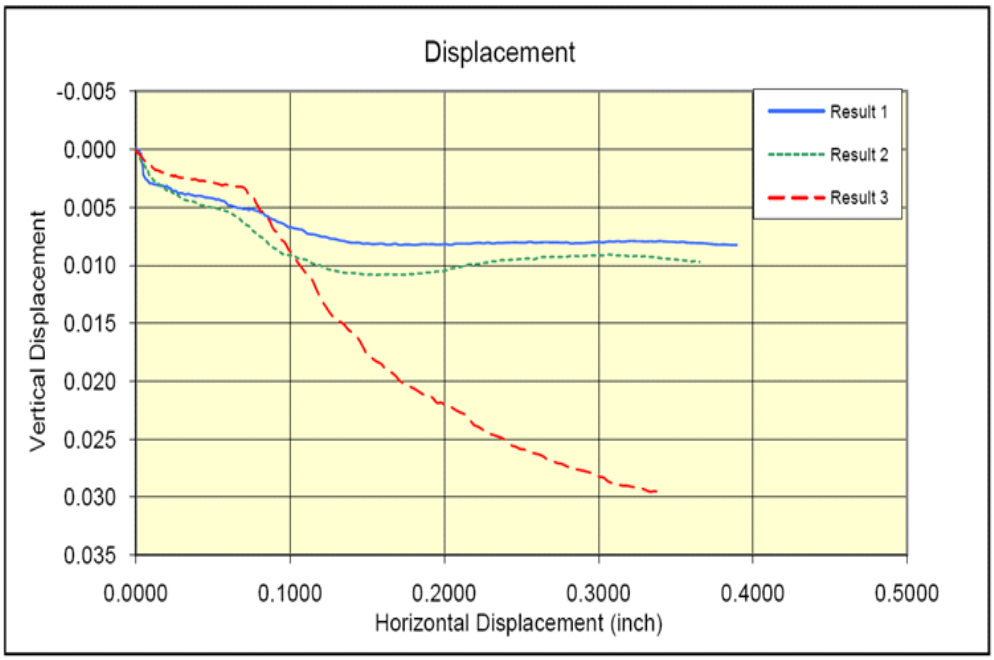
Displacement
Result 1
Result 2
Result 3
Vertical Displacement
-0.005
0.000
0.005
0.010
0.015
0.020
0.025
0.030
0.035
0.0000
0.1000
0.2000
0.3000
0.4000
0.5000
Horizontal Displacement (inch)

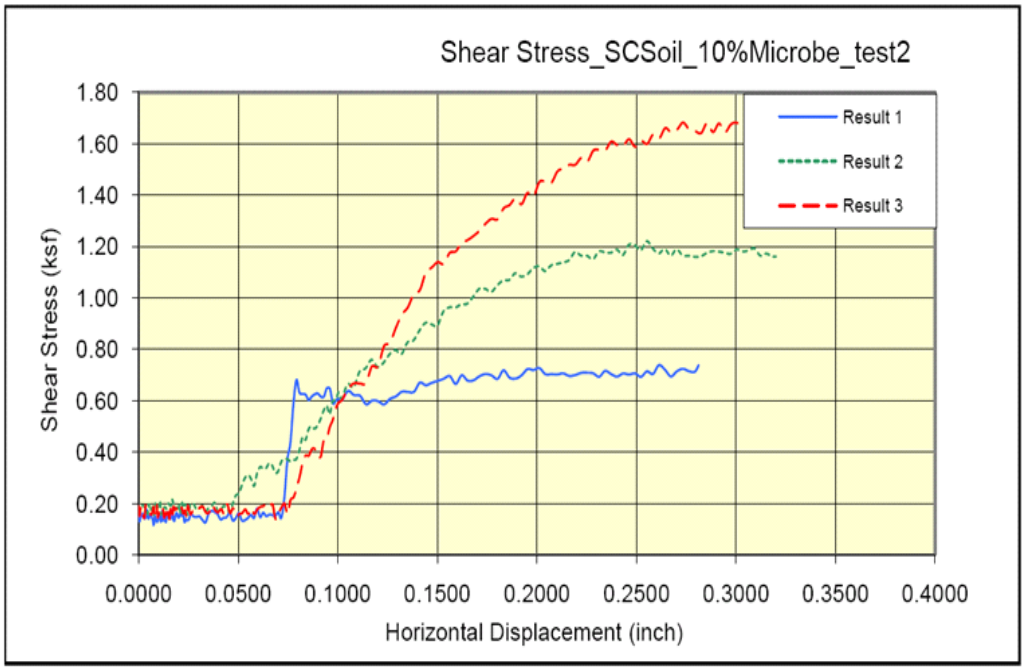
Shear Stress_SCSoil_10%Microbe_test2
Shear Stress (ksf)
1.80
1.60
1.40
1.20
1.00
0.80
0.60
0.40
0.20
0.00
0.0000
0.0500
0.1000
0.1500
0.2000
0.2500
0.3000
0.3500
0.4000
Horizontal Displacement (inch)
Result 1
Result 2
Result 3

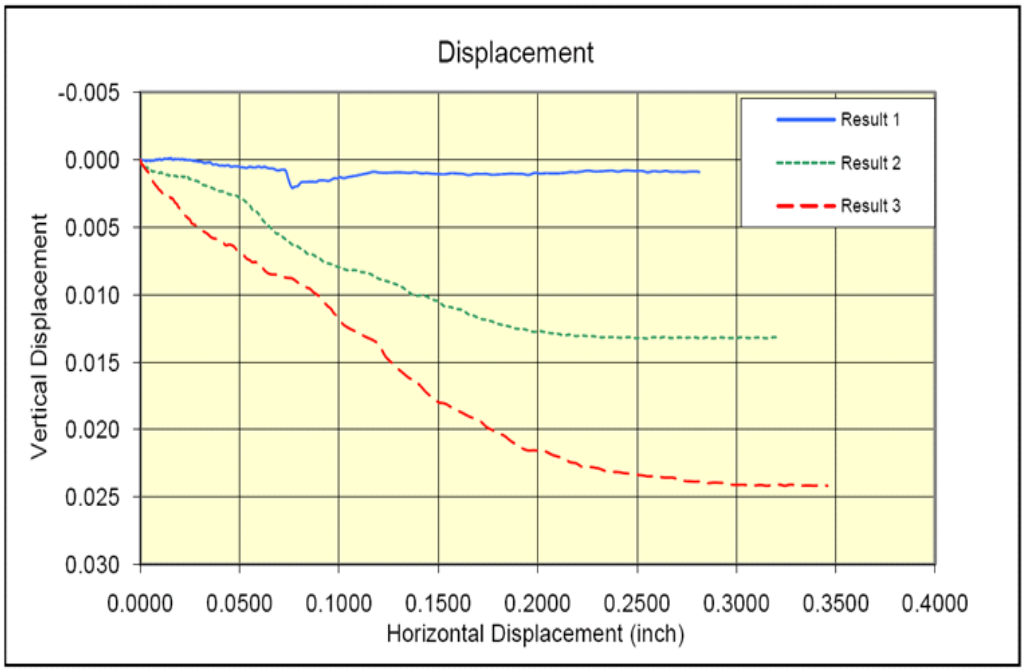
Displacement
Vertical Displacement
-0.005
0.000
0.005
0.010
0.015
0.020
0.025
0.030
0.0000
0.0500
0.1000
0.1500
0.2000
0.2500
0.3000
0.3500
0.4000
Horizontal Displacement (inch)
Result 1
Result 2
Result 3

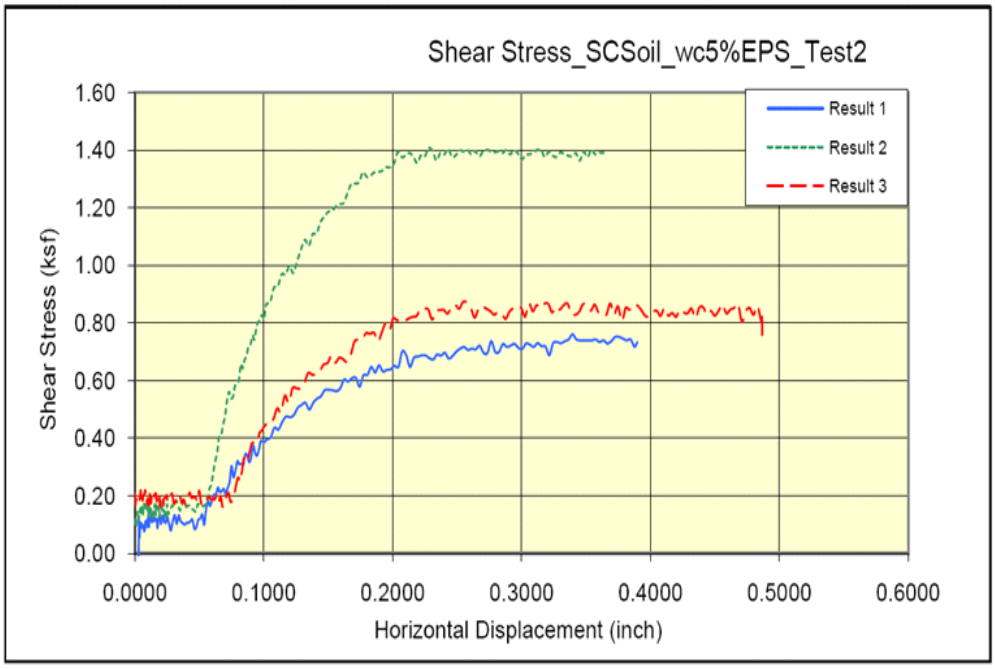
Shear Stress_SCSoil_wc5%EPS_Test2
Result 1
Result 2
Result 3
Shear Stress (ksf)
1.60
1.40
1.20
1.00
0.80
0.60
0.40
0.20
0.00
0.0000
0.1000
0.2000
0.3000
0.4000
0.5000
0.6000
Horizontal Displacement (inch)

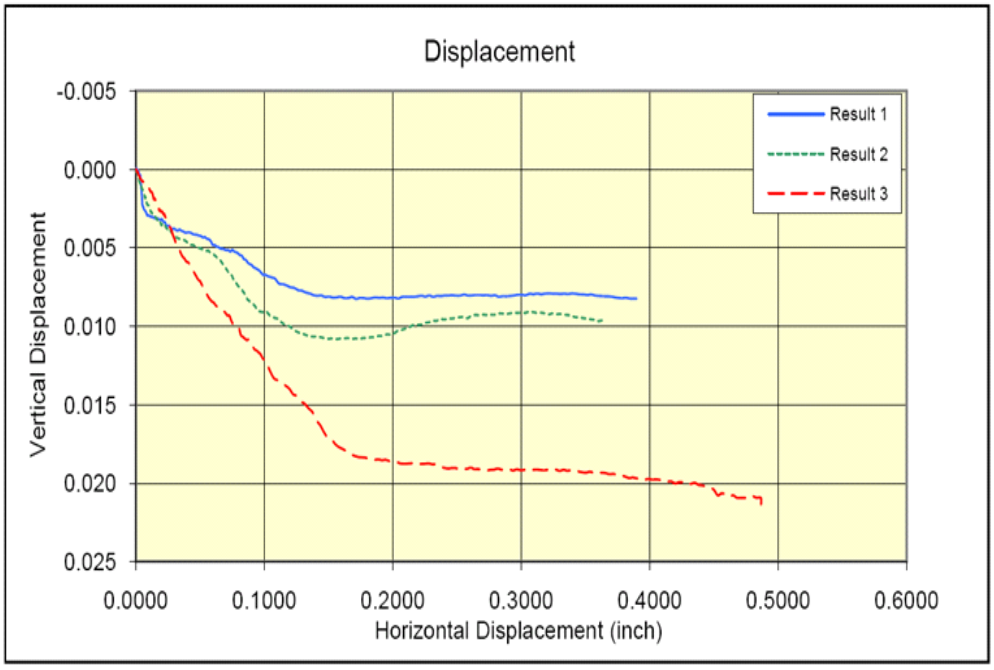
Displacement
Result 1
Result 2
Result 3
Vertical Displacement
-0.005
0.000
0.005
0.010
0.015
0.020
0.025
0.0000
0.1000
0.2000
0.3000
0.4000
0.5000
0.6000
Horizontal Displacement (inch)

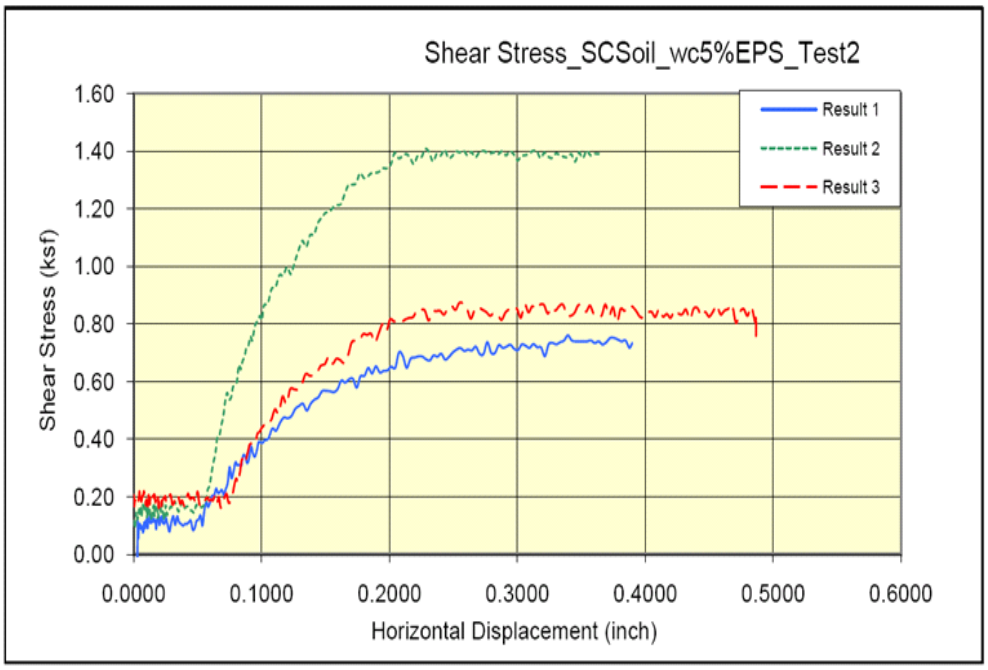
Shear Stress_SCSoil_wc5%EPS_Test2
Result 1
Result 2
Result 3
Shear Stress (ksf)
1.60
1.40
1.20
1.00
0.80
0.60
0.40
0.20
0.00
0.0000
0.1000
0.2000
0.3000
0.4000
0.5000
0.6000
Horizontal Displacement (inch)

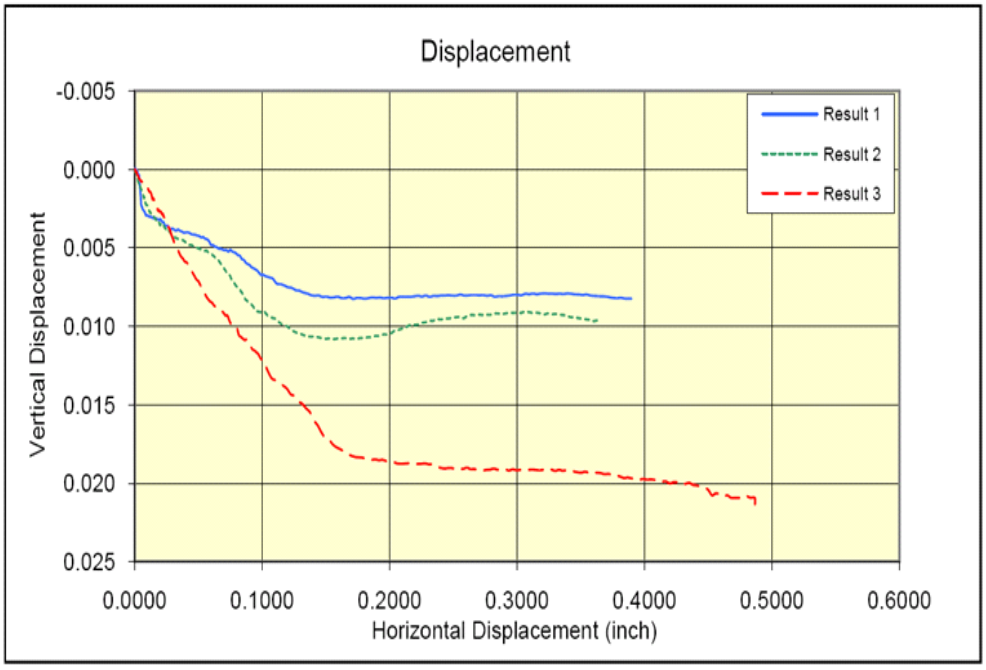
Displacement
Result 1
Result 2
Result 3
Vertical Displacement
-0.005
0.000
0.005
0.010
0.015
0.020
0.025
0.0000
0.1000
0.2000
0.3000
0.4000
0.5000
0.6000
Horizontal Displacement (inch)

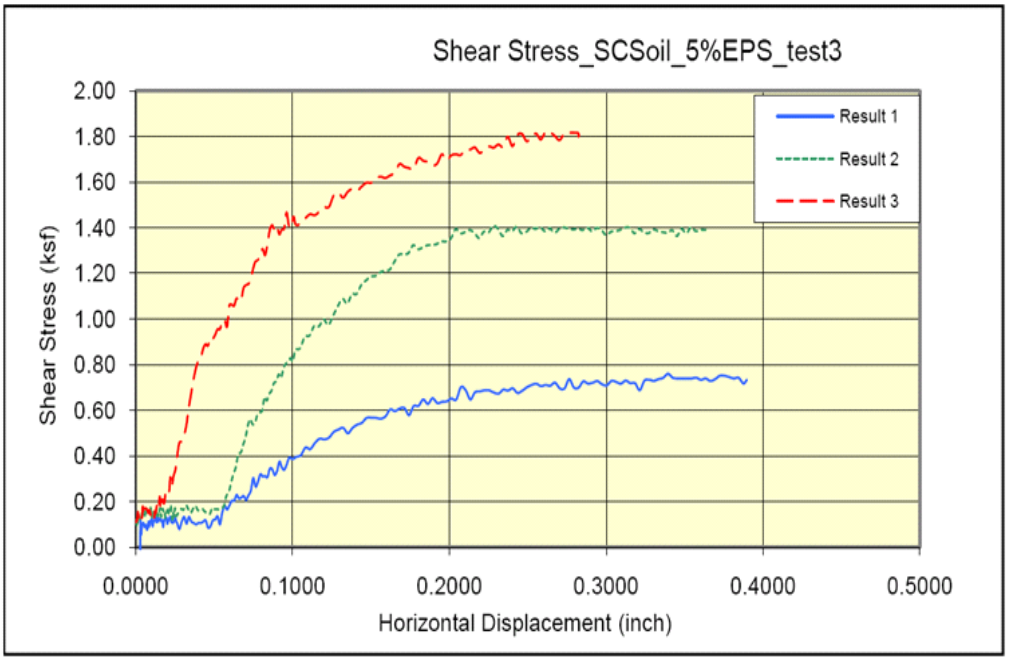
Shear Stress_SCSoil_5%EPS_test3
Shear Stress (ksf)
2.00
1.80
1.60
1.40
1.20
1.00
0.80
0.60
0.40
0.20
0.00
0.0000
0.1000
0.2000
0.3000
0.4000
0.5000
Horizontal Displacement (inch)
Result 1
Result 2
Result 3

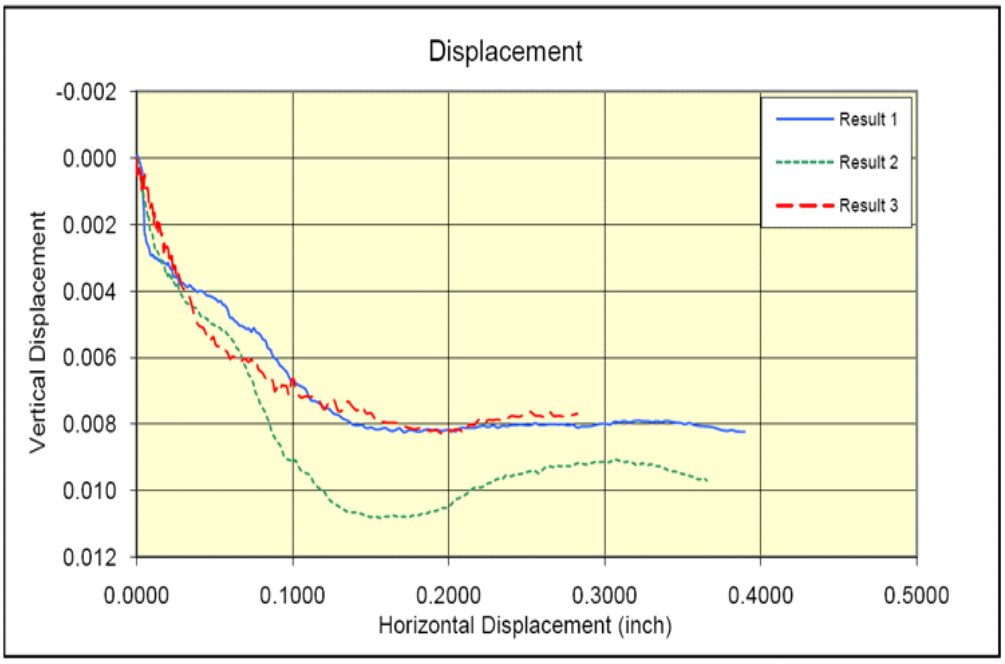
Displacement
Vertical Displacement
-0.002
0.000
0.002
0.004
0.006
0.008
0.010
0.012
0.0000
0.1000
0.2000
0.3000
0.4000
0.5000
Horizontal Displacement (inch)
Result 1
Result 2
Result 3

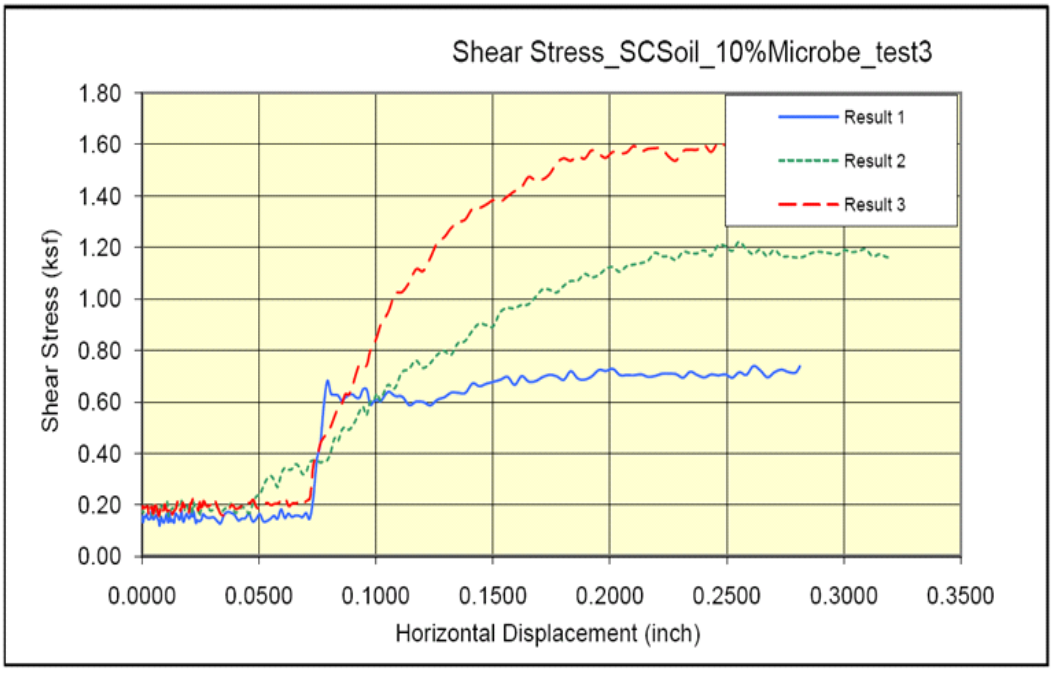
Shear Stress_SCSoil_10%Microbe_test3
Shear Stress (ksf)
1.80
1.60
1.40
1.20
1.00
0.80
0.60
0.40
0.20
0.00
0.0000
0.0500
0.1000
0.1500
0.2000
0.2500
0.3000
0.3500
Horizontal Displacement (inch)
Result 1
Result 2
Result 3

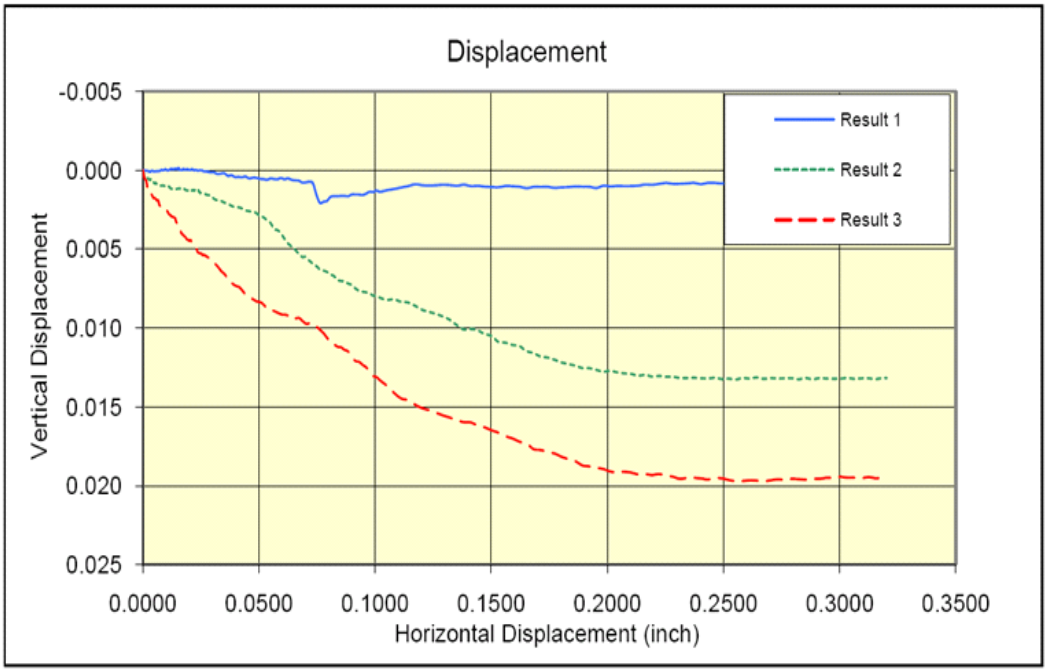
Displacement
Vertical Displacement
-0.005
0.000
0.005
0.010
0.015
0.020
0.025
0.0000
0.0500
0.1000
0.1500
0.2000
0.2500
0.3000
0.3500
Horizontal Displacement (inch)
Result 1
Result 2
Result 3

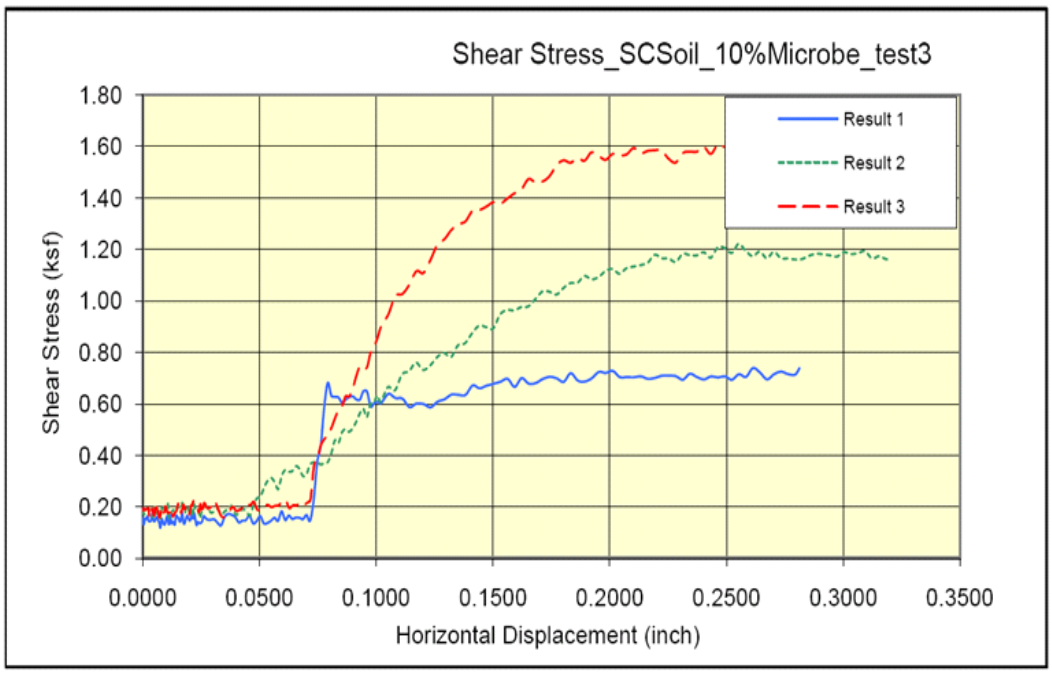
Shear Stress_SCSoil_10%Microbe_test3
Shear Stress (ksf)
1.80
1.60
1.40
1.20
1.00
0.80
0.60
0.40
0.20
0.00
0.0000
0.0500
0.1000
0.1500
0.2000
0.2500
0.3000
0.3500
Horizontal Displacement (inch)
Result 1
Result 2
Result 3

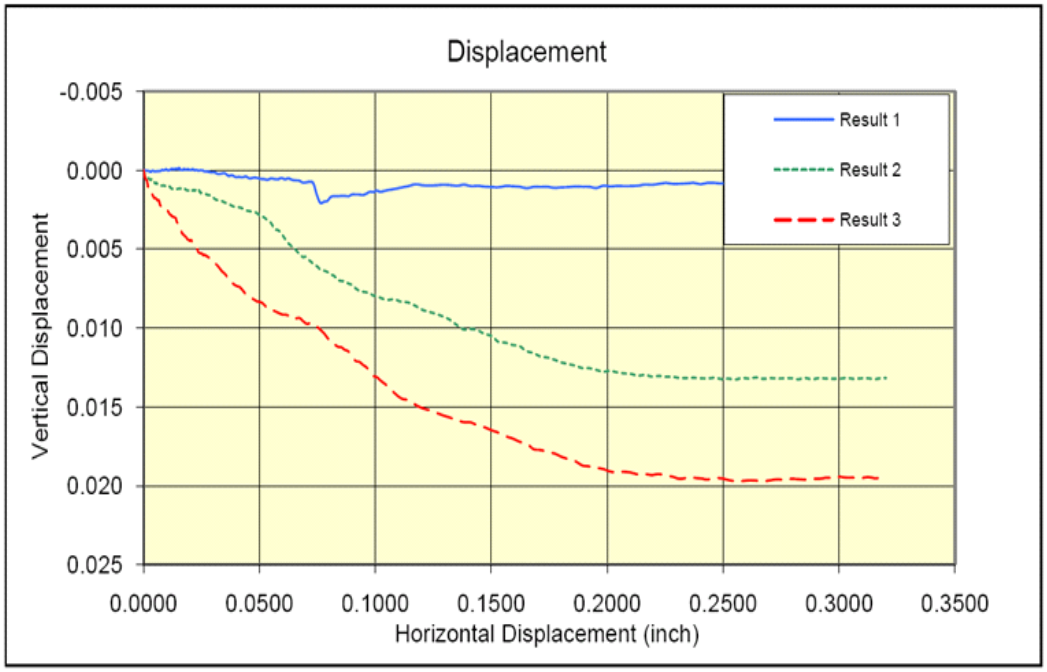
Displacement
Vertical Displacement
-0.005
0.000
0.005
0.010
0.015
0.020
0.025
0.0000
0.0500
0.1000
0.1500
0.2000
0.2500
0.3000
0.3500
Horizontal Displacement (inch)
Result 1
Result 2
Result 3

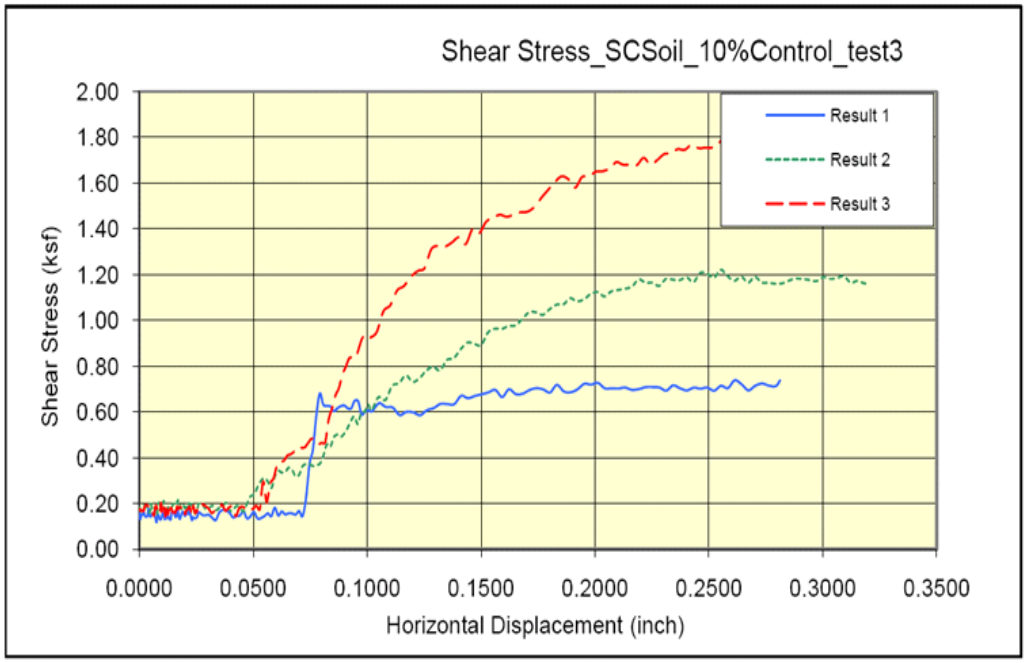
Shear Stress_SCSoil_10%Control_test3
Shear Stress (ksf)
2.00
1.80
1.60
1.40
1.20
1.00
0.80
0.60
0.40
0.20
0.00
0.0000
0.0500
0.1000
0.1500
0.2000
0.2500
0.3000
0.3500
Horizontal Displacement (inch)
Result 1
Result 2
Result 3

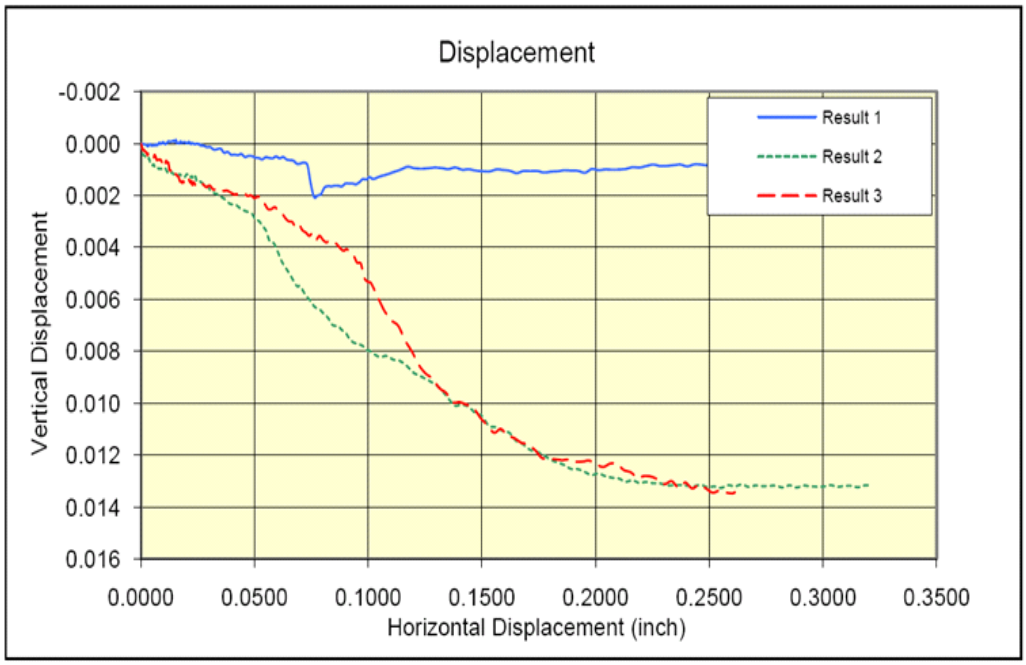
Displacement
Vertical Displacement
-0.002
0.000
0.002
0.004
0.006
0.008
0.010
0.012
0.014
0.016
0.0000
0.0500
0.1000
0.1500
0.2000
0.2500
0.3000
0.3500
Horizontal Displacement (inch)
Result 1
Result 2
Result 3

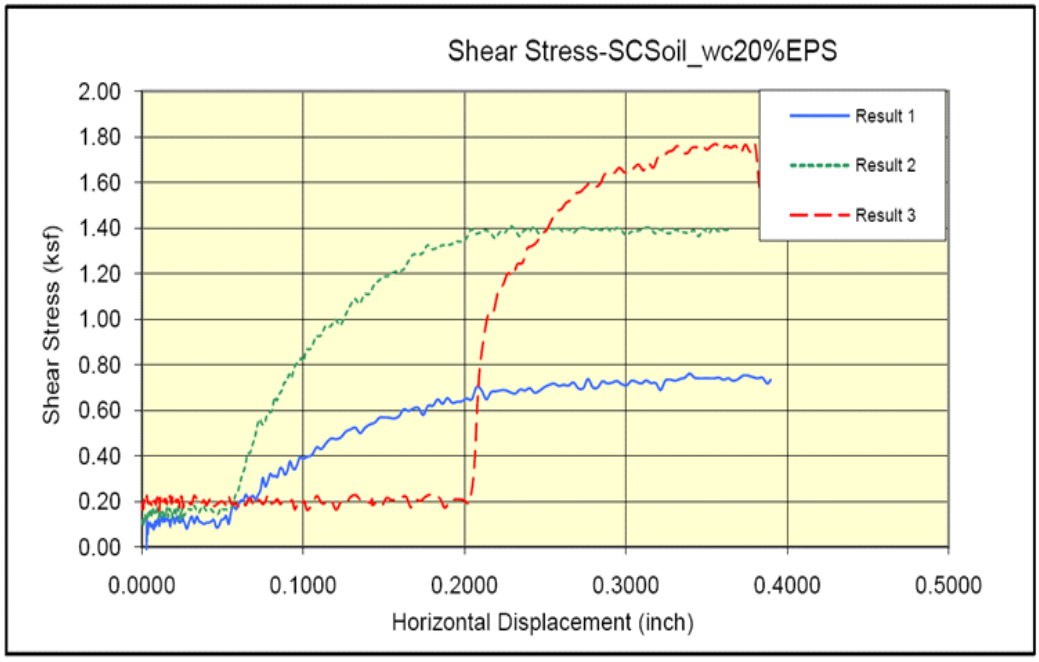
Shear Stress-SCSoil_wc20%EPS
Shear Stress (ksf)
2.00
1.80
1.60
1.40
1.20
1.00
0.80
0.60
0.40
0.20
0.00
0.0000
0.1000
0.2000
0.3000
0.4000
0.5000
Horizontal Displacement (inch)
Result 1
Result 2
Result 3

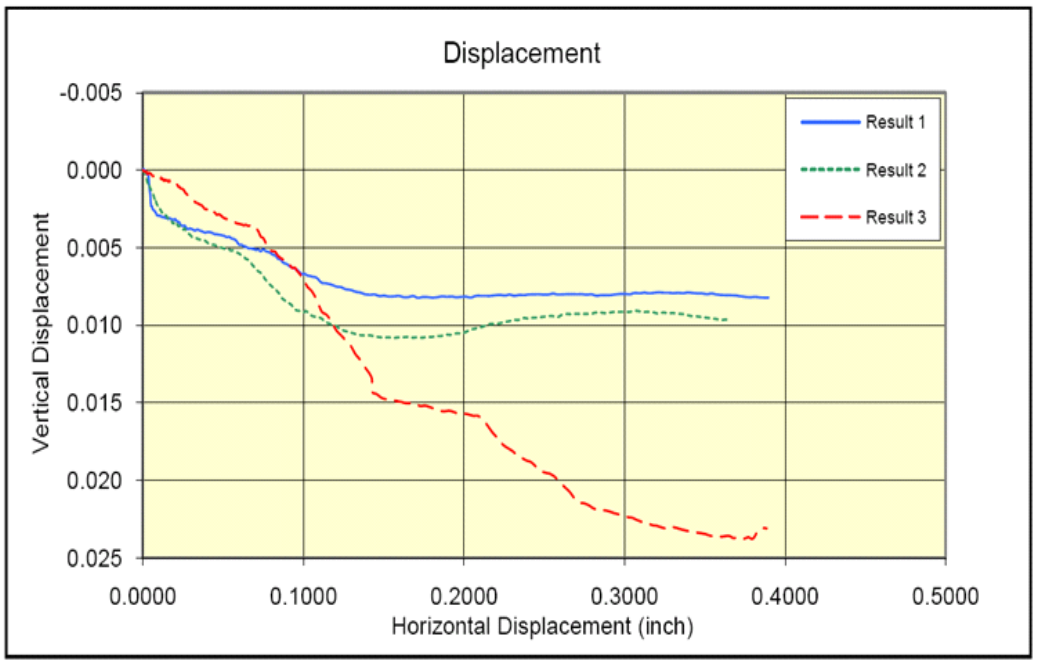
Displacement
Vertical Displacement
-0.005
0.000
0.005
0.010
0.015
0.020
0.025
0.0000
0.1000
0.2000
0.3000
0.4000
0.5000
Horizontal Displacement (inch)
Result 1
Result 2
Result 3

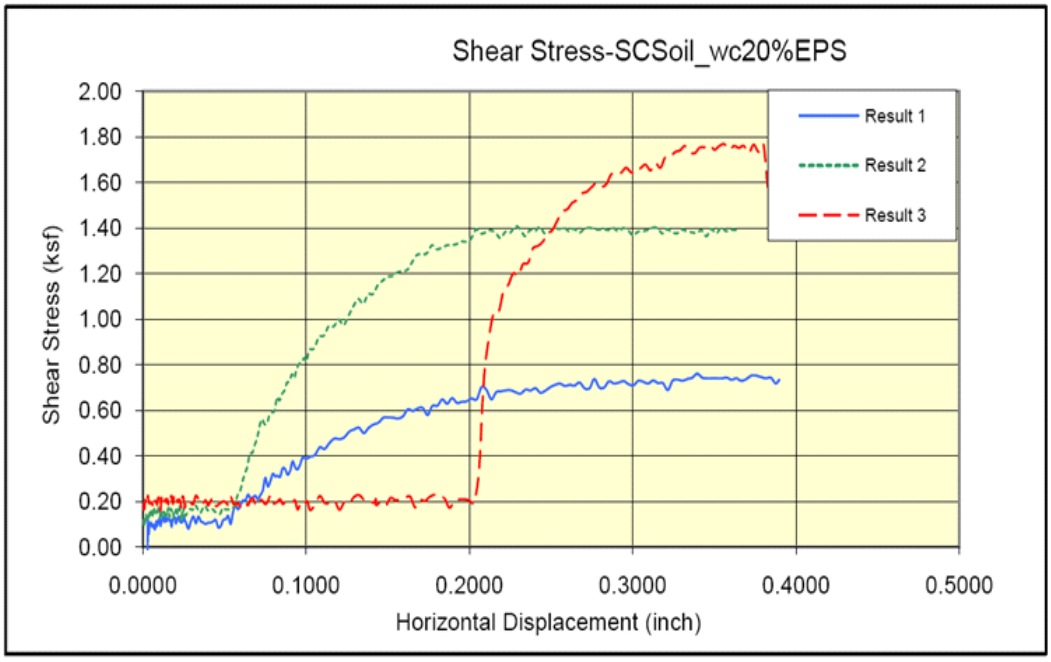
Shear Stress-SCSoil_wc20%EPS
Shear Stress (ksf)
2.00
1.80
1.60
1.40
1.20
1.00
0.80
0.60
0.40
0.20
0.00
0.0000
0.1000
0.2000
0.3000
0.4000
0.5000
Horizontal Displacement (inch)
Result 1
Result 2
Result 3

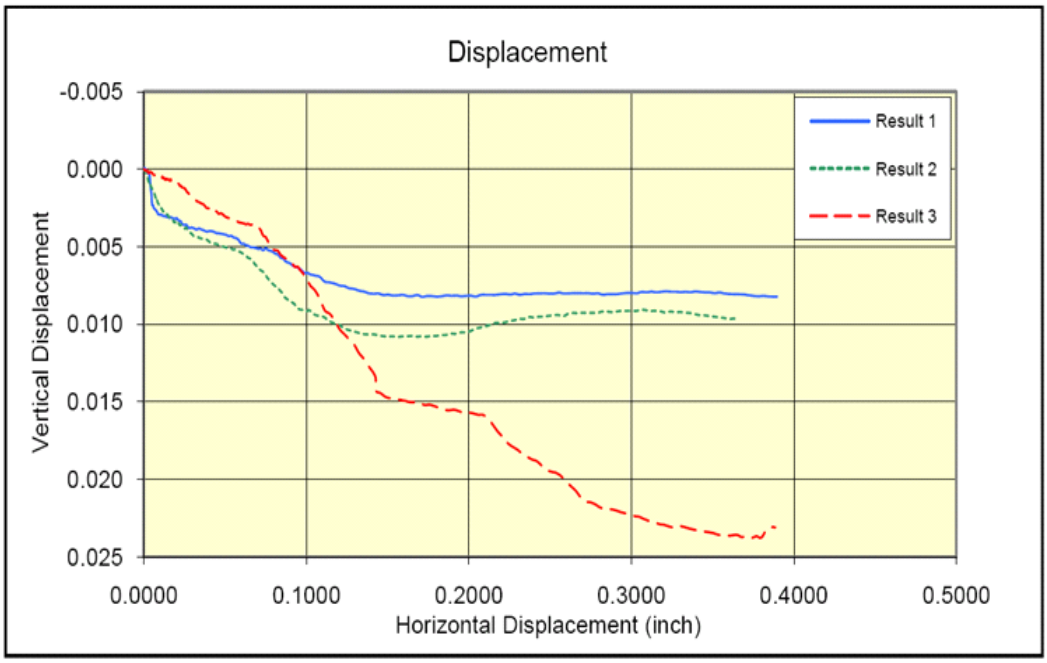
Displacement
Vertical Displacement
-0.005
0.000
0.005
0.010
0.015
0.020
0.025
0.0000
0.1000
0.2000
0.3000
0.4000
0.5000
Horizontal Displacement (inch)
Result 1
Result 2
Result 3

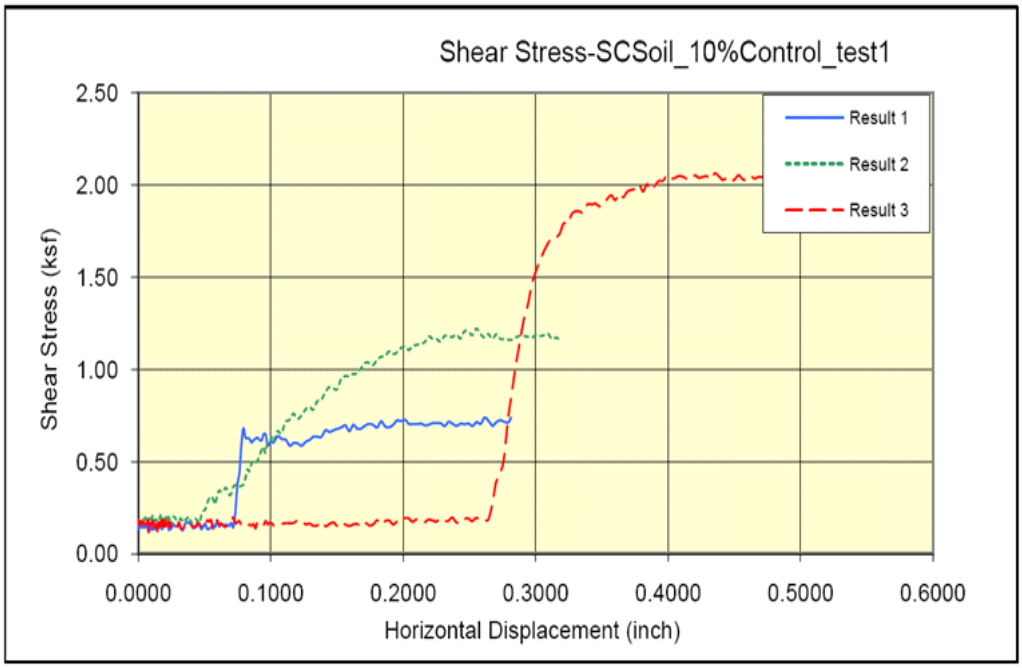
Shear Stress-SCSoil_10%Control_test1
Shear Stress (ksf)
2.50
2.00
1.50
1.00
0.50
0.00
0.0000
0.1000
0.2000
0.3000
0.4000
0.5000
0.6000
Horizontal Displacement (inch)
Result 1
Result 2
Result 3

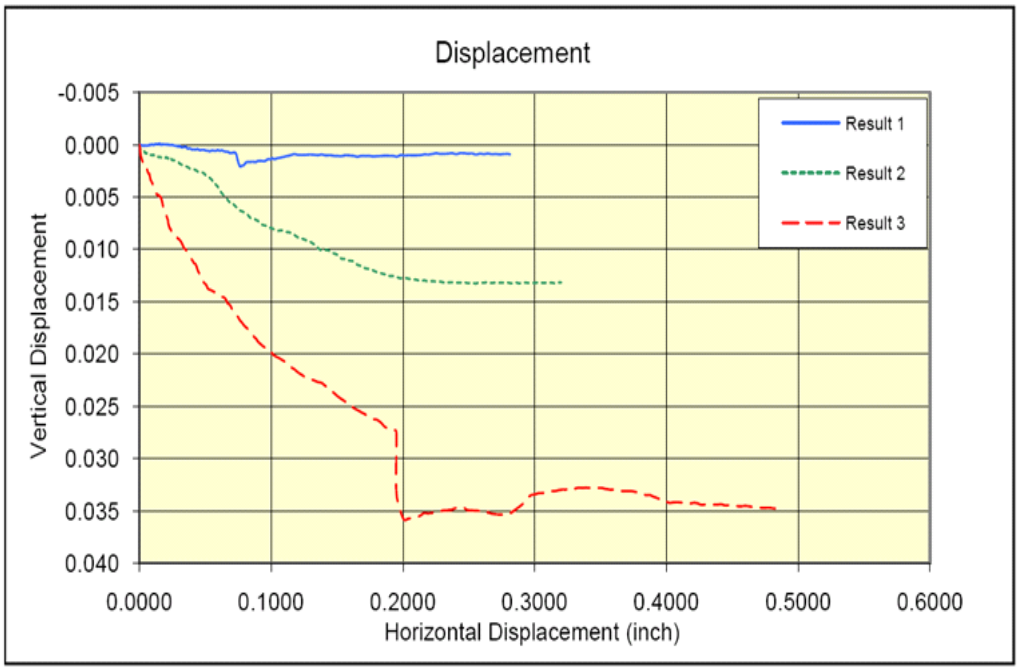
Displacement
Vertical Displacement
-0.005
0.000
0.005
0.010
0.015
0.020
0.025
0.030
0.035
0.040
0.0000
0.1000
0.2000
0.3000
0.4000
0.5000
0.6000
Horizontal Displacement (inch)
Result 1
Result 2
Result 3

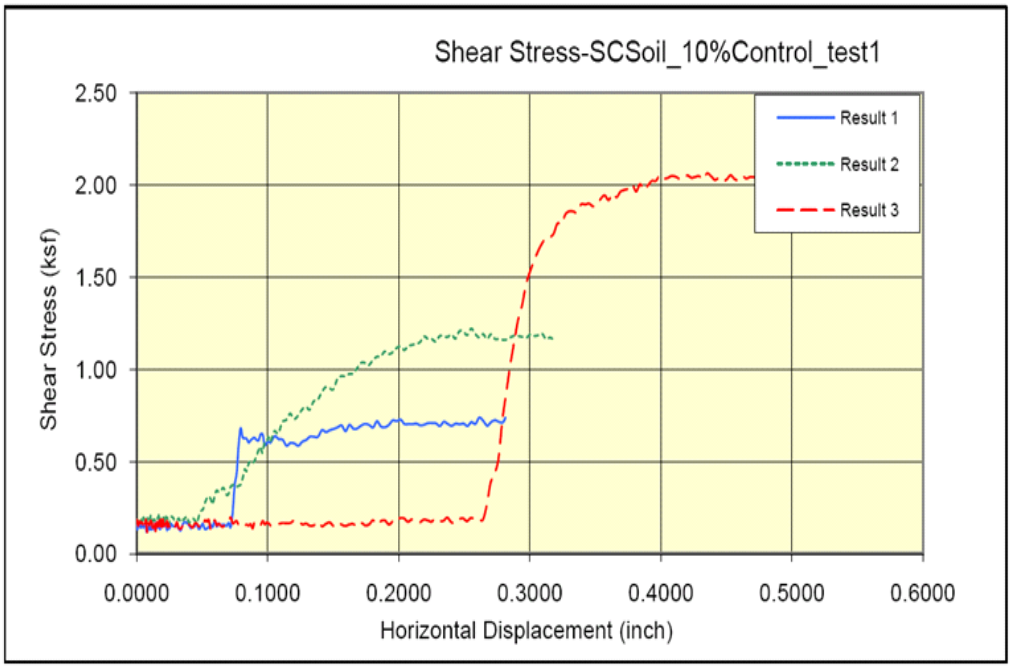
Shear Stress-SCSoil_10%Control_test1
Result 1
Result 2
Result 3
Shear Stress (ksf)
2.50
2.00
1.50
1.00
0.50
0.00
0.0000
0.1000
0.2000
0.3000
0.4000
0.5000
0.6000
Horizontal Displacement (inch)

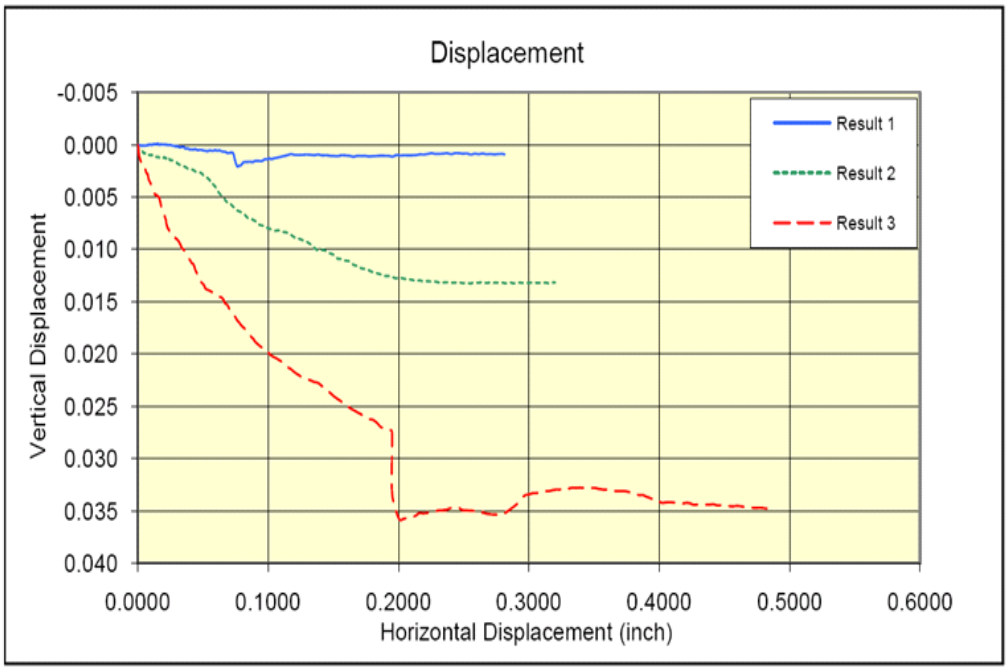
Displacement
Result 1
Result 2
Result 3
Vertical Displacement
-0.005
0.000
0.005
0.010
0.015
0.020
0.025
0.030
0.035
0.040
0.0000
0.1000
0.2000
0.3000
0.4000
0.5000
0.6000
Horizontal Displacement (inch)

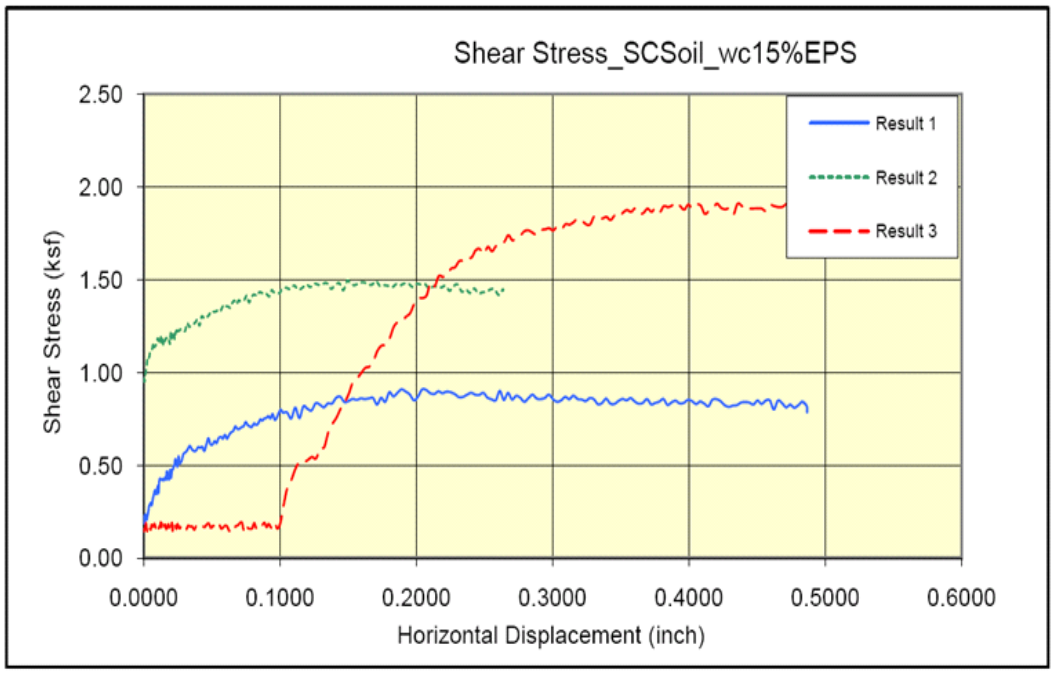
Shear Stress_SCSoil_wc15%EPS
Shear Stress (ksf)
2.50
2.00
1.50
1.00
0.50
0.00
0.0000
0.1000
0.2000
0.3000
0.4000
0.5000
0.6000
Horizontal Displacement (inch)
Result 1
Result 2
Result 3

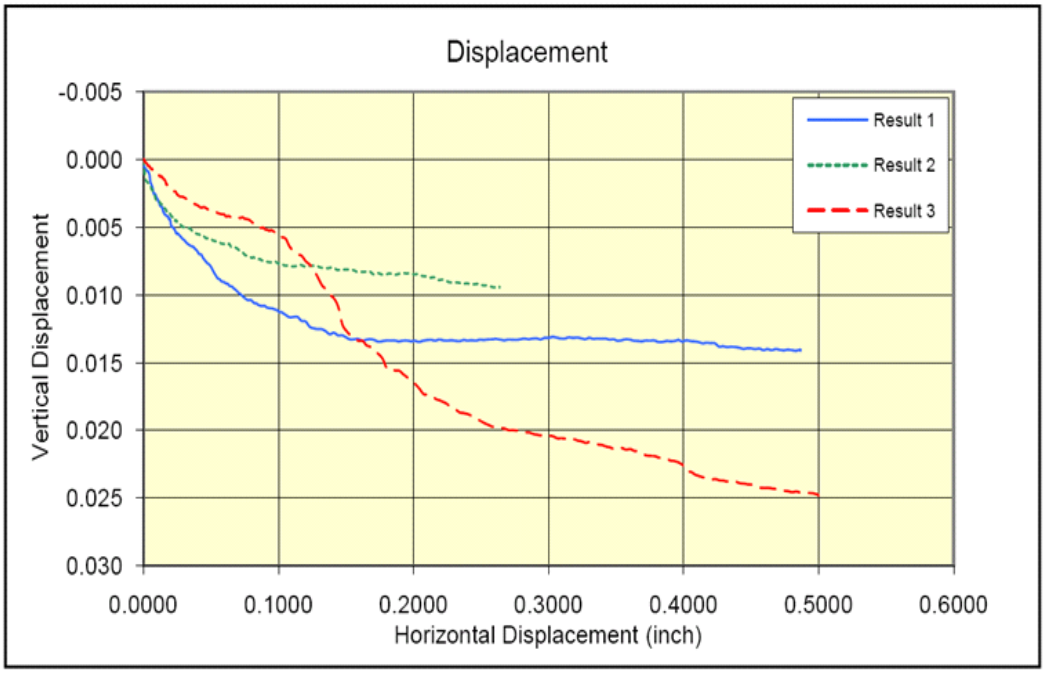
Displacement
Vertical Displacement
-0.005
0.000
0.005
0.010
0.015
0.020
0.025
0.030
0.0000
0.1000
0.2000
0.3000
0.4000
0.5000
0.6000
Horizontal Displacement (inch)
Result 1
Result 2
Result 3

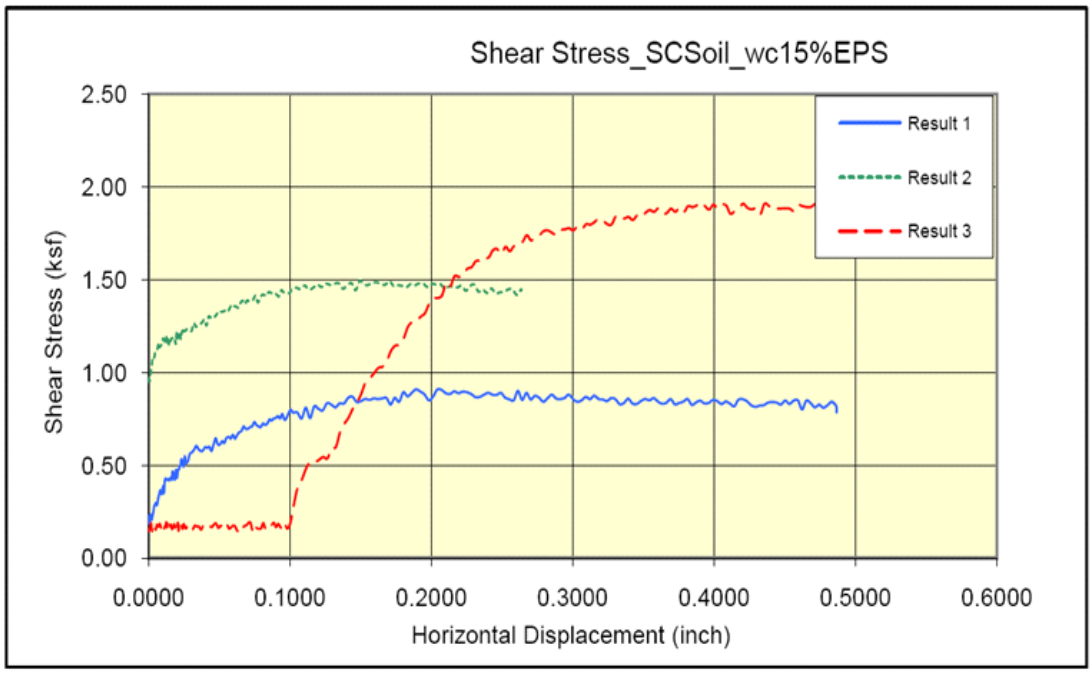
Shear Stress_SCSoil_wc15%EPS
Shear Stress (ksf)
2.50
2.00
1.50
1.00
0.50
0.00
0.0000
0.1000
0.2000
0.3000
0.4000
0.5000
0.6000
Horizontal Displacement (inch)
Result 1
Result 2
Result 3

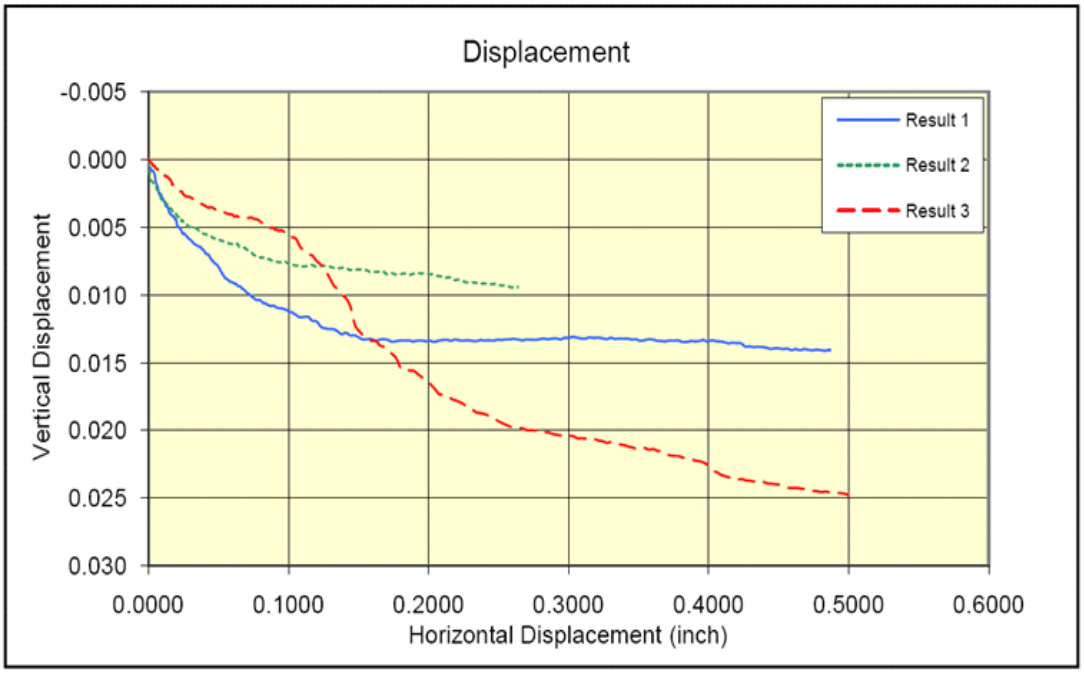
Displacement
Vertical Displacement
-0.005
0.000
0.005
0.010
0.015
0.020
0.025
0.030
0.0000
0.1000
0.2000
0.3000
0.4000
0.5000
0.6000
Horizontal Displacement (inch)
Result 1
Result 2
Result 3

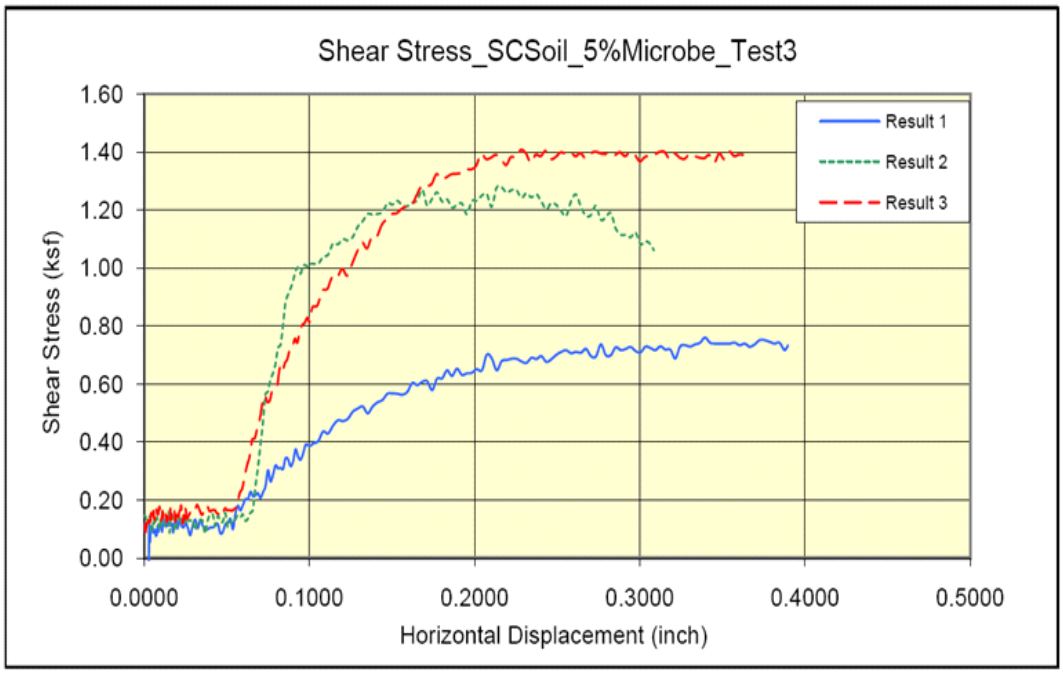
Shear Stress_SCSoil_5%Microbe_Test3
Shear Stress (ksf)
1.60
1.40
1.20
1.00
0.80
0.60
0.40
0.20
0.00
0.0000
0.1000
0.2000
0.3000
0.4000
0.5000
Horizontal Displacement (inch)
Result 1
Result 2
Result 3

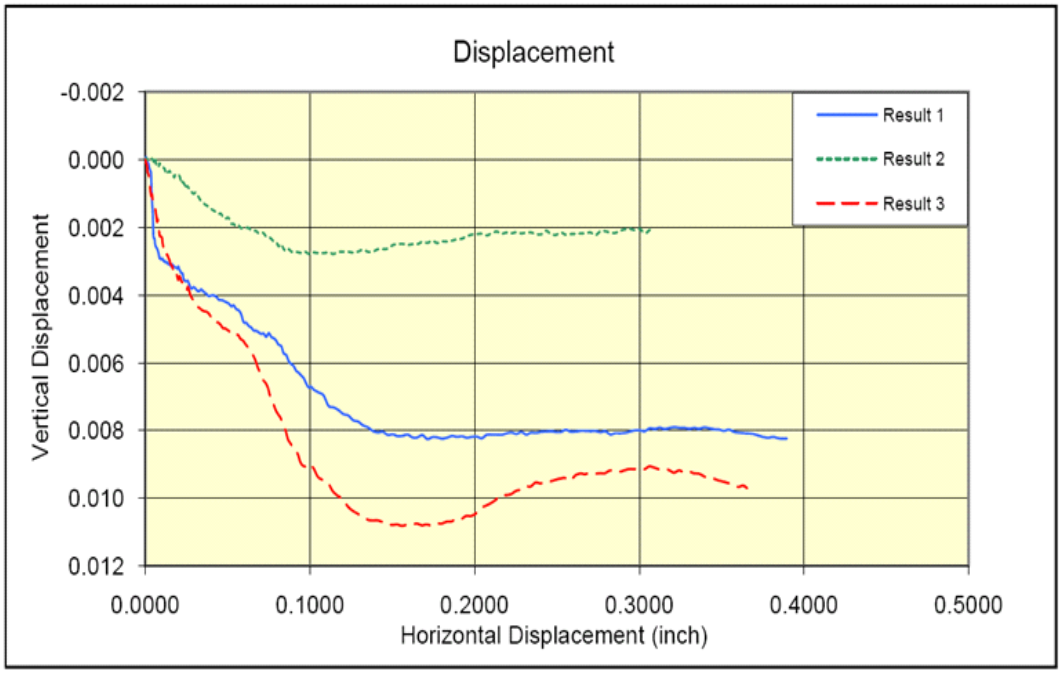
Displacement
Vertical Displacement
-0.002
0.000
0.002
0.004
0.006
0.008
0.010
0.012
0.0000
0.1000
0.2000
0.3000
0.4000
0.5000
Horizontal Displacement (inch)
Result 1
Result 2
Result 3

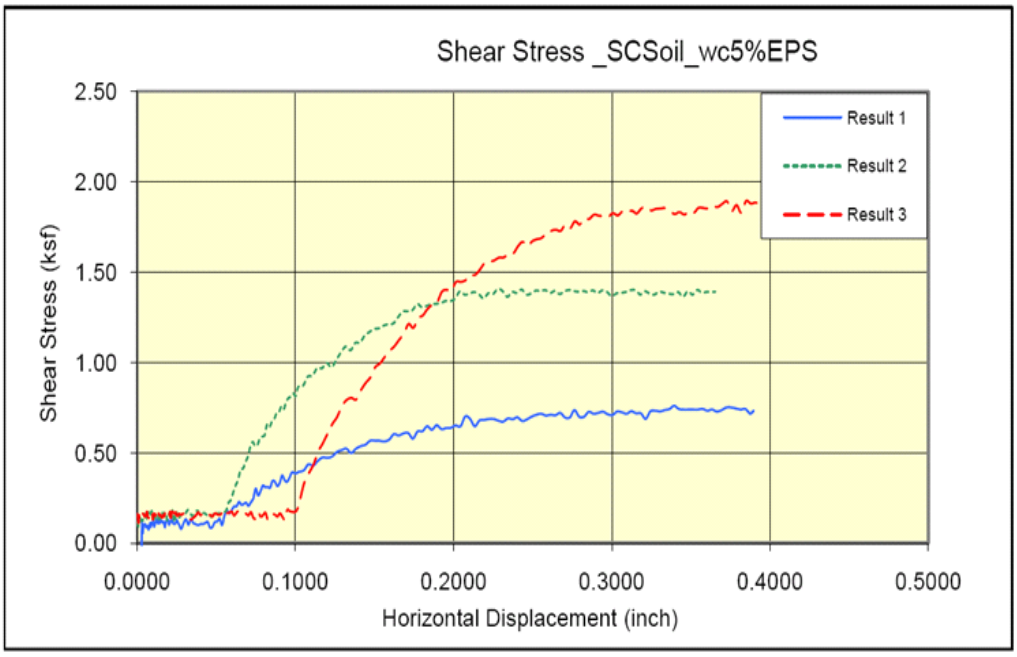
Shear Stress _SCSoil_wc5%EPS
Shear Stress (ksf)
2.50
2.00
1.50
1.00
0.50
0.00
0.0000
0.1000
0.2000
0.3000
0.4000
0.5000
Horizontal Displacement (inch)
Result 1
Result 2
Result 3

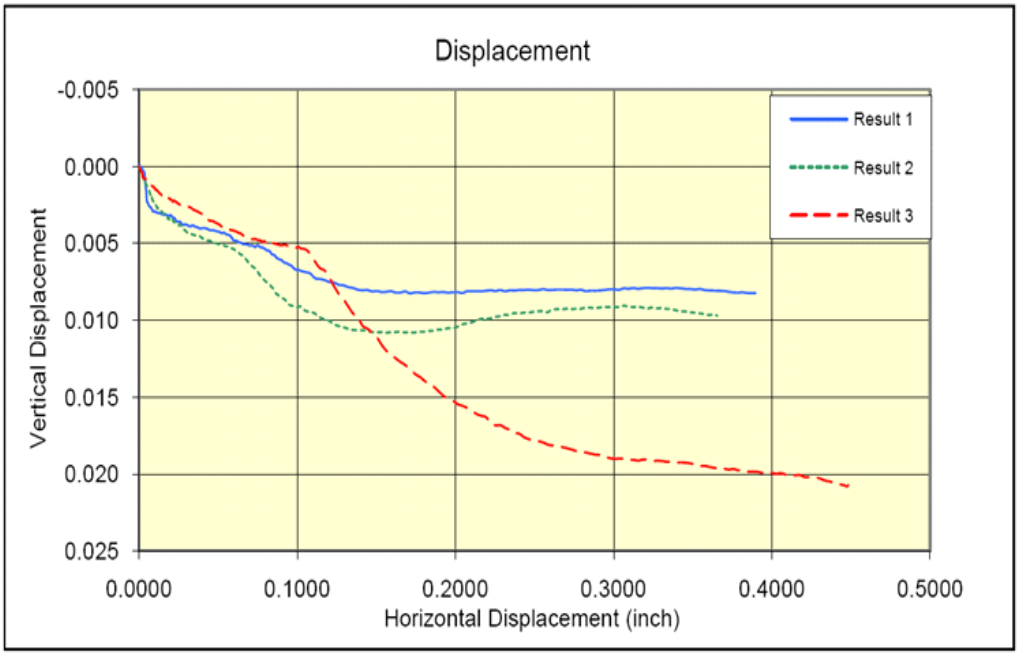
Displacement
Vertical Displacement
-0.005
0.000
0.005
0.010
0.015
0.020
0.025
0.0000
0.1000
0.2000
0.3000
0.4000
0.5000
Horizontal Displacement (inch)
Result 1
Result 2
Result 3

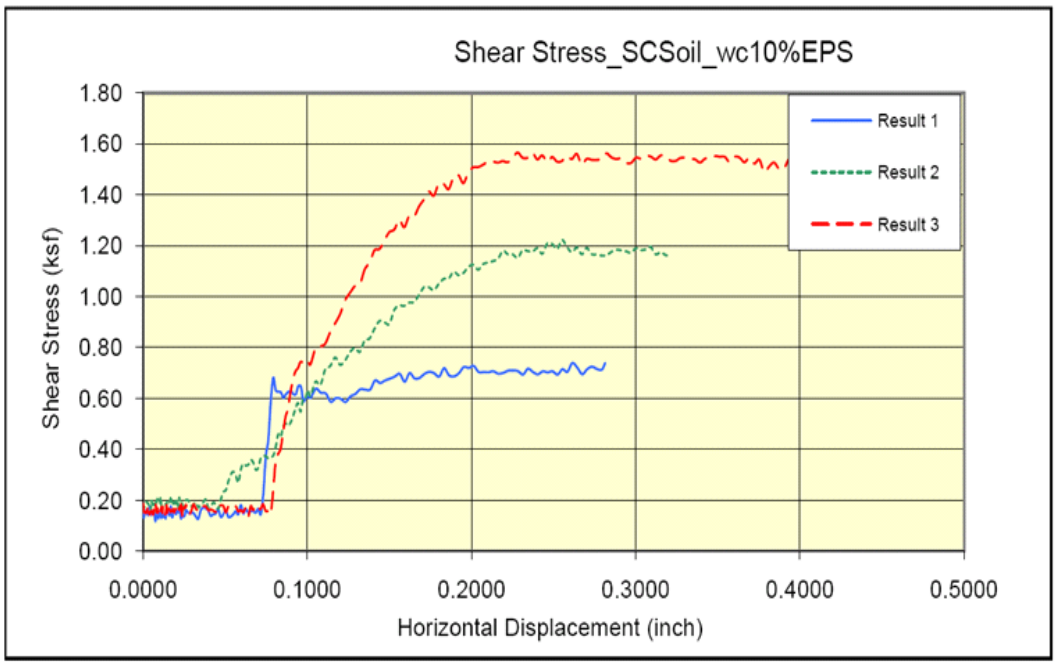
Shear Stress_SCSoil_wc10%EPS
Shear Stress (ksf)
1.80
1.60
1.40
1.20
1.00
0.80
0.60
0.40
0.20
0.00
0.0000
0.1000
0.2000
0.3000
0.4000
0.5000
Horizontal Displacement (inch)
Result 1
Result 2
Result 3

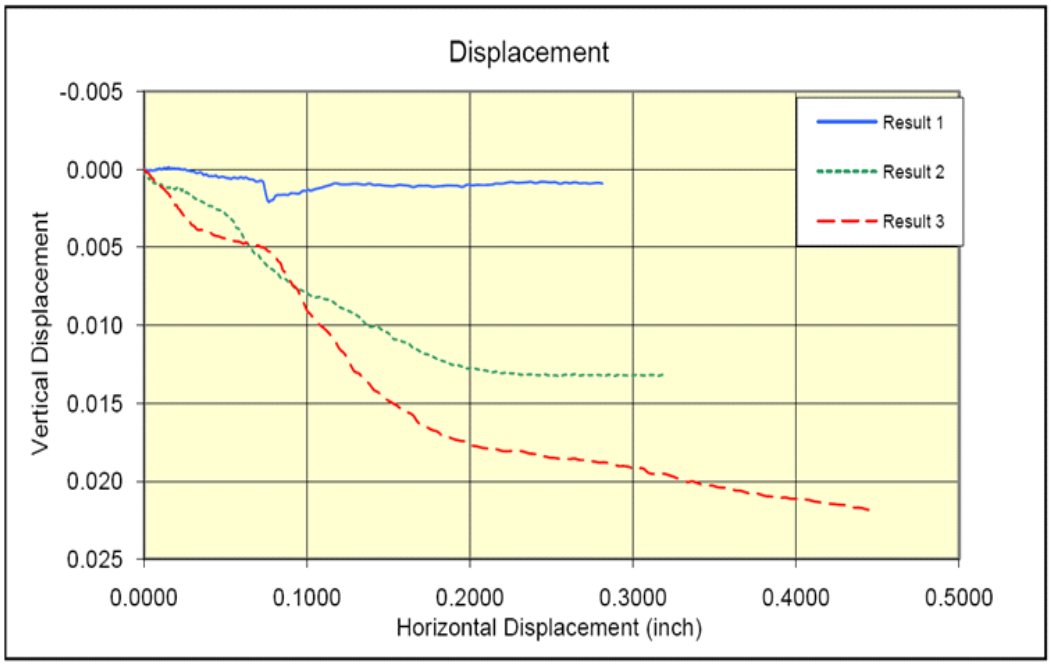
Displacement
Vertical Displacement
-0.005
0.000
0.005
0.010
0.015
0.020
0.025
0.0000
0.1000
0.2000
0.3000
0.4000
0.5000
Horizontal Displacement (inch)
Result 1
Result 2
Result 3

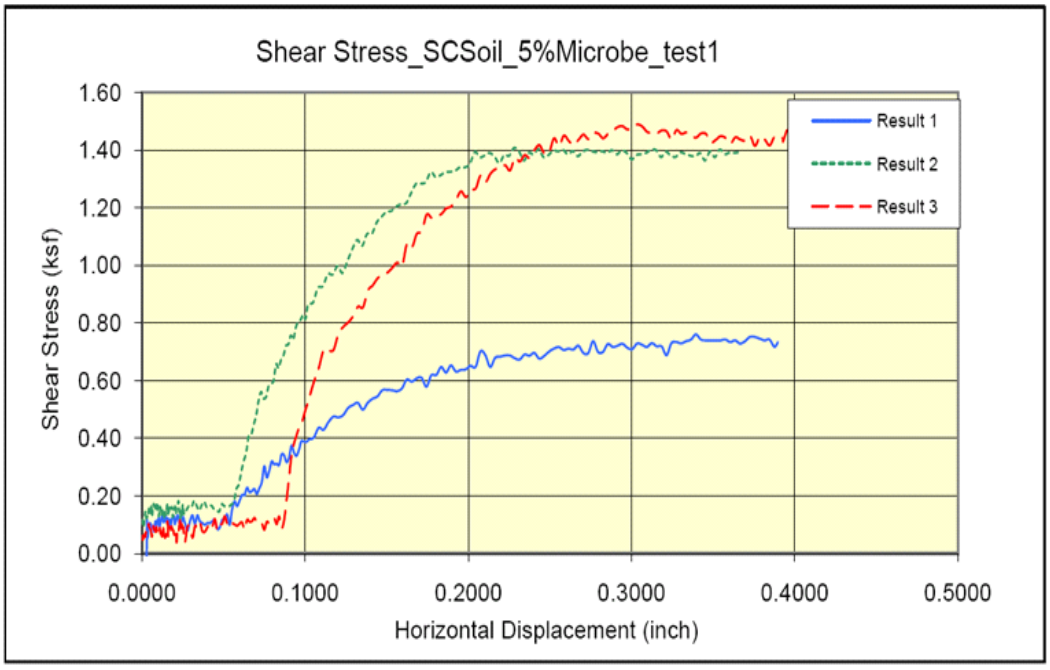
Shear Stress_SCSoil_5%Microbe_test1
Shear Stress (ksf)
1.60
1.40
1.20
1.00
0.80
0.60
0.40
0.20
0.00
0.0000
0.1000
0.2000
0.3000
0.4000
0.5000
Horizontal Displacement (inch)
Result 1
Result 2
Result 3

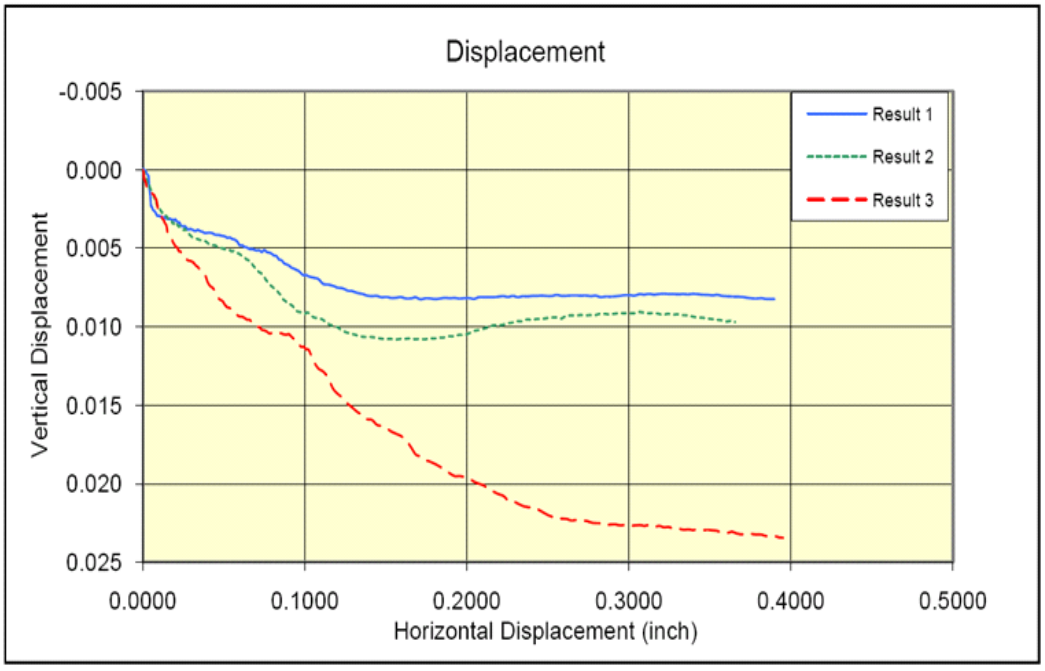
Displacement
Vertical Displacement
-0.005
0.000
0.005
0.010
0.015
0.020
0.025
0.0000
0.1000
0.2000
0.3000
0.4000
0.5000
Horizontal Displacement (inch)
Result 1
Result 2
Result 3

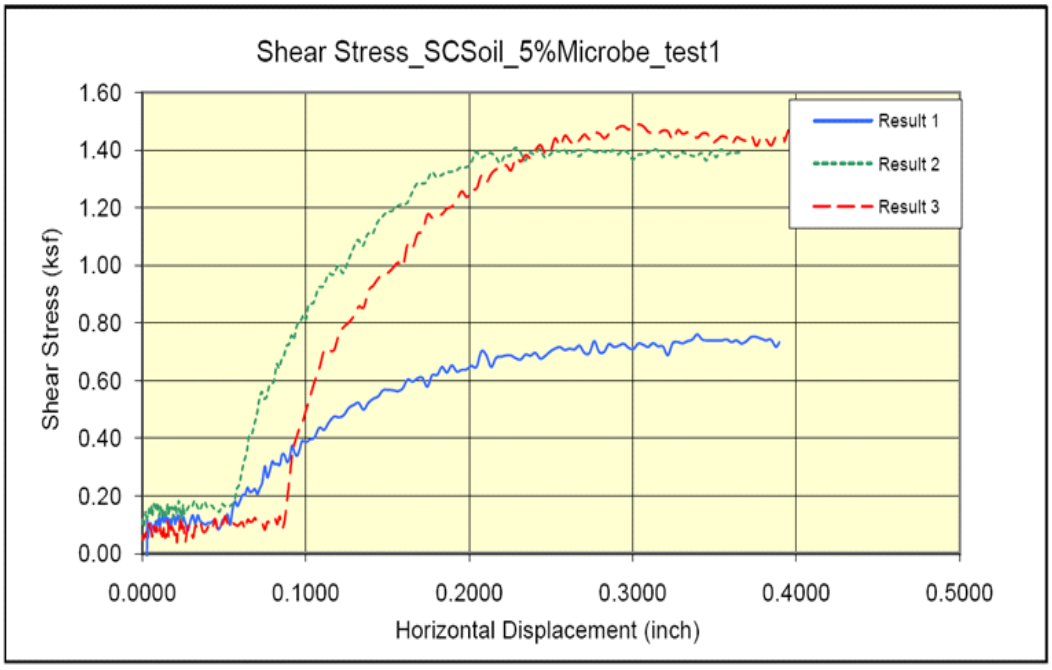
Shear Stress_SCSoil_5%Microbe_test1
Shear Stress (ksf)
1.60
1.40
1.20
1.00
0.80
0.60
0.40
0.20
0.00
0.0000
0.1000
0.2000
0.3000
0.4000
0.5000
Horizontal Displacement (inch)
Result 1
Result 2
Result 3

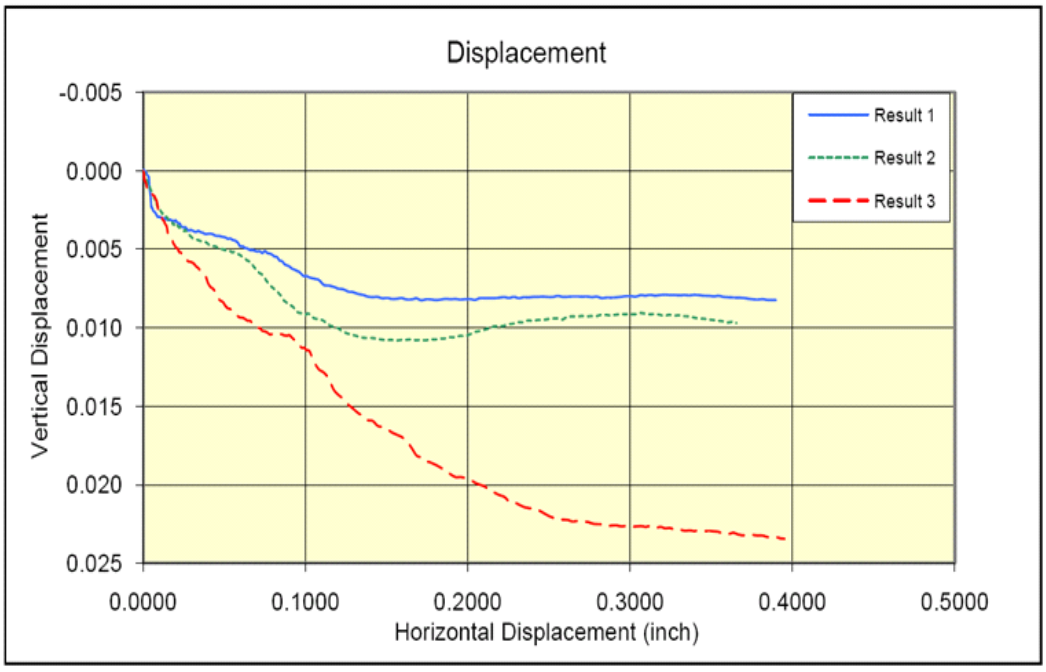
Displacement
Vertical Displacement
-0.005
0.000
0.005
0.010
0.015
0.020
0.025
0.0000
0.1000
0.2000
0.3000
0.4000
0.5000
Horizontal Displacement (inch)
Result 1
Result 2
Result 3

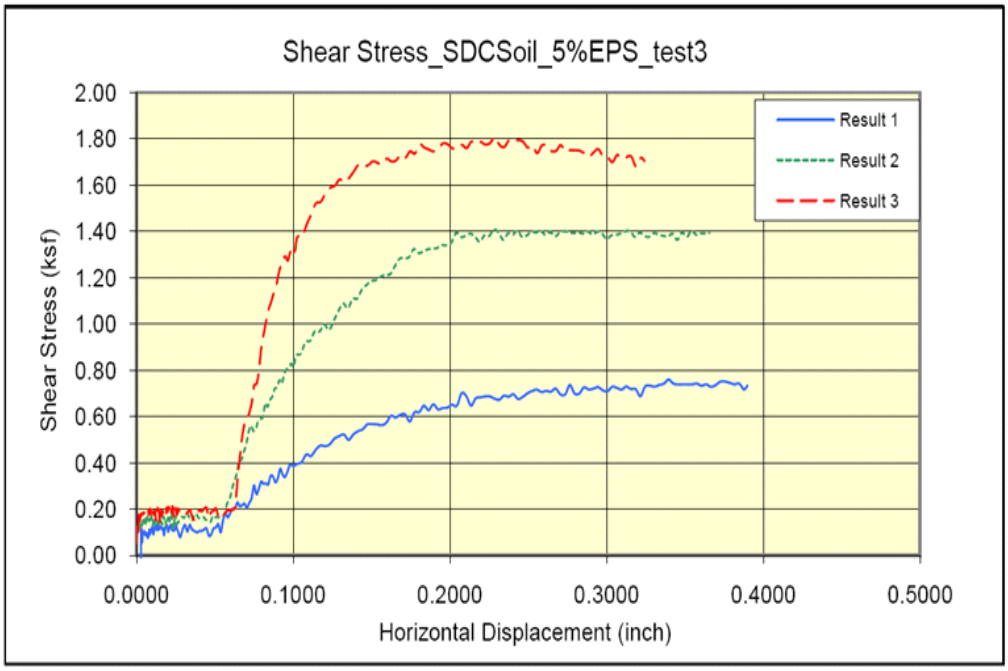
Shear Stress_SDCSoil_5%EPS_test3
Shear Stress (ksf)
2.00
1.80
1.60
1.40
1.20
1.00
0.80
0.60
0.40
0.20
0.00
0.0000
0.1000
0.2000
0.3000
0.4000
0.5000
Horizontal Displacement (inch)
Result 1
Result 2
Result 3

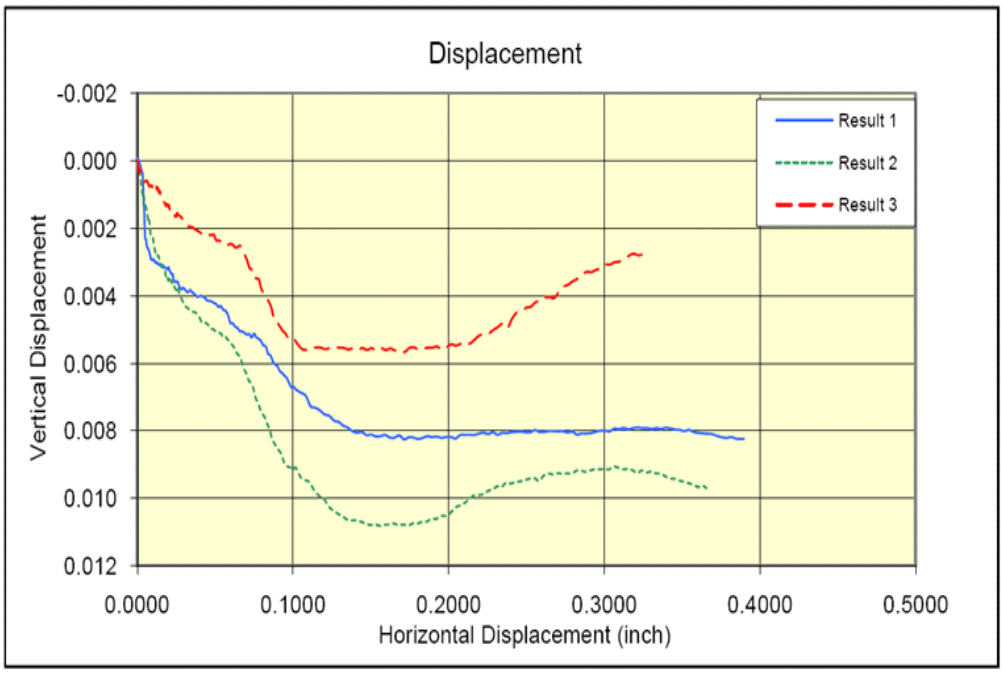
Displacement
Vertical Displacement
-0.002
0.000
0.002
0.004
0.006
0.008
0.010
0.012
0.0000
0.1000
0.2000
0.3000
0.4000
0.5000
Horizontal Displacement (inch)
Result 1
Result 2
Result 3

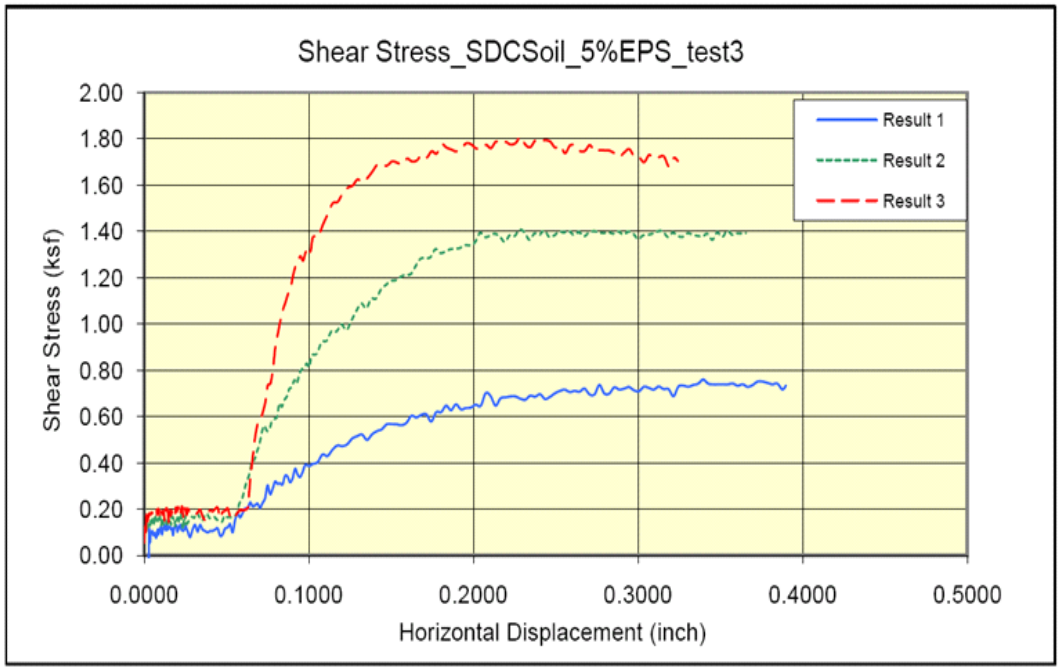
Shear Stress_SDCSoil_5%EPS_test3
Shear Stress (ksf)
2.00
1.80
1.60
1.40
1.20
1.00
0.80
0.60
0.40
0.20
0.00
0.0000
0.1000
0.2000
0.3000
0.4000
0.5000
Horizontal Displacement (inch)
Result 1
Result 2
Result 3

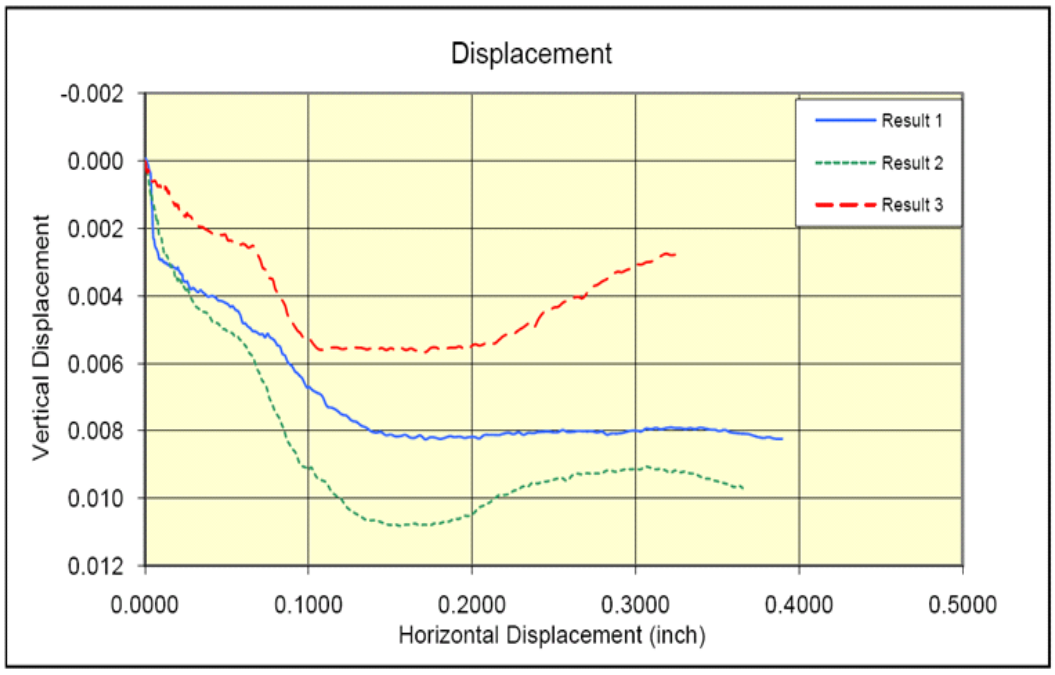
Displacement
Vertical Displacement
-0.002
0.000
0.002
0.004
0.006
0.008
0.010
0.012
0.0000
0.1000
0.2000
0.3000
0.4000
0.5000
Horizontal Displacement (inch)
Result 1
Result 2
Result 3

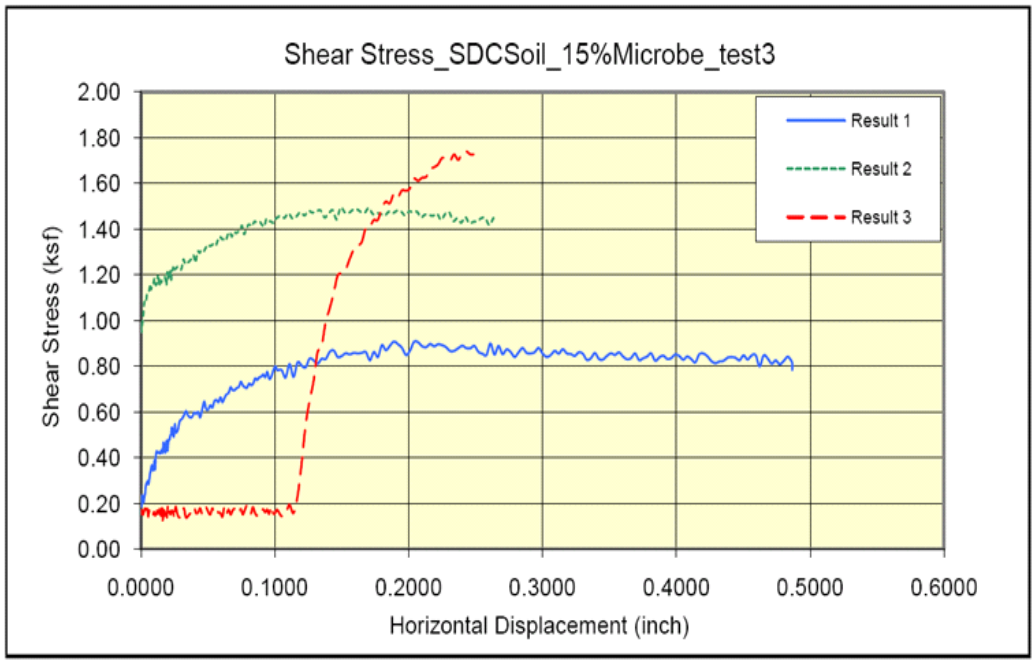
Shear Stress_SDCSoil_15%Microbe_test3
Shear Stress (ksf)
2.00
1.80
1.60
1.40
1.20
1.00
0.80
0.60
0.40
0.20
0.00
0.0000
0.1000
0.2000
0.3000
0.4000
0.5000
0.6000
Horizontal Displacement (inch)
Result 1
Result 2
Result 3

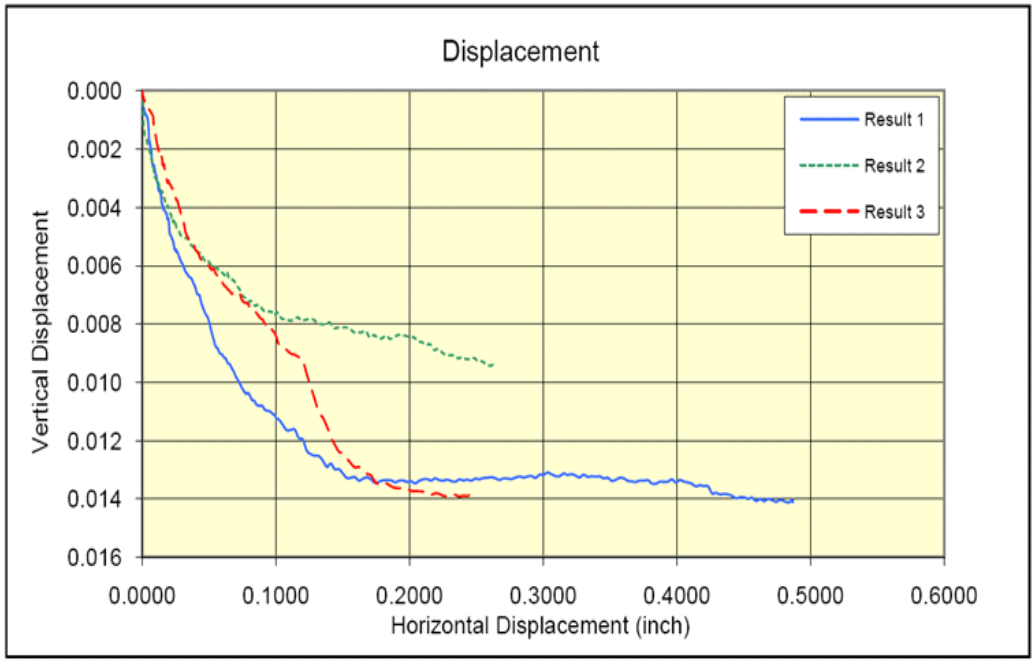
Displacement
Vertical Displacement
0.000
0.002
0.004
0.006
0.008
0.010
0.012
0.014
0.016
0.0000
0.1000
0.2000
0.3000
0.4000
0.5000
0.6000
Horizontal Displacement (inch)
Result 1
Result 2
Result 3

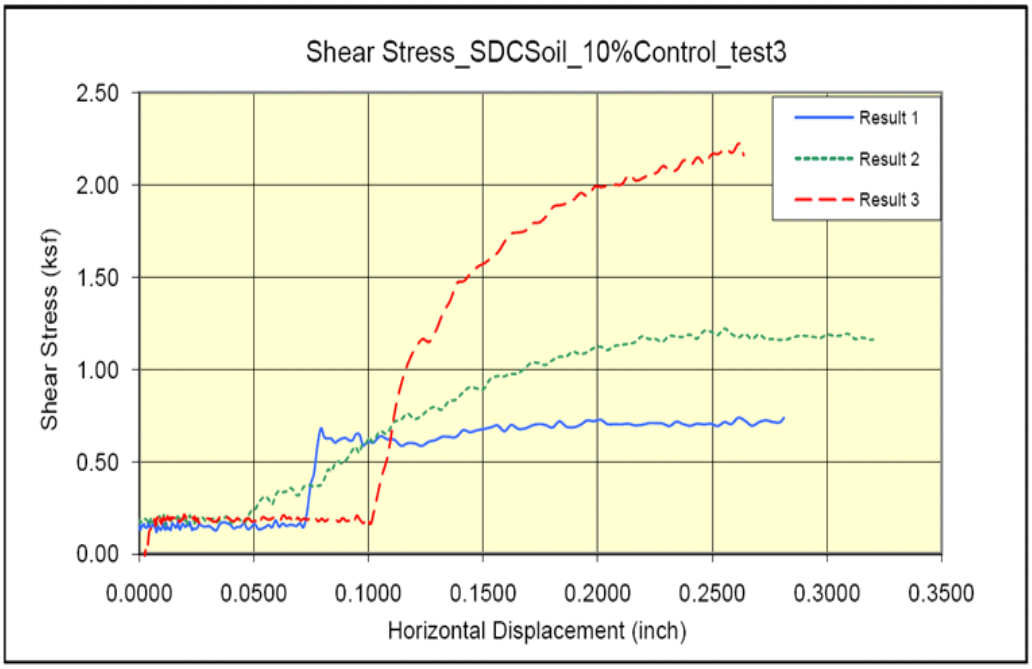
Shear Stress_SDCSoil_10%Control_test3
Shear Stress (ksf)
2.50
2.00
1.50
1.00
0.50
0.00
0.0000
0.0500
0.1000
0.1500
0.2000
0.2500
0.3000
0.3500
Horizontal Displacement (inch)
Result 1
Result 2
Result 3

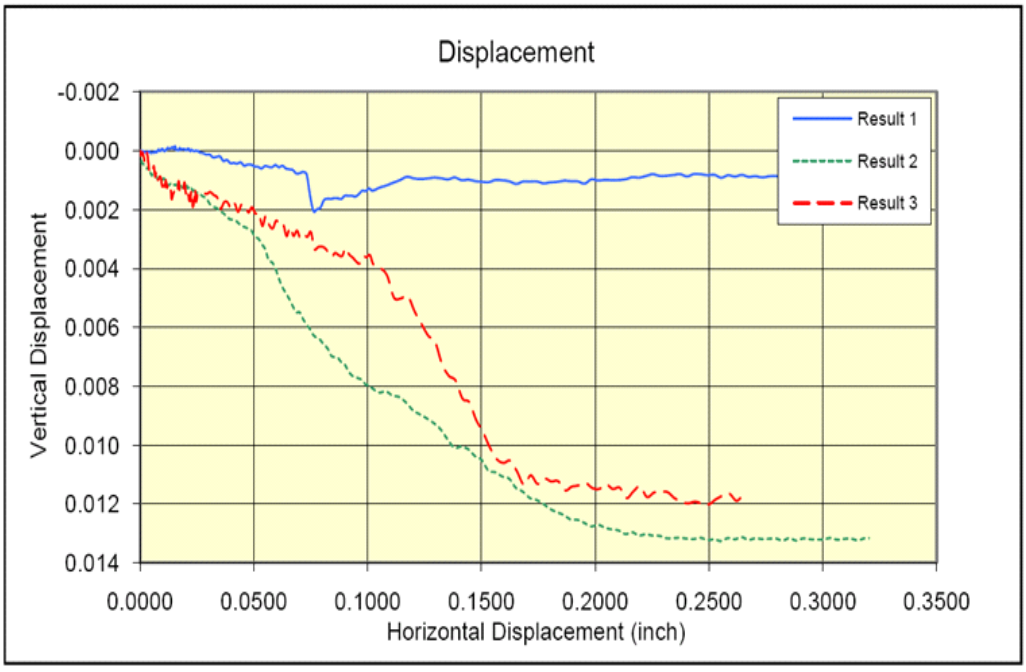
Displacement
Vertical Displacement
-0.002
0.000
0.002
0.004
0.006
0.008
0.010
0.012
0.014
0.0000
0.0500
0.1000
0.1500
0.2000
0.2500
0.3000
0.3500
Horizontal Displacement (inch)
Result 1
Result 2
Result 3

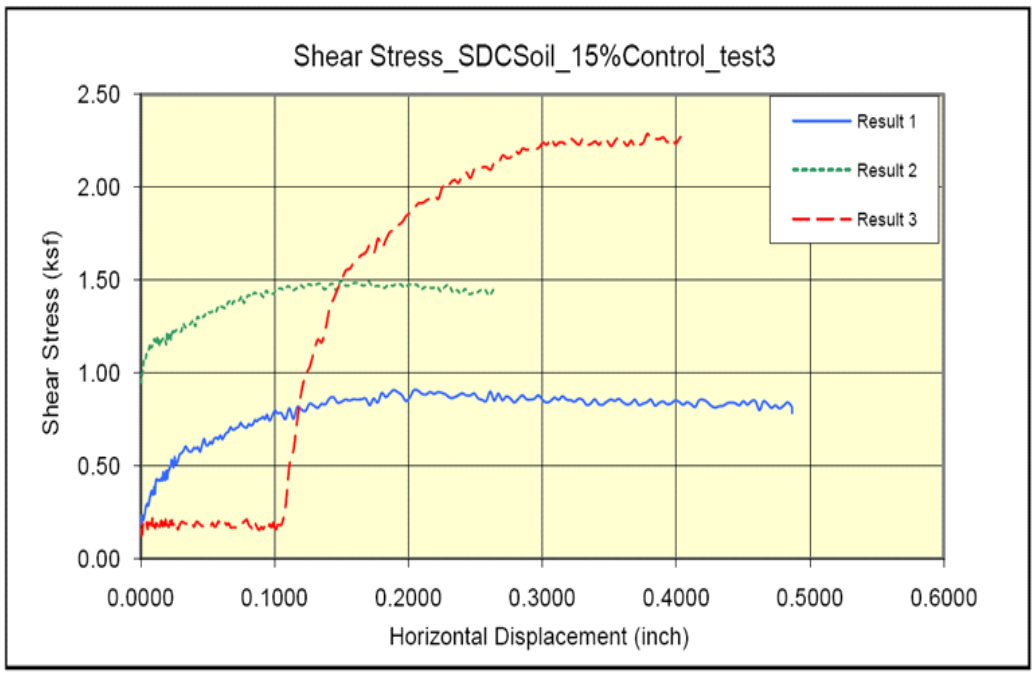
Shear Stress_SDCSoil_15%Control_test3
Shear Stress (ksf)
2.50
2.00
1.50
1.00
0.50
0.00
0.0000
0.1000
0.2000
0.3000
0.4000
0.5000
0.6000
Horizontal Displacement (inch)
Result 1
Result 2
Result 3

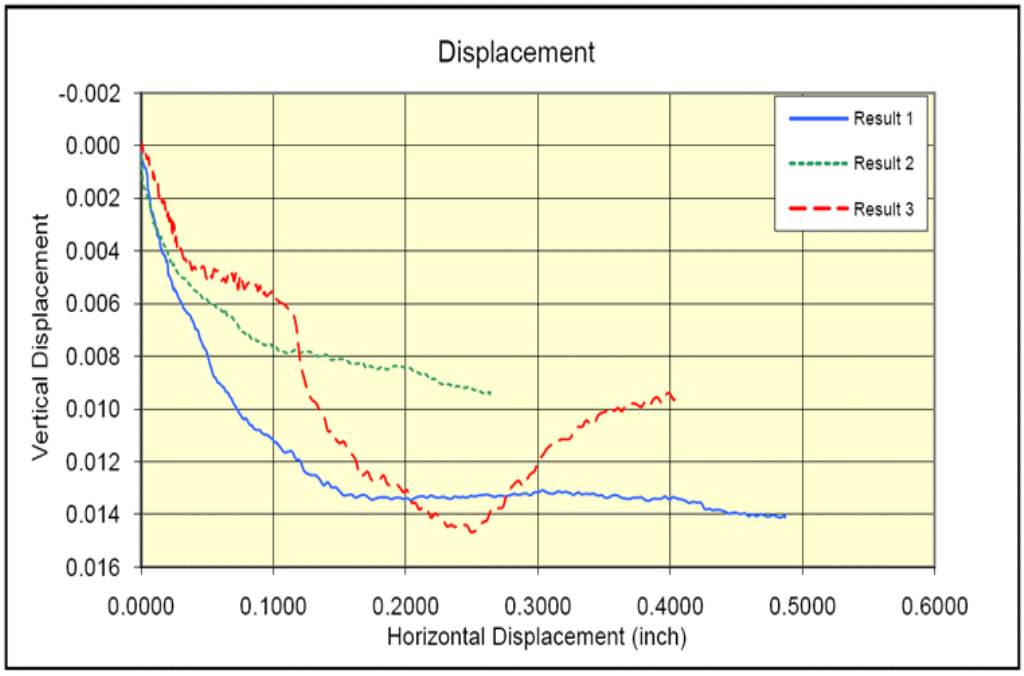
Displacement
Vertical Displacement
-0.002
0.000
0.002
0.004
0.006
0.008
0.010
0.012
0.014
0.016
0.0000
0.1000
0.2000
0.3000
0.4000
0.5000
0.6000
Horizontal Displacement (inch)
Result 1
Result 2
Result 3

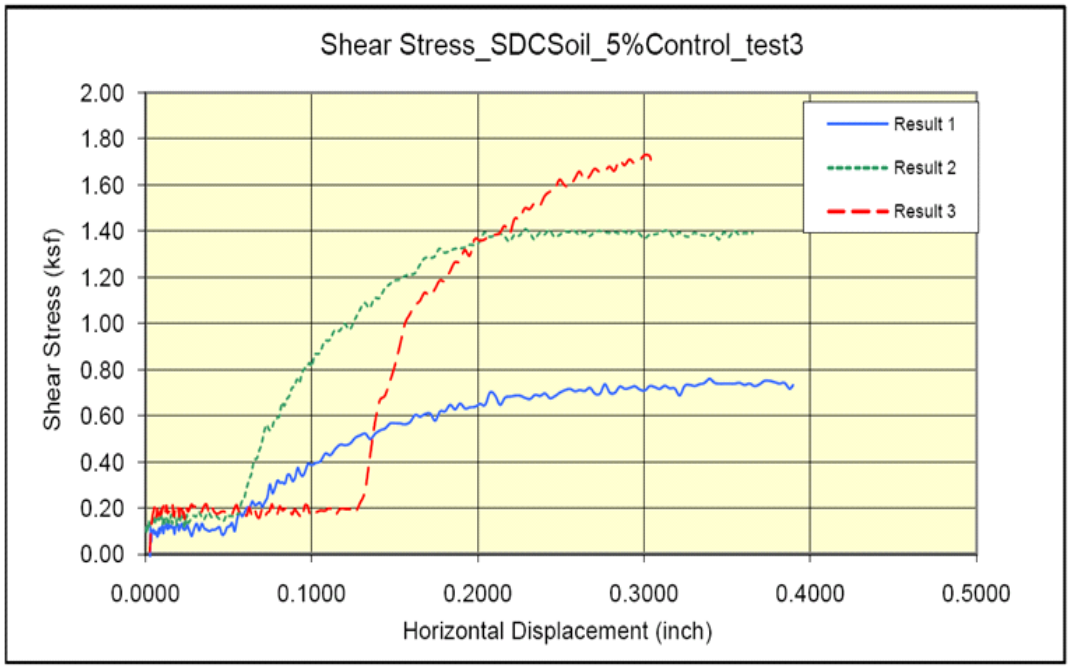
Shear Stress_SDCSoil_5%Control_test3
Shear Stress (ksf)
2.00
1.80
1.60
1.40
1.20
1.00
0.80
0.60
0.40
0.20
0.00
0.0000
0.1000
0.2000
0.3000
0.4000
0.5000
Horizontal Displacement (inch)
Result 1
Result 2
Result 3

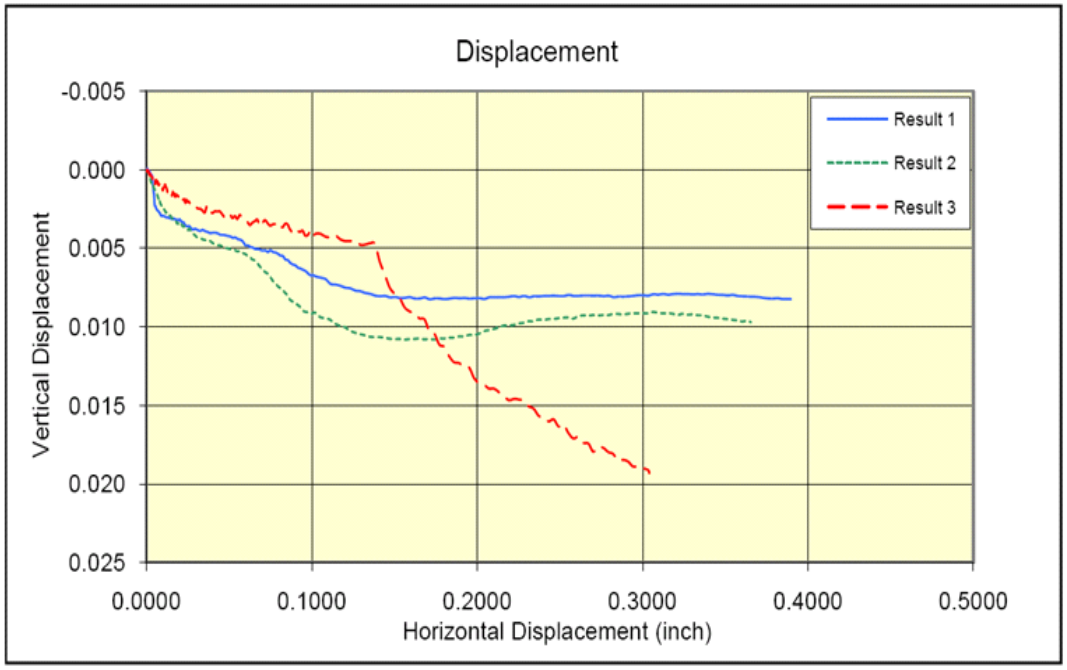
Displacement
Vertical Displacement
-0.005
0.000
0.005
0.010
0.015
0.020
0.025
0.0000
0.1000
0.2000
0.3000
0.4000
0.5000
Horizontal Displacement (inch)
Result 1
Result 2
Result 3

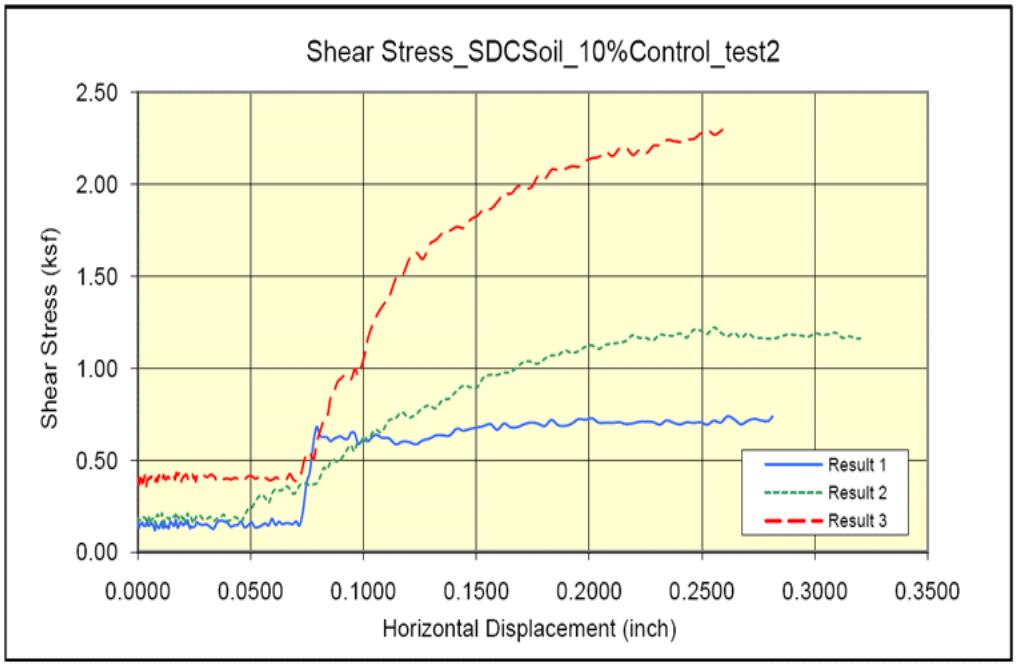
Shear Stress_SDCSoil_10%Control_test2
Shear Stress (ksf)
2.50
2.00
1.50
1.00
0.50
0.00
0.0000
0.0500
0.1000
0.1500
0.2000
0.2500
0.3000
0.3500
Horizontal Displacement (inch)
Result 1
Result 2
Result 3

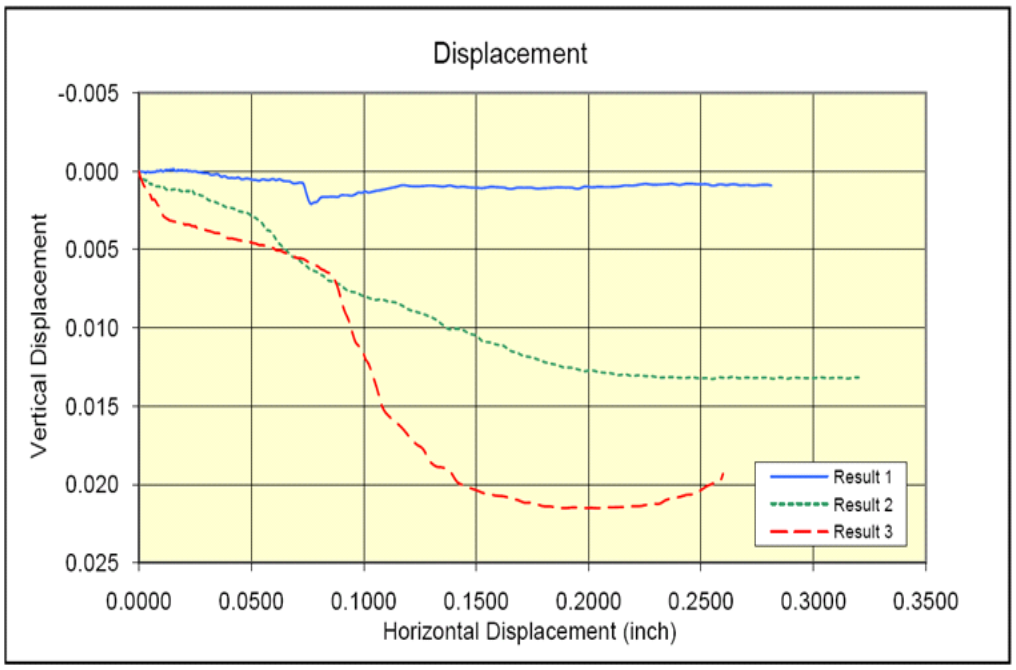
Displacement
Vertical Displacement
-0.005
0.000
0.005
0.010
0.015
0.020
0.025
0.0000
0.0500
0.1000
0.1500
0.2000
0.2500
0.3000
0.3500
Horizontal Displacement (inch)
Result 1
Result 2
Result 3

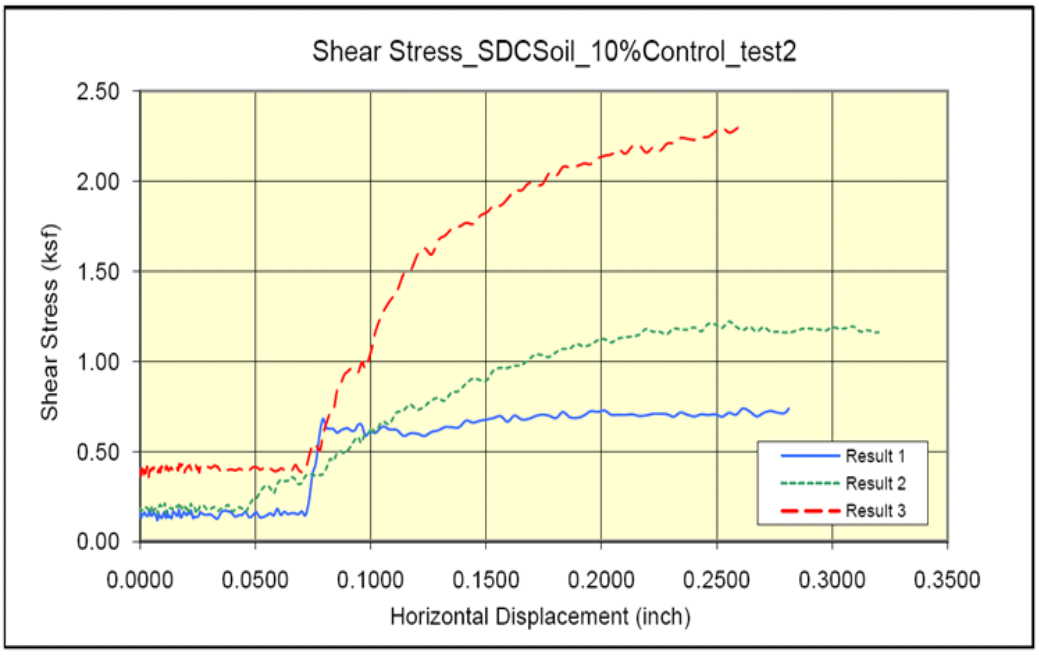
Shear Stress_SDCSoil_10%Control_test2
Shear Stress (ksf)
2.50
2.00
1.50
1.00
0.50
0.00
0.0000
0.0500
0.1000
0.1500
0.2000
0.2500
0.3000
0.3500
Horizontal Displacement (inch)
Result 1
Result 2
Result 3

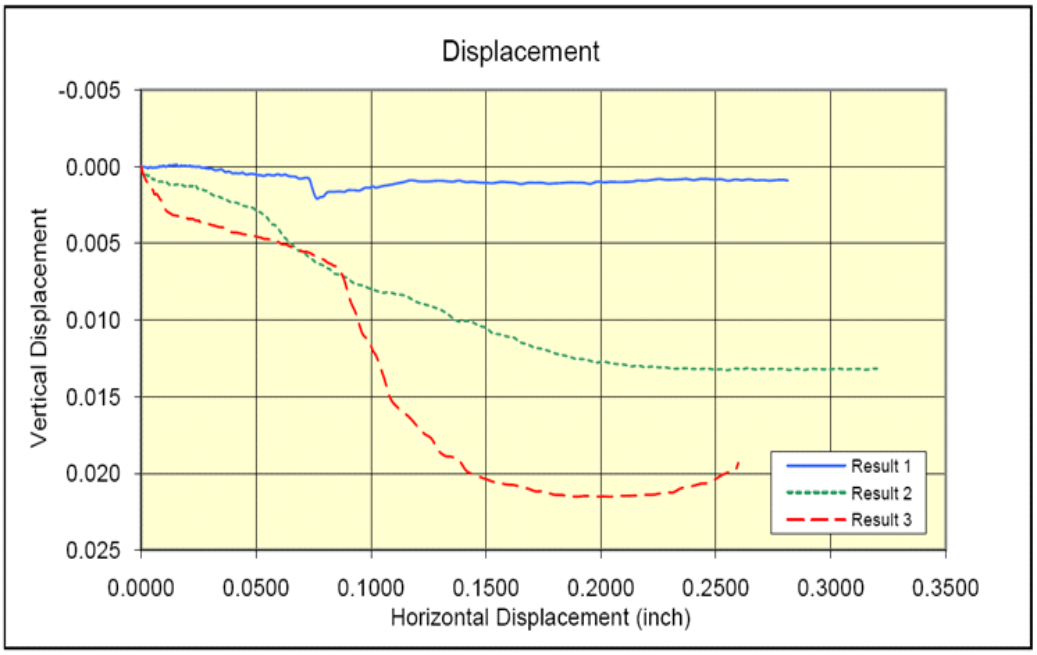
Displacement
Vertical Displacement
-0.005
0.000
0.005
0.010
0.015
0.020
0.025
0.0000
0.0500
0.1000
0.1500
0.2000
0.2500
0.3000
0.3500
Horizontal Displacement (inch)
Result 1
Result 2
Result 3

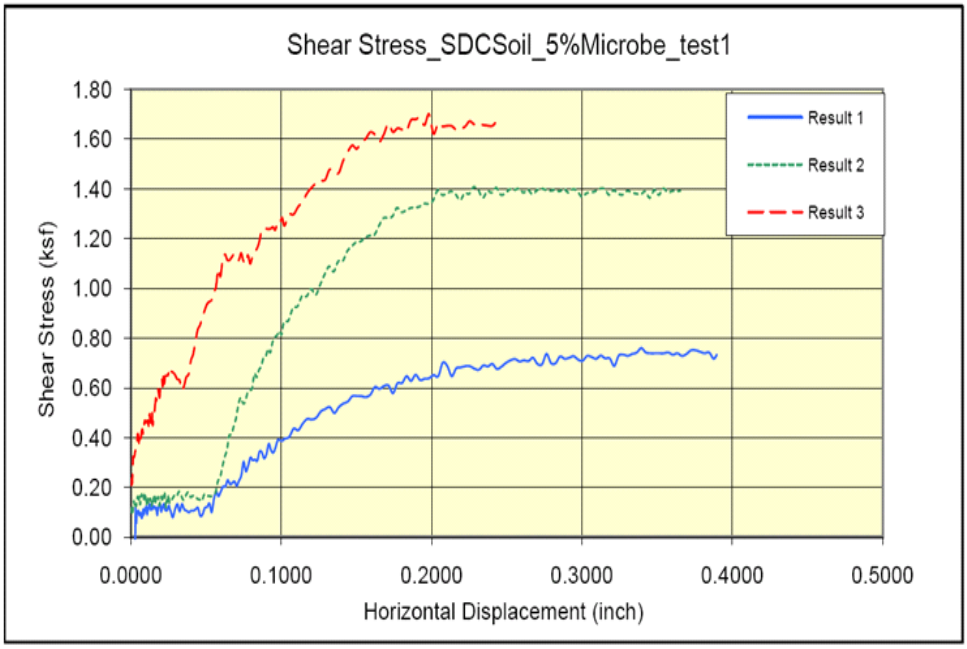
Shear Stress_SDCSoil_5%Microbe_test1
Shear Stress (ksf)
1.80
1.60
1.40
1.20
1.00
0.80
0.60
0.40
0.20
0.00
0.0000
0.1000
0.2000
0.3000
0.4000
0.5000
Horizontal Displacement (inch)
Result 1
Result 2
Result 3

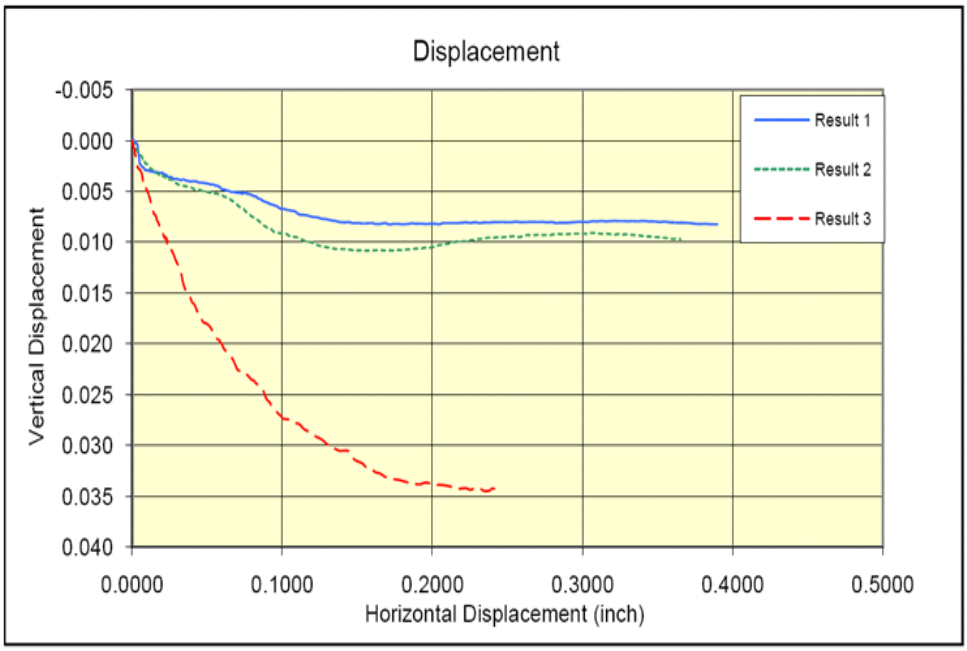
Displacement
Vertical Displacement
-0.005
0.000
0.005
0.010
0.015
0.020
0.025
0.030
0.035
0.040
0.0000
0.1000
0.2000
0.3000
0.4000
0.5000
Horizontal Displacement (inch)
Result 1
Result 2
Result 3

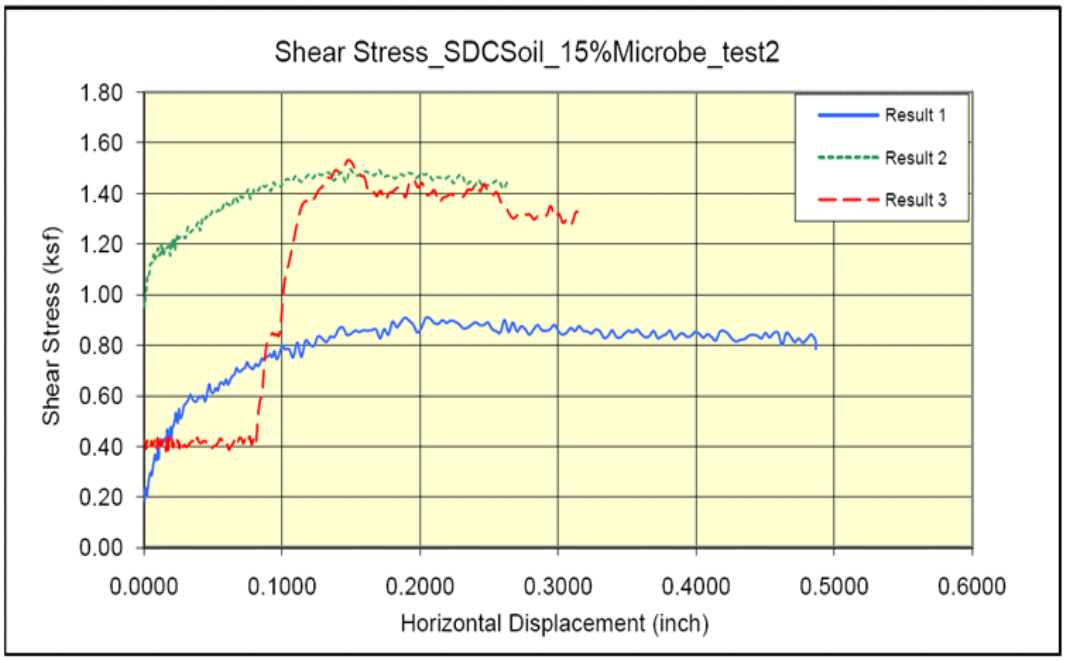
Shear Stress_SDCSoil_15%Microbe_test2
Shear Stress (ksf)
1.80
1.60
1.40
1.20
1.00
0.80
0.60
0.40
0.20
0.00
0.0000
0.1000
0.2000
0.3000
0.4000
0.5000
0.6000
Horizontal Displacement (inch)
Result 1
Result 2
Result 3

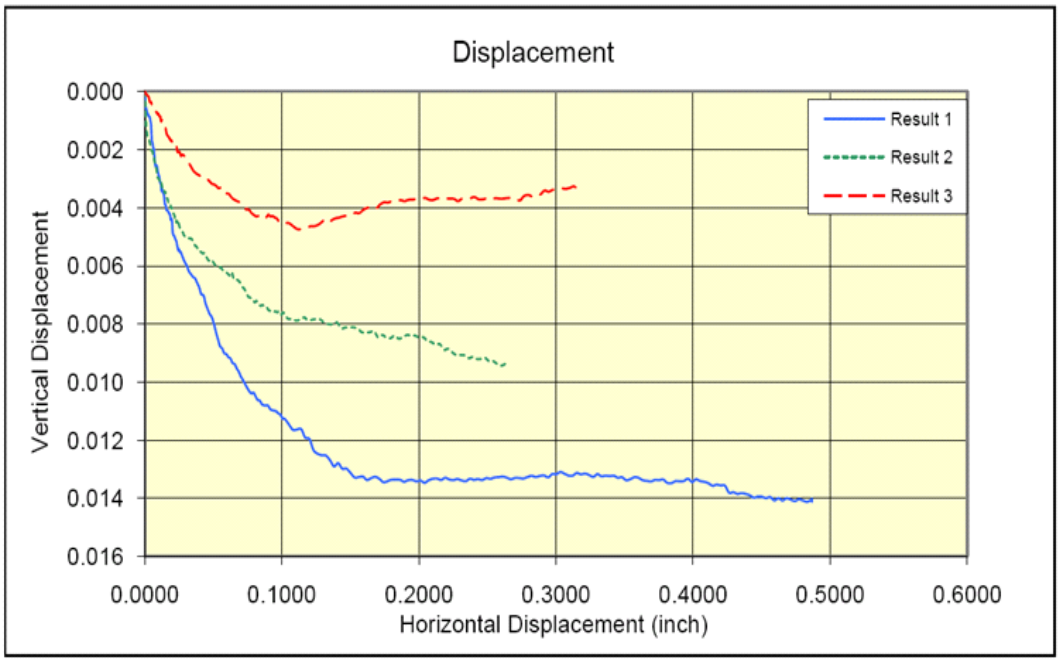
Displacement
Vertical Displacement
0.000
0.002
0.004
0.006
0.008
0.010
0.012
0.014
0.016
0.0000
0.1000
0.2000
0.3000
0.4000
0.5000
0.6000
Horizontal Displacement (inch)
Result 1
Result 2
Result 3

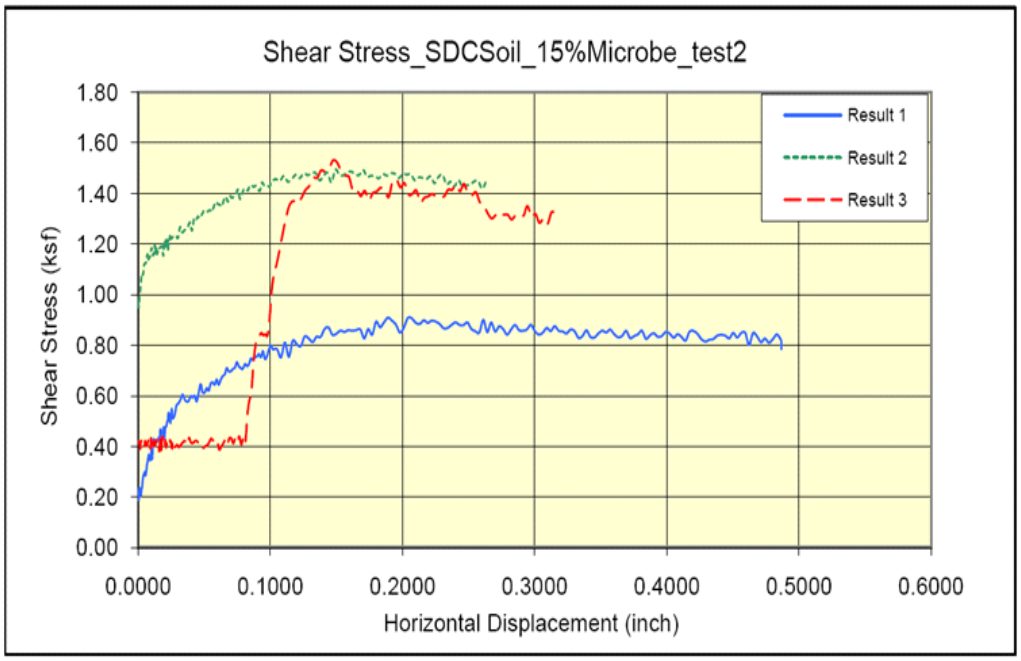
Shear Stress_SDCSoil_15%Microbe_test2
Shear Stress (ksf)
1.80
1.60
1.40
1.20
1.00
0.80
0.60
0.40
0.20
0.00
0.0000
0.1000
0.2000
0.3000
0.4000
0.5000
0.6000
Horizontal Displacement (inch)
Result 1
Result 2
Result 3

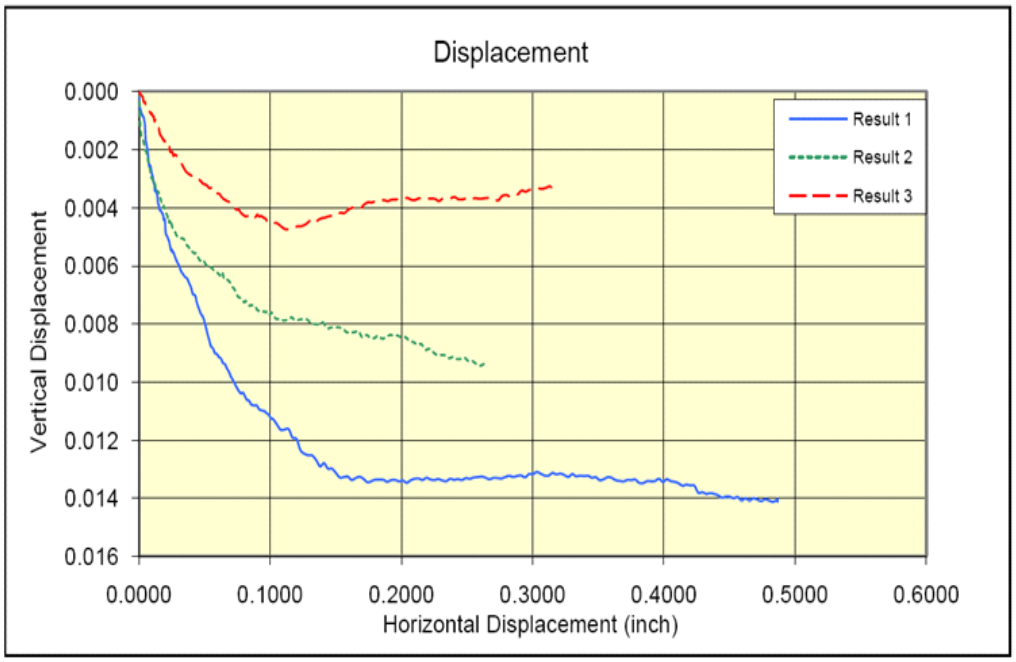
Displacement
Vertical Displacement
0.000
0.002
0.004
0.006
0.008
0.010
0.012
0.014
0.016
0.0000
0.1000
0.2000
0.3000
0.4000
0.5000
0.6000
Horizontal Displacement (inch)
Result 1
Result 2
Result 3

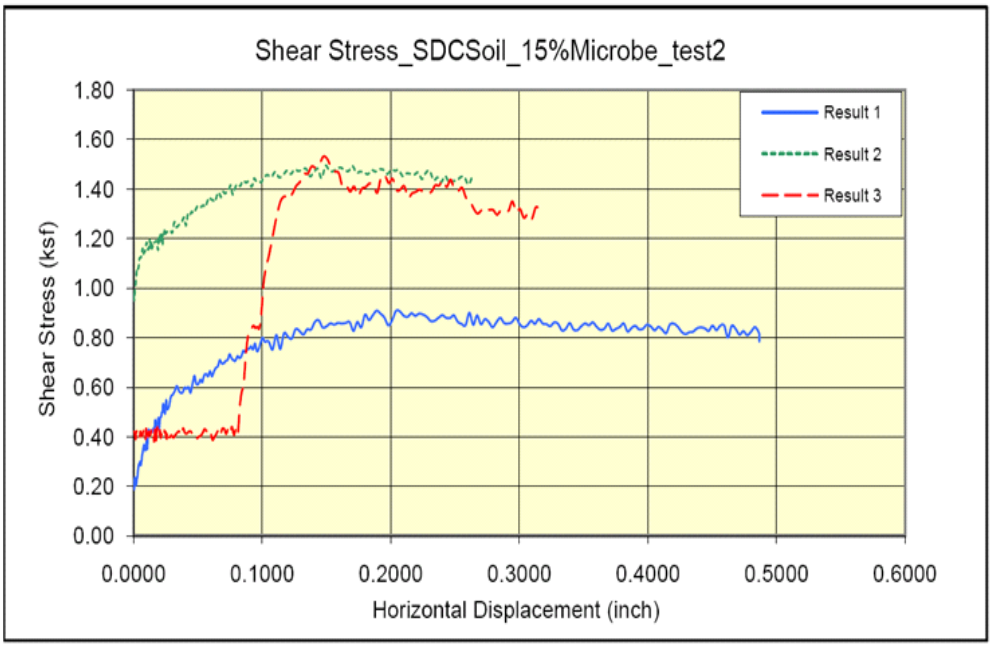
Shear Stress_SDCSoil_15%Microbe_test2
Shear Stress (ksf)
1.80
1.60
1.40
1.20
1.00
0.80
0.60
0.40
0.20
0.00
0.0000
0.1000
0.2000
0.3000
0.4000
0.5000
0.6000
Horizontal Displacement (inch)
Result 1
Result 2
Result 3

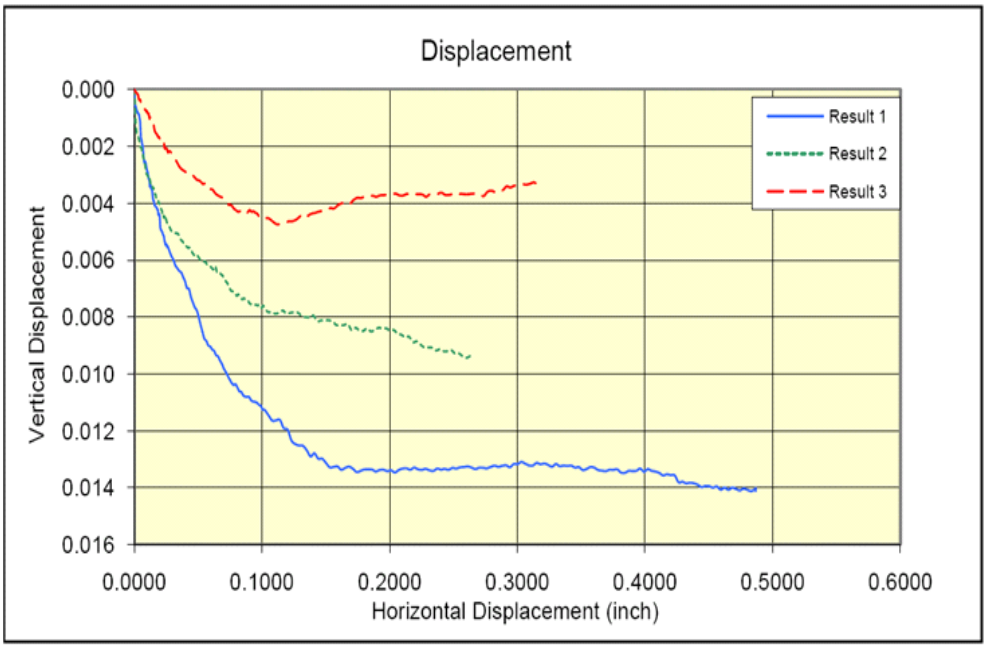
Displacement
Vertical Displacement
0.000
0.002
0.004
0.006
0.008
0.010
0.012
0.014
0.016
0.0000
0.1000
0.2000
0.3000
0.4000
0.5000
0.6000
Horizontal Displacement (inch)
Result 1
Result 2
Result 3

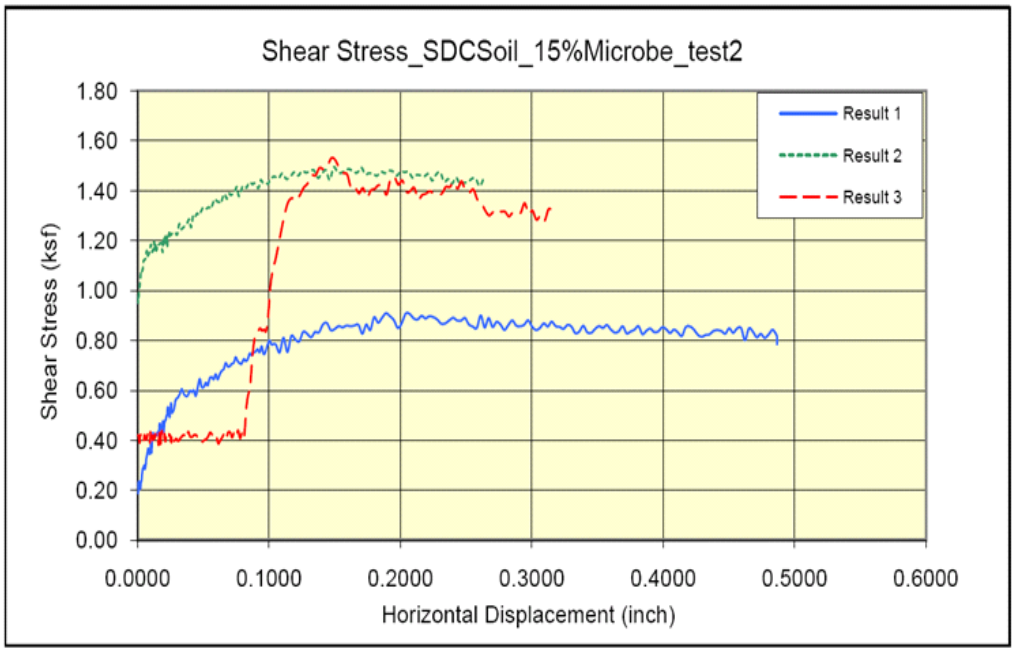
Shear Stress_SDCSoil_15%Microbe_test2
Shear Stress (ksf)
1.80
1.60
1.40
1.20
1.00
0.80
0.60
0.40
0.20
0.00
0.0000
0.1000
0.2000
0.3000
0.4000
0.5000
0.6000
Horizontal Displacement (inch)
Result 1
Result 2
Result 3

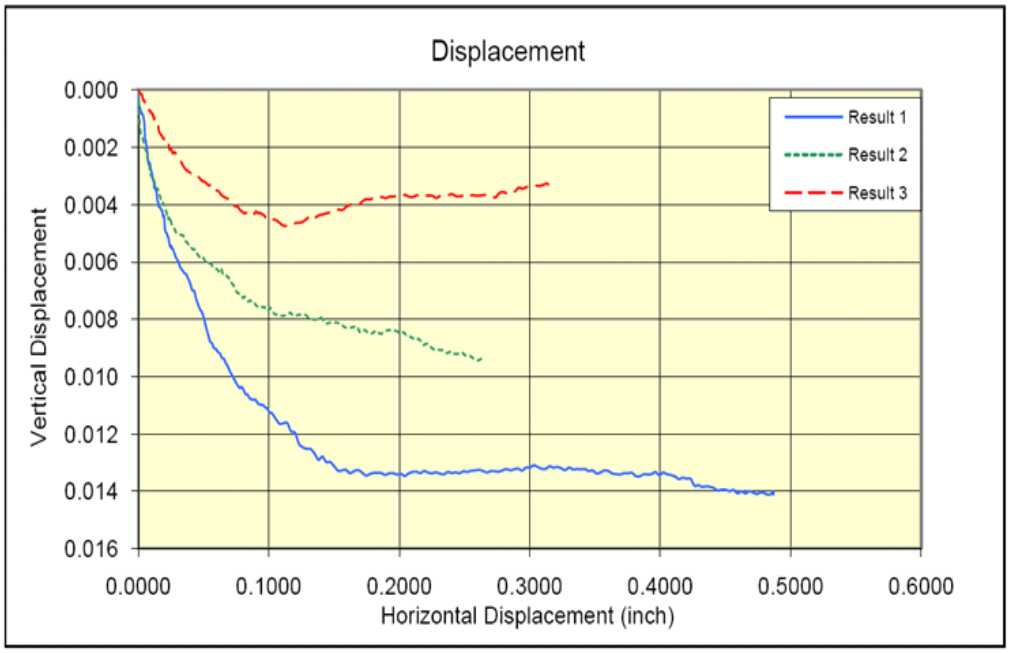
Displacement
Vertical Displacement
0.000
0.002
0.004
0.006
0.008
0.010
0.012
0.014
0.016
0.0000
0.1000
0.2000
0.3000
0.4000
0.5000
0.6000
Horizontal Displacement (inch)
Result 1
Result 2
Result 3

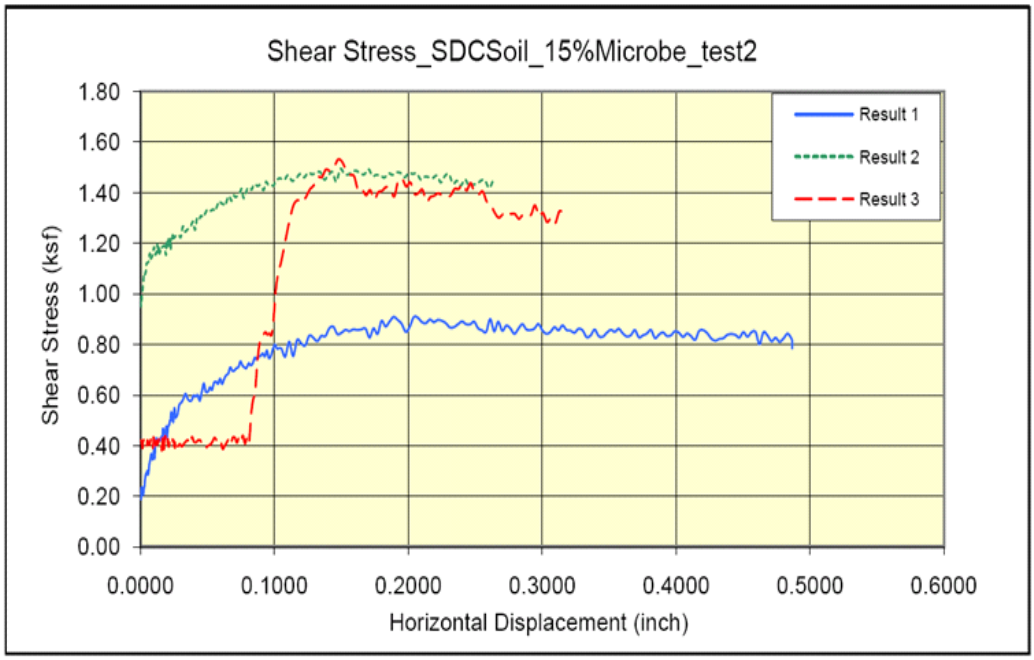
Shear Stress_SDCSoil_15%Microbe_test2
Shear Stress (ksf)
1.80
1.60
1.40
1.20
1.00
0.80
0.60
0.40
0.20
0.00
0.0000
0.1000
0.2000
0.3000
0.4000
0.5000
0.6000
Horizontal Displacement (inch)
Result 1
Result 2
Result 3

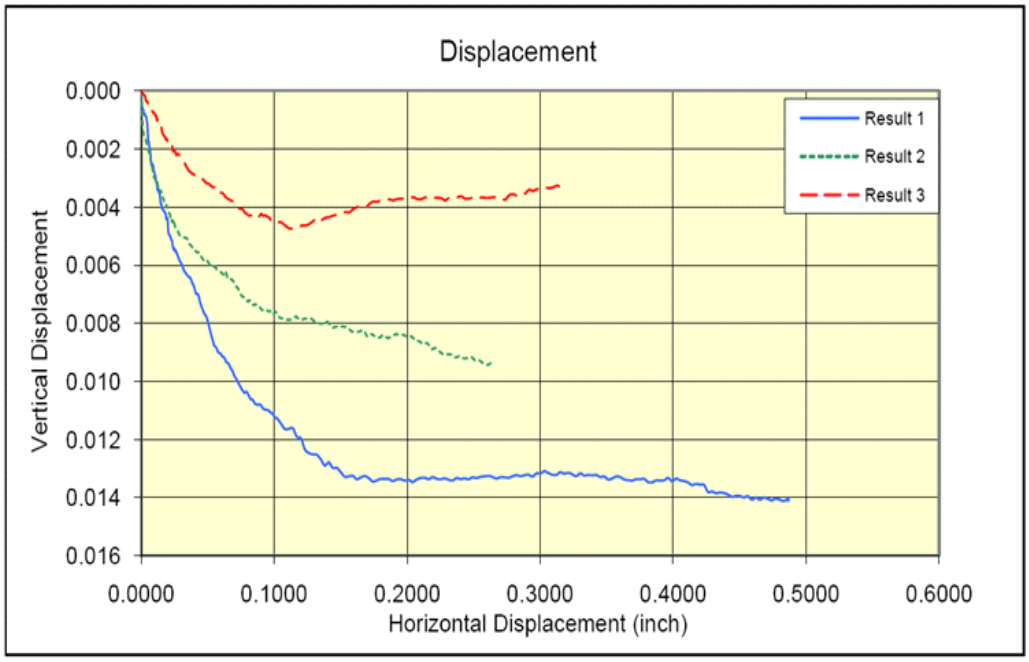
Displacement
Vertical Displacement
0.000
0.002
0.004
0.006
0.008
0.010
0.012
0.014
0.016
0.0000
0.1000
0.2000
0.3000
0.4000
0.5000
0.6000
Horizontal Displacement (inch)
Result 1
Result 2
Result 3

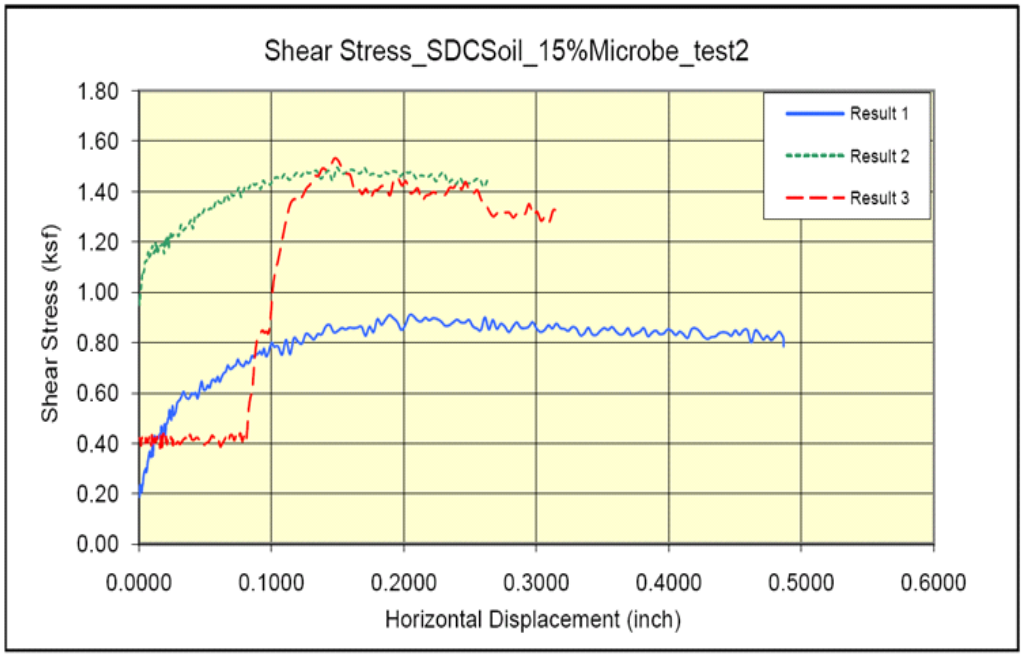
Shear Stress_SDCSoil_15%Microbe_test2
Shear Stress (ksf)
1.80
1.60
1.40
1.20
1.00
0.80
0.60
0.40
0.20
0.00
0.0000
0.1000
0.2000
0.3000
0.4000
0.5000
0.6000
Horizontal Displacement (inch)
Result 1
Result 2
Result 3

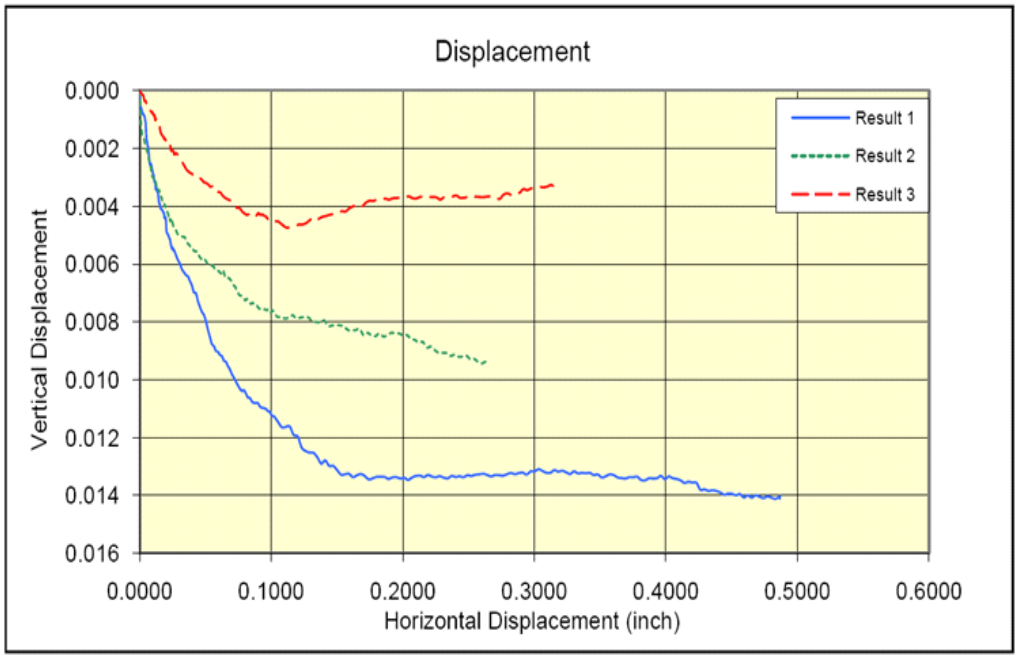
Displacement
Vertical Displacement
0.000
0.002
0.004
0.006
0.008
0.010
0.012
0.014
0.016
0.0000
0.1000
0.2000
0.3000
0.4000
0.5000
0.6000
Horizontal Displacement (inch)
Result 1
Result 2
Result 3

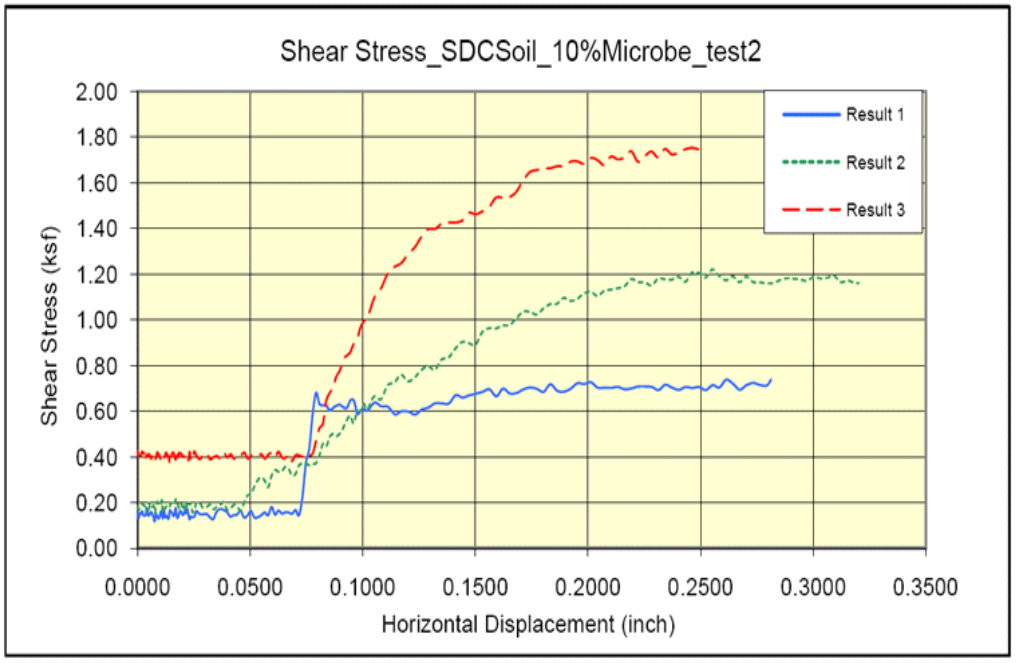
Shear Stress_SDCSoil_10%Microbe_test2
Shear Stress (ksf)
2.00
1.80
1.60
1.40
1.20
1.00
0.80
0.60
0.40
0.20
0.00
0.0000
0.0500
0.1000
0.1500
0.2000
0.2500
0.3000
0.3500
Horizontal Displacement (inch)
Result 1
Result 2
Result 3

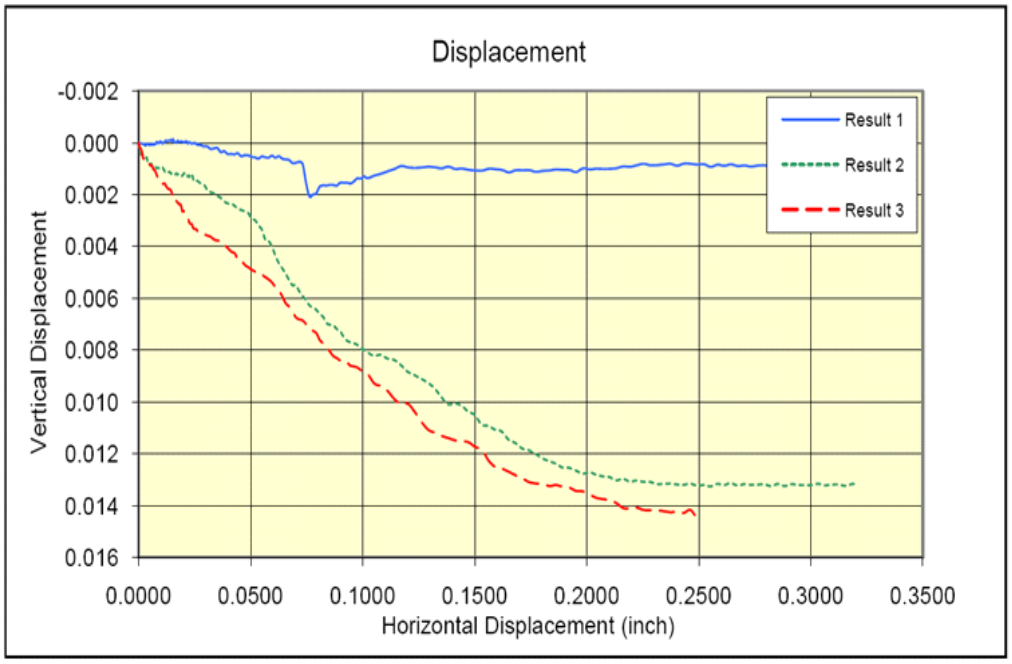
Displacement
Vertical Displacement
-0.002
0.000
0.002
0.004
0.006
0.008
0.010
0.012
0.014
0.016
0.0000
0.0500
0.1000
0.1500
0.2000
0.2500
0.3000
0.3500
Horizontal Displacement (inch)
Result 1
Result 2
Result 3

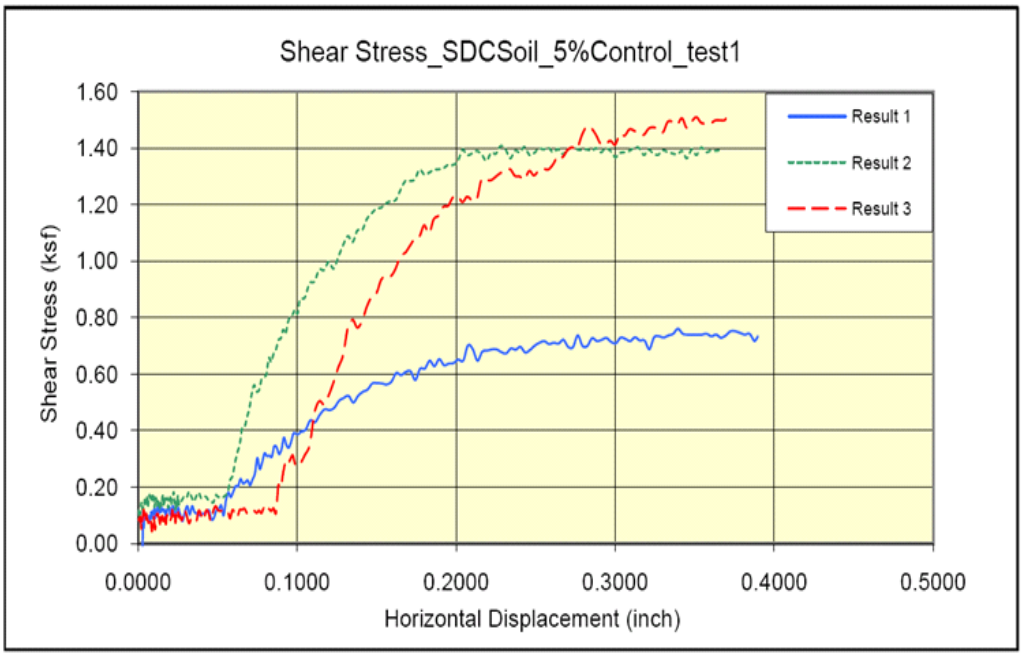
Shear Stress_SDCSoil_5%Control_test1
Shear Stress (ksf)
1.60
1.40
1.20
1.00
0.80
0.60
0.40
0.20
0.00
0.0000
0.1000
0.2000
0.3000
0.4000
0.5000
Horizontal Displacement (inch)
Result 1
Result 2
Result 3

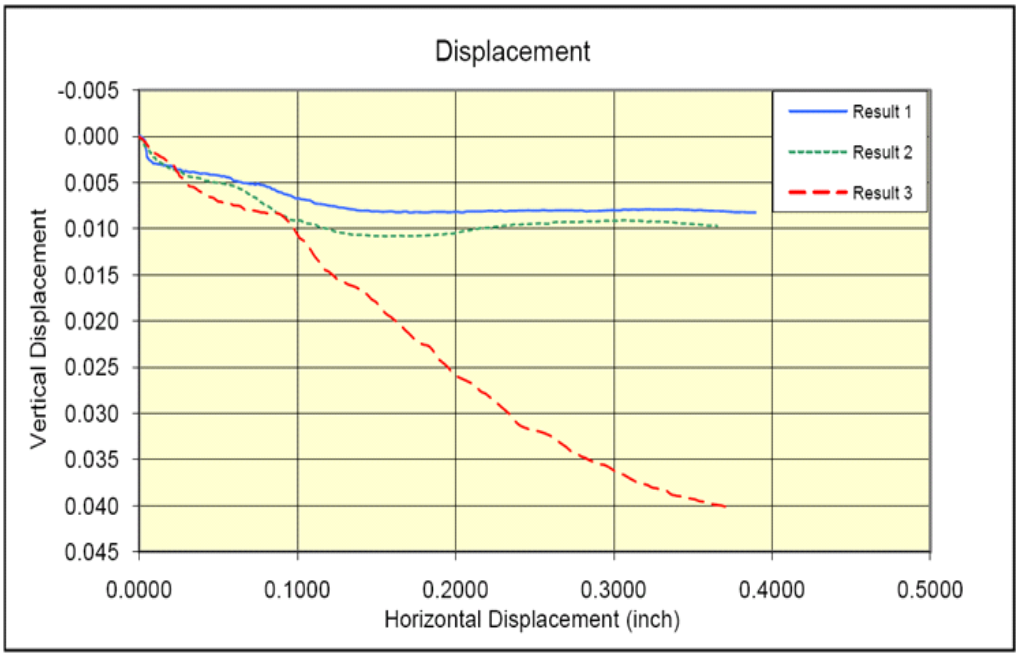
Displacement
Vertical Displacement
-0.005
0.000
0.005
0.010
0.015
0.020
0.025
0.030
0.035
0.040
0.045
0.0000
0.1000
0.2000
0.3000
0.4000
0.5000
Horizontal Displacement (inch)
Result 1
Result 2
Result 3

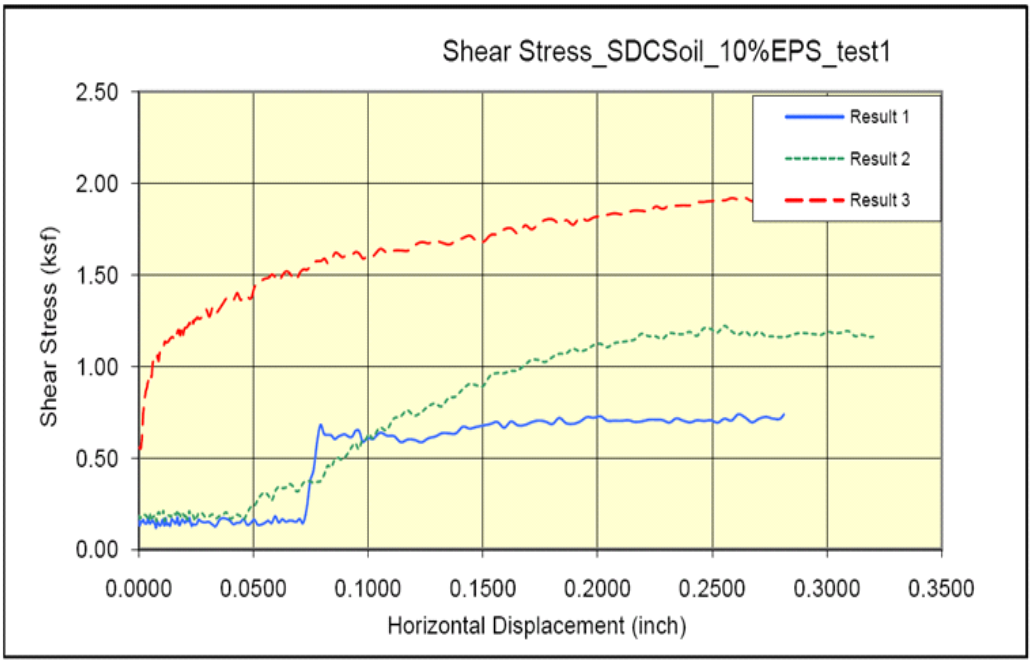
Shear Stress_SDCSoil_10%EPS_test1
Result 1
Result 2
Result 3
Shear Stress (ksf)
2.50
2.00
1.50
1.00
0.50
0.00
0.0000
0.0500
0.1000
0.1500
0.2000
0.2500
0.3000
0.3500
Horizontal Displacement (inch)

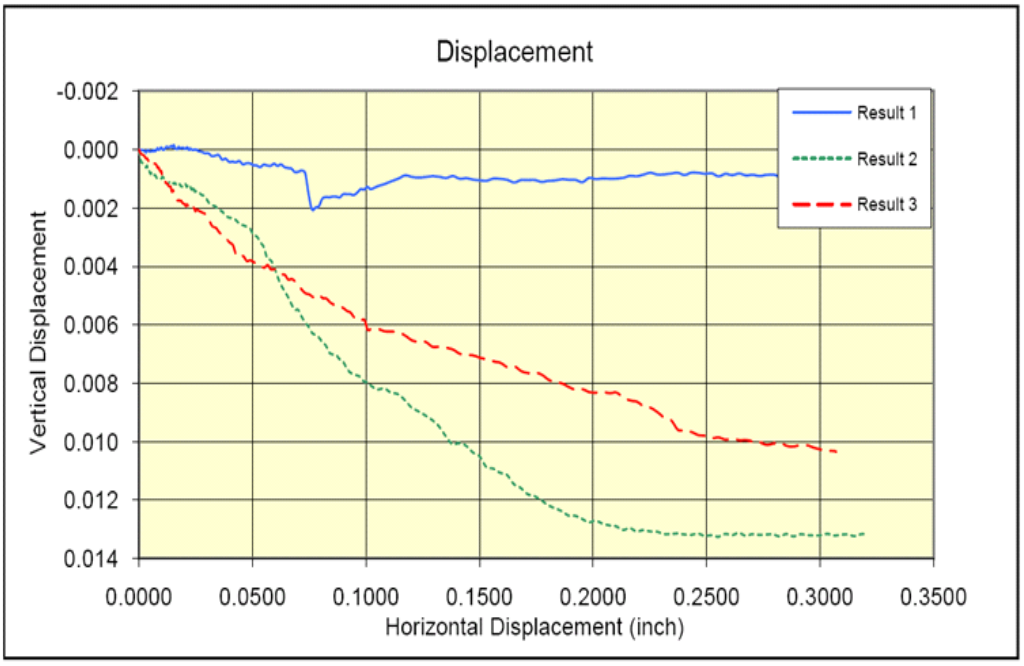
Displacement
Result 1
Result 2
Result 3
Vertical Displacement
-0.002
0.000
0.002
0.004
0.006
0.008
0.010
0.012
0.014
0.0000
0.0500
0.1000
0.1500
0.2000
0.2500
0.3000
0.3500
Horizontal Displacement (inch)

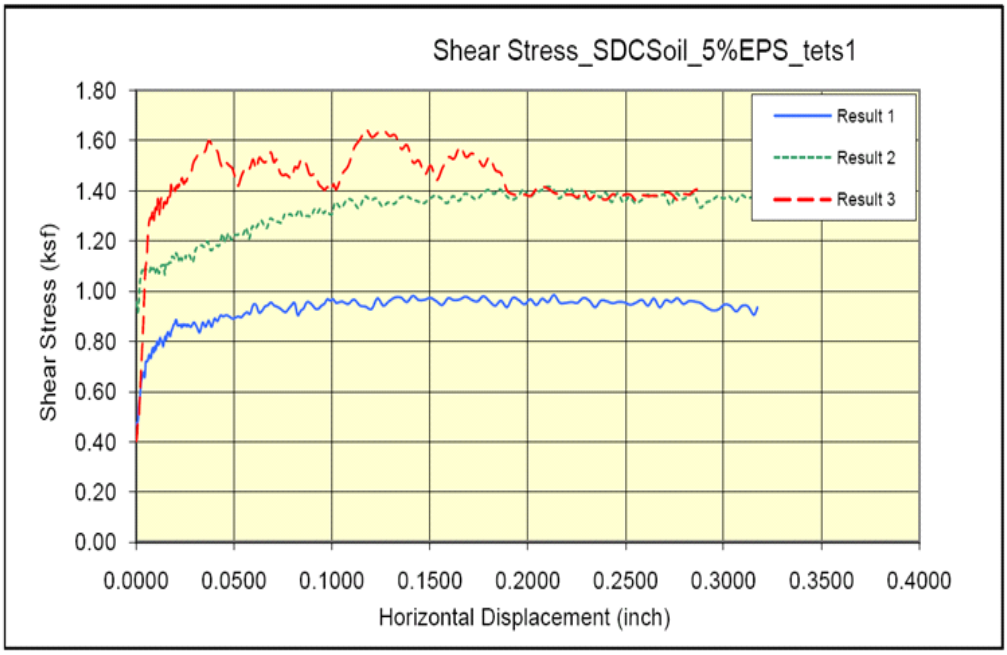
Shear Stress_SDCSoil_5%EPS_tets1
Shear Stress (ksf)
1.80
1.60
1.40
1.20
1.00
0.80
0.60
0.40
0.20
0.00
0.0000
0.0500
0.1000
0.1500
0.2000
0.2500
0.3000
0.3500
0.4000
Horizontal Displacement (inch)
Result 1
Result 2
Result 3

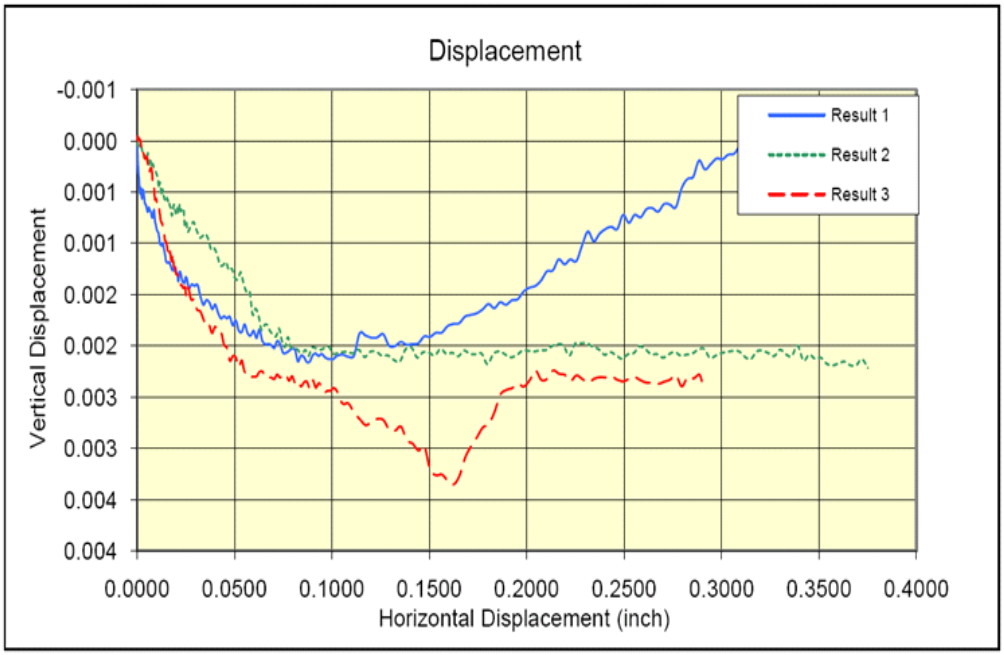
Displacement
Vertical Displacement
-0.001
0.000
0.001
0.001
0.002
0.002
0.003
0.003
0.004
0.004
0.0000
0.0500
0.1000
0.1500
0.2000
0.2500
0.3000
0.3500
0.4000
Horizontal Displacement (inch)
Result 1
Result 2
Result 3

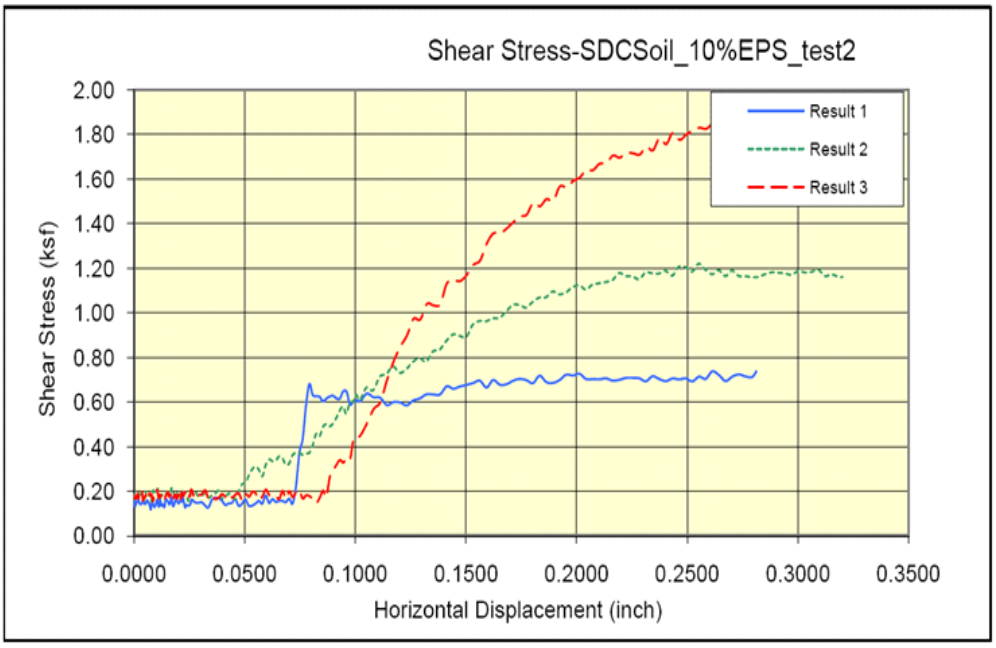
Shear Stress-SDCSoil_10%EPS_test2
Shear Stress (ksf)
2.00
1.80
1.60
1.40
1.20
1.00
0.80
0.60
0.40
0.20
0.00
0.0000
0.0500
0.1000
0.1500
0.2000
0.2500
0.3000
0.3500
Horizontal Displacement (inch)
Result 1
Result 2
Result 3

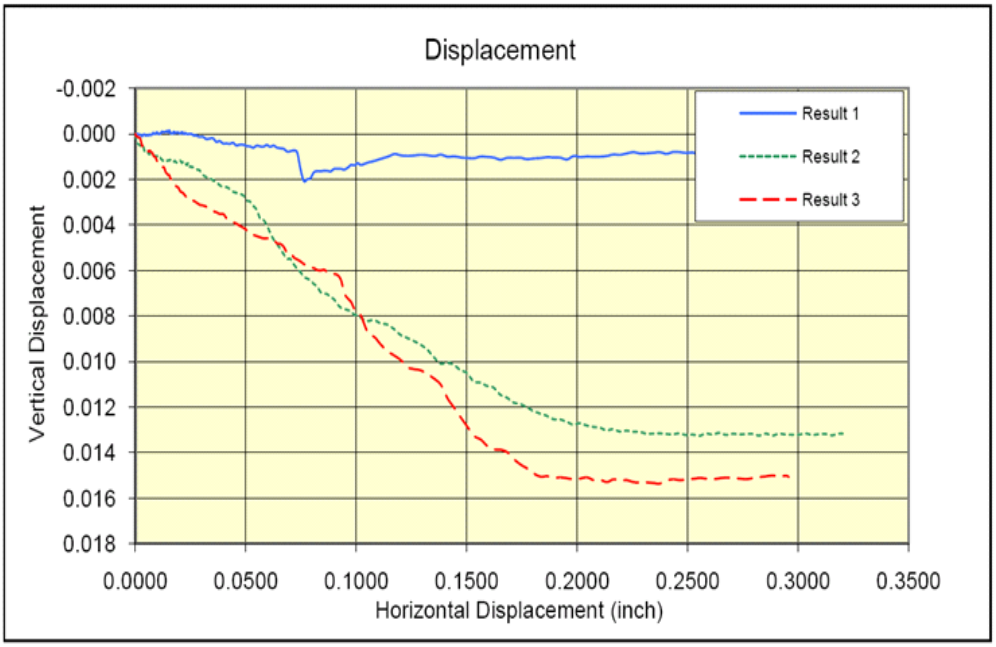
Displacement
Vertical Displacement
-0.002
0.000
0.002
0.004
0.006
0.008
0.010
0.012
0.014
0.016
0.018
0.0000
0.0500
0.1000
0.1500
0.2000
0.2500
0.3000
0.3500
Horizontal Displacement (inch)
Result 1
Result 2
Result 3

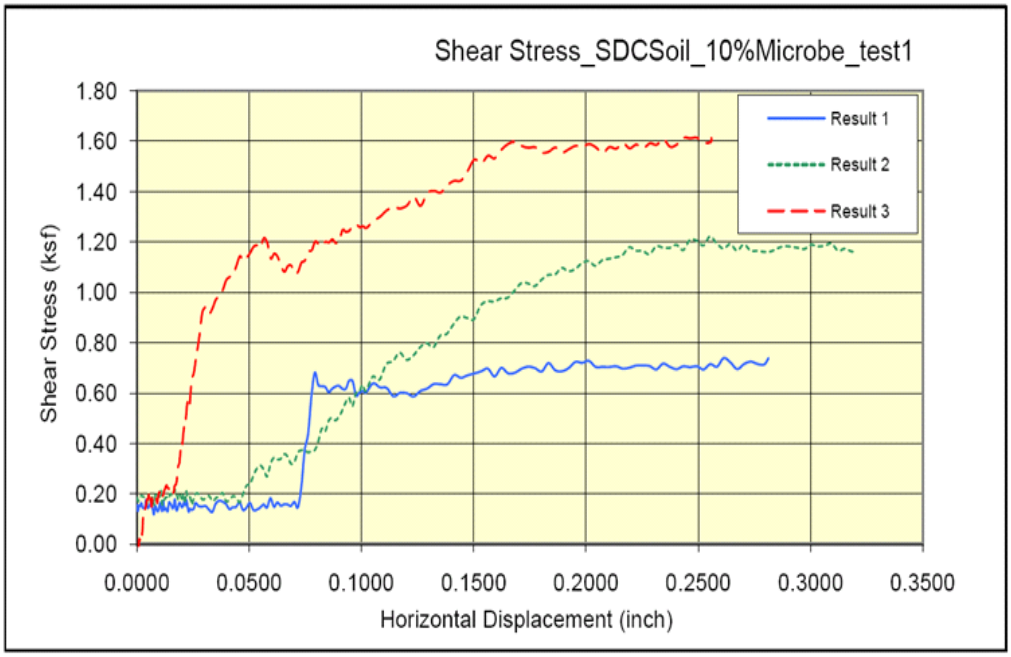
Shear Stress_SDCSoil_10%Microbe_test1
Shear Stress (ksf)
1.80
1.60
1.40
1.20
1.00
0.80
0.60
0.40
0.20
0.00
0.0000
0.0500
0.1000
0.1500
0.2000
0.2500
0.3000
0.3500
Horizontal Displacement (inch)
Result 1
Result 2
Result 3

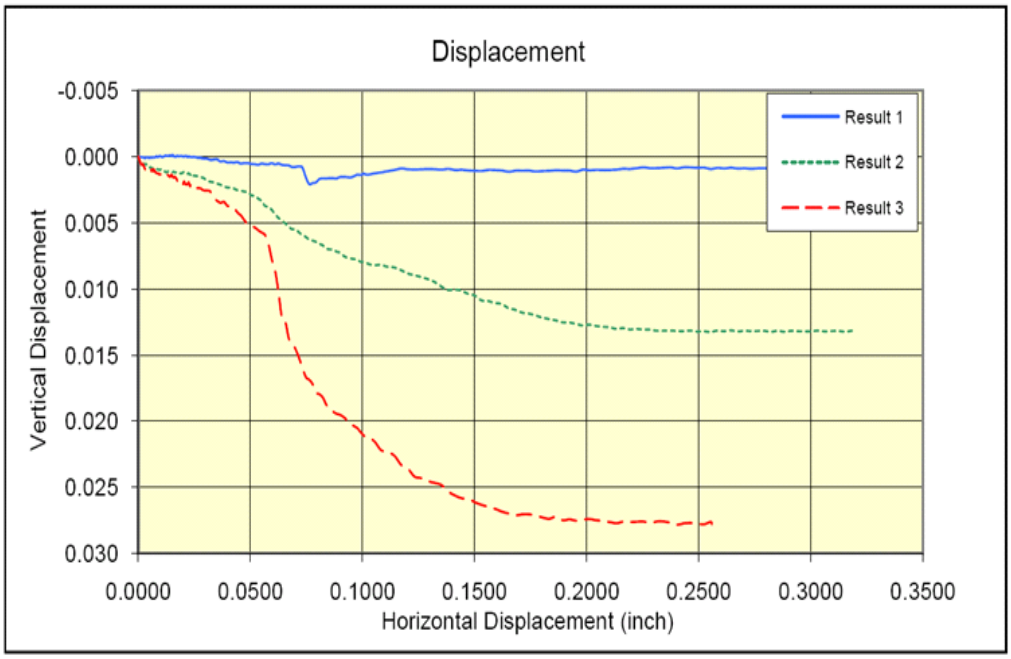
Displacement
Vertical Displacement
-0.005
0.000
0.005
0.010
0.015
0.020
0.025
0.030
0.0000
0.0500
0.1000
0.1500
0.2000
0.2500
0.3000
0.3500
Horizontal Displacement (inch)
Result 1
Result 2
Result 3

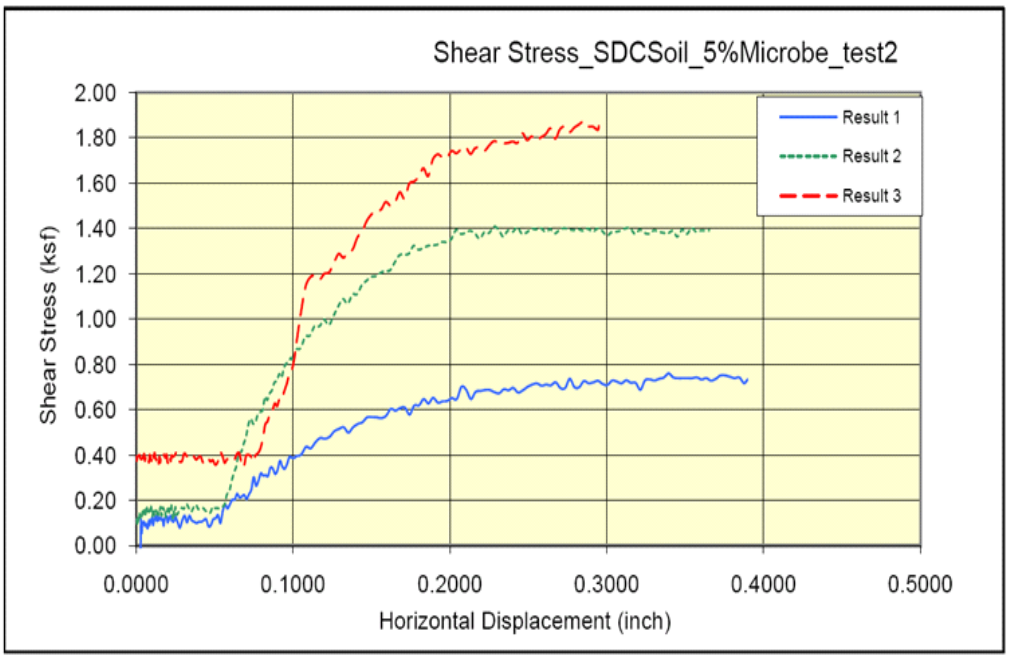
Shear Stress_SDCSoil_5%Microbe_test2
Shear Stress (ksf)
2.00
1.80
1.60
1.40
1.20
1.00
0.80
0.60
0.40
0.20
0.00
0.0000
0.1000
0.2000
0.3000
0.4000
0.5000
Horizontal Displacement (inch)
Result 1
Result 2
Result 3

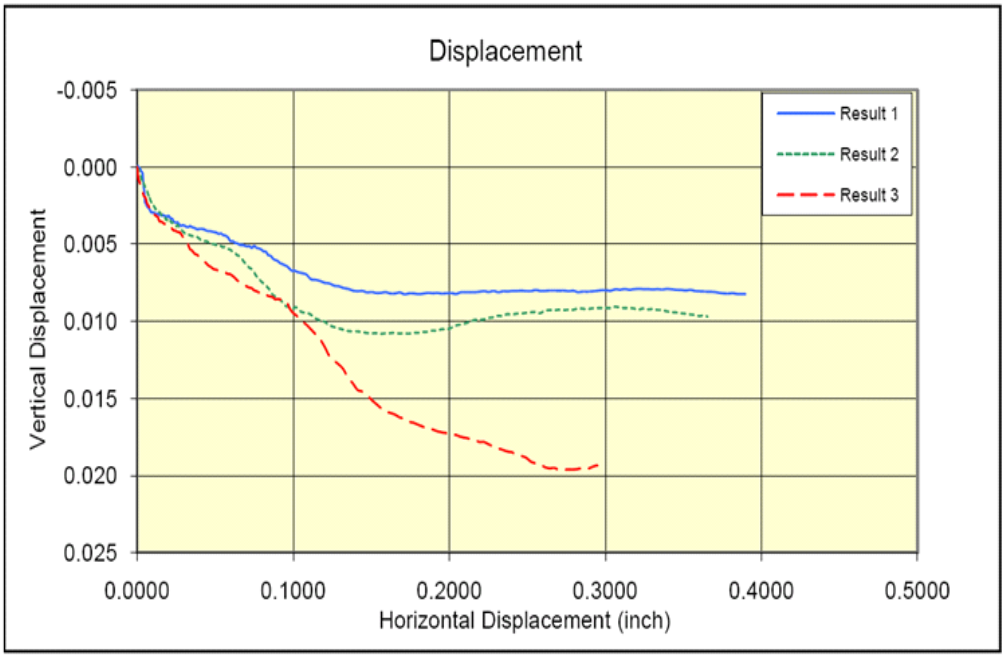
Displacement
Vertical Displacement
-0.005
0.000
0.005
0.010
0.015
0.020
0.025
0.0000
0.1000
0.2000
0.3000
0.4000
0.5000
Horizontal Displacement (inch)
Result 1
Result 2
Result 3

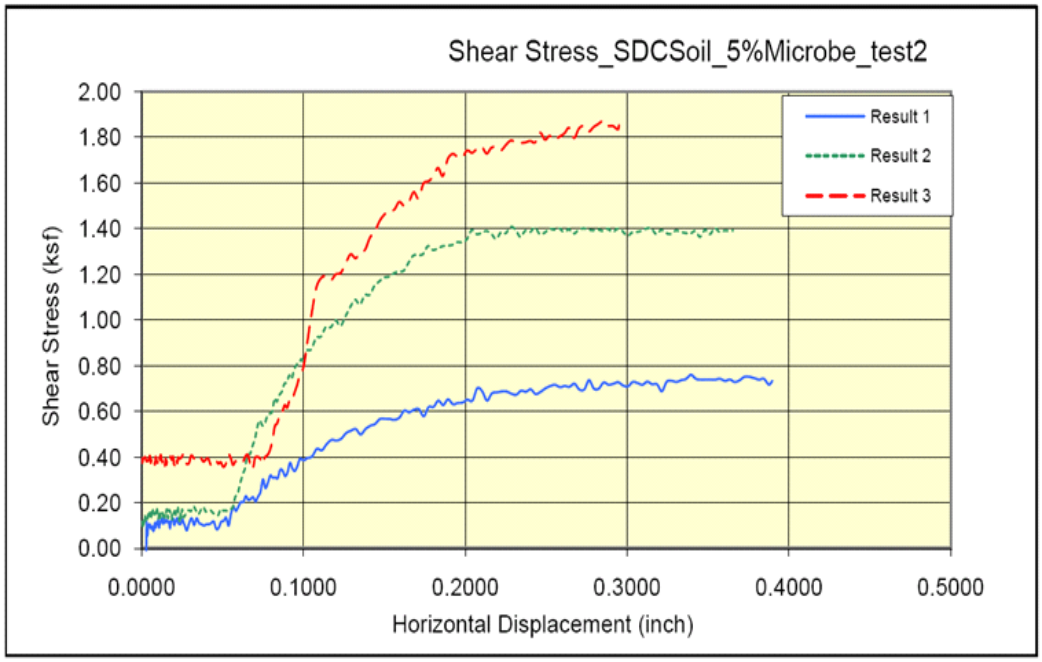
Shear Stress_SDCSoil_5%Microbe_test2
Shear Stress (ksf)
2.00
1.80
1.60
1.40
1.20
1.00
0.80
0.60
0.40
0.20
0.00
0.0000
0.1000
0.2000
0.3000
0.4000
0.5000
Horizontal Displacement (inch)
Result 1
Result 2
Result 3

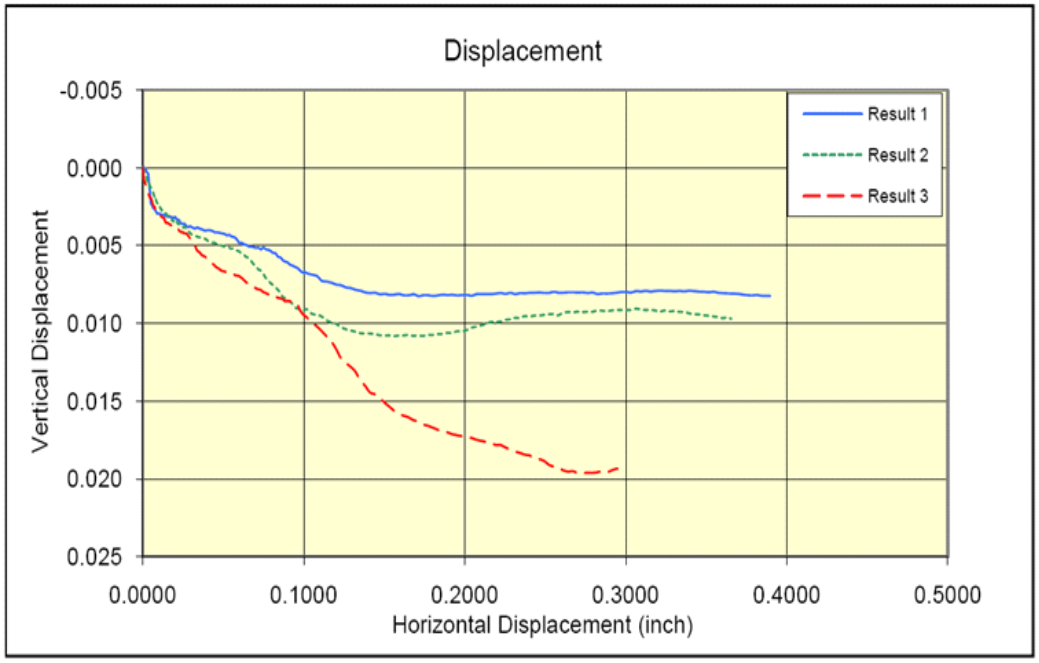
Displacement
Vertical Displacement
-0.005
0.000
0.005
0.010
0.015
0.020
0.025
0.0000
0.1000
0.2000
0.3000
0.4000
0.5000
Horizontal Displacement (inch)
Result 1
Result 2
Result 3

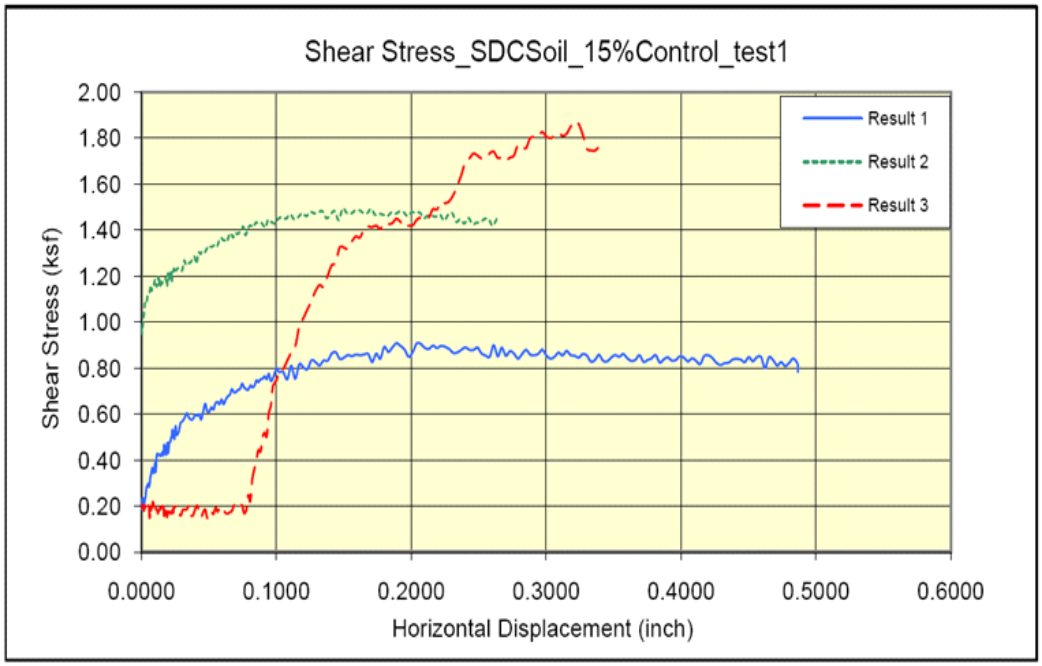
Shear Stress_SDCSoil_15%Control_test1
Shear Stress (ksf)
2.00
1.80
1.60
1.40
1.20
1.00
0.80
0.60
0.40
0.20
0.00
0.0000
0.1000
0.2000
0.3000
0.4000
0.5000
0.6000
Horizontal Displacement (inch)
Result 1
Result 2
Result 3

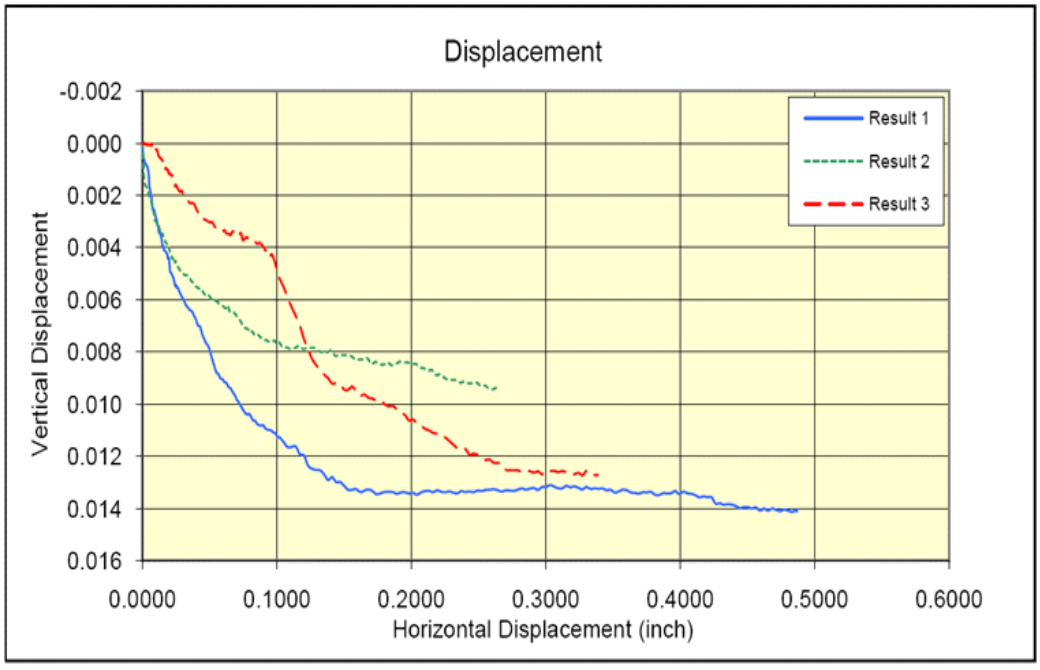
Displacement
Vertical Displacement
-0.002
0.000
0.002
0.004
0.006
0.008
0.010
0.012
0.014
0.016
0.0000
0.1000
0.2000
0.3000
0.4000
0.5000
0.6000
Horizontal Displacement (inch)
Result 1
Result 2
Result 3

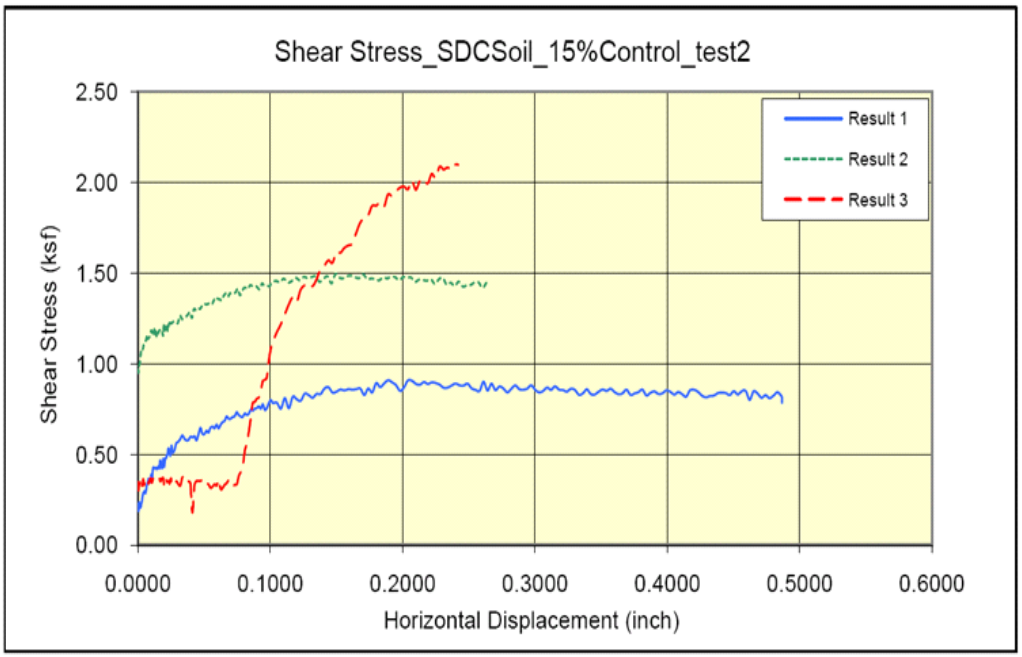
Shear Stress_SDCSoil_15%Control_test2
Shear Stress (ksf)
2.50
2.00
1.50
1.00
0.50
0.00
0.0000
0.1000
0.2000
0.3000
0.4000
0.5000
0.6000
Horizontal Displacement (inch)
Result 1
Result 2
Result 3

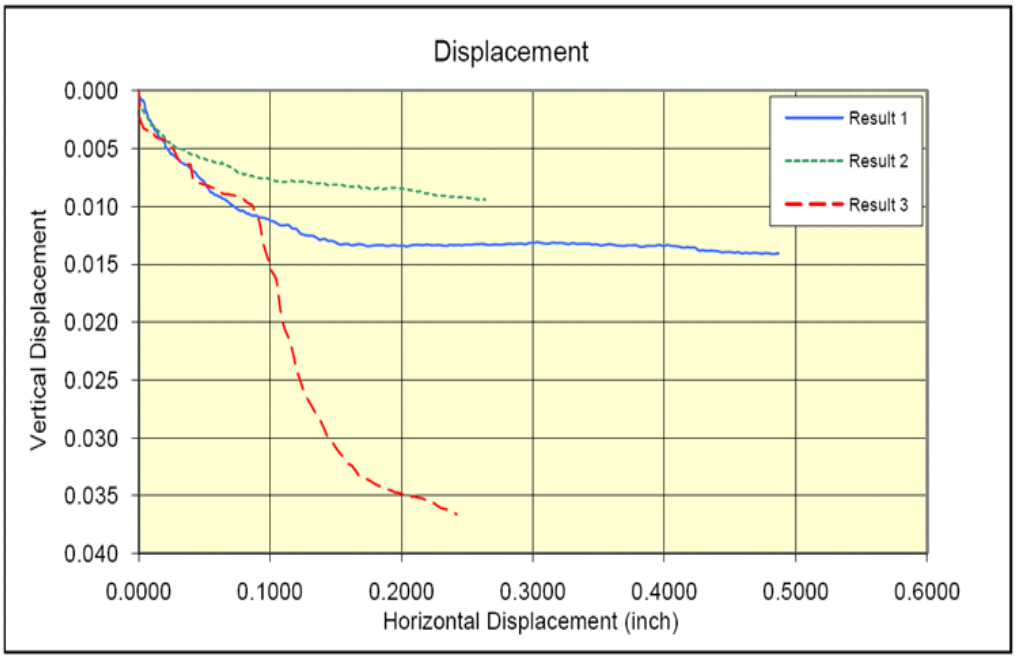
Displacement
Vertical Displacement
0.000
0.005
0.010
0.015
0.020
0.025
0.030
0.035
0.040
0.0000
0.1000
0.2000
0.3000
0.4000
0.5000
0.6000
Horizontal Displacement (inch)
Result 1
Result 2
Result 3

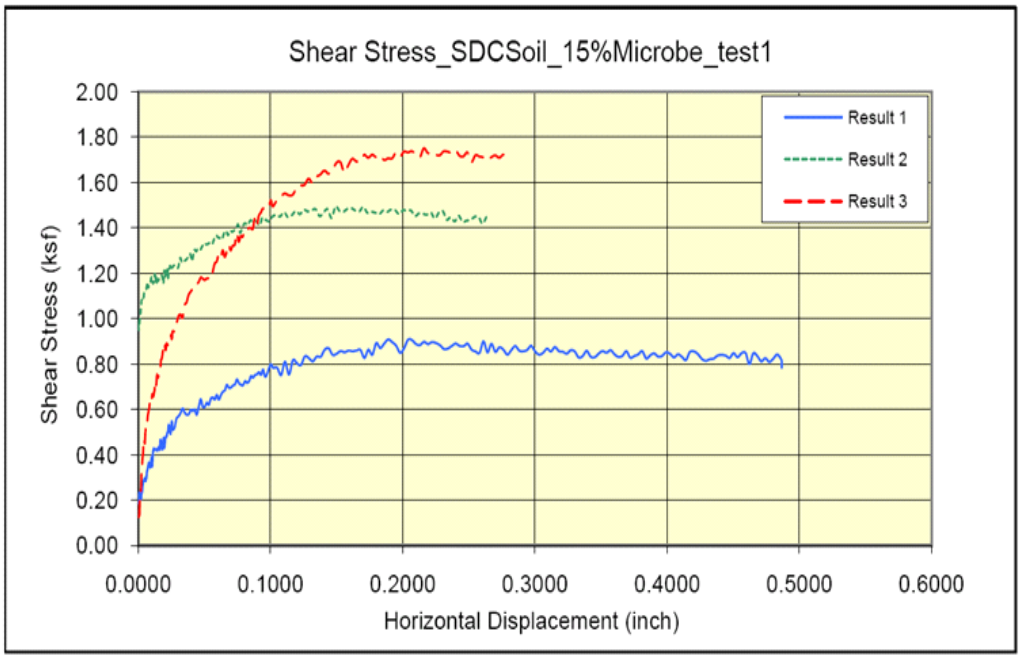
Shear Stress_SDCSoil_15%Microbe_test1
Shear Stress (ksf)
2.00
1.80
1.60
1.40
1.20
1.00
0.80
0.60
0.40
0.20
0.00
0.0000
0.1000
0.2000
0.3000
0.4000
0.5000
0.6000
Horizontal Displacement (inch)
Result 1
Result 2
Result 3

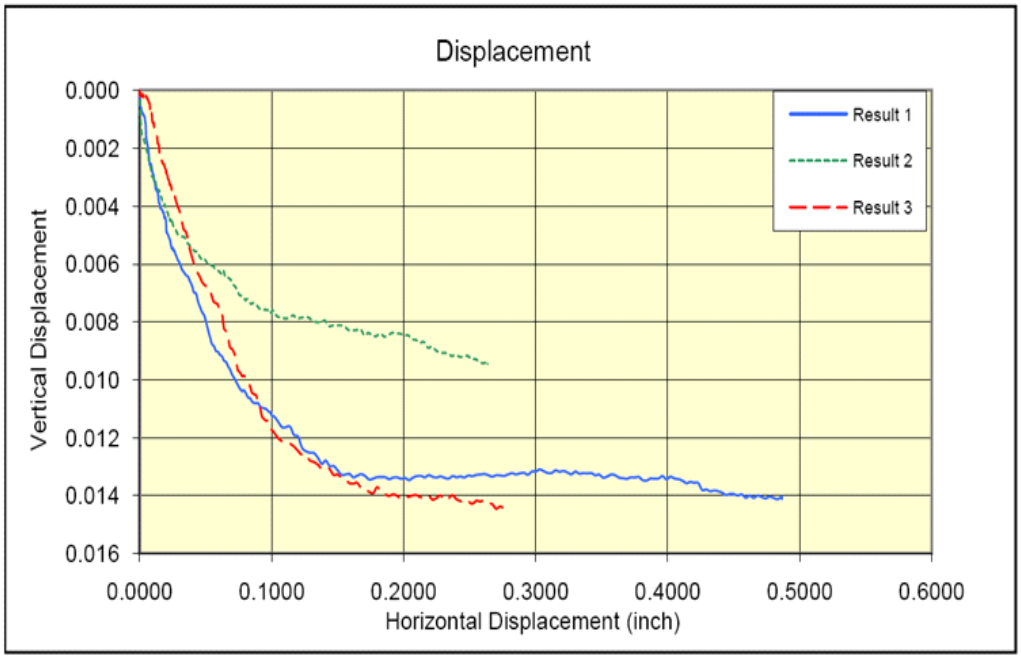
Displacement
Vertical Displacement
0.000
0.002
0.004
0.006
0.008
0.010
0.012
0.014
0.016
0.0000
0.1000
0.2000
0.3000
0.4000
0.5000
0.6000
Horizontal Displacement (inch)
Result 1
Result 2
Result 3

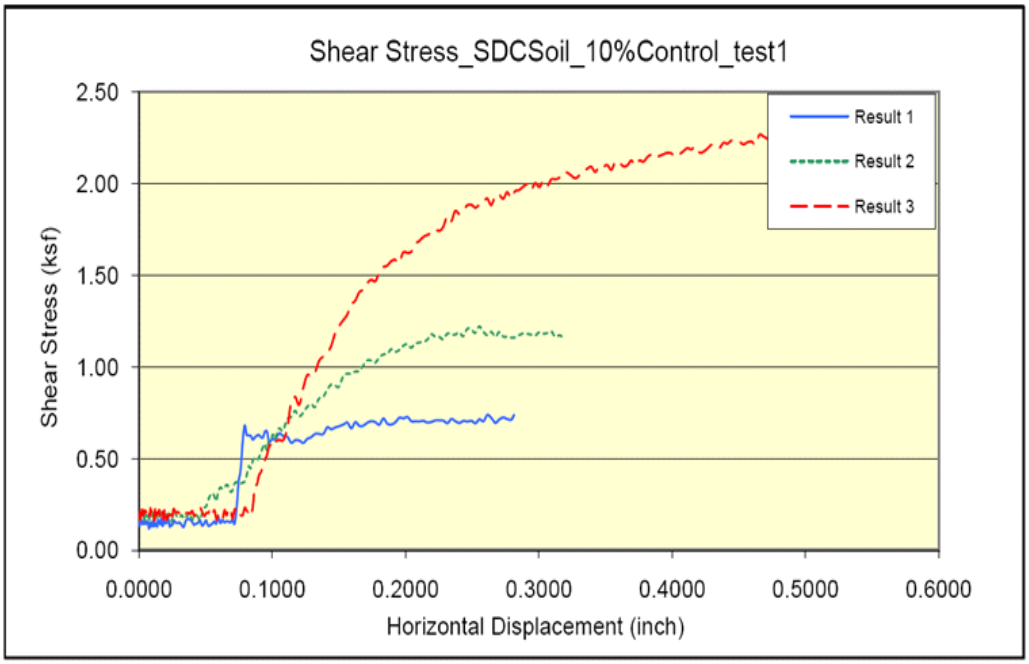
Shear Stress_SDCSoil_10%Control_test1
Shear Stress (ksf)
2.50
2.00
1.50
1.00
0.50
0.00
0.0000
0.1000
0.2000
0.3000
0.4000
0.5000
0.6000
Horizontal Displacement (inch)
Result 1
Result 2
Result 3

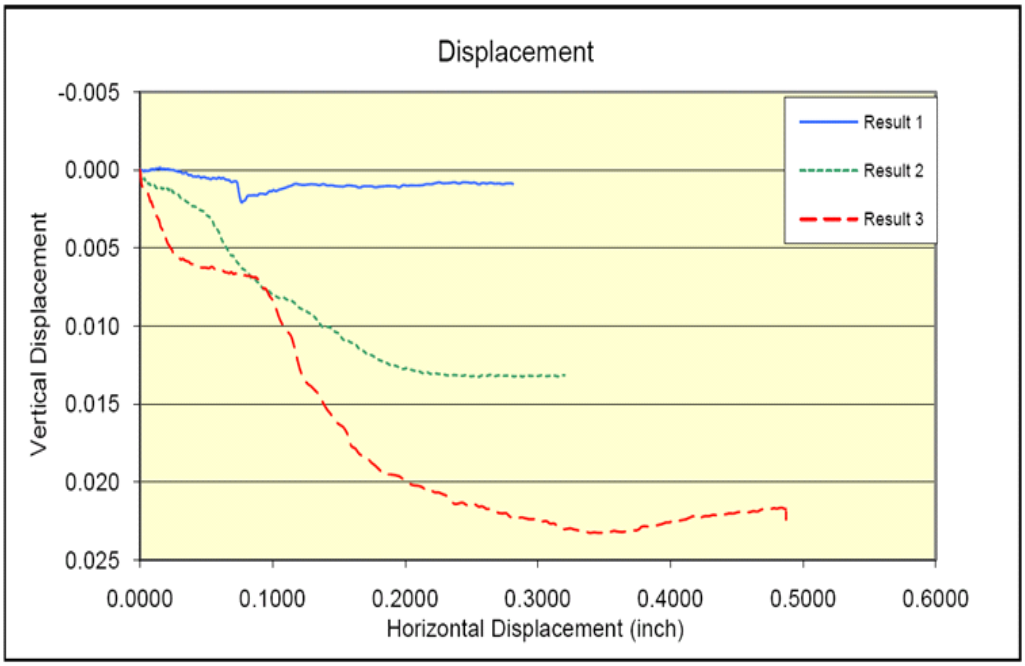
Displacement
Vertical Displacement
-0.005
0.000
0.005
0.010
0.015
0.020
0.025
0.0000
0.1000
0.2000
0.3000
0.4000
0.5000
0.6000
Horizontal Displacement (inch)
Result 1
Result 2
Result 3

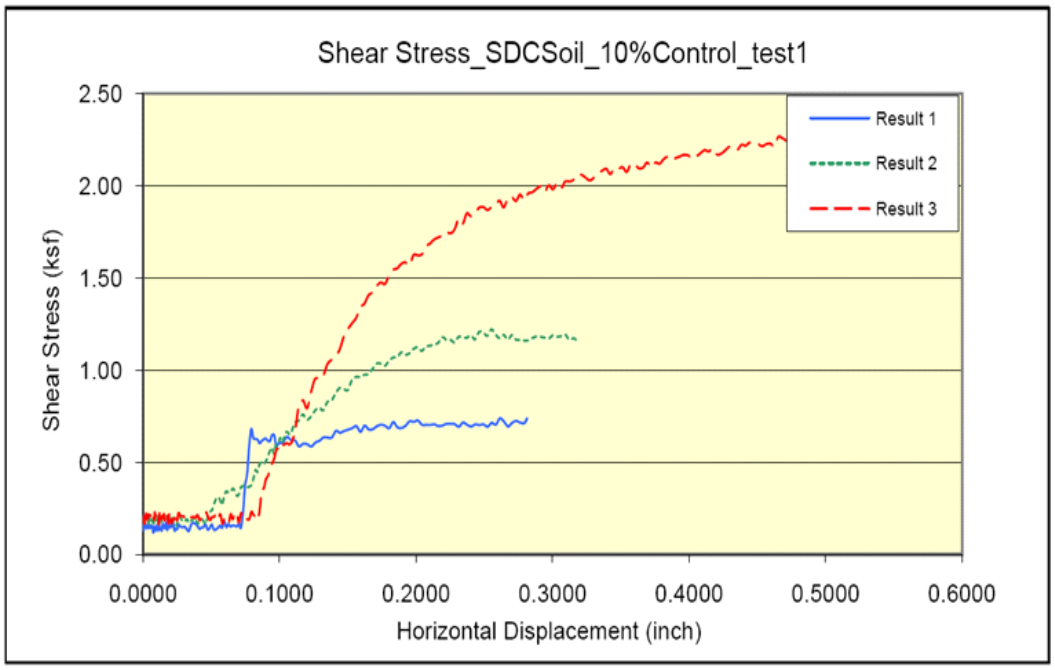
Shear Stress_SDCSoil_10%Control_test1
Shear Stress (ksf)
2.50
2.00
1.50
1.00
0.50
0.00
0.0000
0.1000
0.2000
0.3000
0.4000
0.5000
0.6000
Horizontal Displacement (inch)
Result 1
Result 2
Result 3

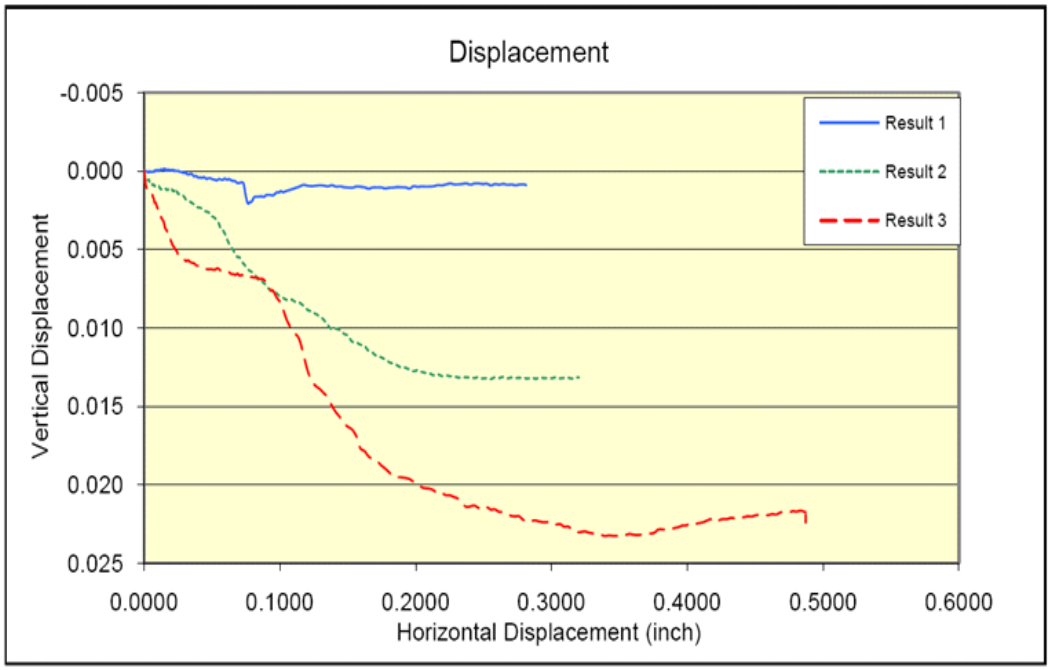
Displacement
Vertical Displacement
-0.005
0.000
0.005
0.010
0.015
0.020
0.025
0.0000
0.1000
0.2000
0.3000
0.4000
0.5000
0.6000
Horizontal Displacement (inch)
Result 1
Result 2
Result 3

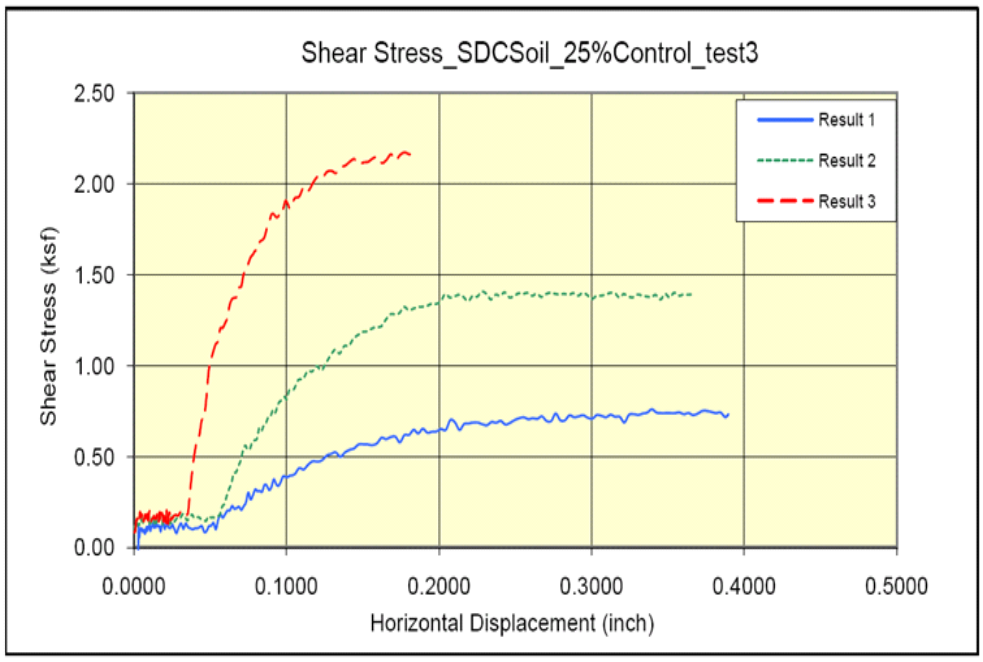
Shear Stress_SDCSoil_25%Control_test3
Shear Stress (ksf)
2.50
2.00
1.50
1.00
0.50
0.00
0.0000
0.1000
0.2000
0.3000
0.4000
0.5000
Horizontal Displacement (inch)
Result 1
Result 2
Result 3

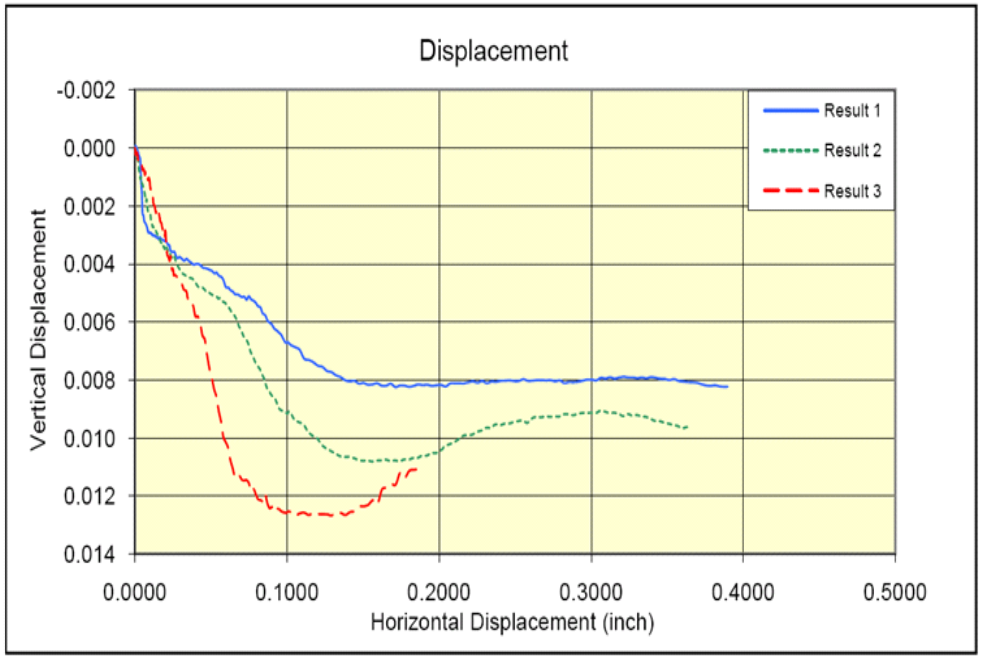
Displacement
Vertical Displacement
-0.002
0.000
0.002
0.004
0.006
0.008
0.010
0.012
0.014
0.0000
0.1000
0.2000
0.3000
0.4000
0.5000
Horizontal Displacement (inch)
Result 1
Result 2
Result 3

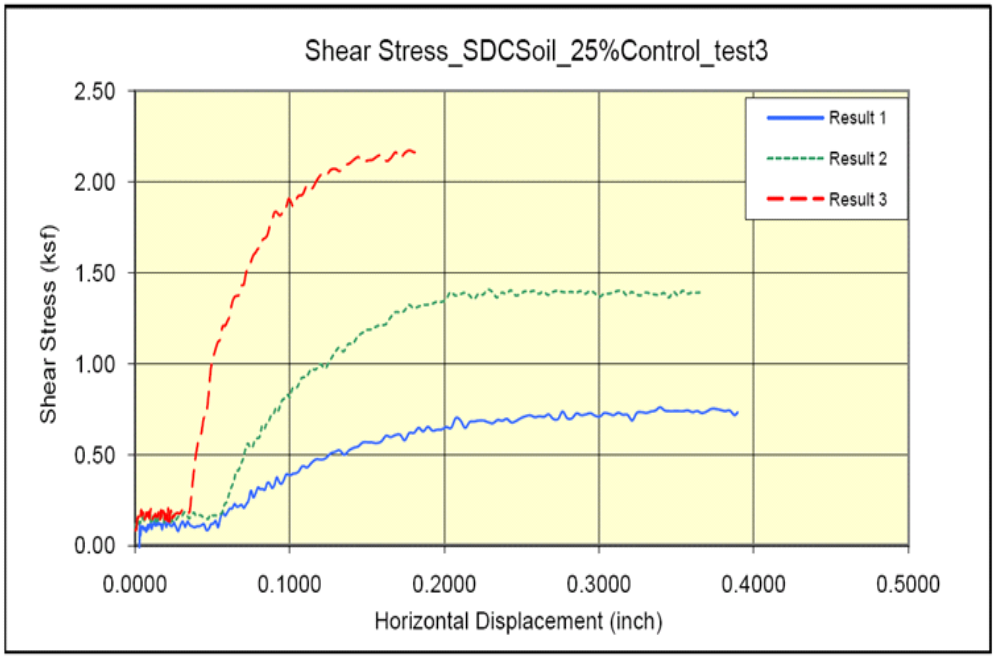
Shear Stress_SDCSoil_25%Control_test3
Shear Stress (ksf)
2.50
2.00
1.50
1.00
0.50
0.00
0.0000
0.1000
0.2000
0.3000
0.4000
0.5000
Horizontal Displacement (inch)
Result 1
Result 2
Result 3

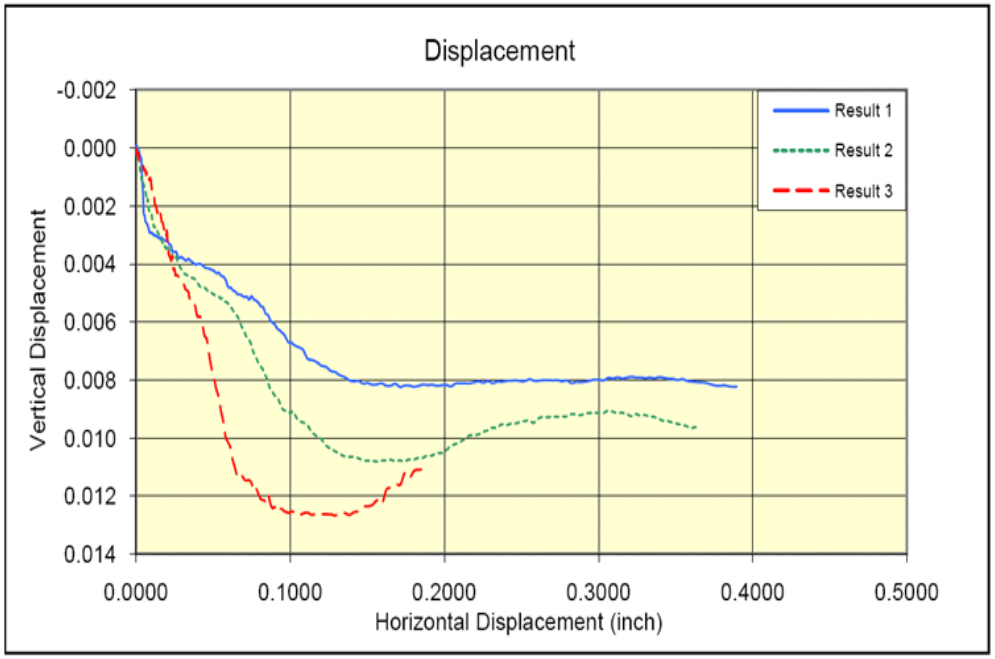
Displacement
Vertical Displacement
-0.002
0.000
0.002
0.004
0.006
0.008
0.010
0.012
0.014
0.0000
0.1000
0.2000
0.3000
0.4000
0.5000
Horizontal Displacement (inch)
Result 1
Result 2
Result 3

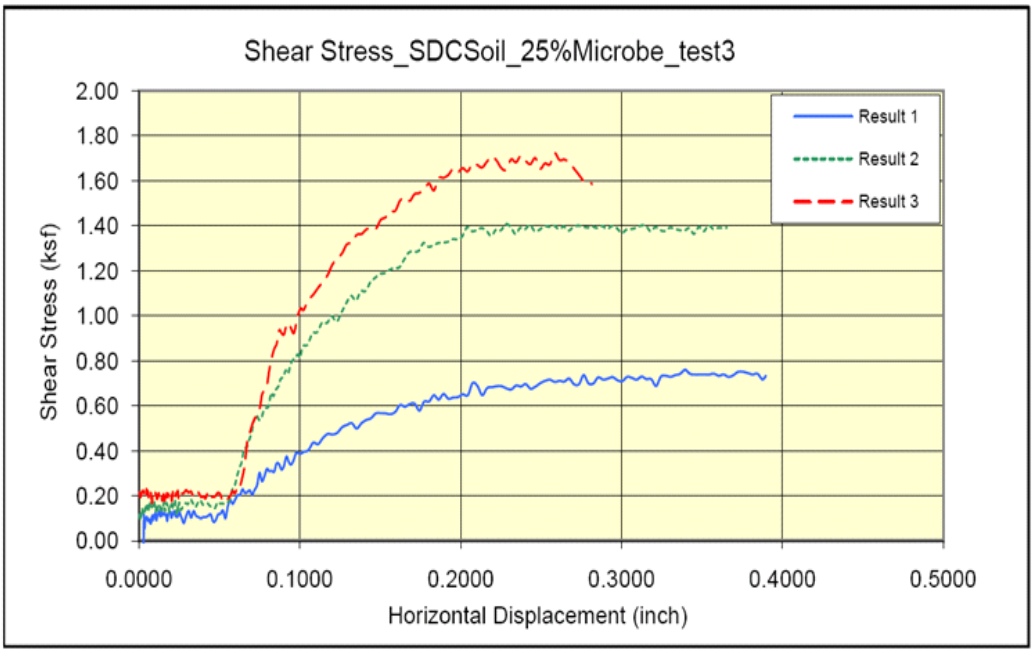
Shear Stress_SDCSoil_25%Microbe_test3
Shear Stress (ksf)
2.00
1.80
1.60
1.40
1.20
1.00
0.80
0.60
0.40
0.20
0.00
0.0000
0.1000
0.2000
0.3000
0.4000
0.5000
Horizontal Displacement (inch)
Result 1
Result 2
Result 3

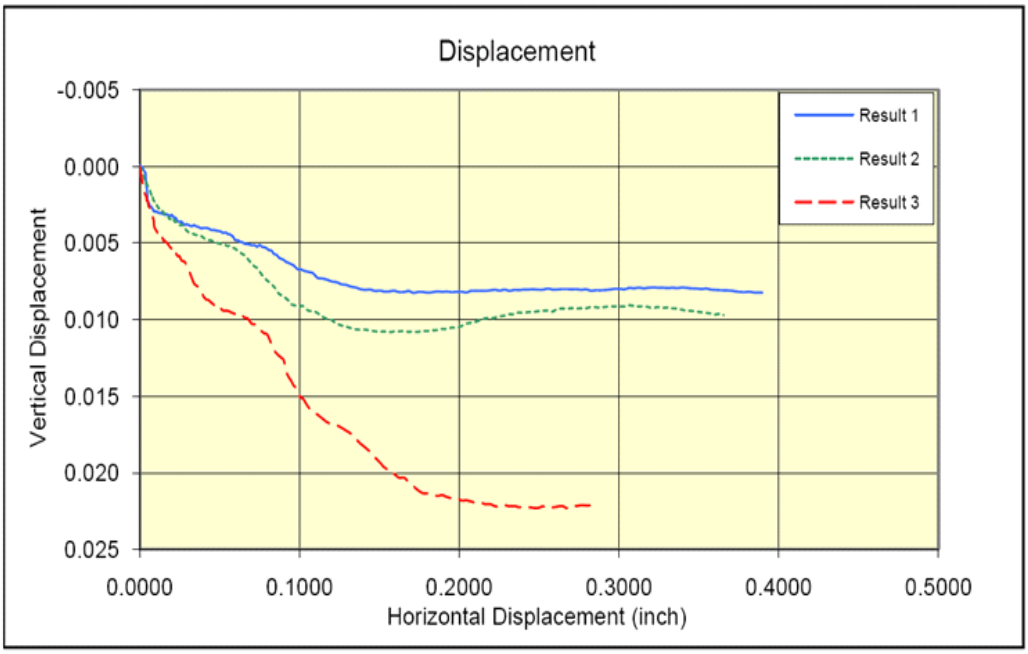
Displacement
Vertical Displacement
-0.005
0.000
0.005
0.010
0.015
0.020
0.025
0.0000
0.1000
0.2000
0.3000
0.4000
0.5000
Horizontal Displacement (inch)
Result 1
Result 2
Result 3

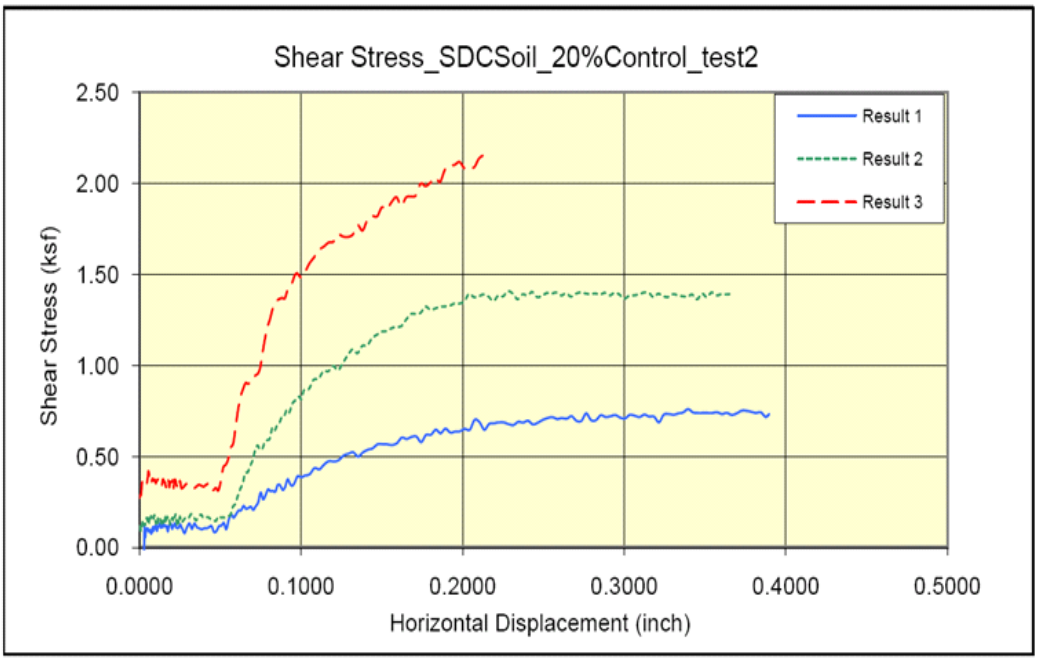
Shear Stress_SDCSoil_20%Control_test2
Shear Stress (ksf)
2.50
2.00
1.50
1.00
0.50
0.00
0.0000
0.1000
0.2000
0.3000
0.4000
0.5000
Horizontal Displacement (inch)
Result 1
Result 2
Result 3

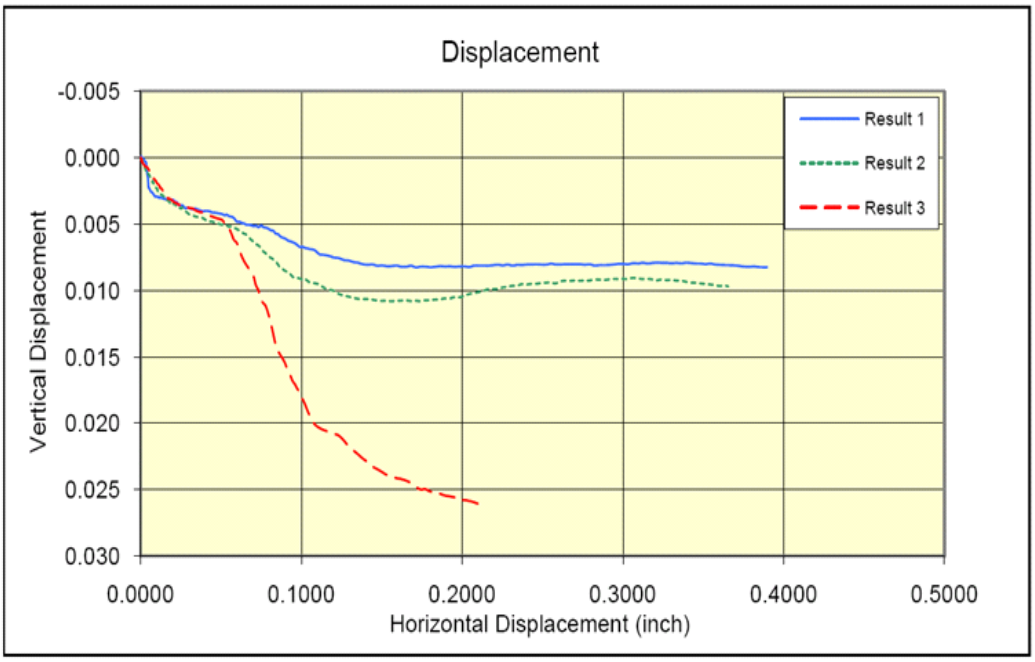
Displacement
Vertical Displacement
-0.005
0.000
0.005
0.010
0.015
0.020
0.025
0.030
0.0000
0.1000
0.2000
0.3000
0.4000
0.5000
Horizontal Displacement (inch)
Result 1
Result 2
Result 3

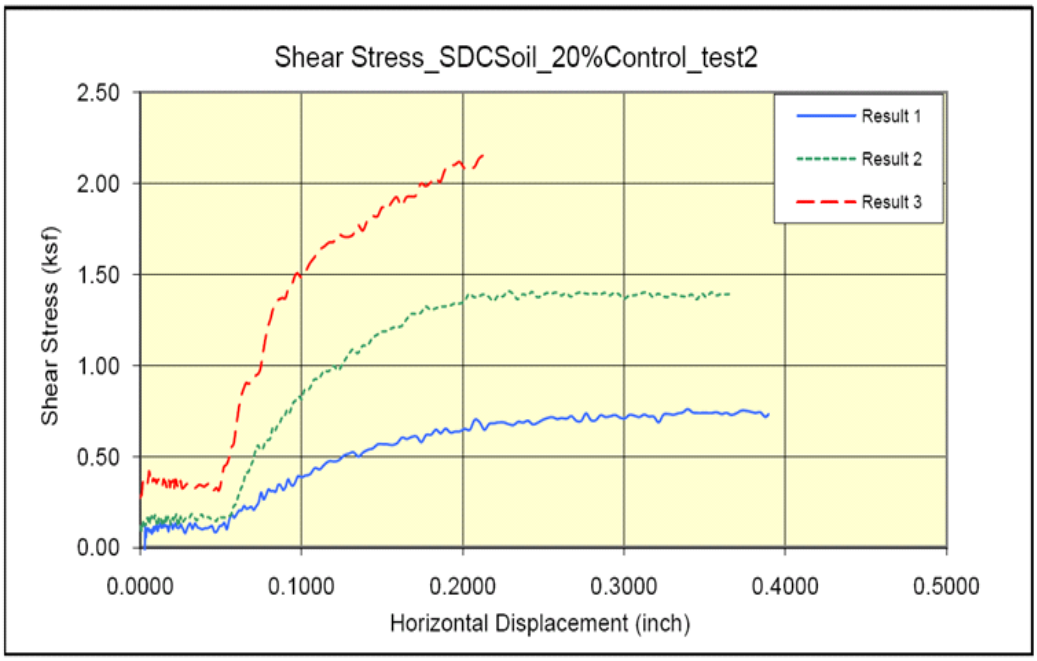
Shear Stress_SDCSoil_20%Control_test2
Shear Stress (ksf)
2.50
2.00
1.50
1.00
0.50
0.00
0.0000
0.1000
0.2000
0.3000
0.4000
0.5000
Horizontal Displacement (inch)
Result 1
Result 2
Result 3

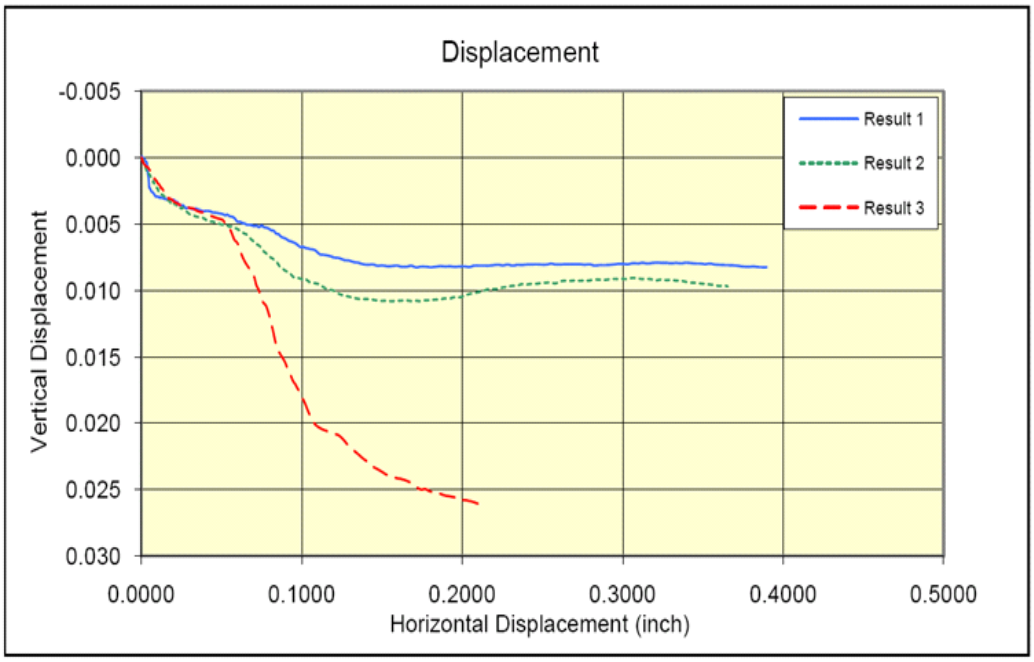
Displacement
Vertical Displacement
-0.005
0.000
0.005
0.010
0.015
0.020
0.025
0.030
0.0000
0.1000
0.2000
0.3000
0.4000
0.5000
Horizontal Displacement (inch)
Result 1
Result 2
Result 3

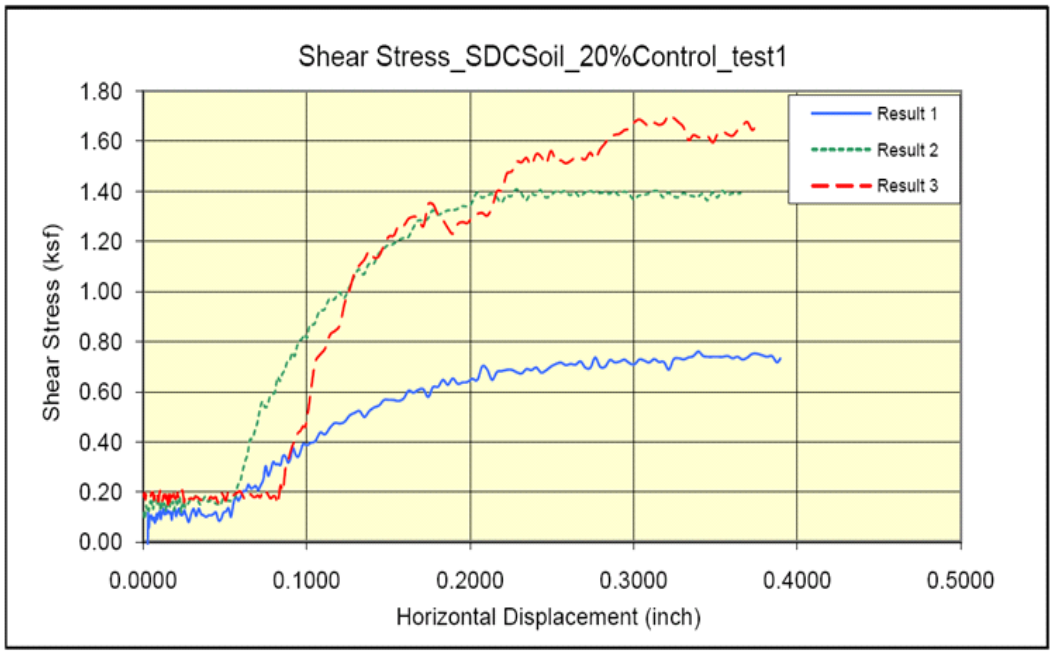
Shear Stress_SDCSoil_20%Control_test1
Shear Stress (ksf)
1.80
1.60
1.40
1.20
1.00
0.80
0.60
0.40
0.20
0.00
0.0000
0.1000
0.2000
0.3000
0.4000
0.5000
Horizontal Displacement (inch)
Result 1
Result 2
Result 3

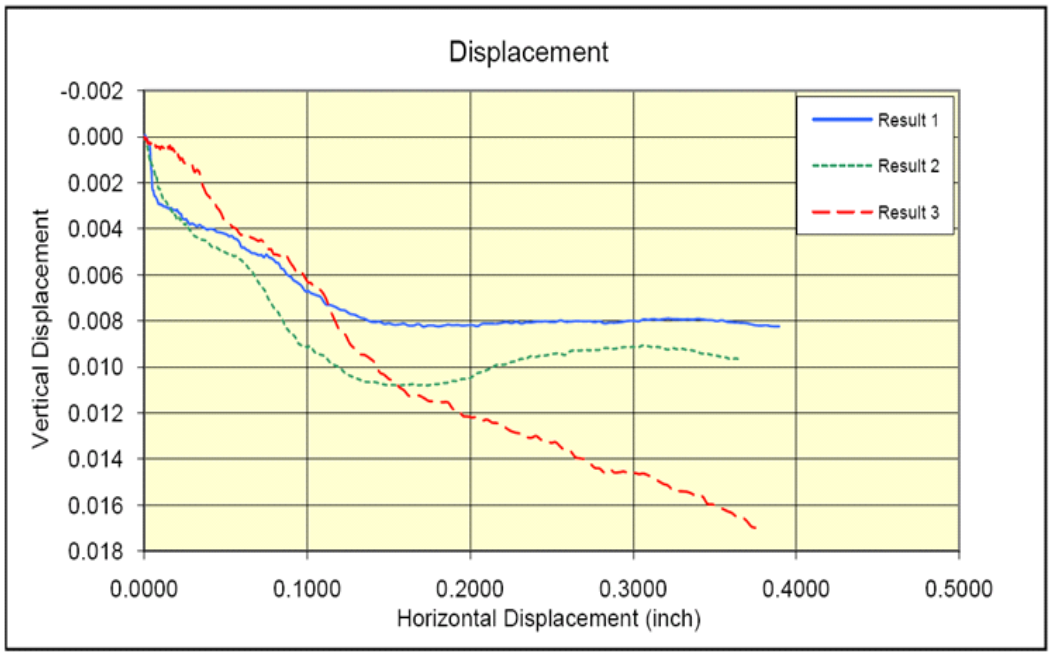
Displacement
Vertical Displacement
-0.002
0.000
0.002
0.004
0.006
0.008
0.010
0.012
0.014
0.016
0.018
0.0000
0.1000
0.2000
0.3000
0.4000
0.5000
Horizontal Displacement (inch)
Result 1
Result 2
Result 3

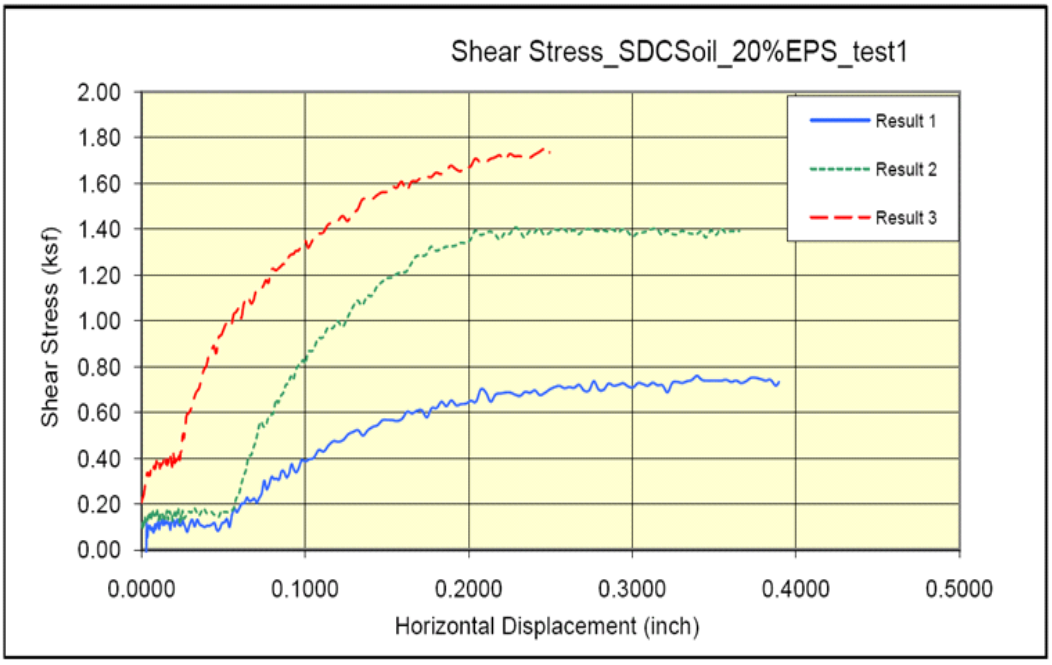
Shear Stress_SDCSoil_20%EPS_test1
Shear Stress (ksf)
2.00
1.80
1.60
1.40
1.20
1.00
0.80
0.60
0.40
0.20
0.00
0.0000
0.1000
0.2000
0.3000
0.4000
0.5000
Horizontal Displacement (inch)
Result 1
Result 2
Result 3

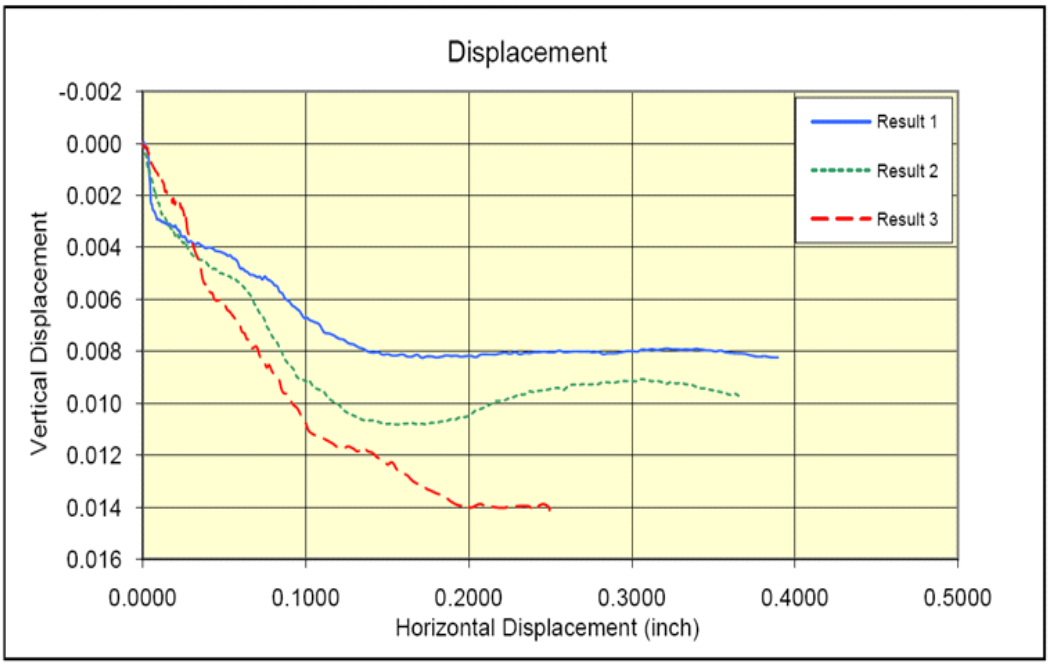
Displacement
Vertical Displacement
-0.002
0.000
0.002
0.004
0.006
0.008
0.010
0.012
0.014
0.016
0.0000
0.1000
0.2000
0.3000
0.4000
0.5000
Horizontal Displacement (inch)
Result 1
Result 2
Result 3

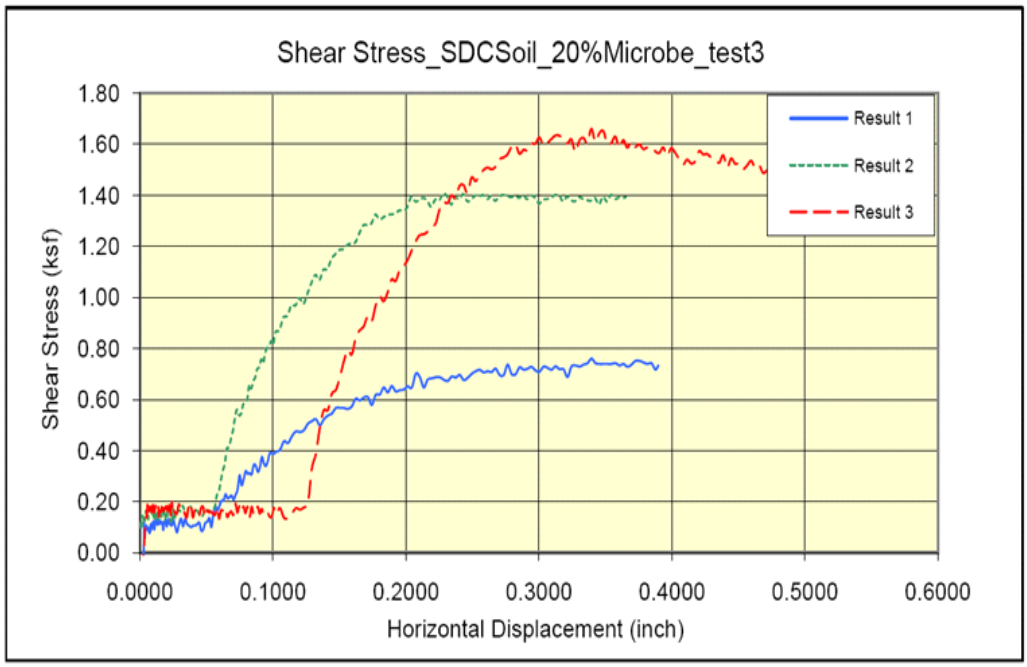
Shear Stress_SDCSoil_20%Microbe_test3
Shear Stress (ksf)
1.80
1.60
1.40
1.20
1.00
0.80
0.60
0.40
0.20
0.00
0.0000
0.1000
0.2000
0.3000
0.4000
0.5000
0.6000
Horizontal Displacement (inch)
Result 1
Result 2
Result 3

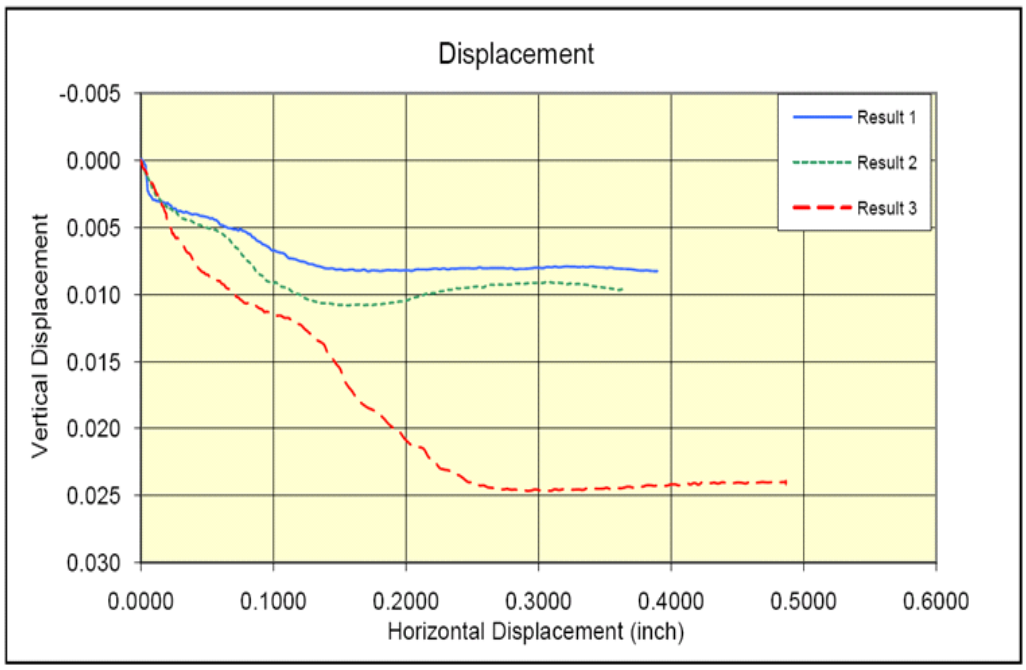
Displacement
Vertical Displacement
-0.005
0.000
0.005
0.010
0.015
0.020
0.025
0.030
0.0000
0.1000
0.2000
0.3000
0.4000
0.5000
0.6000
Horizontal Displacement (inch)
Result 1
Result 2
Result 3

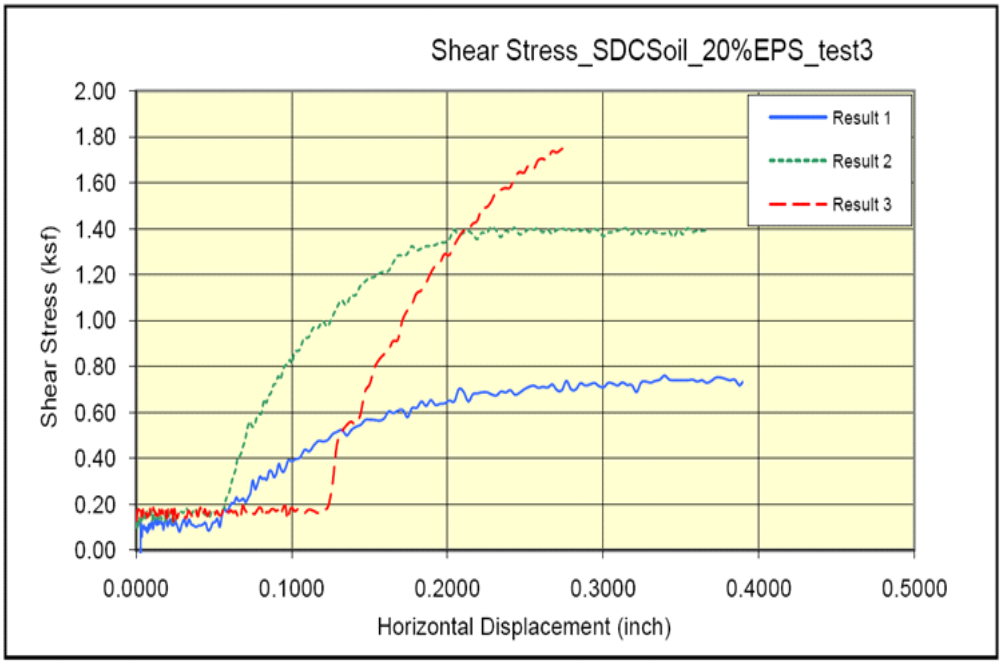
Shear Stress_SDCSoil_20%EPS_test3
Shear Stress (ksf)
2.00
1.80
1.60
1.40
1.20
1.00
0.80
0.60
0.40
0.20
0.00
0.0000
0.1000
0.2000
0.3000
0.4000
0.5000
Horizontal Displacement (inch)
Result 1
Result 2
Result 3

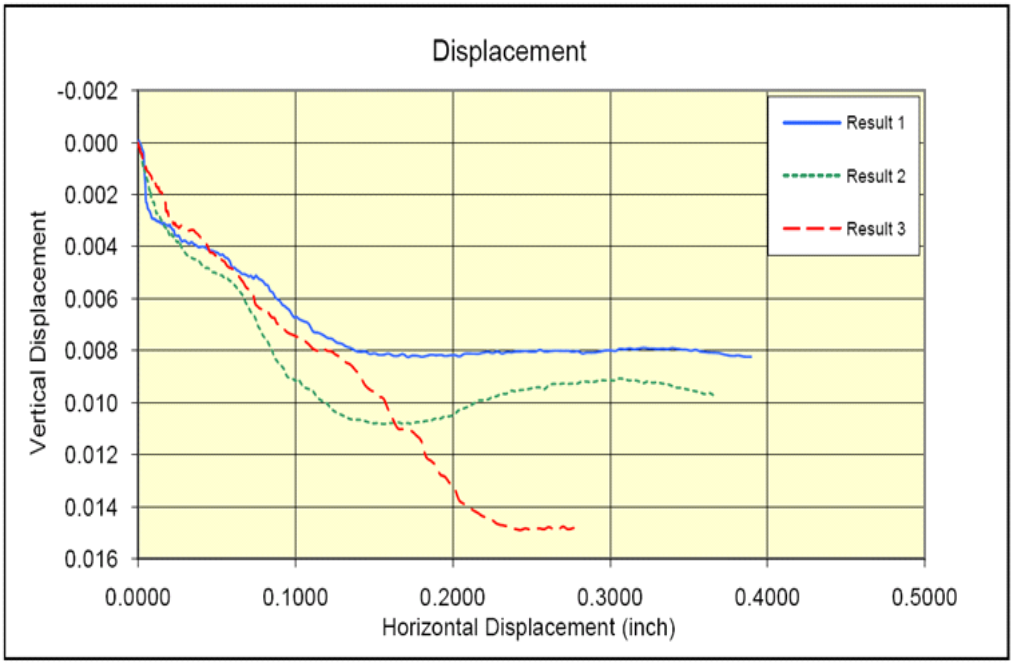
Displacement
Vertical Displacement
-0.002
0.000
0.002
0.004
0.006
0.008
0.010
0.012
0.014
0.016
0.0000
0.1000
0.2000
0.3000
0.4000
0.5000
Horizontal Displacement (inch)
Result 1
Result 2
Result 3

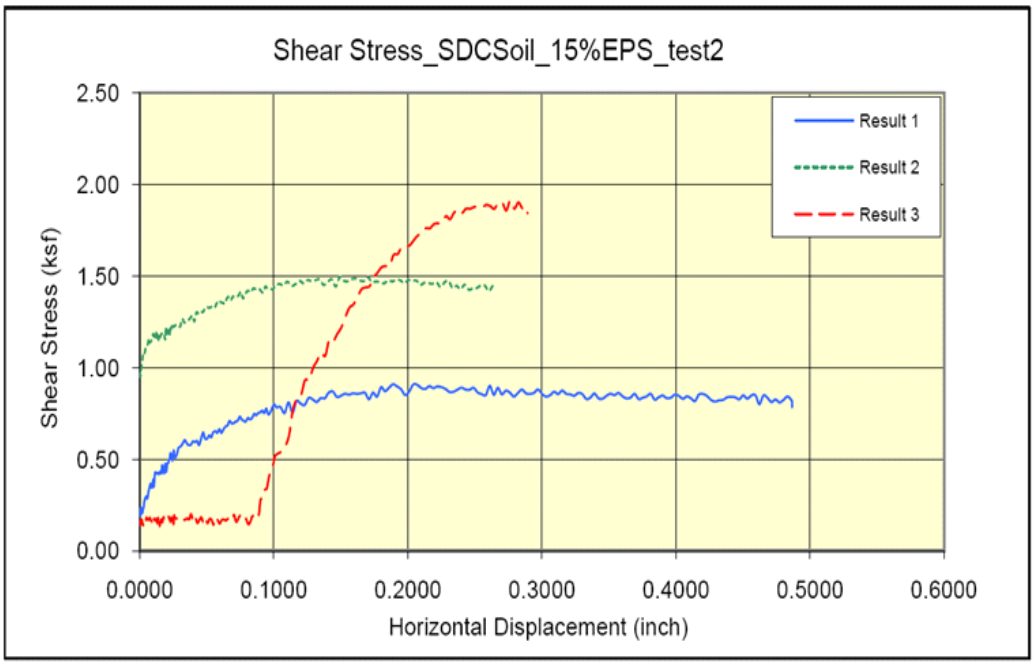
Shear Stress_SDCSoil_15%EPS_test2
Shear Stress (ksf)
2.50
2.00
1.50
1.00
0.50
0.00
0.0000
0.1000
0.2000
0.3000
0.4000
0.5000
0.6000
Horizontal Displacement (inch)
Result 1
Result 2
Result 3

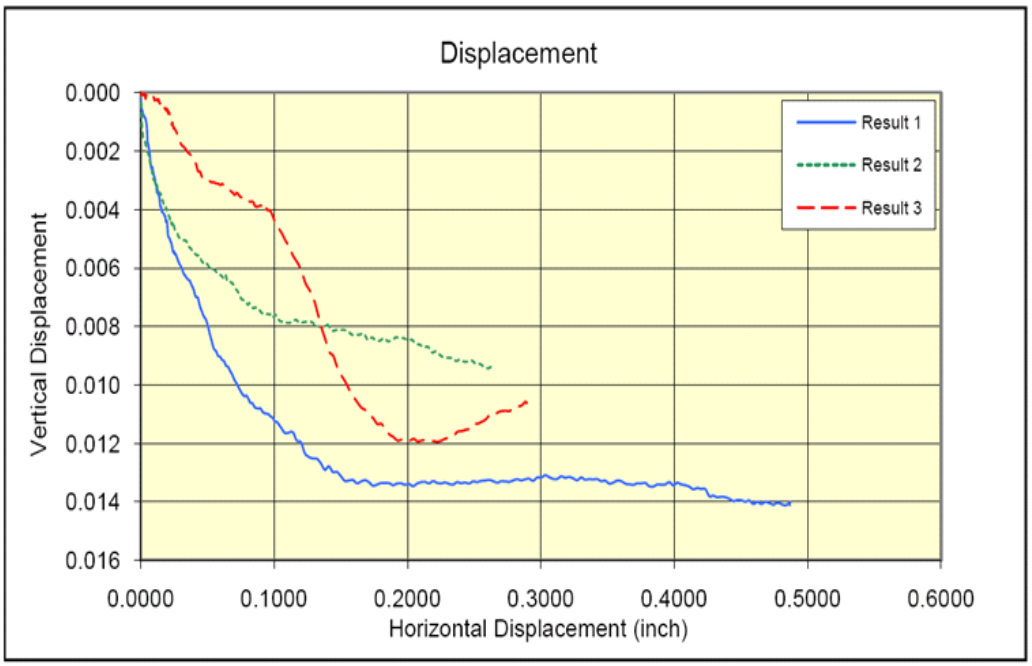
Displacement
Vertical Displacement
0.000
0.002
0.004
0.006
0.008
0.010
0.012
0.014
0.016
0.0000
0.1000
0.2000
0.3000
0.4000
0.5000
0.6000
Horizontal Displacement (inch)
Result 1
Result 2
Result 3

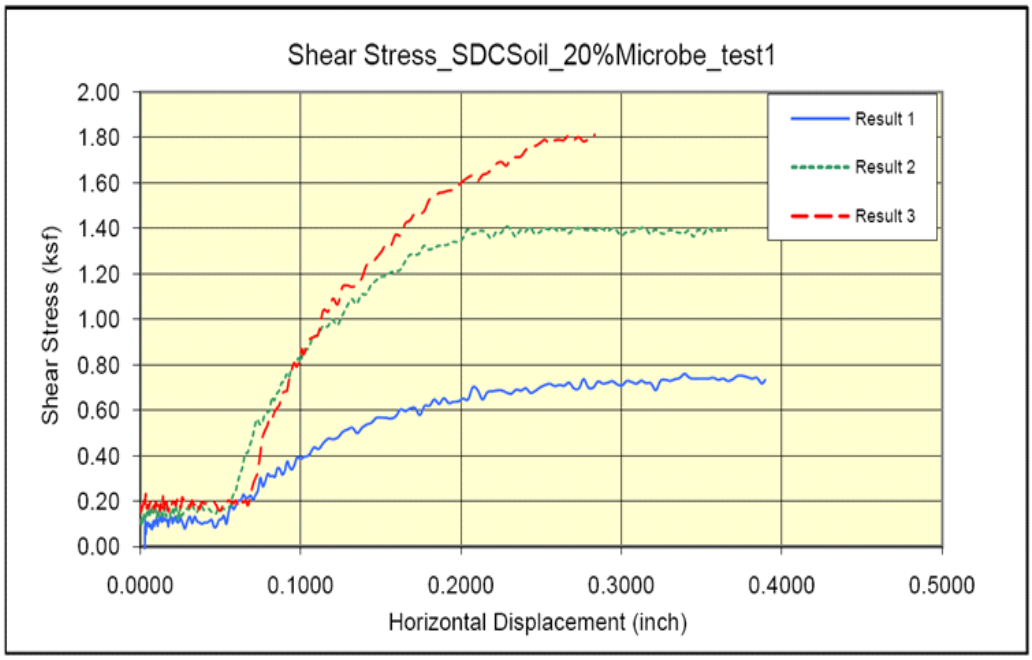
Shear Stress_SDCSoil_20%Microbe_test1
Shear Stress (ksf)
2.00
1.80
1.60
1.40
1.20
1.00
0.80
0.60
0.40
0.20
0.00
0.0000
0.1000
0.2000
0.3000
0.4000
0.5000
Horizontal Displacement (inch)
Result 1
Result 2
Result 3

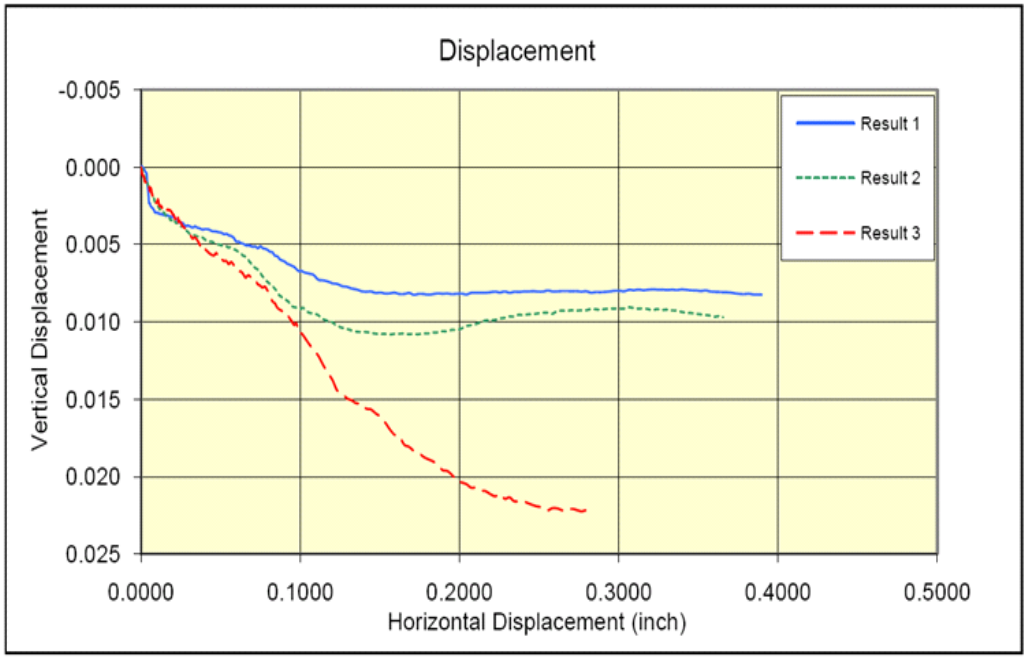
Displacement
Vertical Displacement
-0.005
0.000
0.005
0.010
0.015
0.020
0.025
0.0000
0.1000
0.2000
0.3000
0.4000
0.5000
Horizontal Displacement (inch)
Result 1
Result 2
Result 3

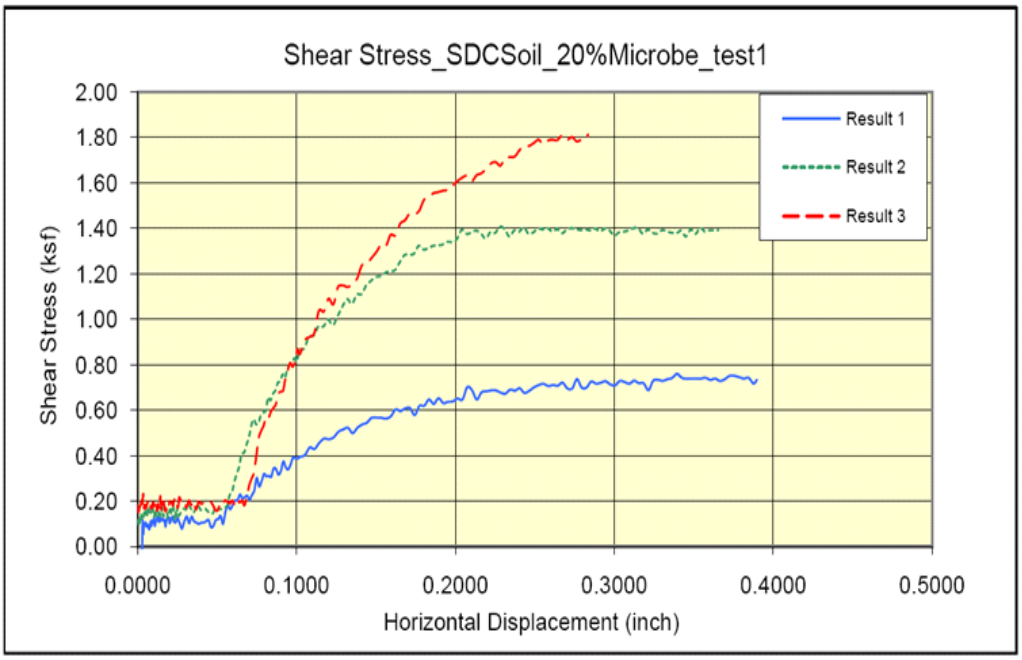
Shear Stress_SDCSoil_20%Microbe_test1
Shear Stress (ksf)
2.00
1.80
1.60
1.40
1.20
1.00
0.80
0.60
0.40
0.20
0.00
0.0000
0.1000
0.2000
0.3000
0.4000
0.5000
Horizontal Displacement (inch)
Result 1
Result 2
Result 3

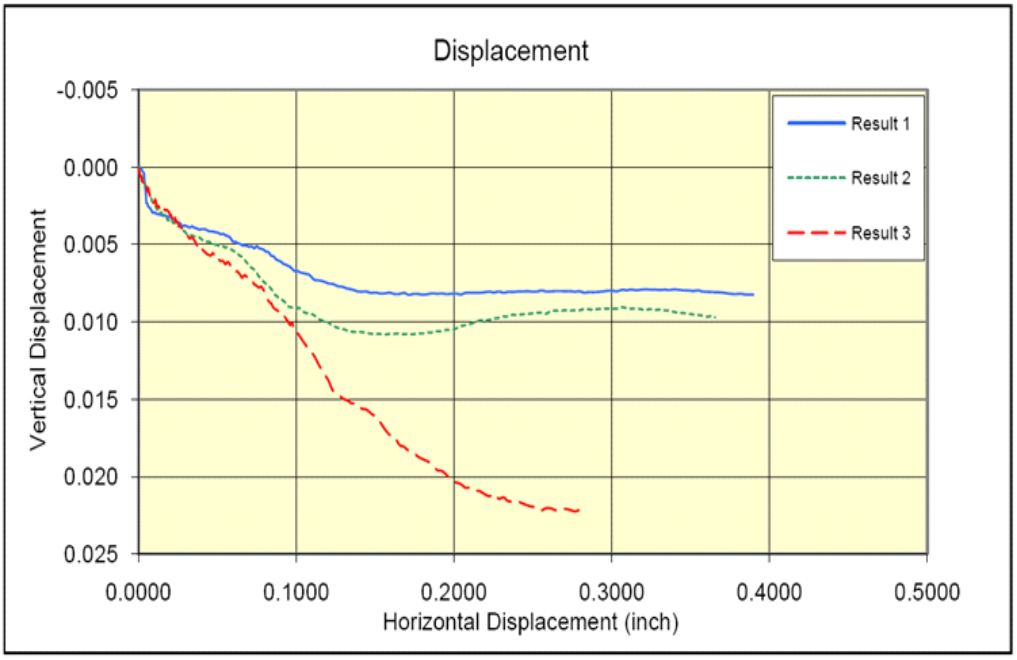
Displacement
Vertical Displacement
-0.005
0.000
0.005
0.010
0.015
0.020
0.025
0.0000
0.1000
0.2000
0.3000
0.4000
0.5000
Horizontal Displacement (inch)
Result 1
Result 2
Result 3

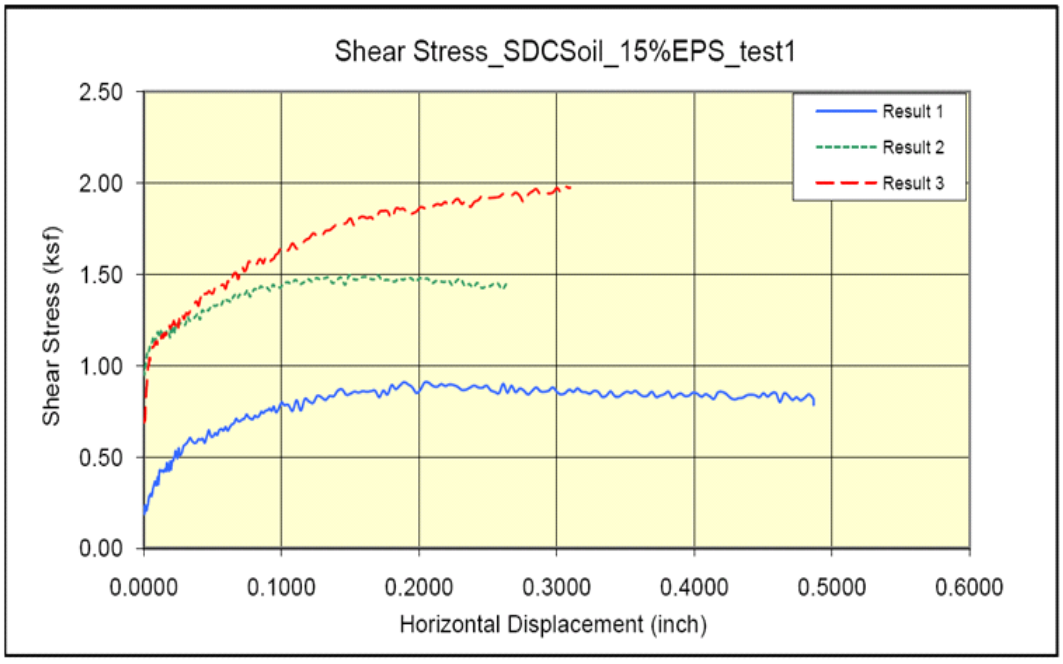
Shear Stress_SDCSoil_15%EPS_test1
Shear Stress (ksf)
2.50
2.00
1.50
1.00
0.50
0.00
0.0000
0.1000
0.2000
0.3000
0.4000
0.5000
0.6000
Horizontal Displacement (inch)
Result 1
Result 2
Result 3

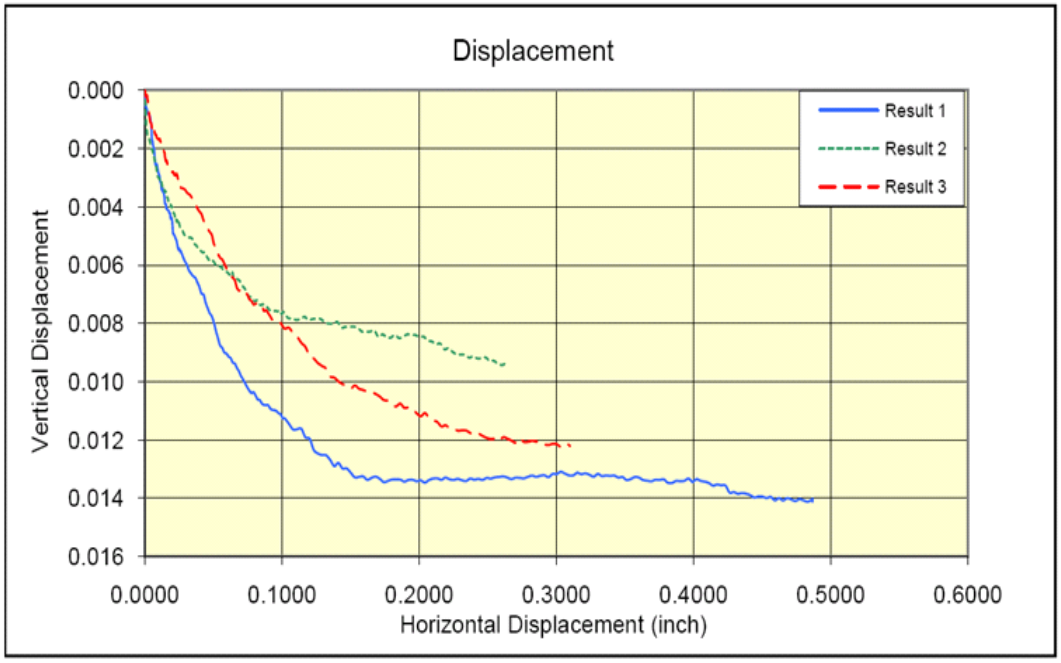
Displacement
Vertical Displacement
0.000
0.002
0.004
0.006
0.008
0.010
0.012
0.014
0.016
0.0000
0.1000
0.2000
0.3000
0.4000
0.5000
0.6000
Horizontal Displacement (inch)
Result 1
Result 2
Result 3

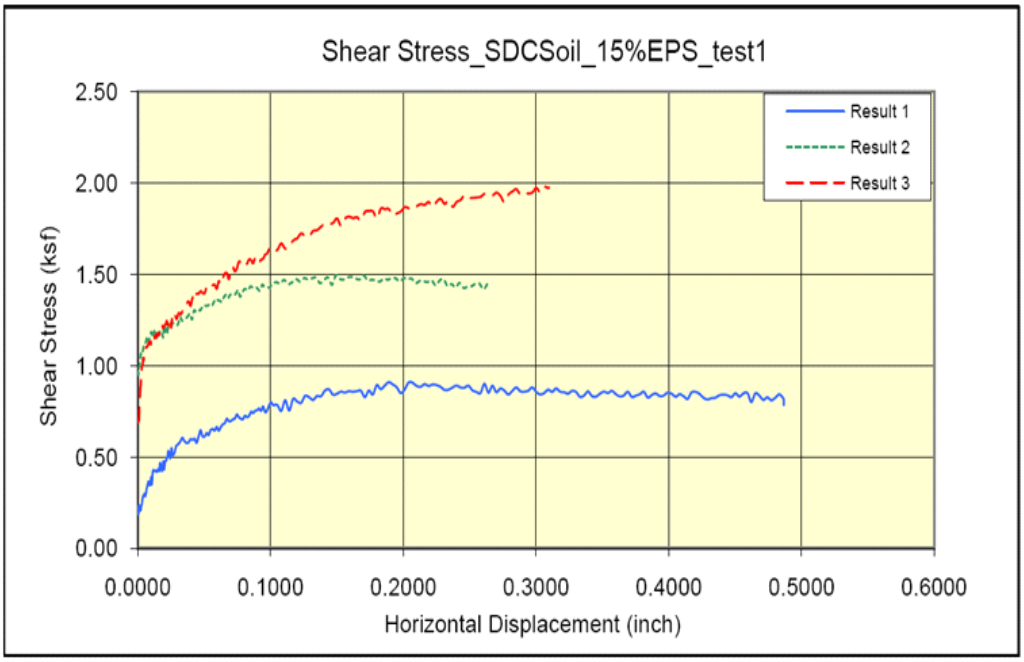
Shear Stress_SDCSoil_15%EPS_test1
Shear Stress (ksf)
2.50
2.00
1.50
1.00
0.50
0.00
0.0000
0.1000
0.2000
0.3000
0.4000
0.5000
0.6000
Horizontal Displacement (inch)
Result 1
Result 2
Result 3

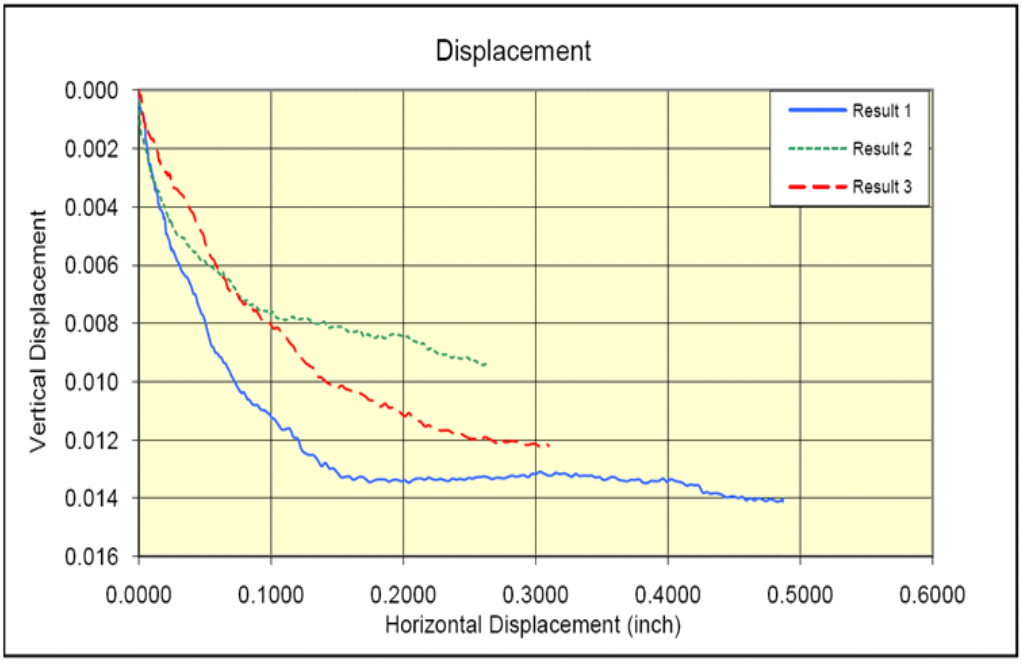
Displacement
Vertical Displacement
0.000
0.002
0.004
0.006
0.008
0.010
0.012
0.014
0.016
0.0000
0.1000
0.2000
0.3000
0.4000
0.5000
0.6000
Horizontal Displacement (inch)
Result 1
Result 2
Result 3

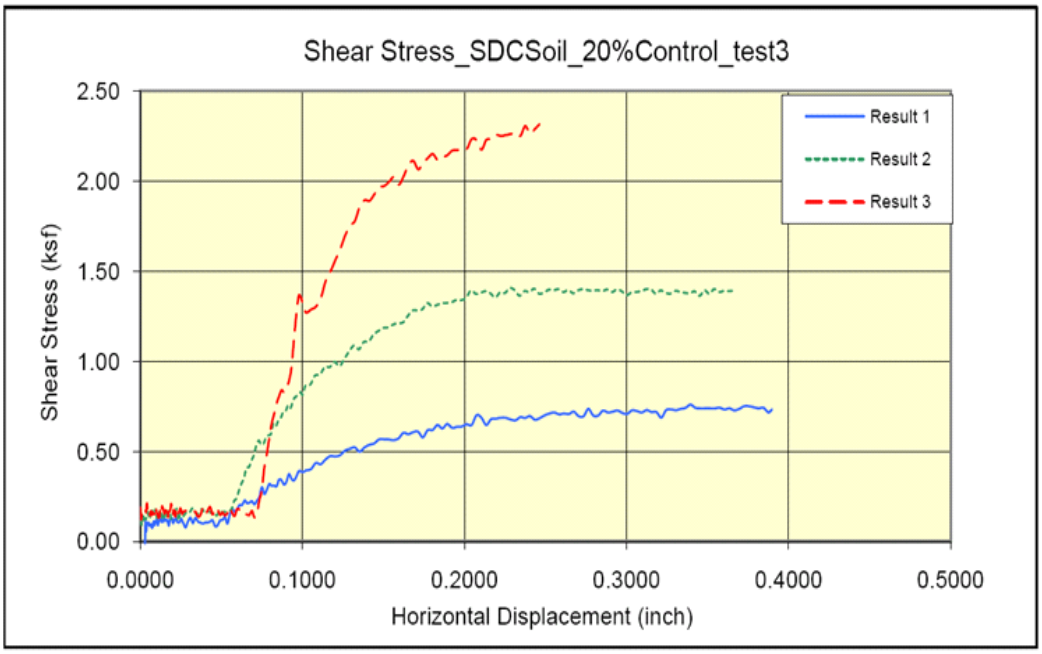
Shear Stress_SDCSoil_20%Control_test3
Shear Stress (ksf)
2.50
2.00
1.50
1.00
0.50
0.00
0.0000
0.1000
0.2000
0.3000
0.4000
0.5000
Horizontal Displacement (inch)
Result 1
Result 2
Result 3

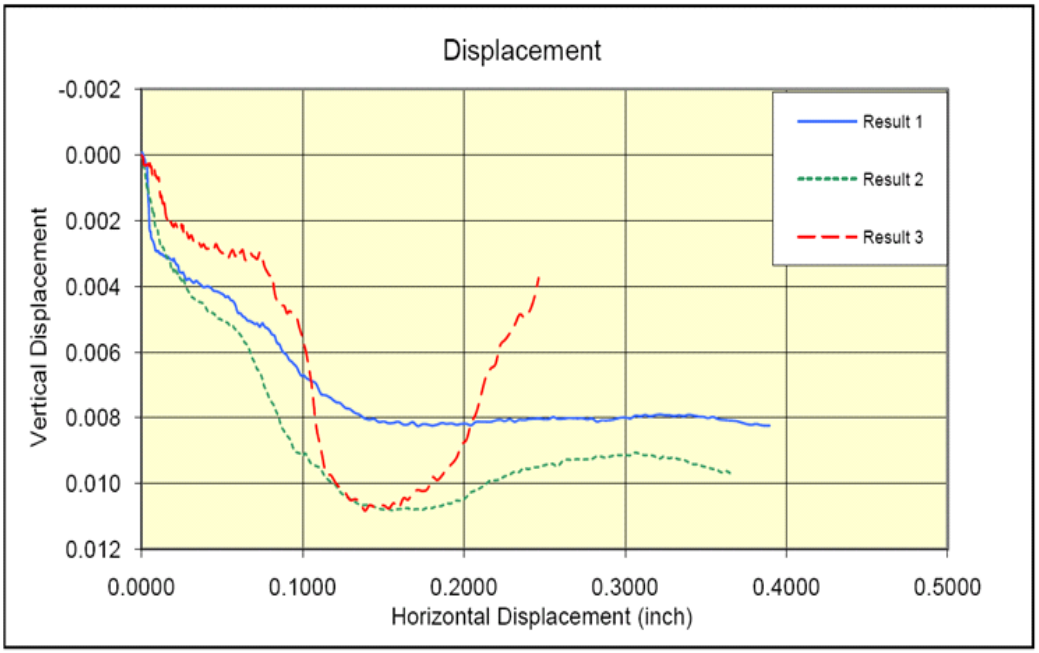
Displacement
Vertical Displacement
-0.002
0.000
0.002
0.004
0.006
0.008
0.010
0.012
0.0000
0.1000
0.2000
0.3000
0.4000
0.5000
Horizontal Displacement (inch)
Result 1
Result 2
Result 3

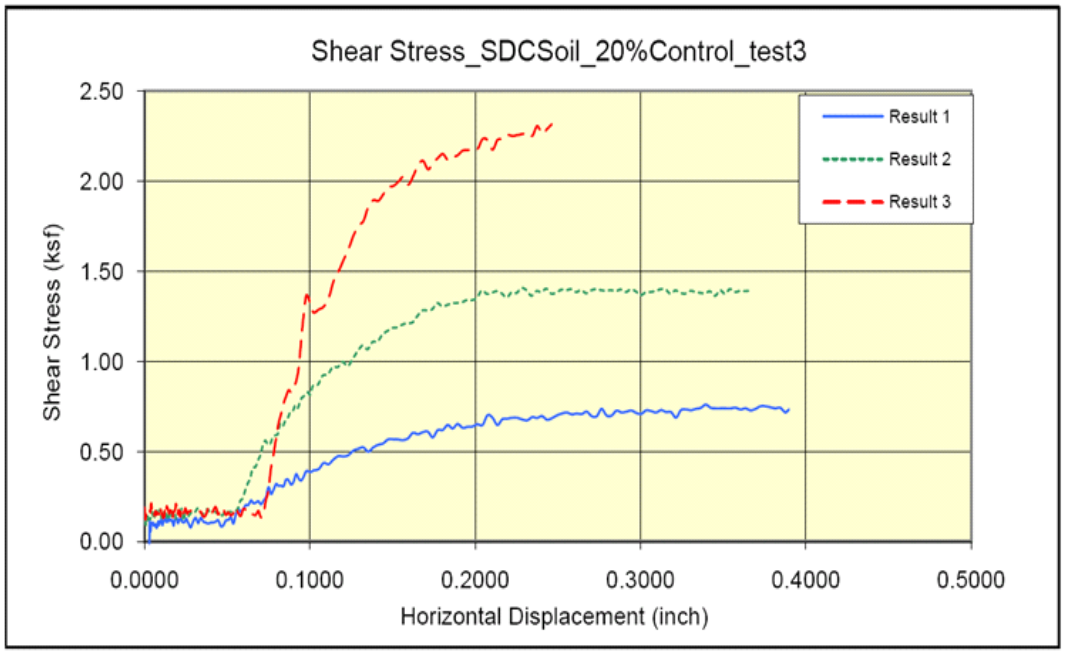
Shear Stress_SDCSoil_20%Control_test3
Shear Stress (ksf)
2.50
2.00
1.50
1.00
0.50
0.00
0.0000
0.1000
0.2000
0.3000
0.4000
0.5000
Horizontal Displacement (inch)
Result 1
Result 2
Result 3

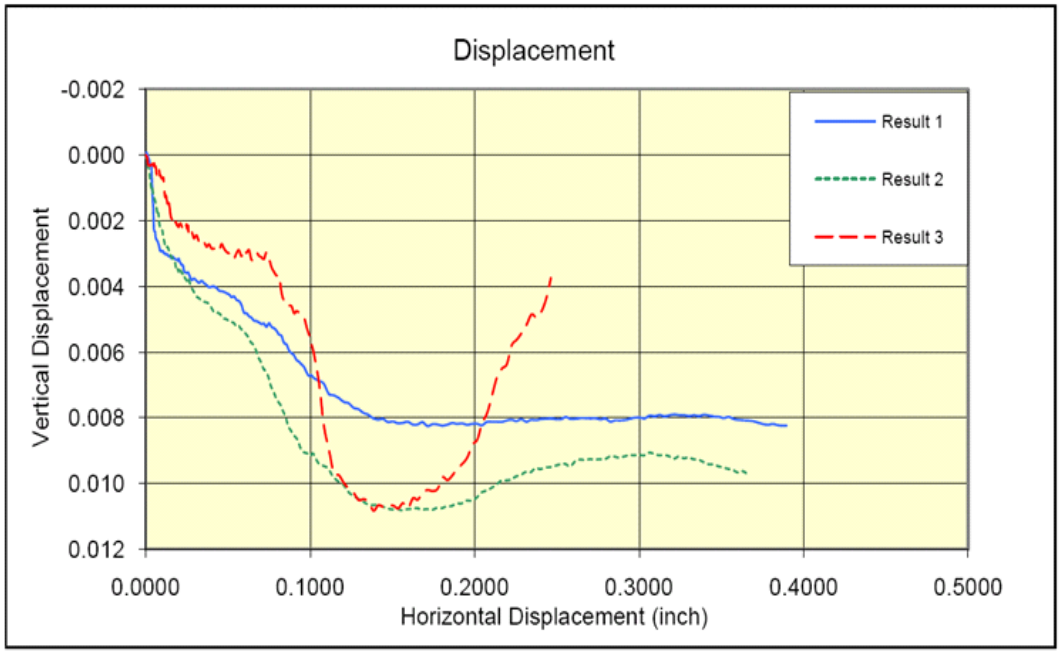
Displacement
Vertical Displacement
-0.002
0.000
0.002
0.004
0.006
0.008
0.010
0.012
0.0000
0.1000
0.2000
0.3000
0.4000
0.5000
Horizontal Displacement (inch)
Result 1
Result 2
Result 3

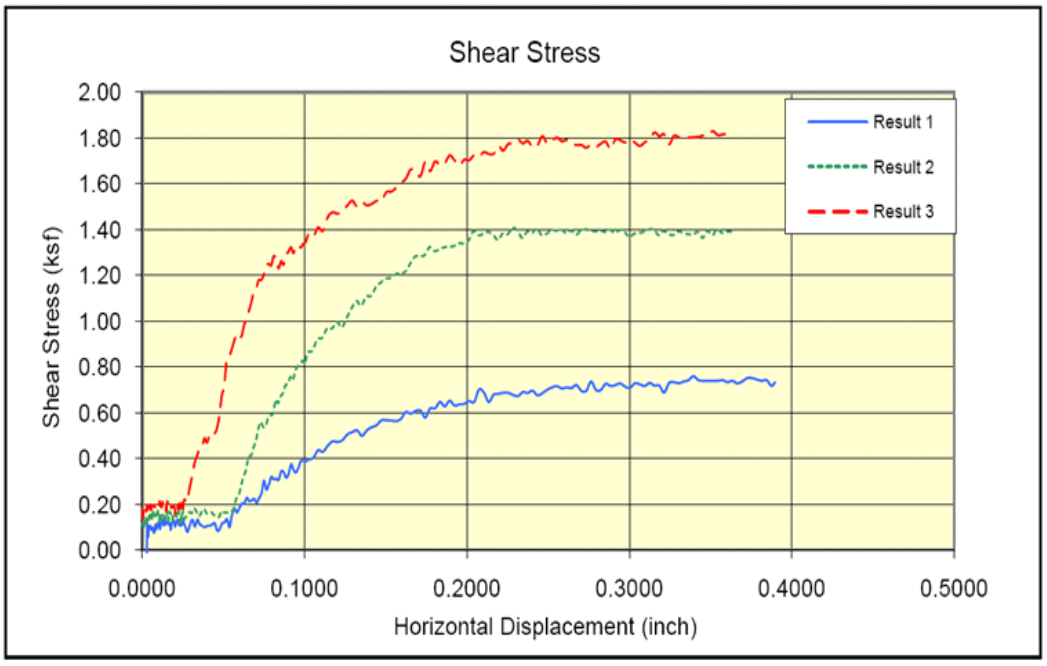
Shear Stress
Shear Stress (ksf)
2.00
1.80
1.60
1.40
1.20
1.00
0.80
0.60
0.40
0.20
0.00
0.0000
0.1000
0.2000
0.3000
0.4000
0.5000
Horizontal Displacement (inch)
Result 1
Result 2
Result 3

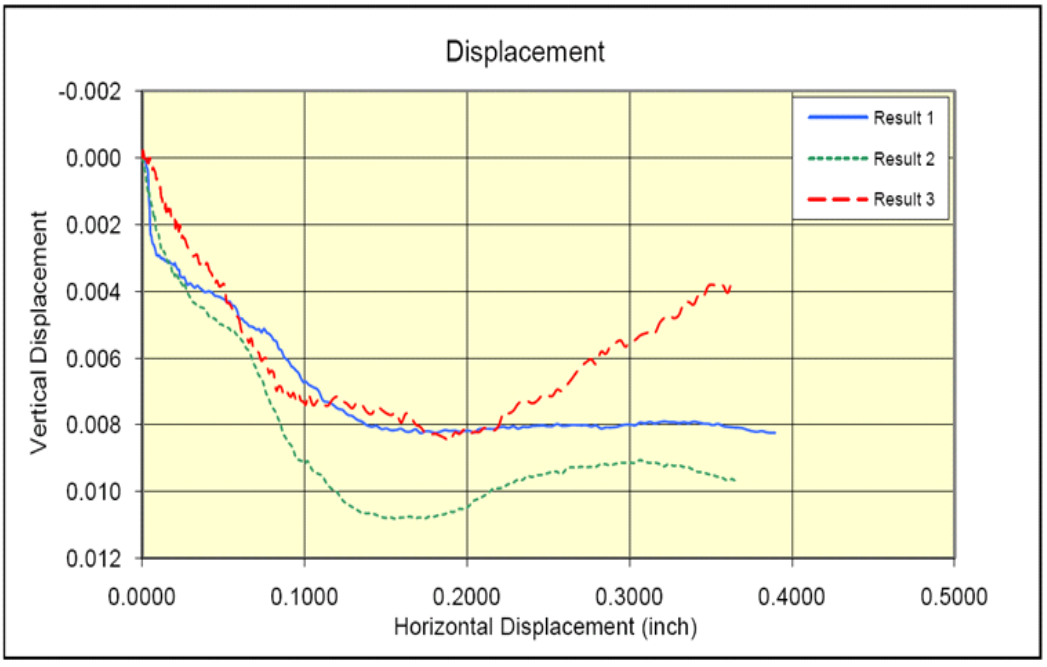
Displacement
Vertical Displacement
-0.002
0.000
0.002
0.004
0.006
0.008
0.010
0.012
0.0000
0.1000
0.2000
0.3000
0.4000
0.5000
Horizontal Displacement (inch)
Result 1
Result 2
Result 3

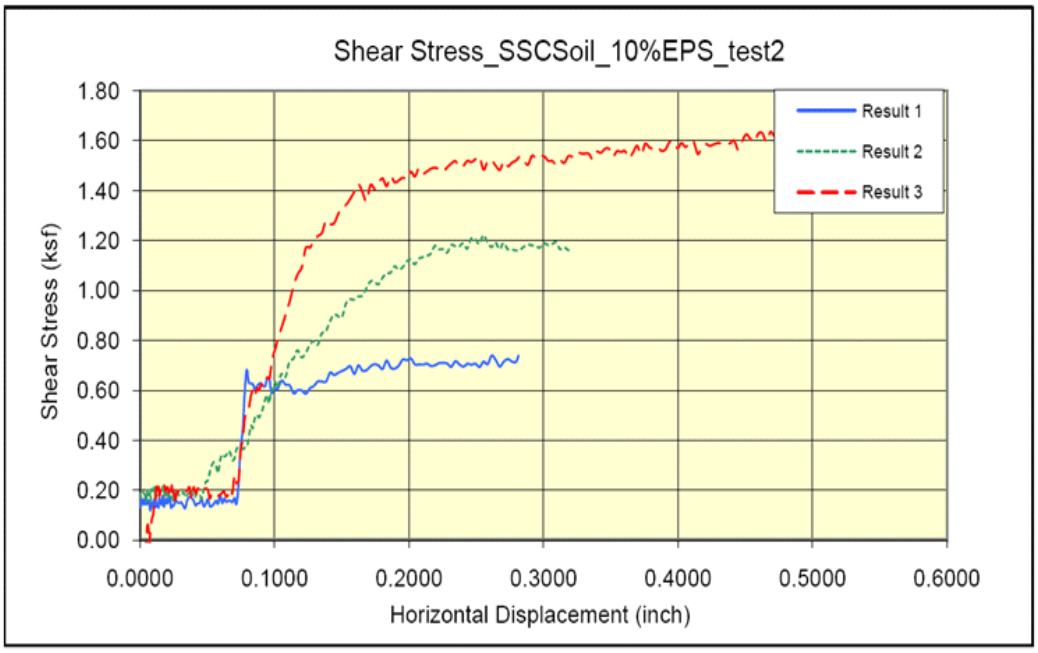
Shear Stress_SSCSoil_10%EPS_test2
Shear Stress (ksf)
1.80
1.60
1.40
1.20
1.00
0.80
0.60
0.40
0.20
0.00
0.0000
0.1000
0.2000
0.3000
0.4000
0.5000
0.6000
Horizontal Displacement (inch)
Result 1
Result 2
Result 3

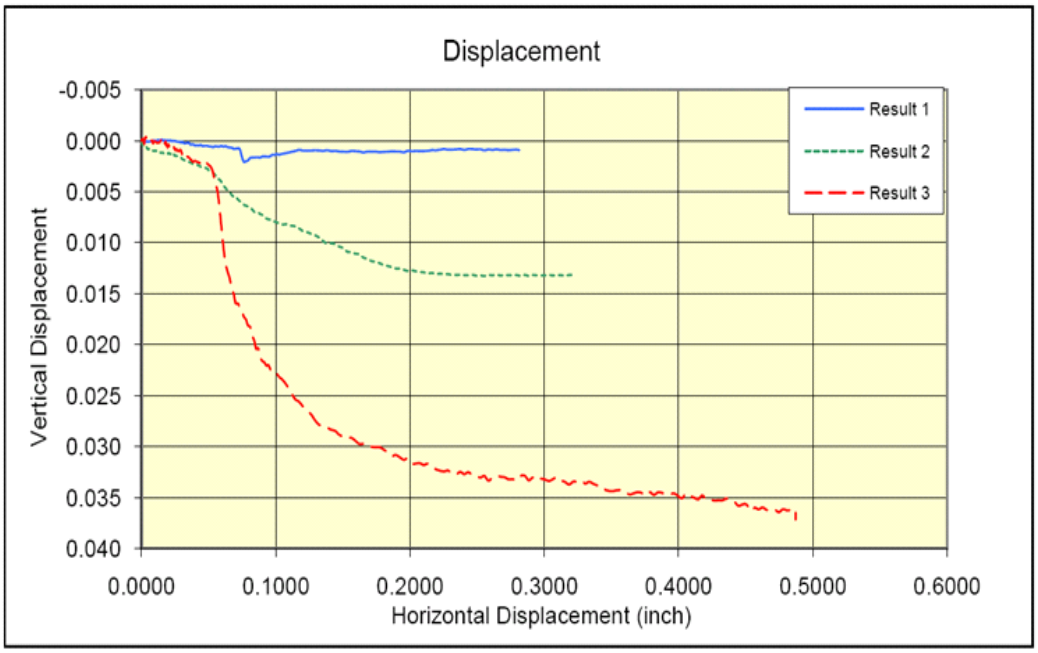
Displacement
Vertical Displacement
-0.005
0.000
0.005
0.010
0.015
0.020
0.025
0.030
0.035
0.040
0.0000
0.1000
0.2000
0.3000
0.4000
0.5000
0.6000
Horizontal Displacement (inch)
Result 1
Result 2
Result 3

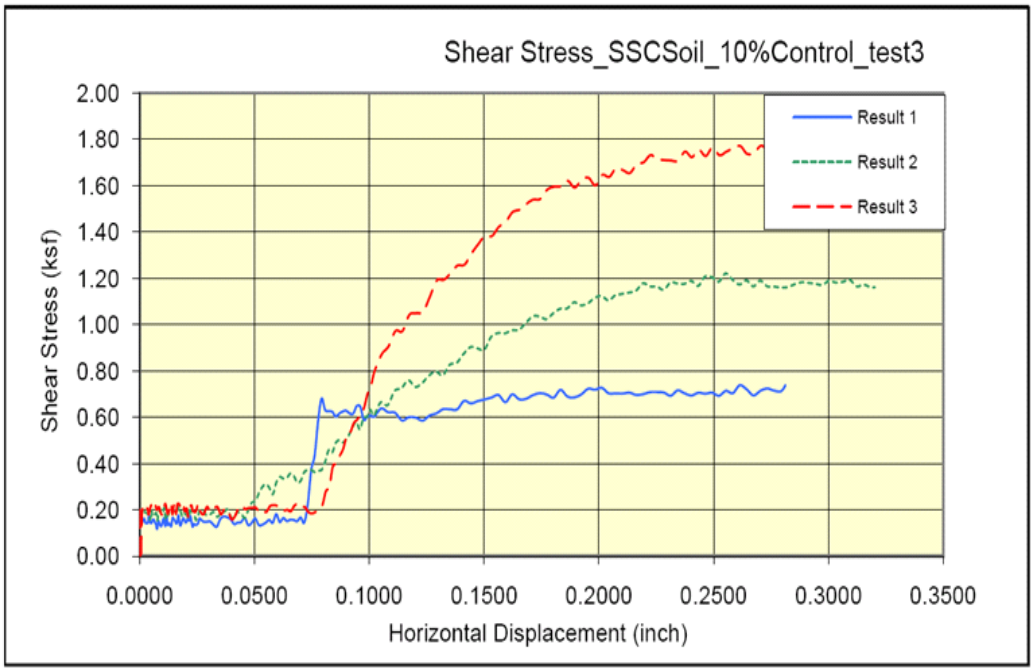
Shear Stress_SSCSoil_10%Control_test3
Shear Stress (ksf)
2.00
1.80
1.60
1.40
1.20
1.00
0.80
0.60
0.40
0.20
0.00
0.0000
0.0500
0.1000
0.1500
0.2000
0.2500
0.3000
0.3500
Horizontal Displacement (inch)
Result 1
Result 2
Result 3

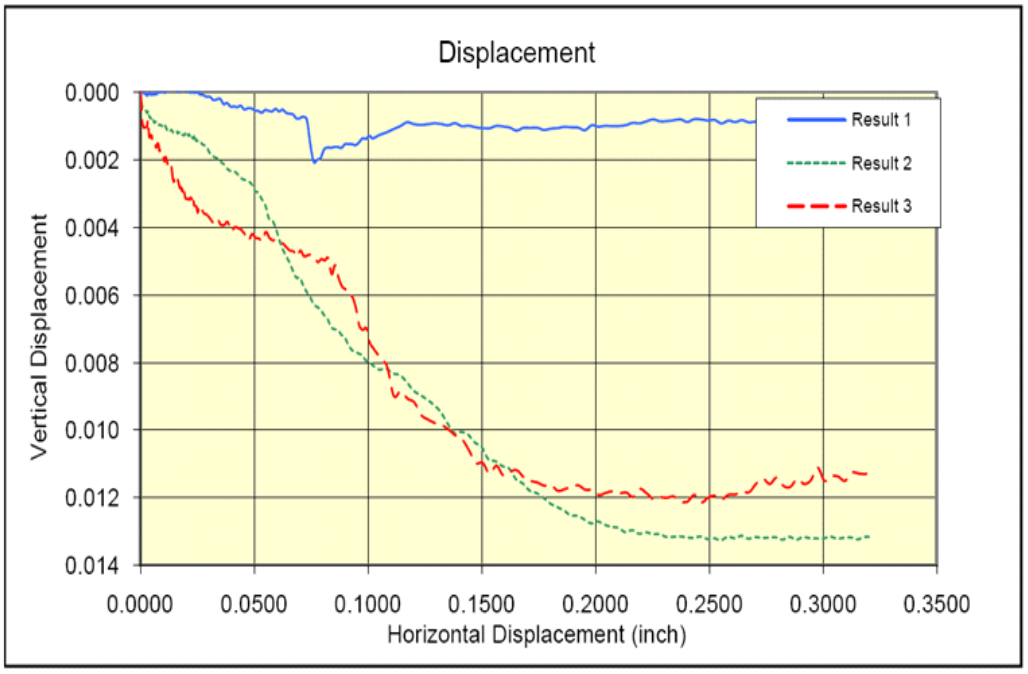
Displacement
Vertical Displacement
0.000
0.002
0.004
0.006
0.008
0.010
0.012
0.014
0.0000
0.0500
0.1000
0.1500
0.2000
0.2500
0.3000
0.3500
Horizontal Displacement (inch)
Result 1
Result 2
Result 3

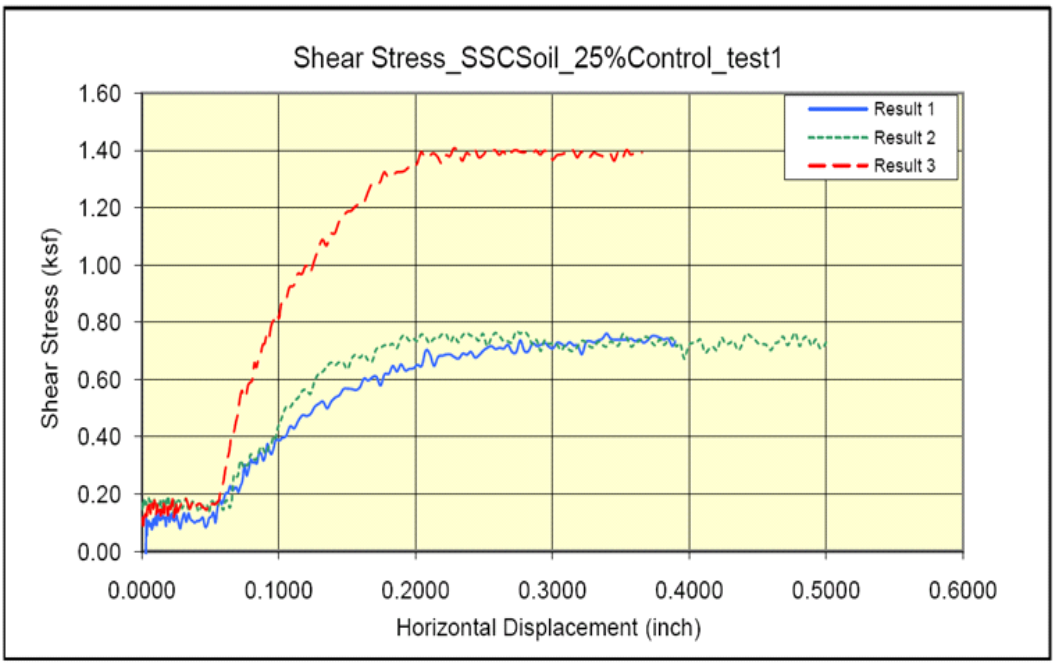
Shear Stress_SSCSoil_25%Control_test1
Shear Stress (ksf)
1.60
1.40
1.20
1.00
0.80
0.60
0.40
0.20
0.00
0.0000
0.1000
0.2000
0.3000
0.4000
0.5000
0.6000
Horizontal Displacement (inch)
Result 1
Result 2
Result 3

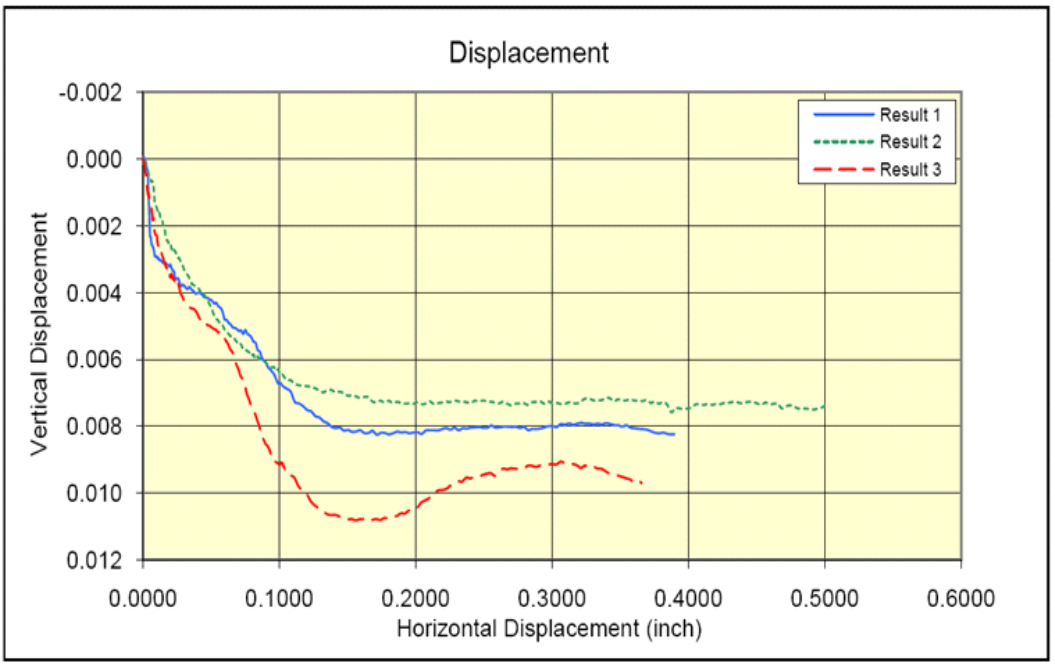
Displacement
Vertical Displacement
-0.002
0.000
0.002
0.004
0.006
0.008
0.010
0.012
0.0000
0.1000
0.2000
0.3000
0.4000
0.5000
0.6000
Horizontal Displacement (inch)
Result 1
Result 2
Result 3

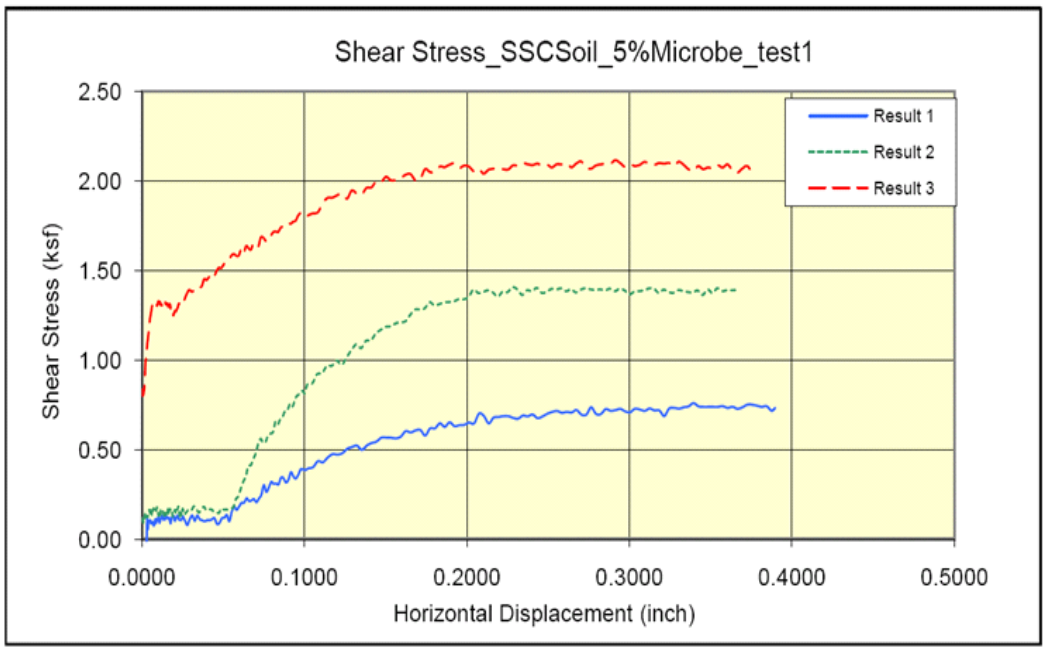
Shear Stress_SSCSoil_5%Microbe_test1
Shear Stress (ksf)
2.50
2.00
1.50
1.00
0.50
0.00
0.0000
0.1000
0.2000
0.3000
0.4000
0.5000
Horizontal Displacement (inch)
Result 1
Result 2
Result 3

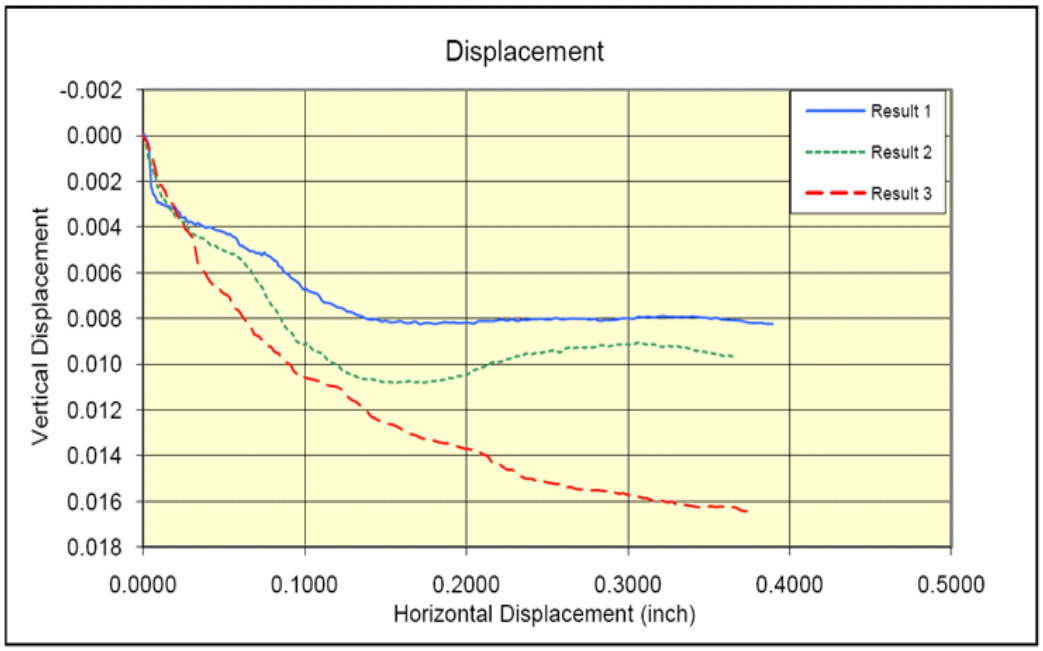
Displacement
Vertical Displacement
-0.002
0.000
0.002
0.004
0.006
0.008
0.010
0.012
0.014
0.016
0.018
0.0000
0.1000
0.2000
0.3000
0.4000
0.5000
Horizontal Displacement (inch)
Result 1
Result 2
Result 3

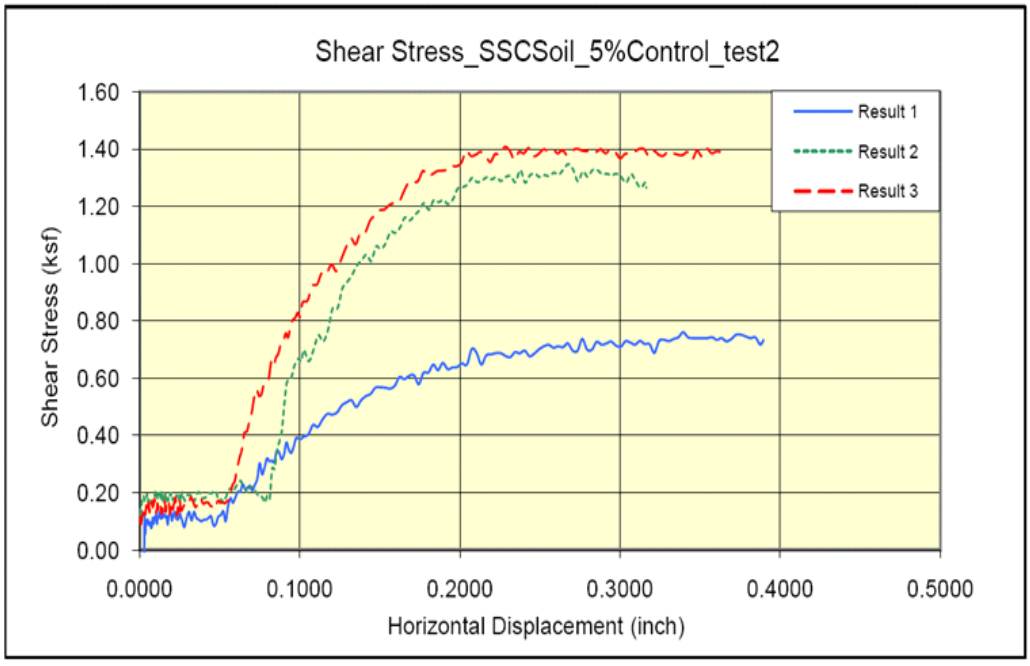
Shear Stress_SSCSoil_5%Control_test2
Shear Stress (ksf)
1.60
1.40
1.20
1.00
0.80
0.60
0.40
0.20
0.00
0.0000
0.1000
0.2000
0.3000
0.4000
0.5000
Horizontal Displacement (inch)
Result 1
Result 2
Result 3

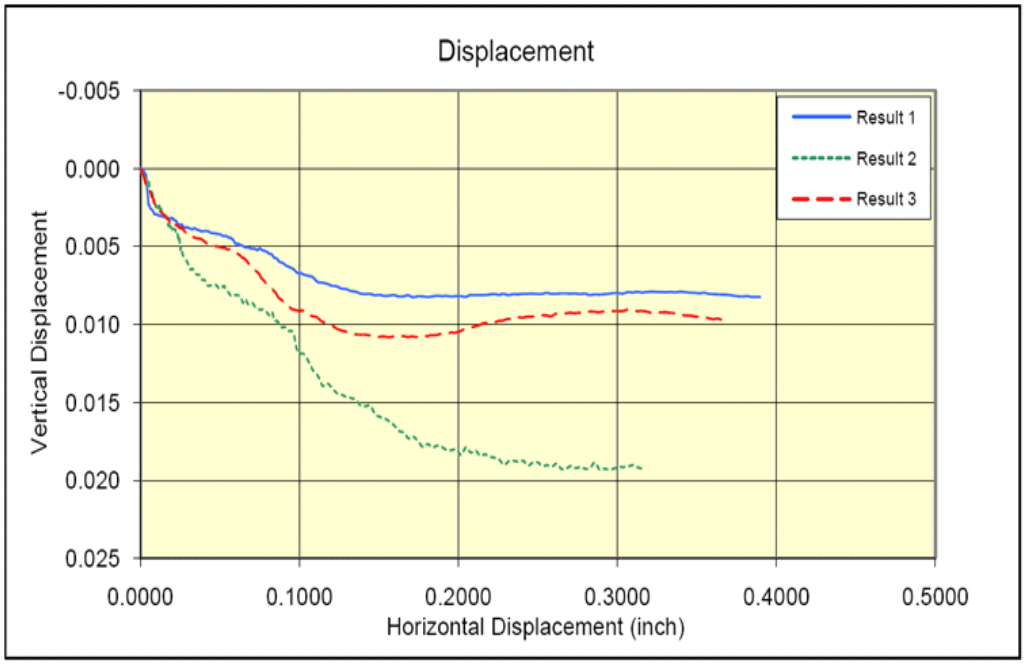
Displacement
Vertical Displacement
-0.005
0.000
0.005
0.010
0.015
0.020
0.025
0.0000
0.1000
0.2000
0.3000
0.4000
0.5000
Horizontal Displacement (inch)
Result 1
Result 2
Result 3

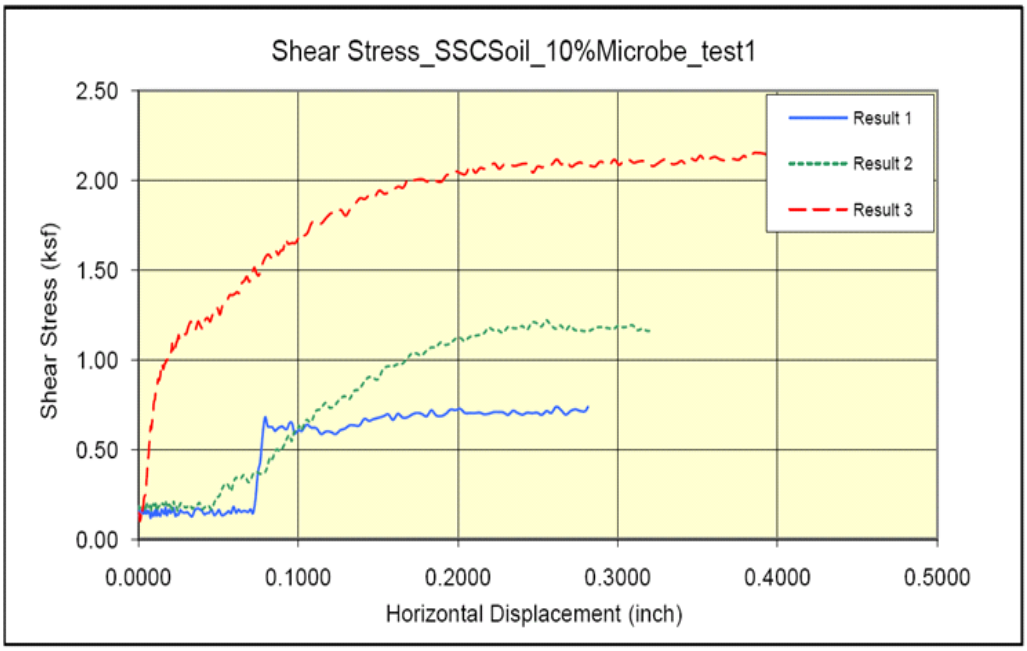
Shear Stress_SSCSoil_10%Microbe_test1
Shear Stress (ksf)
2.50
2.00
1.50
1.00
0.50
0.00
0.0000
0.1000
0.2000
0.3000
0.4000
0.5000
Horizontal Displacement (inch)
Result 1
Result 2
Result 3

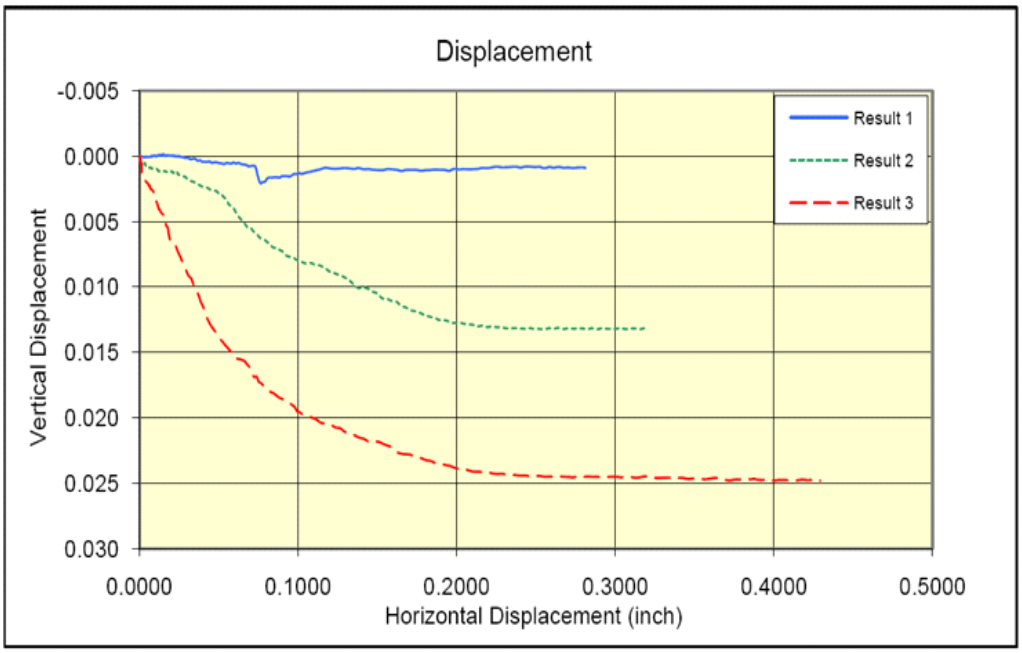
Displacement
Vertical Displacement
-0.005
0.000
0.005
0.010
0.015
0.020
0.025
0.030
0.0000
0.1000
0.2000
0.3000
0.4000
0.5000
Horizontal Displacement (inch)
Result 1
Result 2
Result 3

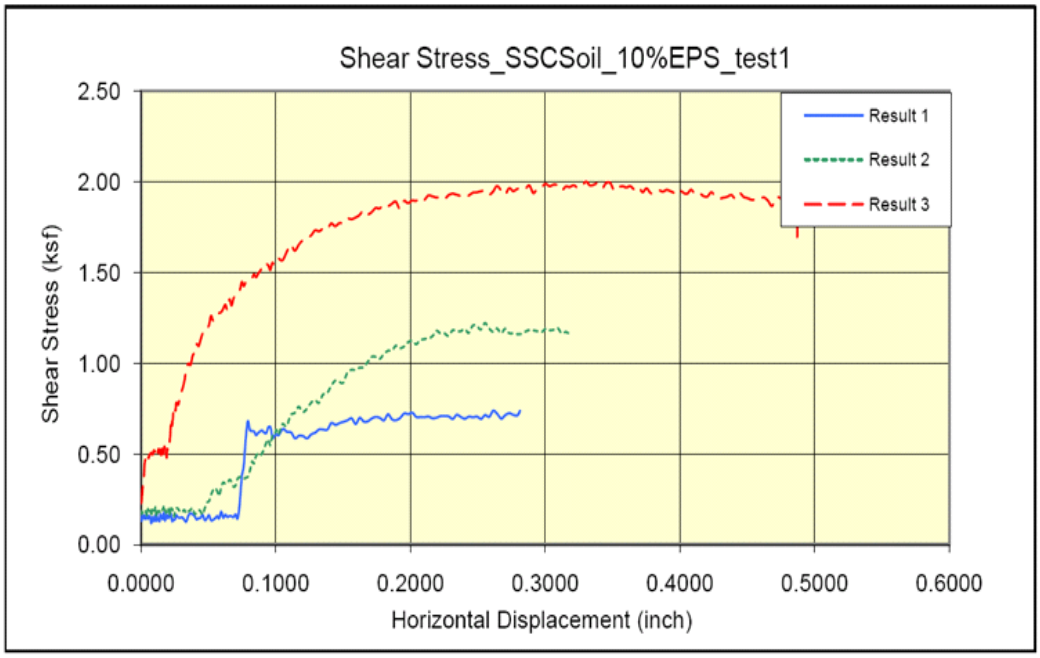
Shear Stress_SSCSoil_10%EPS_test1
Shear Stress (ksf)
2.50
2.00
1.50
1.00
0.50
0.00
0.0000
0.1000
0.2000
0.3000
0.4000
0.5000
0.6000
Horizontal Displacement (inch)
Result 1
Result 2
Result 3

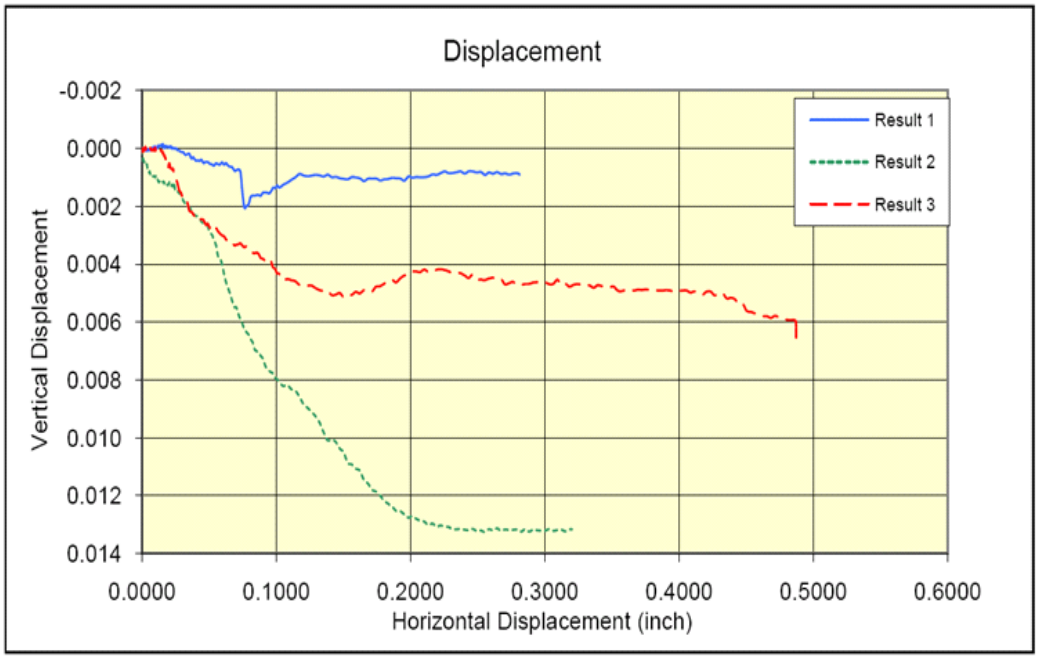
Displacement
Vertical Displacement
-0.002
0.000
0.002
0.004
0.006
0.008
0.010
0.012
0.014
0.0000
0.1000
0.2000
0.3000
0.4000
0.5000
0.6000
Horizontal Displacement (inch)
Result 1
Result 2
Result 3

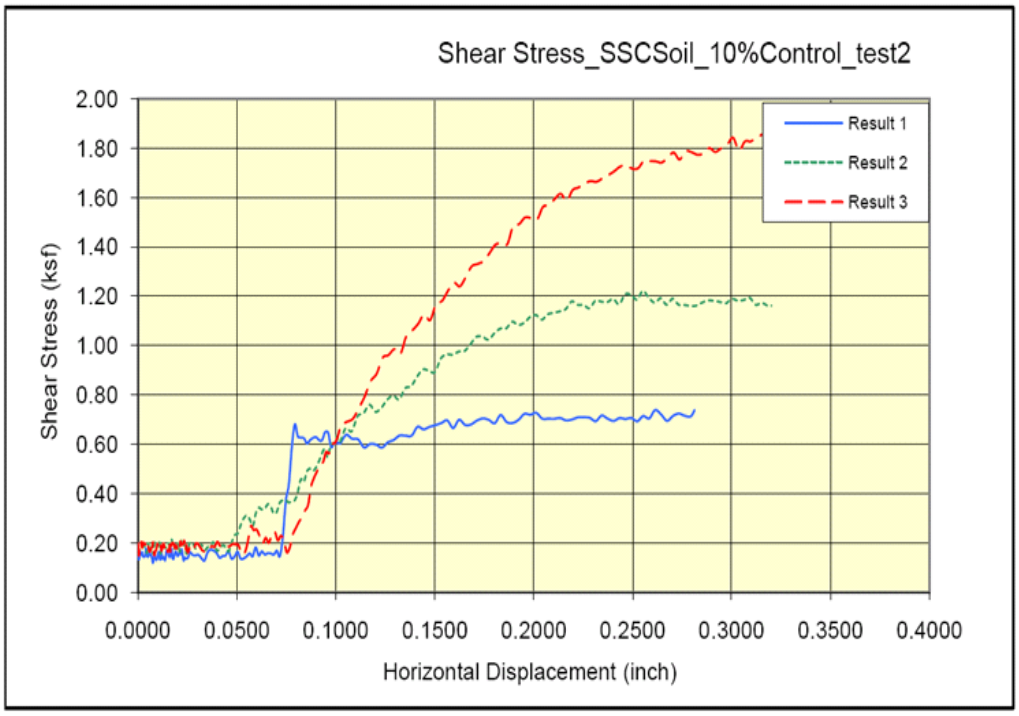
Shear Stress_SSCSoil_10%Control_test2
Shear Stress (ksf)
2.00
1.80
1.60
1.40
1.20
1.00
0.80
0.60
0.40
0.20
0.00
0.0000
0.0500
0.1000
0.1500
0.2000
0.2500
0.3000
0.3500
0.4000
Horizontal Displacement (inch)
Result 1
Result 2
Result 3

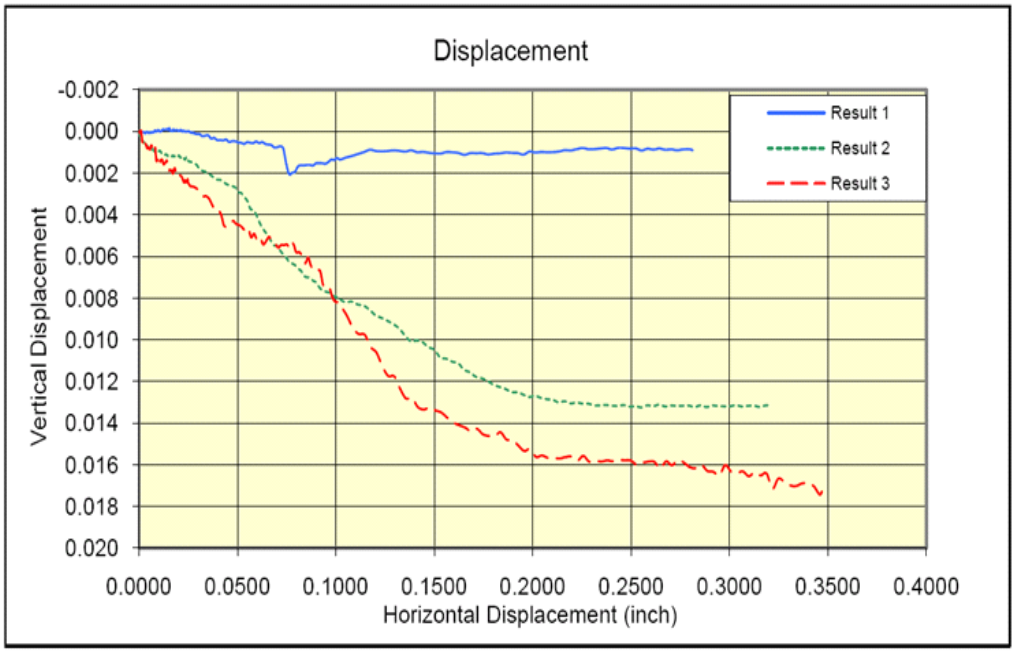
Displacement
Vertical Displacement
-0.002
0.000
0.002
0.004
0.006
0.008
0.010
0.012
0.014
0.016
0.018
0.020
0.0000
0.0500
0.1000
0.1500
0.2000
0.2500
0.3000
0.3500
0.4000
Horizontal Displacement (inch)
Result 1
Result 2
Result 3

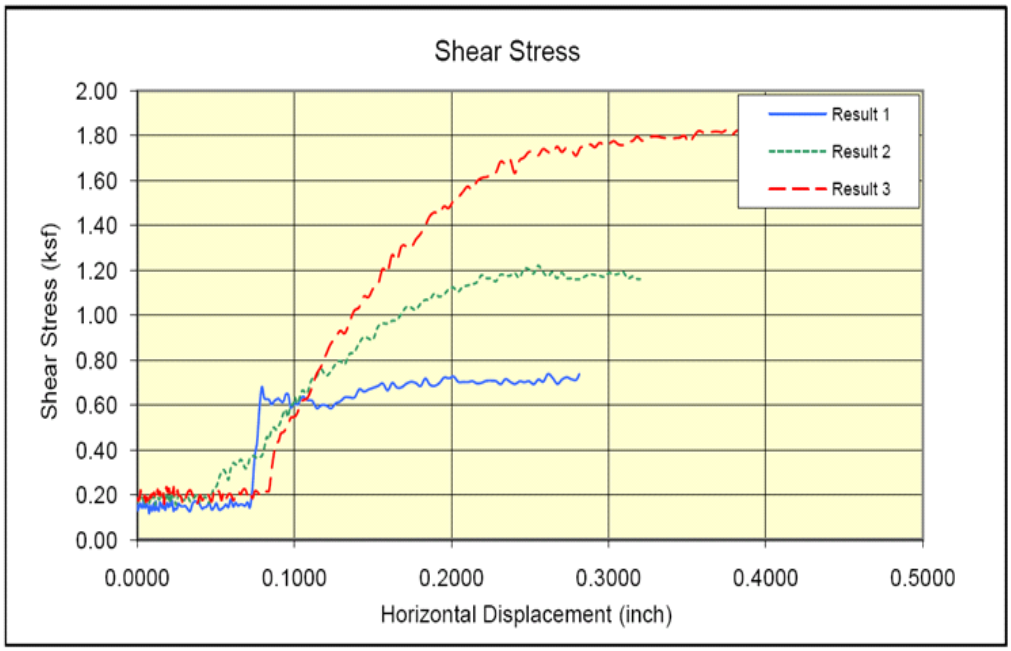
Shear Stress
Shear Stress (ksf)
2.00
1.80
1.60
1.40
1.20
1.00
0.80
0.60
0.40
0.20
0.00
0.0000
0.1000
0.2000
0.3000
0.4000
0.5000
Horizontal Displacement (inch)
Result 1
Result 2
Result 3

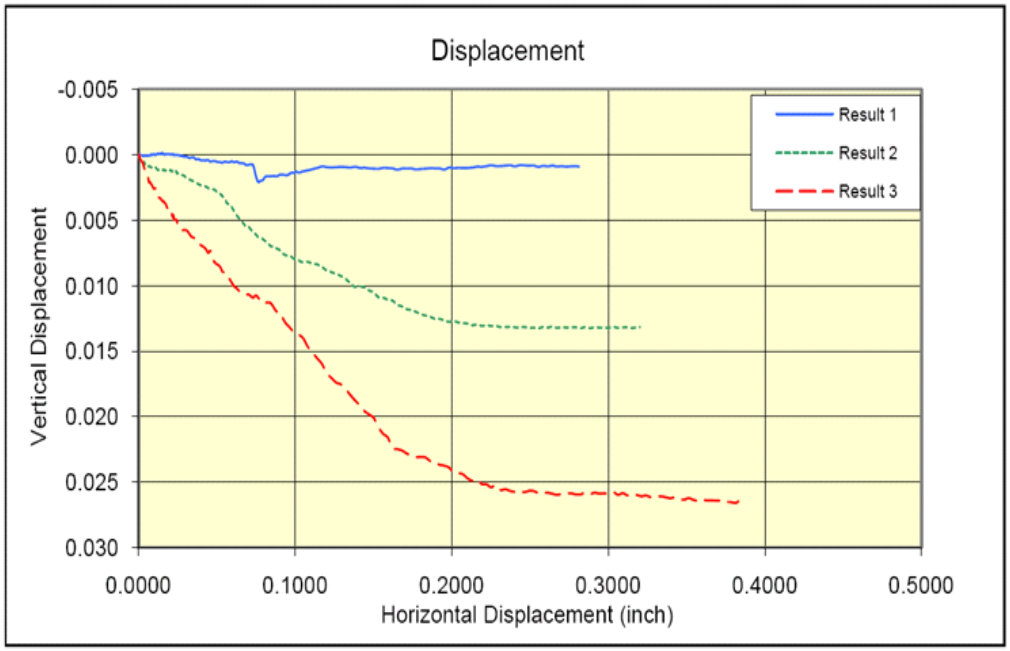
Displacement
Vertical Displacement
-0.005
0.000
0.005
0.010
0.015
0.020
0.025
0.030
0.0000
0.1000
0.2000
0.3000
0.4000
0.5000
Horizontal Displacement (inch)
Result 1
Result 2
Result 3

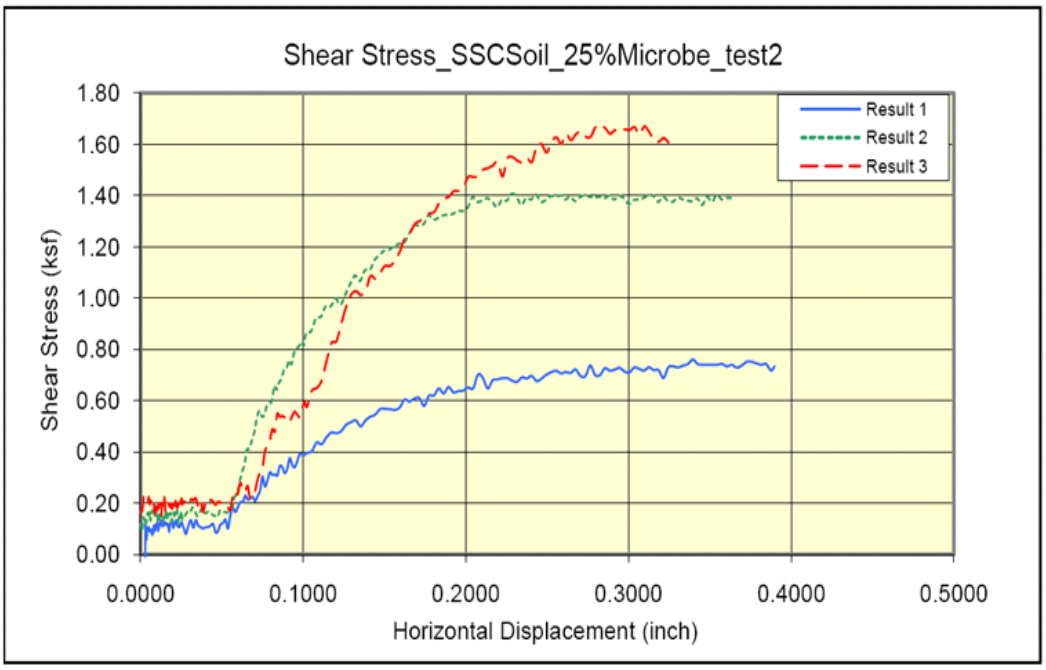
Shear Stress_SSCSoil_25%Microbe_test2
Shear Stress (ksf)
1.80
1.60
1.40
1.20
1.00
0.80
0.60
0.40
0.20
0.00
0.0000
0.1000
0.2000
0.3000
0.4000
0.5000
Horizontal Displacement (inch)
Result 1
Result 2
Result 3

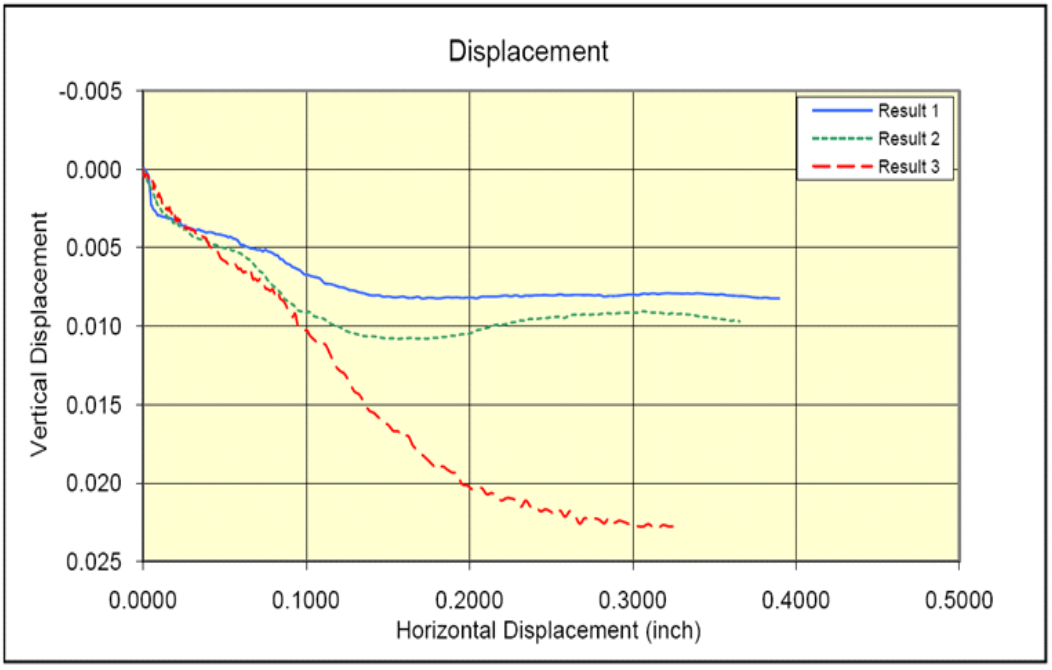
Displacement
Vertical Displacement
-0.005
0.000
0.005
0.010
0.015
0.020
0.025
0.0000
0.1000
0.2000
0.3000
0.4000
0.5000
Horizontal Displacement (inch)
Result 1
Result 2
Result 3

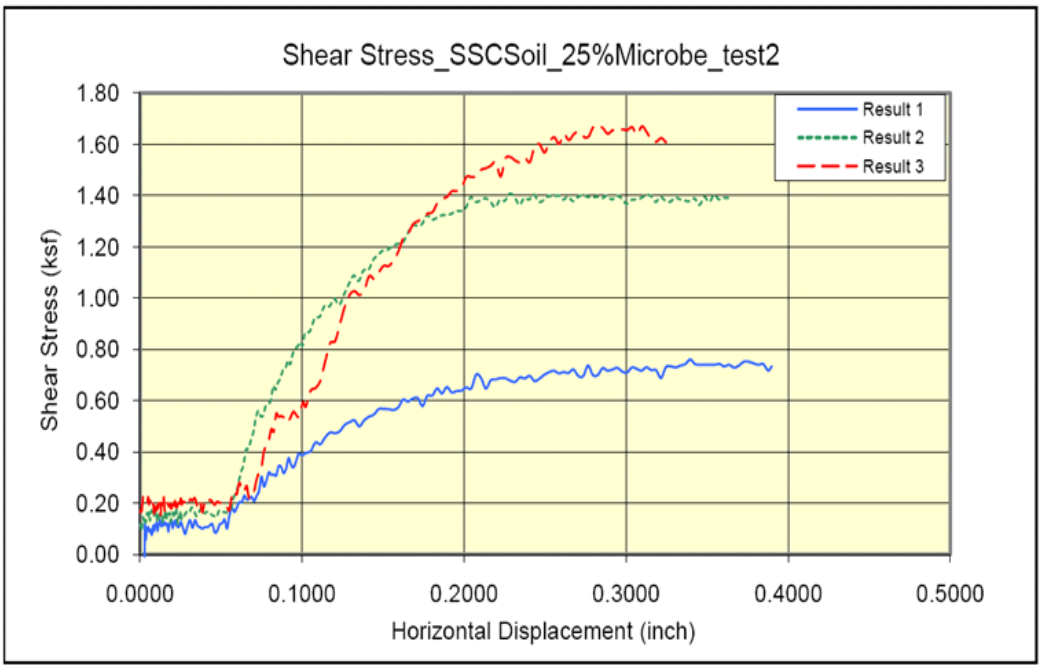
Shear Stress_SSCSoil_25%Microbe_test2
Shear Stress (ksf)
1.80
1.60
1.40
1.20
1.00
0.80
0.60
0.40
0.20
0.00
0.0000
0.1000
0.2000
0.3000
0.4000
0.5000
Horizontal Displacement (inch)
Result 1
Result 2
Result 3

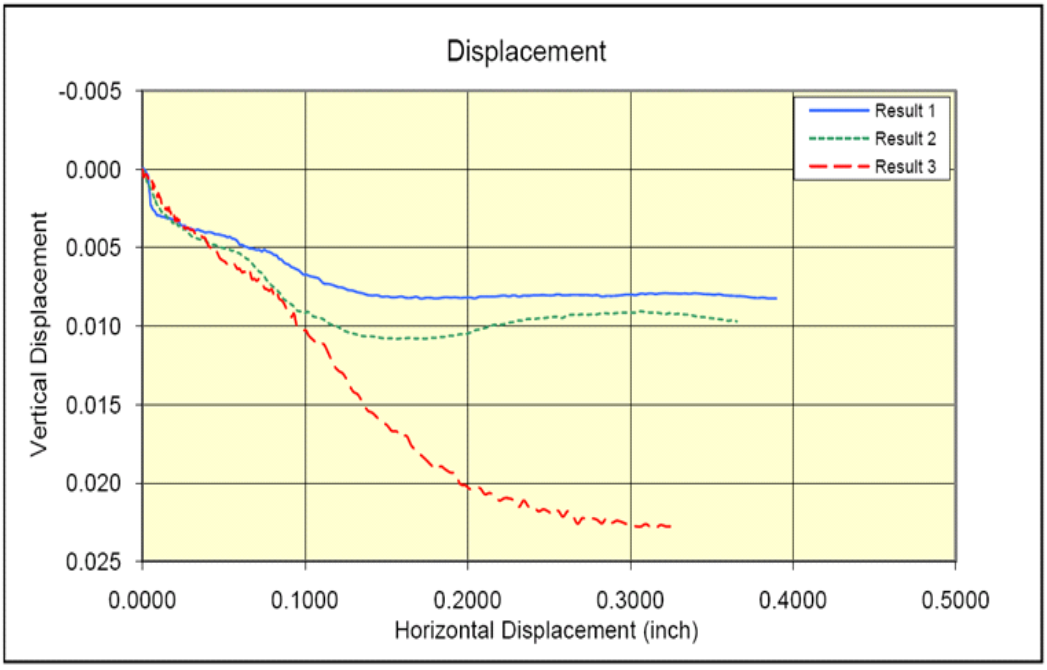
Displacement
Vertical Displacement
-0.005
0.000
0.005
0.010
0.015
0.020
0.025
0.0000
0.1000
0.2000
0.3000
0.4000
0.5000
Horizontal Displacement (inch)
Result 1
Result 2
Result 3

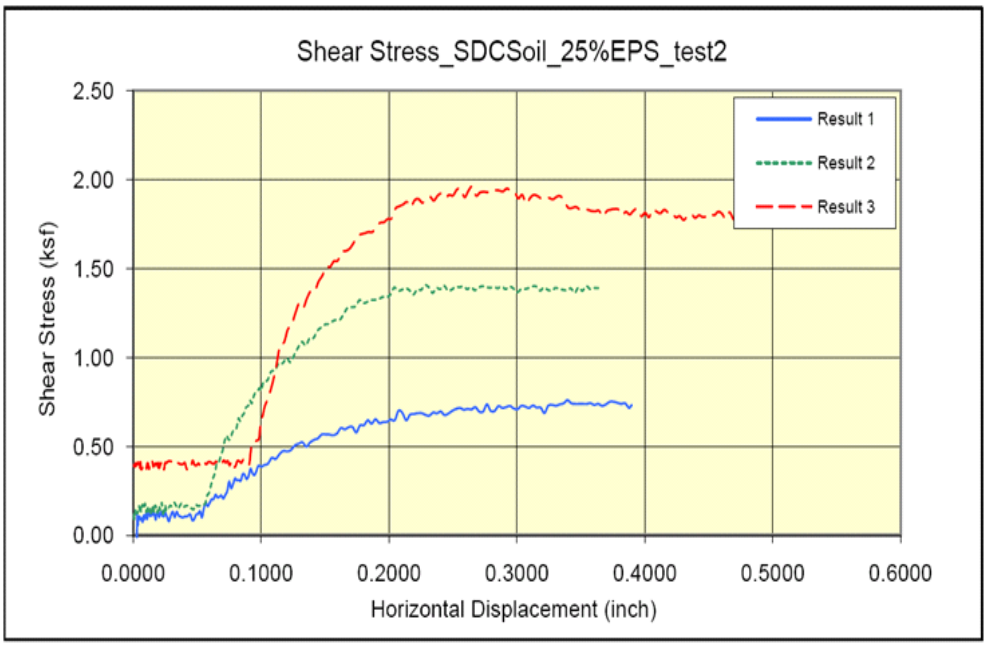
Shear Stress_SDCSoil_25%EPS_test2
Shear Stress (ksf)
2.50
2.00
1.50
1.00
0.50
0.00
0.0000
0.1000
0.2000
0.3000
0.4000
0.5000
0.6000
Horizontal Displacement (inch)
Result 1
Result 2
Result 3

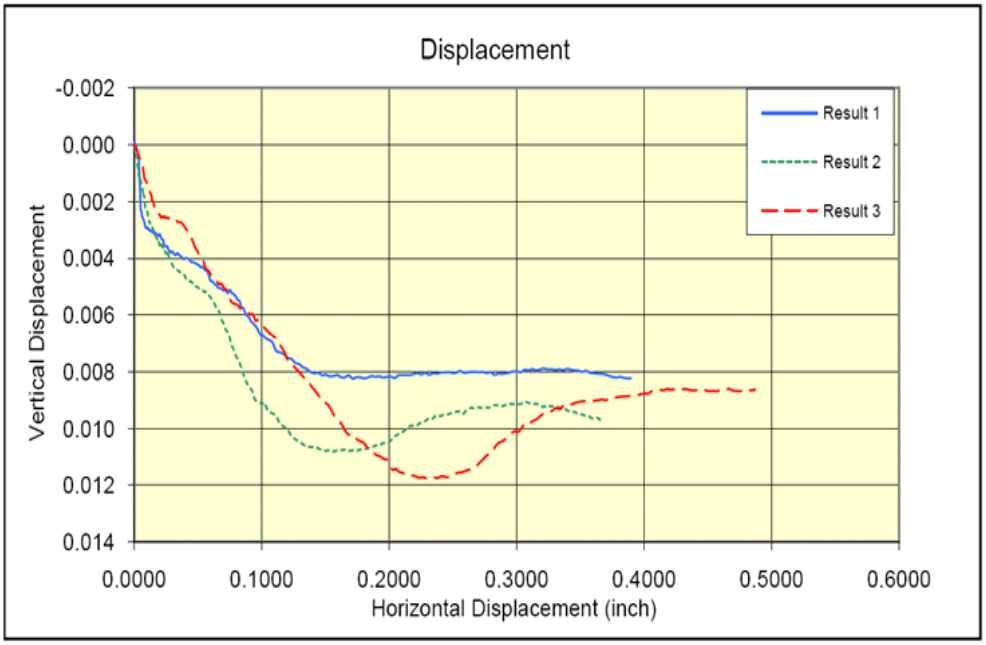
Displacement
Vertical Displacement
-0.002
0.000
0.002
0.004
0.006
0.008
0.010
0.012
0.014
0.0000
0.1000
0.2000
0.3000
0.4000
0.5000
0.6000
Horizontal Displacement (inch)
Result 1
Result 2
Result 3

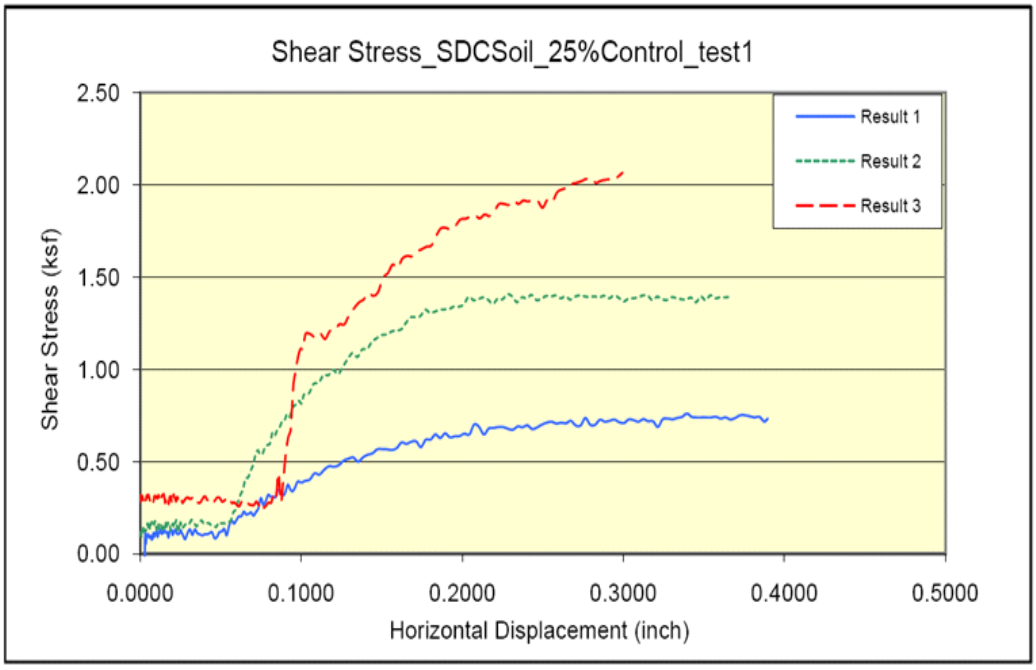
Shear Stress_SDCSoil_25%Control_test1
Shear Stress (ksf)
2.50
2.00
1.50
1.00
0.50
0.00
0.0000
0.1000
0.2000
0.3000
0.4000
0.5000
Horizontal Displacement (inch)
Result 1
Result 2
Result 3

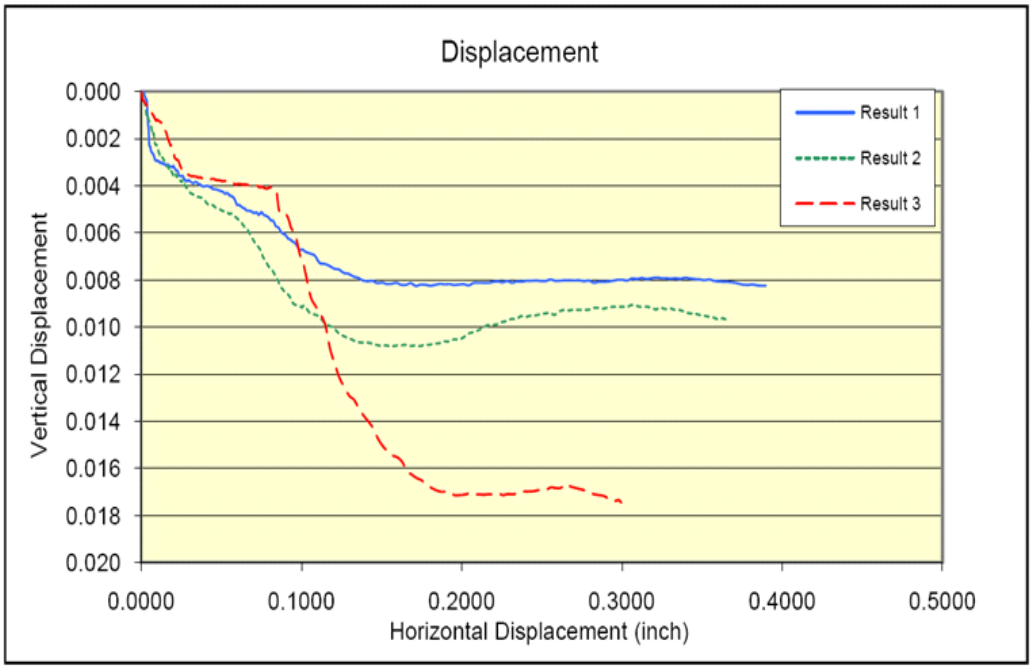
Displacement
Vertical Displacement
0.000
0.002
0.004
0.006
0.008
0.010
0.012
0.014
0.016
0.018
0.020
0.0000
0.1000
0.2000
0.3000
0.4000
0.5000
Horizontal Displacement (inch)
Result 1
Result 2
Result 3

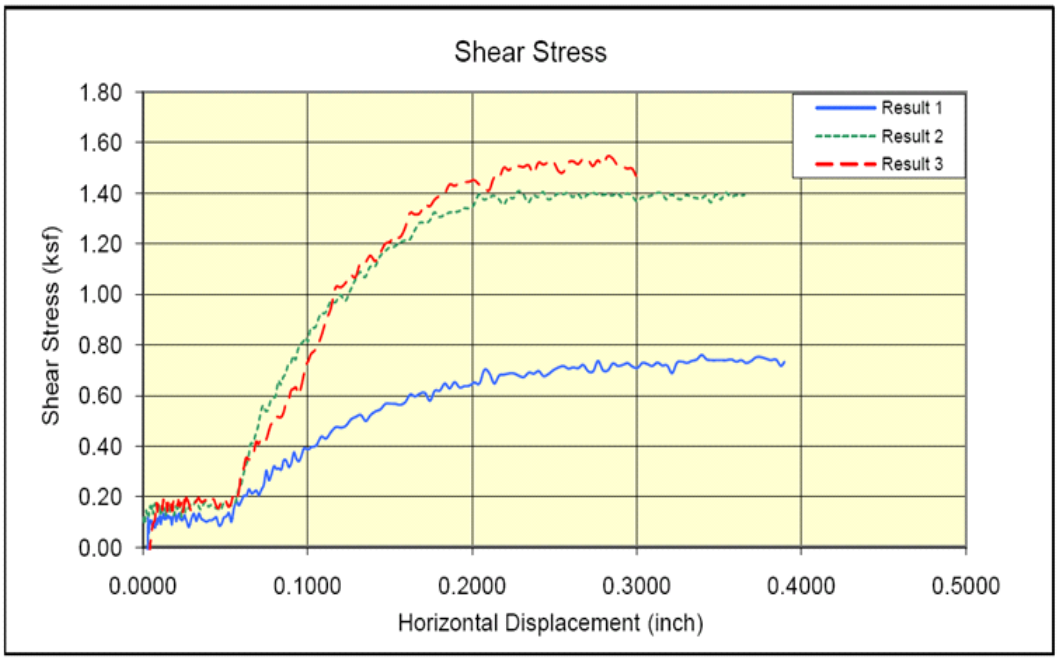
Shear Stress
Shear Stress (ksf)
1.80
1.60
1.40
1.20
1.00
0.80
0.60
0.40
0.20
0.00
0.0000
0.1000
0.2000
0.3000
0.4000
0.5000
Horizontal Displacement (inch)
Result 1
Result 2
Result 3

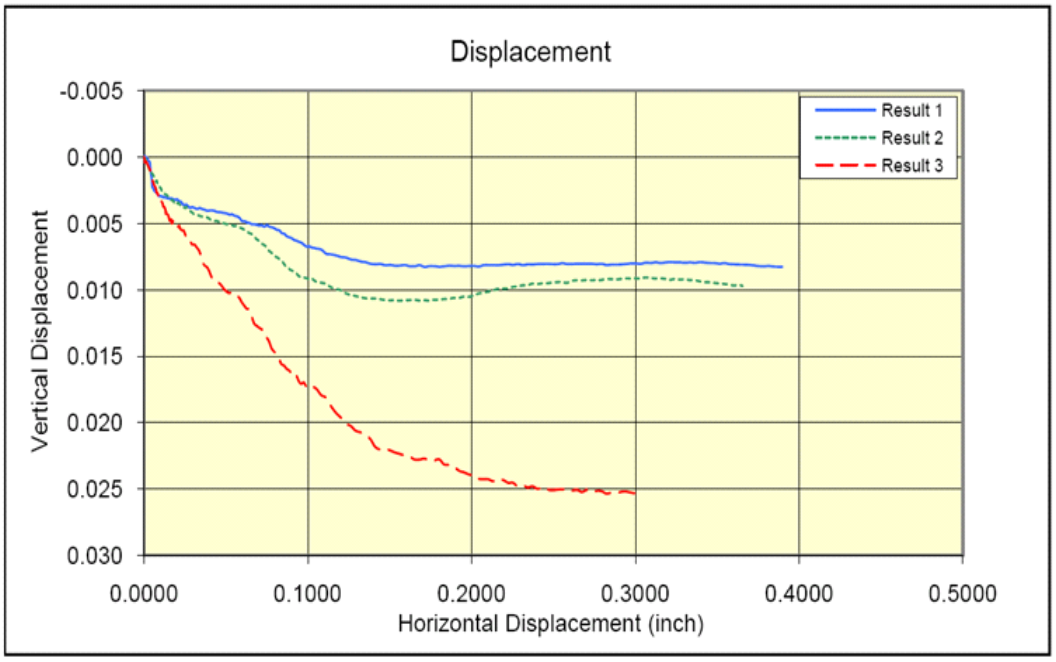
Displacement
Vertical Displacement
-0.005
0.000
0.005
0.010
0.015
0.020
0.025
0.030
0.0000
0.1000
0.2000
0.3000
0.4000
0.5000
Horizontal Displacement (inch)
Result 1
Result 2
Result 3

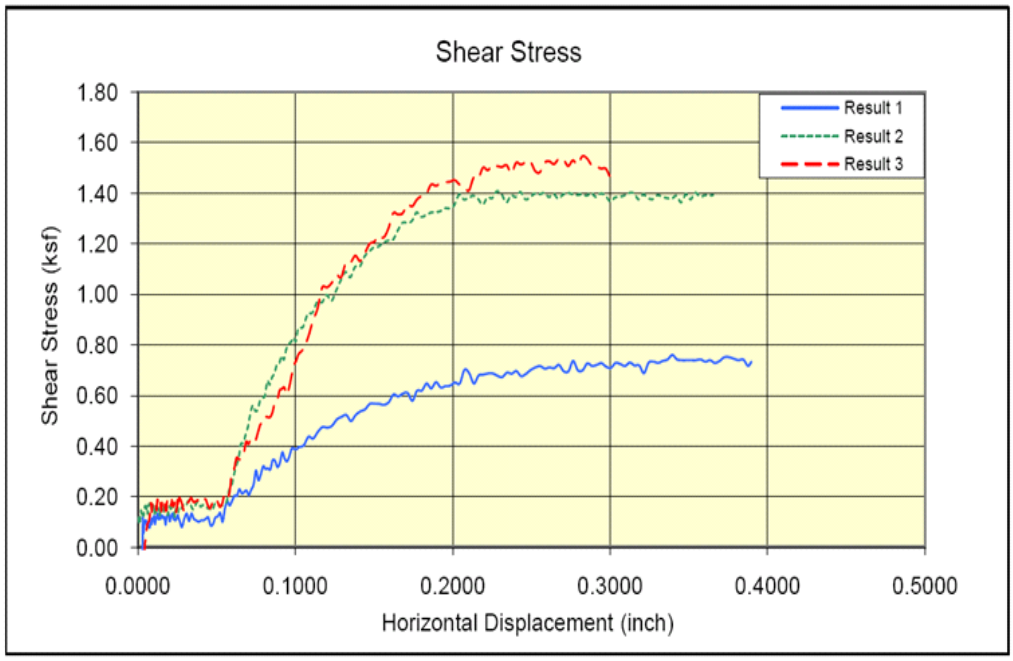
Shear Stress
Shear Stress (ksf)
1.80
1.60
1.40
1.20
1.00
0.80
0.60
0.40
0.20
0.00
0.0000
0.1000
0.2000
0.3000
0.4000
0.5000
Horizontal Displacement (inch)
Result 1
Result 2
Result 3

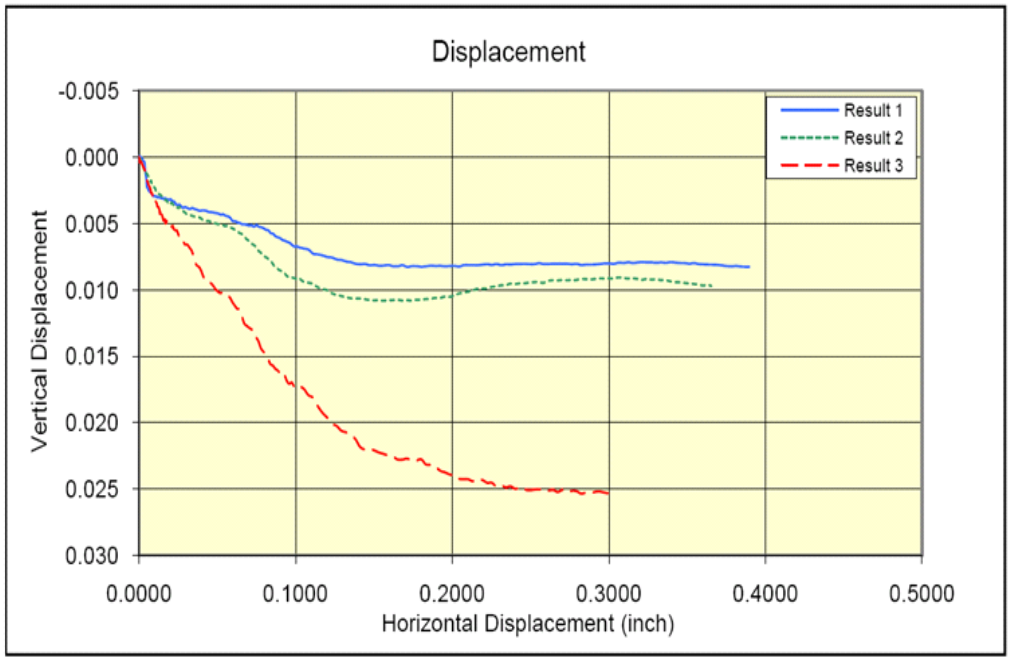
Displacement
Vertical Displacement
-0.005
0.000
0.005
0.010
0.015
0.020
0.025
0.030
0.0000
0.1000
0.2000
0.3000
0.4000
0.5000
Horizontal Displacement (inch)
Result 1
Result 2
Result 3

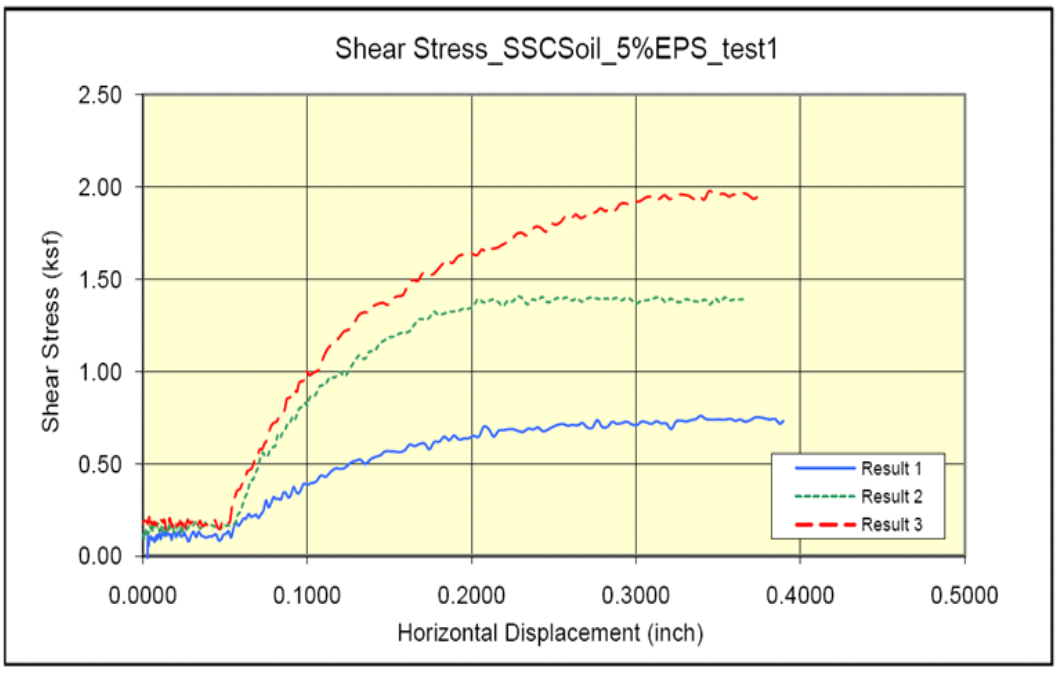
Shear Stress_SSCSoil_5%EPS_test1
Shear Stress (ksf)
2.50
2.00
1.50
1.00
0.50
0.00
0.0000
0.1000
0.2000
0.3000
0.4000
0.5000
Horizontal Displacement (inch)
Result 1
Result 2
Result 3

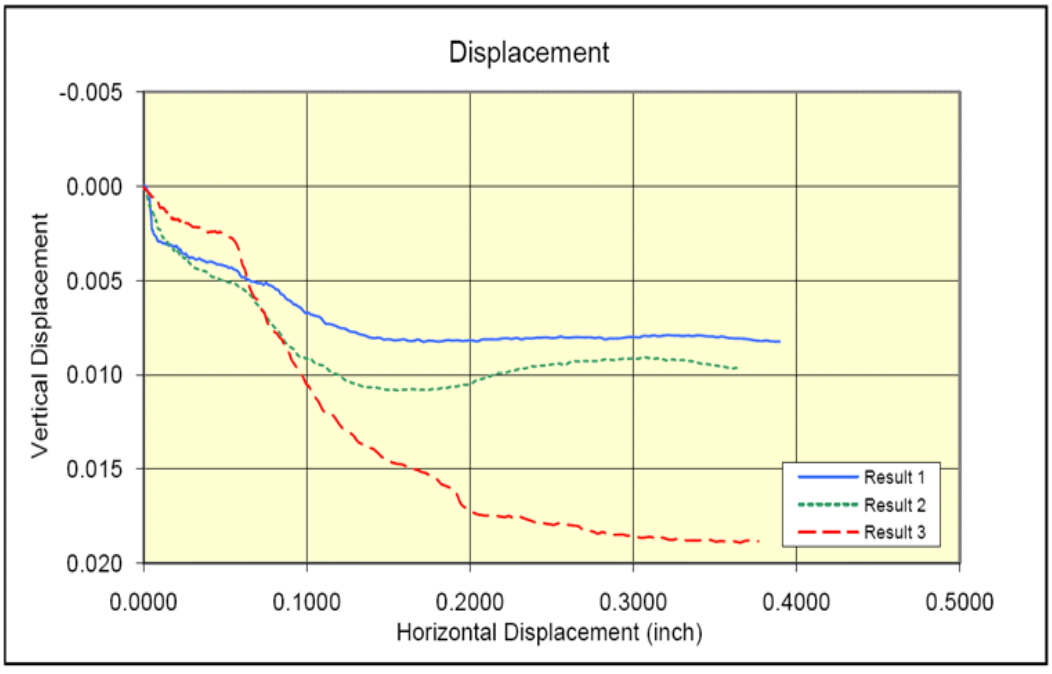
Displacement
Vertical Displacement
-0.005
0.000
0.005
0.010
0.015
0.020
0.0000
0.1000
0.2000
0.3000
0.4000
0.5000
Horizontal Displacement (inch)
Result 1
Result 2
Result 3

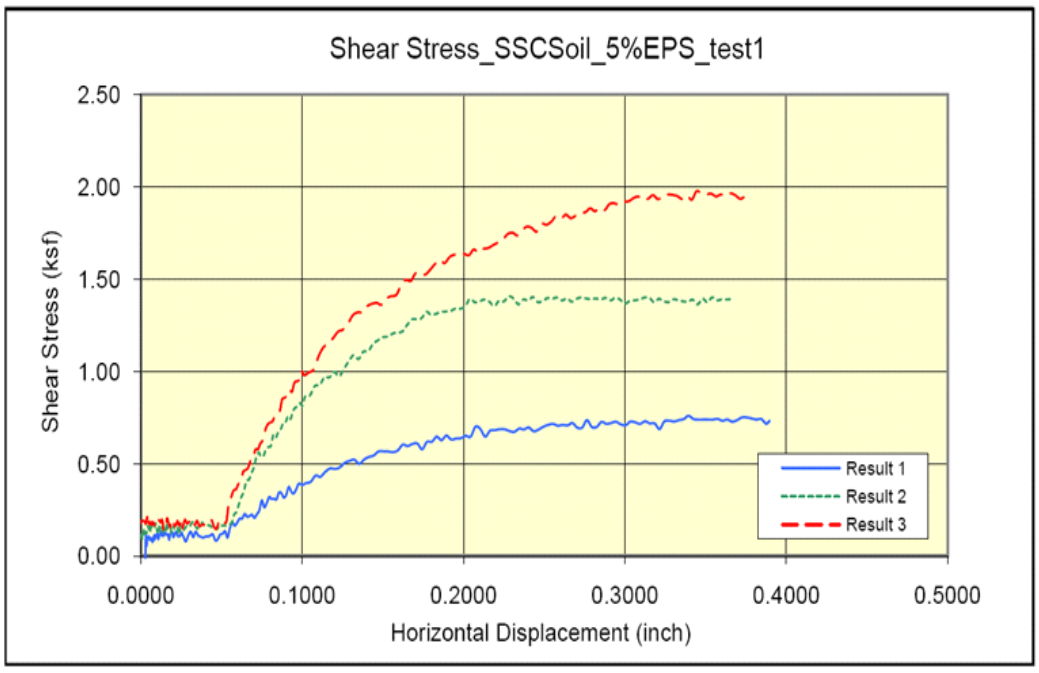
Shear Stress_SSCSoil_5%EPS_test1
Shear Stress (ksf)
2.50
2.00
1.50
1.00
0.50
0.00
0.0000
0.1000
0.2000
0.3000
0.4000
0.5000
Horizontal Displacement (inch)
Result 1
Result 2
Result 3

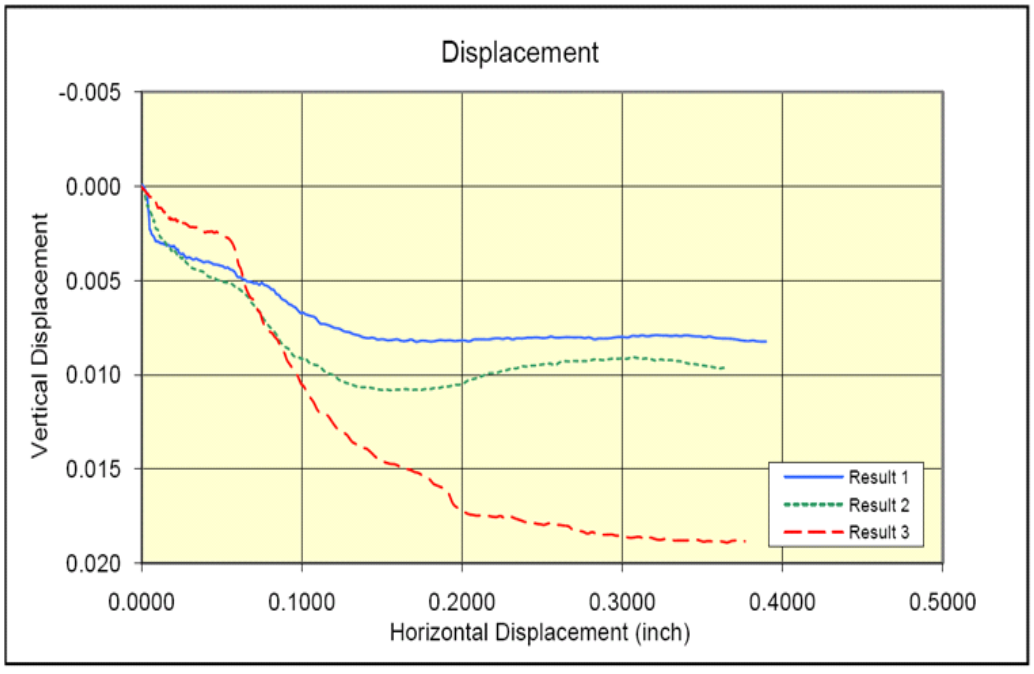
Displacement
Vertical Displacement
-0.005
0.000
0.005
0.010
0.015
0.020
0.0000
0.1000
0.2000
0.3000
0.4000
0.5000
Horizontal Displacement (inch)
Result 1
Result 2
Result 3

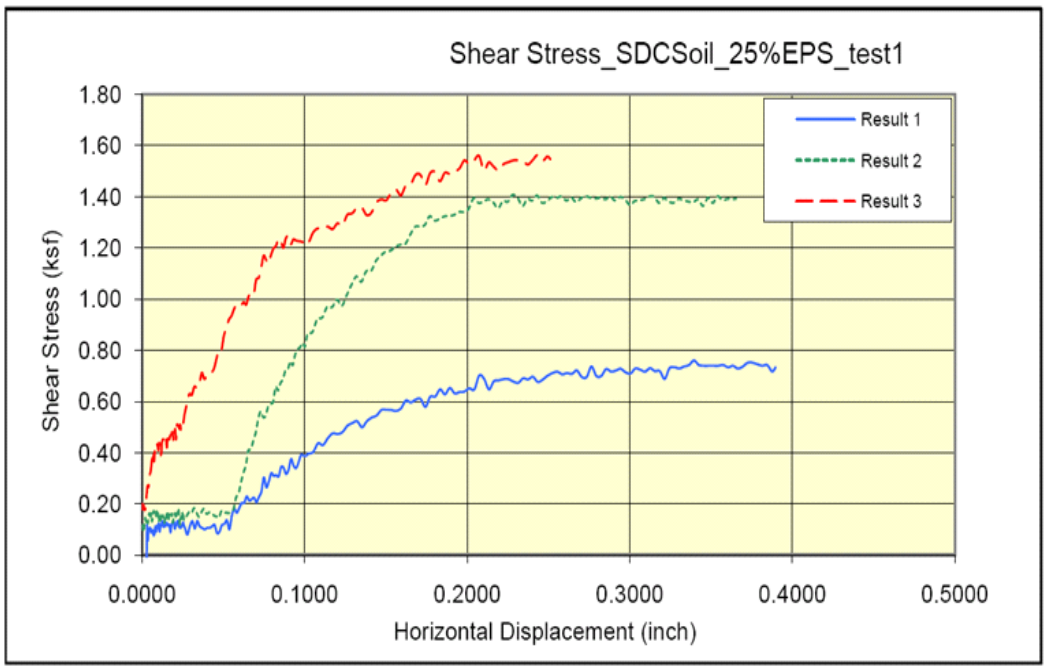
Shear Stress_SDCSoil_25%EPS_test1
Shear Stress (ksf)
1.80
1.60
1.40
1.20
1.00
0.80
0.60
0.40
0.20
0.00
0.0000
0.1000
0.2000
0.3000
0.4000
0.5000
Horizontal Displacement (inch)
Result 1
Result 2
Result 3

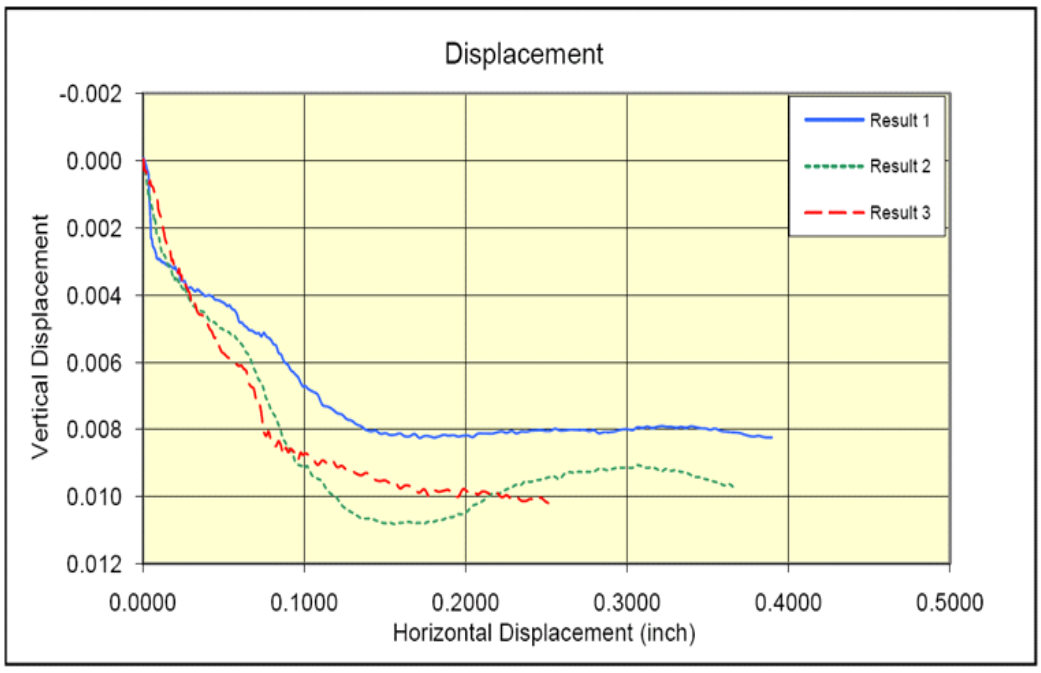
Displacement
Vertical Displacement
-0.002
0.000
0.002
0.004
0.006
0.008
0.010
0.012
0.0000
0.1000
0.2000
0.3000
0.4000
0.5000
Horizontal Displacement (inch)
Result 1
Result 2
Result 3

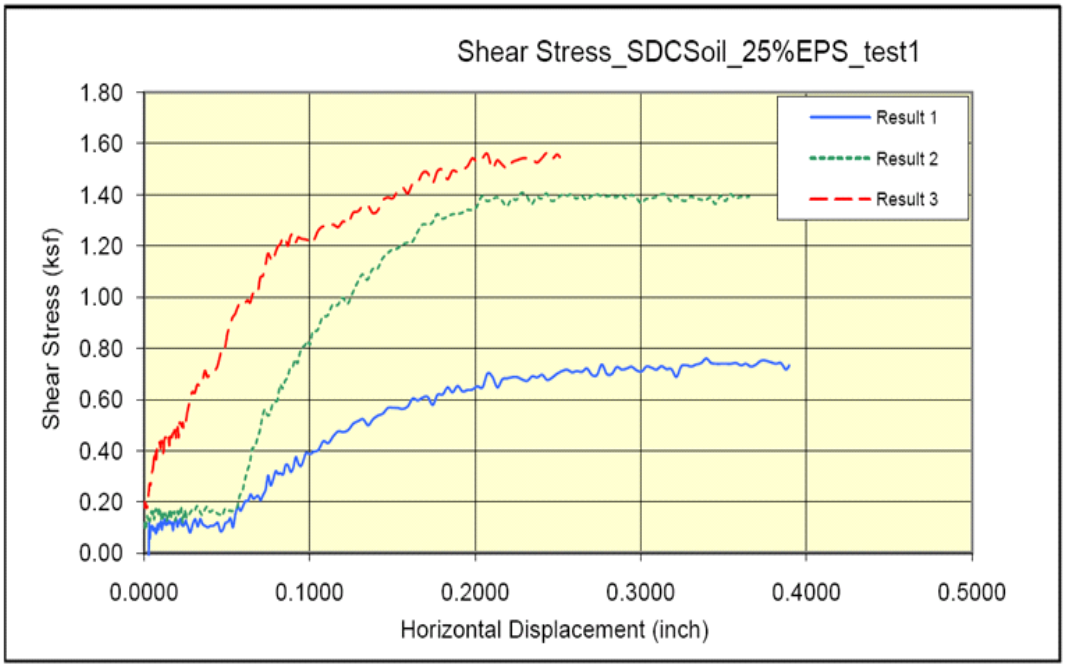
Shear Stress_SDCSoil_25%EPS_test1
Shear Stress (ksf)
1.80
1.60
1.40
1.20
1.00
0.80
0.60
0.40
0.20
0.00
0.0000
0.1000
0.2000
0.3000
0.4000
0.5000
Horizontal Displacement (inch)
Result 1
Result 2
Result 3

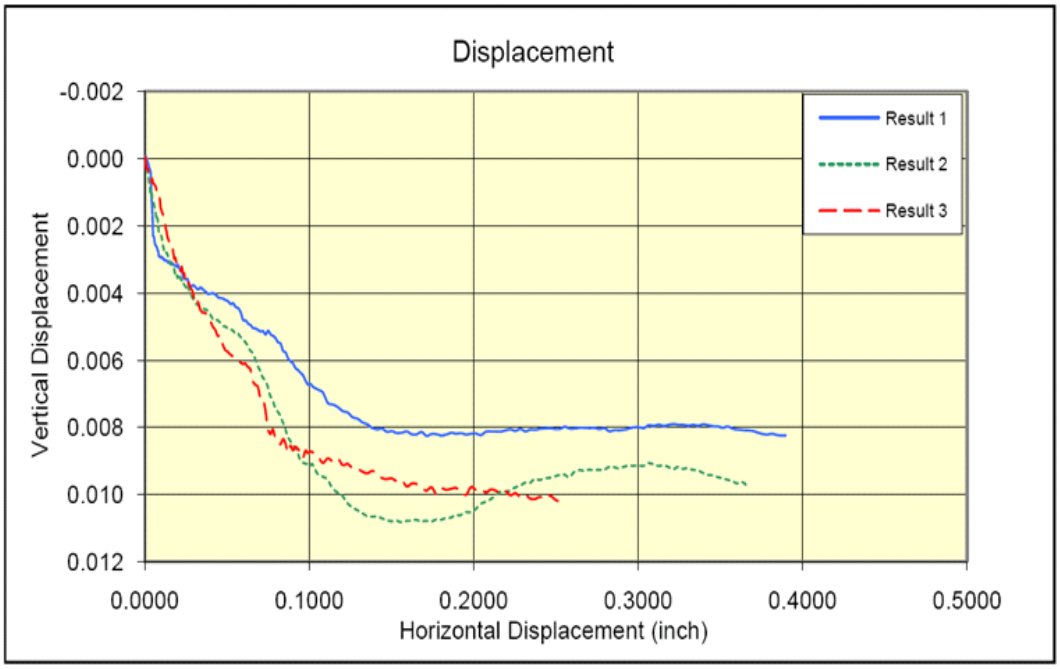
Displacement
Vertical Displacement
-0.002
0.000
0.002
0.004
0.006
0.008
0.010
0.012
0.0000
0.1000
0.2000
0.3000
0.4000
0.5000
Horizontal Displacement (inch)
Result 1
Result 2
Result 3

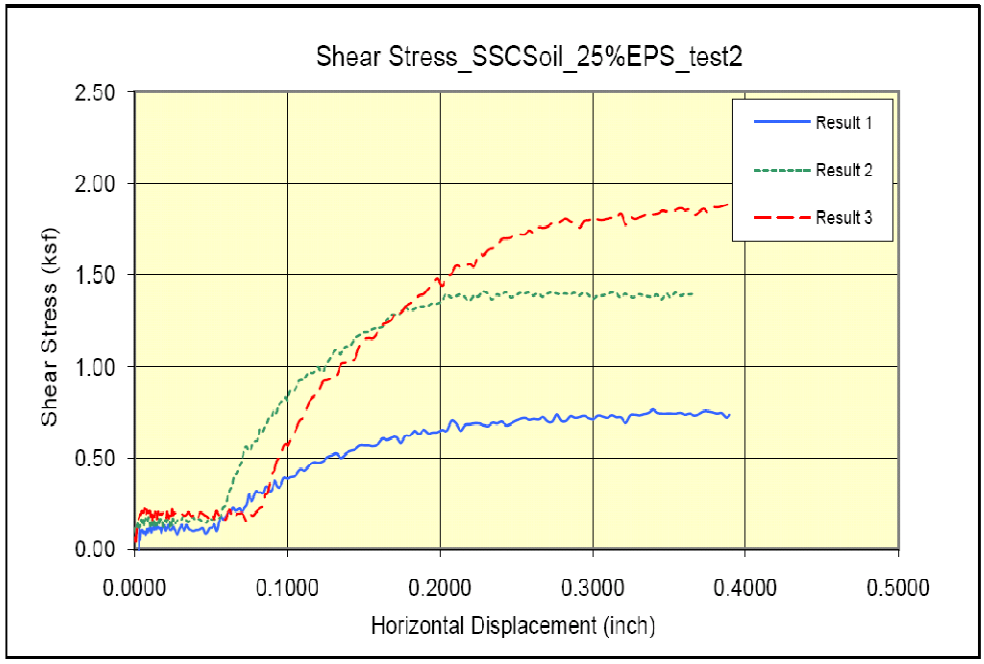
Shear Stress_SSCSoil_25%EPS_test2
Shear Stress (ksf)
2.50
2.00
1.50
1.00
0.50
0.00
0.0000
0.1000
0.2000
0.3000
0.4000
0.5000
Horizontal Displacement (inch)
Result 1
Result 2
Result 3

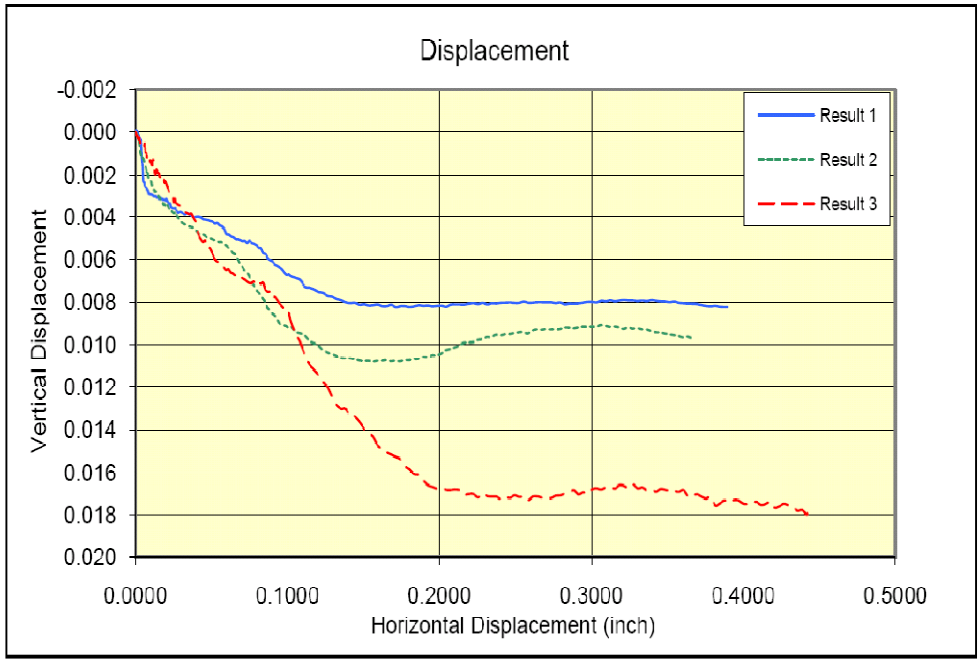
Displacement
Vertical Displacement
-0.002
0.000
0.002
0.004
0.006
0.008
0.010
0.012
0.014
0.016
0.018
0.020
0.0000
0.1000
0.2000
0.3000
0.4000
0.5000
Horizontal Displacement (inch)
Result 1
Result 2
Result 3

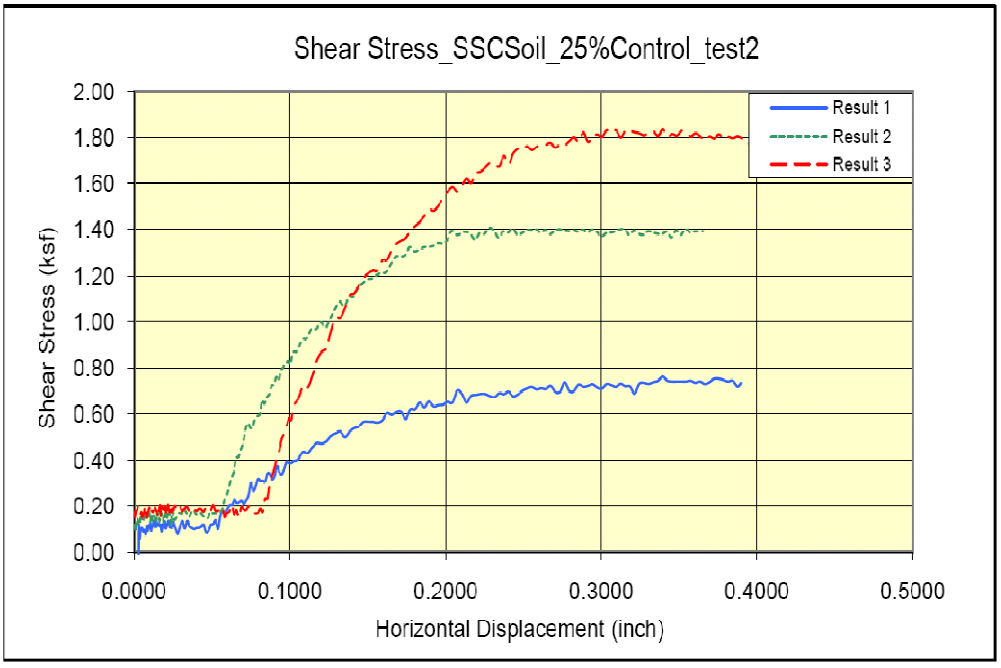
Shear Stress_SSCSoil_25%Control_test2
Shear Stress (ksf)
2.00
1.80
1.60
1.40
1.20
1.00
0.80
0.60
0.40
0.20
0.00
0.0000
0.1000
0.2000
0.3000
0.4000
0.5000
Horizontal Displacement (inch)
Result 1
Result 2
Result 3

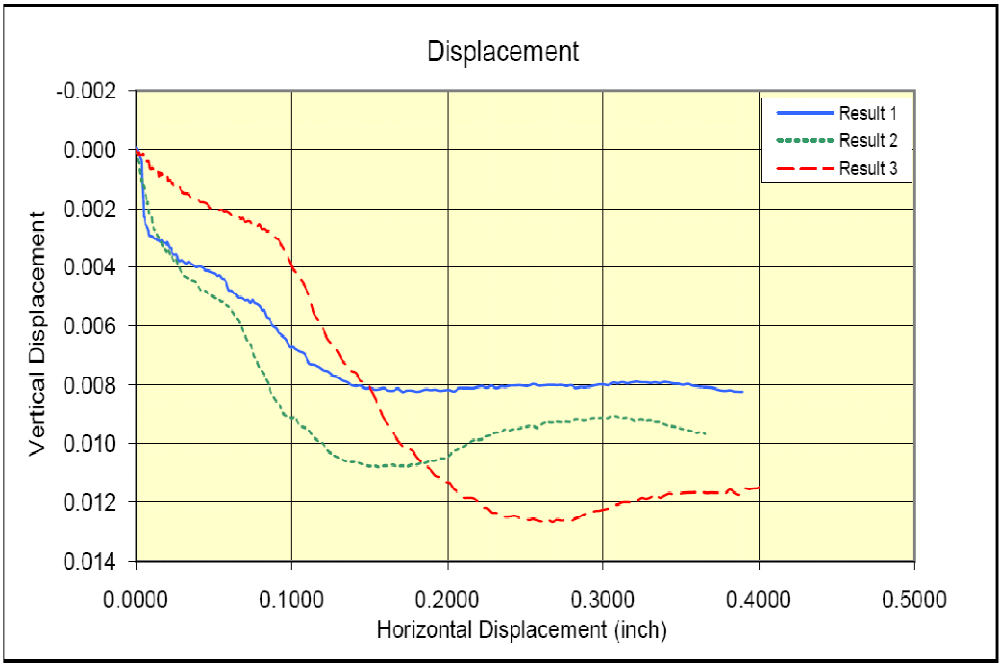
Displacement
Vertical Displacement
-0.002
0.000
0.002
0.004
0.006
0.008
0.010
0.012
0.014
0.0000
0.1000
0.2000
0.3000
0.4000
0.5000
Horizontal Displacement (inch)
Result 1
Result 2
Result 3

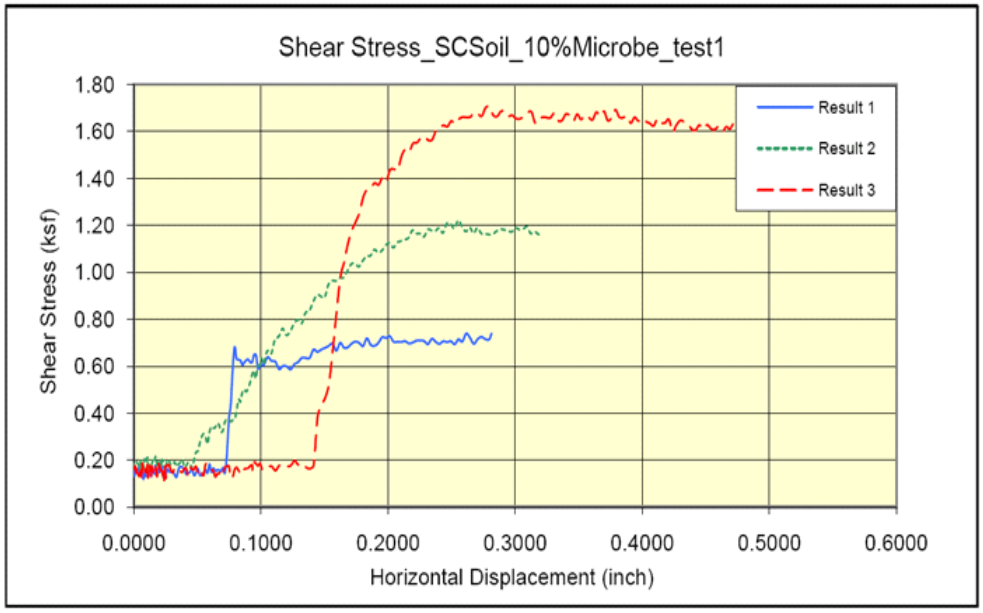
Shear Stress_SCSoil_10%Microbe_test1
Shear Stress (ksf)
1.80
1.60
1.40
1.20
1.00
0.80
0.60
0.40
0.20
0.00
0.0000
0.1000
0.2000
0.3000
0.4000
0.5000
0.6000
Horizontal Displacement (inch)
Result 1
Result 2
Result 3

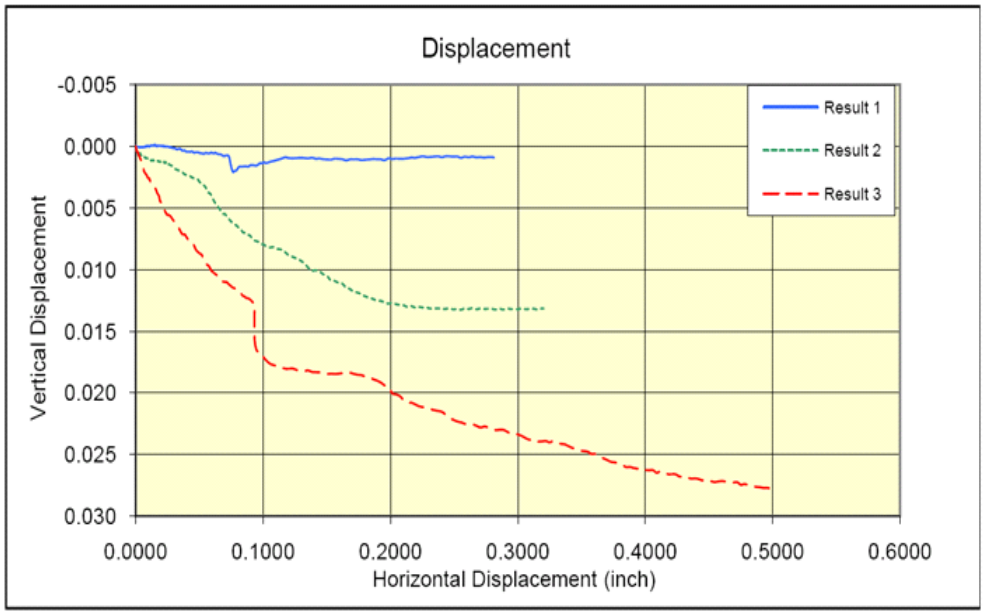
Displacement
Vertical Displacement
-0.005
0.000
0.005
0.010
0.015
0.020
0.025
0.030
0.0000
0.1000
0.2000
0.3000
0.4000
0.5000
0.6000
Horizontal Displacement (inch)
Result 1
Result 2
Result 3

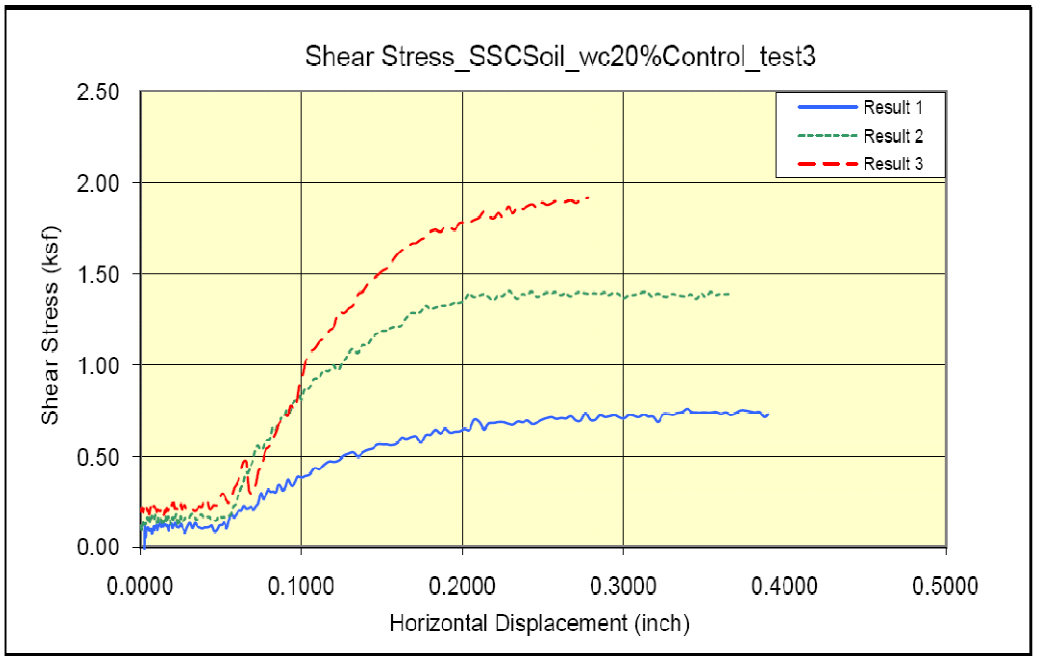
Shear Stress_SSCSoil_wc20%Control_test3
Shear Stress (ksf)
2.50
2.00
1.50
1.00
0.50
0.00
0.0000
0.1000
0.2000
0.3000
0.4000
0.5000
Horizontal Displacement (inch)
Result 1
Result 2
Result 3

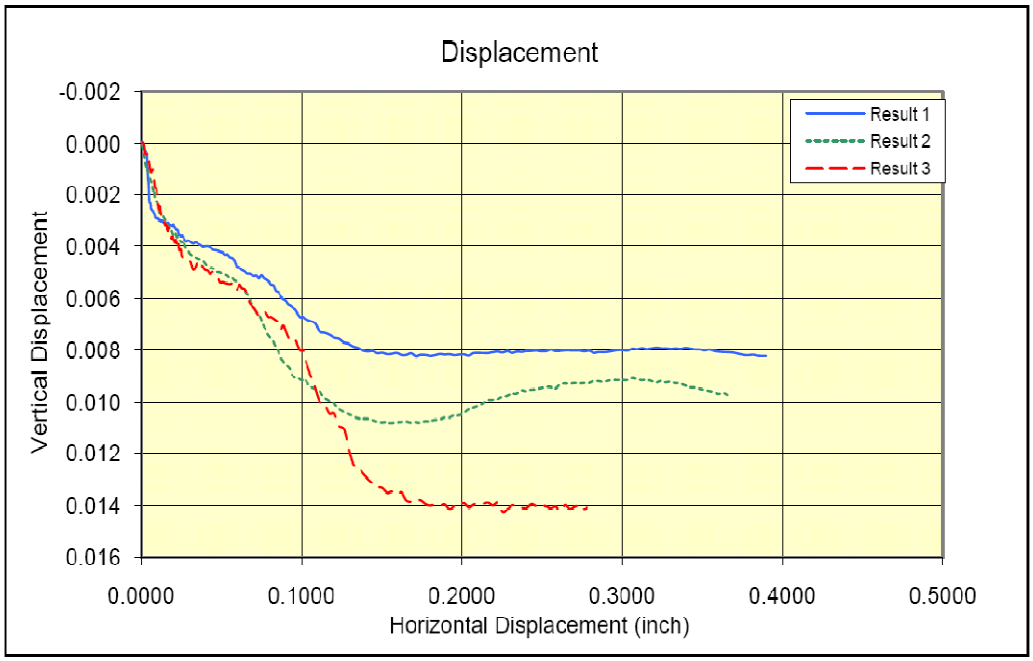
Displacement
Vertical Displacement
-0.002
0.000
0.002
0.004
0.006
0.008
0.010
0.012
0.014
0.016
0.0000
0.1000
0.2000
0.3000
0.4000
0.5000
Horizontal Displacement (inch)
Result 1
Result 2
Result 3

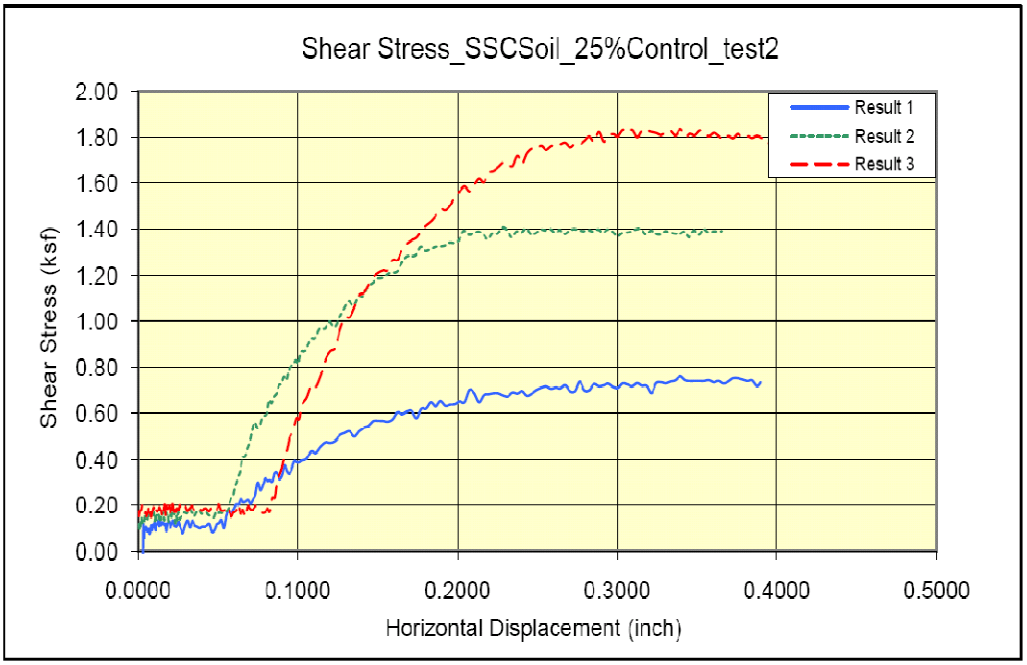
Shear Stress_SSCSoil_25%Control_test2
Shear Stress (ksf)
2.00
1.80
1.60
1.40
1.20
1.00
0.80
0.60
0.40
0.20
0.00
0.0000
0.1000
0.2000
0.3000
0.4000
0.5000
Horizontal Displacement (inch)
Result 1
Result 2
Result 3

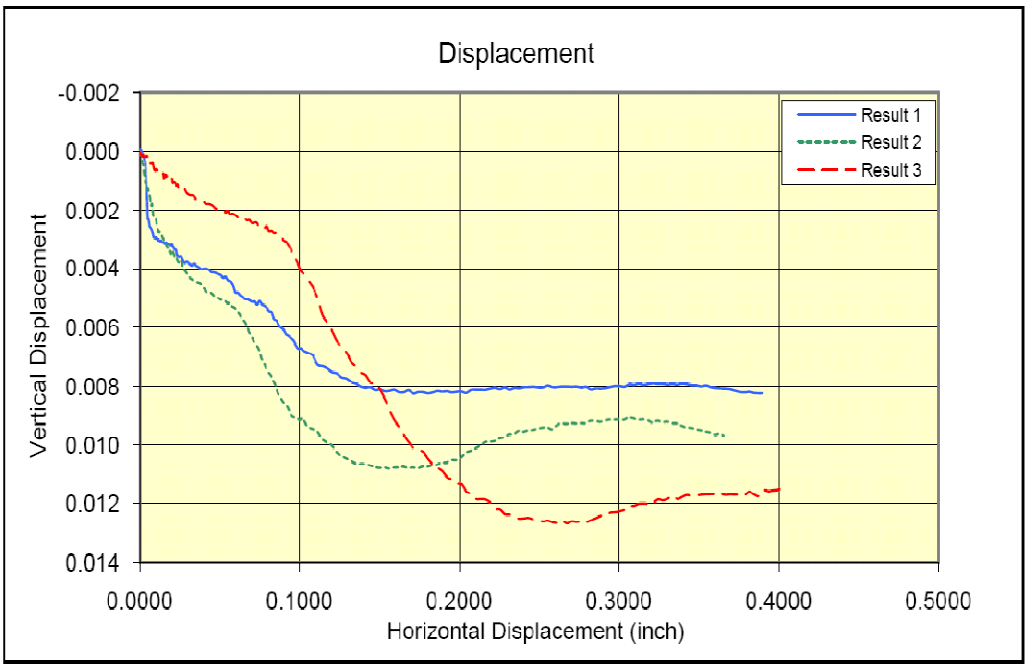
Displacement
Vertical Displacement
-0.002
0.000
0.002
0.004
0.006
0.008
0.010
0.012
0.014
0.0000
0.1000
0.2000
0.3000
0.4000
0.5000
Horizontal Displacement (inch)
Result 1
Result 2
Result 3

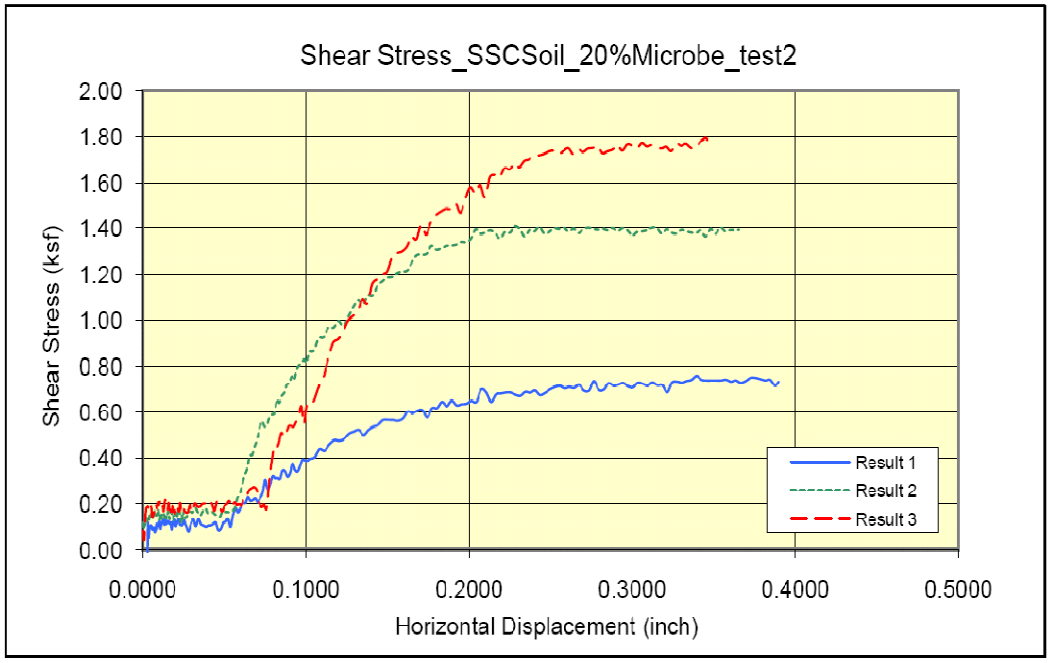
Shear Stress_SSCSoil_20%Microbe_test2
Shear Stress (ksf)
2.00
1.80
1.60
1.40
1.20
1.00
0.80
0.60
0.40
0.20
0.00
0.0000
0.1000
0.2000
0.3000
0.4000
0.5000
Horizontal Displacement (inch)
Result 1
Result 2
Result 3

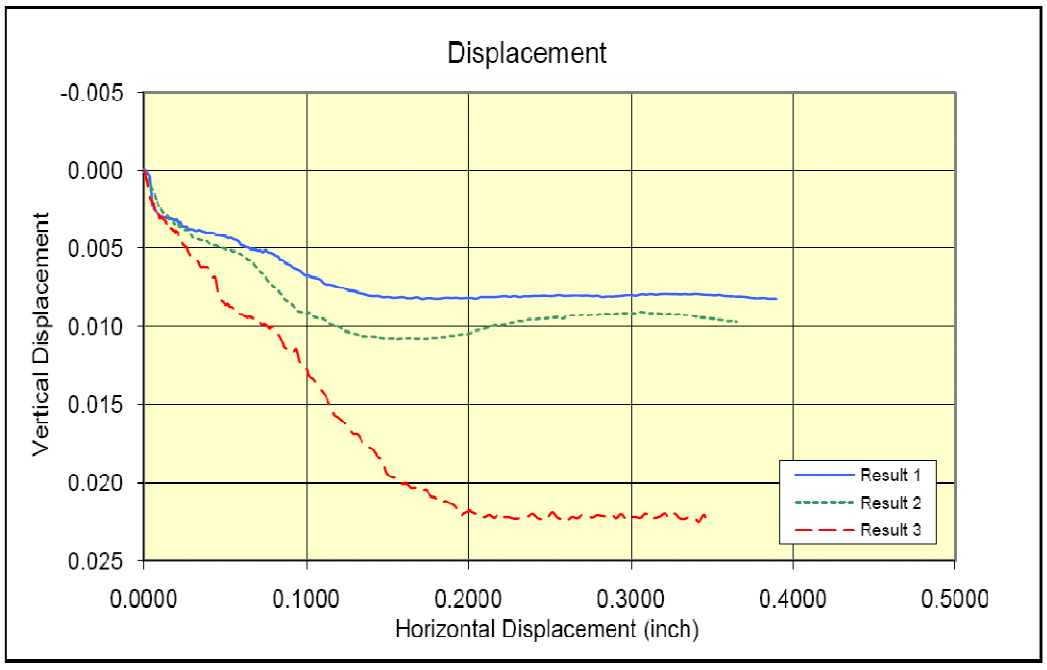
Displacement
Vertical Displacement
-0.005
0.000
0.005
0.010
0.015
0.020
0.025
0.0000
0.1000
0.2000
0.3000
0.4000
0.5000
Horizontal Displacement (inch)
Result 1
Result 2
Result 3

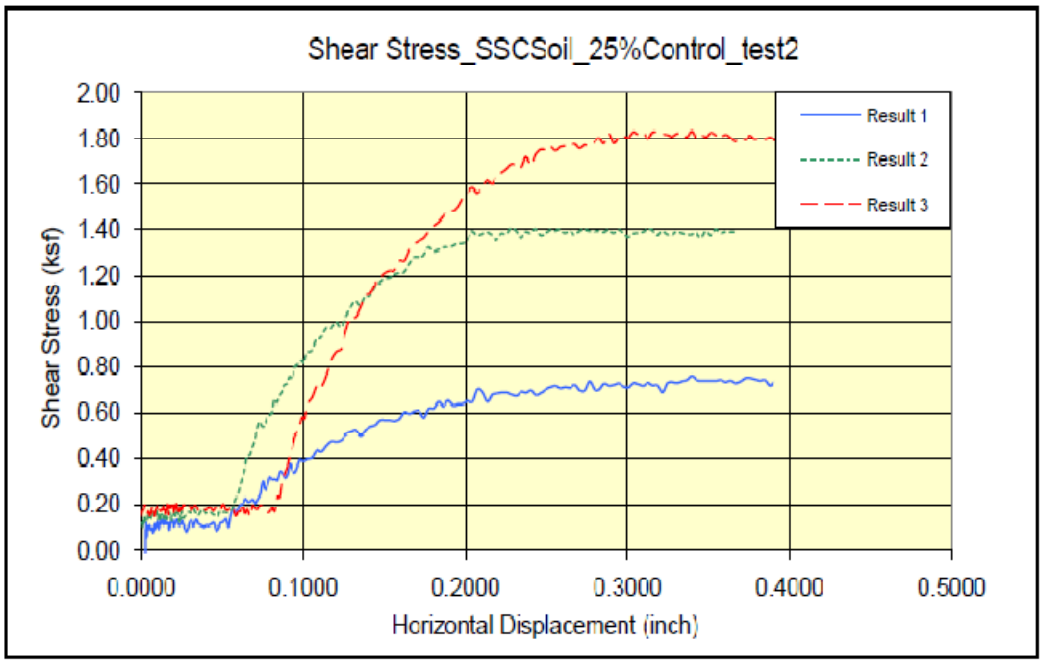
Shear Stress_SSCSoil_25%Control_test2
Shear Stress (ksf)
2.00
1.80
1.60
1.40
1.20
1.00
0.80
0.60
0.40
0.20
0.00
0.0000
0.1000
0.2000
0.3000
0.4000
0.5000
Horizontal Displacement (inch)
Result 1
Result 2
Result 3

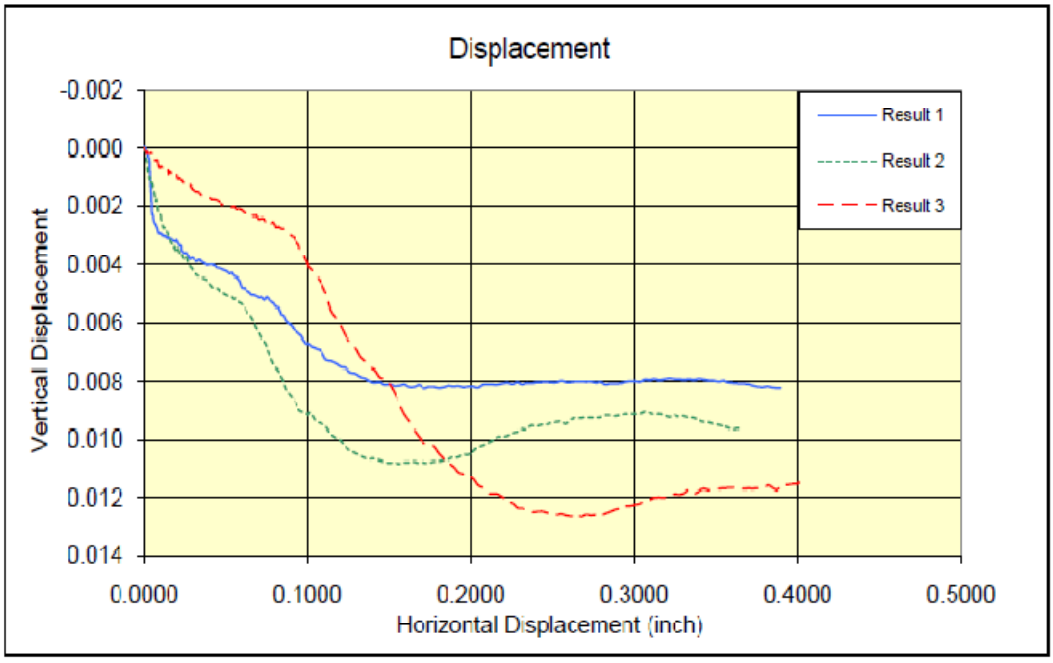
Displacement
Vertical Displacement
-0.002
0.000
0.002
0.004
0.006
0.008
0.010
0.012
0.014
0.0000
0.1000
0.2000
0.3000
0.4000
0.5000
Horizontal Displacement (inch)
Result 1
Result 2
Result 3

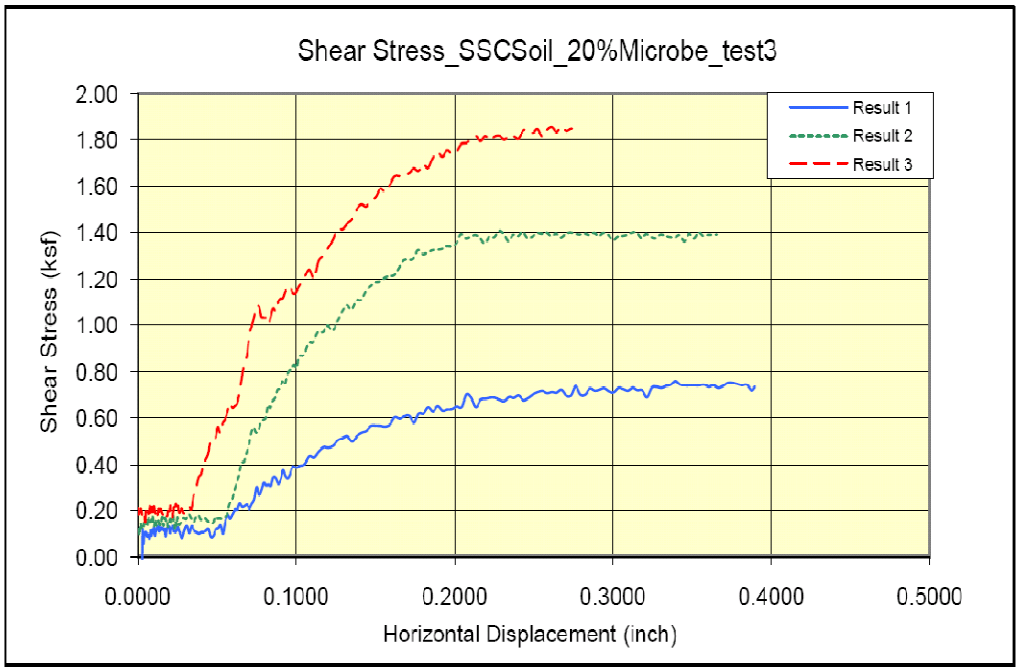
Shear Stress_SSCSoil_20%Microbe_test3
Shear Stress (ksf)
2.00
1.80
1.60
1.40
1.20
1.00
0.80
0.60
0.40
0.20
0.00
0.0000
0.1000
0.2000
0.3000
0.4000
0.5000
Horizontal Displacement (inch)
Result 1
Result 2
Result 3

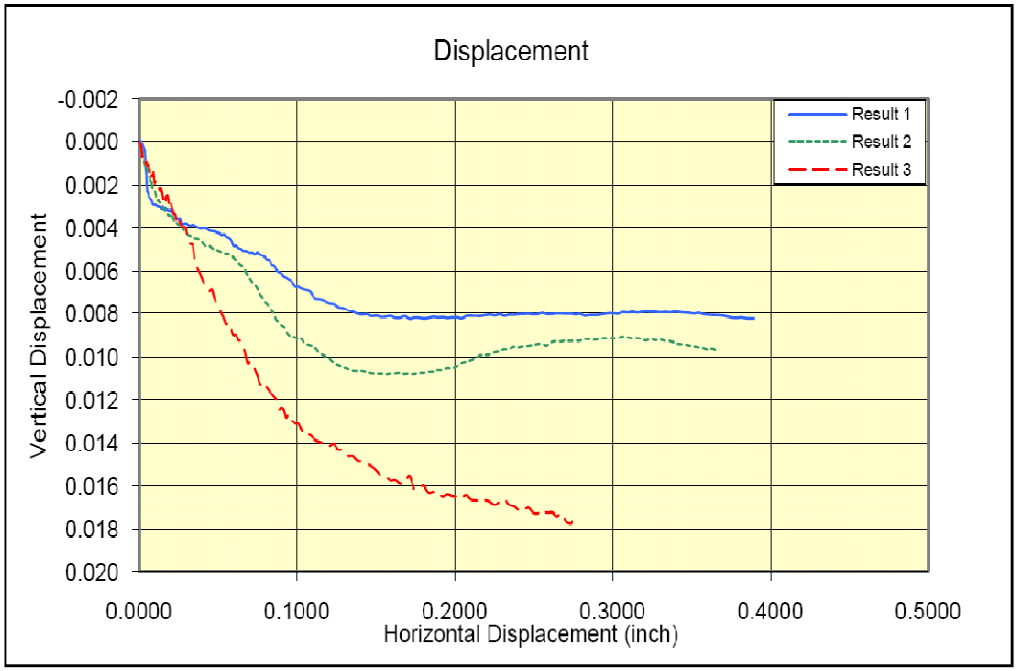
Displacement
Vertical Displacement
-0.002
0.000
0.002
0.004
0.006
0.008
0.010
0.012
0.014
0.016
0.018
0.020
0.0000
0.1000
0.2000
0.3000
0.4000
0.5000
Horizontal Displacement (inch)
Result 1
Result 2
Result 3

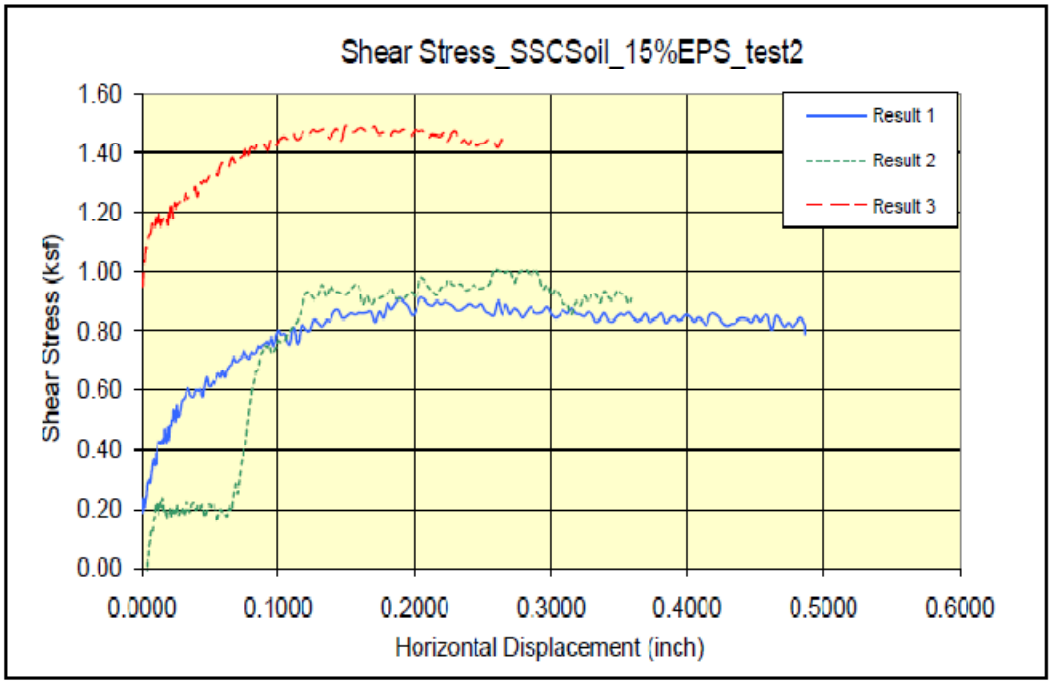
Shear Stress_SSCSoil_15%EPS_test2
Shear Stress (ksf)
1.60
1.40
1.20
1.00
0.80
0.60
0.40
0.20
0.00
0.0000
0.1000
0.2000
0.3000
0.4000
0.5000
0.6000
Horizontal Displacement (inch)
Result 1
Result 2
Result 3

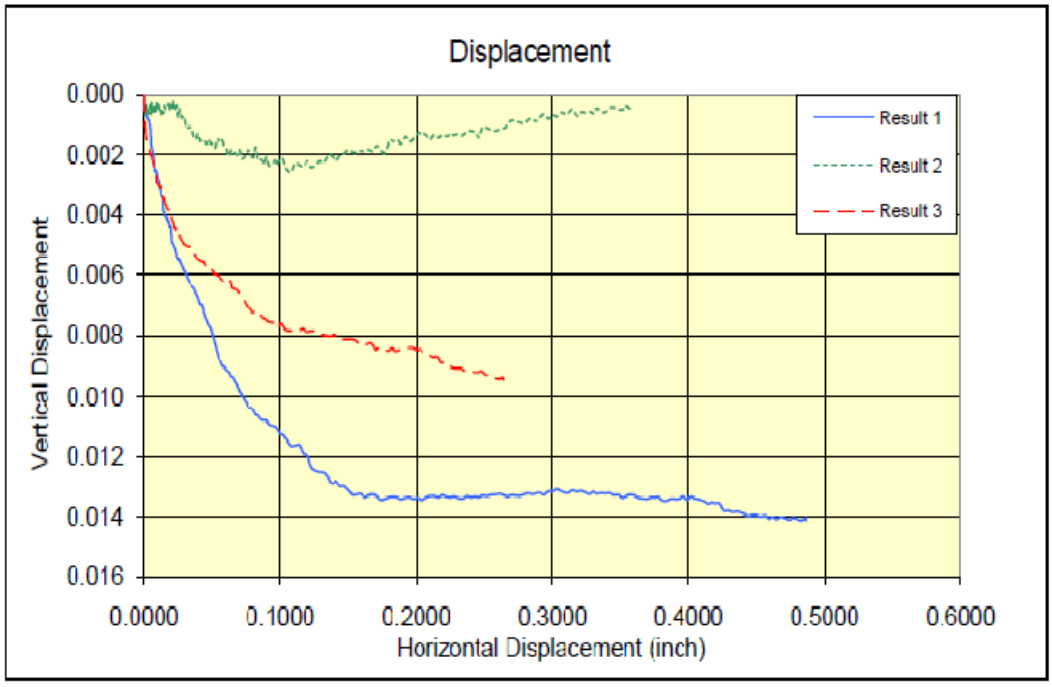
Displacement
Vertical Displacement
0.000
0.002
0.004
0.006
0.008
0.010
0.012
0.014
0.016
0.0000
0.1000
0.2000
0.3000
0.4000
0.5000
0.6000
Horizontal Displacement (inch)
Result 1
Result 2
Result 3

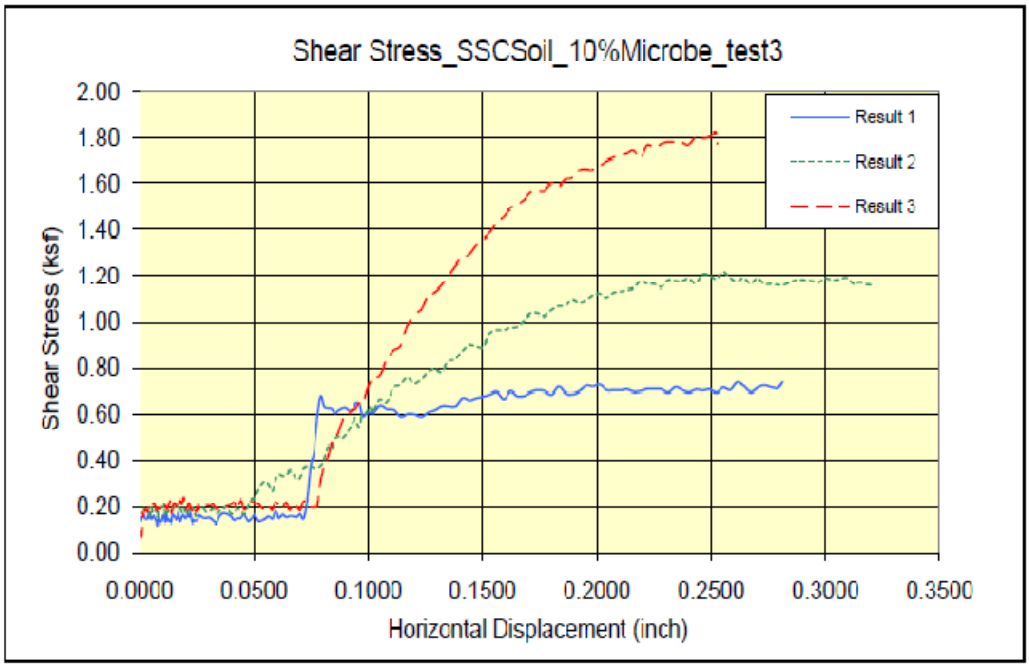
Shear Stress_SSCSoil_10%Microbe_test3
Shear Stress (ksf)
2.00
1.80
1.60
1.40
1.20
1.00
0.80
0.60
0.40
0.20
0.00
0.0000
0.0500
0.1000
0.1500
0.2000
0.2500
0.3000
0.3500
Horizontal Displacement (inch)
Result 1
Result 2
Result 3

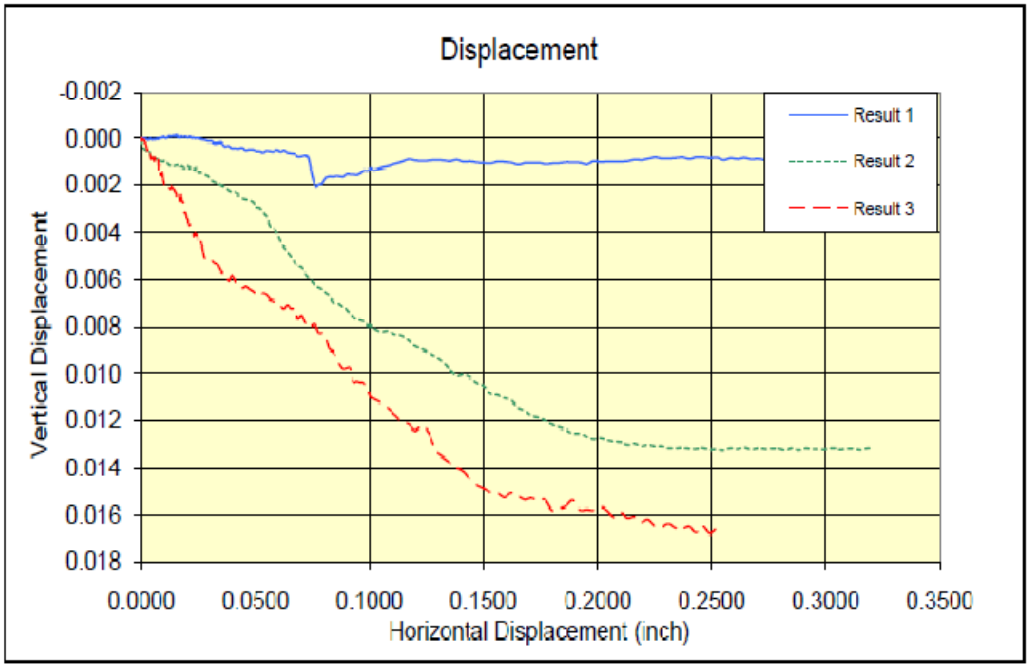
Displacement
Vertical Displacement
-0.002
0.000
0.002
0.004
0.006
0.008
0.010
0.012
0.014
0.016
0.018
0.0000
0.0500
0.1000
0.1500
0.2000
0.2500
0.3000
0.3500
Horizontal Displacement (inch)
Result 1
Result 2
Result 3

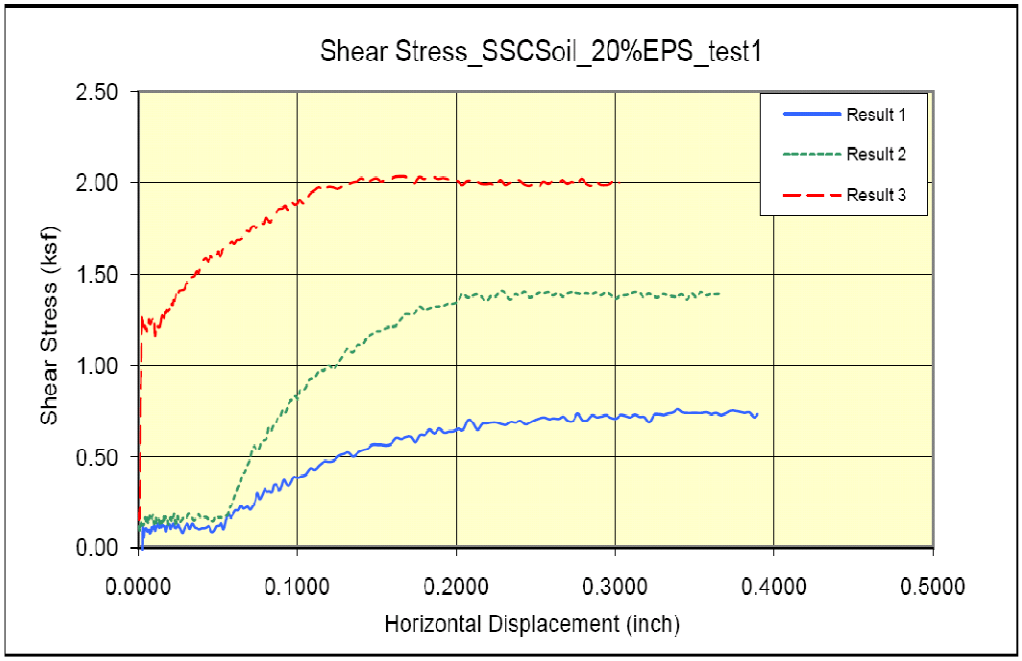
Shear Stress_SSCSoil_20%EPS_test1
Shear Stress (ksf)
2.50
2.00
1.50
1.00
0.50
0.00
0.0000
0.1000
0.2000
0.3000
0.4000
0.5000
Horizontal Displacement (inch)
Result 1
Result 2
Result 3

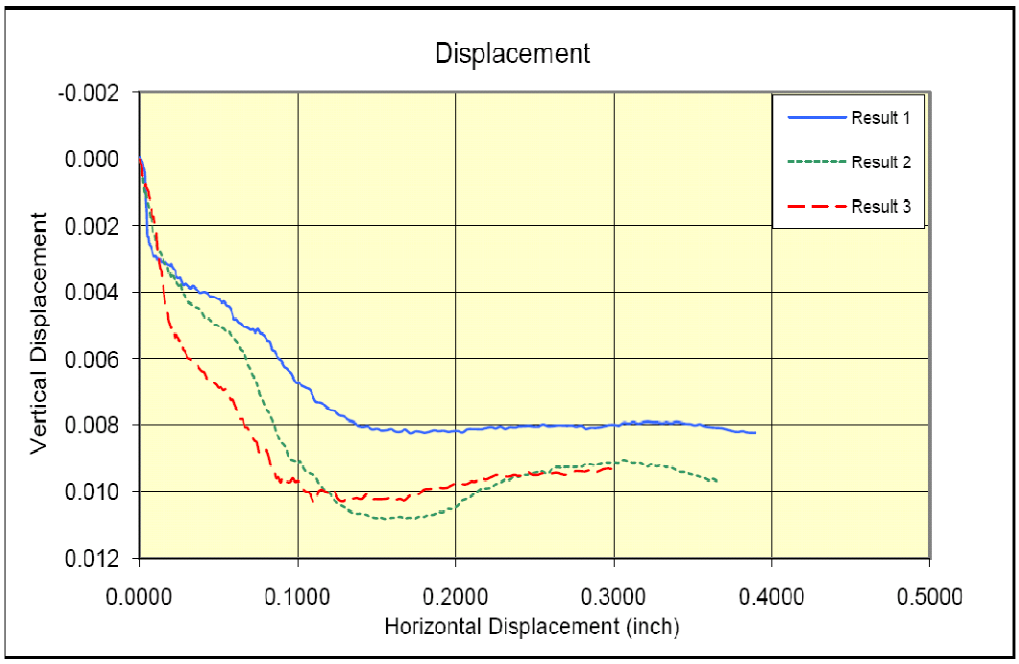
Displacement
Vertical Displacement
-0.002
0.000
0.002
0.004
0.006
0.008
0.010
0.012
0.0000
0.1000
0.2000
0.3000
0.4000
0.5000
Horizontal Displacement (inch)
Result 1
Result 2
Result 3

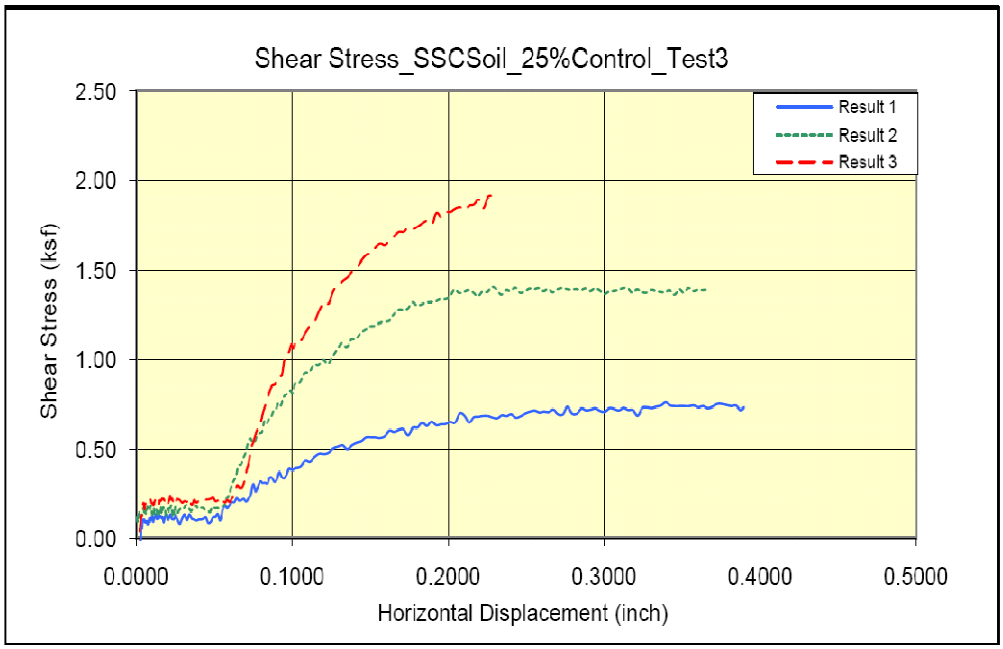
Shear Stress_SSCSoil_25%Control_Test3
Result 1
Result 2
Result 3
Shear Stress (ksf)
2.50
2.00
1.50
1.00
0.50
0.00
0.0000
0.1000
0.2000
0.3000
0.4000
0.5000
Horizontal Displacement (inch)

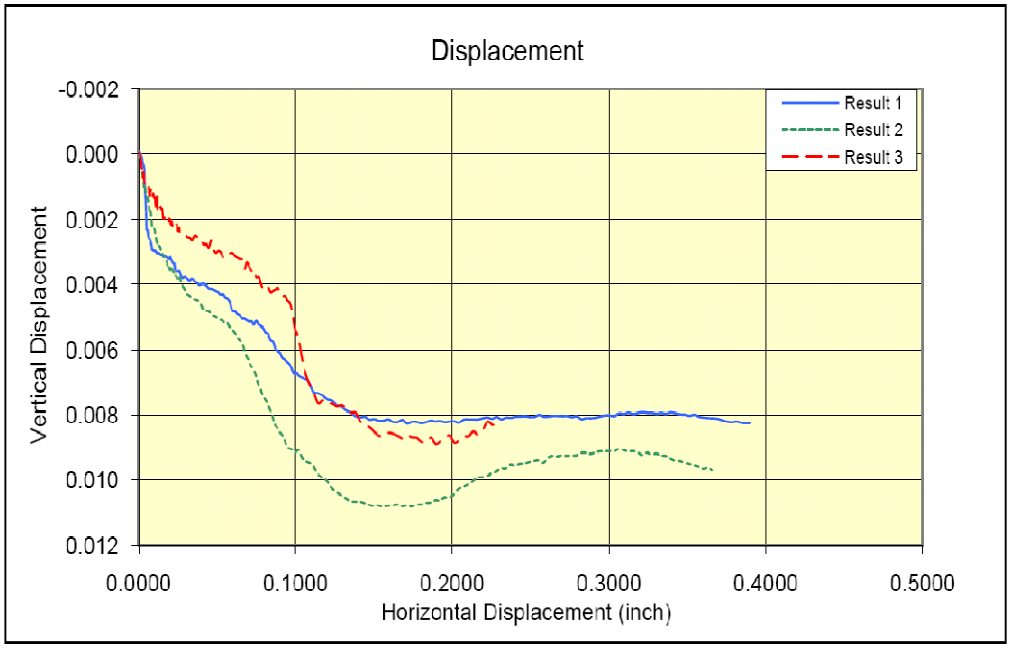
Displacement
Result 1
Result 2
Result 3
Vertical Displacement
-0.002
0.000
0.002
0.004
0.006
0.008
0.010
0.012
0.0000
0.1000
0.2000
0.3000
0.4000
0.5000
Horizontal Displacement (inch)

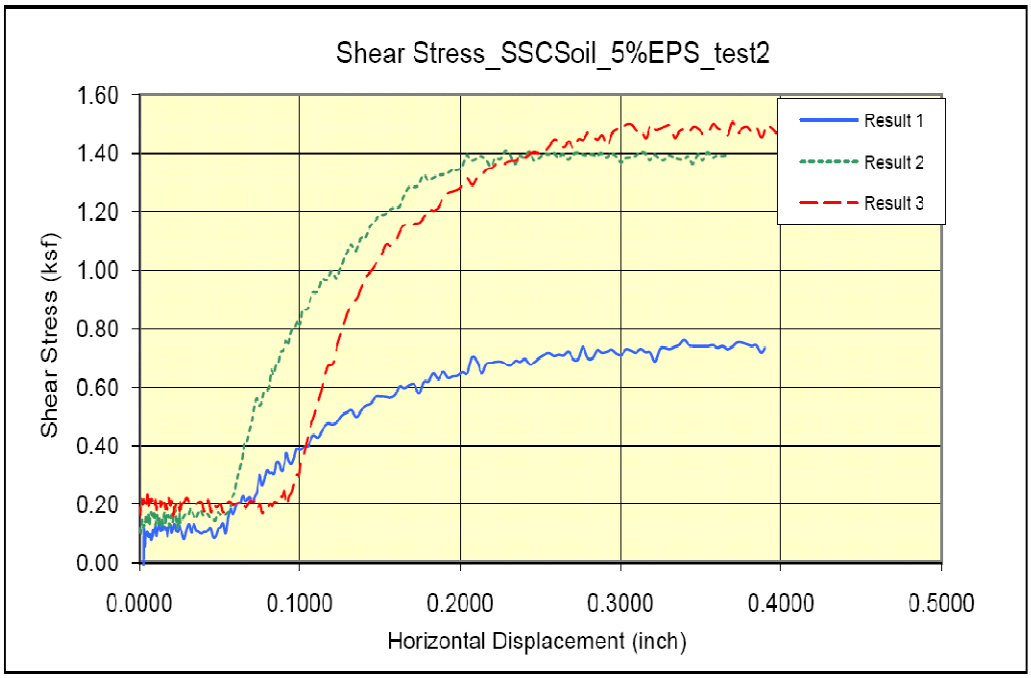
Shear Stress_SSCSoil_5%EPS_test2
Shear Stress (ksf)
1.60
1.40
1.20
1.00
0.80
0.60
0.40
0.20
0.00
0.0000
0.1000
0.2000
0.3000
0.4000
0.5000
Horizontal Displacement (inch)
Result 1
Result 2
Result 3

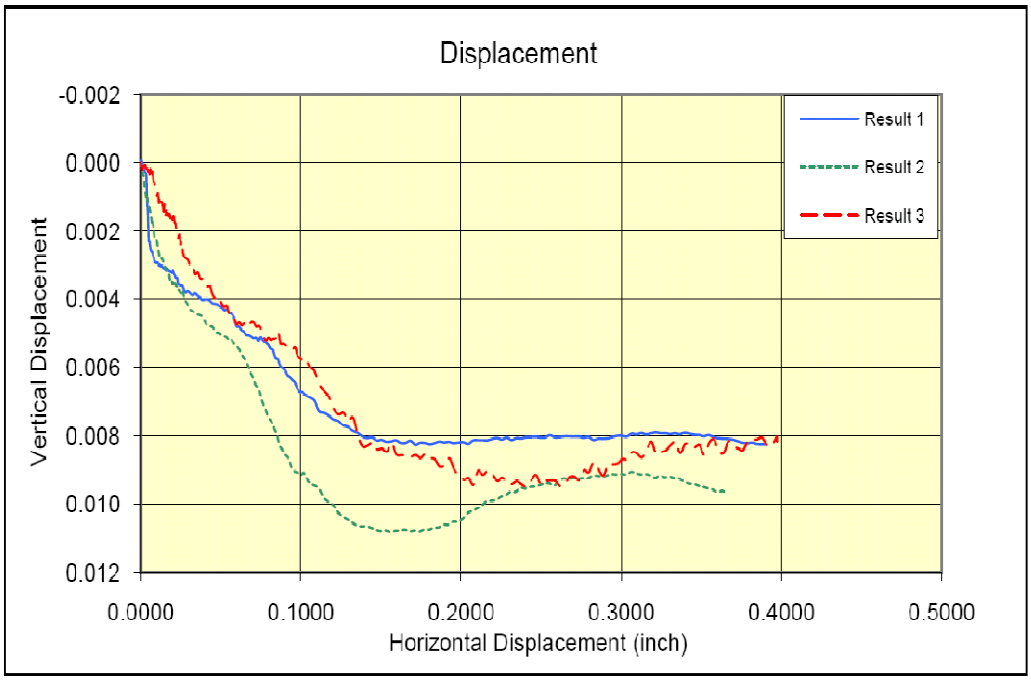
Displacement
Vertical Displacement
-0.002
0.000
0.002
0.004
0.006
0.008
0.010
0.012
0.0000
0.1000
0.2000
0.3000
0.4000
0.5000
Horizontal Displacement (inch)
Result 1
Result 2
Result 3

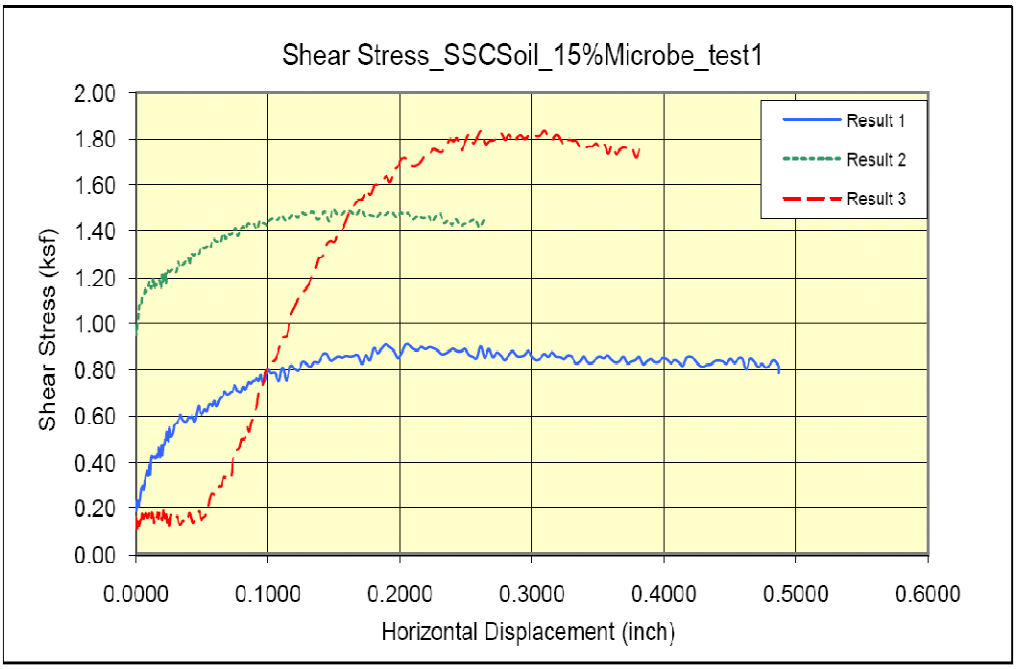
Shear Stress_SSCSoil_15%Microbe_test1
Shear Stress (ksf)
2.00
1.80
1.60
1.40
1.20
1.00
0.80
0.60
0.40
0.20
0.00
0.0000
0.1000
0.2000
0.3000
0.4000
0.5000
0.6000
Horizontal Displacement (inch)
Result 1
Result 2
Result 3

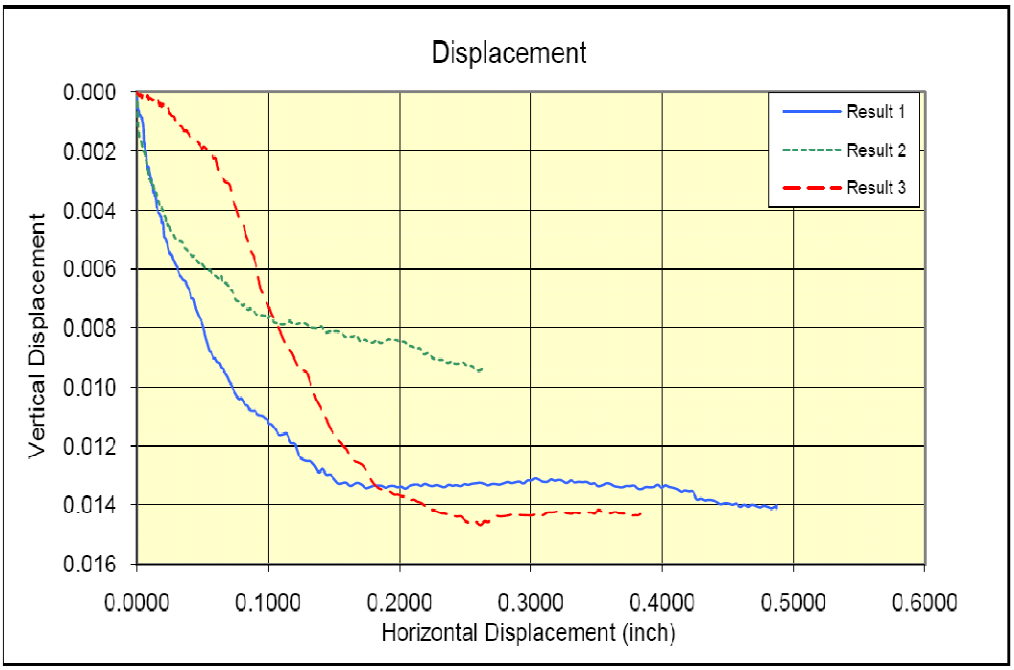
Displacement
Vertical Displacement
0.000
0.002
0.004
0.006
0.008
0.010
0.012
0.014
0.016
0.0000
0.1000
0.2000
0.3000
0.4000
0.5000
0.6000
Horizontal Displacement (inch)
Result 1
Result 2
Result 3

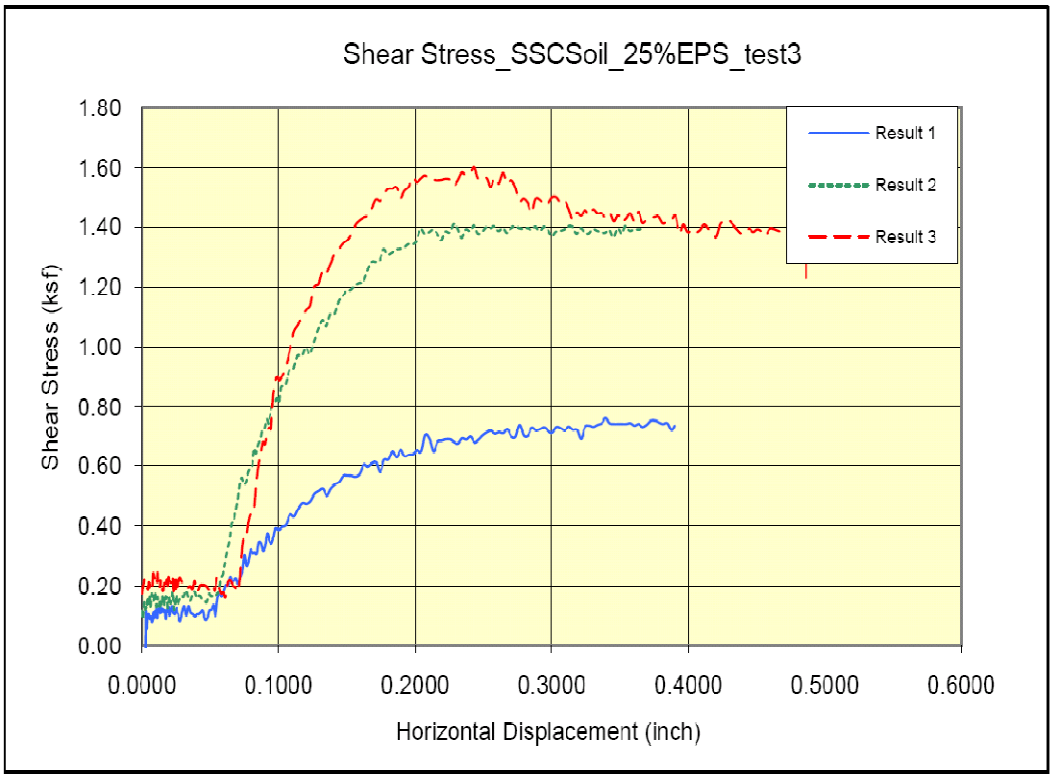
Shear Stress_SSCSoil_25%EPS_test3
Shear Stress (ksf)
1.80
1.60
1.40
1.20
1.00
0.80
0.60
0.40
0.20
0.00
0.0000
0.1000
0.2000
0.3000
0.4000
0.5000
0.6000
Horizontal Displacement (inch)
Result 1
Result 2
Result 3

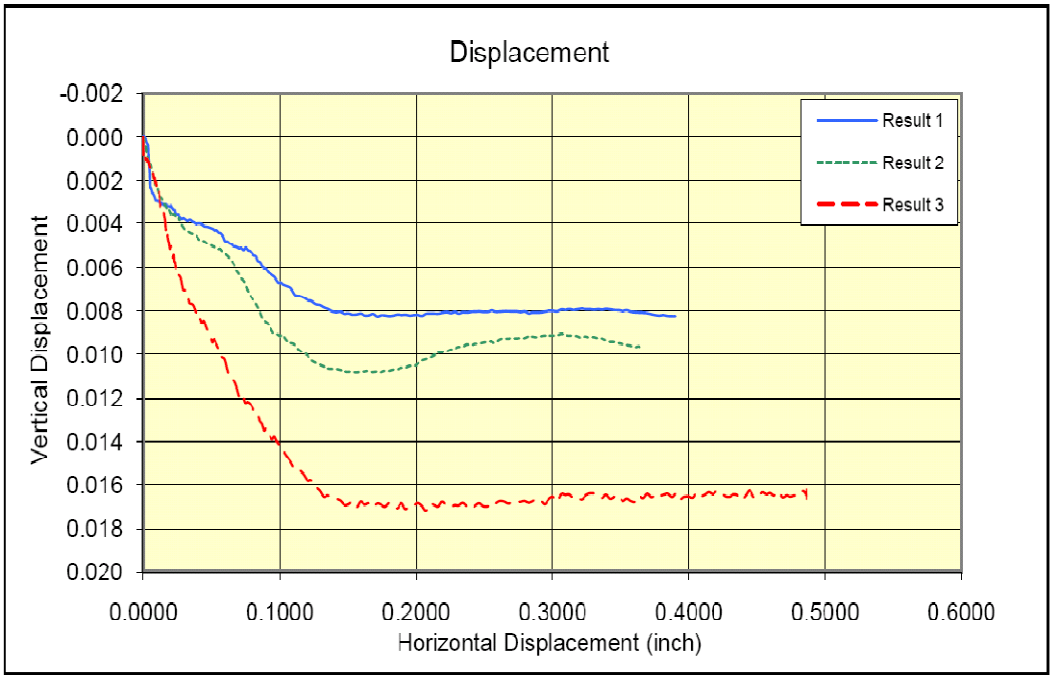
Displacement
Vertical Displacement
-0.002
0.000
0.002
0.004
0.006
0.008
0.010
0.012
0.014
0.016
0.018
0.020
0.0000
0.1000
0.2000
0.3000
0.4000
0.5000
0.6000
Horizontal Displacement (inch)
Result 1
Result 2
Result 3

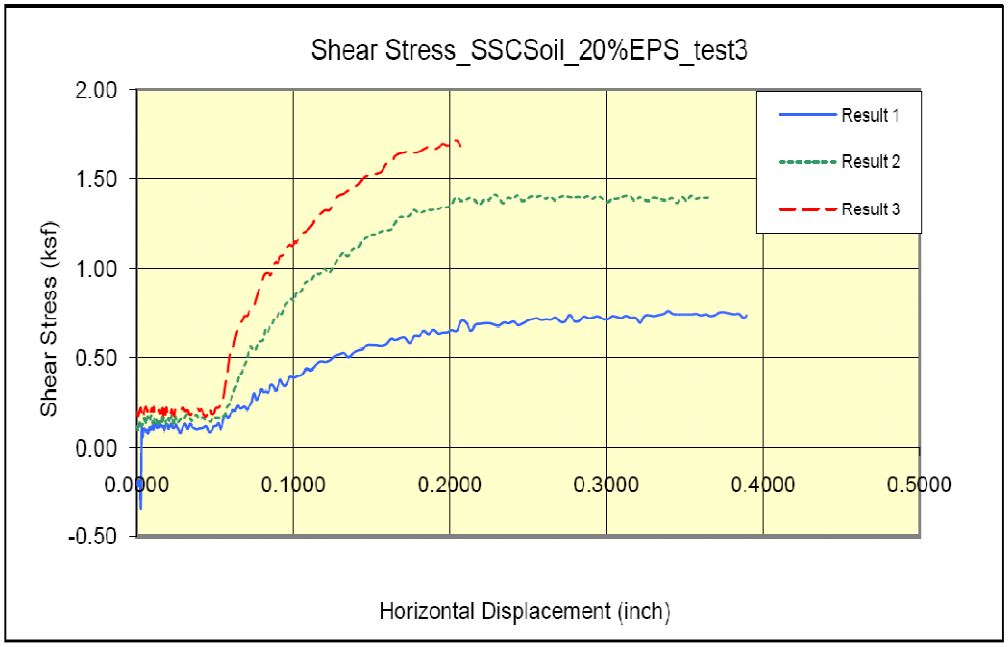
Shear Stress_SSCSoil_20%EPS_test3
Shear Stress (ksf)
2.00
1.50
1.00
0.50
0.00
-0.50
0.0000
0.1000
0.2000
0.3000
0.4000
0.5000
Horizontal Displacement (inch)
Result 1
Result 2
Result 3

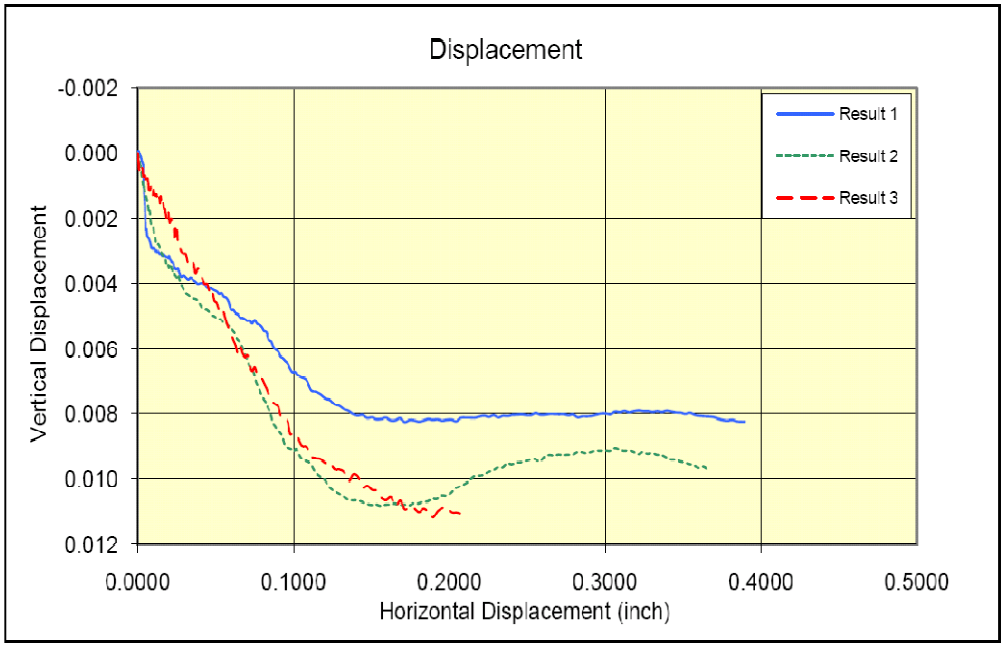
Displacement
Vertical Displacement
-0.002
0.000
0.002
0.004
0.006
0.008
0.010
0.012
0.0000
0.1000
0.2000
0.3000
0.4000
0.5000
Horizontal Displacement (inch)
Result 1
Result 2
Result 3

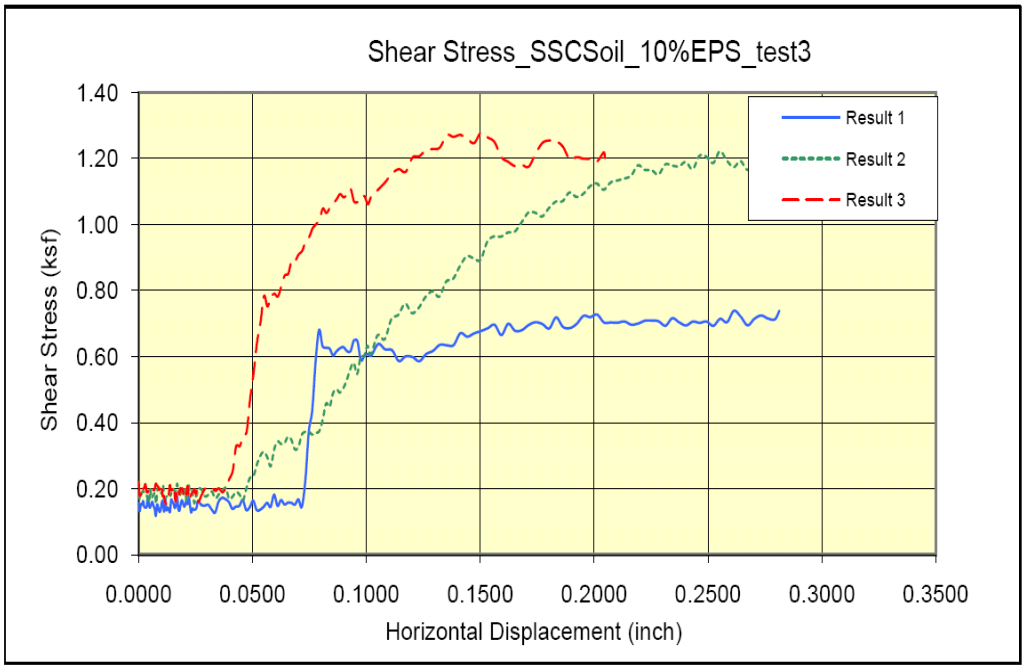
Shear Stress_SSCSoil_10%EPS_test3
Shear Stress (ksf)
1.40
1.20
1.00
0.80
0.60
0.40
0.20
0.00
0.0000
0.0500
0.1000
0.1500
0.2000
0.2500
0.3000
0.3500
Horizontal Displacement (inch)
Result 1
Result 2
Result 3

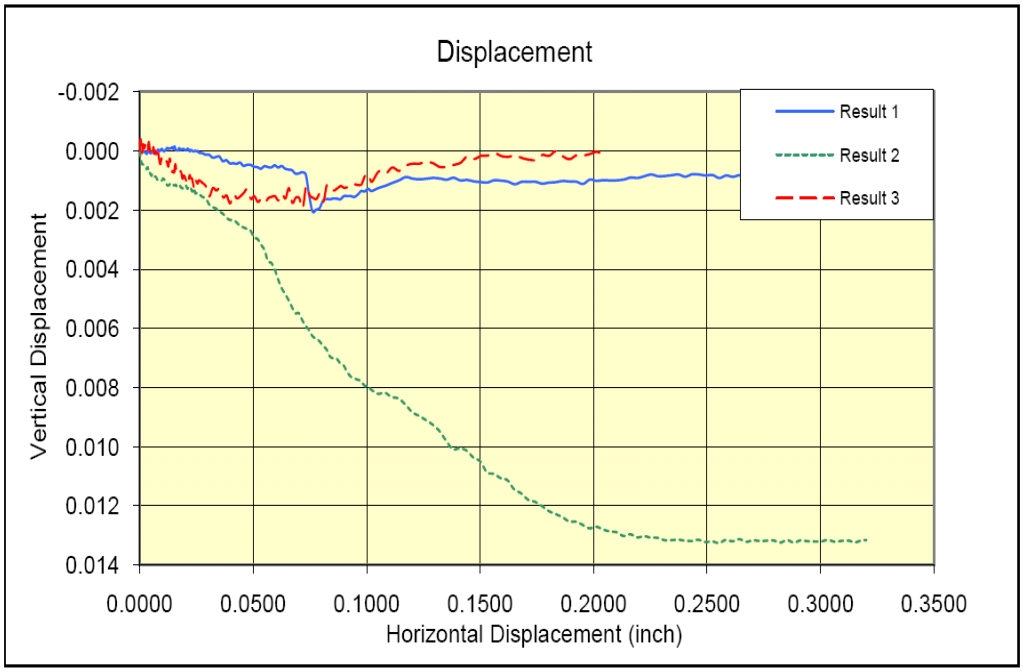
Displacement
Vertical Displacement
-0.002
0.000
0.002
0.004
0.006
0.008
0.010
0.012
0.014
0.0000
0.0500
0.1000
0.1500
0.2000
0.2500
0.3000
0.3500
Horizontal Displacement (inch)
Result 1
Result 2
Result 3

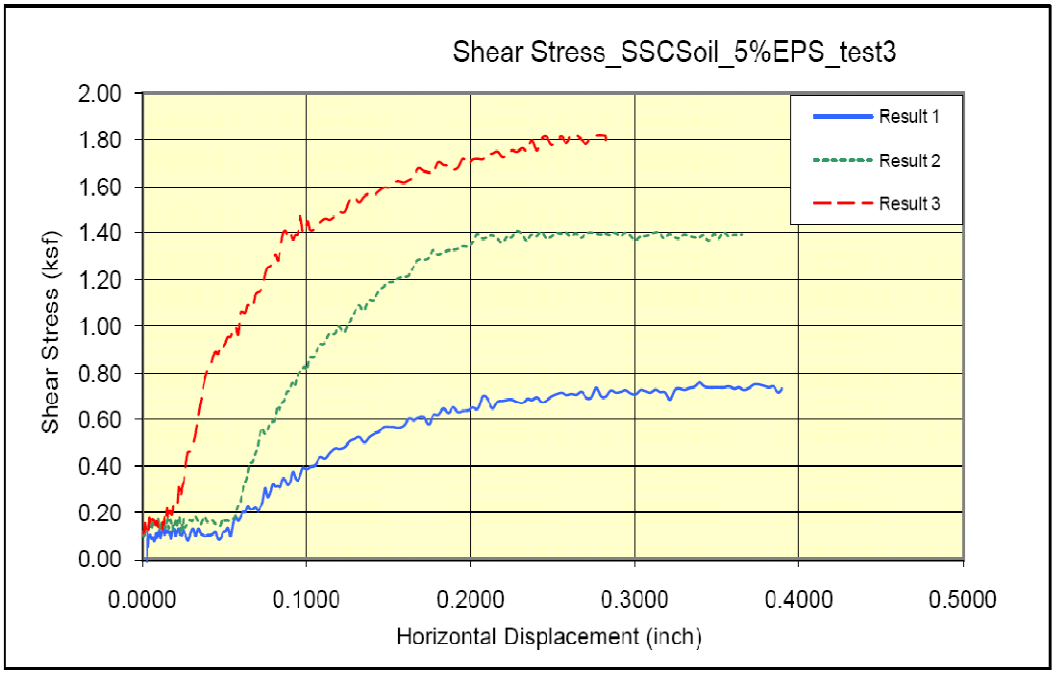
Shear Stress_SSCSoil_5%EPS_test3
Shear Stress (ksf)
2.00
1.80
1.60
1.40
1.20
1.00
0.80
0.60
0.40
0.20
0.00
0.0000
0.1000
0.2000
0.3000
0.4000
0.5000
Horizontal Displacement (inch)
Result 1
Result 2
Result 3

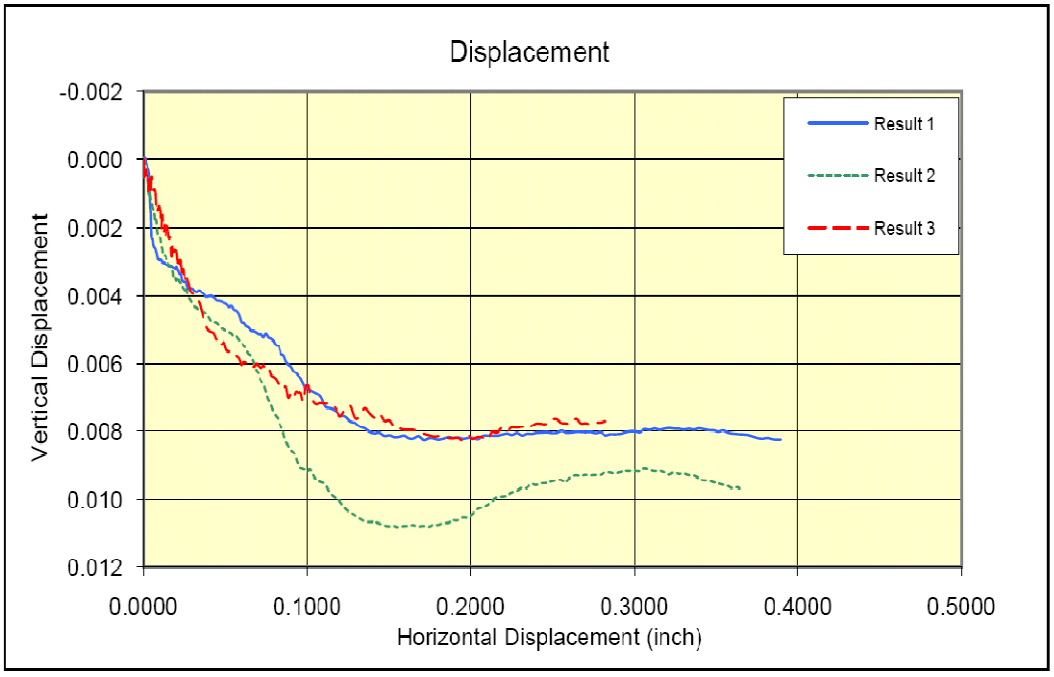
Displacement
Vertical Displacement
-0.002
0.000
0.002
0.004
0.006
0.008
0.010
0.012
0.0000
0.1000
0.2000
0.3000
0.4000
0.5000
Horizontal Displacement (inch)
Result 1
Result 2
Result 3

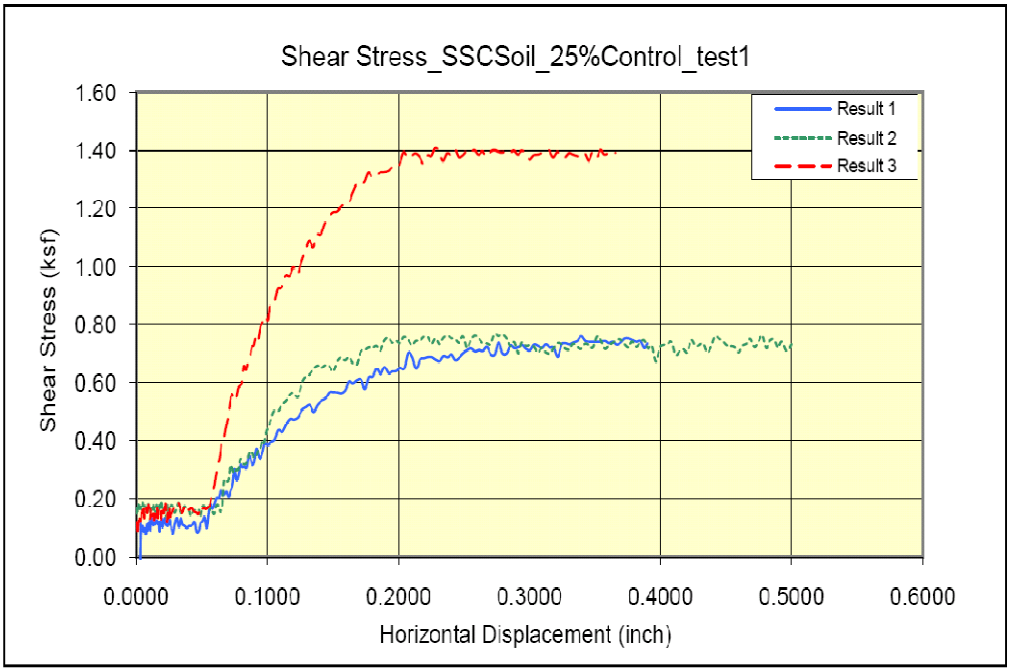
Shear Stress_SSCSoil_25%Control_test1
Result 1
Result 2
Result 3
Shear Stress (ksf)
1.60
1.40
1.20
1.00
0.80
0.60
0.40
0.20
0.00
0.0000
0.1000
0.2000
0.3000
0.4000
0.5000
0.6000
Horizontal Displacement (inch)

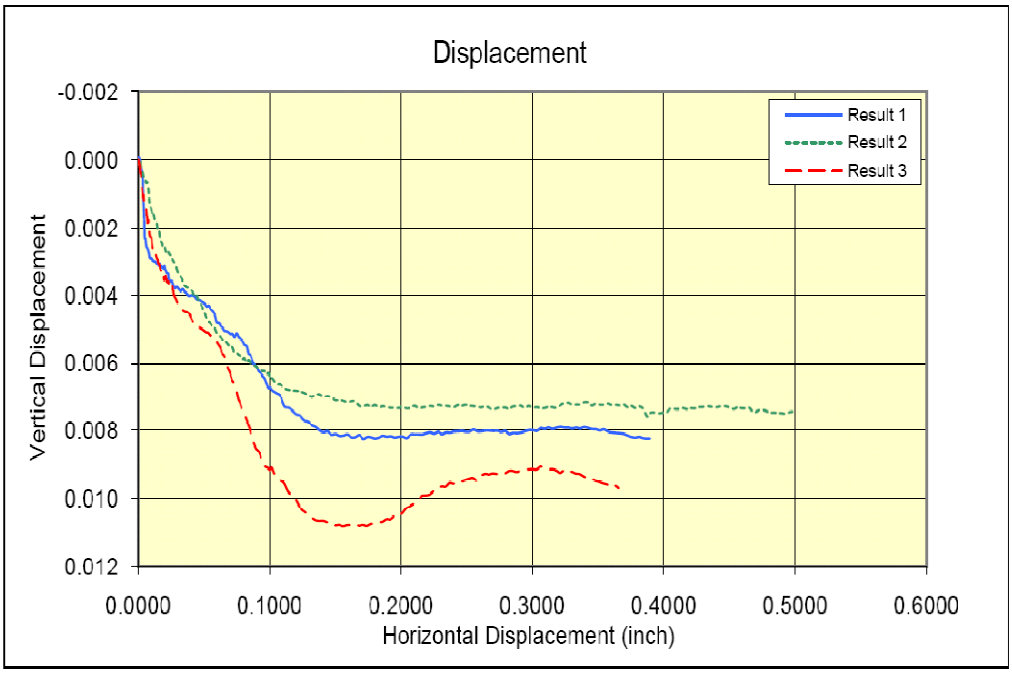
Displacement
Result 1
Result 2
Result 3
Vertical Displacement
-0.002
0.000
0.002
0.004
0.006
0.008
0.010
0.012
0.0000
0.1000
0.2000
0.3000
0.4000
0.5000
0.6000
Horizontal Displacement (inch)

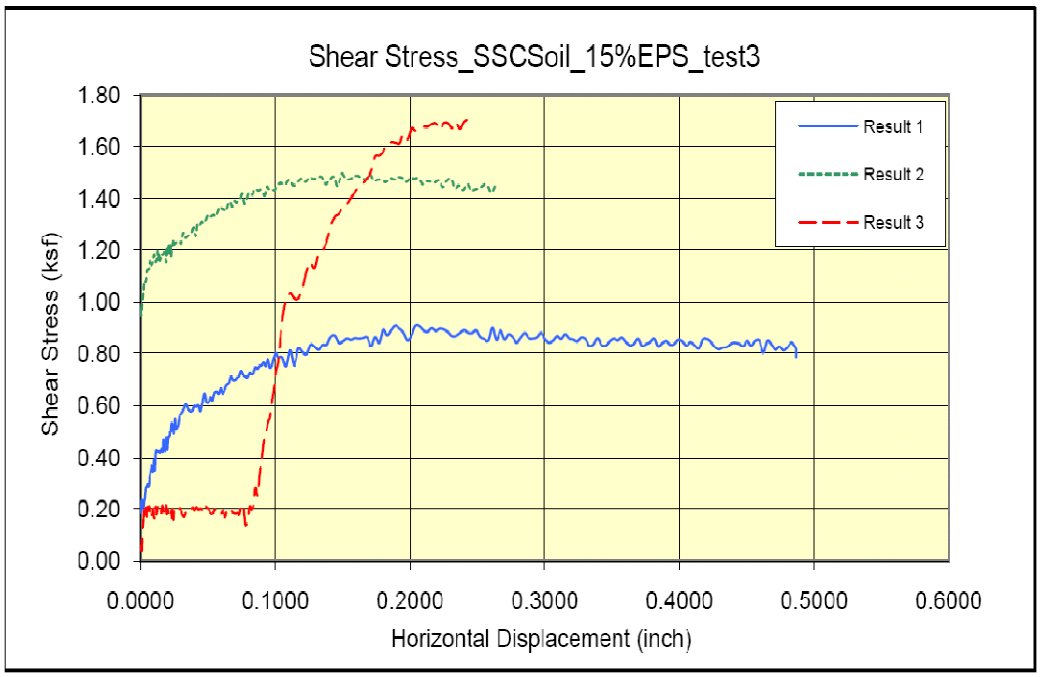
Shear Stress_SSCSoil_15%EPS_test3
Shear Stress (ksf)
1.80
1.60
1.40
1.20
1.00
0.80
0.60
0.40
0.20
0.00
0.0000
0.1000
0.2000
0.3000
0.4000
0.5000
0.6000
Horizontal Displacement (inch)
Result 1
Result 2
Result 3

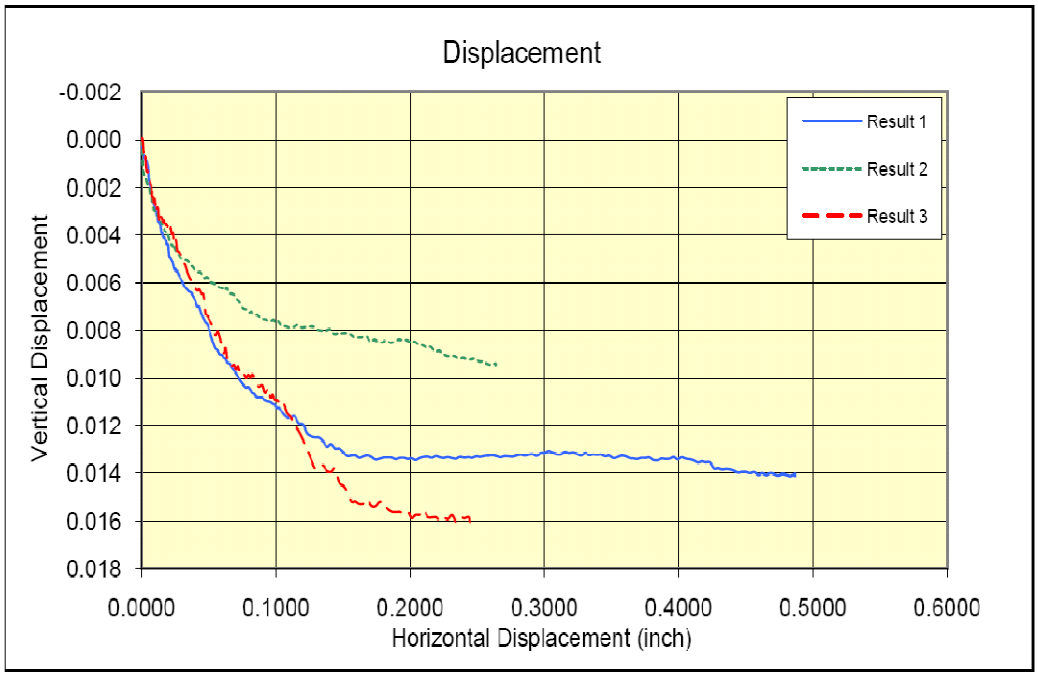
Displacement
Vertical Displacement
-0.002
0.000
0.002
0.004
0.006
0.008
0.010
0.012
0.014
0.016
0.018
0.0000
0.1000
0.2000
0.3000
0.4000
0.5000
0.6000
Horizontal Displacement (inch)
Result 1
Result 2
Result 3

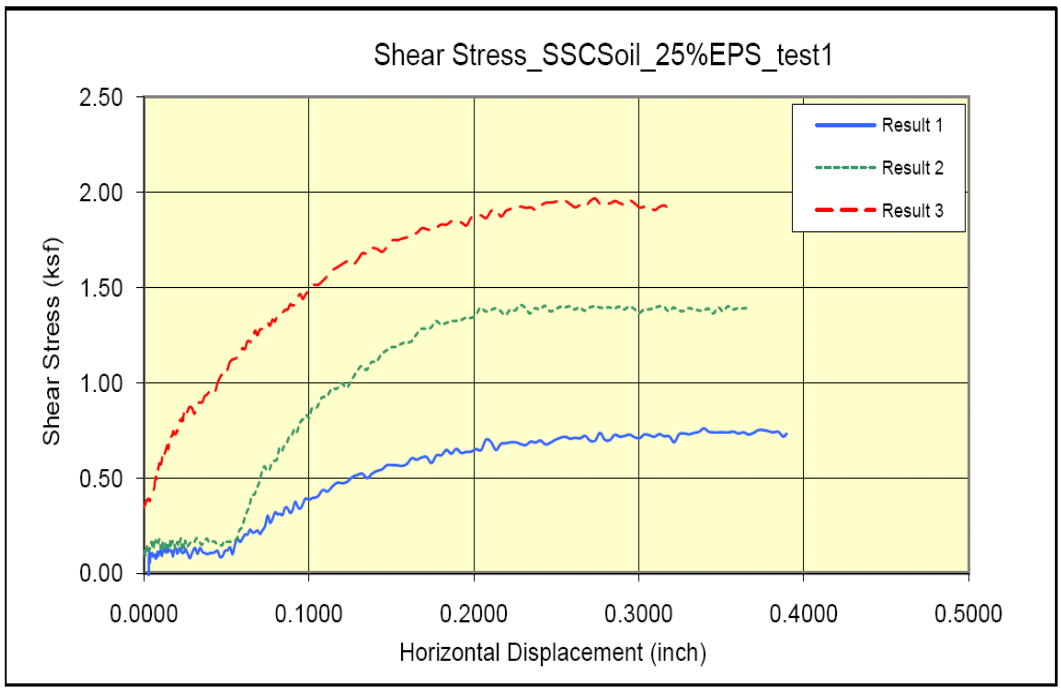
Shear Stress_SSCSoil_25%EPS_test1
Shear Stress (ksf)
2.50
2.00
1.50
1.00
0.50
0.00
0.0000
0.1000
0.2000
0.3000
0.4000
0.5000
Horizontal Displacement (inch)
Result 1
Result 2
Result 3

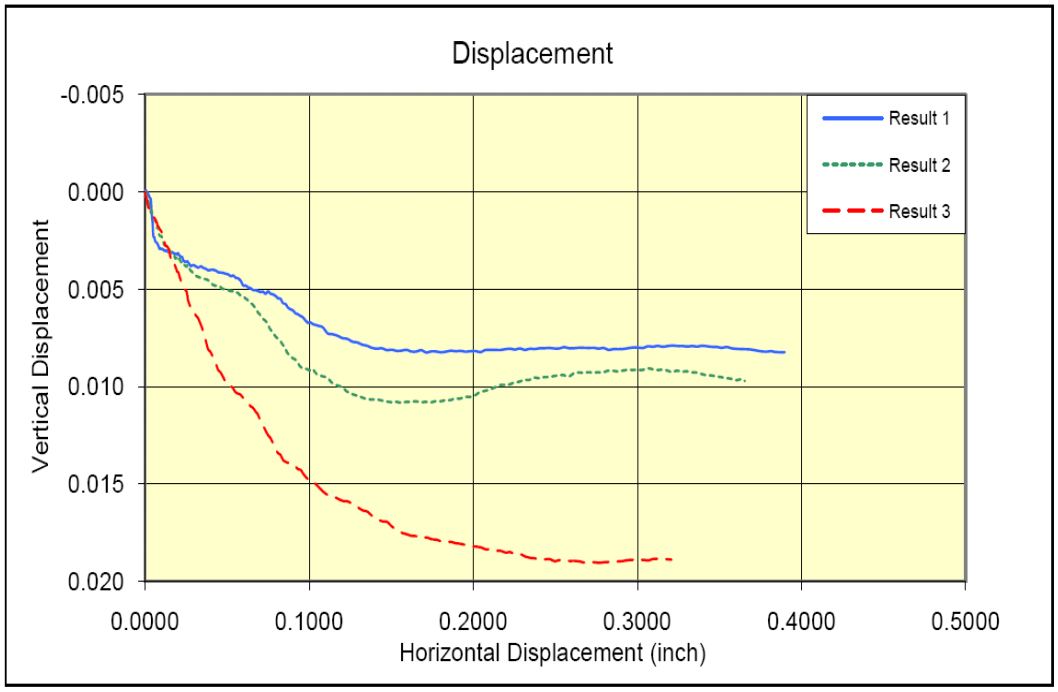
Displacement
Vertical Displacement
-0.005
0.000
0.005
0.010
0.015
0.020
0.0000
0.1000
0.2000
0.3000
0.4000
0.5000
Horizontal Displacement (inch)
Result 1
Result 2
Result 3

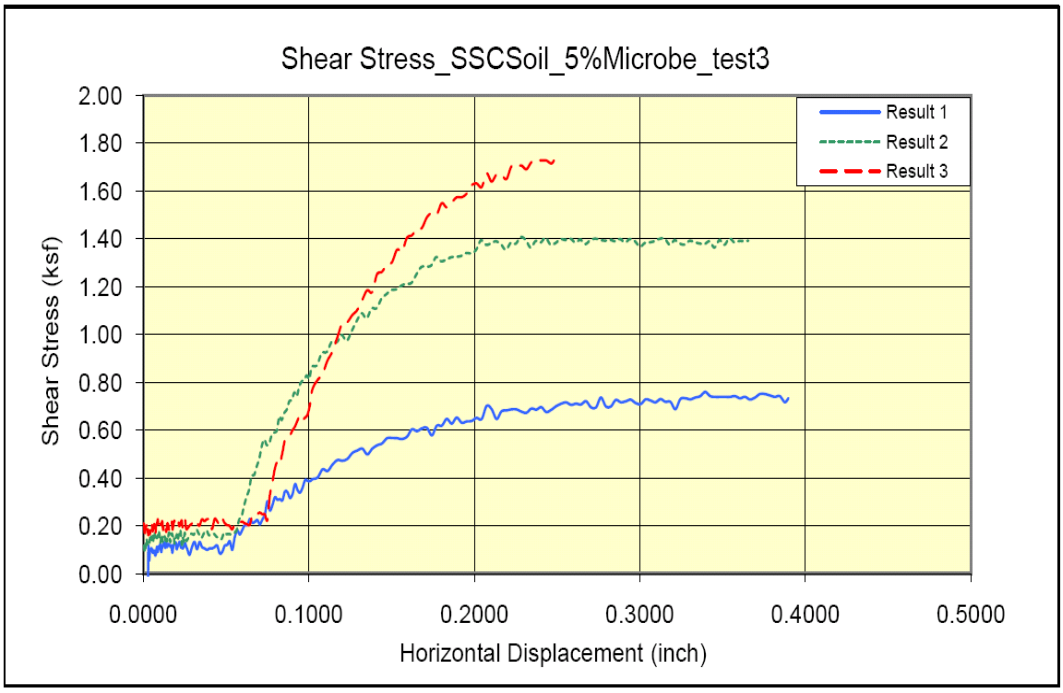
Shear Stress_SSCSoil_5%Microbe_test3
Shear Stress (ksf)
2.00
1.80
1.60
1.40
1.20
1.00
0.80
0.60
0.40
0.20
0.00
0.0000
0.1000
0.2000
0.3000
0.4000
0.5000
Horizontal Displacement (inch)
Result 1
Result 2
Result 3

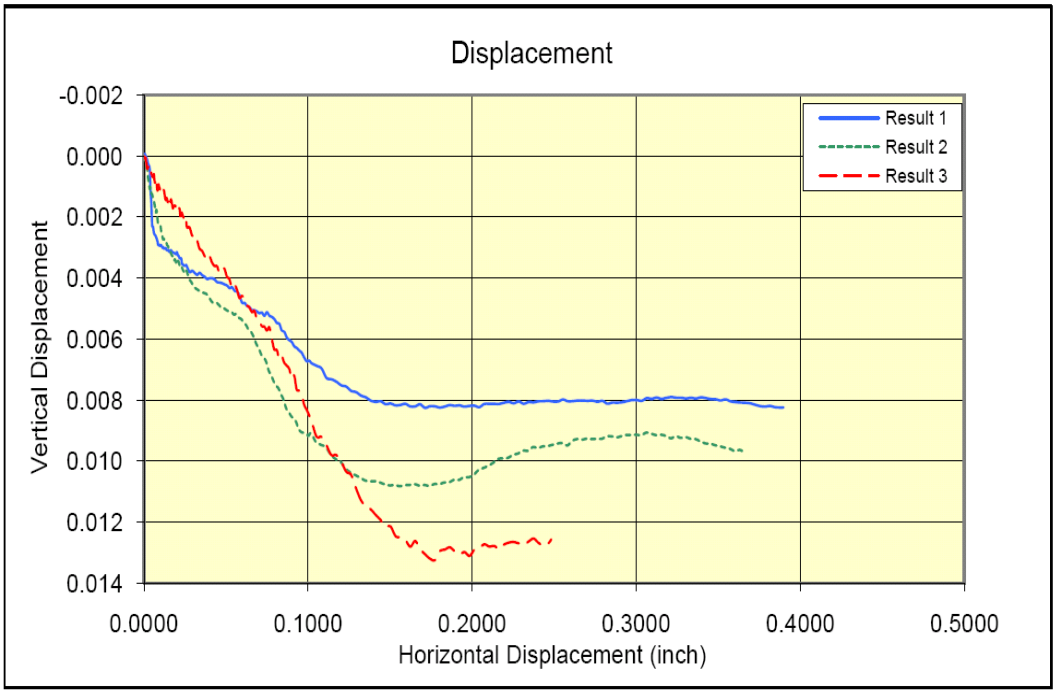
Displacement
Vertical Displacement
-0.002
0.000
0.002
0.004
0.006
0.008
0.010
0.012
0.014
0.0000
0.1000
0.2000
0.3000
0.4000
0.5000
Horizontal Displacement (inch)
Result 1
Result 2
Result 3

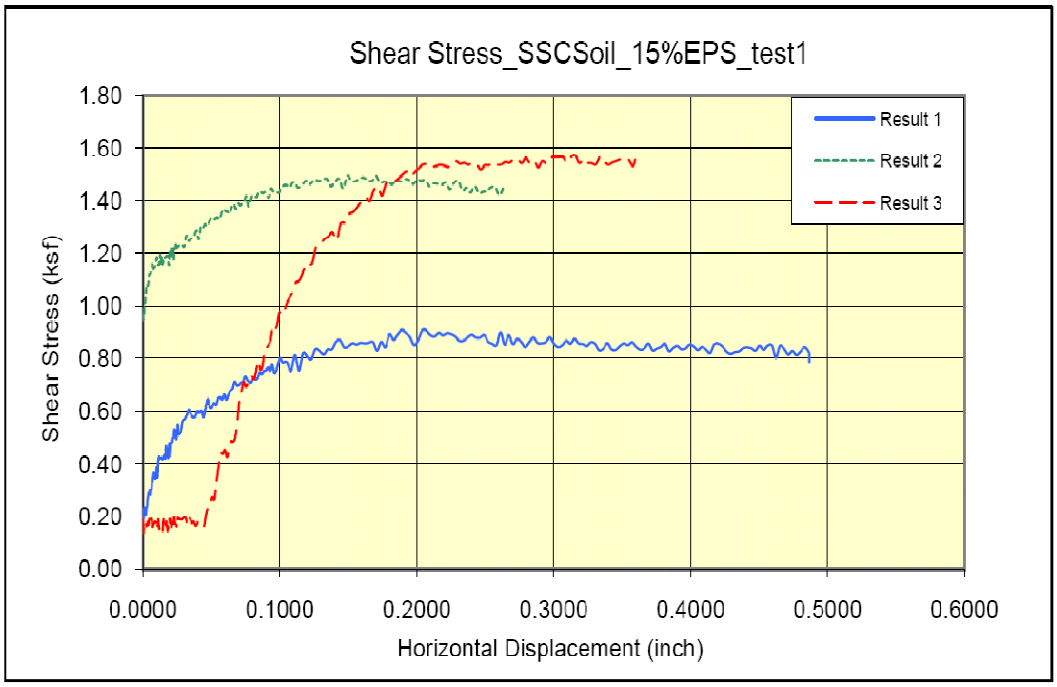
Shear Stress_SSCSoil_15%EPS_test1
Shear Stress (ksf)
1.80
1.60
1.40
1.20
1.00
0.80
0.60
0.40
0.20
0.00
0.0000
0.1000
0.2000
0.3000
0.4000
0.5000
0.6000
Horizontal Displacement (inch)
Result 1
Result 2
Result 3

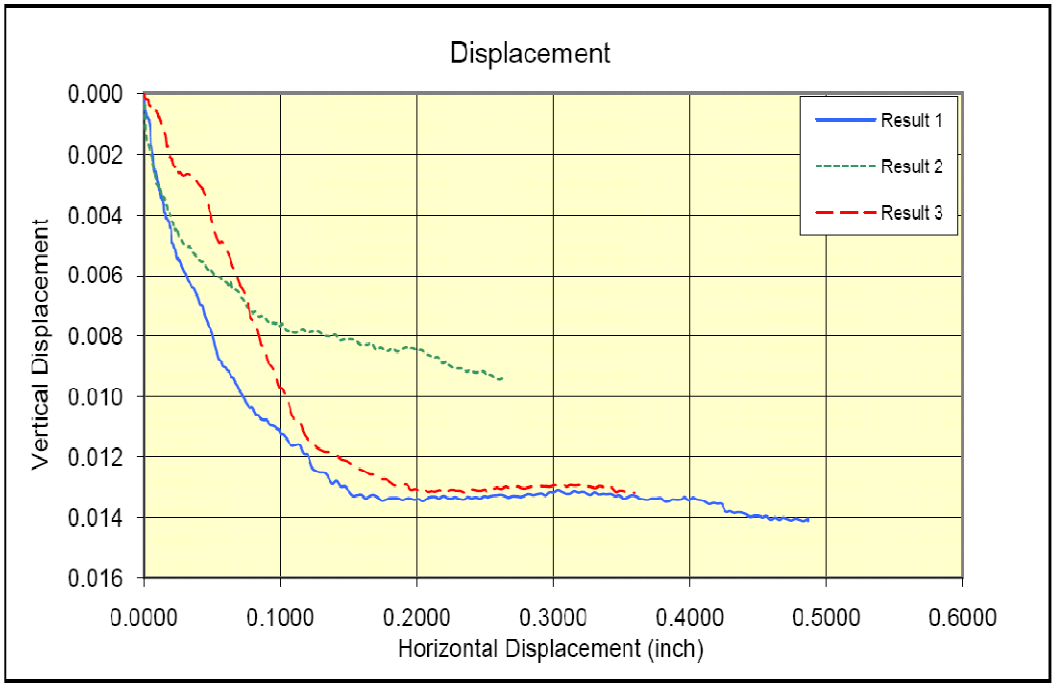
Displacement
Vertical Displacement
0.000
0.002
0.004
0.006
0.008
0.010
0.012
0.014
0.016
0.0000
0.1000
0.2000
0.3000
0.4000
0.5000
0.6000
Horizontal Displacement (inch)
Result 1
Result 2
Result 3

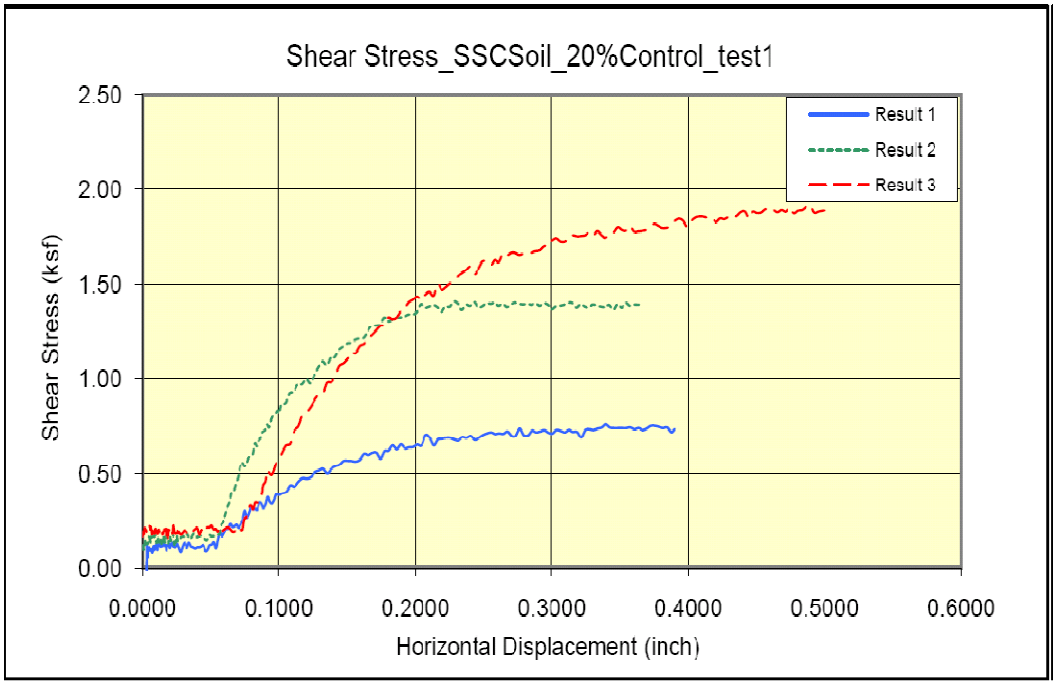
Shear Stress_SSCSoil_20%Control_test1
Shear Stress (ksf)
2.50
2.00
1.50
1.00
0.50
0.00
0.0000
0.1000
0.2000
0.3000
0.4000
0.5000
0.6000
Horizontal Displacement (inch)
Result 1
Result 2
Result 3

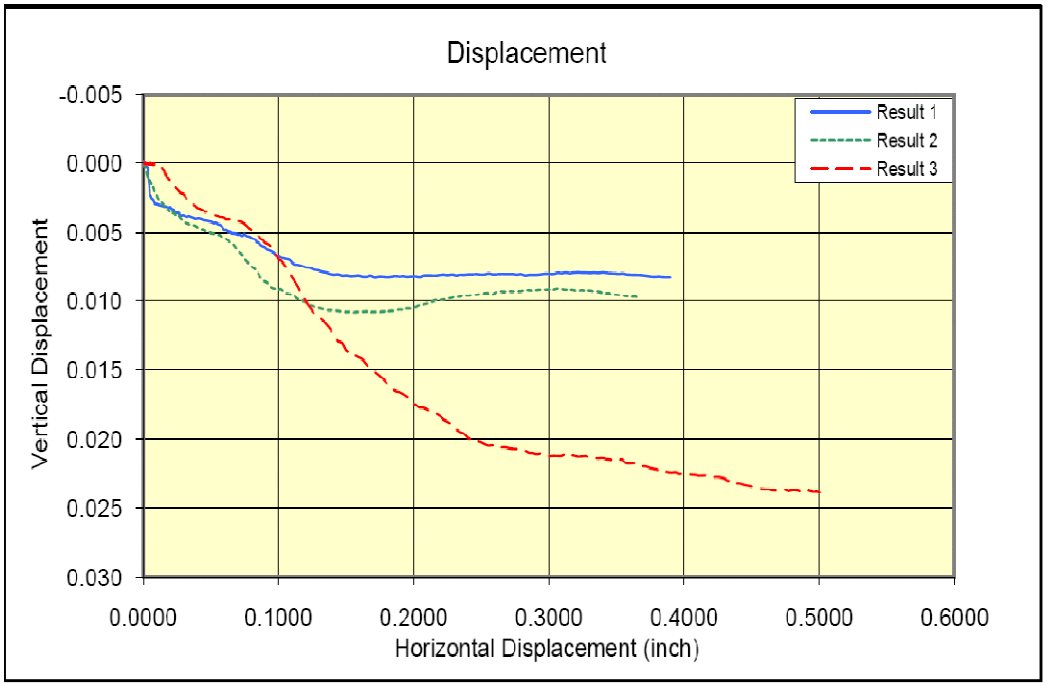
Displacement
Vertical Displacement
-0.005
0.000
0.005
0.010
0.015
0.020
0.025
0.030
0.0000
0.1000
0.2000
0.3000
0.4000
0.5000
0.6000
Horizontal Displacement (inch)
Result 1
Result 2
Result 3

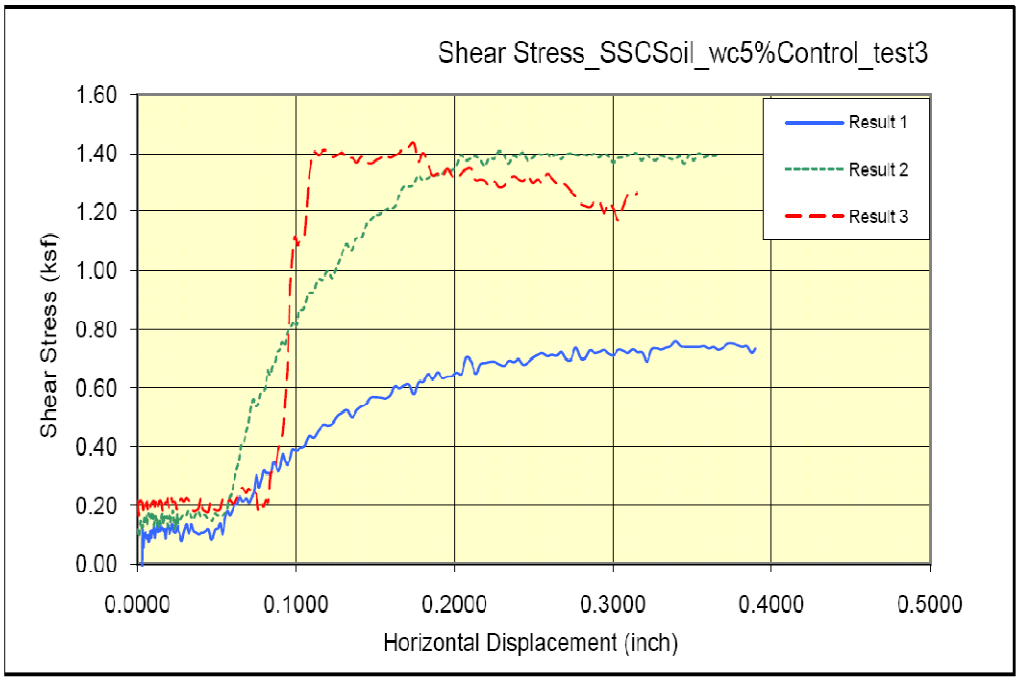
Shear Stress_SSCSoil_wc5%Control_test3
Shear Stress (ksf)
1.60
1.40
1.20
1.00
0.80
0.60
0.40
0.20
0.00
0.0000
0.1000
0.2000
0.3000
0.4000
0.5000
Horizontal Displacement (inch)
Result 1
Result 2
Result 3

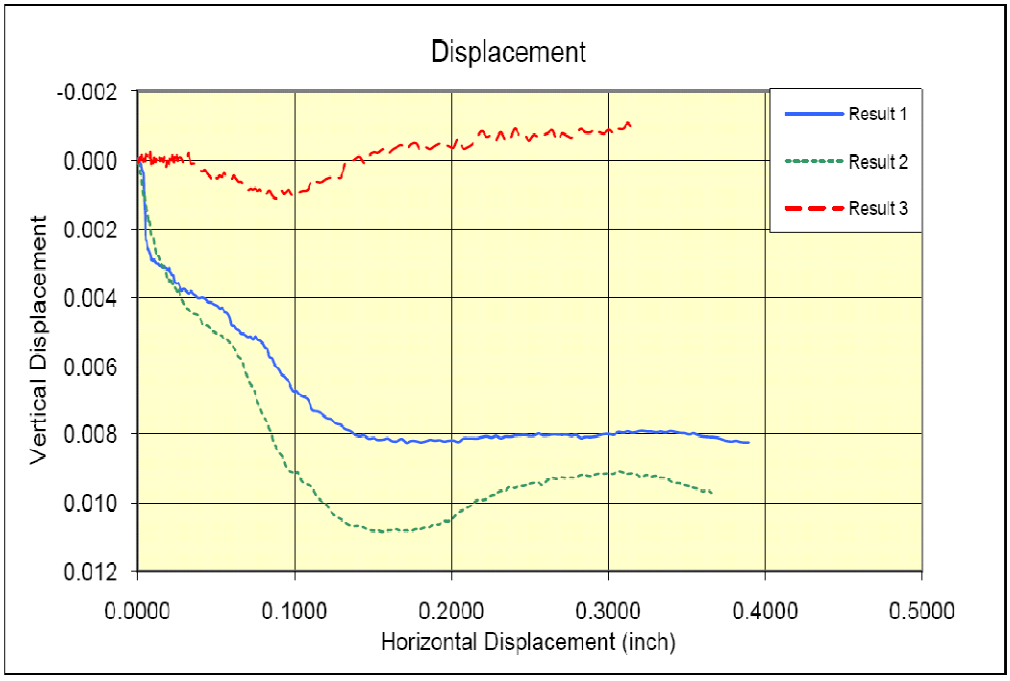
Displacement
Vertical Displacement
-0.002
0.000
0.002
0.004
0.006
0.008
0.010
0.012
0.0000
0.1000
0.2000
0.3000
0.4000
0.5000
Horizontal Displacement (inch)
Result 1
Result 2
Result 3

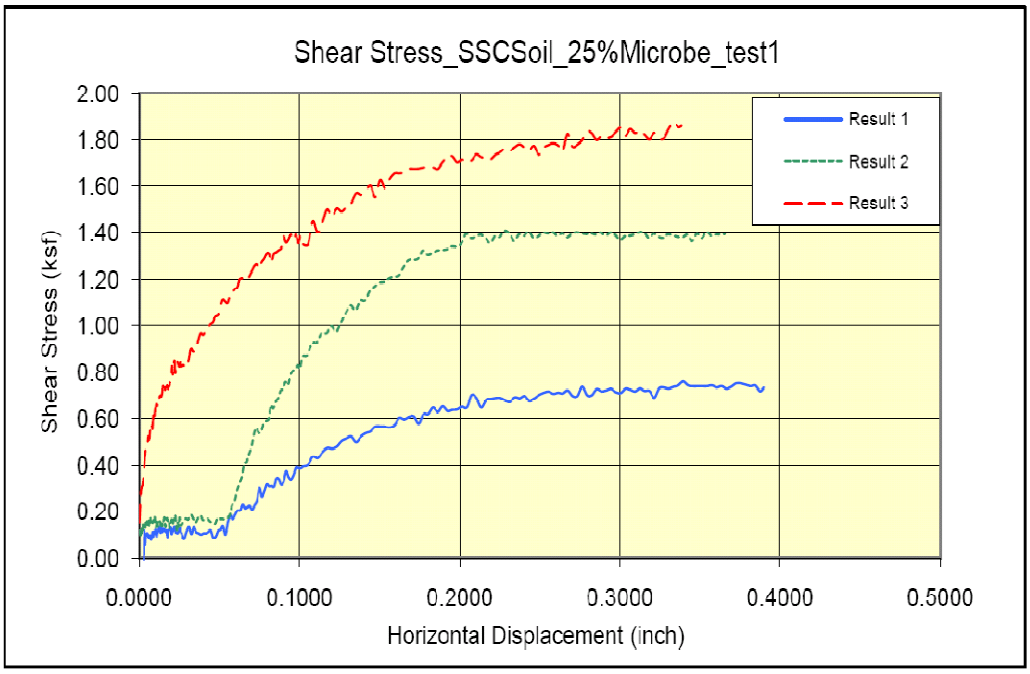
Shear Stress_SSCSoil_25%Microbe_test1
Shear Stress (ksf)
2.00
1.80
1.60
1.40
1.20
1.00
0.80
0.60
0.40
0.20
0.00
0.0000
0.1000
0.2000
0.3000
0.4000
0.5000
Horizontal Displacement (inch)
Result 1
Result 2
Result 3

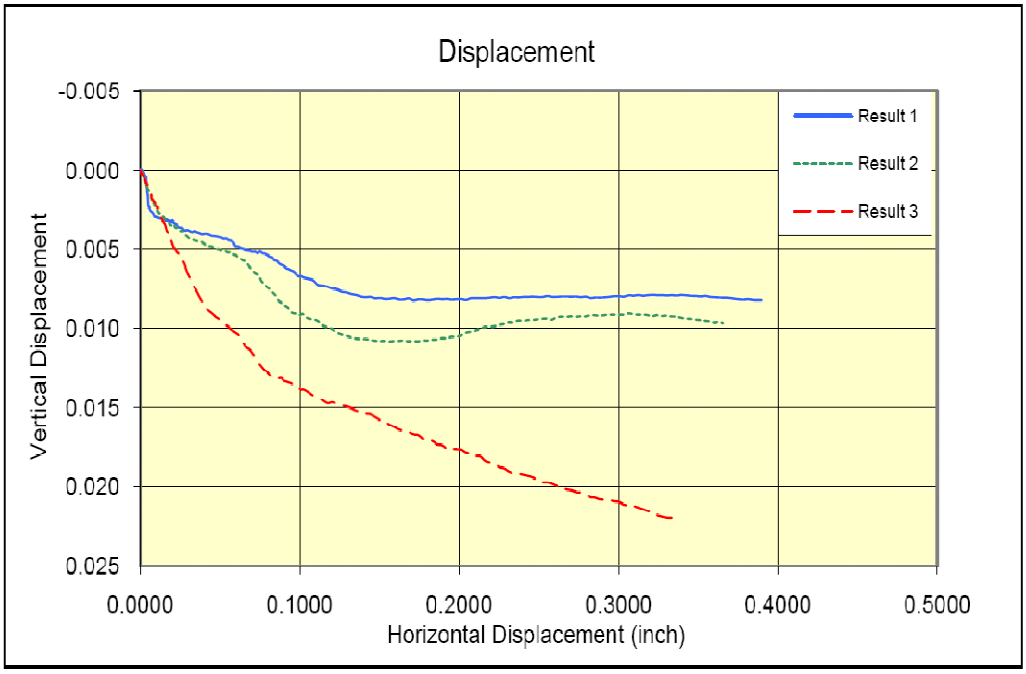
Displacement
Vertical Displacement
-0.005
0.000
0.005
0.010
0.015
0.020
0.025
0.0000
0.1000
0.2000
0.3000
0.4000
0.5000
Horizontal Displacement (inch)
Result 1
Result 2
Result 3